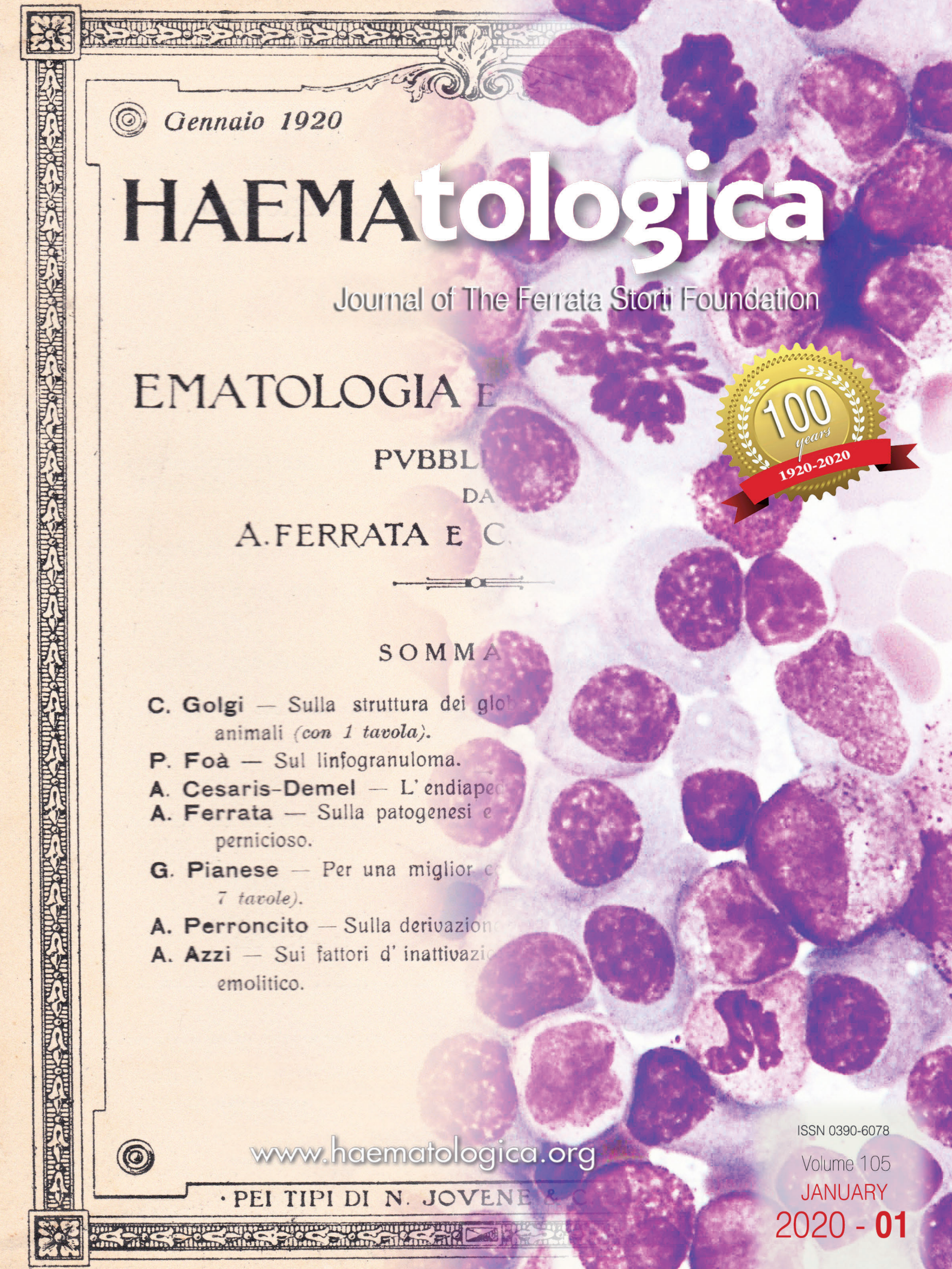

ISSN 0390-6078
Volume 105
JANUARY
2020 - 01

haematologica
Journal of the Ferrata Storti Foundation

haematologica
Journal of the Ferrata Storti Foundation

Information for readers, authors and subscribers

Haematologica (print edition, pISSN 0390-6078, eISSN 1592-8721) publishes peer-reviewed papers on all areas of experimental and clinical hematology. The journal is owned by a non-profit organization, the Ferrata Storti Foundation, and serves the scientific community following the recommendations of the World Association of Medical Editors (www.wame.org) and the International Committee of Medical Journal Editors (www.icmje.org).

Haematologica publishes editorials, research articles, review articles, guideline articles and letters. Manuscripts should be prepared according to our guidelines (www.haematologica.org/information-for-authors), and the Uniform Requirements for Manuscripts Submitted to Biomedical Journals, prepared by the International Committee of Medical Journal Editors (www.icmje.org).

Manuscripts should be submitted online at http://www.haematologica.org/.

Conflict of interests. According to the International Committee of Medical Journal Editors (http://www.icmje.org/#conflicts), "Public trust in the peer review process and the credibility of published articles depend in part on how well conflict of interest is handled during writing, peer review, and editorial decision making". The ad hoc journal's policy is reported in detail online (www.haematologica.org/content/policies).

Transfer of Copyright and Permission to Reproduce Parts of Published Papers. Authors will grant copyright of their articles to the Ferrata Storti Foundation. No formal permission will be required to reproduce parts (tables or illustrations) of published papers, provided the source is quoted appropriately and reproduction has no commercial intent. Reproductions with commercial intent will require written permission and payment of royalties.

Detailed information about subscriptions is available online at www.haematologica.org. Haematologica is an open access journal. Access to the online journal is free. Use of the Haematologica App (available on the App Store and on Google Play) is free.
For subscriptions to the printed issue of the journal, please contact: Haematologica Office, via Giuseppe Belli 4, 27100 Pavia, Italy (phone +39.0382.27129, fax +39.0382.394705, E-mail: info@haematologica.org).

Rates of the International edition for the year 2019 are as following:

	Institutional	*Personal*
Print edition	*Euro 700*	*Euro 170*

Advertisements. Contact the Advertising Manager, Haematologica Office, via Giuseppe Belli 4, 27100 Pavia, Italy (phone +39.0382.27129, fax +39.0382.394705, e-mail: marketing@haematologica.org).

Direttore responsabile: Prof. Carlo Balduini; Autorizzazione del Tribunale di Pavia n. 63 del 5 marzo 1955.
Printing: Press Up, zona Via Cassia Km 36, 300 Zona Ind.le Settevene - 01036 Nepi (VT)

Associated with USPI, Unione Stampa Periodica Italiana.
Premiato per l'alto valore culturale dal Ministero dei Beni Culturali ed Ambientali

haematologica
Journal of the Ferrata Storti Foundation

Table of Contents

Volume 105, Issue 1: January 2020

Editorials

Centenary Review Article

Review Articles

Guideline Article

Articles

Jivi: a new rFVIII with the proven power to protect for up to 7 days

▼**THIS MEDICINAL PRODUCT IS SUBJECT TO ADDITIONAL MONITORING.** Adverse events should be reported. Please report any suspected adverse reaction to the applicable national authority.

JIVI 250 / 500 / 1000 / 2000 / 3000 IU POWDER AND SOLVENT FOR SOLUTION FOR INJECTION
(Refer to full SmPC before prescription.)

COMPOSITION: site specifically PEGylated recombinant human coagulation factor VIII, 250/500/1000/2000/3000 IU/vial (100/200/400/800/1200 IU/ml after reconstitution). *Excipients:* Powder: Sucrose, Histidine, Glycine, Sodium chloride, Calcium chloride dihydrate, Polysorbate 80, glacial acetic acid (for pH adjustment). Solvent: Water for injections. **INDICATION:** Treatment and prophylaxis of bleeding in previously treated patients ≥ 12 years of age with haemophilia A (congenital factor VIII deficiency). **CONTRAINDICATIONS:** Hypersensitivity to the active substance or to any of the excipients. Known allergic reactions to mouse or hamster proteins. **WARNINGS AND PRECAUTIONS:** Allergic type hypersensitivity reactions are possible. Hypersensitivity reactions could also be related to antibodies against polyethylene glycol (PEG). If symptoms of hypersensitivity occur, patients should be advised to discontinue the use of the medicinal product immediately and contact their physician. The formation of neutralising antibodies (inhibitors) to FVIII is a known complication in the management of individuals with haemophilia A. A clinical immune response associated with anti-PEG antibodies, manifested as symptoms of acute hypersensitivity and/or loss of drug effect has been observed primarily within the first 4 exposure days. In patients with existing cardiovascular risk factors, substitution therapy with factor VIII may increase the cardiovascular risk. If a central venous access device (CVAD) is required, risk of CVAD-related complications including local infections, bacteraemia and catheter site thrombosis should be considered. **UNDESIRABLE EFFECTS:** *very common:* headache; *common:* hypersensitivity, insomnia, dizziness, cough, abdominal pain, nausea, vomiting, erythema (incl. erythema and erythema multiforme), rash (incl. rash and rash popular), injection site reactions (incl. injection site pruritus/rash and vessel puncture site pruritus), pyrexia; *uncommon:* FVIII inhibition (previously treated patients), dysgeusia, flushing, pruritus.

ON PRESCRIPTION ONLY.

MARKETING AUTHORISATION HOLDER:
Bayer AG, 51368 Leverkusen, Germany.

DATE OF REVISION OF THE UNDERLYING PRESCRIBING INFORMATION:
November 2018

PP-JIV-ALL-0215-1
February 2019

Jivi®
Recombinant Factor VIII (damoctocog alfa pegol)

LET'S GO

haematologica
Journal of the Ferrata Storti Foundation

REGISTER NOW
AND SUBMIT YOUR ABSTRACT

The science of **today** is the innovation of **tomorrow**

You are invited to attend the 28th Congress of the International Society on Thrombosis and Haemostasis (ISTH). Held in Milan, Italy, from July 11 - 15, 2020, the ISTH 2020 Congress will be the premier meeting in thrombosis, hemostasis and vascular biology and will be attended by thousands of the world's experts.

REGISTRATION AND ABSTRACT SUBMISSION ARE NOW OPEN. SUBMIT YOUR ABSTRACT BY FEBRUARY 4 AT ISTH2020.ORG

#ISTH2020

Plan to attend ISTH 2020 to exchange the latest science, discuss the newest clinical applications and present the recent advances to improve patient outcomes around the world.

MILAN
The science of today is the innovation of tomorrow

ISTH 2020 CONGRESS
JULY 11–15
ISTH2020.ORG

haematologica
Journal of the Ferrata Storti Foundation

Letters to the Editor

Letters are available online only at www.haematologica.org/content/105/1.toc

Comments

Comments are available online only at www.haematologica.org/content/105/1.toc

ANNOUNCING THE AWARDEE 2019

Dr. Ilaria Pagani

Leukaemia Research Group, Cancer Program, SAHMRI, Adelaide, Australia

for her two year project on

'Use of machine learning to integrate clinical data and biomarkers to optimise prediction of TFR'

"It is an honour and a pleasure to be the first John Goldman Research Prize Awardee. Receiving funding support from the European School of Haematology (ESH) is a privilege. It represents a critical step in my career towards becoming an independent investigator and provides the opportunity to build new collaborations.

My project aims to identify bioassays that can be integrated with clinical data in a machine learning system to develop a personalized predictive model for treatment free remission (TFR). I expect it will bring novel insights into the biology of TFR, opening new horizons toward the discovery of targeted therapies and improving TFR patient outcome."

APPLY FOR THE JOHN GOLDMAN AWARD 2020

Submitted projects must:

- aim to develop a method, algorithm or test to reliably identify patients able to benefit from treatment discontinuation, thereby significantly improving the probability of TFR success,
- demonstrate potential to improve healthcare standards for Chronic Myeloid Leukaemia (CML) patients or for patients suffering from other haematological malignancies.

The recipient of this annual award will receive a total of 80 000€ to finance or co-finance a research project on **Treatment Free Remission (TFR).**

DEADLINE FOR SUBMISSION: MARCH 1, 2020

For further information: Didi.jasmin@univ-paris-diderot.fr
European School of Haematology (ESH)
Saint-Louis Research Institute, Saint-Louis Hospital, Paris 75010,France
www.esh.org

Centenary of Haematologica

Carlo L. Balduini

Ferrata-Storti Foundation, Pavia, Italy

E-mail: CARLO L. BALDUINI, - carlo.balduini@unipv.it

doi:10.3324/haematol.2019.244939

The first issue of Haematologica was printed in January 1920. Today, therefore, the journal is 100 years old and represents the oldest hematology journal. The cover of this issue aims to synthesize the 100-years history of Haematologica (Figure 1).

As illustrated by Paolo Mazzarello in the Centenary Review in this issue, Haematologica has played an important role in the dissemination of knowledge on the subject of hematology and has hosted articles that have contributed to writing the history of this branch of medicine.

This was possible thanks to the work of the many generations of editors who, after the founders Adolfo Ferrata and Carlo Moreschi, succeeded one another in the direction of the journal and were able to keep it alive even in dark periods of our recent history characterized by economic crises and a war that devastated the whole world.

The journal, despite its one hundred years, is in excellent health, as demonstrated by the over two thousand papers submitted each year, by the 10 million visits that its website receives and by more than 1 million articles downloaded annually. Moreover, the articles published in Haematologica are among the most cited in the field of hematology.

The Ferrata Storti-Foundation, which owns and publishes Haematologica, is a non-profit organization, and this allows us to keep the costs for the authors low and everything published is available online for free.

The way in which the Foundation intends to celebrate the centenary is in line with this idea of a scientific journal: from January of this year the Haematologica website hosts a new, online Hematology Atlas (Figure 2) that is available for free to all readers. Being involved in this initiative as an editor, I am not allowed to say that it is a good atlas, but I can only report that it has nearly 300 pages and contains 800 images with detailed captions distributed in 35 chapters, each with a brief introduction explaining the diagnostic utility of evaluating peripheral blood and marrow smears. Rosangela Inverizzi, the lead author of the Atlas, and the editor have made every effort to ensure that the images appearing on the screen faithfully reproduce what is seen under the microscope. A printed version is available for those who want to have the atlas next to the microscope.

I believe that the Haematologica centenary is an appropriate occasion to thank all those who have contributed to the success of the journal: authors, editors, associated editors, and reviewers, as well as all members of the editorial staff. Thanks above all to Haematologica readers, who have contributed decisively to its achievements.

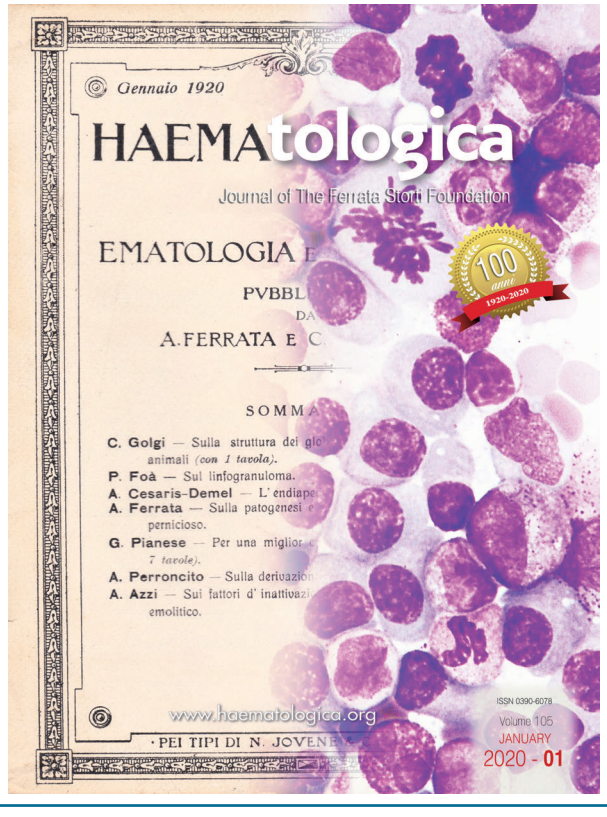

Figure 1. Cover of the Centenary issue.

Figure 2. The Haematologica Atlas.

Defining niche interactions to target chronic myeloid leukemia stem cells

Rebecca Mitchell and Mhairi Copland

Paul O'Gorman Leukaemia Research Centre, Institute of Cancer Sciences, University of Glasgow, Glasgow, UK

E-mail: MHAIRI COPLAND - mhairi.copland@glasgow.ac.uk

doi:10.3324/haematol.2019.234898

In this issue of *Haematologica*, Godavarthy *et al.*[1] describe how the expression of CD44 on the surface of leukemic stem cells (LSC) and E-selectin on bone marrow (BM) endothelium are essential for the engraftment of LSC within the BM niche. They show how this interaction can provide the LSC with protection from imatinib treatment. Importantly, disruption of this axis using an E-selectin inhibitor in combination with imatinib prevents LSC binding to the endothelium and demonstrates superior eradication of LSC in chronic myeloid leukemia (CML) compared with imatinib alone.

CML has been well characterized for a number of years, since the discovery of the Philadelphia chromosome and associated aberrant BCR-ABL signaling. This led to the revolutionary development of BCR-ABL-specific tyrosine kinase inhibitors such as imatinib. Tyrosine kinase inhibitors are highly effective at reducing the leukemic burden and disease progression, inducing remission and prolonging survival of patients with chronic phase CML.[2] Although very good control over the disease is gained in most chronic phase CML patients with tyrosine kinase inhibitor treatment, eradication of the LSC population, which sustains and repopulates the disease in patients, remains elusive.[3]

It has been established that the BM niche provides a sanctuary for LSC in which to thrive and avoid pharmacological interventions. There have been many studies showing how the niche adapts and is exploited during leukemic transformation.[4-6] By gaining, a better understanding of the interactions between LSC and their microenvironment, it may be possible to distinguish factors that favor survival of the leukemic cells and identify targets for improved drug therapy. One such strategy is to inhibit the homing and engraftment of LSC within the BM niche, without affecting normal hematopoietic stem cells (HSC).[7]

The BM microenvironment is complex, due to the array of different cell types which reside there, including osteolineage cells, mesenchymal stem cells, endothelial cells, neurons and hematopoietic cells.[8] In order to control and maintain homeostasis of the healthy BM niche, a multitude of cytokines and chemokines help determine HSC fate.[8] In normal hematopoiesis homing and engraftment of HSC within the BM is a highly coordinated multistep process that requires activation of different adhesion receptors to maintain tight regulation. Selectins and integrins are very important within this process.[9,10] Expression of integrins allows HSC to bind to vascular cell adhesion molecule-1 on BM endothelium and fibronectin on the extracellular matrix. Integrins, such as VLA4, also interact with E- and P-selectins, which are found constitutively expressed on the BM endothelium, and this interaction mediates HSC rolling and homing.[10] Another important factor within this process is CXCL12; this chemkine functions as an HSC chemoattractant through its receptor CXCR4, which through crosstalk with β_1 and β_2 integrins, mediates HSC homing and is required for stable engraftment.[9] CD44 has also been linked to HSC homing; however, HSC that do not express CD44 can still home and engraft normally.[11]

In studies comparing the homing and engraftment of CML LSC to normal HSC, it has been shown that patients with CML have several adhesion abnormalities.[12,13] LSC have defective β_1 integrin function, despite normal expression of VLA4 and VLA5, which decreases LSC adhesion to BM stroma.[13] It has also been shown that primary CML progenitor cells have reduced CXCR4 expression and impaired chemotaxis towards CXCL12, as well as reduced CXCL12-mediated integrin adhesion.[12] Despite these functional defects, LSC can still home and engraft within the BM and therefore must use alternative mechanisms.

Godavarthy *et al.*[1] demonstrate a novel reciprocal link between the external cues from the BM microenvironment and BCR-ABL-specific LSC-intrinsic pathways. They show how this leads to modulation of the expression of LSC adhesion molecules and alters interactions with the vascular niche. The authors confirm the interaction of BCR-ABL$^+$ cells and the vascular endothelium by using very sophisticated *in vivo* microscopy of the calvarium of mice injected with human CML leukocytes. Using time-lapse imaging, they found that the contact time of the leukemic cells to the BM endothelium was reduced in mice treated with an E-selectin inhibitor (GMI-1271).

The authors replicated these findings in a transgenic model, showing that BCR-ABL$^+$ cells were situated significantly further away from the endothelium if treated with GMI-1271 and imatinib. Furthermore, after treatment with GMI-1271 and imatinib, mice had improved survival, and demonstrated reduced numbers of CML-initiating clones, impaired short-term homing to the spleen and the BM, reduced leukocyte counts, BCR-ABL$^+$ myeloid cell counts and spleen size. Further studies showed that inhibition of E-selectin led to non-adhesion and an increase of *Scl/Tal1* expression in BCR-ABL$^+$ leukemia-initiating cells (LIC) *in vitro*. Additionally, *Scl/Tal1* negatively regulated the expression of CD44 on LIC, and overexpression of *Scl/Tal1* on LIC led to prolongation of survival in a murine model of CML, similar to the improved survival with CD44-deficient CML-initiating cells previously demonstrated by Krause *et al.*[14]

In vitro experiments demonstrated that CD44 was highly expressed in BCR-ABL$^+$ cells compared to BCR-ABL$^-$ cells, and that when BCR-ABL$^+$ cells were treated with GMI-1271 alone or in combination with imatinib there was an increase in cells in G2-S-M phase and a decrease in the G0 phase of the cell cycle. This coincided with an increase in cell cycle promoter CDK6 and decreased expression of cell cycle inhibitor p16. Furthermore, BCR-ABL1 phosphorylated SCL/TAL1 via the AKT signaling pathway. SCL/TAL1 regulated the activity of the CD44 regulatory element by

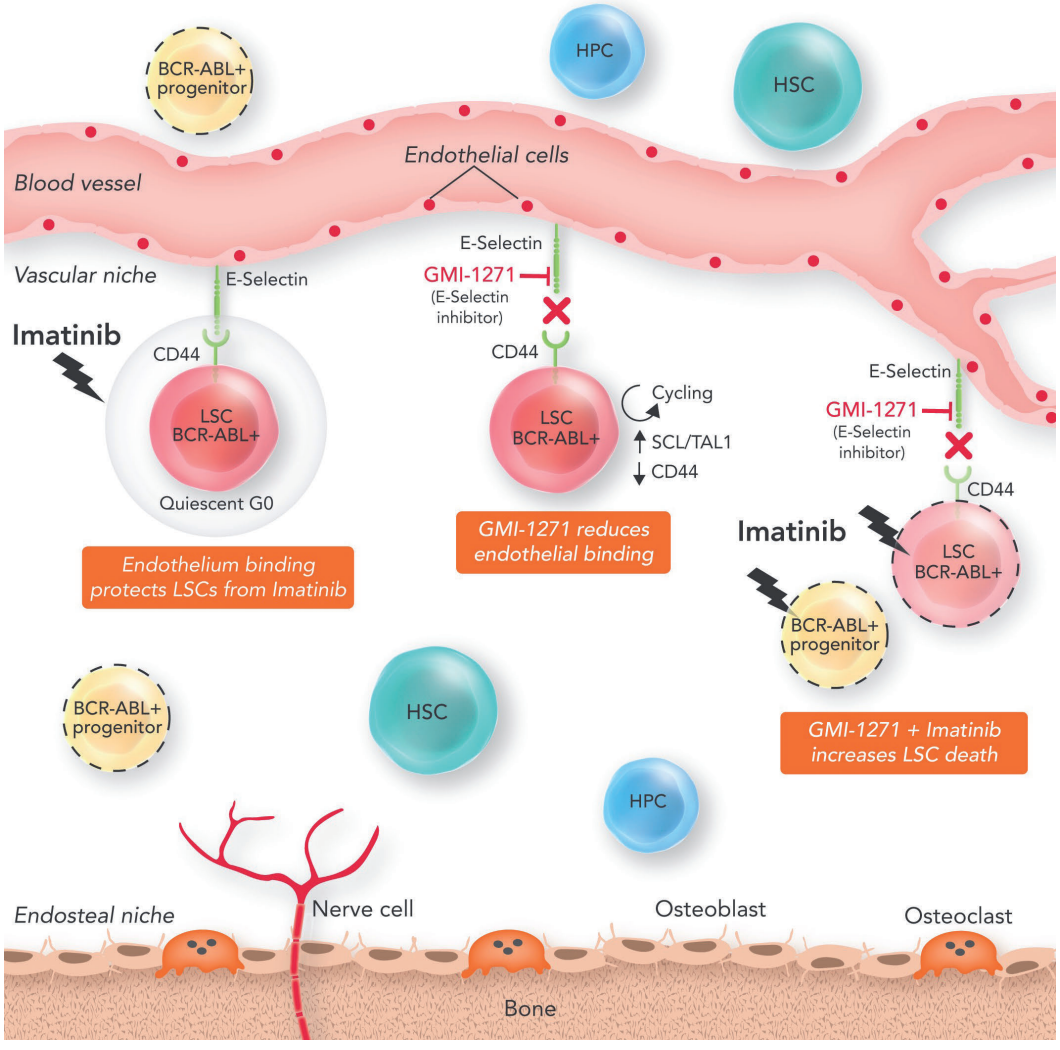

Figure 1. This schematic demonstrates the effects of E-selectin inhibition within the bone marrow microenvironment and the impact upon chronic myeloid leukemia stem cells and mechanistically how this is controlled by the SCL/TAL1 – CD44 axis. HPC: hematopoietic progenitor cell; HSC; hematopoietic stem cell; LSC: leukemic stem cell.

acting as a transcriptional repressor leading to decreased expression of CD44, decreased adhesion to the vascular niche and an increase in cycling LSC.

Interestingly, higher expression of CD44 was demonstrated in BCR-ABL cells specifically harboring the T315I mutation, which correlated with increased binding to E-selectin, with a larger amount of adherent cells in G0. The authors suggest that the increased expression of CD44 and increased binding to E-selectin may contribute to LSC dormancy and resistance to tyrosine kinase inhibitors.

Finally, relevance to human CML was established as leukocytes from patients with CML had higher transcriptional expression of *SCL/TAL1* and lower *CD44* expression compared to those from healthy individuals. Analyses of published datasets suggest a trend that expression of *SCL/TAL1* and *CD44* may correlate with disease stage and survival in CML patients; however, larger cohorts and further experimental data are required to confirm this.

The important experiments presented by Godavarthy *et al.* establish the mechanism of increased expression of CD44 on BCR-ABL1$^+$ cells. They further showed that dislocation of BCR-ABL1$^+$ cells from the niche, via inhibition of E-selectin binding, increased BCR-ABL$^+$ cell cycle progression and increased responsiveness to imatinib therapy.[1]

Inhibition of E-selectin has been shown to have therapeutic utility in other cancer types, such as acute myeloid leukemia and solid tumors in which it is thought to have a role in metastasis.[15] In acute myeloid leukemia, the leukemic blast cells bind to E-selectin on the endothelium and this activates leukemic pathways that contribute to chemotherapy resistance.[16] Currently, GMI-1271 is in a phase I/II clinical trial to treat acute myeloid leukemia in combination with chemotherapy to disrupt leukemia survival pathways and sensitize the leukemic cells to chemotherapy (*ClinicalTrials.gov Identifier: NCT02306291*)

E-selectin has also been implicated in the development of metastasis to the lungs from primary solid tumors, such as breast[17] and colon[18] cancer. It is hypothesized that, during the premetastatic stage, the primary tumors secrete soluble factors, which induce an inflammatory response in the

blood vessels and activate E-selectin on the endothelium, allowing engraftment of immune progenitor cells. This initial binding of E-selectin to its ligand confers firm adhesion, and triggers signaling that leads to permabilization of the endothelium through the dissociation of VE-cadherin/β-catenin. In an attempt to counteract metastasis, the E-selectin inhibitor GMI-1271 is currently being tested in preclinical models and is showing high efficacy.[17] As well as being a therapeutic target, E-selectin is also being screened as a potential biomarker for disease progression and metastasis.[19]

The BM microenvironment is a developing research focus which is showing great importance in disease pathophysiology. Advances in technology, such as the time-lapse intra-vital imaging used in the study by Godavarthy *et al.*,[1] are enabling a greater understanding of the interactions and mechanisms involved in cellular microenvironments This type of pioneering microscopy allows us to see interactions between leukemic cells and the niche, and is providing powerful data, as exemplified by this study as well as many others.[13] Enriching these data, single-cell RNA-sequencing allows for the analysis of the different cell types within the niche, evaluation of their transcriptional regulation and a view of how they may contribute to disease progression, providing important information which may have been masked using bulk sequencing approaches.[20] Through these studies, we continue to build upon our knowledge of the pathophysiology of CML and come ever closer to finding a way of eradicating quiescent LSC.

References

1. Godavarthy PS, Kumar R, Herkt SC, et al. The vascular bone marrow niche influences outcome in chronic myeloid leukemia via the E-selectin - SCL/TAL1 - CD44 axis . Haematologica. 2019;05(1):136-147.
2. Hochhaus A, Larson RA, Guilhot F, et al. Long-term outcomes of imatinib treatment for chronic myeloid leukemia. N Engl J Med. 2017;376(10):917-927.
3. Graham SM, Jørgensen HG, Allan E, et al. Primitive, quiescent, Philadelphia-positive stem cells from patients with chronic myeloid leukemia are insensitive to STI571 in vitro. Blood. 2002;99(1):319-325.
4. Ishikawa F, Yoshida S, Saito Y, et al. Chemotherapy-resistant human AML stem cells home to and engraft within the bone-marrow endosteal region. Nat Biotechnol. 2007;25(11):1315-1321.
5. Schepers K, Pietras EM, Reynaud D, et al. Myeloproliferative neoplasia remodels the endosteal bone marrow niche into a self-reinforcing leukemic niche. Cell Stem Cell. 2013;13(3):285-299.
6. Welner RS, Amabile G, Bararia D, et al. Treatment of chronic myelogenous leukemia by blocking cytokine alterations found in normal stem and progenitor cells. Cancer Cell. 2015;27(5):671-681.
7. Krause DS, Lawarides K, Lewis JB, von Andrian UH, Van Etten RA. Selectins and their ligands are required for homing and engraftment of BCR-ABL1+ leukemic stem cells in the bone marrow niche. Blood. 2014;123(9):1361-1371.
8. Morrison SJ, Scadden DT. The bone marrow niche for haematopoietic stem cells. Nature. 2014;505(7483):327-334.
9. Peled A, Kollet O, Ponomaryov T, et al. The chemokine SDF-1 activates the integrins LFA-1, VLA-4, and VLA-5 on immature human CD34+ cells: role in transendothelial/stromal migration and engraftment of NOD/SCID mice. Blood. 2000;95(11):3289-3296.
10. Frenette PS, Subbarao S, Marzo IB, von Andrian UH, Wagner DD. Endothelial selectins and vascular cell adhesion molecule-1 promote hematopoietic progenitor homing to bone marrow. Proc Natl Acad Sci U S A. 1998;95(24):14423-14428.
11. Oostendorp RAJ, Ghaffari S, Eaves CJ. Kinetics of in vivo homing and recruitment into cycle of hematopoietic cells are organ-specific but CD44-independent. Bone Marrow Transplant. 2000;26(5):559-566.
12. Zhang B, Ho YW, Huang Q, et al. Altered microenvironmental regulation of leukemic and normal stem cells in chronic myelogenous leukemia. Cancer Cell. 2012;21(4):577-592.
13. Bhatia R, Verfaillie CM. The effect of interferon-α on beta-1 integrin mediated adhesion and growth regulation in chronic myelogenous leukemia. Leuk Lymphoma. 1998;28(3-4):241-254.
14. Krause DS, Lazarides K, von Andrian UH, Van Etten RA. Requirement for CD44 in homing and engraftment of BCR-ABL–expressing leukemic stem cells. Nat Med. 2006;12(10):1175-1180.
15. Erbani J, Barbier V, Lowe J, Tay J, Levesque JP, Winkler I. Vascular niche E-selectin promotes acute myeloid leukemia resistance to chemotherapy via its receptors CD44 and CD162. Exp. Hematol. 2018;64:S63.
16. Chien S, Haq SU, Pawlus M, et al. Adhesion of acute myeloid leukemia blasts to E-selectin in the vascular niche enhances Their Survival By Mechanisms Such As Wnt Activation. Blood. 2013;122(21):61.
17. Kang SA, Blache CA, Bajana S, et al. The effect of soluble E-selectin on tumor progression and metastasis. BMC Cancer. 2016;16:331.
18. Köhler S, Ullrich S, Richter U, Schumacher U. E-/P-selectins and colon carcinoma metastasis: first in vivo evidence for their crucial role in a clinically relevant model of spontaneous metastasis formation in the lung. Br J Cancer. 2010;102(3):602-609.
19. Aref S, Salama O, Al-Tonbary Y, Fouda M, Menessy A, El-Sherbiny M. L and E selectins in acute myeloid leukemia: expression, clinical relevance and relation to patient outcome. Hematology. 2002;7(2):83-87.
20. Tikhonova AN, Dolgalev I, Hu H, et al. The bone marrow microenvironment at single-cell resolution. Nature. 2019;569(7755):222-228.

KIT D816V and the cytokine storm in mastocytosis: production and role of interleukin-6

Peter Valent[1,2]

[1]*Department of Internal Medicine I, Division of Hematology and Hemostaseology and* [2]*Ludwig Boltzmann Institute for Hematology and Oncology, Medical University of Vienna, Vienna, Austria*

E-mail: PETER VALENT - peter.valent@meduniwien.ac.at

doi:10.3324/haematol.2019.234864

Mast cell disorders (mastocytosis) are a hematologic neoplasm defined by abnormal expansion and dense accumulation of clonally altered mast cells in various organ systems.[1-5] The disease exhibits a complex pathology and an equally complex pattern of clinical presentations.[1-5] The classification of the World Health Organization (WHO) splits mast cell disorders into cutaneous entities, systemic variants, and localized mast cell tumors.[2-5] In more than 80% of all cases with systemic mastocytosis (SM), a somatic point mutation in *KIT* at codon 816 is detected.[3-6] Whereas patients with indolent forms of the disease have a normal or close-to-normal life expectancy, patients with advanced mast cell neoplasms, including aggressive SM (ASM) and mast cell leukemia (MCL), have an unfavorable prognosis with clearly reduced survival times.[2-5] In a majority of these patients, multiple somatic mutations and/or an associated hematologic neoplasm, such as a myeloid leukemia, can be detected. Regardless of the category of mastocytosis and the serum tryptase level, patients with mast cell disorders may suffer from (more or less severe) mediator-related symptoms and/or osteopathy.[1-5] Depending on co-morbidities, the symptoms in such patients require anti-mediator-type therapy and may be mild, more severe, or even life-threatening.[5]

A number of different mediators and cytokines are produced by mast cells and are involved in the clinical symptoms and pathological features that can be recorded in patients with mastocytosis.[7-12] Histamine is considered one of the most relevant mediators released from activated mast cells in patients with mastocytosis.[1-5,9] In fact, many of the symptoms reported by patients with SM can be kept under control by applying histamine receptor (HR)1 and HR2-targeting drugs.[5] However, mast cells also produce other clinically relevant mediators, such as prostaglandin D2, leukotrienes, heparin and tryptases.[1,9,13,14] In addition, activated mast cells can produce and release a number of functional cytokines, such as tumor necrosis factor (TNF), oncostatin M (OSM), or interleukin-6 (IL-6).[7-14] So far little is known about the mechanisms underlying the production and release of these cytokines in neoplastic mast cells in patients with SM. In many instances, activation of KIT and/or the IgE receptor may play a role in cytokine secretion.[7,9] Correspondingly, most of these cytokines are measurable in the sera of patients with SM and, in several instances, cytokine levels correlate with the variant of SM and with prognosis.[7-12] For example, a clear correlation between the variant of SM and IL-6 levels has been described.[11,12] In addition, in SM, elevated IL-6 levels are regarded as an indicator of a poor prognosis.[11,12]

In this issue of the Journal, Tobío *et al.* report that the D816V-mutated KIT receptor triggers expression and release of IL-6 in neoplastic mast cells.[15] In particular, they were able to show that bone marrow mast cells in patients with KIT D816V$^+$ SM express and release IL-6, and that the levels of IL-6 in cultured mononuclear cells in these patients correlate with the D816V KIT allele burden and with the percentage of mast cells in these samples.[15] In addition, they found that human mast cell lines expressing KIT D816V produce and secrete IL-6. Finally, they deciphered the KIT D816V-dependent signaling machinery that triggers IL-6 production in neoplastic mast cells. It is worth noting that these signaling molecules, like PI3K, AKT, TOR or JAK2-STAT5, represent druggable therapeutic targets.[15] An overview of the concept proposed by Tobío *et al.* is shown in Figure 1.

IL-6 is a multi-functional cytokine that plays a role in various biological and pathological processes. In particular, IL-6 has been implicated as a regulator of inflammatory reactions, infectious diseases and host defense, stromal reactions, and bone metabolism. In various neoplastic states, elevated levels of IL-6 have been reported, and in most disease models, higher IL-6 levels are associated with a poor prognosis.[11,12,16-18] Based on these observations, IL-6 has also been discussed as a new potential therapeutic target in chronic inflammatory and neoplastic disorders.[19]

In mastocytosis, IL-6 has been implicated as a potential mediator of mast cell development and activation, accumulation and function of lymphocytes, bone marrow remodeling, and bone pathology (ostesclerosis, osteopenia/osteoporosis). In addition, high IL-6 levels have been implicated as a prognostic parameter in SM.[11,12] In this regard, it is noteworthy that IL-6 may also act as an autocrine growth factor for neoplastic mast cells (Figure 1).

The observation by Tobío *et al.* confirms the impact of IL-6 in SM and suggests that IL-6 production in neoplastic mast cells is triggered by the oncogenic signaling machinery activated by KIT D816V (Figure 1).[15] This observation may have clinical implications and may lead to the development of new treatment concepts. For example, high IL-6 levels may already be detected in indolent SM (ISM) before the disease progresses to ASM or MCL.[11,12] In these cases, high IL-6 levels may serve as a biomarker of "high risk ISM" where a closer follow up or early interventional therapy may be considered.

There may be several ways to interfere with KIT D816V-dependent signaling in neoplastic mast cells in SM. One is to apply strong inhibitors of KIT D816V, such as midostaurin or avapritinib.[20-23] It will be of great interest to learn whether IL-6 levels decrease during therapy with these KIT-targeting drugs. Another possibility may be to block KIT-downstream signaling molecules involved in IL-6 production, such as JAK2 or PI3K. Indeed, the data of

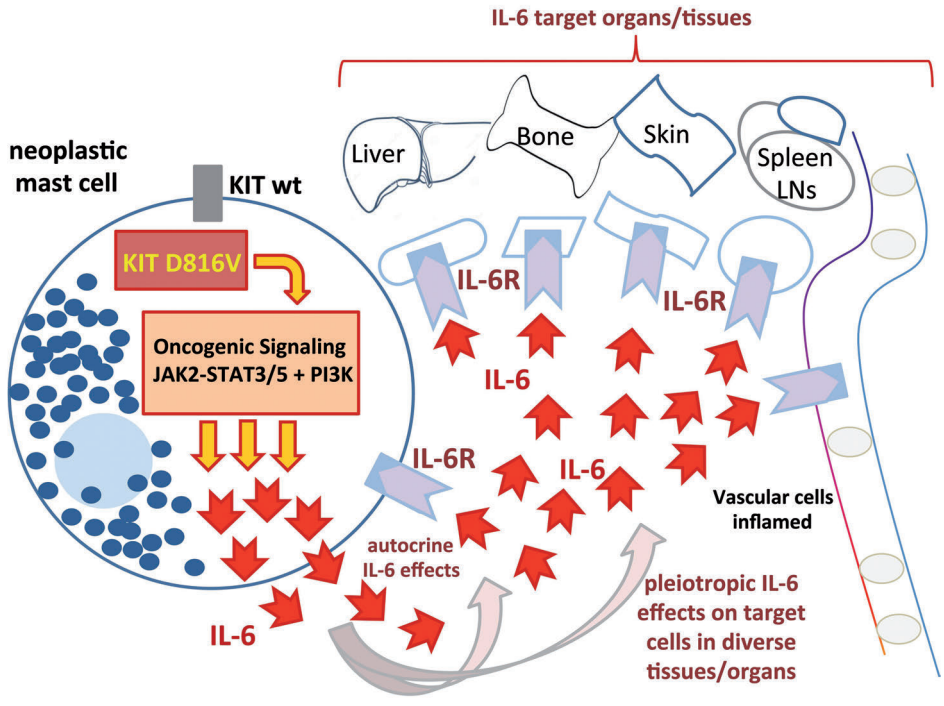

Figure 1. An overview of the concept proposed by Tobío *et al.*[15] of the KIT D816V-dependent signaling machinery that involves PI3K, AKT, TOR, and JAK2-STAT5 and triggers IL-6 production in neoplastic mast cells. In most patients with systemic mastocytosis, the transforming *KIT* mutation D816V is expressed in neoplastic mast cells. The KIT mutant form induces oncogenic signaling pathways which in turn leads to an abnormal production of various effector molecules, including cytokines. One such cytokine is interleukin-6 (IL-6). In contrast to normal mast cells, KIT D816V-transformed mast cells express and release substantial amounts of this cytokine (red arrows). Once released, IL-6 acts as an autocrine growth stimulator as well as a trigger of cell activation and inflammation. The effects of IL-6 on various target cells are exerted *via* specific IL-6 receptors (IL-6R).

Tobío *et al.* suggest that signaling through these target molecules leads to IL-6 production in neoplastic mast cells (Figure 1).[15] Finally, IL-6 effects can directly be blocked by applying antibodies against IL-6 or the IL-6 receptor.[24] However, it remains unclear whether these drugs can block the symptoms and pathologies in patients with SM.

Acknowledgments and Funding

Research by PV and his team is supported by the Austrian Science Fund, grants F4701-B20 and F4704-B20.

References

1. Metcalfe DD. Mast cells and mastocytosis. Blood. 2008;112(4):946-956.
2. Valent P, Horny HP, Escribano L, et al. Diagnostic criteria and classification of mastocytosis: a consensus proposal. Leuk Res. 2001;25(7):603-625.
3. Akin C, Valent P. Diagnostic criteria and classification of mastocytosis in 2014. Immunol Allergy Clin North Am. 2014;34(2):207-218.
4. Valent P, Akin C, Metcalfe DD. Mastocytosis: 2016 updated WHO classification and novel emerging treatment concepts. Blood. 2017;129(11):1420-1427.
5. Valent P, Akin C, Gleixner KV, et al. Multidisciplinary Challenges in Mastocytosis and How to Address with Personalized Medicine Approaches. Int J Mol Sci. 2019;20(12).
6. Arock M, Sotlar K, Akin C, et al. KIT mutation analysis in mast cell neoplasms: recommendations of the European Competence Network on Mastocytosis. Leukemia. 2015;29(6):1223-1232.
7. Hoermann G, Cerny-Reiterer S, Perné A, et al. Identification of oncostatin M as a STAT5-dependent mediator of bone marrow remodeling in KIT D816V-positive systemic mastocytosis. Am J Pathol. 2011;178(5):2344-2356.
8. Rabenhorst A, Christopeit B, Leja S, et al. Serum levels of bone cytokines are increased in indolent systemic mastocytosis associated with osteopenia or osteoporosis. J Allergy Clin Immunol. 2013;132(5):1234-1237.e7.
9. Theoharides TC, Valent P, Akin C. Mast Cells, Mastocytosis, and Related Disorders. N Engl J Med. 2015;373(2):163-172.
10. Hoermann G, Greiner G, Valent P. Cytokine Regulation of Microenvironmental Cells in Myeloproliferative Neoplasms. Mediators Inflamm. 2015;2015:869242.
11. Brockow K, Akin C, Huber M, Metcalfe DD. IL-6 levels predict disease variant and extent of organ involvement in patients with mastocytosis. Clin Immunol. 2005;115(2):216-223.
12. Mayado A, Teodosio C, Garcia-Montero AC, et al. Increased IL6 plasma levels in indolent systemic mastocytosis patients are associated with high risk of disease progression. Leukemia. 2016;30(1):124-130.
13. Galli SJ, Tsai M. Mast cells: versatile regulators of inflammation, tissue remodeling, host defense and homeostasis. J Dermatol Sci. 2008;49(1):7-19.
14. Mukai K, Tsai M, Saito H, Galli SJ. Mast cells as sources of cytokines, chemokines, and growth factors. Immunol Rev. 2018;282(1):121-150.
15. Tobío A, Bandara G, Morris DA, et al. Oncogenic D816V-KIT signaling in mast cells causes persistent IL-6 production. Haematologica. 2019;105(1):124-135.
16. Burger R. Impact of Interleukin-6 in Hematological Malignancies. Transfus Med Hemoth. 2013;40(5):336-343.
17. Taniguchi K, Karin M. IL-6 and related cytokines as the critical lynchpins between inflammation and cancer. Semin Immunol. 2014;26(1):54-74.
18. Hong DS, Angelo LS, Kurzrock R. Interleukin-6 and its receptor in cancer: implications for translational therapeutics. Cancer. 2007;110(9):1911-1928.
19. Rossi JF, Lu ZY, Jourdan M, Klein B. Interleukin-6 as a therapeutic target. Clin Cancer Res. 2015;21(6):1248-1257.
20. Gotlib J, Kluin-Nelemans HC, George TI, et al. Efficacy and Safety of Midostaurin in Advanced Systemic Mastocytosis. N Engl J Med. 2016;374(26):2530-2541.
21. Valent P, Akin C, Hartmann K, et al. Midostaurin: a magic bullet that blocks mast cell expansion and activation. Ann Oncol. 2017;28(10):2367-2376.
22. Arock M, Wedeh G, Hoermann G, et al. Preclinical human models and emerging therapeutics for advanced systemic mastocytosis. Haematologica. 2018;103(11):1760-1771.
23. Lübke J, Naumann N, Kluger S, et al. Inhibitory effects of midostaurin and avapritinib on myeloid progenitors derived from patients with KIT D816V positive advanced systemic mastocytosis. Leukemia. 2019;33(5):1195-1205.
24. Kang S, Tanaka T, Kishimoto T. Therapeutic uses of anti-interleukin-6 receptor antibody. Int Immunol. 2015;27(1):21-29.

A new kid on the block for acute myeloid leukemia treatment? Homoharringtonine interferes with key pathways in acute myeloid leukemia cells

Stefan K. Bohlander

Marijana Kumerich Chair in Leukaemia and Lymphoma Research, Leukaemia and Blood Cancer Research Unit, Department of Molecular Medicine and Pathology, The University of Auckland, Auckland, New Zealand

E-mail: STEFAN K. BOHLANDER - s.bohlander@auckland.ac.nz

doi:10.3324/haematol.2019.234880

Treatment for acute myeloid leukemia (AML) has not changed substantially in the past 40 years. We still largely rely on the substances (antimetabolites and topoisomerase inhibitors) that were introduced for AML treatment in the 1970s. Although treatment outcomes for AML, other than acute promyelocytic leukemia (APM), have improved over the years, these improvements have been slow and incremental and been largely achieved by optimizing dosing schedules and better supportive care.[1] However, substantial improvements in treatment, with high cure rates, have been achieved in genetically well defined subgroups of leukemia like acute promyelocytic leukemia (driven by the PML/RARA fusion)[2] and chronic myeloid leukemia (driven by the BCR/ABL fusion).[3] AML, however, is a different beast. It is not a single disease but a genetically highly heterogeneous group of malignant diseases of the hematopoietic stem cell that have similar phenotypes. The great genetic heterogeneity of AML, which was recognizable even in the early cytogenetic studies, has become very apparent with the advent of next-generation sequencing which has allowed the analysis of AML genomes at base pair resolution.[4,5]

Considering that AML is a highly heterogeneous group of malignant diseases, it is not surprising that a 'one size fits all' standard treatment approach can not achieve satisfactory cure rates. One critical question is: how heterogenous is AML? How many different diseases are we dealing with? If we simply looked at the number of genes that have been shown to harbor somatic mutation in AML and the number of somatic mutations in each AML sample, the number of potential combinations, and thus AML subgroups, would be astronomical. However, this is most likely an overestimate of the heterogeneity and complexity of AML, and there is likely only a much smaller number of crucial pathways that are disrupted in AML pathogenesis. Identifying and targeting these crucial pathways should greatly improve AML therapy.

In their report in this issue of the Journal, Chen *et al.* present convincing evidence that homoharringtonine (HHT) (omacetaxine mepesuccinate), an alkaloid found in the Hainan plum yew,[6] is targeting such a critical pathway in AML pathogenesis.[7] HHT has been used in China for several years for the treatment of AML[8,9] and was approved in 2012 by the US Food and Drug Administration (FDA) for the treatment of chronic myeloid leukemia (CML) with resistance to tyrosine kinase inhibitors.[10] The mode of action of HHT in CML was reported to be through the inhibition of protein synthesis by binding to the A site of the ribosome.[11]

Building on the success of HHT in the treatment of AML patients in China, where a remission rate of 83% was achieved when HHT was used in combination with cytarabine and aclarubicin to treat *de novo* AML patients,[9] Chen *et al.* explored the mechanism of HHT efficacy in murine and human AML cell lines as well as in murine and xenotransplant AML models. HHT treatment led to apoptosis and differentiation in cell lines and resulted in increased survival in murine AML transplantation models and in human AML xenograft models. Then the group set out to elucidate the molecular mechanism responsible for the observed effects of HHT treatment.

In a series of elegant experiments, Chen *et al.* showed that HHT binds to the transcription factor SP1, thereby inhibiting the binding of SP1 to its cognate DNA sequences. However, the route to this discovery was not straightforward. Initially, the group examined global 5-hydroxymethylcytosine (5hmC) levels in cells treated with HHT and noticed a remarkable reduction in global 5hmC levels. 5hmC is generated by the oxidation of methylcytosine groups in DNA through the action of the three dioxygenase enzymes TET1, 2 and 3.[12] As only the expression of the *TET1* gene, and not of *TET2* or *TET3*, was significantly down-regulated after HHT treatment, the authors concluded that the reduction in *TET1* expression, and hence a reduced TET1 enzymatic activity, was probably the cause of the reduced 5hmC levels. Examining the promoter region of TET1, they found multiple binding motifs for the transcription factor SP1 and reasoned that SP1 might be important for the HHT-induced downregulation of TET1 expression. And indeed, they could show that HHT treatment reduced binding of SP1 to its binding motifs in the TET1 promoter region. Furthermore, a drug affinity responsive target stability assay and a cellular thermal shift assay provided strong evidence that HHT is indeed binding to the SP1 protein and preventing SP1 from binding to its recognition sites in the *TET1* promoter region.

What are the consequences of the HHT-induced reduction in *TET1* transcription and, consequently, the global reduction in 5hmC levels? The 5hmC mark is associated with active transcription. Thus, the reduction in 5hmC levels was accompanied by a genome-wide reduction in gene transcription. More than 1,600 genes showed reduced expression. Very interestingly, one of the most strongly repressed genes was *FLT3*, which codes for the tyrosine kinase receptor FLT3. The authors confirmed that the *FLT3* gene was one of the direct targets of TET1 action with chromatin immunoprecipiation-quantitative polymerase chain reaction (ChIP-qPCR). FLT3 signaling is critical in the maintenance of the leukemic phenotype and activates a number of genes, including *HOXA9* and *MEIS1*, which are highly expressed in hematopoietic stem and progenitor cells. There is a positive feed-back

loop between FLT3 and HOXA9 / MEIS1 expression. Enforced *FLT3* expression leads to upregulation of *HOXA9* and *MEIS1*, and enforced expression of *HOXA9* and *MEIS1* in turn results in upregulation of *FLT3*. In addition, looking at all of the genes that had reduced expression after HHT administration, the authors found a significant enrichment of MYC target genes. They were then able to confirm that MYC expression itself was reduced after HHT treatment. Myc is one of the master regulators of cellular growth, increasing ribosome biogenesis and protein synthesis.[13]

SP1 is a transcription factor which has many cognate binding sites in the promoter region of many genes. So what is the evidence that the HHT-mediated inhibition of SP1 binding to the *TET1* promoter is critical for the phenotype observed in AML cells after HHT treatment and not the repression of a number of other genes? Very elegantly, the authors showed that repression of *TET1* phenocopies the effect of HHT treatment.

In summary, by binding to the transcription factor SP1, HHT affects one of the core pathways that are responsible for growth (MYC and targets) and impaired differentiation (HOXA9 and MEIS1) of AML cells. The central players in this pathway are the dioxygenase TET1 and the receptor tyrosine kinase FLT3. FLT3-activating mutations are found in about 40% of AML cases and it is overexpressed in an even larger proportion of AML. Thus, HHT promises to be effective in the majority of AML cases. HHT might thus be efficacious in a larger number of AML patients than several of the more recently introduced targeted AML drugs like FLT3 inhibitors (e.g. midostaurin, gilteritinib), IDH1/2 inhibitors (enasidenib, evosidenib), or hedgehog pathway inhibitors (glasdegib).[14] At the same time, one would hope that it is more specific for AML than conventional chemotherapeutic agents such as nucleoside analogs or anthracyclines, which affect very basic cellular functions like DNA metabolism and are thus highly toxic to normal cells.

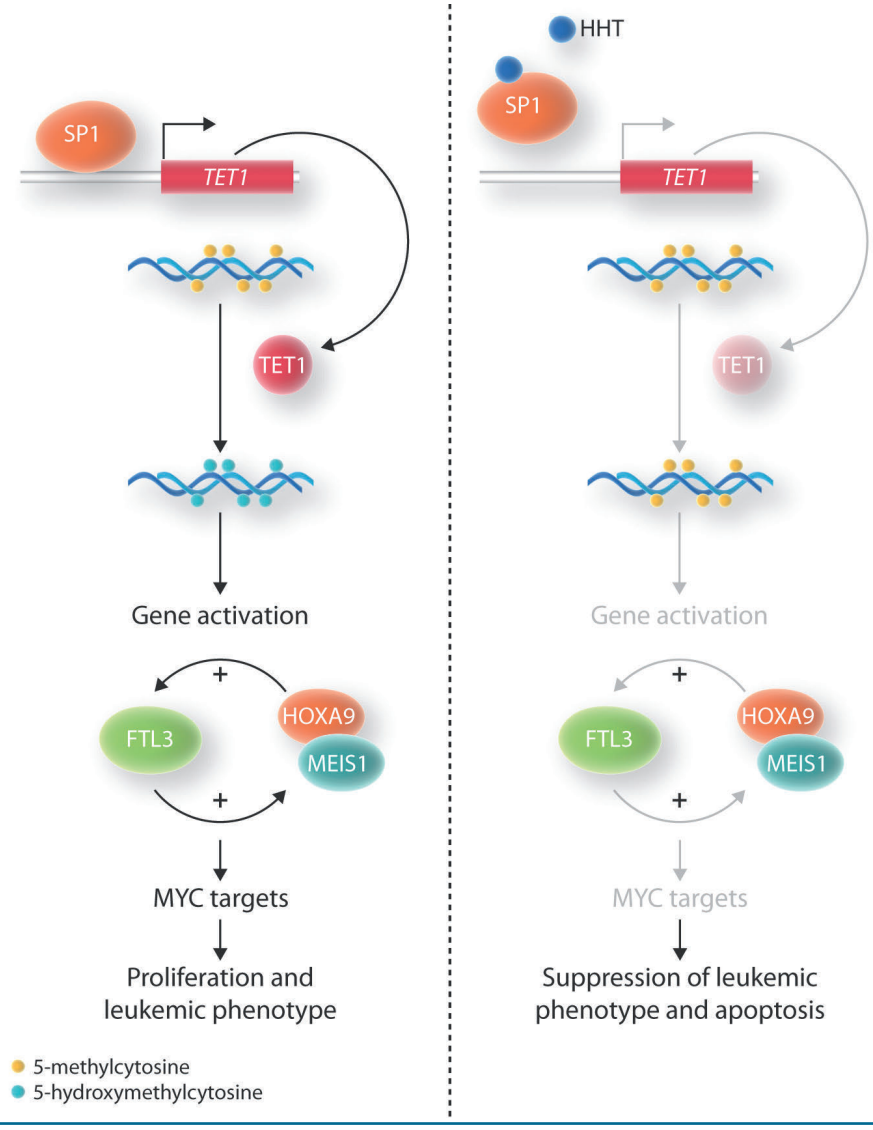

Figure 1. Diagram of the pathways affected by homoharringtonine (HHT). (A) Status of the pathways in the leukemic cells in the absence of HHT. (B) When HHT is present, it binds to SP1 which leads to a reduction of the activity of downstream pathways.

However, as HHT has been shown to bind to SP1, and SP1 is a widely expressed transcription factor whose expression is not restricted to AML cells, it is not surprising that HHT treatment can have considerable side effects, including myelosuppression. Another unanswered question is whether HHT only binds to SP1 or whether it also binds to other cellular proteins which, again, could cause side effects and adverse reactions.

Although it is unlikely that HHT will provide a cure for AML, it could become an important component of ever more diversified and targeted treatment strategies in this disease. The effectiveness of HHT and its therapeutic window need to be assessed rigorously in controlled clinical trials. These should be accompanied by a detailed genetic work up to identify those AML subgroups that are especially responsive to HHT therapy.

References

1. Burnett A, Wetzler M, and Löwenberg B. Therapeutic advances in acute myeloid leukemia. J Clin Oncol. 2011;29(5):487-494.
2. Platzbecker U, Avvisati G, Cicconi L, et al. Improved Outcomes With Retinoic Acid and Arsenic Trioxide Compared With Retinoic Acid and Chemotherapy in Non-High-Risk Acute Promyelocytic Leukemia: Final Results of the Randomized Italian-German APL0406 Trial. J Clin Oncol. 2017;35(6):605-612.
3. Bower H, Björkholm M, Dickman PW, Höglund M, Lambert PC, Andersson TM. Life Expectancy of Patients With Chronic Myeloid Leukemia Approaches the Life Expectancy of the General Population. J Clin Oncol. 2016;34(24):2851-2857.
4. Cancer Genome Atlas Research Network. Genomic and epigenomic landscapes of adult de novo acute myeloid leukemia. N Engl J Med. 2013;368(22):2059-2074.
5. Papaemmanuil E, Gerstung M, Bullinger L, et al. Genomic Classification and Prognosis in Acute Myeloid Leukemia. N Engl J Med. 2016;374(23):2209-2221.
6. Powell RG, Weisleder D, and Smith CR. Antitumor alkaloids for Cephalataxus harringtonia: structure and activity. J Pharm Sci. 1972;61(8):1227-1230.
7. Li C, Dong L, Su R, et al. Homoharringtonine exhibits potent antitumr effect and modulates DNA epigenome n acute myeloid leukemia by targeting SP1/TET1/5hmC. Haematologica. 2020; 105(1):148-160.
8. Jin J, Jiang DZ, Mai WY, et al. Homoharringtonine in combination with cytarabine and aclarubicin resulted in high complete remission rate after the first induction therapy in patients with de novo acute myeloid leukemia. Leukemia. 2006;20(8):1361-1367.
9. Jin J, Wang JX, Chen FF, et al. Homoharringtonine-based induction regimens for patients with de-novo acute myeloid leukaemia: a multicentre, open-label, randomised, controlled phase 3 trial. Lancet Oncol. 2013;14(7):599-608.
10. Nazha A, Kantarjian H, Cortes J, and Quintás-Cardama A. Omacetaxine mepesuccinate (synribo) - newly launched in chronic myeloid leukemia. Expert Opin Pharmacother. 2013;14(14):1977-1986.
11. Gürel G, Blaha G, Moore PB, and Steitz TA. U2504 determines the species specificity of the A-site cleft antibiotics: the structures of tiamulin, homoharringtonine, and bruceantin bound to the ribosome. J Mol Biol. 2009;389(1):146-156.
12. Wu X and Zhang Y. TET-mediated active DNA demethylation: mechanism, function and beyond. Nat Rev Genet. 2017;18(9):517-534.
13. van Riggelen J, Yetil A and Felsher DW. MYC as a regulator of ribosome biogenesis and protein synthesis. Nat Rev Cancer. 2010;10(4):301-309.
14. Tiong IS and Wei AH. New drugs creating new challenges in acute myeloid leukemia. Genes Chromosomes Cancer. 2019;58(12):903-914.

Therapeutic targeting of mutated p53 in acute lymphoblastic leukemia

Frank N. van Leeuwen

Princess Máxima Center for Pediatric Oncology, Utrecht, the Netherlands

E-mail: FRANK N. VAN LEEUWEN - F.N.vanleeuwen@prinsesmaximacentrum.nl

doi:10.3324/haematol.2019.234872

In this issue of *Haematologica*, Demir and colleagues describe a potential novel therapy for *TP53*-mutated acute lymphoblastic leukemia (ALL).[1] *TP53*, the gene encoding p53, is probably the most studied tumor suppressor in cancer biology. In about 50% of all human cancers, a mutation or deletion of *TP53* is observed at some point during tumor development or progression. The high incidence of *TP53* loss of function across human tumors relates to its central role as a transcription factor controlling cell cycle regulation in response to DNA damage, DNA repair, metabolic regulation, stem cell development and cell senescence.[2] In most hematologic malignancies, loss of p53 function is a harbinger of a poor response to therapy, particularly at relapse.[3] In ALL, genetic alterations affecting *TP53* are surprisingly uncommon at diagnosis, with their incidence being less than 5%.[4] A notable exception is a rare ALL subtype known as low hypodiploid ALL (32–39 chromosomes), in which there are almost invariably mutations or deletions affecting *TP53*. In about 50% of patients with low hypodiploid ALL, *TP53* alterations are also present in somatic cells, suggesting that Li-Fraumeni syndrome, an autosomal dominant disorder involving loss of *TP53*, somehow favors the development of low hypodiploid ALL in children.[4]

In relapsed ALL, the frequency of *TP53* mutations or deletions rises to about 10% and represents a strong and independent predictor of treatment failure.[5] *TP53* alterations result in either a loss of protein expression or the generation of protein variants with (partly) impaired function. About 80% of these TP53 variants are the result of missense mutations that affect DNA binding.[3] In most cancers, the *TP53* gene behaves as a classical tumor suppressor, which means that after mutation of one allele, the second allele is lost at a later stage of the disease. However, such a biallelic loss of function is not always observed in ALL, suggesting that dominant-negative effects or haploinsufficiency contribute to leukemogenesis or resistance to therapy.[5] Regardless of whether a wildtype allele is still present, *TP53* mutations or deletions in relapsed ALL predict a highly unfavorable response to therapy. Consequently, the International study for treatment of childhood relapsed ALL (IntReALL), a pan-European study group, now recognizes *TP53*-aberrant ALL relapse as a rare but very high-risk subtype that requires international collaboration in order to design and test novel treatment protocols, which may include drugs targeting p53.

In the absence of cellular stress signals, expression of the p53 protein is strictly controlled by MDM2 and its

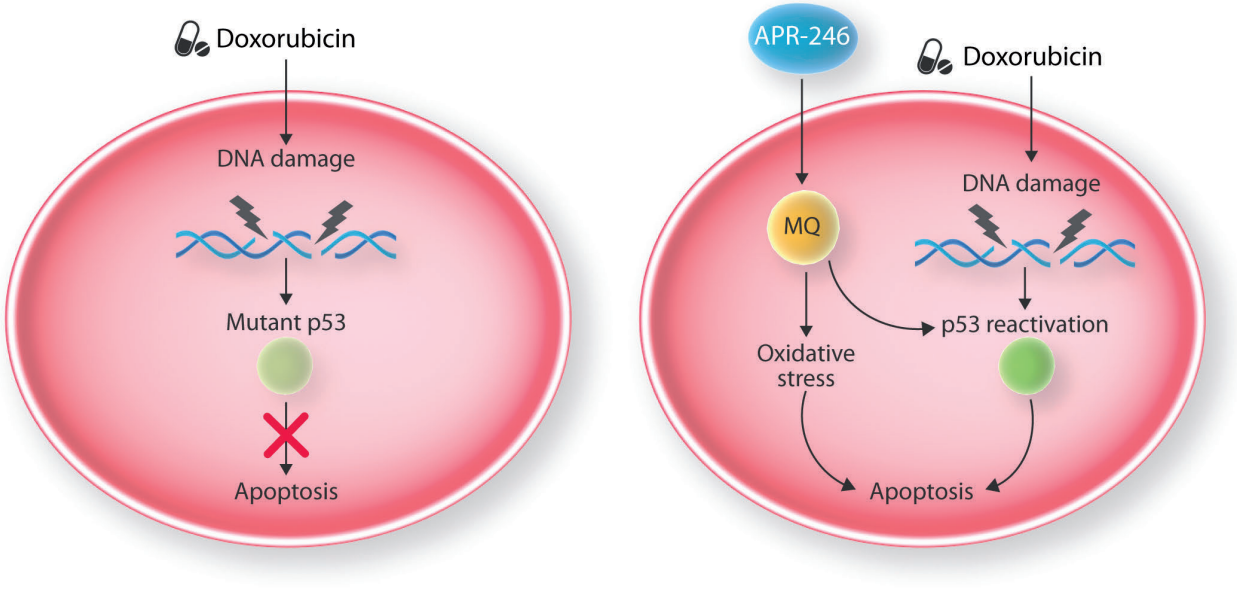

Figure 1. Proposed mechanism of action of APR-246 in TP53-mutated acute lymphoblastic leukemia. Acute lymphoblastic leukemia (ALL) cells expressing mutant p53 are refractory to doxorubicin-induced apoptosis. APR-246 is taken up by cells and metabolized into the reactive electrophile methylene quinuclidinone (MQ). By refolding p53 into an active conformation, MQ restores the apoptosis-inducing effects of doxorubicin. In addition, an increase in oxidative stress brought about by MQ may further enhance apoptosis induction.

homolog MDMX, which together form an E3 ubiquitin ligase complex that targets p53, resulting in nuclear export and subsequent degradation. Small molecule antagonists of MDM2 such as nutlins and related compounds, are under clinical evaluation in a variety of cancers expressing wildtype p53.[6] However, these drugs are ineffective in *TP53*-mutated or -deleted tumors. To target mutant p53, small molecules have been developed that are predicted to correct p53 protein folding, and thereby restore activity, which would re-enable *TP53*-mutated tumor cells to undergo apoptosis in response to (chemo)therapy. For instance, cell-based screening of compound libraries has led to the identification of the alkylating compound "p53 reactivation and induction of massive apoptosis" (PRIMA-1) and its methylated derivative PRIMA-1^{Met}, also known as APR-246. When taken up by cells, APR-246 is converted to the reactive electrophile methylene quinuclidinone (MQ), which is thought to reactivate conformationally unstable p53 mutants by binding to critical cysteine residues in the p53 DNA binding domain.[7] Consistent with such a mechanism of action, expression of p53 target genes is restored by these drugs while strongly promoting the induction of apoptosis. However, since the first descriptions of the proposed mechanism of action of this drug,[7,8] alternative mechanisms of action have been put forward. For instance, it was shown that APR-246 induces apoptosis by increasing intracellular levels of reactive oxygen species (ROS), even in fully p53-deficient cells, a mechanism involving glutathione depletion and MQ-mediated inactivation of the enzyme thioredoxin reductase.[9] Tumor cells expressing only wildtype p53 would be less responsive to these effects, due to the protective role of p53 against oxidative stress.[10] Therefore, irrespective of its precise mechanism of action, APR-246 appears to selectively target cancers with deficient p53 and for this reason it is under clinical evaluation in a number of *TP53*-mutated cancers, including myeloid malignancies such as myelodysplastic syndromes and acute myeloid leukemia.

The paper by Demir and colleagues in this issue of the journal describes the potential clinical use of APR-246 in pediatric *TP53*-mutated ALL.[1] Using both established ALL cell line models and patient-derived xenografts, the authors compared the effects of this drug in wildtype *vs*. *TP53*-mutated cells. They observed that the presence of *TP53* mutations selectively enhanced resistance to the DNA damaging drug doxorubicin, while increasing sensitivity to APR-246. The induction of apoptosis, seen in *TP53*-mutated ALL in response to APR-246, was directly correlated with the upregulation of p53 target genes such as *p21*, *PUMA* and *NOXA*, which is at least consistent with pP53 reactivation contributing to these effects. Moreover, when mutant *TP53* expression was reduced by shRNA-mediated knockdown, the apoptosis-inducing effects of APR-246 were no longer seen, indicating that in these leukemia models, the response to this drug requires the presence of mutant p53. Given the uncertainties pertaining to the precise mechanism of action of APR-246, the authors examined to what extent intracellular ROS levels may contribute to APR-246-induced apoptosis. Indeed, neutralization of ROS using MnTBAP, a synthetic metalloporphyrin with antioxidant activity, was able to partially inhibit the apoptosis-inducing activity of APR-246, suggesting a more complex mode of action for this compound than simply restoring p53 target gene expression.

Since doxorubicin is part of the armamentarium used to treat (relapsed) ALL, *in vivo* synergy between doxorubicin and APR-246 was examined using a *TP53*-mutated ALL xenograft model. Whereas doxorubicin was ineffective as a single agent in prolonging survival, a clear therapeutic benefit was seen from the treatment with APR-246 alone. In addition, and consistent with the observed *ex-vivo* synergy between doxorubicin and APR-246, this drug combination further extended leukemia-free survival in the mice studied. Taken together, the work by Demir and colleagues suggests that ALL patients suffering from relapsed *TP53*-mutated ALL could benefit from the use of APR-246 or similar p53-refolding agents, when used in addition to the current chemotherapy protocol. However, clinical implementation will require a more rigorous characterization of resistance profiles and therapy responses in *TP53*-mutated ALL, such as the inclusion of more patient-derived xenografts and examining potential interactions between APR-246 and other components of the treatment regimen for relapsed ALL. With respect to potential toxicities related to the use of APR-246, it will be important to follow the results of ongoing (phase II/III) trials in acute myeloid leukemia/myelodysplastic syndrome with this drug, either as a single agent or in combination with azacitidine.[11]

References

1. Demir S, Boldrin E, Sun Q, et al. Therapeutic targeting of mutant p53 in pediatric acute lymphoblastic leukemia. Haematologica 2020; 105(1):170-181.
2. Kruiswijk F, Labuschagne CF, Vousden KH. p53 in survival, death and metabolic health: a lifeguard with a licence to kill. Nat Rev Mol Cell Biol. 2015;16(7):393-405.
3. Stengel A, Kern W, Haferlach T, Meggendorfer M, Fasan A, Haferlach C. The impact of TP53 mutations and TP53 deletions on survival varies between AML, ALL, MDS and CLL: an analysis of 3307 cases. Leukemia. 2017;31(3):705-711.
4. Comeaux EQ, Mullighan CG. TP53 mutations in hypodiploid acute lymphoblastic leukemia. Cold Spring Harb Perspect Med. 2017;7(3).
5. Hof J, Krentz S, van Schewick C, et al. Mutations and deletions of the TP53 gene predict nonresponse to treatment and poor outcome in first relapse of childhood acute lymphoblastic leukemia. J Clin Oncol. 2011;29(23):3185-3193.
6. Burgess A, Chia KM, Haupt S, Thomas D, Haupt Y, Lim E. Clinical overview of MDM2/X-targeted therapies. Front Oncol. 2016;6:7.
7. Lambert JM, Gorzov P, Veprintsev DB, et al. PRIMA-1 reactivates mutant p53 by covalent binding to the core domain. Cancer Cell. 2009;15(5):376-388.
8. Bykov VJ, Issaeva N, Shilov A, et al. Restoration of the tumor suppressor function to mutant p53 by a low-molecular-weight compound. Nat Med. 2002;8(3):282-288.
9. Peng X, Zhang MQ, Conserva F, et al. APR-246/PRIMA-1(MET) inhibits thioredoxin reductase 1 and converts the enzyme to a dedicated NADPH oxidase. Cell Death Dis. 2017;8(4):e2751.
10. Sablina AA, Budanov AV, Ilyinskaya GV, Agapova LS, Kravchenko JE, Chumakov PM. The antioxidant function of the p53 tumor suppressor. Nat Med. 2005;11(12):1306-1313.
11. ClinicalTrials.gov [Internet]. Bethesda (MD): National Library of Medicine (US). Available from: http://clinicaltrials.gov/ct/show/NCT00287391/NCT03931291/ NCT03745716

One hundred years of *Haematologica*

Paolo Mazzarello

Department of Brain and Behavioral Sciences and University Museum System, University of Pavia, Italy

E-mail: PAOLO MAZZARELLO - paolo.mazzarello@unipv.it

doi:10.3324/haematol.2019.244350

The historical-scientific background

Hematology as a separate specialty, with its own methodology and hospital wards, only began to emerge between the nineteenth and the twentieth centuries. Before then, the pathophysiology and the clinical practice of hematologic diseases were mainly considered to be simply a part of internal medicine. However, the use of the term 'hematology' was, in fact, much older. In 1743, Thomas Schwencke (1694-1767), professor at the Faculty of Medicine of the University of The Hague, and also a physician to Wolfgang Amadeus Mozart during his concert tour in the Netherlands in 1765, published a volume entitled *Haematologia, sive sanguinis historia*. A book written by Martin Schurig (1656-1733), a doctor from Dresden, was published in 1744 which bore the term 'hematology' in the title: *Haematologia historico-medica, hoc est sanguinis consideratio physico-medico-curiosa etc.*

The turning point that brought hematology into the modern age was the introduction of cell theory in the mid-nineteenth century, according to which all body organs and parts of living beings, including the blood, were composed of many elementary 'bricks', the cells, and by what they produced through their different functions.[1] Although this represents the theoretical prerequisite for the development of this field of medicine, along with biology, its real foundations could only be laid, on the one hand, by the development of modern microscopy (and related cytological staining techniques) and, on the other, by the development of chemical methods to study the blood. The invention of the achromatic microscope by Giovanni Battista Amici (1786-1863) in 1824 and the development of staining procedure in histology based on aniline dyes by Paul Ehrlich (1854-1915) were particularly important.

The second half of the nineteenth century was certainly a crucial period for the investigation of blood components. Although the erythrocytes had been observed by the Italian Marcello Malpighi (1628-1694) in 1665, and clearly described by the Dutch Antoni van Leeuwenhoek (1632-1723) in 1674,[2] they became a subject of functional study in relation to pathological conditions only in the second half of the nineteenth century. An important scientific step in the history of hematology was the discovery of the hematopoietic function of bone marrow by Ernst Neumann (1834-1918) and Giulio Bizzozero (1846-1901) in 1868.[3] Another important development in this field of medicine was the description by Paul Ehrlich (who used the aniline staining technique in his degree thesis) of various types of leukocytes on the basis of their affinity for specific dyes. Although there had been some earlier vague descriptions of platelets, they were clearly observed almost simultaneously by various authors from 1878 to 1882, in particular by Georges Hayem (1841-1933), Ernst Neumann and Giulio Bizzozero. Only the latter, however, was able to consider them as distinct elements unrelated to erythrocytes and leukocytes, and to clarify their fundamental role in the formation of the white thrombus capable of blocking hemorrhage. Moreover, as early as 1869, Bizzozero in Pavia had described the megakaryocytes as "giant cells".[4] However, it was not until 1906 that James Homer Wright (1869-1928) hypothesized that platelets derive from bone marrow megakaryocytes.[5]

Thus, it was during the second half of the nineteenth century that the fundamental cognitive elements from which hematology could develop as an autonomous discipline were laid down. The subsequent explosion of clinical and pathophysiological studies of blood disorders led to the need for specific publishing tools aimed at disseminating the results of the research. And so the first specialized journals for hematologic studies in normal and pathological conditions were founded. One of these that quickly became a focus of attention was *Folia haematologica* founded by Artur Pappenheim (1870-1916), one of the leaders of the emerging field of blood studies in physiology and pathology. Working on the development of erythrocytes in Rudolf Virchow's (1821-1902) Pathological Institute in Berlin, he became the

Figure 1. Guido Bizzozero.

pioneer of the line of inquiry that saw the origin of the erythroid and lymphoid lineages in a common ancestral element: a stem cell (Stammzelle). This was the "unicist" theory of the origin of blood cells, and the journal that Pappenheim had founded became an important means to spread his ideas.

The first two architects of *Haematologica*

An Italian physician, Adolfo Ferrata (1880-1946), joined Artur Pappenheim in 1909 to carry forward his specialization studies in hematology. Ferrata was born in Brescia and studied medicine at the University of Parma. He had very early on shown a marked aptitude for investigating new fields of medical-biological sciences.[6-8] By the time he graduated in 1904, he had already acquired a remarkable mastery of laboratory methods. This was further refined during a first period of study in Germany, in 1907, at the Institute of Pathology under the direction of Julius Morgenroth (1871-1924) who, with his teacher Paul Ehrlich, had introduced the concept of "complement" to indicate that fraction of the blood that favors the immune response. Shortly after his arrival, Adolfo Ferrata was able to demonstrate, through dialysis, the existence of two fractions of the complement (one soluble and the other part of the seroglobulins) that were inactive if taken individually but which reactivated if joined together. Ferrata spent 1908 in Italy but then returned to Germany, this time to the Pappenheim laboratory where he worked on the genesis of the morphological elements of the blood. The result of one year of hard work and intense study was a 130-page monograph, illustrated with four splendid color plates, published in collaboration with his German mentor on *Folia haematologica*. Pappenheim and Ferrata provided persuasive morphological evidence to show that the elements of blood had a unitary origin. This fundamental study began to impose a taxonomic order in a field of study that had become increasingly complex.

Figure 2. Adolfo Ferrata.

In 1912, back in Italy, Ferrata published *Morfologia del sangue normale e patologico*,[9] a book that can be considered to represent the birth of Italian hematology. In Italy, Ferrata very soon became the leader in his field. At the same time, he started his university career, although this was interrupted during the First World War when he became the Director of a military hospital in Brescia. By the beginning of the 1920s, Ferrata was working in Naples at the II Medical Clinic of the University, and very quickly showed he was ready to take a university chair. After other temporary positions, he taught at the University of Pavia between 1924 and 1925, and, he became full professor there in 1926. It was a position he was to hold until his death.

By this time, it had been clearly recognized that what was needed was an Italian journal dedicated to hematology. To help in this, Ferrata found another young scientist who, like him, had spent some of his most important formative years training in Germany: Carlo Moreschi (1876-1921).[10] Born in Cermenate, near Como, Moreschi had studied medicine at the University of Pavia as a member of the Borromeo College. During that time, he regularly attended the General Pathology Laboratory directed by Camillo Golgi (1843-1926). Moreschi quickly adopted the rigorous experimental approach promoted by Golgi and this is clearly evident in his first works, published in 1900, the year he graduated. Moreschi worked as an assistant to the Chair of Medical Pathology in Pavia, but in 1904 began a long scientific collaboration with the prestigious Institute of Hygiene of Königsberg, which continued until 1907. Partnerships with the bacteriologist Richard Pfeiffer (1858-1945), who had isolated *Haemophilus influenzae* in 1892, and the immunologist-hygienist Ernst Friedberger (1875-1932) were both extremely productive. After a brief period of work in Italy in 1907, he returned to Germany and worked in Frankfurt in the laboratory of Paul Ehrlich who, a year later, would receive the Nobel Prize for Medicine. Meanwhile, in 1907 and in 1908, Moreschi published the report of his important scientific discovery, the antiglobulin test. This was rediscovered by Robert (known as Robin) Coombs (1921-2006), Arthur Mourant (1904-1994), and Robert Russell Rice (1907-1984) in 1945. It is now generally referred to as the Coombs test (or the Moreschi-Coombs test). In 1998, recalling this research, Coombs wrote that, when the substantial paper about the rediscovery was ready, "Arthur Mourant, a considerable linguist, came across a paper in the German literature from 1908 by a certain Carlo Moreschi which described enhancement of red cell agglutination with an 'antiserum to serum'. An acknowledgement was added to the proofs as an addendum".[11-13] Back in Italy, Moreschi obtained a position as assistant professor at the University of Pavia, then, as we said before, he worked as a military doctor during the First World War. At the same time, his university career was also progressing. In 1916, he obtained a position as Associate Professor ("Professore Incaricato") of Clinical

Figure 3. Carlo Moreschi.

and Medical Pathology at the University of Sassari, Sardinia, and later the chair of the Medical Clinic in Messina, Sicily.

In 1921, while in Pavia, Moreschi showed the very serious symptoms of hemorrhagic smallpox, probably contracted in Messina while he was visiting a patient, and died on May 24th.

The year before, Ferrata and Moreschi had met in the historic Neapolitan café, the "Gambrinus", and during their discussion, *Haematologica* was founded. It was initially printed in Naples by the publisher "N. Jovene & Co." and then, from 1924, it was edited in Pavia.[14] The two founders became editorial managers of the journal, and from 1922, after the death of Moreschi, Ferrata continued in this role alone. It is evident how the model that inspired them was the journal founded by Pappenheim, *Folia haematologica*.

Haematologica: the beginning of a long story

Haematologica was founded in January 1920 under the best auspices. In fact, the first article had as its author the greatest living revolutionary of Italian medicine and biology, Camillo Golgi, Nobel prize winner in 1906 for his investigation of the structure of the central nervous system. During his life-time, Golgi made an enormous contribution to hematology and clinical pathology. In 1885-1892, he had described with great precision the various stages of development of the malarial parasites in the blood (which became known as the Golgi cycle), identifying the correspondence between the moment of their reproduction with the periodic febrile bouts (Golgi law).[15] So, the first series of articles in *Haematologica* were published under the most authoritative and prestigious name of Italian medicine, and the man who had taught Moreschi. It was a way to guarantee and certify the scientific credibility of the periodical, but also a sign of respect for the old pathologist. Golgi's article was based on a new gold chloride staining method and described the appearance of a central body resembling a kind of nucleus.[16] He immediately distanced himself from those researchers who supported the thesis of a persistence of a real, functionally active nucleus in red blood cells. Among these was Angelo Petrone, who had been defending this concept since 1897 on the basis of experiments conducted using his own particular method. However, Petrone's conclusion had been refuted by work carried out in Golgi's laboratory by Adelchi Negri (1876-1912) in 1899.[15] Petrone subsequently presented new observations that apparently seemed to confirm his old theory. The hypothesis of the existence of a nucleus in the red blood cells of mammals was, therefore, once again of some interest in Italian scientific circles. But Golgi pointed out that his investigations did not support this hypothesis, although he did not provide any alternative functional interpretation of his observation. These findings were subsequently interpreted as artifacts due to the technique used rather than to morphological peculiarities that actually existed in the cell cytoplasm.[17,18] In the same article, Golgi described the presence of the centrosome in white blood cells, while in a subsequent note he addressed the problem of the possible existence of the centrosome in erythrocytes.[19]

Immediately after the authoritative opening of the old master, whose studies were continued by his pupil Costanza Boccadoro (1893-1983),[20,21] the first issue of *Haematologica* contained contributions by some of the exponents of Italian medicine and, in particular, hematology. The pathologist Pio Foà (1848-1923) investigated the

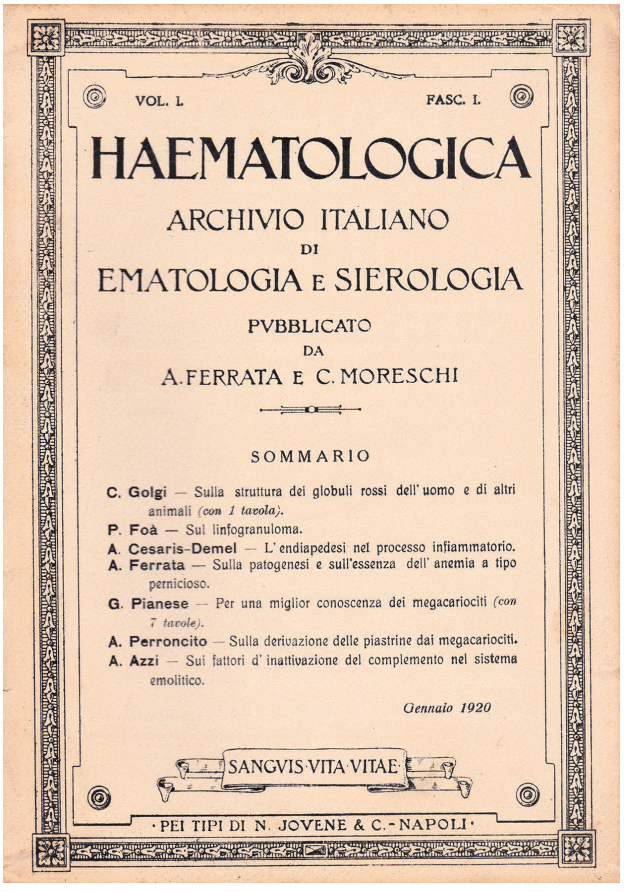
VOL. I. FASC. I.

HAEMATOLOGICA

ARCHIVIO ITALIANO
DI
EMATOLOGIA E SIEROLOGIA

PVBBLICATO
DA
A. FERRATA E C. MORESCHI

SOMMARIO

C. Golgi — Sulla struttura dei globuli rossi dell'uomo e di altri animali *(con 1 tavola)*.
P. Foà — Sul linfogranuloma.
A. Cesaris-Demel — L'endiapedesi nel processo infiammatorio.
A. Ferrata — Sulla patogenesi e sull'essenza dell'anemia a tipo pernicioso.
G. Pianese — Per una miglior conoscenza dei megacariociti *(con 7 tavole)*.
A. Perroncito — Sulla derivazione delle piastrine dai megacariociti.
A. Azzi — Sui fattori d'inattivazione del complemento nel sistema emolitico.

Gennaio 1920

SANGVIS VITA VITAE

PEI TIPI DI N. JOVENE & C. - NAPOLI

Figure 4. First issue of Haematologica.

Figure 5. Camillo Golgi.

nosographic problem of lymphogranuloma and its differentiation from tuberculous granuloma,[22] and another pathologist, Antonio Cesaris-Demel (1866-1938), published a paper on the stages of the diapedesis process.[23] There was also a very important paper by Ferrata on the pathogenesis of pernicious anemia.[24] Ferrata reported the complete disappearance of the megaloblastic erythropoiesis of the embryonic period as soon as the hematopoietic function of the liver begins. Ferrata's paper was a preliminary work which hinted at the therapeutic turning point that occurred a few years later with the introduction of hepatic treatment of pernicious anemia, which results in the rapid disappearance of megaloblastic erythropoiesis; as in the normal embryo, the liver's initial embryonic function makes the megaloblasts disappear. A few years later, Ferrata reviewed this treatment in the light of his 1920 observation in *Haematologica*.* Ferrata probably also made some attempts to treat patients with animal liver, but unfortunately he used cooked tissue, and did not observe any tangible effect.[25] The problem of treating pernicious anemia was taken up in a new way in subsequent works. Enrico Greppi (1896-1969) of the Medical Clinic of the University of Milan reported the case of a young man suffering from pernicious anemia and dyspeptic disorders of a probably infectious nature who was completely cured by transfusion.[26] Another remarkable work on the subject, published in *Haematologica* in German, came from Zoltan Alexander Leitner (1899-1981)[27] of the "Charité" Hospital in Berlin. He discussed the studies of George Richards Minot (1885-1950), George Hoyt Whipple (1878-1976), and William Parry Murphy (1892-1987) on the treatment of pernicious anemia with uncooked liver and with intramuscular liver extracts, which would earn them the Nobel Prize for Medicine in 1934.[28] Leitner suggested that extremely debilitated patients who required urgent intervention, or those in whom the gastro-enteric tract was seriously compromised, thus preventing adequate digestion, needed to receive a blood transfusion.

One of the most hotly debated hematologic arguments at the beginning of the 1920s was the origin of platelets from megakaryocytes. As many as 5 of the 31 articles published in the first volume of *Haematologica* dealt with the genesis of these corpuscles. In Ferrata's 1918 book *Le Emopatie*[29] (The Hemopathies), specific chapters were devoted to the various hypotheses:

– "Are platelets living and independent cells?"
– "Are platelets elements of variable and multiple origin, from erythrocytes, leukocytes and possibly from the vasal endothelium?"

*Carlo Bernasconi, personal communication. Carlo Bernasconi (1929-2014), formerly Professor of Hematology at the University of Pavia.

– "Are platelets derived from leukocytes?"
– "Are platelets derived from erythrocytes?"
– "Are platelets derived from megakaryocytes?"

Although Ferrata openly inclined towards the hypothesis that platelets are the third cellular element of blood and are produced by megakaryocytes, the topic remains a subject of discussion. Some articles published in *Haematologica* in 1920 were particularly relevant. The first written by Giuseppe Pianese (1864-1933) who worked at the Institute of Pathological Anatomy and Histology of Naples, concluded that platelets were not stable elements of blood and did not derive from megakaryocytes, but were formed in particular conditions, just as fibrin is formed from fibrinogen.[30] Golgi's pupil, Aldo Perroncito (1882-1929), who taught General Pathology at the University of Cagliari, Sardinia, had his doubts as to whether platelets where derived from megakaryocytes.[31-34] In fact, he suggested that the morphological evidence that supported this hypothesis was the consequence of experimental artifacts, since the medullary megakaryocytes ingested the platelets. So, since the megakaryocytes contained these corpuscles in their cytoplasm, it seemed that they produced them. In addition, platelets adhere to megakaryocytes and therefore the latter may seem to release them. The origin of the platelets was, therefore, according to Perroncito, still unknown. A precise and determined position in favor of the theory of the origin of platelets from megakaryocytes was taken by Giovanni Di Guglielmo (1886-1961) from Naples in a work performed under the direction of Ferrata.[35] Di Guglielmo observed how megakaryocytes could be present in the blood in some pathological conditions (chronic granulocytic leukemia) and were able to form platelets. He made a very accurate morphological description of this process, demonstrating that Perroncito's critical observations were wrong. In some beautiful color illustrations he showed the formation and release of platelets from megakaryocytes both through the fragmentation of their cytoplasm and *via* the emission of long cytoplasmic extroflexions.

In the years immediately following its foundation, *Haematologica* published numerous other works on the genesis of platelets.[36-41] Their derivation from megakaryocytes received increasing accreditation, although there was still room for alternative hypotheses. In the end, it was again Di Guglielmo who wrote the most lucid work on the origin of these corpuscles, reaffirming the correct thesis of their derivation from megakaryocytes.[42] He also confirmed his previous observations that these cells can enter peripheral blood in pathological conditions. The theory that megakaryocytes are present in the circulatory system (not only in pathological conditions but also in healthy subjects) and contribute to the formation of platelets has been definitively confirmed very recently with the documentation, in the mouse, of the release of platelets by the megakaryocytes migrated through the circulatory stream in the lung.[43]

From the start, serology and serodiagnosis of infectious diseases have always found a place in *Haematologica*.[44-50] But topics of a more hematologic nature continued to be at the center of the interests of the researchers who contributed to the journal. Following the cytological study of Golgi, some works published in the journal dealt with speculative (and sometime bizarre) hypotheses about the structure and shape of red blood cells.[51-54] Other investigations sparked a controversy over the priority of identifying the granule-filamentous substance in erythrocytes.[55] *Haematologica* has always published studies aimed at the chemical-physical characteristics of blood and hemoglobin.[56] One of the most important was a long article written by the physiologist Mario Camis (1878-1946) dedicated to the aggregating properties of hemoglobin that were rigorously studied under different conditions;[57] he also published a paper on the ultramicroscopic aspect of pure colloidal hemoglobin solutions studied, once again, under different conditions by means of the Zeiss microscope model which had been developed by Richard Adolf Zsigmondy (1865-1929) and Henry Siedentopf (1872-1940).[58]

However, the nature of megakaryocytes and their role in the production of platelets continued to be at the center of interest. The particular "budding" shape of the nucleus of megakaryocytes had opened up a specific question. Some cytologists/hematologists, like Ferrata and Pappenheim, believed that this aspect was the consequence of nuclear divisions not followed by cell separation. Other authors thought that megakaryocytes derived from the fusion of several cells. This was one of the most important topics of study at the Medical Clinic of Pavia. In the mid-20s, immediately following the arrival of

Figure 6. Giovanni di Guglielmo.

Ferrata as director and of his assistant Di Guglielmo, the Clinic had immediately become the most important center of hematology in the whole of Italy. The liberal environment assured by Ferrata's honest scientific attitude promoted the cultivation of very different ideas (although these were not always shared by the boss!). Thus, Di Guglielmo was able to argue that megakaryocytes derived from a process of cell fusion that eventually gave rise to their multi-nuclear appearance;[59] an idea shared by others.[60] There were also those who, playing devil's advocate, proposed the hypothesis of the dual origin of megakaryocytes, both by fusion and by nuclear "budding".[61,62]

From its first volume, *Haematologica* continued to publish many works dedicated to the clinical practice and clinical pathology of hematologic diseases. Of course, the founder of the journal, Ferrata, contributed works that resulted from his collaboration with members of the scientific school that was being formed around him (first in Naples, and then in Siena and Pavia), in particular with his most brilliant pupil at that time, Di Guglielmo. In addition to articles on pernicious anemia, studies appeared on the histogenesis of granulocytic leukemia.[63,64] on cytological changes in the malarial spleen,[65] and on histiocytic syndromes.[66] Di Guglielmo wrote an important work on erythremia for *Haematologica*, a field of study he personally introduced.[67] The paper described in depth two cases of acute erythremia (Di Guglielmo's disease) that had already been presented to the Medical-Surgical Society of Pavia in 1926, variously studied from different clinical, hematologic, and anatomical-pathological points of view. Many other areas of clinical hematology and related fields of study were also touched on, including: paroxysmal hemoglobinuria, the clinical and biological significance of Bence-Jones proteinuria, the pathogenesis of Gaucher disease, studies on leukemia, investigation of the forensic applications of hematology, and so on.

Haematologica has also always provided a means of making research performed outside Italy available to a wider readership, with works published in French, German and English. Thanks to the credibility and high professional profile of the director, Ferrata, the prestige of the journal immediately attracted the publication of studies produced by illustrious European names in the medical sciences. In 1924, Otto Lubarsch (1860-1933), director of the Institute of Pathology of the University of Berlin (known for defining carcinoid tumors) published a paper on the pathogenesis of thrombosis and embolism.[68] Shortly afterwards, the well-known pathologist Felix Marchand (1846-1928), who worked in Leipzig, published an article on the histology of the omentum.[69] An important paper was published in 1922 by Hal Downey (1877-1959) of the Department of Animal Biology of the University of Minnesota, in the US, a researcher who would become known the following year for the description of reactive lymphocytes (also known as "Downey cells"). The paper dealt with the structure and origin of lymph sinuses of mammalian lymph nodes.[70] In its first ten years, other studies were sent for publication in *Haematologica* from France,[71] Hungary,[72] Switzerland,[73,74] Austria,[75] Romania,[76,77] Belgium,[78] Russia,[79] Czechoslovakia,[80] and Brazil.[81]

Ups and downs

In ten years, Ferrata's management of *Haematologica* had allowed it to gain a position of great international prestige in the study of the physiology and pathology of the blood. Between the end of the 1920s and the beginning of the following decade, Ferrata's pupils from Pavia began to publish regularly in the journal. Many were destined to have important careers in Italian Hematology and Medical Clinic departments. Aminta Fieschi (1904-1991) was an active contributor to both clinical research and in cytological studies. Besides working at the Medical Clinic of Pavia, he also worked at the hospital in Cremona and, from 1930, at the Pavia Institute of Anatomy and Comparative Physiology.[82-87] Another important pupil of Ferrata was Paolo Introzzi (1898-1990), who worked for a time in Berlin with Zoltan Alexander Leitner and started to publish in *Haematologica* in the mid-'20s.** In one article, he proposed spleen puncture as a diagnostic procedure for pernicious anemia instead of bone marrow biopsy, a method that he proposed also applied to malignant granuloma.[88,89] The spleen remained his particular focus of interest and with Ferrata he proposed splenectomy to treat a case of primitive follicle-hyperplastic splenomegaly; the patient recovered.[90] In *Haematologica* he published studies in collaboration with Caterina Dessylla[91] of the Pediatric Clinic of Bologna and, above all, with Jörgen Nilsen Schaumann (1879-1953) of the Finsen-Institutet of Stockholm (who would give his name to Besnier-Boeck-Schaumann disease), with whom he studied the alterations of hematopoietic organs in acute lupus erythematosus.[92]

In 1931, Edoardo Storti (1909-2006) made his debut for *Haematologica* with a work on experimental anemia during an infection with *Botriocephalus*.[93] At the time he was a student of the Ghislieri College at the University of Pavia and attended the Institute of Anatomy and Comparative Physiology to prepare his degree thesis. A few years later he would become one of the main collaborators of Ferrata[94-96] and his last scientific heir.[97] At the same Institute of Anatomy and Comparative Physiology, his fellow student at the Ghislieri College, Vittorio Erspamer (1909-1999), also took his first steps in scientific research. In 1934, *Haematologica* published his study on schistosomiasis anemia in Libyan patients who he had examined during a scientific expedition.[98] Three years later he discovered serotonin in the intestines of experimental animals.[99,100]

Important works were published in the journal by the principal Italian hematologists of the day. Among them was Ferdinando Micheli (1872-1937), director of the Medical Clinic of the University of Turin, whose contribution was a paper on hemolytic anemia with hemoglobinuria and hemosiderinuria[101] (at the time called Marchiafava disease, but later to be known as Marchiafava-Micheli disease) and Giovanni De Toni (1895-1973), from the Pediatric Clinic of Bologna (whose

***Leitner was a friend of Ferrata who invited him to Pavia to hold some academic lessons. The Italian hematologist then asked him to host Introzzi in Berlin for a period of training. I got this information from Peter Schwartz, former Professor of Cardiology in Pavia and cousin of Zoltan Alexander Leitner.*

name is linked to De Toni-Fanconi-Debré syndrome), who investigated the possible relationship between Jennerian vaccination and the alterations of hematopoiesis.[102]

In the '30s, *Haematologica* continued to host articles also from various foreign countries, including the United States (Harvard University and Jefferson Medical College of Philadelphia).[103-110] The journal was at that time the fundamental forum for activities related to hematology in Italy and in 1935 became the official journal of the Italian Society of Hematology, publishing its acts, statutes and regulatory guidelines.

In 1940, with Europe thrown into the turmoil of the Second World War, *Haematologica* celebrated its twentieth anniversary with an impressive volume in honor of the founder Adolfo Ferrata, promoted by his most illustrious pupil Di Guglielmo. Di Guglielmo undersigned the introduction, dedicated with great affection to his teacher, and was himself the author of an extensive study of the pathology of the spleen.[111] Of course, the war completely interrupted the flow of scientific contributions from abroad. Among the many works that came from Italy, one stood out clearly and was signed by Edoardo Storti with his collaborator Mario Brotto (who had graduated just two years before).[112] It was a statistical and clinical-pathological study of 157 cases of leukemias which clearly took a position in favor of the old hypothesis, sustained between the nineteenth and the twentieth centuries by Hugo Ribbert (1855-1920), Guido Banti (1852-1925) and other pathologists, that leukemias were neoplastic diseases, in stark contrast to the view presented by Ferrata, Otto Naegeli (1871-1938), and other clinicians who instead claimed them to be hyperplastic illnesses. This testifies to the liberal atmosphere that so characterized the Pavia Medical Clinic and the original *raison d'être* of *Haematologica* directed by Ferrata, who, in honor of the freedom of research, allowed one of his pupils to advocate ideas diametrically opposed to those he himself supported. The topic was

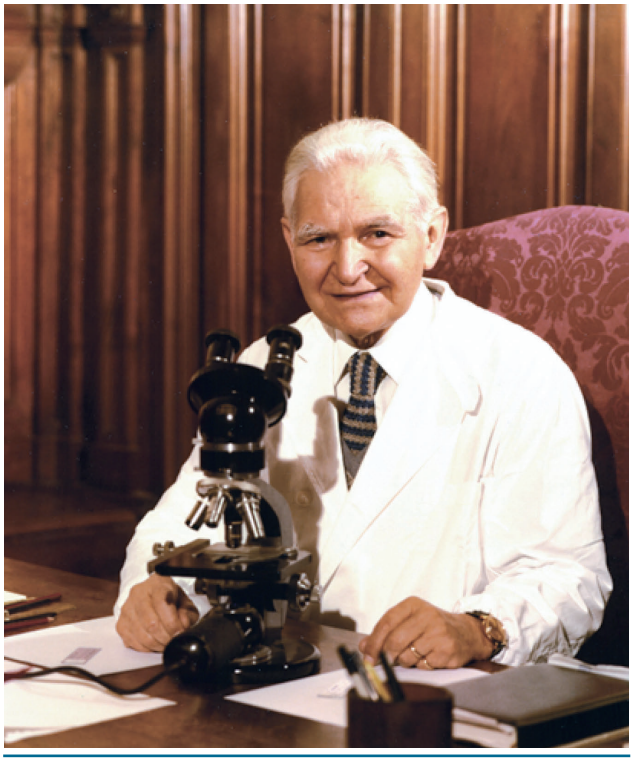

Figure 7. Edoardo Storti.

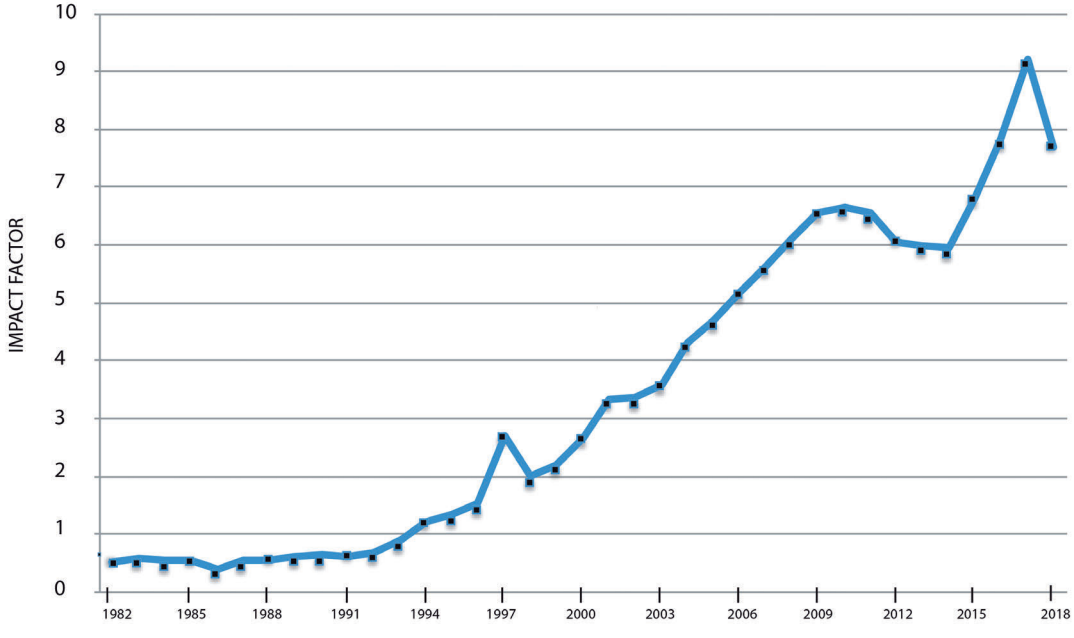

Table 1. *Haematologica Impact Factor for the years 1982-2018.*

immediately discussed in the following months,[113] and very soon the idea of the neoplastic origin of leukemias became a fact adopted by the international community of hematologists.

In the following years, the journal continued to publish significant works on many areas of blood morphology and pathology, for example, on the relationship between pulmonary tuberculosis and hematopoiesis,[114,115] in splenectomy in aplastic myelosis,[116] on a form of familial leukemia,[117] on chronic erythremic myelosis,[118] and others. The number of articles was, however, drastically reduced, and there were no published contributions from foreign research centers.

Ferrata died suddenly in 1946, and the direction of *Haematologica* was assigned to Giovanni Di Guglielmo (from 1946 to 1960) and then to Paolo Introzzi (from 1961 to 1973). However, the negative trend steadily continued and the decline also affected the other traditional European hematologic journals, like *Blut, Folia haematologica*, *Le sang*, that stopped publishing and disappeared from the scene. At the beginning of the '70s, *Haematologica* had only about a hundred subscribers divided between libraries and Italian hematologists, mostly related to the Ferrata school. This was the editorial situation in 1973 when Edoardo Storti became president of the Italian Society of Haematology and director of the journal.

A second beginning

Storti decided that it was worth attempting to revive the magazine and co-opted his pupils Sergio Perugini (1925-1979) as Assistant Editor and Edoardo Ascari as Scientific Secretary.[119] With a respected publisher, "Il Pensiero Scientifico Editore", which could ensure the continuity and regularity of publication, the new adventure began. From the beginning, Storti decided to promote the diffusion of the journal on the national and international stage, trying to increase the number of articles published in English, or, at least, to always provide a summary of the work in English. The journal management selected some Italian and foreign hematologists to ensure a rigorous and proper peer review of the articles submitted. Having taken these first steps, and seeing the credibility of the journal subsequently increase, from 1978, *Haematologica* was placed under an observation procedure by the Institute of Scientific Information. Its bibliometric impact, however, was initially very low.

In 1983, Storti, in agreement with the heirs of Ferrata, gave birth to the "Ferrata Storti Foundation", becoming its first president, and providing it with a substantial financial endowment. Its purpose was "to promote and encourage studies and research on blood diseases and their treatment".[120,121] One of the aims of the Foundation was "the support and the strengthening of *Haematologica*", which in the meantime had become the oldest surviving journal on blood diseases. Meanwhile, the number of articles coming from abroad was steadily increasing. Ferrata's heirs, who were the owners of *Haematologica*, donated it to the Ferrata Storti Foundation, and from 1985, the journal began to be published completely in English. In 1990, Storti passed the role of Editor to Edoardo Ascari with Mario Cazzola as Assistant Editor. At the same time, the journal was elected as the official organ of the Italian Society of Hematology and, since 1997, also of the Spanish Society of Hematology and Hemotherapy. Mario Cazzola became Editor of the journal in 2002 and, thanks to the endeavors of Emili Montserrat and Robin Foà, in 2005, *Haematologica* became the official organ of the European Hematology Association.[122] In that same year, Robin Foà became co-editor of the journal with Cazzola, joined by a team of 12 Associate Editors.

Ever since *Haematologica* has been published online, the management of the magazine and the Ferrata Storti Foundation have adopted the Open Access publishing mode. In the '80s and '90s, the Impact Factor (IF), which by the first evaluations was very low (in 1982 it was 0.409), grew slowly but steadily,[123] then to increase strongly in the first decade of the new century, thanks also to the commitment of Cazzola during the period of his management of the journal between 2002 and the end of 2011.

From the first of January 2012, Jan Cools was appointed Editor-in-Chief of *Haematologica* with Luca Malcovati as Deputy Editor. The Ferrata Storti Foundation has continued to promote and financially support the journal under the presidency of Edoardo Ascari (since 2002) and subsequently of Carlo Balduini. The last change in management of *Haematologica* came in 2018, when Luca Malcovati became Editor-in-Chief.

The last twenty years have seen a major transformation of the journal and it has become a reference point for studies in every field of hematology. All those who have contributed to making *Haematologica* great in the past hundred years, thanks to the scientific contributions they have made to the journal, have laid the foundations for an equally radiant second centenary.

A great past is the hope for an equally great future.

Acknowledgments

I would like to thank Carlo Balduini, president of the Ferrata Storti Foundation, for his great help in preparing this article.

References

1. Mazzarello P. A unifying concept: the history of cell theory. Nat. Cell. Biol. 1999;1(1):E13-E15.
2. Harris H. The birth of the cell. Yale University Press, New Haven and London, 2000.
3. Mazzarello P, Calligaro AL, Calligaro A. Giulio Bizzozero: a pioneer of cell biology. Nat Rev Mol Cell Biol. 2001;2(10):776-781.
4. Bizzozero G. [Sul midollo delle ossa]. Il Morgagni 1869;11:465-481;617-646.
5. Re L, Young RH, Castleman B. James Homer Wright: a biography of the enigmatic creator of the Wright stain on the occasion of its centennial. Am J Surg Pathol. 2002;26(1):88-96.
6. Storti E. Adolfo Ferrata: one of the fathers of hematology on the 50th anniversary of his death. Haematologica. 1996;81(2):101-104.
7. Mazzarello P, Calligaro A, Vannini V. [L'ematologo Adolfo Ferrata: un profilo]. Medicina nei Secoli 2005;17(3):747-768.
8. Ascari E. [La scuola ematologica pavese]. Fondazione Ferrata Storti, Pavia, 2007.
9. Ferrata A. [Morfologia del sangue normale e patologico]. Società Editrice Libraria, Milano, 1912.
10. Garbarino C. [Moreschi, Carlo]. Dizionario Biografico degli Italiani. 2012;76:692-694.
11. Coombs RRA. Historical note: past, present and future of the antiglobulin test. Vox Sang. 1998;74(2):67-73.
12. McCann SR. A History of haematology: from Herodotus to HIV. Oxford University Press, Oxford, 2016.
13. Pamphilon DH, Scott ML. Robin Coombs: his life and contribution to haematology and transfusion medicine. Brit J Haematol. 2007;137(5):401-408.

14. Di Guglielmo G. [Nel ventennale di "Haematologica"]. Haematologica. 1940;21 (1):V-VI.
15. Mazzarello P. Golgi. Oxford University Press, Oxford & New York, 2010.
16. Golgi C. [Sulla struttura dei globuli rossi dell'uomo e di altri mammiferi]. Haematologica. 1920;1(1):1-16.
17. Pensa A. [Trattato di istologia generale] Società Editrice Libraria, Milano, 1961.
18. Cesaris Demel A. [Sulle formazioni endoglobulari pseudonucleari e sugli anelli di "Cabot" messi in rilievo nei globuli rossi normali colla ipercolorazione]. Haematologica. 1921;2:125-146.
19. Golgi C. [Il centrosoma dei globuli rossi del sangue circolante dell'uomo e di altri animali]. Haematologica. 1920;1:333-359.
20. Boccadoro C. [Contributo allo studio delle alterazioni degli elementi del sangue in diversi stati patologici]. Haematologica. 1921;2:280-310.
21. Boccadoro C. [Di una particolare alterazione dei globuli rossi nella colemia]. Haematologica. 1923;4:428-432.
22. Foà P. [Sul linfogranuloma]. Haematologica. 1920;1:17-32.
23. Cesaris Demel A. [L'endiapedesi nel processo infiammatorio]. Haematologica. 1920;1(1):33-47.
24. Ferrata A. [Sulla patogenesi e sulla essenza delle anemie a tipo pernicioso]. Haematologica. 1920;1(1):48-60.
25. Ferrata A. [La terapia epatica dell'anemia perniciosa e suo probabile meccanismo d'azione nelle anemie a tipo pernicioso]. Boll Soc med Chir. Pavia 1929;43:171-182.
26. Greppi E. [Anemia perniciosa ed emopatie infettive]. Haematologica. 1927;8:253-282.
27. Obituaries in Lancet 1981;2(8258):1299-1300, and British Medical Journal 1982;284:130-131.
28. Leitner Z. Zur Behandlung der perniciösen Anaemie mit Bluttransfusion und Leberdiät. Haematologica. 1929;10:15-31.
29. Ferrata A. [Le emopatie, Trattato per medici e studenti]. Società Editrice Libraria, Milano, 1918.
30. Pianese G. [Per una miglior conoscenza dei megacariociti]. Haematologica. 1920;1(1):61-110.
31. Perroncito A. [Sulla derivazione delle piastrine dai megacariociti]. Haematologica. 1920;1:111-125.
32. Perroncito A. [Sulla derivazione delle piastrine]. Haematologica. 1920; 1(1):265-272.
33. Lapidari M. [La genesi e l'evoluzione della cellula gigante di Bizzozero]. Haematologica. 1929;10:171-184.
34. Introzzi P. [La funzione fagocitaria dei megacariociti]. Haematologica. 1929;10:195-204.
35. Di Guglielmo G. [Megacariociti e piastrine]. Haematologica. 1920;1:303-332.
36. Polettini B. [Sulla preesistenza delle piastrine nel sangue circolante]. Haematologica. 1921;2:47-64.
37. Perroncito A. [Sulla derivazione delle piastrine]. Haematologica. 1921;2:510-526.
38. Marchesini R. [Cellule di Bizzozero o megacariociti e Piastrine]. Haematologica. 1922;3:193-214.
39. Bétancès LM. Quelques images dites artificielles dans les frottis du sang. Haematologica. 1922;3:486-507.
40. Cesaris Demel A. [Fatti ed ipotesi sulla origine delle piastrine]. Haematologica. 1924;4:104-146.
41. Perroncito A. [Sulla derivazione delle piastrine]. Haematologica. 1926;7:87-96.
42. Di Guglielmo G. [I megacariociti nel sangue periferico]. Haematologica. 1923;4:182-205.
43. Lefrançais E, Ortiz-Muñoz G, Caudrillier A, et al. The lung is a site of platelet biogenesis and a reservoir for haematopoietic progenitors. Nature. 2017;544 (7648):105-109.
44. Azzi A. [Sui fattori d'inattivazione del complemento nel sistema emolitico]. Haematologica. 1920;1(1):126-140.
45. Moreschi C. [Sul significato e sul valor clinico della reazione Sachs-Georgi per la diagnosi della sifilide]. Haematologica. 1920;1:222-242.
46. Signorelli E. [Il potere complementare del siero durante la proteino-terapia dei morbi infettivi]. Haematologica. 1920;1:466-473.
47. Izar G. [Sul metodo di Kaup per la prova della fissazione del complemento nella sifilide]. Haematologica. 1920;1:508-521.
48. Luridiana P. [La reazione di Meinicke]. Haematologica. 1920;2:228-241.
49. Marassini A, Andriani S. [Sulla cosidetta legge di ripartizione nelle reazioni tra antigene e siero immune]. Haematologica. 1921;2:311-322.
50. Armuzzi G. [La sierodiagnosi nella sifilide sperimentale]. Haematologica. 1928;9:1-38.
51. Gamna C. [Ricerche e considerazioni sulla costituzione normale e patologica dei globuli rossi]. Haematologica. 1920;1:360-387.
52. Sabbatani L. [Osservazioni sui globuli rossi trattati col permanganato di potassio]. Haematologica. 1920;1:485-507.
53. Triolo C. [Nuova concezione sulla struttura del sangue]. Haematologica. 1922;3:29-37.
54. Mirone G. [Di un particolare morfologico dell'emazia dimostrabile coll'inchiostro di China]. Haematologica. 1925;6:26-28.
55. Ferrata A. [Sulla sostanza granulo-filamentosa dei globuli rossi]. Haematologica. 1928;9:207-210.
56. Chistoni A. [Ricerche sulla reazione attuale del siero di sangue]. Haematologica. 1921;2:213-227.
57. Camis M. [Ricerche chimico-fisiche sull'emoglobina con particolare riguardo alla dottrina dell'aggregazione molecolare]. Haematologica. 1921;2:149-211.
58. Camis M. [Osservazioni ultramicroscopiche sull'emoglobina]. Haematologica. 1927;8:155-176.
59. Di Guglielmo G. [Sul sistema delle cellule giganti midollari]. Haematologica. 1925;6:156-195.
60. Gandolfo S. [Policariociti e megacariociti negli organi embrionali di mammiferi e nelle anemie sperimentali]. Haematologica. 1925;6:244-262.
61. Fabris A. [Osservazioni sopra le eterotopie mieloidi negli avvelenamenti da saponina]. Haematologica. 1926;7:229-266.
62. Morone G. [Di alcune osservazioni sulla genesi e sulla formazione dei megacariociti]. Haematologica. 1928;9:117-155.
63. Ferrata A. [Studi sulle emopatie: I Sulla istogenesi della leucemia granulocitica]. Haematologica. 1921;2:242-279.
64. Ferrata A. [Studi sulle emopatie: II Ancora sulla istogenesi della leucemia granulocitica]. Haematologica. 1924;5:228-241.
65. Ferrata A, Negreiros-Rinaldi U. [Emoistioblasti e monociti nella milza malarica]. Haematologica. 1920;1:243-259.
66. Ferrata A, Reitano D. [Sindromi istiocitemiche (emoistioblastiche)]. Haematologica. 1923;4:385-393.
67. Di Guglielmo G. [Le eritropatie]. Haematologica. 1928;9:301-347.
68. Lubarsch O. [Zur Lehre von der Thrombose und Embolie]. Haematologica. 1924;5:91-103.
69. Marchand F. [Aeltere und neuere Beobachtungen zur Histologie des Omentum]. Haematologica. 1924;5:304-348.
70. Downey H. The structure and origin of the lymph sinuses of mammalian lymph nodes and their relations to endothelium and reticulum. Haematologica. 1922;3:431-468.
71. Bétancès LM. [Relation pathogénique entre les leucémies et certaines dermopathies]. Haematologica. 1920;1:196-221.
72. Liebermann L, Acél D. [Ueber Resistenzänderungen der roten Blutkörperchen bei physischer Arbeit]. Haematologica. 1922;3:15-28.
73. Alder A. [Ueber einen Fall akuter Promyelozytenleukämie]. Haematologica. 1923;4:423-427.
74. Knoll W. [Jollykörper in menschlichen Erythroblasten phylogenetisch betrachtet]. Haematologica. 1925;6:81-93.
75. Hittmair A, Rittmann R. [Ueber azuro-, eosinophile Leukozyteneinlagerungen Ein Beitrag zur Kenntnis der akuten Myelose mit Zelleinschlüssen]. Haematologica. 1926;7:149-188.
76. Vasiliu T. [Contribution à l'étude des cellules migrantes primitives: Hémohistioblastes de Ferrata]. Haematologica. 1924;5:34-40.
77. Jonesco D, Valter B. [Recherches hématologiques et cliniques dans la rage humaine]. Haematologica. 1927;8:213-220.
78. Lambin P. [Recherches sur le role hématopoiétique du système réticulo-endothélial]. Haematologia 1927;8:349-402.
79. Wjereszinski A, O. [Ueber die freien Zellen der serösen Exsudate, ihren Ursprung, ihre genetischen Wechselbeziehungen und ihre prospektiven Potenzen]. Haematologica. 1924;5:41-90.
80. Engel H, Kaznelson P. [Ueber die Bedeutung der Regeneration und Haemolyse bei der Anaemia perniciosa (Kritik der Therapie)]. Haematologica. 1928;9:257-294.
81. De Souza Aranha ME. [Cellule istioidi nel sangue circolante nel paludismo cronico]. Haematologica. 1925;6:328-336.
82. Fieschi A. [Sopra un caso di cloroma]. Haematologica. 1930;11:129-150
83. Fieschi A. [Ricerche morfologiche sugli elementi cellulari della linfa]. Haematologica. 1930;11:429-435.
84. Flarer F, Fieschi A. [Reticolo-endoteliosi cutanea sistematica con eritrodermia ed emoistiosi lenta]. Haematologica. 1933;14:125-143.
85. Fieschi A, Bertola A. [Il glicogeno dei leucociti nelle leucemie.] Haematologica. 1934;15:253-264.
86. Fieschi A. [Composizione chimica di alcune milze umane patologiche aspartate chirurgicamente]. Haematologica. 1936;17:291-305.
87. Fieschi A, Malamani V. [Il decorso dei processi autolitici studiato in alcune milze umane patologiche aspartate chirurgicamente]. Haematologica. 1939;20:185-205.
88. Introzzi P. [La puntura della milza nella anemia perniciosa progressiva. Suo valore diagnostico]. Haematologica. 1929;10:431-457.
89. Introzzi P. [La puntura della milza nel granuloma maligno. Suo valore diagnostico]. Haematologica. 1932;13:571-586.
90. Ferrata A, Introzzi P. [Splenomegalia primitiva follicolo-iperplastica. Splenectomia]. Guarigione. Haematologica. 1933;14:159-171
91. Introzzi P, Dessylla C. [Contributo allo studio degli elementi reticolo-istiocitari del sangue circolante]. Haematologica. 1932;13:127-143.

92. Schaumann J, Introzzi P. [Sulla eziologia e sulle alterazioni sistematiche degli organi ematopoietici del lupus eritematoso acuto]. Haematologica. 1931;12:635-717.
93. Storti E. [Anemia sperimentale da Botriocefalo]. Haematologica. 1931;12:237-261.
94. Storti E. [L'allacciatura dell'arteria splenica e la splenectomia. Studio sperimentale e disamina clinica]. Haematologica. 1934;15:107-189.
95. Fieschi A, Storti E. [Ricerche di citometria nelle leucemie]. Haematologica. 1935;16:345-366.
96. Storti E. [Contributo allo studio della mielosi eritremica]. Haematologica. 1936;17:393-460.
97. [Ricordo di Edoardo Storti]. Fondazione Ferrata-Storti, Pavia, 2006.
98. Erspamer V. [Ricerche ematologiche sulla Schistosomiasi vescicale (Ricerche compiute nel Fezzan)]. Haematologica. 1934;15:633-644.
99. Mazzarello P. Vittorio Erspamer: a student's experience at the Ghislieri College, in Memory of Vittorio Erspamer (L. Negri, P. Melchiorri, T. Hökfelt, G. Nisticò Eds) Exorma, Roma (2010), pp. 37-63.
100. Mantovani D, Mazzarello P. [Il merito e la passione]. Vittorio Erspamer e Pietro Ciapessoni al Collegio Ghislieri di Pavia. Cisalpino, Milano, 2011.
101. Micheli F. [Anemia (splenomegalia) emolitica con emoglobinuria-emosiderinuria tipo Marchiafava]. Haematologica. 1931;12:101-123.
102. De Toni G. [Sull'esistenza di possibili rapport tra la vaccinazione jenneriana e la patologia dell'apparato emopoietico]. Haematologica. 1931;12:125-211.
103. Miculicich jun FG. Beitrag zur Technik der Vitalfärbung der retikulozyten (Granulofilozyten). Haematologica. 1932;13:457-475.
104. Stewart HL, Tocantins LM, Jones HW. Granulopenia. A bacteriological and experimental study with a review of the literature. Haematologica. 1933;14:373-401.
105. Bemelmans E. Zur Krise in der Problemlage der Purpura. Haematologica. 1935;16:369-407:461-524.
106. Phillips JH. The Hemopoietic response of Necturus maculosus to intraperitoneal injections of liver extract, of Alpha dinitrophenol, and of liver extract together with alpha dinitrophenol. Haematologica. 1936;17:461-482.
107. Frey J. The appearance of Kurloff's cells in azoimide-poisoning. Haematologica. 1937;18:493-498.
108. Voorhoeve HC. [Diagnostic du Paludisme au moyen de ponction sternale]. Haematologica. 1937;18:739-747.
109. Émile-Weil P, Isch-Wall P, Perlès S. [La puntura della milza. Sua importanza dal punto di vista chirurgico]. Haematologica. 1937;18:727-738.
110. Frey J. The effect of cyclohexanone upon the hematopoietic system. Haematologica. 1939;20:725-733.
111. Di Guglielmo G. [La patologia della milza]. Haematologica. 1940;21:1-28.
112. Storti E, Brotto M. [Studio statistico, clinico-anatomopatologico su 157 casi di leucemia]. Haematologica;1940;21:37-107
113. Forconi A, Carere-Comes O. [Leucemie e tumori]. Haematologia 1940;22:187-256.
114. Quattrin N. [Tubercolosi polmonare ed emopoiesi]. Haematologica. 1941;23:177-194.
115. Quattrin N, Filla E. [Tubercolosi polmonare ed emopoiesi]. Haematologica. 1941;23:331-348.
116. Ferrata A, Fieschi A. [Risultati e insegnamenti della splenectomia nelle mielosi aplastiche]. Haematologica. 1941;23:979-1009.
117. Cotti L. [La leucemia a forma familiare]. Hematologica. 1941;23:1107-1133.
118. Di Guglielmo G, Quattrin N. [Mielosi eritremica cronica]. Haematologica. 1942;24:1-59.
119. Ascari E. The history of Haematologica. Haematologica. 2015;100(1):1-3.
120. Fondazione Ferrata Storti: 1984-1999. [Quindici anni di attività]. Fondazione Ferrata Storti, Pavia, 1999.
121. Ascari E. [Clinici e patologi medici dell'Università di Pavia, 1883-2003]. Fondazione Ferrata Storti, Pavia, 2004.
122. Cazzola M. New blood in Haematologica. Haematologica. 2011;96(12):1741-1742.
123. Cazzola M. Haematologica's impact factor. Haematologica. 2000;85(9):898.

REVIEW ARTICLE

Ferrata Storti Foundation

Understanding intrinsic hematopoietic stem cell aging

Eva Mejia-Ramirez[1,2] **and Maria Carolina Florian**[1,3]

[1]Center for Regenerative Medicine in Barcelona (CMRB), Bellvitge Institute for Biomedical Research (IDIBELL), Barcelona, Spain; [2]Center for Networked Biomedical Research on Bioengineering, Biomaterials and Nanomedicine (CIBER-BBN), Madrid, 28029, Spain and [3]Institute of Molecular Medicine and Stem Cell Aging, Ulm University, Ulm, Germany

EM-R and MCF contributed equally to this work.

Haematologica 2019
Volume 105(1):22-37

Correspondence:

MARIA CAROLINA FLORIAN
cflorian@cmrb.eu or
carolina.florian@uni-ulm.de

Received: July 14, 2019.

Accepted: November 14, 2019.

Pre-published: December 5, 2019.

doi:10.3324/haematol.2018.211342

Check the online version for the most updated information on this article, online supplements, and information on authorship & disclosures: www.haematologica.org/content/105/1/22

ABSTRACT

Hematopoietic stem cells (HSC) sustain blood production over the entire life-span of an organism. It is of extreme importance that these cells maintain self-renewal and differentiation potential over time in order to preserve homeostasis of the hematopoietic system. Many of the intrinsic aspects of HSC are affected by the aging process resulting in a deterioration in their potential, independently of their microenvironment. Here we review recent findings characterizing most of the intrinsic aspects of aged HSC, ranging from phenotypic to molecular alterations. Historically, DNA damage was thought to be the main cause of HSC aging. However, over recent years, many new findings have defined an increasing number of biological processes that intrinsically change with age in HSC. Epigenetics and chromatin architecture, together with autophagy, proteostasis and metabolic changes, and how they are interconnected, are acquiring growing importance for understanding the intrinsic aging of stem cells. Given the increase in populations of older subjects worldwide, and considering that aging is the primary risk factor for most diseases, understanding HSC aging becomes particularly relevant also in the context of hematologic disorders, such as myelodysplastic syndromes and acute myeloid leukemia. Research on intrinsic mechanisms responsible for HSC aging is providing, and will continue to provide, new potential molecular targets to possibly ameliorate or delay aging of the hematopoietic system and consequently improve the outcome of hematologic disorders in the elderly. The niche-dependent contributions to hematopoietic aging are discussed in another review in this same issue of the Journal.

Introduction

Aging is the largest risk factor for many chronic diseases and disabilities. Not surprisingly, aging is also the major risk factor for several hematologic syndromes and malignancies, such as myelodysplastic syndromes (MDS) and acute myeloid leukemia (AML).[1] Moreover, aging has a negative impact on HSC regenerative capacity, and for this reason, cell-intrinsic mechanisms of aging are important putative targets for therapeutic interventions in order to ameliorate the consequences of aging on HSC and on the hematopoietic system.[2] Understanding the mechanisms of HSC aging will provide the scientific community with new tools to improve the regenerative capacity of healthy HSC and thus the function of the hematopoietic system in the elderly.

The elderly population is growing rapidly worldwide. In addition, hematologic disorders and leukemia are exponentially growing with aging, without an equivalent acceptable growth in the therapeutic management of these diseases in the elderly; this is in sharp contrast to the increase in successful therapies for leukemia in younger patients. So far, with conventional induction therapy, many elderly patients experience a very poor overall survival rate, while requiring substantial social and medical assistance during their few remaining months of life, at a significant cost to the health service.[3,4]

A focussed understanding of the biology of aging in HSC and new therapeutic approaches is, therefore, mandatory.

Intrinsic aging drivers

Hematopoietic stem cells are the cornerstone of the hematopoietic system. Like other adult stem cells, they need to be localized in special niches that support and control the main stem cell functions: self-renewal and differentiation. Since HSC are so critical to the hematopoietic system and have to be functional during the entire life-span of the organism to maintain blood homeostasis, it is logical to think that somehow they require special protection from aging. Several studies have been trying to address how HSC can endure the effects of aging. However, investigating HSC function in living organisms is extremely challenging, since HSC constitute a rare cell population that, for most of the time, remain quiescent, undergoing very few divisions during the life-span of the organism (reviewed by Chandel *et al.*[5] and Singh *et al.*[6]). During aging, changes occur both in the niche, defined as extrinsic, and within the HSC, therefore dependent exclusively on the stem cell itself and, by definition, transplantable.

Working on human aging, especially in the hematopoietic system, has important experimental limitations and for this reason most of the research has been performed in model systems, particularly mouse models. Although some aging characteristics can be translated from mice into the human system, some phenotypes and their mechanistic investigation do not find a parallel in humans. Therefore, the development and establishment of possible new therapies must involve research on humans, or at least on models more similar to humans, such as non-human primates. Throughout this review, we discuss findings obtained in murine studies and we highlight some results obtained from studies carried out also in non-human primates and humans.

In general terms, a set of phenotypic and functional alterations have been consistently reported to characterize aged HSC (Figure 1).

Increase in phenotypic HSC number and decrease regenerative capacity

The number and frequency of HSC in the bone marrow of mice and humans increase with aging, while their regenerative capacity measured in transplantation assays is clearly reduced. It is accepted among researchers that this phenotype is caused primarily by cell-intrinsic mechanisms,[7-9] even though an aged microenvironment can further aggravate it.[10-12]

Myeloid skewing

Aged HSC show an increased differentiation potential to the myeloid lineage and a decrease in the potential to differentiate into the lymphoid lineage.[9,13,14] Moreover, even though the number of myeloid cells is higher, their quality is compromised.[15,16] Interestingly, experiments dealing with single cell transplantations in mice[17] and scRNA-sequencing (scRNA-seq) profiling[18] have shown that HSC differentiation potential is not as homogenous as it was thought. In particular, "myeloid-restricted repopulating progenitors" (MyRP) have been characterized within the young HSC compartment.[17] This MyRP subpopulation increases dramatically with age, in contrast with the moderate increase in the amount of multipotent HSC.[17,18] Intriguingly, within this MyRP subpopulation, a subset of cells called "latent-HSC" can revert to the multipotent HSC state upon secondary transplants only in the aged samples.[17] Consequently, it would be interesting to know if this subpopulation exists, and if it has the same behavior and features in the human bone marrow as in mice, in order to optimize transplantation therapies involving aged patients. These results highlight the potential importance of single cell profiling, at the molecular and at the cellular level, in order to better characterize also the human HSC compartment.

DNA damage

Accumulation of DNA damage is a common feature of aging in different tissues in many organisms, including humans.[19] Although HSC have many mechanisms that enhance their capacity for protecting their genome from DNA alterations,[20,21] some specific mutations have been shown to be highly recurrent in HSC.[10] In addition, upon aging, some of these somatic mutations are fixed and expand within the aged HSC compartment and are thought to be causally involved in the emergency of specific clones, which are the biggest contributors to replenishing the hematopoietic system.[22] It is possible that some of these mutated clones could eventually progress to blood malignancies such as MDS or AML, although this is not necessarily the case.[23]

Clonality

In a young individual, hematopoiesis is normally supported by different HSC clones with similar potential. This has been demonstrated by limiting-dilution transplantation experiments.[10] However, in the elderly, even though there is an increase in the number of HSC in the bone marrow niche,[8] there is a smaller number of HSC clones that disproportionally contribute to the peripheral blood production (reviewed by Akunuru and Geiger[2]). This phenomenon is termed Clonal Hematopoiesis of Indeterminate Potential (CHIP)[24] and is frequently detected in individuals over 55-60 years of age, being associated with an increased risk of hematopoietic malignancies and enhanced cardiovascular risk.[25] In recent years, there has been increasing interest in studying how CHIP develops over time and eventually evolves into hematopoietic malignancies, given that this might prove useful in developing therapeutic approaches.[23,26]

Epigenetic drift

Specific changes occur in the epigenome and chromatin organization of aged HSC compared to young HSC. These changes include DNA methylation,[27] specific histone post-translational modifications, and chromatin reorganization.[28]

Cell polarity

Several molecules appear to be polar within the cell and the nucleus in young HSC when compared with aged HSC. For some of these molecules, both their polarity feature and the functional relevance are conserved from *Drosophila* to humans. In recent years, a few studies have demonstrated that the impairment in the function and stem potential of HSC upon aging are directly related to the loss of polarity of selected biomolecules within the cell.[12,15,29,30]

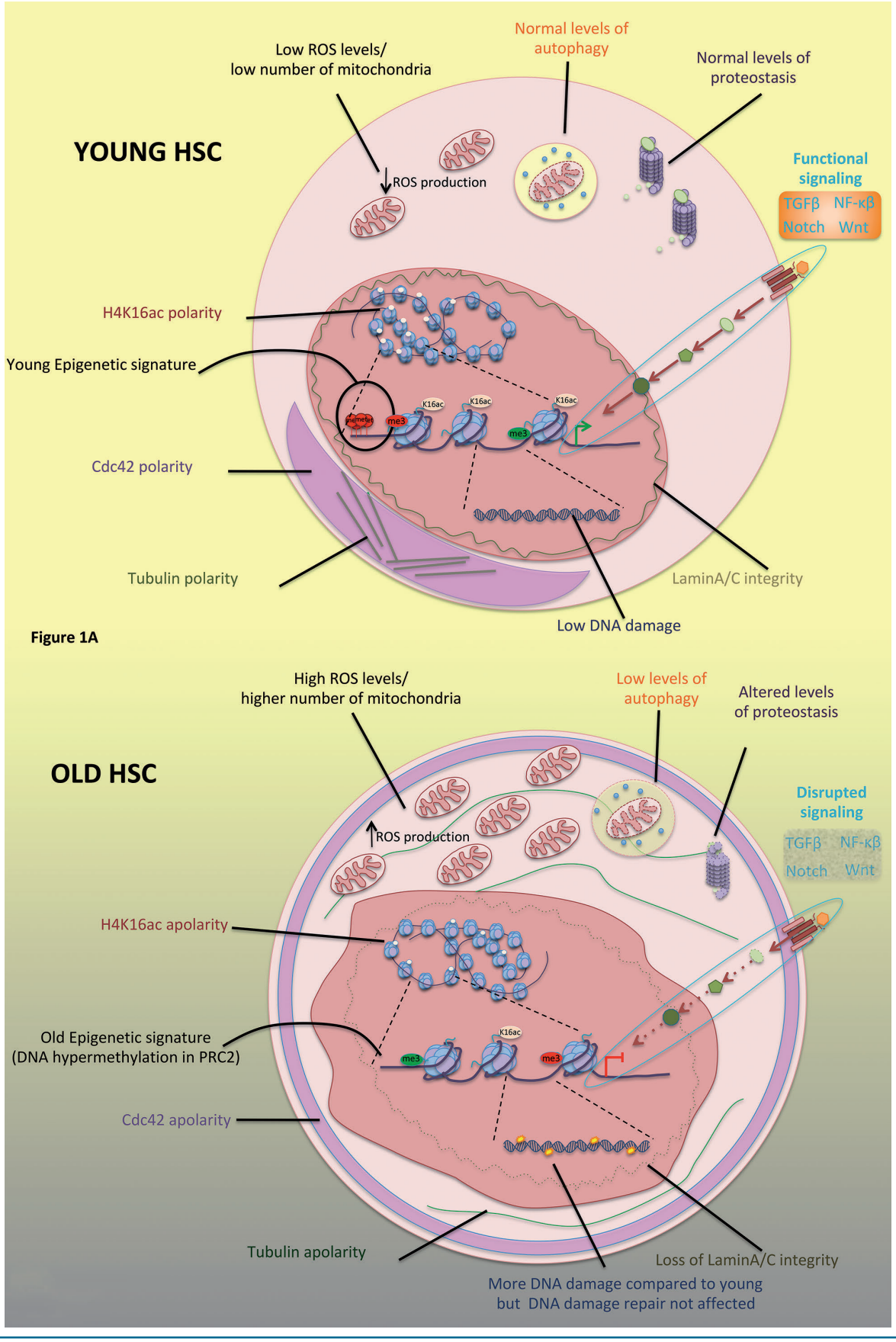

Figure 1. Intrinsic hallmarks of hematopoietic stem cells (HSC) aging. (A) Representative features of young HSC. (B) Representative features of aged HSC. K16ac: H4K16ac; met: DNA methylated; green me3: H3K4me3; red me3: H3K27me3. ROS: Reactive oxidative species; PRC2: Polycomb Repressive Complex 2.

Metabolic alterations and impaired autophagy

Hematopoietic stem cells are characterized by having a low metabolic rate, being essentially glycolytic while quiescent.[5,31] Upon activation, young HSC change towards a more oxidative metabolism that can be reverted when they return to quiescence (reviewed by Verovskaya *et al.*[32]). However, in aged HSC, basal metabolism is shifted to a higher level of oxidative metabolism (reviewed by Verovskaya *et al.*[32]), which increases reactive oxidative species (ROS) leading to oxygen related-stress, accompanied by impaired regenerative potential (reviewed by Chandel *et al.*[5]). Metabolic stress can fire autophagy in the cell, which is a "housekeeping" mechanism involved in self-degrading components of the cell in response to a specific stress.[33] The process consists of enclosing organelles or portions of the cytosol within double membrane vesicles, which later fuse with the lysosome, where the degradation takes place.[33,34] Autophagy deregulation has been related with aging and with age-related diseases such as cancer.[34,35]

Altered proteostasis

Proteostasis or protein homeostasis is described as the situation of balanced levels of protein biogenesis and degradation.[36] Proteostasis is regulated by several mechanisms such as autophagy, the ubiquitination proteasome system (UPS), the unfolded protein control system (UPR), and the proper levels of protein translation.[37] As mentioned above, autophagy is impaired with age, but also UPS and UPR levels are reduced leading to a situation of protein stress that contributes to loss of regenerative potential of aged HSC.[36,38,39]

Alterations in intrinsic signaling pathways

Signaling pathways such as TGF1-β, Notch, NF-κB or Wnt have an essential role in modulating the response of the hematopoietic system within the hematopoietic niche, tightly regulating the balance between quiescence and differentiation.[40-43] These pathways are intrinsically altered in aged HSC, with a consequent effect on their function.[15,28,44,45]

The hallmarks of intrinsic HSC aging cover a very diverse group of biological characteristics that might nevertheless be all interconnected. Here, we will focus on some of these intrinsic molecular aspects, that are implied in driving functional and phenotypical alterations of HSC upon aging.

Is DNA damage a driver of HSC aging?

DNA damage and genomic instability are thought to be primary causes of mutation accumulation upon aging, leading to cancer or premature aging of tissues.[19]

Here we summarize what is known about the effects of DNA damage on aging of HSC under a different perspective, with consideration of new data generated by state-of-the-art techniques.

From DNA damage to hematopoietic clonality

There are premature aging syndromes, such as Werner or Bloom syndrome, in which the cause of the disease is the accumulation of mutations due to an inefficient DNA damage repair. The accumulated mutations in these syndromes lead to different kinds of cancer to arise at early age together with some premature aging phenotypes such as immunosenescence, skin fragility and osteoporosis. However, these syndromes recapitulate only some physiological aging characteristics, but not all.[46]

In the case of HSC, work performed on mice deficient in DNA repair proteins shows an expected reduction in HSC repopulation potential together with a decrease in their self-renewal capacity, driving a reduction of the whole HSC pool.[31,47,48] As one of the most evident phenotypes occurring upon chronological aging is the expansion of HSC, the phenotype observed in mice deficient in DNA repair proteins sharply contrast with physiological HSC aging. More recently, it was elegantly shown by genetic barcoding and clonal functional evaluation of young and aged HSC followed by induced pluripotent stem cells (iPSC) generations and re-differentiation that, despite the heterogeneity of the aged HSC pool, several functional aspects of HSC aging could be reversed to a young-like state. These data strongly support the view that accumulations of DNA mutations in genes critical for hematopoiesis would not be the principal mechanism for the aged-dependent functional decline of HSC,[49] although they might contribute to clonality.[22,23]

Still, mutations occur in every tissue and they are shown to accumulate with age. It has been calculated that somatic mutations in human HPSC occur and accumulate in life in a linear rate of 14bp base substitutions per year, which is similar to or even lower than other tissues.[50]

γH2A has been historically interpreted as being a marker of DNA damage in general, and in HSC in particular, since it is one of the first signals occurring at the damaged site and it is needed for subsequent DNA repair.[48,51] Aged HSC present with increased numbers of γH2A foci compared to young HSC.[48] Therefore, it was logical to conclude that there is deficiency in DNA repair in old HSC because of the persistence of γH2A. Interestingly, γH2A foci have been demonstrated to be not only markers of double strand breaks (DSB). γH2A also signals DNA replication stress (i.e. replication fork collapse) and it accumulates at rDNA in old quiescent HSC. Furthermore, in aged murine HSC, γH2A cannot be removed by the specific phosphatase (PP4c) as efficiently as it is removed in young HSC because PP4c is mis-localized.[21]

Moreover, murine young and old HSC have been demonstrated to be equally efficient in repairing DNA under induced DNA damage.[20,21,52] HSC make this possible by having the main DNA repair pathways attenuated while quiescent and reactivating them once they re-enter the cell cycle.[20] In addition, when young and old HSC are subjected to DNA damage, they lack G1-S arrest and their apoptosis rate increases in order to minimize the acquisition of mutations.[52]

In spite of the ability of HSC to avoid mutation accumulation through age, a series of point mutations have been found in humans to be predominant with age, as is the case of mutations in the epigenetic regulators *DNMT3*, *TET2* and *ASXL1*, among others.[53-56] These mutations appear frequently in healthy older individuals and they are also found over-represented in MDS and AML patients.[23] It can be hypothesized that these mutations confer a competitive advantage that leads to clonal hematopoiesis. This is supported by some studies in the murine hematopoietic system in which the loss of *Dnmt3a* or *Tet2* enhances the self-renewal potential of HSC.[57] DNMT3a and TET2 are epigenetic modifiers: DNMT3s catalyze DNA methylation (mC) and TET2 oxidizes mC to hydroximethyl-C,

which leads to de-methylation of DNA (reviewed by Zhang *et al.*[58]). As has been demonstrated in mouse models, TET2 seems to contribute to both differentiation and self-renewal through gene activation and repression, and DNMT3a might contribute to the same functions by repressing HSC genes and generating substrates for TET2 action.[58] The overall result is that both DNMT3 and TET2 co-operate to prevent activation of lineage-specific transcription factors in HSC.[58] As for ASXL1, it seems that by binding to chromatin when mutated it can alter the epigenome, increasing the tendency towards CHIP or even leukemic transformation in mice.[59] Mutations in the human homologs of these genes have also been found to be related to clonal hematopoiesis and MDS.[60,61]

However, these mutations in humans do not necessarily involve the development of malignancy (although this might occur), probably in combination with other unknown events.[23,62] In addition, MDS does not necessarily always lead to the development of AML. The combination of different mutations might be critical to allow the development of sub-clones with higher competitive advantage implied in the final establishment of MDS or AML.[23]

Telomere shortening is a special kind of DNA damage in which the low activity of telomerase or its absence makes the length of telomeres shorter after every division cycle and leaves the DNA ends unprotected, activating the DNA damage response and DNA repair pathways (reviewed by Behrens *et al.*[63]). Since telomeres become shorter every cycle, their length is intimately related to the life-span of a cell. Based on this assumption, there have been many attempts to understand if and how telomere length is related to life-span of the entire organism. Experimental observations indicate that the lower the rate of telomere shortening, the higher the life expectancy.[64,65] As for HSC, it has long been known that they can only be serially transplanted 4-6 times in mice before they start showing loss of multi-lineage reconstitution capacity.[66] This outcome was linked to limited replicative potential due to telomere shortening. However, it has been reported that HSC telomere length does not decrease in serial transplantation assays,[67,68] and the overexpression of telomerase in mice does not lead to prolonged HSC transplantation capacity.[67] The difference between mice and humans is remarkable in how the hematopoiesis system is affected by telomere attrition. For example, only the fifth generation on a Tert$^{-/-}$ mouse background develops anemia.[69] This might be due to the elevated tolerance of murine HSC to accumulate alterations in their genome upon telomere shortening, either by entering in a senescence state or by undergoing apoptosis.[70] In contrast, human patients of telomeropathies like *Dyskeratosis congenita* or adults with telomere gene mutations display very early bone marrow failure and severe aplastic anemia,[71] which make the patients dependent on transplantation therapy.

Interestingly, a recent study with mice has shown that the loss of expression of Pot1a, a ssDNA binding protein part of the shelterin complex that binds telomeres, diminishes the potential of LT-HSC *in vitro* and *in vivo*, and its overexpression increases the contribution of LT-HSC to peripheral blood and bone marrow after secondary transplant, even rescuing the myeloid skewing in aged mice.[72] Importantly, Hosokawa et al. included data showing that also the human homolog, POT1, improved *ex vivo* culturing of human cord blood HSC.[72]

Clonal hematopoiesis seems to stem out as a consequence of HSC mutation accumulation during aging (Figure 2). As has been shown in mice, the HSC compartment has a clonal dynamic nature that changes over time, with individual clones that expand or shrink, disappear or appear.[26] However, there are differences between the results obtained in mice and those obtained in other model organisms, such as non-human primates. An extensive study dealing with the impact of aging on non-human primate hematopoiesis was recently published. It was demonstrated by lentiviral barcoding and high-throughput sequencing that aged macaques show a delay in the emergence of hematopoietic contribution in transplantations of autologous HSPC compared to mice, together with a persistent output from both B-cell and myeloid-biased clones.[73] These results on clonal behavior of aged non-human primate HSC is of special importance for diagnosis and therapy in humans, since it is unfeasible to clonal-track HSC in healthy patients. Mainly, information on human clonality and its progression upon aging comes from studies of "end-point" clonal population in healthy aged patients[62] or by tracking existing clones from MDS patients to monitor their progression to AML over time.[23] Importantly, a very interesting simulation tool has been recently reported in order to understand clonal contribution to hematopoiesis that can be applied to different species, from mice to humans.[74]

Under the premise that clonality is the result of specific mutations that give rise to "fitter" hematopoietic clones which are more successful after the selective process, one last question continues to be asked: does clonality result from intrinsic changes in aged HSC, or is it rather that clones are selected by the microenvironment?[75] Still, it is possible that the impairment of hematopoiesis upon aging might be the result simply of fewer contributing fit HSC which did not undergo intrinsic changes and which somehow resist microenvironment pressure.

In order to address clonal hematopoiesis and the predisposition to develop blood malignancies with age, many laboratories have tried to engineer AML mouse models. It has been shown that, for example, the deletion of Tet2, in mice leads to deregulated hematopoiesis and subsequent development of blood malignancies;[76] however, the phenotype that is observed in aged human patients is not recapitulated completely in the murine models, either because of the onset of the disease, its penetrance, or the malignancy of the developed disease.[76,77] New molecular biology approaches and a deeper understanding of the HSC aging process might be critical to improve the tools that are currently available.[77]

Epigenetic changes: DNA methylation, histone marks and chromatin architecture

Genome-wide expression profiling of murine young and aged HSC has shown that there are transcriptional alterations associated with aging in HSC which affect myeloid and lymphoid differentiation.[7,28,43,78] Single-cell RNA sequencing (scRNAseq) has become a powerful tool to identify variations in transcriptional profiling between different cells from the same compartment, as in the case of HSC in the murine bone marrow. The information retrieved from scRNAseq from young and aged murine HSC has revealed that there is a molecular bias priming

platelet genes expression at the expense of lymphopoietic genes, confirming the well-known myeloid skewing feature of aged HSC.[18,79]

The suggested mechanisms underlying such a genome-wide transcriptional change are related to the epigenomic regulation. Indeed, there is much evidence to support this hypothesis. For example, by reprogramming young and aged murine hematopoietic progenitors, the repopulation potential is indistinguishable between young and aged derived iPS into all hematopoietic lineages in chimera individuals and in HSC transplantations.[49,78] These data imply that reprogramming is resetting the epigenetic state of the HSC regardless of the age at which the cells are reprogrammed. Moreover, these data also suggest that epigenetic alterations that occur upon aging are reversible.[80,81]

The epigenomic landscape of HSC has been shown to change with respect to DNA methylation, histone modifications and chromatin architecture (Figure 2).

DNA methylation changes from young to aged hematopoietic stem cells

Global hypomethylation occurs in most somatic cells and in primary cells during aging.[19,81] In contrast, the majority of DNA methylation signatures during HSC aging in mice are highly conserved.[27,28,82] However, the overall methylation change of aged HSC compared with young HSC is different depending on the study. The studies performed using reduce-representation bisulfite sequencing (RRBS)[27,28] showed a slight tendency to hypermethylation with aging. In contrast Taiwo *et al.* reported a slight but significant (5%) global loss of DNA methylation by MeDIP-seq. Taiwo *et al.* argue that the difference could be explained by the difference in coverage of each technique. Bisulfite-sequencing provides generally 5-10% genome coverage, in contrast with 60% provided by MeDIP-seq.[82]

Interestingly, independently from the overall hypo- or hypermethylation detected, all studies so far report high similarities in the alterations at specific loci that gained or lost methylation. One of the clearest examples involves polycomb repressive complex (PRC2) target genes, which are hypermethylated in aged HSC.[27,82] It has been demonstrated in a human cell line that PRC2 cannot bind to chromatin if the DNA is hypermethylated.[83] Moreover, some PRC2 complex subunits in aged and proliferative stressed HSC resulted in being down-regulated as measured by RT-qPCR[27] and RNA sequencing.[28] These observations

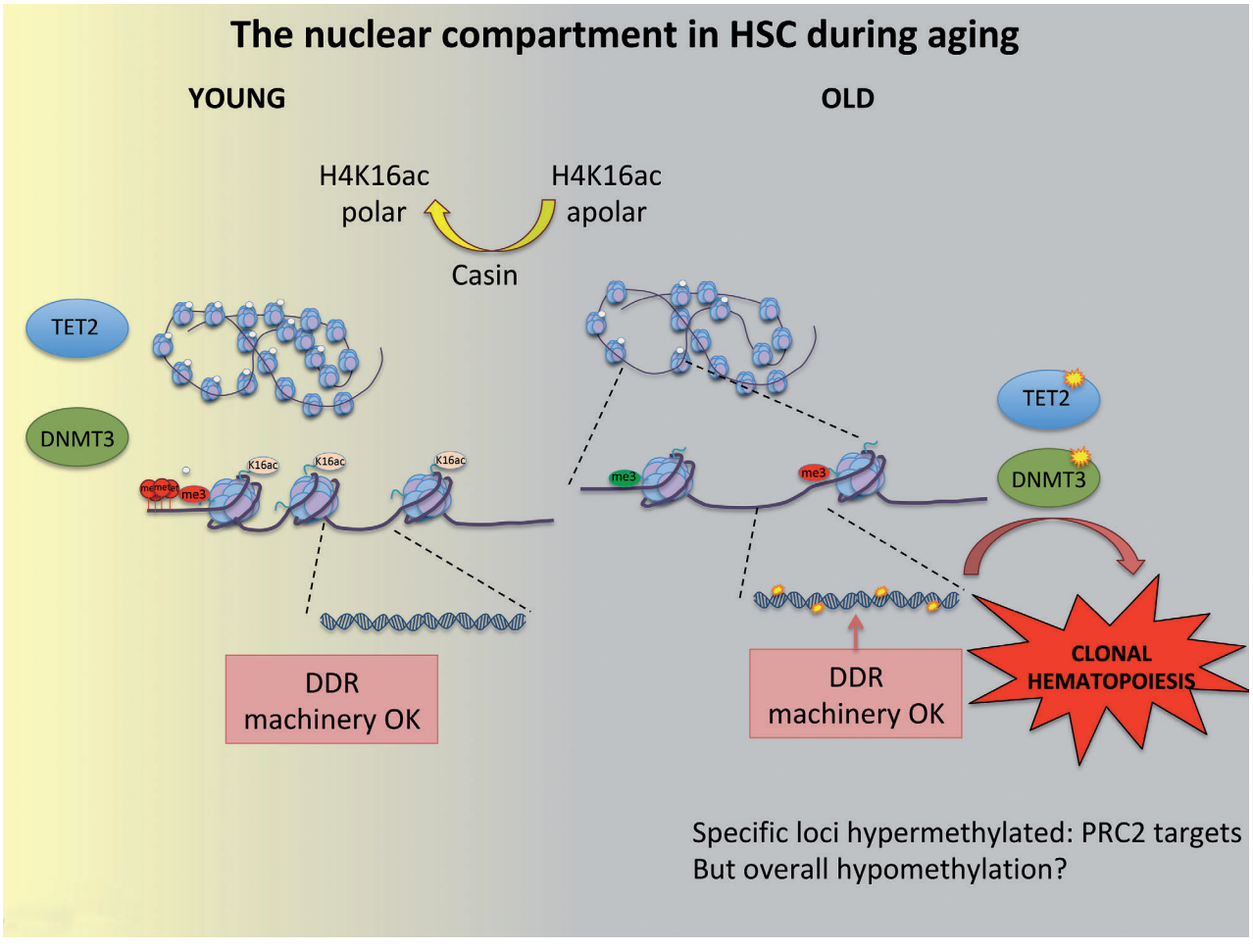

Figure 2. The nuclear compartment in hematopoietic stem cells (HSC) during aging. The nuclear compartment undergoes several changes through aging, ranging from changes in histone post-translational modifications and DNA methylation to alterations of epi-polarity and chromatin architecture. Although the DNA damage repair (DDR) machinery is functional when entering in cycle from quiescence, DNA mutation and hematopoietic clonality can be detected and increase in frequency over time. CASIN treatment of aged HSC restores epi-polarity of H4K16ac, a nuclear hallmark of young HSC. K16ac: H4K16ac; met: DNA methylated; green me3: H3K4me3; red me3: H3K27me3. DDR: DNA damage repair.

might suggest that the methylation machinery in old HSC might access PRC2 target sites merely as a consequence of the reduced levels of PCR2 itself, which normally occupies these specific targets inducing their transcriptional down-regulation. However, this hypothesis has yet to be demonstrated.

A possible explanation for the limitation to a more global and prominent hypomethylation on HSC during aging is linked to their quiescence during adult life. When murine young or old HSC are transplanted, and are therefore subjected to an induced proliferative stress, global hypomethylation occurs.[27] This observation agrees with reports for aging in human somatic cells and tissues (reviewed by Gonzalo[81] and Jones *et al.*[84]). However, even in this case, the hypermethylation of PRC2 targets is still detectable in mice, suggesting that aging and exhaustion promote distinct alterations on the DNA methylation landscape.[27]

It is worth noting that differentially methylated genes in aged HSC compared to young HSC are expressed or highly expressed in progenitor cells downstream in murine hematopoietic differentiation.[27] This observation suggests that the impact of alterations in DNA methylation during aging is not probably manifested until HSC differentiate, and never in HSC themselves. This aspect is also demonstrated by the work of Scadden's team, who elegantly showed in mice that the differences in enhancer methylation between distinct HSC clones in the same individual has no effect on gene expression until stem cells differentiate into subsequent hematopoietic sub-compartments.[26]

Histone post-translational modifications upon hematopoietic stem cell aging

A number of histone tail modifiers have been involved in HSC function and also have a role in chromatin remodeling, which supports the concept that changes in the chromatin state within the HSC compartment are important for blood homeostasis in both mice and human systems. Among them, we can find PRC2 subunits such as Ezh2, Suz12 and Eed,[85-87] histone specific lysine-demethylases such as Jarid1b/KDM5b,[88] UTX/KDM6a[89] or Lsd1/KDM1a,[90] or histone methyltransferases such as SUV39H1.[91]

Moreover, it is known that the expression levels of some of these proteins change upon aging,[27,28,43,91] suggesting that histone modifications are different in old HSC when compared to young HSC.

Goodell's group performed one of the most accurate studies of epigenomic modifications in murine HSC upon aging. Some of the principal regulatory histone marks were profiled by ChIP-seq in HSCs from 4-month old and 24-month old mice. Although the dataset revealed only moderate changes, some interesting unique features were reported. For example, regarding H3K4me3, there was only an increment of 6.3% in peak deposition in old *versus* young HSC, but most of the peaks were generally broader.

As for H3K27me3, peak counts remained similar but an increase in the length of coverage by 29% was detected upon HSC aging. Moreover, the intensity of the signal increased by 50%. In relation to H3K36me3, the peaks moved from the TSS to the transcription termination site, and H3K36me3 and H3K27me3 behaved in a mutually exclusive manner. A strong positive correlation between transcriptome changes and the three histone marks analyzed in the study was also reported.[28]

Regarding other histone marks, H4K16ac levels and localization have been demonstrated to change with age in murine HSC. H4K16ac shows a prominent distribution in one pole of the nucleus in young HSC by single cell 3-dimensional (3D) immunofluorescence analysis. This characteristic is defined as "epigenetic polarity" or "epipolarity". Old HSC show reduced levels of H4K16ac, which also displays apolarity and localizes evenly all over the nucleus.[14,15,29] The polarity and levels of several other histone marks such as H3K4me1, H3K4me3, H4K8ac, H3K27ac and H4K5ac showed no aged-dependent changes in murine HSC and ST-HSC.[29] Interestingly, the loss of epipolarity and the reduction of global H4K16ac deposition upon aging in HSC did not primarily correlate with global changes in gene expression.[15] H4K16ac was associated to the modulation of higher-order chromatin and protein interactions between chromatin and non-histone proteins,[92] and was shown to be targeted by inhibiting Cdc42 activity and LaminA/C expression. H4K16ac role in chromatin architecture in HSC will be further discussed below.

In the context of human AML, H4K16ac levels seem to be linked to the nuclear localization of PAK4, a target of the orphan gene *C3orf54/INKA1*, which promotes self-renewal by inhibiting differentiation of cord blood HSC.[93] *C3orf54/INKA1* seems to be up-regulated in leukemic stem cells in AML patients, while PAK4 is an effector of Cdc42 in humans.[94]

Altogether, the results obtained over the last decade suggest that aging has an effect on histone mark landscape in HSC. However, the specific alteration of histone marks upon aging not always correlates with global change on gene expression in HSC themselves, but it rather affects the expression of genes in downstream progeny during the differentiation program, as we stated above also for the methylation profile.[15,26,27] Altogether, this makes epigenetic studies extremely cumbersome in HSC and subtle differences within this cell population might indeed make a functional impact visible only under specific challenges.

Chromatin architecture changes

Over recent years, chromatin architecture has become more important for gene expression, cell division, fate determination, growth and development, disease and even genome evolution (reviewed by Kong and Zhang[95]). Recent studies have proposed the existence of two different but related ways of 3D chromatin organization: the cohesin-dependent CTCF loops and the small compartmental domains that are formed as a consequence of transcription and chromatin state (reviewed by Rowley and Corces[96]). In this regard, and in relation to HSC biology, some disease-associated mutations in humans that affect proteins involved in establishing or preserving chromatin architecture have been described, for example, proteins belonging to the cohesin complex, such as Stag2, Rad21 and Smc3, which have been associated with AML and MDS particularly in the elderly.[97,98]

Chromatin accessibility changes upon HSC aging have just started to be investigated. Recently, we performed single-cell ATAC-seq on HSC daughter pairs from young and old mice. The results showed that there was a greater difference between young pairs, more "asymmetrical", as based on quantity of ATAC-seq peaks, than those coming from aged pairs, which were, therefore, more "symmetrical". This observation was correlated to H4K16ac distribu-

tion in daughter cells that was more asymmetric in young compared to old pairs. Signature-based, daughter stem cells were in general associated to an overall lower amount of ATAC-seq peaks, suggesting a progressive increase in chromatin accessibility upon differentiation.[15] Interestingly, both young and aged daughter stem cells preserved open chromatin regions linked to glycolysis and small RhoGTPases signatures. Aging was found to impact prominently on the specific signature of open regions associated to critical signaling pathways in HSC (Wnt signaling was associated with aged HSC, while young cells were enriched for VEGF, TGFβ and EGF signaling). In addition, daughter progenitors maintained signatures linked to lipid metabolism and platelet homeostasis in both young and aged cells, while mostly they differed again for open regions linked to specific signaling pathways (interferon, IFG1 and IL2 were characterizing young cells and TNF was enriched in aged cells).[15]

Specific chromatin architectural alterations affecting broader alterations have also been detected in aged murine HSC, such as the relative position of chromosomes. We have observed that chromosome 11 homolog proximity changes upon aging specifically in HSC. This chromosomal rearrangement is dependent on LaminA/C expression and Cdc42 activity.[29] Indeed, we demonstrated that upon aging and in chronologically young LaminA/C knock-out HSC, chromosome 11 homolog proximity was altered and this correlated with the functional impairment of stem cells. Inhibiting Cdc42 activity could restore LaminA/C expression and localization, and also chromosome 11 homolog proximity. Overall, these findings support the functional relevance of chromatin architecture also for HSC aging and, most importantly, show for the first time that is possible to pharmacologically target the chromatin architecture to rejuvenate aged HSC function.[29]

Aging and the epigenetic drift

Epigenetic drift is the term that covers all changes that have a general effect on the epigenome and the chromatin architecture.[99,100] Recently, an exciting report of the epigenetic drift in murine aging across tissues has been published. Benayoun *et al*. showed that the aged-related alterations observed in the epigenome and transcriptome landscape lead to induction of inflammatory responses, mainly interferon related, across different tissues upon aging.[100] In humans, the epigenetic drift has been studied at the single-cell level on peripheral blood mononuclear cells from subjects of different ages.[101] In agreement with previous studies performed on bulked murine HSC,[27,28] they observed an increment of H3K4me3 and H3K27me3 with age. These variations were reflected in transcriptional alterations and an association of H3K4me3 with DNA breakage and translocation was also observed.[102]

The fact that the observed epigenetic drift is consistent between mice and humans suggests that it is a conserved phenomenon in mammals. However, its ultimate manifestation seems very heterogeneous, even within cells and tissues of the same individual. This has been demonstrated using different approaches such as the generation of a multi-color Hue mouse model as a clonal tracking tool[26] and single-cell transcriptomics to study the transcriptional behavior of each clone.[26,103] These two studies agreed in identifying (based on transcriptome analysis) distinct clones in aged individuals that have different regulatory states as a consequence of the epigenetic drift occurred upon aging.[26,103]

Metabolism and hematopoietic stem cell aging

Hematopoietic stem cells are quiescent during most of their lifespan and their metabolic needs are relatively low. However, one of the aging hallmarks is the dysregulation of metabolic pathways, and this aspect might indeed be critical for HSC function, too. Here we detail some of the key metabolic aspects related to HSC aging (Figure 3).

Effects of oxidative stress and mitochondria homeostasis in hematopoietic stem cell aging

It has been shown that artificially altering mitochondrial function can lead to acquiring aging phenotypes in HSC, such as loss of self-renewal and lymphoid/myeloid skewing. Sometimes these mitochondrial-related aging phenotypes can be reverted by the addition of redox scavenger compounds [N-acetylcysteine (NAC), rapamycin or MAPK inhibitors]. Normally, rapamycin and calorie restriction can only partially rescue the effects of aging due to intrinsic deteriorated mitochondrial activity (reviewed by Chandel *et al.*[5]).

Reactive oxygen species (ROS) are the natural side-product of oxygen-based metabolism and are produced mainly by mitochondria. The effect of ROS in aging has been historically attributed only to the oxidation of DNA, RNA and proteins, but it has an important role in cell signaling, too. ROS can be detected by redox sensors that ultimately fire oxidative stress response such as enzymes and transcription factors (reviewed by Bigarella *et al.*[104]).

In HSC, high levels of ROS can generate oxidative stress and lead to loss of quiescence in the cells; therefore, ROS levels have to be tightly controlled (reviewed by Bigarella *et al.*[104]). Quiescent HSC have a low metabolic rate, which involves low levels of reactive oxygen species (ROS).[105] It has been shown in mice that the frequency of HSC with low levels of ROS decreases with age, suggesting that ROS generation/accumulation is a distinctive characteristic of aging.[106] Increments of ROS levels in adult HSC have consequences that are somewhat similar to the aging phenotype such as myeloid lineage skewing and defective long-term repopulation activity, as has been demonstrated in the case of FoxO transcription factors depletion in mice.[107,108] It is very interesting that high levels of ROS in the FoxO depleted HSC can be rescued by the addition of the antioxidant NAC,[108] but only for some weeks.[107] The importance of FoxO3 in LT-HSC function goes beyond regulation of ROS levels since it is essential for activation of the autophagy gene program.[109]

Reactive oxygen species are also augmented in HSC of aged SIRT3 knockout (KO) mice, negatively affecting their function, but not in young SIRT3 KO mice. Intriguingly, overexpression of SIRT3 rescues functional aged-related defects in HSC. SIRT3 is a deacetylase that regulates mitochondrial protein acetylation in mammalian cells and it is enriched in young compared to aged HSC. Therefore, the role of SIRT3 in the maintenance of proper ROS levels in HSC is essential during aging.[110]

Mitochondrial homeostasis refers to the correct regulation of the mitochondria function within the cell. Studies using "mutator mice" (proof reading mutant for PolγA, the catalytic subunit of mtDNA polymerase that is encoded in the nuclear genome) showed phenotypes indicative of

premature aging,[111] including features of MDS.[112] Trifunovic *et al.* concluded that there might be a causative link between mtDNA mutations in these mice and the aging phenotype.[111] However, deep insights in the phenotype and molecular signatures of aged HSC demonstrated that they are different from this 'mutator' strain, concluding that aging is primarily independent of the accumulation of mitochondrial mutations.[105] What is, indeed, observed is that aged HSC show deregulation that deteriorates mitochondrial activity (reviewed by Oh *et al.*[113]).

Maintenance of mitochondrial homeostasis within the cell is also dependent on the regulation of nuclear mitochondrial gene expression. For example, Mohrin et al. showed that SIRT7, a histone deacetylase, is normally located at the proximal promoters of ribosomal proteins and mitochondrial transcription factors within the nuclear genome. It also binds directly to NRF1, the master transcription factor of mitochondria. Eventually, SIRT7 leads to the inhibition of the expression of mitochondrial proteins in young HSC.[114] Aged HSC have lower levels of SIRT7, thus allowing an increment in the expression of mitochondrial proteins. This, in turn, activates the PFSmt (mitochondrial protein folding stress), a metabolic checkpoint that reduces HSC quiescence. Therefore, overexpression of SIRT7 in aged murine HSC was shown to decrease the levels of mitochondrial protein expression associated with mitochondrial stress and to improve aged HSC function.[114]

Autophagy

Autophagy is a major regulator of mitochondria homeostasis and a suppressor of the metabolism. It is regulated by nutrient-sensing pathways like mTOR or AMPK, which inhibit and activate autophagy, respectively. In general, autophagy decreases with aging, due to either the downregulation or the upregulation of critical autophagy proteins. In HSC, the age-related decrease in autophagy has been associated with lower capacity of glucose intake; mitochondrial autophagy would be attenuated in order to maintain necessary energy levels in old HSC and is rapidly induced by FoxO3 transcription factor when HSC are under metabolic stress.[109]

Genetic tools were instrumental in revealing the critical role of autophagy upon HSC aging.[115] For example, in

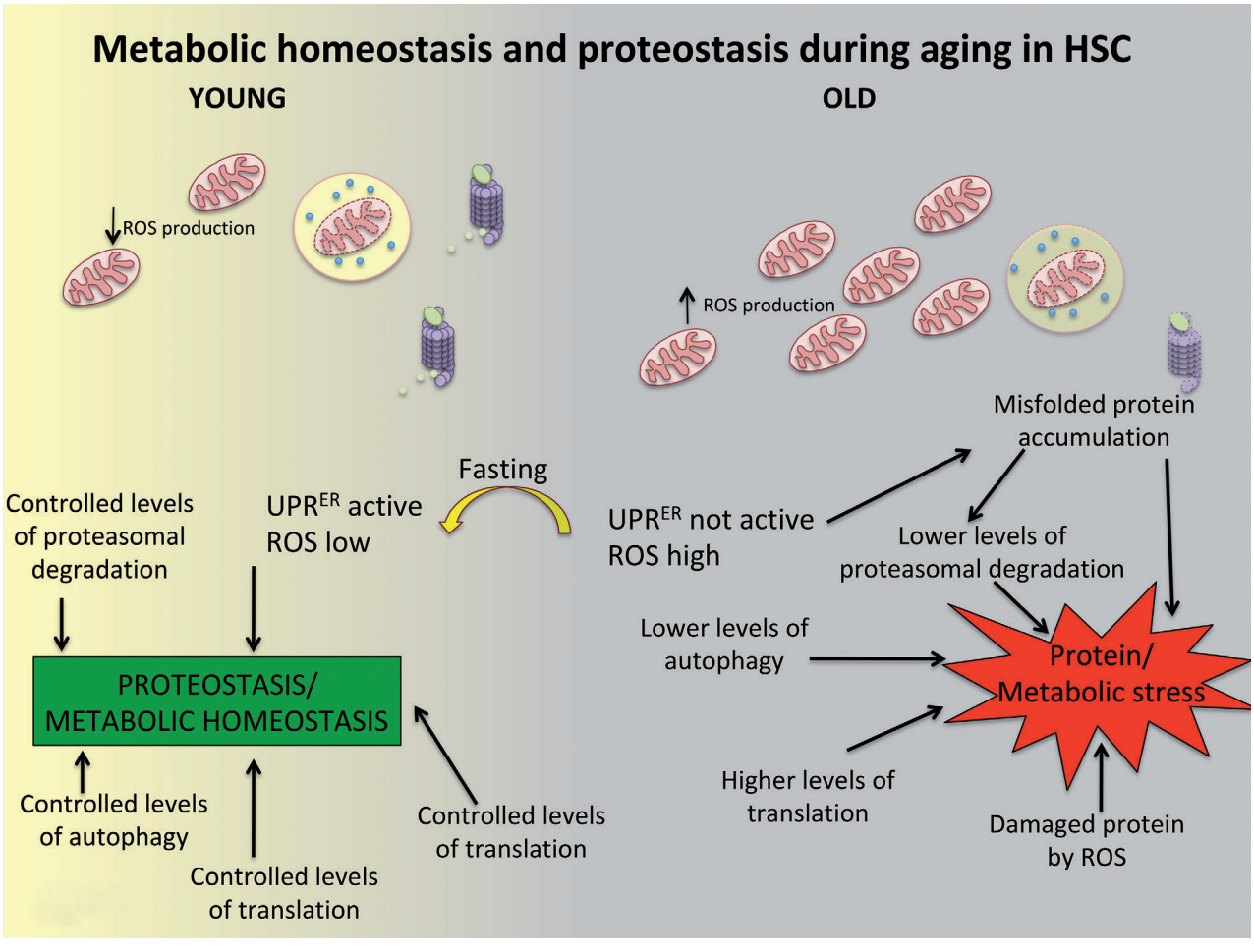

Figure 3. Metabolic homeostasis and proteostasis during aging in hematopoietic stem cells (HSC). Young HSC fine-tune several biological processes: they maintain a low metabolic rate, control protein degradation and regulate autophagy. Aged HSC show an unbalanced scenario where these processes lose their metabolic homeostasis and proteostasis, converging into a status of metabolic and protein stress. Fasting is able to restore at least partially the activity of the UPR^{ER} and proteostasis in aged HSC. ROS: reactive oxygen species; UPR: unfolded protein response.

Atg1scKO mice, autophagy is deregulated and aged HSC present with reduced quiescence, an increased rate of differentiation biased toward the myeloid lineage, and an increment in OXPHOS rates. In HSC from conditional knockout Atg12 mice, changes in the methylome of essential genes for the formation of autophagosomes have been reported. These changes could be explained by the alterations of metabolite levels caused by the loss of autophagy, such as reduction of S-adenylmethionine (SAM), methyl-donor co-substrate for methylases, and an increment in alpha-ketoglutrate (αKG), a co-factor for demethylases.[35,116]

Intriguingly, it was also reported that a fraction of aged HSC showing high levels of autophagy displayed higher resistance to exhaustion, as demonstrated by secondary transplants in mice. These data suggest that, although aged HSC are apparently phenotypically equal, there might be a subset that maintains the autophagy levels of young HSC and are consequently resilient to aging, preserving their stemness and regenerative potential.[35]

Nowadays, autophagy represents a target for therapeutic interventions *in vitro* and *in vivo*, with clinical trials ongoing for several aged-related hematopoietic disorders, such as AML.[117,118] A number of these autophagy-targeting approaches are based on the use of different mTOR pathway inhibitors[119] and could offer a potential therapeutic approach to improve healthy aging as well.

Proteostasis role in hematopoietic stem cell aging

Homeostasis of proteins, also called proteostasis, indicates a situation in which the proteome within the cell reaches an equilibrium by balancing the elimination of misfolded or damaged proteins while preserving at the same time the necessary levels of properly assembled proteins.[36]

Proteostasis relys in part on protein translation, that is, it is directly dependent on ribosomal levels and biogenesis. Transcription of rRNA genes is regulated by the methylation state of the rRNA genes themselves. Interestingly, it has been shown that ribosomal biogenesis is a target of aging with hypo-methylation of rRNA genes and higher levels of transcription in aged HSC.[28]

Cell polarity and aging

Cell polarity is a universal biological feature, and age seems to be a factor contributing to the loss of cell polarity regulation.[120] Polarity can be defined as the asymmetric distribution of cellular components, biomolecules and structures within the cells. The number of genes linking polarity and aging is strikingly increasing and, consequently, the number of targets to be investigated in order to ameliorate aging is growing.[121] For instance, in the baker yeast *S. cerevisiae*, it has been demonstrated that damaged and aggregated proteins are retained in the mother cell establishing an asymmetry that marks which of the cells is aged. The lysine deacetylase Sir2p is responsible for this, since it regulates the ultimate correct folding of actin in order to keep the protein aggregates in the mother (aged) cell.[122] This mechanism is highly conserved among organisms, as is shown in *Drosophila* larval and adult stem cells (female germline and intestinal stem cells). Here, proteostasis seems to be, at least in part, regulated by asymmetric division: the shortest life-span daughter inherits the majority of damaged proteins leaving the stem cell daughter as damage-free as possible.[123] This is particularly important in adult stem cells, since the accumulation of damaged or misfolded proteins can contribute to aging.[36,124] Asymmetry has been described in HSCs for several proteins such as Cdc42, Dlg, Crumb3, Scribble, H4K16ac, LaminA/C. Polarity of these proteins is characteristic of young HSC and apolarity is more prominent in aged stem cells.[14,15,29,44,125] CD71, the transferrin receptor, and CD53 and CD63, endosomal-associated proteins are also described to be polar and confer asymmetry during division of HSC, being characteristic of the most primitive population of HSC when they are together with the stem marker CD133.[126]

In summary, despite the wide experimental evidence linking loss of cell polarity and the proteostasis decay upon aging, only a few pharmacological approaches have been proposed so far. For example, CASIN was successfully used to recover HSC cell polarity and rejuvenate function of aged stem cells in mice.[14]

Protein degradation systems and folding stress response

The ubiquitin proteasome system (UPS) is a complex of factors responsible for tagging proteins for signaling or for degradation, and is, therefore, implied in regulating proteostasis in eukaryotic cells.[39] It has been shown that HSC function can be affected by the absence or malfunction of different UPS system factors, such as E3 ligases or deubiquitinases. This happens in an indirect way, affecting the accumulation of its protein targets, like STAT5, c-myc or Notch, and promoting exacerbated responses.[39] Moreover, the UPS regulates the degradation of histone modifying enzymes such as HDAC1 and DNMT1.[127] This means that the epigenetic changes observed might be a consequence of the proteasome decay occurring with aging.[128]

Another system controlling proteostasis is the unfolded protein response that occurs in the endoplasmic reticulum (UPR^{ER}). This system preferentially induces apoptosis under ER (endoplasmic reticulum) stress in HSPC compared to closely related progenitors. The biological relevance of this mechanism relys on the elimination by apoptosis of those HSC that are under ER stress due to accumulation of misfolded proteins.[129] Intimately related with the UPR^{ER}, protein chaperones function by enhancing the correct folding of proteins, and, in turn, protecting against UPR-induced apoptosis. For example, the overexpression of the UPR^{ER} factor ATF4 and the co-chaperone ERFJ4 in HSC isolated from human cord blood samples confers greater repopulation capacity compared to non-modified HSC or progenitor cells.[129]

UPR^{ER} is up-regulated in intestinal stem cells (ISC) in *Drosophila* with aging and oxidative stress, which leads to age-related dysplasia and proliferation,[130] although in other biological organisms, such as *C. elegans*, it promotes longevity.[131] In mice, UPR^{ER} is transiently hyper-activated after fasting-re-feeding periods as has been observed by the overexpression of Xbp1, a transcription factor that activates the expression of the UPR^{ER} components. Furthermore, Xbp1 overexpression leads to hypoglycemia due to an improvement in insulin sensitivity and triggers lipolysis in the liver.[132] Adaptation to fasting is linked to the UPR^{ER} system through IRE1α, a protein

located in the ER that splices Xbp1 mRNA to a form that activates UPR^{ER}.[133] Prolonged fasting has a direct effect on the UPR^{ER} system that influences the self-renewal and differentiation potential of stem cells.[134] However, the effects of fasting in HSC have so far only been investigated from a different perspective. Prolonged fasting in mice protects HSC and progenitors within the bone marrow after chemotoxicity and promotes balanced hematopoietic regeneration, also in the absence of chemotherapy treatment. The effect of prolonged fasting on HSC is mediated by the low levels of expression of IGF1 (insulin-like growth factor 1) and PKAα in starved mice.[135]

Signaling pathways influencing intrinsic hematopoietic stem cell aging

Hematopoietic stem cells are located in a very special microenvironment: the bone marrow niche. Communication between the HSC and niche cells is essential for a correct functioning of the whole hematopoietic system.[136] Hence, it is very important that the signaling pathways between HSC and the niche are functioning correctly throughout the life-span of the organisms. Since we are dealing here with intrinsic alterations of HSC upon aging, we will focus on some examples of signaling factors and pathways within stem cells that are particularly compelling in the context of intrinsic aging.

Tgf-β related

Transcriptome data analysis showed reduced TGF-β signaling upon aging in HSC.[15,28] Sun *et al.* calculated that TGF-β-regulated genes were five times more likely to be down-regulated compared to all other genes affected by age.[28] Among the TGF-β downstream genes down-regulated in the study, more than half (63%) are related to biological functions that somehow sustain hematopoiesis.[43,137] In agreement with these findings, scATACseq experiments comparing young and old HSC have shown that TGF-β signaling is specifically enriched in young HSC, meaning that they are in a more accessible chromatin context, and consequently, more likely to be expressed in young when compared to old cells.[15] TGF1-β signaling is also modulated by the regulation of the stability of its receptor upon aging. Tif1-γ (transcription intermediary factor 1γ) regulates TGF1-βR turn over via its ubiquitin ligase activity. Tif1-γ was reported to be down-regulated in aged HSC, while knock out of Tif1-γ promoted premature HSC aging. Consequently, the amount of TGF1-βR is higher in aged HSC, making the cells more sensitive to TGF1-β.[45]

Wnt related

Wnt signaling has been described to have an important role in aging in different stem cell systems such as muscle stem cells, adult neural stem cells or skin stem cells.[138-140] In the case of muscle stem cells, with age, canonical Wnt signaling is activated, leading to impaired muscle regeneration and augmented fibrosis.[139] For adult neural stem cells, it has been shown that aging leads to the overexpression of the Wnt antagonist Dickkopf-1 in order to reduce neurogenesis. When Dickkopf-1 is conditionally ablated, neurogenesis increases.[138] Regarding skin stem cells, the Wnt antagonist Klotho protects against aging by blocking Wnt signaling.[140] Wnt family members also have a role in bone marrow function, since different members are expressed in hematopoietic cells and in non-hematopoietic stromal cells.[141] It has been shown that Wnt signaling is involved in the maintenance of the balance between quiescence and activation of HSC in the bone marrow.[40,142] In murine HSC, it has been shown that there is an intrinsic increased expression of Wnt5a, shifting the signaling from canonical to non-canonical in aged HSC.[44] The non-canonical Wnt pathway resulted in Cdc42 activation and induced aging-like phenotypes when Wnt5a was added to young LT-HSC, including apolarity and loss of epigenetic asymmetry at division.[15,44] In contrast, the haploinsufficiency of Wnt5 showed attenuation of aging phenotypes in old HSC $Wnt5a^{+/-}$ mice.[44] However, Wnt signaling in aging also has an extrinsic role in the bone marrow since haploinsufficient $Wnt5a^{+/-}$ recipient mice regenerate dysfunctional HSC upon secondary transplantation.[143] This apparent incongruence suggests that Wnt5a might exert both an autocrine and a paracrine effect on HSC.

Notch related

It is known that Notch is important for the maintenance of murine muscle stem cells since loss of Notch signaling pathway causes impairment in regeneration of muscle.[144] In fact, the loss of satellite cells that occurs in aged *mdx mice*, a murine model for the Duchenne-Muscular-Disthropy that involves the downregulation of the Notch signaling pathway, can be ameliorated when Notch signaling pathway is restored.[145] Recently, it was also demonstrated in murine muscle stem cells that ligands of Notch activate p53 during normal regeneration, while this axis is impaired in aged mice leading to cell death due to mitotic catastrophe.[146]

There is also evidence of the implication of Notch2, and not Notch1 in the specific Ventricular-subVentricular Zone (V-SVZ) adult neural stem cells, where it represses cell cycle preserving quiescence.[147]

In the case of the hematopoietic system, there are conflicting results from different studies making this a subject of intense debate (reviewed by Lampreia[42] and Weber and Calvi[148]). On one hand, the function of Notch signaling in murine HSC has been reported several times as favoring HSC self-renewal and expansion by *in vitro* stimulation of the Notch pathway, such as the transduction of the active intracellular portion of Notch1 or its targets, *Hes1*[149,150] and *in vivo* by the deletion of a E3 ubiquitin ligase that negatively regulates Notch receptor degradation.[151] However, most studies based on *in vivo* loss-of-function models seem to argue against these results, since Notch signaling pathway is not essential for adult hematopoiesis in mice.[152,153] Notch involvement in human HSC function is also controversial.[42] On one side, inhibition of Notch by transducing human HSCs with dnMAML1 leads to blockage of maintenance/expansion and T-cell development *in vitro*, while *in vivo* engraftment seems not to be affected.[154] However, by using γ-secretase inhibitor (DAPT) to inhibit Notch signaling, it has been shown that Notch pathway is important for the repopulation capacity of human HSC.[155]

NF-κB related

Constitutive NF-κB activation has been involved in aging in several murine tissues, including bone marrow,[156] and in age-related myeloid malignancies like AML

(reviewed by Zhou *et al.*[157]). A very interesting integrative study combining human and mice datasets from young and aged fibroblasts has revealed that NF-κB enforces the aging phenotype and it can be targeted, at least in mice, to revert the aged phenotype.[158] Also, NF-κB signaling seems to be activated in aged tissues and it negatively regulates autophagy (reviewed by Salminen *et al.*[159]).

More recently, NF-κB signaling activation in the hematopoietic system has been studied under inflammation stimuli in mice showing that aged LT-HSC present with an altered myeloid-biased response to inflammation.[18]

In another study, carried out in mice, aged HSC were shown to be failing in down-regulating NF-κB signaling when an acute inflammatory stimulus occurs,[43,160] and that this is dependent on the levels of Rad21/cohesin.[160]

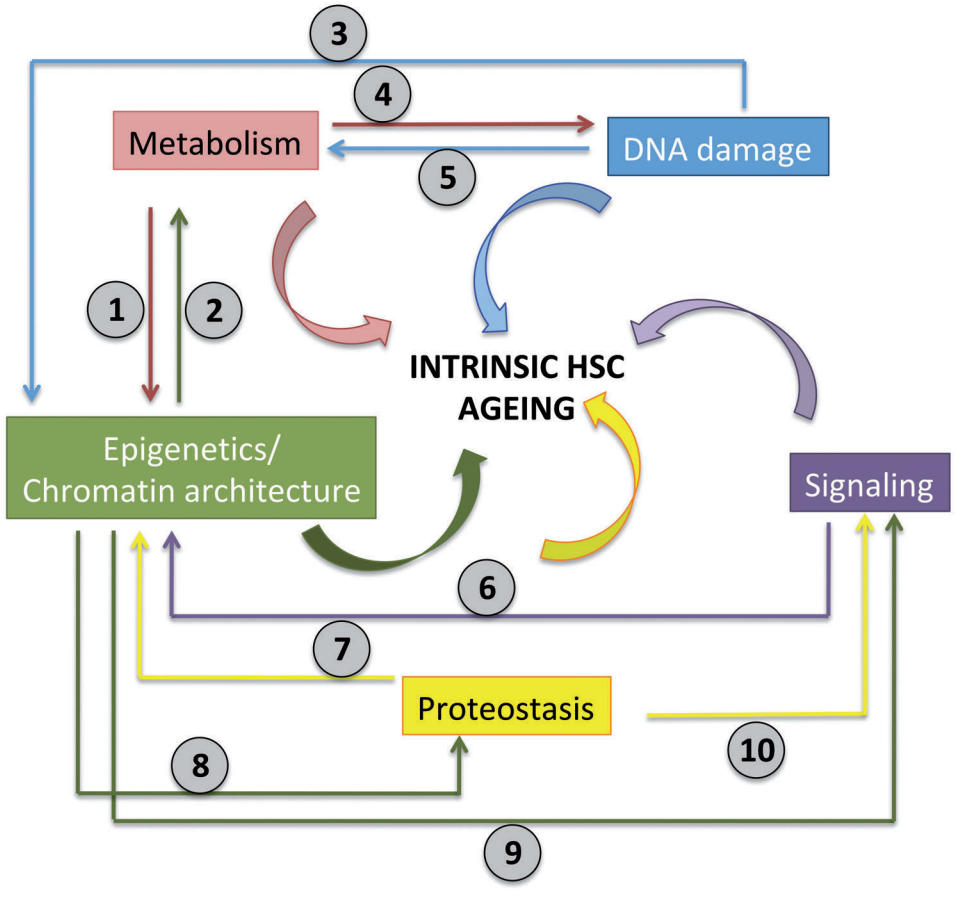

Figure 4. Interconnections between different biological processes involved in intrinsic hematopoietic stem cell (HSC) aging. We have defined five biological processes affected during aging that cannot be compartmentalized from each other. They are interconnected and a change in one of the processes might affect the others, and all of them converge in the final outcome of intrinsic aging. Specific documented interconnections between different biological processes involved in intrinsic HSC aging are numbered (1 to 10).

Table 1. Details of documented connections between different biological processes involved in intrinsic hematopoietic stem cell aging.

Connection	Process	Reference
1	-Change in some metabolite levels affect to the activity of methylases on DNA methylation	(35)
2	-SIRT7 overexpression in aged HSC, preserves against mitochondrial stress	(114)
3	-Specific mutations in epigenetic regulators such as DNMT3, TET2 or ASXL2 tend to appear upon ageing	(53-56)
4	-Accumulation of ROS is related to augmented DNA damage	(107)
5	-Pot1 has a dual role inhibiting ATR-dependent DNA damage repair at telomeres at the same time that it controls the expression of genes involved in ROS reduction and mTOR signaling	(72)
6	-Wnt non-canonical pathway activates Cdc42 in young HSC inducing ageing-like phenotypes	(12,44)
7	-The UPS malfunctions in aged HSC which inhibits the correct degradation of histone modifying enzymes such as HDAC1 and DNMT1	(127,128)
8	-rRNA genes are hypomethylated in aged HSC which involves increased rRNA transcription, more ribosomal biogenesis and higher levels of protein translation	(28)
9	-TGF-β signaling-related genes are enriched in young HSC by ATAC-seq and Wnt signaling-related genes are enriched in old HSC by ATAC-seq	(15,28)
10	-The UPS malfunctions in aged HSC which inhibits the correct degradation of Notch signaling-related factors	(39,45)

HSC: hematopoietic stem cell; ROS: reactive oxygen species; UPS: ubiquitin proteasome system.

Perspectives for rejuvenation and therapeutic strategies

In this review, we have summarized some of the most recent and relevant information about the intrinsic factors that affect HSC upon aging. In general, we can identify at least five biological processes, which we would define as intrinsic HSC aging mechanisms (Table 1 and Figure 4). DNA damage, metabolism, epigenetics/chromatin architecture, proteostasis, and signaling. However, the cell cannot compartmentalize hermetically each one of these processes. This is the reason why the interconnections between these biological processes will be a key aspect in deciphering the extent of the impact of aging on HSC. For instance, the levels of several metabolites like SAM or ketoglutharate affect the activity of methylases, which in turn have an effect on the epigenetics of the cell.[35] Investigating and understanding cellular and molecular mechanisms of HSC aging will increase the possibility of defining new pharmacological targets to reduce the negative effects of aging and promote "healthy aging".

We are aware that most aging mechanisms that we have reviewed here have been studied in the murine or in non-human systems. Nevertheless, we would like to emphasize the progress achieved so far and the importance of pursuing an integrative research approach, to connect all the aspects affecting stem cell aging. A broader view of this process might indeed be central in bridging the gap to translation in the human system.

Acknowledgment

This work was supported by the Deutsche Forschungsgemeinschaft (DFG or German Research Foundation) FOR2674 and SFB1074 to MCF and by Ministerio de Ciencia, Innovación y Universidades (Spanish Ministry of Science, Innovation and University) PGC2018-102049-B-I00 and RYC2018-025979-I to MCF.

References

1. Klepin HD. Myelodysplastic Syndromes and Acute Myeloid Leukemia in the Elderly. Clin Geriatr Med. 2016;32(1):155-173.
2. Akunuru S, Geiger H. Aging, Clonality, and Rejuvenation of Hematopoietic Stem Cells. Trends Mol Med. 2016;22(8):701-712.
3. Preussler JM, Meyer CL, Mau LW, et al. Healthcare Costs and Utilization for Patients Age 50 to 64 Years with Acute Myeloid Leukemia Treated with Chemotherapy or with Chemotherapy and Allogeneic Hematopoietic Cell Transplantation. Biol Blood Marrow Transplant. 2017;23(6):1021-1028.
4. Meyers J, Yu Y, Kaye JA, Davis KL. Medicare fee-for-service enrollees with primary acute myeloid leukemia: an analysis of treatment patterns, survival, and healthcare resource utilization and costs. Appl Health Econ Health Policy. 2013;11(3):275-286.
5. Chandel NS, Jasper H, Ho TT, Passegue E. Metabolic regulation of stem cell function in tissue homeostasis and organismal ageing. Nat Cell Biol. 2016;18(8):823-832.
6. Singh AK, Althoff MJ, Cancelas JA. Signaling Pathways Regulating Hematopoietic Stem Cell and Progenitor Aging. Current Stem Cell Rep. 2018;4(2):166-181.
7. Rossi DJ, Bryder D, Zahn JM, et al. Cell intrinsic alterations underlie hematopoietic stem cell aging. Proc Natl Acad Sci U S A. 2005;102(26):9194-9199.
8. Sudo K, Ema H, Morita Y, Nakauchi H. Age-Associated Characteristics of Murine Hematopoietic Stem Cells. J Exp Med. 2000;192(9):1273-1280.
9. Pang WW, Price EA, Sahoo D, et al. Human bone marrow hematopoietic stem cells are increased in frequency and myeloid-biased with age. Proc Natl Acad Sci U S A. 2011;108(50):20012-20017.
10. Vas V, Senger K, Dorr K, Niebel A, Geiger H. Aging of the microenvironment influences clonality in hematopoiesis. PLoS One. 2012;7(8):e42080.
11. Ergen AV, Boles NC, Goodell MA. Rantes/Ccl5 influences hematopoietic stem cell subtypes and causes myeloid skewing. Blood. 2012;119(11):2500-2509.
12. Guidi N, Sacma M, Standker L, et al. Osteopontin attenuates aging-associated phenotypes of hematopoietic stem cells. EMBO J. 2017;36(7):840-853.
13. Beerman I, Maloney WJ, Weissmann IL, Rossi DJ. Stem cells and the aging hematopoietic system. Curr Opin Immunol. 2010;22(4):500-506.
14. Florian MC, Dorr K, Niebel A, et al. Cdc42 activity regulates hematopoietic stem cell aging and rejuvenation. Cell Stem Cell. 2012;10(5):520-530.
15. Florian MC, Klose M, Sacma M, et al. Aging alters the epigenetic asymmetry of HSC division. PLoS Biol. 2018;16(9):e2003389.
16. Signer RA, Montecino-Rodriguez E, Witte ON, McLaughlin J, Dorshkind K. Age-related defects in B lymphopoiesis underlie the myeloid dominance of adult leukemia. Blood. 2007;110(6):1831-1839.
17. Yamamoto R, Wilkinson AC, Ooehara J, et al. Large-Scale Clonal Analysis Resolves Aging of the Mouse Hematopoietic Stem Cell Compartment. Cell Stem Cell. 2018;22(4):600-607.
18. Mann M, Mehta A, de Boer CG, et al. Heterogeneous Responses of Hematopoietic Stem Cells to Inflammatory Stimuli Are Altered with Age. Cell Rep. 2018;25(11):2992-3005.
19. Lopez-Otin C, Blasco MA, Partridge L, Serrano M, Kroemer G. The hallmarks of aging. Cell. 2013;153(6):1194-1217.
20. Beerman I, Seita J, Inlay MA, Weissman IL, Rossi DJ. Quiescent hematopoietic stem cells accumulate DNA damage during aging that is repaired upon entry into cell cycle. Cell Stem Cell. 2014;15(1):37-50.
21. Flach J, Bakker ST, Mohrin M, et al. Replication stress is a potent driver of functional decline in ageing haematopoietic stem cells. Nature. 2014;512(7513):198-202.
22. Akunuru S, Geiger H. Aging, Clonality, and Rejuvenation of Hematopoietic Stem Cells. Trends Mol Med. 2016;22(8):701-712.
23. Chen J, Kao YR, Sun D, et al. Myelodysplastic syndrome progression to acute myeloid leukemia at the stem cell level. Nat Med. 2019;25(1):103-110.
24. Steensma DP, Bejar R, Jaiswal S, et al. Clonal hematopoiesis of indeterminate potential and its distinction from myelodysplastic syndromes. Blood. 2015;126(1):9-16.
25. Jaiswal S, Natarajan P, Silver AJ, et al. Clonal Hematopoiesis and Risk of Atherosclerotic Cardiovascular Disease. N Engl J Med. 2017;377(2):111-121.
26. Yu VWC, Yusuf RZ, Oki T, et al. Epigenetic Memory Underlies Cell-Autonomous Heterogeneous Behavior of Hematopoietic Stem Cells. Cell. 2016;167(5):1310-1322.
27. Beerman I, Bock C, Garrison BS, et al. Proliferation-dependent alterations of the DNA methylation landscape underlie hematopoietic stem cell aging. Cell Stem Cell. 2013;12(4):413-425.
28. Sun D, Luo M, Jeong M, et al. Epigenomic Profiling of Young and Aged HSCs Reveals Concerted Changes during Aging that Reinforce Self-Renewal. Cell Stem Cell. 2014;14(5):673-688.
29. Grigoryan A, Guidi N, Senger K, et al. LaminA/C regulates epigenetic and chromatin architecture changes upon aging of hematopoietic stem cells. Genome Biol. 2018;19(1):189.
30. Maryanovich M, Zahalka AH, Pierce H, et al. Adrenergic nerve degeneration in bone marrow drives aging of the hematopoietic stem cell niche. Nat Med. 2018;24(6):782-791.
31. Ito K, Suda T. Metabolic requirements for the maintenance of self-renewing stem cells. Nat Rev Mol Cell Biol. 2014;15(4):243-256.
32. Verovskaya EV, Dellorusso PV, Passegué E. Losing Sense of Self and Surroundings: Hematopoietic Stem Cell Aging and Leukemic Transformation. Trends Mol Med. 2019;25(6):494-515.
33. He C, Klionsky DJ. Regulation mechanisms and signaling pathways of autophagy. Annu Rev Genet. 2009;43:67-93.
34. Kaushik S, Cuervo AM. The coming of age of chaperone-mediated autophagy. Nat Rev Mol Cell Biol. 2018;19(6):365-381.
35. Ho TT, Warr MR, Adelman ER, et al. Autophagy maintains the metabolism and function of young and old stem cells. Nature. 2017;543(7644):205-210.
36. Vilchez D, Simic MS, Dillin A. Proteostasis and aging of stem cells. Trends Cell Biol. 2014;24(3):161-170.
37. Noormohammadi A, Calculli G, Gutierrez-Garcia R, Khodakarami A, Koyuncu S,

Vilchez D. Mechanisms of protein homeostasis (proteostasis) maintain stem cell identity in mammalian pluripotent stem cells. Cell Mol Life Sci. 2018;75(2):275-290.
38. Chapple RH, Hu T, Tseng YJ, et al. ERalpha promotes murine hematopoietic regeneration through the Ire1alpha-mediated unfolded protein response. Elife. 2018;7.
39. Moran-Crusio K, Reavie LB, Aifantis I. Regulation of hematopoietic stem cell fate by the ubiquitin proteasome system. Trends Immunol. 2012;33(7):357-363.
40. Fleming HE, Janzen V, Lo Celso C, et al. Wnt signaling in the niche enforces hematopoietic stem cell quiescence and is necessary to preserve self-renewal in vivo. Cell Stem Cell. 2008;2(3):274-283.
41. Blank U, Karlsson S. TGF-beta signaling in the control of hematopoietic stem cells. Blood. 2015;125(23):3542-3550.
42. Lampreia FP, Carmelo JG, Anjos-Afonso F. Notch Signaling in the Regulation of Hematopoietic Stem Cell. Curr Stem Cell Rep. 2017;3(3):202-209.
43. Chambers SM, Shaw CA, Gatza C, Fisk CJ, Donehower LA, Goodell MA. Aging hematopoietic stem cells decline in function and exhibit epigenetic dysregulation. PLoS Biol. 2007;5(8):e201.
44. Florian MC, Nattamai KJ, Dorr K, et al. A canonical to non-canonical Wnt signalling switch in haematopoietic stem-cell ageing. Nature. 2013;503(7476):392-396.
45. Quere R, Saint-Paul L, Carmignac V, et al. Tif1gamma regulates the TGF-beta1 receptor and promotes physiological aging of hematopoietic stem cells. Proc Natl Acad Sci U S A. 2014;111(29):10592-10597.
46. de Renty C, Ellis NA. Bloom's syndrome: Why not premature aging?: A comparison of the BLM and WRN helicases. Ageing Res Rev. 2017;33:36-51.
47. Parmar K, Kim J, Sykes SM, et al. Hematopoietic stem cell defects in mice with deficiency of Fancd2 or Usp1. Stem Cells. 2010;28(7):1186-1195.
48. Rossi DJ, Bryder D, Seita J, Nussenzweig A, Hoeijmakers J, Weissman IL. Deficiencies in DNA damage repair limit the function of haematopoietic stem cells with age. Nature. 2007;447(7145):725-729.
49. Wahlestedt M, Erlandsson E, Kristiansen T, et al. Clonal reversal of ageing-associated stem cell lineage bias via a pluripotent intermediate. Nat Commun. 2017;8:14533.
50. Osorio FG, Rosendahl Huber A, Oka R, et al. Somatic Mutations Reveal Lineage Relationships and Age-Related Mutagenesis in Human Hematopoiesis. Cell Rep. 2018;25(9):2308-2316.
51. Rogakou EP, Pilch DR, Orr AH, Ivanova VS, Bonner WM. DNA double-stranded breaks induce histone H2AX phosphorylation on serine 139. J Biol Chem. 1998;273(10):5858-5868.
52. Moehrle BM, Nattamai K, Brown A, et al. Stem Cell-Specific Mechanisms Ensure Genomic Fidelity within HSCs and upon Aging of HSCs. Cell Rep. 2015;13(11):2412-2424.
53. Beerman I. Accumulation of DNA damage in the aged hematopoietic stem cell compartment. Semin Hematol. 2017;54(1):12-18.
54. Busque L, Patel JP, Figueroa ME, et al. Recurrent somatic TET2 mutations in normal elderly individuals with clonal hematopoiesis. Nat Genet. 2012;44(11):1179-1181.
55. Genovese G, Kahler AK, Handsaker RE, et al. Clonal hematopoiesis and blood-cancer risk inferred from blood DNA sequence. N Engl J Med. 2014;371(26):2477-2487.
56. Jaiswal S, Fontanillas P, Flannick J, et al. Age-related clonal hematopoiesis associated with adverse outcomes. N Engl J Med. 2014;371(26):2488-2498.
57. Challen GA, Sun D, Mayle A, et al. Dnmt3a and Dnmt3b have overlapping and distinct functions in hematopoietic stem cells. Cell Stem Cell. 2014;15(3):350-364.
58. Zhang X, Su J, Jeong M, et al. DNMT3A and TET2 compete and cooperate to repress lineage-specific transcription factors in hematopoietic stem cells. Nat Genet. 2016;48(9):1014-1023.
59. Nagase R, Inoue D, Pastore A, et al. Expression of mutant Asxl1 perturbs hematopoiesis and promotes susceptibility to leukemic transformation. J Exp Med. 2018;215(6):1729-1747.
60. Buscarlet M, Provost S, Zada YF, et al. DNMT3A and TET2 dominate clonal hematopoiesis and demonstrate benign phenotypes and different genetic predispositions. Blood. 2017;130(6):753-762.
61. Cargo CA, Rowbotham N, Evans PA, et al. Targeted sequencing identifies patients with preclinical MDS at high risk of disease progression. Blood. 2015;126(21):2362-2365.
62. Young AL, Challen GA, Birmann BM, Druley TE. Clonal haematopoiesis harbouring AML-associated mutations is ubiquitous in healthy adults. Nat Commun. 2016;7:12484.
63. Behrens A, van Deursen JM, Rudolph KL, Schumacher B. Impact of genomic damage and ageing on stem cell function. Nat Cell Biol. 2014;16(3):201-207.
64. Shepherd BE, Kiem HP, Lansdorp PM, et al. Hematopoietic stem-cell behavior in nonhuman primates. Blood. 2007;110(6):1806-1813.
65. Whittemore K, Vera E, Martínez-Nevado E, Sanpera C, Blasco MA. Telomere shortening rate predicts species life span. Proc Natl Acad Sci U S A. 2019;116(30):15122-15127.
66. Harrison DE, Astle CM. Loss of stem cell repopulating ability upon transplantation. Effects of donor age, cell number, and transplantation procedure. J Exp Med. 1982;156(6):1767-1779.
67. Allsopp RC, Morin GB, Horner JW, DePinho R, Harley CB, Weissman IL. Effect of TERT over-expression on the long-term transplantation capacity of hematopoietic stem cells. Nat Med. 2003;9(4):369-371.
68. Sekulovic S, Gylfadottir V, Vulto I, et al. Prolonged self-renewal activity unmasks telomerase control of telomere homeostasis and function of mouse hematopoietic stem cells. Blood. 2011;118(7):1766-1773.
69. Raval A, Behbehani GK, Nguyen lX, et al. Reversibility of Defective Hematopoiesis Caused by Telomere Shortening in Telomerase Knockout Mice. PLoS One. 2015;10(7):e0131722.
70. Wang J, Lu X, Sakk V, Klein CA, Rudolph KL. Senescence and apoptosis block hematopoietic activation of quiescent hematopoietic stem cells with short telomeres. Blood. 2014;124(22):3237-3240.
71. Townsley DM, Dumitriu B, Young NS. Bone marrow failure and the telomeropathies. Blood. 2014;124(18):2775-2783.
72. Hosokawa K, MacArthur BD, Ikushima YM, et al. The telomere binding protein Pot1 maintains haematopoietic stem cell activity with age. Nat Commun. 2017;8(1):804.
73. Yu KR, Espinoza DA, Wu C, et al. The impact of aging on primate hematopoiesis as interrogated by clonal tracking. Blood. 2018;131(11):1195-1205.
74. Xu J, Wang Y, Guttorp P, Abkowitz JL. Visualizing hematopoiesis as a stochastic process. Blood Adv. 2018;2(20):2637-2645.
75. Rozhok AI, DeGregori J. The evolution of lifespan and age-dependent cancer risk. Trends Cancer. 2016;2(10):552-560.
76. Li Z, Cai X, Cai CL, et al. Deletion of Tet2 in mice leads to dysregulated hematopoietic stem cells and subsequent development of myeloid malignancies. Blood. 2011;118(17):4509-4518.
77. Almosailleakh M, Schwaller J. Murine Models of Acute Myeloid Leukaemia. Int J Mol Sci. 2019;20(2).
78. Wahlestedt M, Norddahl GL, Sten G, et al. An epigenetic component of hematopoietic stem cell aging amenable to reprogramming into a young state. Blood. 2013;121(21):4257-4264.
79. Grover A, Sanjuan-Pla A, Thongjuea S, et al. Single-cell RNA sequencing reveals molecular and functional platelet bias of aged haematopoietic stem cells. Nat Commun. 2016;7:11075.
80. Wahlestedt M, Bryder D. The slippery slope of hematopoietic stem cell aging. Exp Hematol. 2017;56:1-6.
81. Gonzalo S. Epigenetic alterations in aging. J Appl Physiol (1985). 2010;109(2):586-597.
82. Taiwo O, Wilson GA, Emmett W, et al. DNA methylation analysis of murine hematopoietic side population cells during aging. Epigenetics. 2013;8(10):1114-1122.
83. Brinkman AB, Gu H, Bartels SJ, et al. Sequential ChIP-bisulfite sequencing enables direct genome-scale investigation of chromatin and DNA methylation cross-talk. Genome Res. 2012;22(6):1128-1138.
84. Jones MJ, Goodman SJ, Kobor MS. DNA methylation and healthy human aging. Aging Cell. 2015;14(6):924-932.
85. Kramer A, Challen GA. The epigenetic basis of hematopoietic stem cell aging. Semin Hematol. 2017;54(1):19-24.
86. Lee SC, Miller S, Hyland C, et al. Polycomb repressive complex 2 component Suz12 is required for hematopoietic stem cell function and lymphopoiesis. Blood. 2015;126(2):167-175.
87. Xie H, Xu J, Hsu JH, et al. Polycomb repressive complex 2 regulates normal hematopoietic stem cell function in a developmental-stage-specific manner. Cell Stem Cell. 2014;14(1):68-80.
88. Cellot S, Hope KJ, Chagraoui J, et al. RNAi screen identifies Jarid1b as a major regulator of mouse HSC activity. Blood. 2013;122(9):1545-1555.
89. Thieme S, GyárfásT, Richter C, et al. The histone demethylase UTX regulates stem cell migration and hematopoiesis. Blood. 2013;121(13):2462-2473.
90. Kerenyi MA, Shao Z, Hsu YJ, et al. Histone demethylase Lsd1 represses hematopoietic stem and progenitor cell signatures during blood cell maturation. Elife. 2013;2:e00633.
91. Djeghloul D, Kuranda K, Kuzniak I, et al. Age-Associated Decrease of the Histone Methyltransferase SUV39H1 in HSC Perturbs Heterochromatin and B Lymphoid Differentiation. Stem Cell Rep. 2016;6(6):970-984.
92. Shogren-Knaak M, Ishii H, Sun JM, Pazin MJ, Davie JR, Peterson CL. Histone H4-K16 acetylation controls chromatin structure and protein interactions. Science. 2006;311(5762):844-847.
93. Kaufmann KB, Garcia-Prat L, Liu Q, et al. A stemness screen reveals C3orf54/INKA1 as a promoter of human leukemia stem cell latency. Blood. 2019;133(20):2198-2211.
94. Abo A, Qu J, Cammarano MS, et al. PAK4, a

novel effector for Cdc42Hs, is implicated in the reorganization of the actin cytoskeleton and in the formation of filopodia. EMBO J. 1998;17(22):6527-6540.
95. Kong S, Zhang Y. Deciphering Hi-C: from 3D genome to function. Cell Biol Toxicol. 2019;35(1):15-32.
96. Rowley MJ, Corces VG. Organizational principles of 3D genome architecture. Nat Rev Genet. 2018;19(12):789-800.
97. Galeev R, Larsson J. Cohesin in haematopoiesis and leukaemia. Curr Opin Hematol. 2018;25(4):259-265.
98. Viny AD, Ott CJ, Spitzer B, et al. Dose-dependent role of the cohesin complex in normal and malignant hematopoiesis. J Exp Med. 2015;212(11):1819-1832.
99. Choudry FA, Frontini M. Epigenetic Control of Haematopoietic Stem Cell Aging and Its Clinical Implications. Stem Cells Int. 2016;2016:5797521.
100. Benayoun BA, Pollina EA, Singh PP, et al. Remodeling of epigenome and transcriptome landscapes with aging in mice reveals widespread induction of inflammatory responses. Genome Res. 2019;29(4):697-709.
101. Cheung P, Vallania F, Warsinske HC, et al. Single-Cell Chromatin Modification Profiling Reveals Increased Epigenetic Variations with Aging. Cell. 2018;173(6):1385-1397.
102. Burman B, Zhang ZZ, Pegoraro G, Lieb JD, Misteli T. Histone modifications predispose genome regions to breakage and translocation. Genes Dev. 2015;29(13):1393-1402.
103. Kirschner K, Chandra T, Kiselev V, et al. Proliferation Drives Aging-Related Functional Decline in a Subpopulation of the Hematopoietic Stem Cell Compartment. Cell Rep. 2017;19(8):1503-1511.
104. Bigarella CL, Liang R, Ghaffari S. Stem cells and the impact of ROS signaling. Development. 2014;141(22):4206-4218.
105. Norddahl GL, Pronk CJ, Wahlestedt M, et al. Accumulating mitochondrial DNA mutations drive premature hematopoietic aging phenotypes distinct from physiological stem cell aging. Cell Stem Cell. 2011;8(5):499-510.
106. Jang YY, Sharkis SJ. A low level of reactive oxygen species selects for primitive hematopoietic stem cells that may reside in the low-oxygenic niche. Blood. 2007;110(8):3056-3063.
107. Rimmele P, Liang R, Bigarella CL, et al. Mitochondrial metabolism in hematopoietic stem cells requires functional FOXO3. EMBO Rep. 2015;16(9):1164-1176.
108. Tothova Z, Kollipara R, Huntly BJ, et al. FoxOs are critical mediators of hematopoietic stem cell resistance to physiologic oxidative stress. Cell. 2007;128(2):325-339.
109. Warr MR, Binnewies M, Flach J, et al. FOXO3A directs a protective autophagy program in haematopoietic stem cells. Nature. 2013;494(7437):323-327.
110. Brown K, Xie S, Qiu X, et al. SIRT3 reverses aging-associated degeneration. Cell Rep. 2013;3(2):319-327.
111. Trifunovic A, Wredenberg A, Falkenberg M, et al. Premature ageing in mice expressing defective mitochondrial DNA polymerase. Nature. 2004;429(6990):417-423.
112. Chen F, Liu Y, Wong NK, Xiao J, So KF. Oxidative Stress in Stem Cell Aging. Cell Transplant. 2017;26(9):1483-1495.
113. Oh J, Lee YD, Wagers AJ. Stem cell aging: mechanisms, regulators and therapeutic opportunities. Nat Med. 2014;20(8):870-880.
114. Mohrin M, Shin J, Liu Y, et al. Stem cell aging. A mitochondrial UPR-mediated metabolic checkpoint regulates hematopoietic stem cell aging. Science. 2015;347(6228):1374-1377.
115. Rubinsztein David C, Mariño G, Kroemer G. Autophagy and Aging. Cell. 2011;146(5):682-695.
116. Schvartzman JM, Thompson CB, Finley LWS. Metabolic regulation of chromatin modifications and gene expression. J Cell Biol. 2018;217(7):2247-2259.
117. Auberger P, Puissant A. Autophagy, a key mechanism of oncogenesis and resistance in leukemia. Blood. 2017;129(5):547-552.
118. Rothe K, Porter V, Jiang X. Current Outlook on Autophagy in Human Leukemia: Foe in Cancer Stem Cells and Drug Resistance, Friend in New Therapeutic Interventions. Int J Mol Sci. 2019;20(3).
119. Willems L, Chapuis N, Puissant A, et al. The dual mTORC1 and mTORC2 inhibitor AZD8055 has anti-tumor activity in acute myeloid leukemia. Leukemia. 2012;26(6):1195-1202.
120. Macara IG, Mili S. Polarity and differential inheritance--universal attributes of life? Cell. 2008;135(5):801-812.
121. Budovsky A, Fraifeld VE, Aronov S. Linking cell polarity, aging and rejuvenation. Biogerontology. 2011;12(2):167-175.
122. Liu B, Larsson L, Caballero A, et al. The polarisome is required for segregation and retrograde transport of protein aggregates. Cell. 2010;140(2):257-267.
123. Bufalino MR, DeVeale B, van der Kooy D. The asymmetric segregation of damaged proteins is stem cell-type dependent. J Cell Biol. 2013;201(4):523-530.
124. Yamashita YM, Yuan H, Cheng J, Hunt AJ. Polarity in stem cell division: asymmetric stem cell division in tissue homeostasis. Cold Spring Harb Perspect Biol. 2010;2(1):a001313.
125. Mohr J, Dash BP, Schnoeder TM, et al. The cell fate determinant Scribble is required for maintenance of hematopoietic stem cell function. Leukemia. 2018;32(5):1211-1221.
126. Beckmann J, Scheitza S, Wernet P, Fischer JC, Giebel B. Asymmetric cell division within the human hematopoietic stem and progenitor cell compartment: identification of asymmetrically segregating proteins. Blood. 2007;109(12):5494-5501.
127. Zou C, Mallampalli RK. Regulation of histone modifying enzymes by the ubiquitin–proteasome system. Biochim Biophys Acta. 2014;1843(4):694-702.
128. Tomaru U, Takahashi S, Ishizu A, et al. Decreased proteasomal activity causes age-related phenotypes and promotes the development of metabolic abnormalities. Am J Pathol. 2012;180(3):963-972.
129. van Galen P, Kreso A, Mbong N, et al. The unfolded protein response governs integrity of the haematopoietic stem-cell pool during stress. Nature. 2014;510(7504):268-272.
130. Wang L, Zeng X, Ryoo HD, Jasper H. Integration of UPRER and oxidative stress signaling in the control of intestinal stem cell proliferation. PLoS Genet. 2014;10(8):e1004568.
131. Henis-Korenblit S, Zhang P, Hansen M, et al. Insulin/IGF-1 signaling mutants reprogram ER stress response regulators to promote longevity. Proc Natl Acad Sci U S A. 2010;107(21):9730-9735.
132. Deng Y, Wang ZV, Tao C, et al. The Xbp1s/GalE axis links ER stress to postprandial hepatic metabolism. J Clin Invest. 2013;123(1):455-468.
133. Shao M, Shan B, Liu Y, et al. Hepatic IRE1Œ± regulates fasting-induced metabolic adaptive programs through the XBP1s-PPARŒ± axis signalling. Nat Commun. 2014;5:3528.
134. Chaube R. Can UPR integrate fasting and stem cell regeneration? Front Chem. 2015;3:5.
135. Cheng CW, Adams GB, Perin L, et al. Prolonged fasting reduces IGF-1/PKA to promote hematopoietic-stem-cell-based regeneration and reverse immunosuppression. Cell Stem Cell. 2014;14(6):810-823.
136. Wei Q, Frenette PS. Niches for Hematopoietic Stem Cells and Their Progeny. Immunity. 2018;48(4):632-648.
137. Challen GA, Boles NC, Chambers SM, Goodell MA. Distinct hematopoietic stem cell subtypes are differentially regulated by TGF-beta1. Cell Stem Cell. 2010;6(3):265-278.
138. Seib DR, Corsini NS, Ellwanger K, et al. Loss of Dickkopf-1 restores neurogenesis in old age and counteracts cognitive decline. Cell Stem Cell. 2013;12(2):204-214.
139. Brack AS, Conboy MJ, Roy S, et al. Increased Wnt signaling during aging alters muscle stem cell fate and increases fibrosis. Science. 2007;317(5839):807-810.
140. Liu H, Fergusson MM, Castilho RM, et al. Augmented Wnt signaling in a mammalian model of accelerated aging. Science. 2007;317(5839):803-806.
141. Malhotra S, Kincade PW. Wnt-related molecules and signaling pathway equilibrium in hematopoiesis. Cell Stem Cell. 2009;4(1):27-36.
142. Dijksterhuis JP, Petersen J, Schulte G. WNT/Frizzled signalling: receptor-ligand selectivity with focus on FZD-G protein signalling and its physiological relevance: IUPHAR Review 3. Br J Pharmacol. 2014;171(5):1195-1209.
143. Schreck C, Istvanffy R, Ziegenhain C, et al. Niche WNT5A regulates the actin cytoskeleton during regeneration of hematopoietic stem cells. J Exp Med. 2017;214(1):165-181.
144. Conboy IM, Conboy MJ, Wagers AJ, Girma ER, Weissman IL, Rando TA. Rejuvenation of aged progenitor cells by exposure to a young systemic environment. Nature. 2005;433(7027):760-764.
145. Jiang C, Wen Y, Kuroda K, Hannon K, Rudnicki MA, Kuang S. Notch signaling deficiency underlies age-dependent depletion of satellite cells in muscular dystrophy. Dis Model Mech. 2014;7(8):997-1004.
146. Liu L, Charville GW, Cheung TH, et al. Impaired Notch Signaling Leads to a Decrease in p53 Activity and Mitotic Catastrophe in Aged Muscle Stem Cells. Cell Stem Cell. 2018;23(4):544-556.
147. Engler A, Rolando C, Giachino C, et al. Notch2 Signaling Maintains NSC Quiescence in the Murine Ventricular-Subventricular Zone. Cell Rep. 2018;22(4):992-1002.
148. Weber JM, Calvi LM. Notch signaling and the bone marrow hematopoietic stem cell niche. Bone. 2010;46(2):281-285.
149. Calvi LM, Adams GB, Weibrecht KW, et al. Osteoblastic cells regulate the haematopoietic stem cell niche. Nature. 2003;425(6960):841-846.
150. Karanu FN, Murdoch B, Gallacher L, et al. The Notch Ligand Jagged-1 Represents a Novel Growth Factor of Human Hematopoietic Stem Cells. J Exp Med. 2000;192(9):1365-1372.
151. Rathinam C, Matesic LE, Flavell RA. The E3 ligase Itch is a negative regulator of the homeostasis and function of hematopoietic stem cells. Nat Immunol. 2011;12(5):399-407.
152. Maillard I, Koch U, Dumortier A, et al. Canonical notch signaling is dispensable for

the maintenance of adult hematopoietic stem cells. Cell Stem Cell. 2008;2(4):356-366.
153. Mancini SJ, Mantei N, Dumortier A, Suter U, MacDonald HR, Radtke F. Jagged1-dependent Notch signaling is dispensable for hematopoietic stem cell self-renewal and differentiation. Blood. 2005;105(6):2340-2342.
154. Benveniste P, Serra P, Dervovic D, et al. Notch signals are required for in vitro but not in vivo maintenance of human hematopoietic stem cells and delay the appearance of multipotent progenitors. Blood. 2014;123(8):1167-1177.
155. Anjos-Afonso F, Currie E, Palmer HG, Foster KE, Taussig DC, Bonnet D. CD34(-) cells at the apex of the human hematopoietic stem cell hierarchy have distinctive cellular and molecular signatures. Cell Stem Cell. 2013;13(2):161-174.
156. Spencer NF, Poynter ME, Im SY, Daynes RA. Constitutive activation of NF-kappa B in an animal model of aging. Int Immunol. 1997;9(10):1581-1588.
157. Zhou J, Ching YQ, Chng WJ. Aberrant nuclear factor-kappa B activity in acute myeloid leukemia: from molecular pathogenesis to therapeutic target. Oncotarget. 2015;6(8):5490-5500.
158. Adler AS, Sinha S, Kawahara TL, Zhang JY, Segal E, Chang HY. Motif module map reveals enforcement of aging by continual NF-kappaB activity. Genes Dev. 2007;21(24):3244-3257.
159. Salminen A, Hyttinen JM, Kauppinen A, Kaarniranta K. Context-Dependent Regulation of Autophagy by IKK-NF-κB Signaling: Impact on the Aging Process. Int J Cell Biol. 2012;2012:849541.
160. Chen Z, Amro EM, Becker F, et al. Cohesin-mediated NF-κB signaling limits hematopoietic stem cell self-renewal in aging and inflammation. J Exp Med. 2019;216(1):152-175.

REVIEW ARTICLE

Ferrata Storti Foundation

Microenvironmental contributions to hematopoietic stem cell aging

Ya-Hsuan Ho[1,2] and Simón Méndez-Ferrer[1,2]

[1]Wellcome Trust-Medical Research Council Cambridge Stem Cell Institute and Department of Haematology, University of Cambridge, Cambridge and [2]National Health Service Blood and Transplant, Cambridge Biomedical Campus, Cambridge, UK

Haematologica 2020
Volume 105(1):38-46

ABSTRACT

Hematopoietic stem cell (HSC) aging was originally thought to be essentially an HSC-autonomous process, which is the focus of another review in the same issue of *Haematologica*. However, studies on the microenvironment that maintains and regulates HSC (HSC niche) over the past 20 years have suggested that microenvironmental aging contributes to declined HSC function over time. The HSC niches comprise a complex and dynamic molecular network of interactions across multiple cell types, including endothelial cells, mesenchymal stromal cells, osteoblasts, adipocytes, neuro-glial cells and mature hematopoietic cells. Upon aging, functional changes in the HSC niches, such as microenvironmental senescence, imbalanced bone marrow mesenchymal stromal cell differentiation, vascular remodeling, changes in adrenergic signaling and inflammation, coordinately and dynamically influence the fate of HSC and their downstream progeny. The end result is lymphoid deficiency and myeloid skewing. During this process, aged HSC and their derivatives remodel the niche to favor myeloid expansion. Therefore, the crosstalk between HSC and the microenvironment is indispensable for the aging of the hematopoietic system and might represent a therapeutic target in age-related pathological disorders.

Correspondence:

YA-HSUAN HO
yhh29@medschl.cam.ac.uk

SIMÓN MÉNDEZ-FERRER
sm2116@cam.ac.uk

Received: July 8, 2019.

Accepted: November 14, 2019.

Pre-published: December 5, 2019.

doi:10.3324/haematol.2018.211334

Check the online version for the most updated information on this article, online supplements, and information on authorship & disclosures: www.haematologica.org/content/105/1/38

Introduction to hematopoietic stem cell aging

Adult hematopoiesis takes place in the bone marrow (BM), where hematopoietic stem cells (HSC) can self-renew, proliferate and differentiate to replenish the blood and immune systems. Given that most HSC are quiescent under homeostasis, mature blood and immune cell production is believed to derive mainly under steady state from progenitor cells (rather than HSC), which differentiate to produce mature blood cells. Cumulative studies have demonstrated that HSC are heterogeneous and contain subsets with distinct myeloid, platelet or lymphoid-biased potentials, although the existence of lymphoid-biased HSC has long been debated and remains controversial.[1-5] Additionally, recent studies have shown that HSC can bypass the intermediate steps to generate mature progenies under certain conditions, such as chronic inflammation and aging.

Upon aging, HSC increase in number but their functions are impaired, characterized by reduced regenerative and homing capacity, loss of cell polarity, and myeloid-biased differentiation at the expense of lymphopoiesis.[6-9] These changes were initially thought to cause only cell-intrinsic dysregulation,[10] such as epigenetic deregulation,[11] replication stress,[12] deficient DNA repair,[13] and transition from canonical to non-canonical Wnt signaling.[14] Old HSC also suffer metabolic changes,[15,16] impaired autophagy[17] and altered protein homeostasis,[18] which contribute to the decline of their regenerative potential. However, current studies are revealing that the BM microenvironment may contribute to HSC aging. This hypothesis is supported by an elegant study in which old HSC transplanted into young recipients exhibited reduced myeloid output as compared those transplanted into old recipients, suggesting that the old BM microenvironment contributes to myeloid skewing.[19] This review will cover microenvironmental contributions to

HSC aging, provide hypotheses for BM niche remodeling based on current knowledge, and discuss the potential implications for age-related myeloid malignancies. HSC-intrinsic aging mechanisms are the focus of a separate complementary review in this issue of *Haematologica* and will not be discussed here.

Evolving views on hematopoietic stem cell niches

HSC are surrounded by numerous cell types and the associated extracellular matrix in the BM, which form a unique microenvironment known as the "HSC niche". Osteoblasts were the first niche cells found to be involved in hematopoiesis. Early studies indicated that osteoblasts differentiate from BM osteoprogenitor cells, secrete hematopoietic cytokines and can maintain HSC in culture.[20] In 2003, two studies described for the first time that transplanted HSC localize to the bone surface of BM and their numbers are regulated by osteoblastic cells. Long-term HSC were found to adhere to spindle-shaped N-cadherin$^+$CD45$^-$ osteoblastic (SNO) cells, which control HSC size by BMP signaling.[21] A recent study has shown that N-cadherin$^+$ cells maintain a population of highly quiescent reserve HSC,[22] suggesting the possibility that different BM niches might regulate steady-state *vs.* stress hematopoiesis. Another study showed that osteoblasts activated with parathyroid hormone/parathyroid hormone-related protein receptor produce high levels of Notch ligand Jagged 1 and increase HSC numbers.[23] Later studies further identified Tie2/angiopoietin-1 signaling and thrombopoietin/MPL signaling as important regulators of HSC quiescence through interactions with osteoblasts.[24,25] A high calcium concentration in the endosteum also plays an indispensable role, maintaining HSC in the endosteal niche, since calcium-sensing receptor knockout HSC fail to migrate to the endosteal BM surface after transplantation.[26] In addition, the endosteal BM area is enriched in CXCL12[27] and stem cell factor,[28] two of the most important molecules supporting hematopoiesis, strengthening the hypothesis that the endosteum is a major reservoir for HSC. However, the osteoblastic niche was thereafter challenged in studies in which osteoblastic-specific deletion of Cxcl12 or Scf only affected the maintenance of early lymphoid progenitors but had little impact on HSC.[29] Furthermore, N-cadherin expression in osteolineage cells seems to be dispensable for HSC maintenance under homeostasis.[30] Whereas N-cadherin might not be essential for HSC, N-cadherin$^+$ cells appear necessary to maintain a reservoir population of quiescent HSC.[22] Studies on these aspects raise the possibility that different niches might exist for activated/quiescent HSC, and/or for HSC contributing to steady-state/emergency hematopoiesis. The BM is highly vascularized, and the close developmental relationship between hematopoietic and endothelial lineages together suggest that HSC are housed and regulated in perivascular regions. To date, at least two functionally distinct perivascular niches that highly express Cxcl12 and Scf to dictate HSC cell fate have been identified in mice: (i) the arteriolar niches, composed mainly of arterioles (found throughout the BM) or endosteal transition-zone vessels, both of which are associated with sympathetic nerve fibers, Nestin-GFP^{bright} and/or NG2$^+$ cells; and (ii) the sinusoidal niches, where sinusoid-associated Cxcl12-abundant reticular cells,

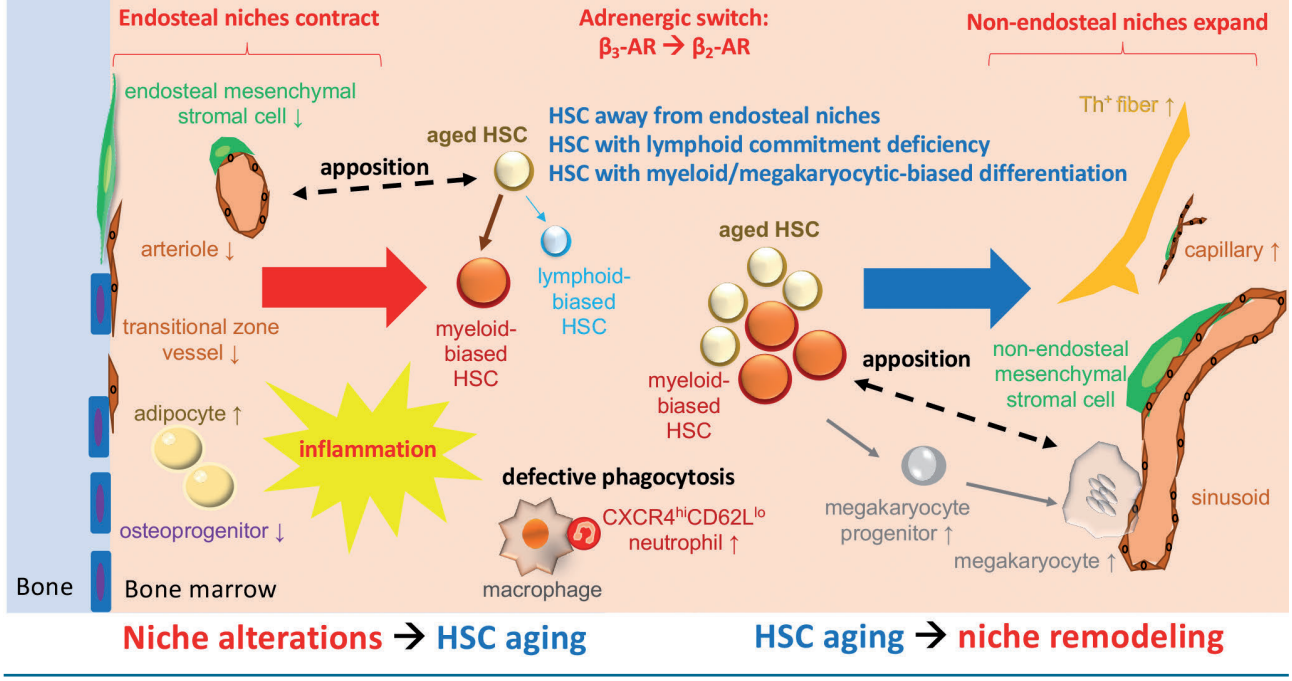

Figure 1. Schematic model of the interplay between hematopoietic stem cells and the microenvironment during aging. Loss of β_3-adrenergic receptor (β_3-AR) activity reduces endosteal niches, pushes hematopoietic stem cells (HSC) away from the endosteum and favors myeloid bias at the expense of lymphopoiesis. Accumulation of aged HSC in the central bone marrow and increased β_2-AR activity causes expansion of central capillaries, myeloid cells and megakaryocytes, which locate farther from HSC.

Nestin-GFP^{dim} and LepR^{+} cells are located.[31] Recent studies also reveal that megakaryocytes, which are mostly adjacent to sinusoids, regulate HSC quiescence through transforming growth factor-β, thrombopoietin and platelet factor-4 secretion.[32-34] Currently, it remains controversial which specialized niches predominantly regulate HSC quiescence. It is possible that HSC quiescence is differently regulated between steady-state and emergency and/or malignant hematopoiesis. However, lineage commitment appears to be influenced by the location of HSC and their derivatives in the BM. Accumulating evidence suggests that lymphopoiesis preferentially occurs near the endosteum, while myelopoiesis/erythropoiesis/megakaryopoiesis mostly takes place in non-endosteal BM regions. Supporting this concept, a recent study using *Vwf-eGFP* to label different HSC populations demonstrated that Vwf^{+} platelet/myeloid-biased HSC are associated with megakaryocytes, whereas Vwf^{-} lymphoid/unbiased HSC are located close to arterioles.[35] Therefore, alterations in specialized niches might directly affect myeloid/lymphoid output, and the imbalanced production of mature hematopoietic cells at specific niches might in turn remodel the local microenvironment for these cells.

Hematopoietic stem cells change location as niches are remodeled during aging

A growing body of evidence has indicated that HSC redistribute within the BM upon aging. For instance, aged HSC locate away from the bone surface (endosteum), compared with young HSC, upon BM transplantation.[36] This abnormal homing behavior correlates with increased BM HSC numbers and enhanced HSC egress into the circulation.[37] Recent studies using whole-mount immunofluorescence staining of murine long bones further revealed that aged HSC are more distant from the endosteum, arterioles, Nestin-GFP^{high} cells and megakaryocytes, but HSC distance from sinusoids and Nestin-GFP^{low} cells appears unchanged, compared with that of young HSC.[38-40] These results strongly suggest that the BM microenvironment is altered with age, favoring HSC lodging near non-endosteal (central) niches, over endosteal niches. The following sections will discuss current studies on age-related BM niche remodeling, the key microenvironmental players and the associated mechanisms by which HSC localization and function are regulated.

Dysfunction of bone marrow mesenchymal stromal cells

Studies regarding the absolute number of BM mesenchymal stromal cells (MSC) during aging have yielded controversial results, with some suggesting an overall increase,[41,42] while others suggest unchanged[43,44] or reduced numbers.[45] It is noteworthy that BM MSC are heterogeneous, and the heterogeneity in the markers used to define BM MSC immunophenotypically might explain some of these controversies. Using *Nestin-gfp* to label murine BM MSC, different studies have reported reduced endosteal Nestin-GFP^{+} cells in the aged BM,[39,40] consistent with reduced numbers of arteriolar αSMA^{+}, PDGFRβ^{+} and NG2^{+} cells.[38] The age-related contraction of endosteal BM might initiate lymphoid deficiency, since lymphoid niches have been previously described near bone.[29,46-48] However, this notion has been refined more recently after elucidating dynamic interactions between B-cell progenitors and perivascular BM MSC, which provide key signals for B lymphopoiesis (such as Cxcl12 and Il7), both in endosteal and central sinusoidal BM niches.[49-52] Functionally, old BM MSC exhibit reduced colony-forming unit-fibroblast (CFU-F) capacity *in vitro* and reduced expression of HSC niche factors.[38] In this regard, revitalizing BM MSC to restore HSC niche factors has been proposed as a strategy to prevent DNA damage in cultured HSC.[53]

BM MSC exhibit reduced osteogenesis with age, which is associated with lower osteopontin secretion to the extracellular matrix.[54] Osteopontin negatively regulates HSC proliferation,[55-57] and its decline might accelerate HSC divisions during aging. Supporting this idea, treatment with thrombin-cleaved osteopontin partially reverses the age-associated phenotype of HSC.[54]

CC-chemokine ligand 5 (CCL5), a pro-inflammatory cytokine involved in bone remodeling,[58] is reportedly increased with age. Researchers also reported a direct contribution to myeloid-biased differentiation at the cost of T cells by CCL5,[19] suggesting that CCL5 is important for aging of the hematopoietic system and the microenvironment. In contrast, old BM MSC show adipocyte skewing.[59] Adipocytes are a BM niche component that promotes HSC regeneration after irradiation, although their roles in hematopoiesis under homeostasis seem to be dispensable.[60] However, altered functions of adipose tissue, including ectopic lipid deposition, insulin resistance and increased inflammation, have been described during aging.[61] Accumulation of BM adipocytes upon aging not only reduces hematopoietic reconstitution, but also disrupts bone fracture repair.[62] The latter likely contributes to the increased risk of osteoporosis and bone fracture in the elderly population.[63,64]

BM aging is also associated with senescence of BM MSC, evidenced by increased p53/p21-mediated DNA damage, upregulation of p16(INK4a) and elevated levels of reactive oxygen species.[65-67] An age-dependent shortening of telomeres was found in telomerase-deficient (*Terc*$^{-/-}$) BM MSC; consequently, lethally-irradiated *Terc*$^{-/-}$ mice carrying wildtype BM cells display accelerated myelopoiesis.[68] More recently, proteome analyses of human BM have unraveled nitric oxide synthesis and the urea cycle pathways as potential mediators for the crosstalk between old BM MSC and HSC.[69] Murine BM MSC show comparatively higher mRNA expression of neuronal nitric oxide synthase (encoded by the *Nos1* gene), as compared with other nitric oxygen synthase isoforms, and *Nos1*$^{-/-}$ mice develop certain features of premature aging, such as remodeled BM vasculature and myeloid skewing.[39] Given the importance of nitric oxide in vascular biology and balanced inflammatory responses, it is likely that nitric oxide pathways participate in the aged vascular remodeling and myeloid expansion partly by modulating inflammation.

Remodeling of bone marrow vasculature and endothelial cell functions

During aging, remodeling of the BM endothelial vasculature is notable. Studies using whole-mount confocal imaging, two-photon intravital microscopy and flow cytometry analysis demonstrated overall increased vascular density in aged mice.[38,70] Yet distinct vascular beds show different, or even opposite alterations with age. Arterioles appear to be decreased, while sinusoids seem

Table 1. Microenvironmental players contributing to hematopoietic stem cell aging.

Players	Size	Functions/Mechanisms
Mesenchymal lineages	Decreased endosteal Nestin-GFP^{+} cells Increased non-endosteal Nestin-GFP^{+} cells Decreased αSMA^{+} cells, NG2^{+} cells, PDGFβ^{+} cells	Increased adipogenesis Decreased osteogenic differentiation Cellular senescence Altered nitric oxide, urea cycle pathways Reduced secretion of niche factors HSC closer to non-endosteal niches, away from endosteal niches
Endothelial cells	Increased overall vascular density Decreased arterioles; shortened arteriole segments Unchanged/preserved sinusoids Decreased transitional zone vessels Increased small capillaries	Increased vascular leakiness Vasodilation Decreased angiogenic potential Decreased Notch activity HSC away from arterioles HSC preserved in sinusoids DLL4 regulating HSC myeloid skewing Sinusoidal Jag2 regulating HSC proliferation
Inflammatory cytokines	Increased IL-1, IL-3, IL-6, TNFα, INFγ, TGFβ	IL-1β regulating HSC myeloid-skewing IL-6 regulating megakaryocyte differentiation TNFα protecting HSC from necroptosis TGF-β regulating megakaryopoiesis IFN regulating megakaryocytic bias
Sympathetic nervous system	Increased Th^{+} nerve fibers	β_2-AR activation regulating HSC myeloid-skewing toward platelet production β_3-AR inactivation regulating niche remodeling, HSC lymphoid deficiency Functional switch of β adrenergic signaling (β_2-AR overriding β_3-AR)
Others	Increased megakaryocytes Accumulation of CXCR4^{high}CD62L^{low} senescent neutrophils	Megakaryocytes closer to sinusoids HSC away from megakaryocytes Macrophages with impaired phagocytosis

GFP: green fluorescent protein; αSMA: alpha smooth muscle actin; PDGFβ: platelet-derived growth factor; HSC: hematopoietic stem cells; IL: interleukin; TNFα: tumor necrosis factor alpha; INFγ: interferon gamma; TGFβ: transforming growth factor beta; DLL4: delta-like 4; Jag2: Jagged 2; AR: adrenergic receptor.

unchanged upon aging.[39] Consistent with these observations, arteriole segments covered by Nestin-GFP^{bright} cells appear shortened.[38] Transitional zone vessels containing type-H endomucin (EMNC)-high endothelial cells (which are enriched in the murine trabecular BM, where they support developmental bone growth[71]) are reduced in old mice.[39,70] In contrast, small capillaries (CD31^{high}EMCN^{-} cells <6 μm in diameter) are notoriously expanded in the central marrow.[39]

The functionality of vascular endothelium declines with age, as manifested by increased vascular leakiness, increased levels of reactive oxygen species and decreased angiogenic potential.[72] Poulos *et al.* previously reported that HSC purified from young mice and co-cultured with endothelial cells from old mice lack long-term hematopoietic multilineage reconstitution, while old HSC co-cultured with young endothelial cells maintain their self-renewal ability.[72] Infusion of young endothelial cells into aged, conditioned mice revives the old hematopoietic system. Kusumbe *et al.* identified high Notch activity in type-H endothelial cells and their associated subendothelial/perivascular cells,[70] suggesting that contraction of endosteal vessels upon aging concomitantly occurs with impaired Notch signaling. Overexpression of the Notch ligand Dll4 in vascular endothelial cells can prevent myeloid skewing of hematopoietic progenitors[73] but cannot completely rescue HSC aging,[70] perhaps consistent with the finding of another study in which Dll4 was unchanged in the aged murine BM.[40] A common finding is reduced endosteal activity of Notch ligand, since the latter study reported reduced expression of Jagged2 (Jag2) ligand in aged Nestin-GFP^{high} cells. In contrast, Jag2 levels seem increased in the sinusoids, or their associated Nestin-GFP^{low} cells. Moreover, Jag2 blockade induces proliferation and clustering of aged HSC near the sinusoids. Therefore, whereas the specific role of Dll4 during aging is not clear, alterations of Notch signaling do seem to be important for hematopoietic aging. Together, these results strongly suggest that altered Notch signaling critically contributes to HSC aging in different ways depending on the niche: in the endosteal vessels, Notch signaling appears to regulate HSC lineage commitment, whereas it is required in the sinusoids to preserve old HSC (since HSC accumulate in sinusoidal niches as a function of age).[40]

Inflammation

Aging of the BM microenvironment is associated with increased pro-inflammatory cytokines, both in mice and humans.[74] Several lines of evidence have indicated that these inflammatory cytokines drive myeloid/megakaryocytic differentiation. In aged-related myeloid malignancies, such as myeloid proliferative neoplasms and chronic myelogenous leukemia, serum interleukine (IL)-1β and IL-6 levels are elevated.[75,76] Pietras *et al.* reported that chronic IL-1 exposure induces HSC myeloid skewing at the expense of self-renewal.[77] IL-1α/β regulates thrombopoiesis *in vitro*,[78,79] possibly explaining high platelet counts in aged mice.[80] Defective phagocytosis of macrophages during aging induces expansion of platelet-biased HSC through Il-1β signaling.[81] Il-6 promotes thrombopoiesis either through a direct effect on BM megakaryocyte differentiation[39] or indirectly upregulating hepatic

thrombopoietin levels.[82] Yamashita *et al.* demonstrated that transient stimulation of tumor necrosis factor-α prevents HSC from necroptosis, and proposed that constitutive activation might lead to hyperproliferation of HSC and exacerbated myelopoiesis in aging and myeloproliferative disorders.[83] Megakaryocytes express transforming growth factor-β to regulate HSC quiescence, while megakaryocyte-derived transforming growth factor-β also stimulates thrombopoietin synthesis by BM stromal cells to enhance megakaryopoiesis.[84] An elegant study by Haas *et al.* found that acute inflammation induces proliferation of the stem cell-like megakaryocyte progenitor to quickly replenish platelet loss, and the process is in part mediated through the interferon family.[85]

Despite the well-known lymphocyte deficiency associated with aging, only the frequency and function (but not the absolute number of lymphoid-biased/balanced HSC) appear to decline with age.[86] In fact, during aging both platelet/myeloid-biased and lymphoid-biased HSC expand, but exhibit altered gene expression programs and myeloid and platelet-skewing.[80] These findings suggest a cell fate change of HSC upon aging, and the net outcome is an increase of the myeloid/platelet compartment at the expense of the lymphoid compartment. Two possible non-mutually exclusive explanations are: (i) different HSC suffer the same intrinsic abnormalities upon aging and (ii) microenvironmental alterations specifically influence HSC and direct their cell fate. In support of the second possibility, distinct HSC subpopulations respond differently to inflammatory challenges during aging.[87] Moreover, old lymphoid-biased/balanced HSC seem to retain normal lymphoid commitment potential when removed from an old microenvironment.[5] Exogenous addition of IL-1 can block lymphocyte differentiation from old lymphoid-biased HSC, confirming the indispensable role of IL-1 in HSC fate decisions. Consistently with this notion, IL-1 blockade seems sufficient to revert the age-dependent increase of megakaryocytic-biased HSC *in vitro*.[81] IL-1 blockade can also attenuate myeloid expansion and inflammatory arthritis associated with the elderly.[88]

However, whether the inflamed BM niche is the cause or the consequence of HSC aging remains debated. It is notable that mature myeloid/megakaryocytic cells are a major source of inflammatory cytokines.[89] Therefore, exacerbated myelopoiesis during aging might induce myeloid/megakaryocytic HSC skewing through inflammatory remodeling of the BM microenvironment. Many different cytokines directly affecting HSC (e.g., IL-6, tumor necrosis factor and interferon) increase during aging. A positive feedback loop between the myeloid cells and their derived inflammatory cytokines might increase both myelopoiesis and the cytokine storm. Future studies are needed to clarify the roles of other inflammatory cytokines, such as IL-6, in the regulation of HSC during aging.

Neuronal regulation by sympathetic adrenergic signaling

It has been reported that BM sympathetic stimulation of β_2 or β_3 adrenergic receptors (AR) regulates the egress and granulocyte – colony-stimulating factor -induced mobilization of HSC.[90-92] A recent publication has suggested that noradrenergic nerve fibers are reduced in old murine BM.[38] The study also indicated that surgical denervation of young BM induces premature aging of the hematopoietic system, although the inflammation caused by the surgical denervation might have had a certain influence. A similar reduction of nerve fibers was found in a mouse model of an age-related blood disorder, myeloproliferative neoplasm,[75] suggesting that BM neuropathy might predispose to myeloid malignancies with age. However, a recent study did not find such a reduction of BM noradrenergic fibers in aged mice.[93] Moreover, whole-mount imaging and three-dimensional reconstruction of different bones has revealed doubled BM area covered by noradrenergic nerve fibers in aged mice.[39] This result is consistent with the well-known increase in sympathetic activity in the elderly, manifested for instance by an increased concentration of noradrenaline in the human plasma with age.[94-97] Increased sympathetic activity causes myeloid skewing of old HSC through activating β_2-AR, since exacerbated thrombopoiesis is present in old wildtype mice but absent in old *Adrb2*$^{-/-}$ mice or *Adrb2*$^{-/-}$*Adrb3*$^{-/-}$ mice.[39] A previous study showed that α-AR directly regulated megakaryocyte migration, adhesion and proplatelet formation under stress, but α-AR did not affect the earlier commitment of progenitor cells to the megakaryocyte lineage.[98] Therefore, the age-dependent increase in sympathetic innervation might activate different AR as hematopoietic progenitor cells differentiate along the megakaryocyte lineage. Additionally, the sympathetic nervous system is known to control inflammation in a context-dependent manner.[99] The concentration of catecholamines and the levels of expression of different AR influence the inflammatory state of innate immune cells. Increased sympathetic activity during aging might contribute to the cytokine storm by activating inflammatory cells, and subsequently affect lineage-bias of HSC.

Interestingly, β_3-AR exhibits opposite effects on lympho-myeloid skewing, compared with β_2-AR. Adult *Adrb3*$^{-/-}$ mice show a decreased frequency of endosteal lymphoid-biased HSC and/or lymphoid multipotent progenitors.[38,39] Age-related remodeling of vasculature, such as reduced transitional zone vessels and expanded small capillaries, possibly explains the lymphoid deficiency in these mice.[39] Altogether, these results suggest that lack of β_3-AR in the microenvironment might accelerate aging of the hematopoietic system. One study suggested that administration of a β_3-AR agonist to old mice rejuvenates most features of HSC aging, but overall changes of hematopoiesis in peripheral blood were not reported in this study.[38] The same β_3-AR agonist reduced myeloid expansion in a mouse model of myeloproliferative neoplasm[75] and a murine model of Hutchinson-Gilford progeria syndrome (HGPS).[39] However, hematopoietic rejuvenation was not detected in the peripheral blood of mice treated with this β_3-AR agonist over 40 weeks in another study.[75] Likewise, elderly individuals with myeloproliferative neoplasms who received a β_3-AR agonist over 24 weeks did not show rejuvenation in the peripheral blood counts in a human study.[100] Five-month old mice lacking β_3-AR reportedly showed normal peripheral blood counts[39] or premature, lymphoid deficiency and myeloid skewing.[38] The discrepancies between these studies suggest that modulating a single neuronal pathway might not be sufficient to rejuvenate overall hematopoiesis. This may be due to the multiple compensatory/adjustment mechanisms of the autonomic nervous system revealed, for instance, in the cardio-

vascular system.[101] It is worth mentioning that myeloid and lymphoid cells are also a source of catecholamines.[102] Adrenal gland-derived adrenaline and immune cell-derived (nor)adrenaline might contribute to increased levels of adrenaline and noradrenaline in the circulation of aged individuals[94-97] which, together with the increased BM noradrenergic innervation, might activate BM AR. We propose that sympathetic regulation of lympho-myeloid skewing pivots on activation or inactivation of different AR. A functional switch of neurotransmission (β_2-AR overriding β_3-AR) with age, rather than a general decline of BM noradrenergic innervation,[38] might initiate BM niche remodeling and subsequently promote HSC myeloid skewing toward platelet production. Further investigation of other adrenergic and/or cholinergic signaling pathways possibly influencing aging is warranted.

Other players in the bone marrow microenvironment

Emerging data suggest that the progeny of HSC can feed back to regulate their activity under homeostasis, raising the possibility that mature hematopoietic cells (or their interactions with others) also contribute to HSC aging. For instance, clearance of senescent CD62L^{low}CXCR4^{high} neutrophils by macrophages has been reported to modulate HSC niches.[103] Frisch *et al.* discovered that aged macrophages are unable to engulf senescent neutrophils, leading to expansion of megakaryocytic-biased HSC through IL-1β signaling.[81] Another key player is the megakaryocyte, reportedly expressing CXCL4, thrombopoietin and transforming growth factor-β to control HSC proliferation/quiescence.[32-34] In murine BM, around 20% of HSC are spatially associated with megakaryocytes,[32] and depletion of megakaryocytes expands platelet-biased HSC.[35] During aging, megakaryocytes are found in increased numbers, lodging closer to sinusoids, and abundantly forming pseudopodial extensions (likely to be proplatelets).[39] Of note, the distance between HSC and megakaryocytes increases substantially,[38,39] suggesting a remodeling of megakaryocyte niches with age. It is possible that megakaryocytes with these morphological changes fail to anchor HSC, inducing HSC hyperproliferation and lineage bias. However, whether and how age-related alterations of megakaryocytes regulate HSC aging is still unknown and requires further investigation.

Premature aging in Hutchinson-Gilford progeria syndrome

In HGPS, aberrant splicing of the *LMNA* gene (encoding lamin A and C) leads to nuclear assembly of the truncated protein, prelamin A (progerin).[104,105] Certain hallmarks of murine hematopoietic aging, such as increased platelet counts, have been observed in HGPS.[106] Given that cells aging naturally also express increased levels of progerin,[107] it is possible that normal physiological conditions and progeria might share some aging mechanisms. Grigoryan *et al.* recently reported that HSC deficient of LMNA display a premature aging-like phenotype,[108] suggesting a prominent role of lamin A/C in hematopoiesis at the level of HSC. The strong impact of progeria on growth and sexual maturation might be paralleled by altered endocrine regulation of HSC, since growth hormones and sex hormones regulate HSC survival, proliferation and lineage commitment.[109-112] However, it remains unknown whether premature hematopoietic aging in HGPS is a consequence of progerin accumulation in HSC, other hematopoietic cells and/or the microenvironment. Using the *Lmna*$^{G609G/G609G}$ mouse model,[113] we found that primary *Lmna*$^{G609G/G609G}$ mice exhibit features of premature hematopoietic aging; however, premature hematopoietic aging is not observed in wildtype recipients carrying *Lmna*$^{G609G/G609G}$ hematopoietic cells.[39] Microenvironmental alterations are observed in *Lmna*$^{G609G/G609G}$ mice, some of which are shared between normally aged mice, such as elevated levels of pro-inflammatory cytokines (IL-3, IL-6, IL-1, interferon-γ), increased megakaryocytes with pro-platelet-like structure and megakaryocyte apposition to BM sinusoids. Of note, β_3-AR agonism improves exacerbated myeloid expansion and restores the apposition of HSC to megakaryocytes. These results suggest that premature hematopoietic aging in HGPS is not HSC-autonomous, and certain aging features can be rejuvenated by targeting the microenvironment.[39]

Aged hematopoietic stem cells/ microenvironment: chicken or egg?

One remaining key question relates to whether microenvironmental alterations initiate HSC aging and/or whether old HSC cause niche remodeling. It is noteworthy that HSC aging is not characterized by a single cellular feature, and different aging features might emerge individually at different developmental stages. For instance, in murine aging, defective lymphopoiesis starts early, at the age of 8 months old,[114] while increased platelet counts do not seem to be pronounced until 18 months.[39] BM noradrenergic nerve fibers appear to be decreased in adult, 8-month old mice[75] (Supplementary Figure 5B in the report of that study), but these fibers appear increased in aged (20-month old) mice, when β_3-AR signaling is already strongly reduced.[39] A deficiency in β_3-AR accelerates the loss of endosteal lymphoid-biased HSC in 4-month old mice, but it does not aggravate HSC aging in old mice.[39] In contrast, a deficiency in β_2-AR impairs megakaryopoiesis in young and old mice, and double knockout mice for β_2-AR and β_3-AR recapitulate the hematopoietic phenotype of single β_2-AR-deficient mice. These results suggest that β_2-AR overrides β_3-AR during aging, and that this adrenergic remodeling contributes to imbalanced lymphoid/myeloid output. We propose that a lack of β_3-AR activity near endosteum initiates the contraction of endosteal niches, which attenuates lymphopoiesis, favors myeloid bias and pushes HSC away from the endosteum. An adrenergic switch from β_3-AR to β_2-AR could feed back to worsen the reduction of endosteal niches, since activation of β_2-AR on osteoblasts is known to restrain bone formation.[115] However, the cell types expressing β_2-AR and/or β_3-AR involved in aged hematopoiesis are still elusive. Chances are that cells highly expressing β_2-AR replace those with high expression of β_3-AR over time, or BM niche cells ubiquitously increase β_2-AR while decreasing β_3-AR upon aging. These and other hypotheses need to be validated in future studies[116] since the experiments were performed using global knockouts. Tissue-specific deletion of β_2-AR and/or β_3-AR will provide further insights into the mechanisms of β-adrenergic switching during aging. Importantly, β_2-AR and β_3-AR have different affinities for noradrenaline and adrenaline; whereas β_3-AR

shows higher affinity for noradrenaline over adrenaline, the opposite is true for β_2-AR.[117] Another possibility might be that BM concentrations of both neurotransmitters differ in aging, leading to imbalanced stimulation of the two receptors. The observation that old HSC home in the BM away from endosteal regions suggests that HSC-driven niche remodeling mainly occurs in non-endosteal domains. For instance, skewed myelopoiesis leading to increased numbers of neutrophils and defective phagocytosis of marrow macrophages might modulate the microenvironment favoring myeloid bias during aging.[81] Increased myeloid cells might provide an additional source of catecholamines in a feed-forward loop promoting megakaryocyte differentiation by activating β_2-AR. We propose that accumulation of old HSC results in microenvironmental remodeling by reinforcing adrenergic activity, expansion of non-endosteal niches and enhanced myeloid/megakaryocyte differentiation. As a secondary outcome, alteration of megakaryocyte niches (increased megakaryocyte numbers, proplatelet formation and apposition to sinusoids) might release HSC from their state of quiescence, further promoting HSC proliferation with age.

Niche alterations might predispose to hematologic neoplasms

The risk of developing myeloid malignancies increases significantly in individuals harboring clonal hematopoiesis-related somatic mutations. In fact some of these mutations are oncogenic drivers of myeloid malignancies.[118] However, the factors limiting clonal expansion or, instead, allowing the mutant clones to become dominant and, in some cases, cause disease, remain unclear. Interestingly, similar niche alterations are shared between aging and myeloid disorders associated with age, which is an important selection pressure to expand aberrant HSC clones. For instance, a damaged neuro-MSC circuit promotes the development of a cytokine storm created by the mutant HSC, aggravating the progression of myeloproliferative neoplasms.[75] In myelodysplastic syndromes, abnormal production of cytokines from the microenvironment, dysfunction of MSC and osteolineage cells, and vascular remodeling have been associated with disease initiation and progression.[119,120] Targeting the abnormal microenvironment could be a promising complementary therapeutic approach to treat hematologic cancers in the future, especially when early diagnosis becomes available.

Conclusive remarks

Aging of the hematopoietic system might result from both HSC-intrinsic and microenvironmental alterations with changes in the location, function and regulation of HSC and their progeny. Future studies will determine the relative contribution of the aged microenviroment to altered hematopoiesis and increased incidence of age-related disorders originating in the BM.

Acknowledgments

Y-HH received fellowships from Alborada Scholarship (University of Cambridge), Trinity-Henry Barlow Scholarship (University of Cambridge) and R.O.C. Government Scholarship to Study Abroad (GSSA). This work was supported by core support grants from the Wellcome Trust and the MRC to the Cambridge Stem Cell Institute, National Health Service Blood and Transplant (United Kingdom), European Union's Horizon 2020 research (ERC-2014-CoG-64765) and a Programme Foundation Award from Cancer Research UK to SM-F The authors regret that some relevant literature could not be discussed because of space constrictions.

References

1. Carrelha J, Meng Y, Kettyle LM, et al. Hierarchically related lineage-restricted fates of multipotent haematopoietic stem cells. Nature. 2018;554(7690):106-111.
2. Weksberg DC, Chambers SM, Boles NC, Goodell MA. CD150- side population cells represent a functionally distinct population of long-term hematopoietic stem cells. Blood. 2008;111(4):2444-2451.
3. Kiel MJ, Yilmaz OH, Morrison SJ. CD150-cells are transiently reconstituting multipotent progenitors with little or no stem cell activity. Blood. 2008;111(8):4413-4414; author reply 4414-4415.
4. Kent DG, Copley MR, Benz C, et al. Prospective isolation and molecular characterization of hematopoietic stem cells with durable self-renewal potential. Blood. 2009;113(25):6342-6350.
5. Montecino-Rodriguez E, Kong Y, Casero D, et al. Lymphoid-biased hematopoietic stem cells are maintained with age and efficiently generate lymphoid progeny. Stem Cell Reports. 2019;12(3):584-596.
6. Liang Y, Van Zant G, Szilvassy SJ. Effects of aging on the homing and engraftment of murine hematopoietic stem and progenitor cells. Blood. 2005;106(4):1479-1487.
7. Mohrin M, Shin J, Liu Y, et al. Stem cell aging. A mitochondrial UPR-mediated metabolic checkpoint regulates hematopoietic stem cell aging. Science. 2015;347(6228):1374-1377.
8. Rossi DJ, Bryder D, Zahn JM, et al. Cell intrinsic alterations underlie hematopoietic stem cell aging. Proc Natl Acad Sci U S A. 2005;102(26):9194-9199.
9. Sudo K, Ema H, Morita Y, Nakauchi H. Age-associated characteristics of murine hematopoietic stem cells. J Exp Med. 2000;192(9):1273-1280.
10. Dykstra B, Olthof S, Schreuder J, Ritsema M, de Haan G. Clonal analysis reveals multiple functional defects of aged murine hematopoietic stem cells. J Exp Med. 2011;208(13):2691-2703.
11. Chambers SM, Shaw CA, Gatza C, et al. Aging hematopoietic stem cells decline in function and exhibit epigenetic dysregulation. PLoS Biol. 2007;5(8):e201.
12. Flach J, Bakker ST, Mohrin M, et al. Replication stress is a potent driver of functional decline in ageing haematopoietic stem cells. Nature. 2014;512(7513):198-202.
13. Rossi DJ, Bryder D, Seita J, et al. Deficiencies in DNA damage repair limit the function of haematopoietic stem cells with age. Nature. 2007;447(7145):725-729.
14. Florian MC, Nattamai KJ, Dorr K, et al. A canonical to non-canonical Wnt signalling switch in haematopoietic stem-cell ageing. Nature. 2013;503(7476):392-396.
15. Ito K, Suda T. Metabolic requirements for the maintenance of self-renewing stem cells. Nat Rev Mol Cell Biol. 2014;15(4):243-256.
16. Chandel NS, Jasper H, Ho TT, Passegue E. Metabolic regulation of stem cell function in tissue homeostasis and organismal ageing. Nat Cell Biol. 2016;18(8):823-832.
17. Ho TT, Warr MR, Adelman ER, et al. Autophagy maintains the metabolism and function of young and old stem cells. Nature. 2017;543(7644):205-210.
18. Vilchez D, Simic MS, Dillin A. Proteostasis and aging of stem cells. Trends Cell Biol. 2014;24(3):161-170.
19. Ergen AV, Boles NC, Goodell MA. Rantes/Ccl5 influences hematopoietic stem cell subtypes and causes myeloid skewing. Blood. 2012;119(11):2500-2509.
20. Taichman RS, Emerson SG. Human osteoblasts support hematopoiesis through the production of granulocyte colony-stimulating factor. J Exp Med. 1994;179(5):1677-1682.
21. Zhang J, Niu C, Ye L, et al. Identification of the haematopoietic stem cell niche and control of the niche size. Nature. 2003;425

(6960):836-841.
22. Zhao M, Tao F, Venkatraman A, et al. N-cadherin-expressing bone and marrow stromal progenitor cells maintain reserve hematopoietic stem cells. Cell Rep. 2019;26 (3):652-669.
23. Calvi LM, Adams GB, Weibrecht KW, et al. Osteoblastic cells regulate the haematopoietic stem cell niche. Nature. 2003;425 (6960):841-846.
24. Arai F, Hirao A, Ohmura M, et al. Tie2/angiopoietin-1 signaling regulates hematopoietic stem cell quiescence in the bone marrow niche. Cell. 2004;118(2):149-161.
25. Yoshihara H, Arai F, Hosokawa K, et al. Thrombopoietin/MPL signaling regulates hematopoietic stem cell quiescence and interaction with the osteoblastic niche. Cell Stem Cell. 2007;1(6):685-697.
26. Adams GB, Chabner KT, Alley IR, et al. Stem cell engraftment at the endosteal niche is specified by the calcium-sensing receptor. Nature. 2006;439(7076):599-603.
27. Sugiyama T, Kohara H, Noda M, Nagasawa T. Maintenance of the hematopoietic stem cell pool by CXCL12-CXCR4 chemokine signaling in bone marrow stromal cell niches. Immunity. 2006;25(6):977-988.
28. Kinashi T, Springer TA. Steel factor and c-kit regulate cell-matrix adhesion. Blood. 1994;83(4):1033-1038.
29. Ding L, Morrison SJ. Haematopoietic stem cells and early lymphoid progenitors occupy distinct bone marrow niches. Nature. 2013;495(7440):231-235.
30. Greenbaum AM, Revollo LD, Woloszynek JR, Civitelli R, Link DC. N-cadherin in osteolineage cells is not required for maintenance of hematopoietic stem cells. Blood. 2012;120(2):295-302.
31. Boulais PE, Frenette PS. Making sense of hematopoietic stem cell niches. Blood. 2015;125(17):2621-2629.
32. Bruns I, Lucas D, Pinho S, et al. Megakaryocytes regulate hematopoietic stem cell quiescence through CXCL4 secretion. Nat Med. 2014;20(11):1315-1320.
33. Zhao M, Perry JM, Marshall H, et al. Megakaryocytes maintain homeostatic quiescence and promote post-injury regeneration of hematopoietic stem cells. Nat Med. 2014;20(11):1321-1326.
34. Nakamura-Ishizu A, Takubo K, Fujioka M, Suda T. Megakaryocytes are essential for HSC quiescence through the production of thrombopoietin. Biochem Biophys Res Commun. 2014;454(2):353-357.
35. Pinho S, Marchand T, Yang E, et al. Lineage-biased hematopoietic stem cells are regulated by distinct niches. Dev Cell. 2018;44(5): 634-641.
36. Florian MC, Dorr K, Niebel A, et al. Cdc42 activity regulates hematopoietic stem cell aging and rejuvenation. Cell Stem Cell. 2012;10(5):520-530.
37. Xing Z, Ryan MA, Daria D, et al. Increased hematopoietic stem cell mobilization in aged mice. Blood. 2006;108(7):2190-2197.
38. Maryanovich M, Zahalka AH, Pierce H, et al. Adrenergic nerve degeneration in bone marrow drives aging of the hematopoietic stem cell niche. Nat Med. 2018;24(6):782-791.
39. Ho YH, Del Toro R, Rivera-Torres J, et al. Remodeling of bone marrow hematopoietic stem cell niches promotes myeloid cell expansion during premature or physiological aging. Cell Stem Cell. 2019;25(3):407-418.
40. Sacma M, Pospiech J, Bogeska R, et al. Haematopoietic stem cells in perisinusoidal niches are protected from ageing. Nat Cell Biol. 2019;21(11):1309-1320.
41. Stolzing A, Jones E, McGonagle D, Scutt A. Age-related changes in human bone marrow-derived mesenchymal stem cells: consequences for cell therapies. Mech Ageing Dev. 2008;129(3):163-173.
42. Garcia-Prat L, Sousa-Victor P, Munoz-Canoves P. Functional dysregulation of stem cells during aging: a focus on skeletal muscle stem cells. FEBS J. 2013;280(17):4051-4062.
43. Siegel G, Kluba T, Hermanutz-Klein U, et al. Phenotype, donor age and gender affect function of human bone marrow-derived mesenchymal stromal cells. BMC Med. 2013;11:146.
44. Wagner W, Bork S, Horn P, et al. Aging and replicative senescence have related effects on human stem and progenitor cells. PloS One. 2009;4(6):e5846.
45. Ganguly P, El-Jawhari JJ, Burska AN, et al. The analysis of in vivo aging in human bone marrow mesenchymal stromal cells using colony-forming unit-fibroblast assay and the CD45(low)CD271(+) Phenotype. Stem Cells Int. 2019;2019: 5197983.
46. Visnjic D, Kalajzic Z, Rowe DW, et al. Hematopoiesis is severely altered in mice with an induced osteoblast deficiency. Blood. 2004;103(9):3258-3264.
47. Zhu J, Garrett R, Jung Y, et al. Osteoblasts support B-lymphocyte commitment and differentiation from hematopoietic stem cells. Blood. 2007;109(9):3706-3712.
48. Wu JY, Purton LE, Rodda SJ, et al. Osteoblastic regulation of B lymphopoiesis is mediated by Gs{alpha}-dependent signaling pathways. Proc Natl Acad Sci U S A. 2008;105(44):16976-16981.
49. Zehentmeier S, Pereira JP. Cell circuits and niches controlling B cell development. Immunol Rev. 2019;289(1):142-157.
50. Fistonich C, Zehentmeier S, Bednarski JJ, et al. Cell circuits between B cell progenitors and IL-7(+) mesenchymal progenitor cells control B cell development. J Exp Med. 2018;215(10):2586-2599.
51. Cordeiro Gomes A, Hara T, Lim VY, et al. Hematopoietic stem cell niches produce lineage-instructive signals to control multipotent progenitor differentiation. Immunity. 2016;45(6):1219-1231.
52. Balzano M, De Grandis M, Vu Manh TP, et al. Nidogen-1 contributes to the interaction network involved in pro-B cell retention in the peri-sinusoidal hematopoietic stem cell niche. Cell Rep. 2019;26(12):3257-3271.
53. Nakahara F, Borger DK, Wei Q, et al. Engineering a haematopoietic stem cell niche by revitalizing mesenchymal stromal cells. Nat Cell Biol. 2019;21(5):560-567.
54. Guidi N, Sacma M, Standker L, et al. Osteopontin attenuates aging-associated phenotypes of hematopoietic stem cells. EMBO J. 2017;36(7):840-853.
55. Nilsson SK, Johnston HM, Whitty GA, et al. Osteopontin, a key component of the hematopoietic stem cell niche and regulator of primitive hematopoietic progenitor cells. Blood. 2005;106(4):1232-1239.
56. Stier S, Ko Y, Forkert R, et al. Osteopontin is a hematopoietic stem cell niche component that negatively regulates stem cell pool size. J Exp Med. 2005;201(11):1781-1791.
57. Haylock DN, Nilsson SK. Osteopontin: a bridge between bone and blood. Br J Haematol. 2006;134(5):467-474.
58. Wintges K, Beil FT, Albers J, et al. Impaired bone formation and increased osteoclastogenesis in mice lacking chemokine (C-C motif) ligand 5 (Ccl5). J Bone Miner Res. 2013;28(10):2070-2080.
59. Kim M, Kim C, Choi YS, et al. Age-related alterations in mesenchymal stem cells related to shift in differentiation from osteogenic to adipogenic potential: implication to age-associated bone diseases and defects. Mech Ageing Dev. 2012;133(5):215-225.
60. Zhou BO, Yu H, Yue R, et al. Bone marrow adipocytes promote the regeneration of stem cells and haematopoiesis by secreting SCF. Nat Cell Biol. 2017;19(8):891-903.
61. Mancuso P, Bouchard B. The impact of aging on adipose function and adipokine synthesis. Front Endocrinol (Lausanne). 2019; 10:137.
62. Ambrosi TH, Scialdone A, Graja A, et al. Adipocyte accumulation in the bone marrow during obesity and aging impairs stem cell-based hematopoietic and bone regeneration. Cell Stem Cell. 2017;20(6): 771-784.
63. Fazeli PK, Horowitz MC, MacDougald OA, et al. Marrow fat and bone--new perspectives. J Clin Endocrinol Metab. 2013;98 (3):935-945.
64. Schwartz AV. Marrow fat and bone: review of clinical findings. Front Endocrinol (Lausanne). 2015;6:40.
65. Zhang DY, Wang HJ, Tan YZ. Wnt/beta-catenin signaling induces the aging of mesenchymal stem cells through the DNA damage response and the p53/p21 pathway. PloS One. 2011;6(6):e21397.
66. Zheng Y, He L, Wan Y, Song J. H3K9me-enhanced DNA hypermethylation of the p16INK4a gene: an epigenetic signature for spontaneous transformation of rat mesenchymal stem cells. Stem Cells Dev. 2013;22(2):256-267.
67. Kornicka K, Marycz K, Tomaszewski KA, Maredziak M, Smieszek A. The effect of age on osteogenic and adipogenic differentiation potential of human adipose derived stromal stem cells (hASCs) and the impact of stress fctors in the course of the differentiation process. Oxid Med Cell Longev. 2015;2015: 309169.
68. Ju Z, Jiang H, Jaworski M, et al. Telomere dysfunction induces environmental alterations limiting hematopoietic stem cell function and engraftment. Nat Med. 2007;13 (6):742-747.
69. Hennrich ML, Romanov N, Horn P, et al. Cell-specific proteome analyses of human bone marrow reveal molecular features of age-dependent functional decline. Nat Commun. 2018;9(1):4004.
70. Kusumbe AP, Ramasamy SK, Itkin T, et al. Age-dependent modulation of vascular niches for haematopoietic stem cells. Nature. 2016;532(7599):380-384.
71. Kusumbe AP, Ramasamy SK, Adams RH. Coupling of angiogenesis and osteogenesis by a specific vessel subtype in bone. Nature. 2014;507(7492):323-328.
72. Poulos MG, Ramalingam P, Gutkin MC, et al. Endothelial transplantation rejuvenates aged hematopoietic stem cell function. J Clin Invest. 2017;127(11):4163-4178.
73. Tikhonova AN, Dolgalev I, Hu H, et al. The bone marrow microenvironment at single-cell resolution. Nature. 2019;569(7755):222-228.
74. Kovtonyuk LV, Fritsch K, Feng X, Manz MG, Takizawa H. Inflamm-aging of hematopoiesis, hematopoietic stem cells, and the bone marrow microenvironment. Front Immunol. 2016;7:502.
75. Arranz L, Sanchez-Aguilera A, Martin-Perez D, et al. Neuropathy of haematopoietic

stem cell niche is essential for myeloproliferative neoplasms. Nature. 2014;512(7512):78-81.
76. Reynaud D, Pietras E, Barry-Holson K, et al. IL-6 controls leukemic multipotent progenitor cell fate and contributes to chronic myelogenous leukemia development. Cancer Cell. 2011;20(5):661-673.
77. Pietras EM, Mirantes-Barbeito C, Fong S, et al. Chronic interleukin-1 exposure drives haematopoietic stem cells towards precocious myeloid differentiation at the expense of self-renewal. Nat Cell Biol. 2016;18(6):607-618.
78. Beaulieu LM, Lin E, Mick E, et al. Interleukin 1 receptor 1 and interleukin 1beta regulate megakaryocyte maturation, platelet activation, and transcript profile during inflammation in mice and humans. Arterioscler Thromb Vasc Biol. 2014;34(3):552-564.
79. Nishimura S, Nagasaki M, Kunishima S, et al. IL-1alpha induces thrombopoiesis through megakaryocyte rupture in response to acute platelet needs. J Cell Biol. 2015;209(3):453-466.
80. Grover A, Sanjuan-Pla A, Thongjuea S, et al. Single-cell RNA sequencing reveals molecular and functional platelet bias of aged haematopoietic stem cells. Nat Commun. 2016;7:11075.
81. Frisch BJ, Hoffman CM, Latchney SE, et al. Aged marrow macrophages expand platelet-biased hematopoietic stem cells via interleukin1B. JCI Insight. 2019;5.pii:124213.
82. Kaser A, Brandacher G, Steurer W, et al. Interleukin-6 stimulates thrombopoiesis through thrombopoietin: role in inflammatory thrombocytosis. Blood. 2001;98(9):2720-2725.
83. Yamashita M, Passegue E. TNF-alpha Coordinates hematopoietic stem cell survival and myeloid regeneration. Cell Stem Cell. 2019;25(3):357-372.
84. Sakamaki S, Hirayama Y, Matsunaga T, et al. Transforming growth factor-beta1 (TGF-beta1) induces thrombopoietin from bone marrow stromal cells, which stimulates the expression of TGF-beta receptor on megakaryocytes and, in turn, renders them susceptible to suppression by TGF-beta itself with high specificity. Blood. 1999;94(6):1961-1970.
85. Haas S, Hansson J, Klimmeck D, et al. Inflammation-induced emergency megakaryopoiesis driven by hematopoietic stem cell-like megakaryocyte progenitors. Cell Stem Cell. 2015;17(4):422-434.
86. Beerman I, Bhattacharya D, Zandi S, et al. Functionally distinct hematopoietic stem cells modulate hematopoietic lineage potential during aging by a mechanism of clonal expansion. Proc Natl Acad Sci U S A. 2010;107(12):5465-5470.
87. Mann M, Mehta A, de Boer CG, et al. Heterogeneous responses of hematopoietic stem cells to inflammatory stimuli are altered with age. Cell Rep. 2018;25(11):2992-3005.
88. Hernandez G, Mills TS, Rabe JL, et al. Pro-inflammatory cytokine blockade attenuates myeloid expansion in a murine model of rheumatoid arthritis. Haematologica. 2019 May 17. [Epub ahead of print]
89. Pietras EM. Inflammation: a key regulator of hematopoietic stem cell fate in health and disease. Blood. 2017;130(15):1693-1698.
90. Mendez-Ferrer S, Battista M, Frenette PS. Cooperation of beta(2)- and beta(3)-adrenergic receptors in hematopoietic progenitor cell mobilization. Ann N Y Acad Sci. 2010;1192:139-144.
91. Katayama Y, Battista M, Kao WM, et al. Signals from the sympathetic nervous system regulate hematopoietic stem cell egress from bone marrow. Cell. 2006;124(2):407-421.
92. Mendez-Ferrer S, Lucas D, Battista M, Frenette PS. Haematopoietic stem cell release is regulated by circadian oscillations. Nature. 2008;452(7186):442-447.
93. Chartier SR, Mitchell SAT, Majuta LA, Mantyh PW. The changing sensory and sympathetic innervation of the young, adult and aging mouse femur. Neuroscience. 2018;387:178-190.
94. Hart EC, Charkoudian N. Sympathetic neural regulation of blood pressure: influences of sex and aging. Physiology (Bethesda). 2014;29(1):8-15.
95. Ng AV, Callister R, Johnson DG, Seals DR. Age and gender influence muscle sympathetic nerve activity at rest in healthy humans. Hypertension. 1993;21(4):498-503.
96. Veith RC, Featherstone JA, Linares OA, Halter JB. Age differences in plasma norepinephrine kinetics in humans. J Gerontol. 1986;41(3):319-324.
97. Ziegler MG, Lake CR, Kopin IJ. Plasma noradrenaline increases with age. Nature. 1976;261(5558):333-335.
98. Chen S, Du C, Shen M, et al. Sympathetic stimulation facilitates thrombopoiesis by promoting megakaryocyte adhesion, migration, and proplatelet formation. Blood. 2016;127(8):1024-1035.
99. Pongratz G, Straub RH. The sympathetic nervous response in inflammation. Arthritis Res Ther. 2014;16(6):504.
100. Drexler B, Passweg JR, Tzankov A, et al. The sympathomimetic agonist mirabegron did not lower JAK2-V617F allele burden, but restored nestin-positive cells and reduced reticulin fibrosis in patients with myeloproliferative neoplasms: results of phase II study SAKK 33/14. Haematologica. 2019;104(4):710-716.
101. Triposkiadis F, Karayannis G, Giamouzis G, et al. The sympathetic nervous system in heart failure physiology, pathophysiology, and clinical implications. J Am Coll Cardiol. 2009;54(19):1747-1762.
102. Cosentino M, Marino F, Maestroni GJ. Sympathoadrenergic modulation of hematopoiesis: a review of available evidence and of therapeutic perspectives. Front Cell Neurosci. 2015;9:302.
103. Casanova-Acebes M, Pitaval C, Weiss LA, et al. Rhythmic modulation of the hematopoietic niche through neutrophil clearance. Cell. 2013;153(5):1025-1035.
104. De Sandre-Giovannoli A, Bernard R, Cau P, et al. Lamin a truncation in Hutchinson-Gilford progeria. Science. 2003;300(5628):2055.
105. Eriksson M, Brown WT, Gordon LB, et al. Recurrent de novo point mutations in lamin A cause Hutchinson-Gilford progeria syndrome. Nature. 2003;423(6937):293-298.
106. Merideth MA, Gordon LB, Clauss S, et al. Phenotype and course of Hutchinson-Gilford progeria syndrome. N Engl J Med. 2008;358(6):592-604.
107. Scaffidi P, Misteli T. Lamin A-dependent nuclear defects in human aging. Science. 2006;312(5776):1059-1063.
108. Grigoryan A, Guidi N, Senger K, et al. LaminA/C regulates epigenetic and chromatin architecture changes upon aging of hematopoietic stem cells. Genome Biol. 2018;19(1):189.
109. Heo HR, Chen L, An B, et al. Hormonal regulation of hematopoietic stem cells and their niche: a focus on estrogen. Int J Stem Cells. 2015;8(1):18-23.
110. Stewart MH, Gutierrez-Martinez P, Beerman I, et al. Growth hormone receptor signaling is dispensable for HSC function and aging. Blood. 2014;124(20):3076-3080.
111. Sanchez-Aguilera A, Arranz L, Martin-Perez D, et al. Estrogen signaling selectively induces apoptosis of hematopoietic progenitors and myeloid neoplasms without harming steady-state hematopoiesis. Cell Stem Cell. 2014;15(6):791-804.
112. Nakada D, Oguro H, Levi BP, et al. Oestrogen increases haematopoietic stem-cell self-renewal in females and during pregnancy. Nature. 2014;505(7484):555-558.
113. Osorio FG, Navarro CL, Cadinanos J, et al. Splicing-directed therapy in a new mouse model of human accelerated aging. Sci Transl Med. 2011;3(106):106ra107.
114. Young K, Borikar S, Bell R, et al. Progressive alterations in multipotent hematopoietic progenitors underlie lymphoid cell loss in aging. J Exp Med. 2016;213(11):2259-2267.
115. Kajimura D, Hinoi E, Ferron M, et al. Genetic determination of the cellular basis of the sympathetic regulation of bone mass accrual. J Exp Med. 2011;208(4):841-851.
116. Raaijmakers M. Aging of the hematopoietic stem cell niche: an unnerving matter. Cell Stem Cell. 2019;25(3):301-303.
117. Hoffmann C, Leitz MR, Oberdorf-Maass S, Lohse MJ, Klotz KN. Comparative pharmacology of human beta-adrenergic receptor subtypes--characterization of stably transfected receptors in CHO cells. Naunyn Schmiedebergs Arch Pharmacol. 2004;369(2):151-159.
118. Deininger MWN, Tyner JW, Solary E. Turning the tide in myelodysplastic/myeloproliferative neoplasms. Nat Rev Cancer. 2017;17(7):425-440.
119. Li AJ, Calvi LM. The microenvironment in myelodysplastic syndromes: niche-mediated disease initiation and progression. Exp Hematol. 2017;55:3-18.
120. Wang C, Yang Y, Gao S, et al. Immune dysregulation in myelodysplastic syndrome: clinical features, pathogenesis and therapeutic strategies. Crit Rev Oncol Hematol. 2018;122:123-132.

Clinical applications of donor lymphocyte infusion from an HLA-haploidentical donor: consensus recommendations from the Acute Leukemia Working Party of the EBMT

Bhagirathbhai Dholaria,[1] Bipin N. Savani,[1] Myriam Labopin,[2] Leo Luznik,[3] Annalisa Ruggeri,[4] Stephan Mielke,[5] Monzr M. Al Malki,[6] Piyanuch Kongtim,[7] Ephraim Fuchs,[8] Xiao-Jun Huang,[9] Franco Locatelli,[10] Franco Aversa,[11] Luca Castagna,[12] Andrea Bacigalupo,[13] Massimo Martelli,[14] Didier Blaise,[15] Patrick Ben Soussan,[16] Yolande Arnault,[17] Rupert Handgretinger,[18] Denis-Claude Roy,[19] Paul O'Donnell,[20] Asad Bashey,[21] Scott Solomon,[21] Rizwan Romee,[22] Philippe Lewalle,[23] Jorge Gayoso,[24] Michael Maschan,[25] Hillard M. Lazarus,[26] Karen Ballen,[27] Sebastian Giebel,[28] Frederic Baron,[29] Fabio Ciceri,[30] Jordi Esteve,[31] Norbert-Claude Gorin,[32] Alexandros Spyridonidis,[33] Christoph Schmid,[34] Stefan O. Ciurea,[35] Arnon Nagler[36] and Mohamad Mohty[37]

[1]Department of Hematology-Oncology, Vanderbilt University Medical Center, Nashville, TN, USA: [2]Department of Haematology and EBMT Paris study office / CEREST-TC, Saint Antoine Hospital, Paris, France; [3]Department of Oncology Hematologic Malignancies, Johns Hopkins University School of Medicine, Baltimore, MD, USA; [4]Department of Pediatric Hematology/Oncology and Cell and Gene Therapy, IRCCS Ospedale Pediatrico Bambino Gesù, Rome, Italy; [5]Department of Laboratory Medicine, CAST, Karolinska Institutet and University Hospital, Stockholm, Sweden; [6]Department of Hematology and Hematopoietic Cell Transplantation, City of Hope National Medical Center, Duarte, CA, USA; [7]Stem Cell Transplant and Cellular Therapy, Thammasat University, Pathumthani, Thailand; [8]Johns Hopkins University, Sidney Kimmel Comprehensive Cancer Center, Baltimore, MD, USA; [9]Peking University People's Hospital, Peking University Institute of Hematology, Beijing China; [10]Department of Pediatric Hematology/Oncology, IRCCS Ospedale Pediatrico Bambino Gesù, Rome, Sapienza, University of Rome, Italy; [11]Department of Medicine and Surgery, University of Parma, Parma, Italy; [12]Instituto Clinico Humanitas, Rozzano Milano, Italy; [13]Fondazione Policlinico Universitario Gemelli IRCCS, Università Cattolica del Sacro Cuore, Rome, Italy; [14]University of Perugia, Sant'Andrea Delle Fratte, Perugia Italy; [15]Department of Hematology, Institut Paoli Calmettes, Marseille France; [16]Department of Clinical Psychology, Paoli-Calmettes Institute, Marseille, France; [17]Institut Paoli-Calmette, département de psychologie clinique, Marseille, France; [18]Department of Hematology and Oncology, University Children's Hospital Tübingen, Tübingen Germany; [19]Division of Hematology and Medical Oncology, Hospital Maisonneuve-Rosemont, Montreal, QC, Canada; [20]Hematology-Oncology, Massachusetts General Hospital, Harvard Medical School, Boston, MA, USA; [21]Blood and Marrow Transplant Program at Northside Hospital, Atlanta, GA, USA; [22]Dana Farber Cancer Institute, Harvard Medical School, Boston, MA, USA; [23]Hematology Department, Institut Jules Bordet, Université Libre de Bruxelles, Brussels, Belgium; [24]HGU Gregorio Marañón, Instituto de Investigación Sanitaria Gregorio Marañón, Madrid, Spain; [25]Oncology and immunology, Dmitriy Rogachev National Medical Center of pediatric hematology, Moscow, Russia; [26]Adult Hematologic Malignancies & Stem Cell Transplant Section, University Hospitals Seidman Cancer Center, Cleveland, OH, USA; [27]Division of hematology/oncology, University of Virginia Health System, Charlottesville, VA, USA; [28]Dept. of Bone Marrow Transplantation and Onco-Hematology, Maria Sklodowska-Curie Institute - Oncology Center, Gliwice Branch, Gliwice, Poland; [29]Laboratory of Hematology, University of Liège, Liège, Belgium; [30]Hematology and Bone Marrow Transplantation Unit, San Raffaele Scientific Institute, Milano Italy; [31]Hematology department, Hospital Clínic de Barcelona, Barcelona Spain; [32]Service d'hématologie et thérapie cellulaire Centre international greffes APHP-EBMT-INCa Hospital, Saint Antoine Hospital, Paris France; [33]Bone Marrow Transplantation Unit and CBMDP Donor Center, University Hospital of Patras, Patras, Greece; [34]Department of Hematology and Oncology, Klinikum Augsburg, Augsburg, Germany; [35]Stem Cell Transplant and Cellular Therapy, The University of Texas MD Anderson Cancer Center, Houston, TX, USA; [36]Chaim Sheba Medical Center, Tel Aviv University, Tel-Hashomer, Israel and EBMT ALWP office, Saint Antoine Hospital , Paris, France and [37]Service d'Hématologie Clinique et Thérapie Cellulaire, Hôpital Saint-Antoine, AP-HP, Sorobonne University, and INSERM UMRs 938, Paris, France

Ferrata Storti Foundation

Haematologica 2020
Volume 105(1):47-58

Correspondence:

BHAGIRATHBHAI DHOLARIA
bhagirathbhai.r.dholaria@vumc.org

Received: February 17, 2019.

Accepted: September 19, 2019.

Pre-published: September 19, 2019.

doi:10.3324/haematol.2019.219790

Check the online version for the most updated information on this article, online supplements, and information on authorship & disclosures: www.haematologica.org/content/105/1/47

ABSTRACT

Donor lymphocyte infusion has been used in the management of relapsed hematologic malignancies after allogeneic hematopoietic cell transplantation. It can eradicate minimal residual disease or be used to rescue a hematologic relapse, being able to induce durable remissions in a subset of patients. With the increased use of haploidentical

hematopoietic cell transplantation, there is renewed interest in the use of donor lymphocytes to either treat or prevent disease relapse post transplant. Published retrospective and small prospective studies have shown encouraging results with therapeutic donor lymphocyte infusion in different haploidentical transplantation platforms. In this consensus paper, finalized on behalf of the Acute Leukemia Working Party of the European Society for Blood and Marrow Transplantation, we summarize the available evidence on the use of donor lymphocyte infusion from haploidentical donor, and provide recommendations on its therapeutic, pre-emptive and prophylactic use in clinical practice.

Introduction

Allogeneic hematopoietic cell transplantation (allo-HCT) remains an important therapeutic option for a wide number of both hematologic malignancies and non-hematologic disorders. With improvements in conditioning regimens, graft-*versus*-host disease (GvHD) prophylaxis and supportive care, leading to a reduced risk of transplant-related mortality, disease relapse has become the foremost cause of mortality after allo-HCT. The cumulative incidence of relapse (CIR) after allo-HCT for acute leukemia can be as high as 40-50% with only 10-15% long-term survival in patients experiencing leukemia recurrence.[1-3] Strategies aimed at preventing and/or treating disease relapse have the greatest potential to improve transplant outcomes. Donor-lymphocyte infusion (DLI) has an established role in the management of disease relapse after allo-HCT. Unmanipulated DLI is a form of immunotherapy, which can induce durable remissions by enhancing the graft-*versus*-tumor (GvT) effect.[4-6] Efficacy of DLI varies by type and burden of the disease.[7] DLI is more effective in chronic myeloid leukemia (CML), leading to complete remission (CR) in 70-80% of patients in hematologic or cytogenetic CML relapse, whereas less than 40% of acute leukemia patients respond to DLI.[8,9] A study by Schmid *et al.* using the European Society for Blood and Marrow Transplantation (EBMT) registry showed DLI was associated with improved survival of patients with AML in the first hematologic relapse after allo-HCT, but 2-year overall survival (OS) was only 15% if DLI was given in the setting of active disease.[10] Pre-emptive DLI for mixed chimerism or molecular disease relapse and prophylactic DLI for high-risk hematologic malignancies have also been studied with promising results in the setting of human leukocyte antigen (HLA)-matched allo-HCT.[11-13]

Allo-HCT from an HLA-haploidentical related donor (haplo-HCT) has emerged as a suitable alternative for those patients who need an allograft but who lack an HLA-matched related or unrelated donor.[14,15] Several T-cell depleted and T-cell replete haploidentical transplant strategies are applied today. In T-cell replete haploidentical stem cell transplantation, the use of post-transplant cyclophosphamide (PTCy) has rapidly increased across the globe due to its logistical simplicity and efficacy.[2] Another T-cell replete haplo-HCT platform is granulocyte colony stimulating factor (GCSF)-antithymocyte globulin (ATG)-based or "GIAC" protocol' [GCSF-stimulation of the donor; intensified immunosuppression through post-transplantation cyclosporine (CSA), mycophenolate mofetil (MMF), and short-course methotrexate (MTX); anti-thymocyte globulin (ATG); and combination of peripheral blood stem cells (PBSC) and bone marrow (BM) allografts] initially developed at the Peking University.[16] Today's T-cell depleted strategies derive from the mega-dose CD34$^+$ protocol developed at the Perugia University[17] and represent a historical standard in T-cell depletion. From this platform, several other T-cell depleted strategies have evolved, such as CD3/CD19 cell depletion[18] and α-β-T/CD19-B cell depletion.[19] The adoptive transfer of selectively allo-depleted[20] or gene-modified T cells with a suicide switch[21,22] after T-cell depleted transplantation have further optimized this transplant form and are now being investigated in large randomized trials in comparison with PTCy.

Haplo-HCT with PTCy has shown comparable clinical outcomes to matched unrelated donor allo-HCT in retrospective analyses with a significantly lower risk of chronic GvHD in myeloid and lymphoid malignancies, regardless of whether the graft was obtained from BM or mobilized PBSC.[23-26] There is concern that DLI from a haploidentical donor (haplo-DLI) may pose an increased risk for GvHD, given the higher degree of HLA disparity between the donor and recipient. However, a greater HLA-disparity may also be beneficial in promoting a stronger GvT effect.[27] Another advantage is that a related haploidentical donor is, in most cases, readily available and collection is faster than a registry-based unrelated donor. While the experience with haplo-DLI is limited, and there are many uncertainties around its clinical application, it can be a powerful tool to manage a disease relapse after haplo-HCT. Nonetheless, it should be emphasized that haplo-DLI after T-cell depleted transplantation without full immune reconstitution may have very different effects than after T-cell replete transplantation and may require completely different dosing strategies. Therefore, in the absence of data from prospective clinical trials, general recommendations cannot be made.

In this review, we summarize the published experience with haplo-DLI and provide recommendations regarding its use in various clinical settings (therapeutic *vs.* pre-emptive *vs.* prophylactic DLI), use of chemotherapy before DLI, optimal cell dose, and concurrent immunosuppression management. Newer strategies using cellular engineering, donor-derived natural killer (NK) cells and pharmacological immunomodulation are also discussed.

Therapeutic haplo-donor-lymphocyte infusion: hematologic relapse

Previously published retrospective studies have suggested that outcomes of haplo-DLI in patients with hematologic relapse are comparable to standard DLI from an HLA-matched donor. The incidence of DLI-associated GvHD also appears to be similar regardless of donor type.[28-30] Possible explanations, at least when used late post transplant, are the use of lower cell dose and presence of donor-derived tolerogenic cells in the recipient,

which may reduce their alloreactivity and, thus, the risk of GvHD. The type of haplo-HCT protocol may influence outcomes of subsequent haplo-DLI. The current therapeutic haplo-DLI experience is limited to haplo-HCT/PTCy or a 'GCSF-ATG-based protocol'. Table 1 summarizes the published studies using DLI from a haploidentical donor.

Therapeutic donor-lymphocyte infusion in T-cell replete haplo-hematopoietic cell transplantation

Zeidan *et al*. retrospectively reported results of haplo-DLI in 40 patients [minimal residual disease (MRD)/loss of chimerism (LOC): n=5; hematologic relapse: n=35] after a haplo-HCT/PTCy with BM graft. At the median follow up of seven months, CR was achieved in 30% of patients (CR after a hematologic relapse: 26%) and acute GvHD (aGvHD) occurred in 25% of them. At time of last follow up, six patients were alive in CR for over a year after the intervention. The cell dose in most DLI was $1x10^6$ $CD3^+$ cells/kg and the majority of patients received cytoreductive chemotherapy before DLI.[28] Subsequently, two similar reports showed that haplo-DLI after chemotherapy successfully resulted in CR in approximately 30% of the patients with a subset of long-term survivors.[29,30] The incidence of grade 2-4 aGvHD was approximately 30%, and only 5% of patients developed grade 3-4 aGvHD. No patient (0%) developed extensive chronic GvHD (cGvHD).[29,30] None of these studies used immunosuppression for GvHD prophylaxis after haplo-DLI. Disease responses and GvHD rates were comparable between patients who received BM *versus* a PBSC graft.[30] Patients with relapsed Hodgkin lymphoma appear to have relatively better disease responses to haplo-DLI compared to those with acute leukemia (40% *vs.* 33%).[29] In a smaller retrospective study (n=21) published by Goldsmith *et al.*, the authors showed that patients with extra-medullary disease relapse had a better relapse-free survival (RFS) compared to those with marrow relapse (4-month RFS 43% *vs*. 8%).[30] The group at Peking University has developed a haplo-DLI protocol using GCSF-primed peripheral blood progenitor cells (GBPC) with short-term immunosuppression. They have used a higher cell dose ($1x10^7$ to $1x10^8$ $CD3^+$ cells/kg) than that used in haplo-DLI in the setting of allo-HCT/PTCy ($1x10^5$ to $1x10^6$ $CD3^+$ cells/kg).[31-37] An earlier prospective study using GBPC without immunosuppression resulted in a high incidence of severe GvHD (grade 3-4 aGvHD 30%, extensive cGvHD 30%), resulting in 2-year disease-free survival (DFS) of 40% and non-relapse mortality (NRM) of 25%.[38] Subsequent studies used cytoreductive chemotherapy before GBPC infusion (chemo-DLI) followed by GvHD prophylaxis with low-dose weekly MTX or CSA for 6-8 weeks. A retrospective report by Yan *et al.* on 55 patients with relapsed acute leukemia showed 3-year DFS, NRM, and OS of 24%,13%, and 25%, respectively. A total of 76% of patients achieved CR (MRD negative CR: 55%).[39] Relapse after achieving CR following chemo-DLI was a major problem, resulting in poor long-term survival. In spite of the limitations of cross-study comparison, outcomes of chemo-GBPC infusion with short-course immunosuppression are comparable to unmanipulated haplo-DLI after haplo-HCT/PTCy.

Pre-emptive haplo-donor-lymphocyte infusion: minimal residual disease, mixed-donor chimerism

Impact of minimal residual disease and mixed-chimerism on haplo-hematopoietic cell transplantation outcomes

Strategies are being explored to reliably predict the risk of disease relapse after an allo-HCT in the hope of implementing pre-emptive treatments. The presence of MRD before or after allo-HCT is associated with significantly increased risk of relapse and reduced survival in both acute lymphoblastic leukemia (ALL) and acute myeloid leukemia (AML).[40,41] Canaani *et al.* looked at pre-haplo-HCT MRD positivity in AML patients and showed its negative correlation with leukemia-free survival.[42] Low donor T-cell chimerism [mixed-chimerism (MC)] after an allo-HCT is also associated with poor donor-derived immune reconstitution and increased risk of disease relapse, especially after myeloablative conditioning. In patients with AML/MDS who underwent myeloablative allo-HCT, donor T-cell chimerism <85% at day (d)+90 and d+120 was associated with increased risk of 3-year disease progression (HR=2.1, P=0.04).[43] Koreth *et al.* reported that d+100 total donor chimerism <90% was associated with increased risk of relapse (HR= 2.54, P<0.001) and lower OS (HR=1.50, P=0.009) in patients after a reduced-intensity allo-HCT.[44] Pre-emptive DLI from a full matched donor for MRD and MC appears to be safe and effective in improving disease-specific outcomes.[45,46]

Pre-emptive donor-lymphocyte infusion in T-cell replete haplo-hematopoietic cell transplantation

In the previously mentioned retrospective study by Zeidan *et al.*, 3 of 4 patients who received haplo-DLI for MRD entered CR.[28] Similarly, other reports showed higher response rates in patients who received haplo-DLI for MRD or MC compared to the administration at the time of hematologic relapse.[29,30] Yan *et al.* reported comparative outcomes of prospective studies of standard-risk acute leukemia and MDS patients with persistent MRD after allo-HCT (haploidentical donor, n=29; matched donor, n=27), who received low-dose interleukin-2 (IL-2) or pre-emptive DLI. The latter was associated with reduced 3-year CIR compared to IL-2 alone (28% *vs*. 64%; P=0.001).[31] In another retrospective study by Mo *et al.*, 101 patients (haplo-HCT, n=56) received chemo-DLI for persistent MRD after an allo-HCT. Three-year CIR, NRM, and OS were 40%, 10%, and 52%, respectively. Patients who cleared their MRD within 30 days after pre-emptive chemo-DLI had lower relapse rates compared to those with persistent MRD beyond 30 days (20% *vs*. 47%; P=0.001).[36] It should be noted that the published data on pre-emptive haplo-DLI for MC is limited to a few patients[28,30] and further studies are needed to establish its role in preventing disease relapse.

It is important to monitor for MRD after allo-HCT as DLI is probably more effective when administered for MRD only compared overt hematologic relapse.[47] Retrospective studies have shown that persistent MRD post-transplant is associated with high relapse rate and poor outcomes,[48] and the eradication of MRD improves survival.[46] Comparative studies are needed between DLI and other systemic therapies in order to develop disease-

Table 1. Donor-lymphocyte infusion from a haploidentical donor.

Study	N. of patients (prospective/ retrospective)	Diagnosis	Indication for DLI	Treatments before DLI	$CD3^+$ dose/kg	N. of DLI (median)	Disease response	Rate of GvHD	Survival	Notes
T-cell depleted haplo-HCT										
Lewalle *et al.* (2003)[65]	12 (prospective)	AML=5 ALL=3 CML=1 Other=3	Prophylactic=12	None	1-4x10^4			58%	1-yr RFS=50%, 1-yr OS=50%, NRM=0%	T-/B-cell depleted graft
Dodero *et al.* (2009)[62]	23 (prospective)	Lymphoma CLL ALL MM AML	Prophylactic-23	None	2-15x10^4	2	NA	aGvHD=26% (grade 3-4=9%) cGvHD=15% (extensive=12%)	2-yr PFS=45% 2-yr OS=44% NRM=26%	$CD8^+$ T-cell depleted DLI
Martelli *et al.* (2014)[61]	43 (prospective)	AML=33 ALL=10	Prophylactic-43	None	T_{reg}=2.5x10^6±1.1 T_{con}=1.1x10^6±0.6	1	NA	aGvHD (grade ≥2)=15% cGvHD=16% (extensive=7%)	CI NRM=40% 46-m relapse =5%	T_{reg} on day-4, T_{con} on day 0
Gilman *et al.* (2018)[60]	34 (prospective)	AML/MDS=13 ALL=10 Other=11	Prophylactic-34	None	3-5x10^4	1	NA	aGvHD (grade 3-4)=4% cGvHD=16% (extensive=7%)	2-yr OS=63% 2-yr NRM=25%	Post-DLI-GvHD ppx=100%
T-cell replete haplo-HCT										
Or *et al.* (2006)[106]	28 (haplo-26,MMUD-2) (retrospective)	AML=12 ALL=7 CML=5 Other=3	Prophylactic-6 Therapeutic- 22	None	1x10^2 to 15x10^8	1-7 (1)	CR=18%	46%	NRM=11%	
Huang *et al.* (2007)[38]*	20 (prospective)	AML=7 ALL=10 CML=3	Therapeutic=20	CT=9 TKI=2	0.07-4.39x10^8	1-3 (1)	CR=75%	aGvHD=55% (grade 3-4=30%) cGvHD=64% (extensive=30%)	2-yr DFS=40% NRM=25%	Post-DLI-GvHD ppx=55%
Yan *et al.* (2012)[31]*	56 (haplo-29, matched related-26, MUD-1) (prospective)	AML=32 ALL=21 MDS=3	Pre-emptive=56 (MRD)	CT=32	0.75-2x10^8	1	NA	aGvHD=31% (grade 3-4=8%) cGvHD=43% (extensive=34%)	3-yr DFS=56% 3-yr OS=58% 3-yr NRM=14%	Post-DLI-GvHD ppx=100%
Yan *et al.* (2012)[69]*	124 (retrospective)	AML=49 ALL=59 MDS=5 CML=11	Prophylactic=74 Therapeutic/ pre-emptive= 50(MRD)	CT=27 (MRD+) All relapsed pts received CT.	0.13-2.11x10^8	1-4(1)	NA	aGvHD=53% (grade 3-4=28%)	2-yr CIR=35% 2-yr OS=47% 2-yr NRM=34% In disease relapse, 2-yr CIR=45% 2-yr OS=19% 2-yr NRM=37%	Post-DLI-GvHD ppx=100%
Wang *et al.* (2012)[66]*	61 (retrospective)	AML=42 ALL=19	Prophylactic=61	CT=0%	0.9-7.2x10^8	1	NA	aGvHD=48% (grade 3-4=10%) cGvHD=39% (extensive=31%)	3-yr DFS=22% 3-yr OS=31% 2-yr NRM=38%	Post-DLI-GvHD ppx=100%
Yan *et al.* (2013)[33]*	50 (retrospective)	AML=29 ALL=21	Therapeutic=50	CT=100%	0.11-2.07x10^8	NA	CR=64%	aGvHD=66% (grade 3-4=40%) cGvHD=44% (extensive=42%)	1-yr DFS=36% 1-yr OS=36% 1-yr NRM=14%	Post-DLI-GvHD ppx=100%
Yan *et al.* (2015)[39]*	55 (retrospective)	AML=18 ALL=23	Therapeutic=55	CT=100%	0.19-0.74x10^8	NA	CR=76% MRD negative CR=55%	aGvHD=44% (grade 3-4=11%) cGvHD=49% (extensive=42%)	3-yr DFS=24% 3-yr OS=25% 3-yr NRM=13%	Post-DLI-GvHD ppx=100%
Mo *et al.* (2016)[36]*	101 (haplo=58) (retrospective)	AML/MDS=69 ALL=32	Pre-emptive =101(MRD)	CT=100%	1.7-7.4x10^7	NA	CR=76%	aGvHD=9% (grade 3-4=4%) cGvHD=59%	AML/MDS, 3-yr DFS=57% 3-yr NRM=7% ALL, 3-yr DFS=49% 3-yr NRM=11%	Post-DLI-GvHD ppx=100%

continued on the next page

continued from the previous page

Study T-cell depleted haplo-HCT	N of patients (prospective/ retrospective)	Diagnosis	Indication for DLI	Treatments before DLI	CD3+ dose/kg	N. of DLI (median)	Disease response	Rate of GvHD	Survival	Notes
Yan *et al.* (2016)[57]*#	47 (haplo=31) (prospective)	AML=25 ALL=22	Pre-emptive=47 (MRD)	CT=100%	1.5-6.4x10^7	1-4	NA	aGvHD =19% (grade 3-4=6%) cGvHD=79% (≥moderate=66%)	1-yr DFS=71% 1-yr NRM=9% 1-yr OS=78%	Post-DLI-GvHD ppx=100%
Yan *et al.* (2017)[32]*	100 (haplo=62) (prospective)	AML=59 ALL=41	Prophylactic=100	CT=0%	1.8-6.6x10^7	NA	NA	Haplo-HCT, aGvHD =47% (grade 3-4=10%) cGvHD=63% (≥moderate=59%)	Haplo-HCT, 3-yr DFS=51% 3-yr NRM=18% 3-yr OS=49%	Post-DLI-GvHD ppx=100%
Ma *et al.* (2017)[34]*	36 (retrospective)	AML/ALL/ MDS/CML	Therapeutic=36	CT/TKI =100%	NA	NA	CR=56%	Grade 3-4 aGvHD=25%) Extensive cGvHD=36%	3-yr DFS=11% 3-yr OS=14%	Post-DLI-GvHD ppx=100%
Gao *et al.* (2018)[54]*	31 (retrospective)	AML=21 ALL=5 CML=2 Other=3	Prophylactic=31	CT=0%	0.4-6.9x10^7	1	NA	aGvHD=58% (Grade 3-4=7%) cGvHD=39% (Mod-severe=29%)	2-yr RFS=32% 2-yr NRM=33% 2-yr OS=40%	Post-DLI-GvHD ppx=100%
Zeidan *et al.* (2014)[28+]	40 (retrospective)	AML=16 ALL=3 CML=1 Lymphoma=11 Other=9	Therapeutic=35 Pre-emptive=5 (MRD+/MC)	CT/RT= 70%	1x10^5 to 1x10^8	1-4(1)	CR=30% (MRD=75%, Relapse=26%)	aGvHD=25% (grade 3-4=15%) cGvHD=8% (extensive=5%)	8/12 responders (67%) alive, in CR at 17.5 months	
Ghiso *et al.* (2015)[29+]	42 (retrospective)	AML=22 ALL=9 HL=10 MM=1	Therapeutic=22 Pre-emptive=20 (MRD)	CT/RT= 100%	1x10^3 to 1x10^7	1-6 (mean-2.5)	CR=36% CR in MRD =45%	aGvHD=33% (grade 3-4=5%) cGvHD=0%	Leukemia, median response=4m(2-10), median survival =7m(1-15) HL, median response =9m(3-28), median survival =18m(4-34)	
Jaiswal *et al.* (2016)[56§]	21 (prospective)	AML=21	Prophylactic=21	CT=0%	9.2-110x10^7	1-3	NA	Cum incident aGvHD =31% cGvHD=41%	1.5-yr PFS=62% 1.5-yr CIR=21% 1.5-yr OS=71%	Post-DLI-GvHD ppx=100%
Goldsmith *et al.* (2017)[30+]	21 (retrospective)	AML/MDS=16 ALL=2 CML=2 Lymphoma=11 Other=9	Therapeutic=19 Pre-emptive=2(MC)	CT=76%	0.01-3x10^7	1-5	CR=32%	aGvHD=33% (grade 3-4=5%) cGvHD=26% (extensive=0%)	Hematologic relapse, 4-m RFS=8% 4-m OS=29% EM relapse, 4-m RFS=43% 4-m OS=71%	PBSC haplo-HCT
Cauchois *et al.* (2018)[67+]	36 (retrospective)	AML/MDS=25 ALL=2 Lymphoma=6 Other=3	Prophylactic=36	CT=0%	0.1-2.5x10^6	1-3	NA	1-yr CI of mod-severe GvHD=33%	1-yr PFS=83% 1-yr NRM=9% 1-yr OS=76%	PBSC graft=31

N: number; AML: acute myeloid leukemia; ALL: acute lymphoblastic leukemia; CML: chronic myeloid leukemia; MDS: myelodysplastic syndromes; MMUD: mismatched unrelated donor; GvHD ppx: graft-*versus*-host disease prophylaxis; aGvHD: acute GvHD; cGvHD: chronic GvHD; OS: overall survival; DFS: disease-free survival; PFS: progression-free survival; NRM: non-relapse mortality; CT: chemotherapy; TKI: tyrosine kinase inhibitor; MRD: minimal residual disease; MC: mixed-chimerism; NA: not available; RT: radiation therapy; PBSC: peripheral blood stem cell; EM: extra-medullary relapse; RFS: relapse-free survival; haplo-HCT: haploidentical-hematopoietic cell transplant; matched: HLA-matched allo-HCT; MUD: HLA-matched unrelated donor; T_{reg}: regulatory T-cell; T_{con}: conventional T-cells; CI: cumulative incidence; yr: year; m: months; NA: not available. *Granulocyte colony-stimulating factor (GCSF)-anti-thymocyte globulin (ATG)-based protocol and G-CSF-primed peripheral blood progenitor cell (GBPC). §Haplo-HCT with post-transplant cyclophosphamide (PTCy) and GBPC. +Haplo-HCT with PTCy and standard donor-lymphocyte infusion (DLI). #Patients had salvage chemotherapy + therapeutic DLI for hematologic relapse, followed by pre-emptive DLI for persistent minimal residual disease (MRD). pt: patient; mod: moderate; cum: cumulative; HL: Hodgkin lymphoma.

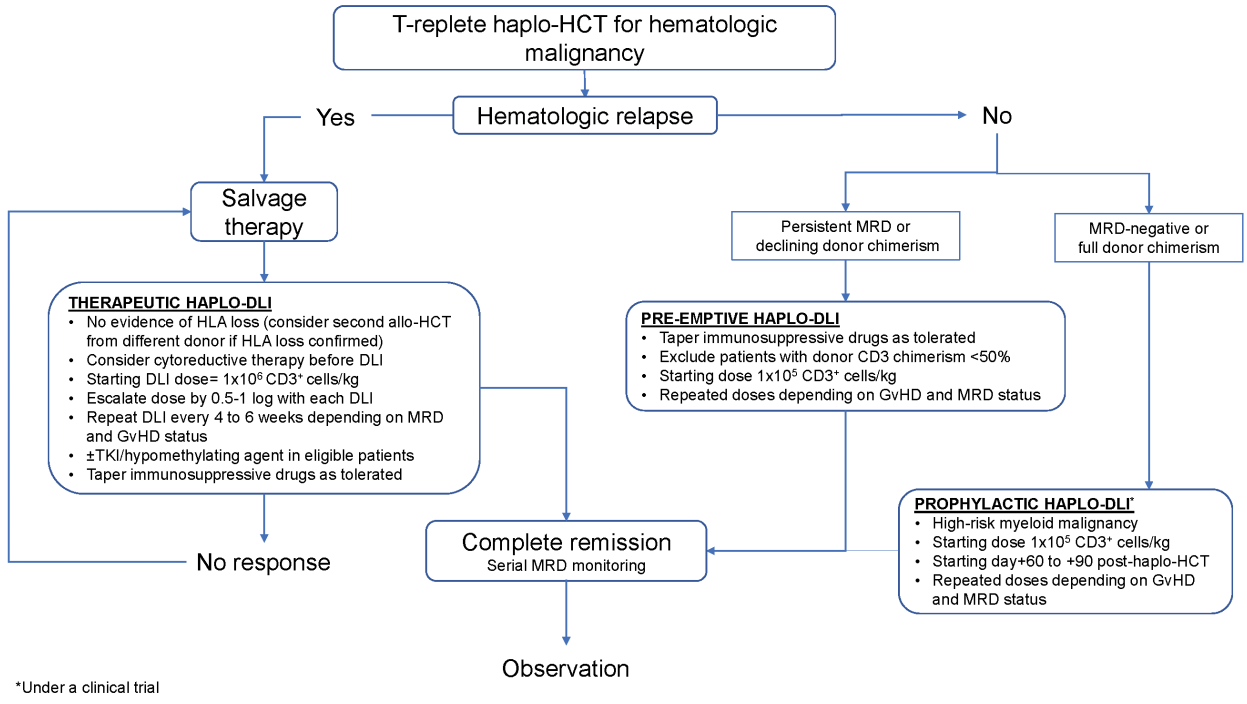

Figure 1. Proposed treatment algorithm of therapeutic, pre-emptive and prophylactic donor-lymphocyte infusion (DLI) following T-cell replete haploidentical hematopoietic cell transplantation (HCT). HLA: human leukocyte antigen; MRD: minimal residual disease; GvHD: graft-*versus*-host disease; TKI: tyrosine kinase inhibitor.

specific MRD management strategies. DLI should not be used in patients who have converted to host chimerism due to increased risk of marrow aplasia.[49] An alternative strategy for such patients would be to undergo a second allo-HCT from the same or from a different donor. It is important to weigh the risk of GvHD and marrow aplasia *versus* the potential benefit of reducing the disease relapse when considering pre-emptive DLI for MRD or MC.

Prophylactic haplo-donor-lymphocyte infusion

Prophylactic DLI from a matched donor has been studied in patients with high-risk myeloid malignancies and was associated with improved disease-specific outcomes and low NRM.[11,50,51] It can contribute to immune reconstitution and reduce the risk of infection,[52] which is a major challenge after a T-cell depleted haplo-HCT. A matched-pair analysis by the EBMT showed improved OS in high-risk AML recipients who received prophylactic DLI from a matched donor (70% *vs.* 40% in controls; P=0.027).[53] Inclusion criteria differ among published studies in their definition of high-risk disease. Most reports included patients with primary induction failure acute leukemia, high disease risk index, active disease before allo-HCT or the presence of high-risk mutations (i.e. TP53, ASXL1, RUNX1) in myeloid malignancies.[54-57] One of the first experiences with prophylactic haplo-DLI was in the setting of autologous-HCT. Nagler *et al.* reported outcomes of 26 patients who received multiple haplo-DLI (with/without IL-2) after an autologous-HCT. This approach was feasible in inducing GvHD, but higher cell doses led to increased toxicity.[58] The timing of prophylactic-DLI is also important as decreasing the interval between allo-HCT and DLI will likely increase the risk of aGvHD.[13] The activity of ATG, given as a part of conditioning, may persist for weeks, and residual ATG may negatively impact prophylactically infused donor lymphocytes.[59] At the same time, the administration of haplo-DLI as early as d+45 was feasible in single center studies.[32,56] It may be reasonable to administer prophylactic haplo-DLI before d+90 given that median time to relapse after allo-HCT is approximately three months.

Prophylactic donor-lymphocyte infusion in T-cell depleted haplo-hematopoietic cell transplantation

Early experience with prophylactic haplo-DLI was with T-cell-depleted haplo-HCT where donor lymphocytes were infused after a CD34⁺ cell-selected graft to enhance immune reconstitution.[60-62] Perruccio *et al.* showed that infusion of donor-derived non-alloreactive T cells specific for cytomegalovirus (CMV) and aspergillus resulted in the rapid development of T-cell responses against these pathogens without inducing GvHD.[63] Another prospective study utilized CD8⁺ T-cell depleted DLI, which resulted in aGvHD in 26% of patients with 2-year PFS of 45%.[62] Donor-derived T regulatory cells (T_{regs}), co-infused with conventional T cells (T_{cons}) were shown to protect recipients against GvHD.[64] In a prospective study, patients received T_{regs} (d -4) followed by a megadose of CD34⁺cells and T_{cons} on d0 from a haploidentical donor without any post-transplant immunosuppression. Only 15% of the patients developed ≥grade 2 aGvHD and DFS was 56% at 18 months.[61] In another prospective study by Gilman *et al.*, 34 pediatric patients were infused an unmanipulated prophylactic haplo-DLI with MTX between d+30 and d+42 after a T-cell depleted/CD34⁺ selected haplo-HCT. The intervention was safe and 2-year NRM

and OS were 25% and 63%, respectively.[60] Lewalle *et al.* reported the outcomes of 12 patients who received prophylactic haplo-DLI starting on d+28 after T-/B-cell depleted haplo-HCT in a prospective study. One-year RFS, NRM, and OS were 50%, 0%, and 50%, respectively.[65] Despite the encouraging results with prophylactic infusion of T-cell subset after a T-cell deplete/CD34$^+$ selected haplo-HCT, its widespread adoption has been challenging as cell selection remains a labor-intensive and expensive process.

Prophylactic donor-lymphocyte infusion in T-cell replete haplo-hematopoietic cell transplantation

The Chinese group has led the way by incorporating prophylactic GBPC in high-risk malignancies after a haplo-HCT with the GCSF-ATG-based protocol. In a retrospective study by Wang *et al.*, [61] patients with high-risk leukemia who underwent GBPC infusion were compared to 27 patients who received routine care after an haplo-HCT. Prophylactic GBPC was associated with lower relapse rate (36% *vs*. 55%; *P*=0.017) and superior estimated 3-year survival (31% *vs*. 11%; *P*=0.001) compared to routine care. There was no difference in NRM between the two groups.[66] A prospective study by the same group enrolled 62 patients with high-risk acute leukemia. All patients received prophylactic GPBC between d+45 and d+60 and further DLI were guided by MRD and GvHD status. Three-year DFS, NRM, and OS were 51%, 18%, and 49%, respectively. Acute and chronic GvHD were seen in 47% and 63% patients, respectively. Outcomes were similar between recipients of haploidentical (n=62) *versus* matched donor (n=38) prophylactic DLI.[32]

Jaiswal *et al.* reported their prospective experience with prophylactic GBPC in the T-cell replete haplo-HCT/PTCy setting. Twenty-one patients with AML (not in remission) received up to three doses of haplo-GPBC (d+21, d+35 and d+60). They were compared with 20 patients who received routine monitoring after haplo-HCT. At 18 months, CIR, PFS, and OS were 21% *versus* 66%; 62% *versus* 25% and 71% *versus* 35% in DLI and routine care cohorts, respectively. Incidence of aGvHD was 31%, while incidence of chronic GvHD was 41% after GBPC infusions. NRM was equivalent between the groups.[56] Recently, Cauchios *et al.* reported outcomes of 36 patients who received prophylactic haplo-DLI after a haplo-HCT/PTCy. One-year PFS and OS were 76% and 83%, respectively. The cumulative incidence of relapse was 16% and the incidence of DLI-associated GvHD was 33%.[67]

Practical aspects of haplo-donor-lymphocyte infusion

Cell dose

The CD3$^+$ T-cell dose ranged from 0.01 to 8.8x10^8 mononuclear cells/kg in reports on therapeutic DLI from a matched donor.[7] A study reported a relatively lower rate of GvHD with an escalating cell dose regimen *versus* a single bulk infusion of DLI from HLA-matched donors. Disease responses were similar between the two approaches.[68] There was no dose-response relationship with GvHD or disease response rates in haplo-DLI in the setting of T-cell depleted haplo-HCT.[28,29] The average starting dose for therapeutic haplo-DLI in the T-cell replete haplo-HCT/PTCy setting was 1 or 2 log lower than the standard DLI dose (1x10^7 CD3$^+$ cells/kg) from HLA-matched donors. In a report on 40 patients, a cell dose of 1x10^6 CD3$^+$ cells/kg was associated with grade 2-4 aGvHD in 17% of patients, and a CR rate of 27%.[28] Goldsmith *et al.* used the same dose in 21 patients; only seven (33%) developed aGvHD (grade 3-4 aGvHD in 1 patient).[30] These incidences of aGvHD were lower than those reported by the Chinese group using haplo-GBPC at 1 to 2 log higher cell dose with the GCSF-ATG-based protocol. A starting cell dose of 1x10^7 to 1x10^8 CD3$^+$ cells/kg was associated with grade 2-4 aGvHD in 50-60% (grade 3-4 aGvHD approximately 30%) of patients.[31,38,69] Subsequent reports by Yan *et al.* showed a reduced incidence of aGvHD with the routine use of short-term GvHD prophylaxis after GBPC infusion.[39] Available data suggest that 1x10^6 CD3$^+$cells/kg is a reasonable starting dose with appropriate repeated dose escalation every 4-6 weeks based on disease response and GvHD for therapeutic haplo-DLI in T-replete haplo-HCT with PTCy. Clinical trials are needed to establish the optimal timing and cell dose in prophylactic and T-cell depleted haplo-HCT settings. Published studies have used wide-ranging repeated non-escalating cell doses for pre-emptive or prophylactic DLI.[32,37,54]

The end point of donor-lymphocyte infusion therapy

It is important to establish the goal of DLI therapy beforehand as each DLI is associated with increased risk of GvHD. Patients with DLI-responsive relapse usually respond within 2-3 months.[7] Repeated infusions of escalating doses of therapeutic DLI can be administered until CR is achieved (ideally an MRD-negative status) or the patient develops clinically significant GvHD. Patients should be evaluated for GvHD, donor chimerism and disease response after each DLI. Pre-emptive DLI for MRD persistence after allo-HCT may be stopped once the achievement of MRD negativity, significant GvHD or a hematologic relapse occurs. Donor chimerism should be assessed after each pre-emptive DLI for MC. Pre-emptive DLI may be stopped once ≥90% donor chimerism is achieved. As noted above, DLI can result in marrow aplasia in those patients who have converted to host chimerism. There is no standard duration of prophylactic DLI outside a clinical trial. In these circumstances, each dose of prophylactic haplo-DLI should be used with caution, balancing the risk of disease relapse and GvHD.

Traditional donor-lymphocyte infusion *versus* granulocyte colony-stimulating factor-primed peripheral blood progenitor cell infusion

Standard DLI uses freshly collected unmanipulated donor lymphocytes. This approach privileges tumor alloreactivity over the risk of GvHD. GCSF promotes T-cell hypo-responsiveness in marrow grafts by increasing the number of plasmacytoid dendritic cells and monocytes. It also reduces the expression of co-stimulatory CD28/B7 on monocytes, B and T cells,[70] promotes macrophage[71] and T-cell polarization in the BM graft towards the more tolerogenic pattern. This property is maintained even after *in vitro* mixture of G-CSF primed BM and PBSC grafts.[72,73] The Chinese group has reported their extensive experience with using GBPC instead of unmanipulated DLI. Huang *et al.* reported the outcomes of 20 patients who received therapeutic GBPC from hap-

loidentical donors (the majority of whom received salvage therapy prior to GBPC infusion); CR was achieved in 75% of patients and the rates of acute and chronic GvHD were 55% and 64%, respectively.[38] In another study of pre-emptive GBPC infusion for MRD after an allo-HCT (haploidentical related donor: n=29; matched-related donor: n=26), the incidences of acute and chronic GvHD were 31% and 43%, respectively. Routine debulking chemotherapy and short-term immunosuppression were used in most studies using GBPC.[31] A prospective observational study by Jaiswal *et al.* used prophylactic-GBPC in the setting of T-cell replete haplo-HCT/PTCy.[56] The incidence of aGvHD was comparable but cGvHD was higher than that reported with unmanipulated haplo-DLI in the PTCy setting.[28-30] A recent report from Mexico showed that administration of G-CSF-primed whole blood units (median cell count $6.7x10^6$ $CD3^+$ cells/kg) from haploidentical donors is safe, with disease responses and improvement in MC in a subset of patients.[74] Whole blood units can potentially reduce the cost associated with haplo-DLI in developing countries. Long-term immune tolerance after PTCy may be enough to overcome the immunological barrier of haplo-DLI, and GCSF priming may not be required in this setting. Comparative studies between unmanipulated DLI *versus* GBPC in the setting of haplo-HCT/PTCy are needed.

Role of concurrent immunosuppression

Graft-*versus*-host disease is the main limiting toxicity of DLI, and short-term immunosuppression with DLI may improve the safety of DLI. Yan *et al.* reported aGvHD in 31% of patients after pre-emptive GBPC infusion for MRD persistence after T-cell replete haplo-HCT.[31] All patients received CSA or low-dose MTX for 6-8 weeks after GBPC. There was no difference in acute and chronic GvHD rates between CSA and MTX. MTX was associated with lower relapse rate (38% *vs*. 81%; *P*=0.029) and better DFS (52% *vs*. 16%; *P*=0.06). Patients who received MTX had higher absolute lymphocyte count compared to those who received CSA, which may have contributed to better GvT effect.[39] The same group also showed that patients receiving GvHD prophylaxis for 6-8 weeks had a lower cumulative incidence of grade 3-4 aGvHD than patients receiving prophylaxis for 4-6, 2-4, and <2 weeks (9%, 14%, 32%, and 50%, respectively; *P*=0.018).[69] In a retrospective study, Mo *et al.* used pre-emptive chemo-DLI for MRD persistence along with routine prophylaxis with CSA or MTX (haploidentical donor 6-8 weeks; matched donor 4-6 weeks). The incidence of aGvHD was only 9% (grade 3-4 aGvHD: 4%) in their cohort of 101 patients.[36] It is important to note here that haplo-DLI without concurrent immunosuppression in the T-cell replete haplo-HCT/PTCy setting has been reported to have a similar incidence of GvHD compared to the GCSF-ATG-based haplo-HCT protocol, which routinely uses prophylactic immunosuppression with DLI.[28] The potential impairment of the DLI-mediated GvT effect by CSA or MTX is a concern when managing a hematologic relapse. It is reasonable to add short-term MTX after a pre-emptive or prophylactic haplo-DLI, especially in patients with a history of GvHD.[56] There are no data available on concurrent immunosuppression with therapeutic haplo-DLI in the T-cell replete haplo-HCT/PTCy setting.

Combination of systemic therapies with donor-lymphocyte infusion

Administration of salvage therapy before the infusion of DLI may improve its efficacy by reducing the tumor burden and supporting *in vivo* expansion of infused T cells. In this regard, chemotherapy helps eliminate regulatory donor T cells and create a favorable immunological environment for DLI by increasing serum levels of IL-7 that favors peripheral expansion of T cells.[75] In the retrospective study by Zeidan *et al.*, patients who received a cytoreductive therapy had better CR rates compared to those who received unmanipulated haplo-DLI without any preceding therapy (39% *vs*. 8%).[28] This beneficial effect of pre-DLI chemotherapy was not seen in a similar report by Goldsmith *et al*.[30]

The downside of pre-DLI chemotherapy is tissue injury and inflammatory cytokine surge which may increase the risk of GvHD, especially when used closer to the allo-HCT.[76] Intensive chemotherapy after an allo-HCT is poorly tolerated, and infectious complications are common.[34,76] Recently, hypomethylating agents (i.e. azacitidine, decitabine) have been used with DLI for relapsed AML/MDS. Azacitidine can induce allogeneic $CD8^+$ T-cell response by enhancing the expression of epigenetically silenced tumor-associated antigens.[77] A combination of a hypomethylating agent and DLI is safe with no apparent increase in GvHD or infection risk compared to DLI-alone.[78,79] In a prospective study using azacitidine with DLI for relapsed disease after HLA-matched allo-HCT, the CR rate was 23% and the 2-year OS was 17%.[80] Another retrospective study utilizing decitabine followed by DLI for relapsed myeloid malignancies showed an overall response rate of 25% with 2-year OS of 11%.[81] Drugs targeting specific molecular anomalies (*BCR-ABL1*, *FLT3-ITD*, *IDH1*, *IDH2*) are increasingly being incorporated in the treatment of disease relapse or as maintenance therapy after allo-HCT.[82,83] These drugs are safer compared to traditional salvage chemotherapy and may provide benefit when administered in combination with DLI.[84]

Immune escape after haplo-hematopoietic cell transplantation

Recent data have shed light on mechanisms of immune escape causing disease relapse after haplo-HCT. In haplo-SCT, HLA haplotype mismatched in the donor/recipient pair was replaced by a shared parent haplotype (uniparental disomy) in 5 of 17 patients with relapsed AML post-haplo-HCT.[85] In a subsequent retrospective analysis of 69 patients who relapsed after haplo-HCT, mismatched-HLA haplotype loss accounted for 33% of the relapses.[86] Based on retrospective studies, a second allo-HCT using a donor with a different mismatched haplotype or a mismatched unrelated donor may induce a better GvT effect compared to same donor from the first haplo-HCT.[86,87] At present, there is no standardized method of detecting loss of mismatched HLA haplotype in leukemic cells. HLA-allele specific quantitative polymerase chain reaction is required to quantify recipient- and donor-specific alleles to confirm uniparental disomy in low-burden disease relapse.[86,88]

Historically speaking, most patients receiving therapeutic DLI relapse and succumb to their disease. Close monitoring of MRD and donor chimerism after a successful therapeutic haplo-DLI is important to identify the

patients who are at high-risk of subsequent relapses. Mo *et al.* reported that patients with persistent MRD after DLI had increased relapse risk (P=0.001), resulting in poor DFS (P=0.004).[36] In a prospective study of 47 patients (66% received haplo-HCT), MRD-guided repeated administration of pre-emptive chemo-DLI was effective in reducing the risk of subsequent relapse after achieving initial disease response. The one-year CIR, DFS, and OS were 22%, 71%, and 78%, respectively (Figure 1).[57]

Future directions

Donor-derived natural killer cells

Natural killer cells may play a role in tumor alloreactivity in the setting of mismatched or haploidentical transplant. A recent study showed a marked reduction in donor-derived NK cells in the recipients of PTCy, leading to blunting of NK-cell alloreactivity.[89] In a pilot study, prophylactic infusion of CD56$^+$/CD3$^+$ cells after haplo-HCT/PTCy in patients with refractory active disease was safe and associated with rapid immune reconstitution.[55] The same group used prophylactic DLI primed with abatacept (CTLA4Ig), which selectively suppresses T-cell alloreactivity without interfering with NK-cell activation. Abatacept with DLI was associated with reduced incidence of aGvHD (10% *vs*. 31%) and improved relapse-free survival compared to prophylactic DLI alone.[90] In a phase I study by Ciurea *et al.*, donor-derived NK cells expanded *ex vivo* were infused prophylactically before and after haplo-HCT in high-risk myeloid malignancies. The intervention was safe and associated with improved NK-cell number and function, lower viral infections, and low relapse rate when compared to a historical control group.[91] Several methods to enhance NK-cell alloreactivity, including combination with immunomodulatory drugs,[92] use of cytokine-activated NK cells,[93] and selection of alloreactive single KIR$^+$ NK cells,[94] are under investigation.

Engineered donor-lymphocyte infusion

Different strategies are being explored to modify DLI composition and reduce the risk of GvHD while maintaining antitumor activity. ATIR101© is a haplo-DLI product with alloreactive T cells depleted by *ex vivo* photodepletion.[20] In a pooled analysis of two prospective trials, 37 patients received prophylactic ATIR101© after T-cell depleted haplo-HCT. One-year relapse rate, NRM and OS were 8%, 33% and 58%, respectively. Interestingly, aGvHD (grade 3-4) and severe cGvHD were seen in 5% and 0% of the patients, respectively.[95] Alloanergized DLI generated *ex vivo* was infused on d+35 after a CD34$^+$ selected haplo-HCT in a phase I study. These donor lymphocytes with the reduced donor-specific alloreactivity expanded *in vivo* and contributed to immune reconstitution.[96] Another strategy is to insert an inducible suicide gene in donor lymphocytes so that they can be selectively eliminated to treat DLI-associated GvHD.[21,97] A recent analysis on 100 children with acute leukemia given a titrated number of donor T cells transduced with the inducible caspase-9 safety switch after haplo-HSCT showed an 82% probability of relapse-free survival.[98]

Chimeric antigen receptor T-cell (CAR-T) therapy has emerged as a potent form of adoptive cellular therapy. Two CD19 CAR-T-cell therapies have been approved by the US Food and Drug Administration (FDA) and the European Medicines Agency (EMA) for relapsed/refractory high-grade B-cell lymphoma and B-ALL.[99,100] Prophylactic infusion of CD19 CAR-T cells from a haploidentical donor was found to be safe with only mild aGvHD in one report.[101] There are reports of therapeutic or pre-emptive donor-derived CAR-T-cell infusion with a small number of patients achieving durable remissions. CAR-T-cell-associated GvHD appears to be rare and of mild severity.[102] Selective depletion of CD3$^+$ αβ-TCR$^+$ T cells (thought to be the principal mediators of GvHD) to enrich DLI with CD3$^+$ γδ-TCR$^+$ T cells and CD3$^-$ CD56$^+$ NK cells is also an attractive strategy to reduce the risk of GvHD while maintaining tumor alloreactivity.[103] Maschan *et al.* infused low-dose (1x10^5 CD3$^+$cells/kg) CD45RA-depleted DLI (memory T cell) in 25 patients after TCR α/β-depleted haplo-HCT. The intervention was safe and associated with the expansion of cytomegalovirus-specific T cells in the recipients.[52]

Donor-lymphocyte infusion with immunomodulatory drugs

Immunomodulation with checkpoint inhibitors and targeted agents may enhance the efficacy of DLI. This may allow lower CD3$^+$ cell dose while maintaining tumor alloreactivity. Blinatumomab (a CD19-CD3 bispecific T-cell engager) has been used with DLI for relapsed B-ALL. In a recent report of 14 patients, it appears to be safe with high response rates.[104] In a prospective phase II study, DLI was administered with azacitidine and lenalidomide in patients with molecular or hematologic relapse of myeloid malignancies. The combination was relatively safe and the CR rates were 67% in MRD and 43% in hematologic relapse.[80] Interferon-γ (IFNγ) induced re-expression of epigenetically silenced MHC class II antigens in relapsed AML clones after allo-HCT.[105] One could hypothesize that treating a patient with IFNγ before haplo-DLI may result in better tumor alloreactivity, although it may also increase the risk of GvHD.

Conclusions

- Unmanipulated DLI from a haploidentical donor appears to be relatively safe and reasonably effective in patients who relapse after a T-cell replete haplo-HCT. Patients given haplo-DLI should be enrolled in a clinical trial whenever possible, as data regarding optimal cell dose, timing and role of concurrent systemic therapies with haplo-DLI are limited. Information about the application of unmanipulated DLI after T-cell depleted transplantation is limited, which is why dosing should be managed with caution.
- The risk of GvHD after unmanipulated DLI in the haplo-HCT/PTCy setting is comparable to an unmanipulated DLI from an HLA-matched donor.
- Cytoreductive therapy prior to DLI from a haploidentical donor should be considered in patients with a hematologic relapse after haplo-HCT.
- Pre-emptive haplo-DLI may play a role in reducing disease relapse in patients with persistent MRD or mixed-donor chimerism after haplo-HCT; however, more studies are needed.
- Patients with high-risk myeloid malignancies may benefit from a prophylactic haplo-DLI, which should ide-

ally be used in the setting of a clinical trial.

• The administration of manipulated DLI after T-cell depleted or T-cell replete haploidentical transplantation, such as allodepleted or gene-modified T cells, should only be performed in the setting of a clinical trial.

• Patients should be monitored closely with frequent disease-specific MRD testing and donor-chimerism after DLI administration.

• Mismatched-HLA allele loss was detected in one-third of leukemia relapses after a haplo-HCT. Such patients are unlikely to benefit from DLI from the original donor. A second allo-HCT from a related donor with a different mismatched haplotype or a mismatched unrelated donor may be considered if HLA-loss is confirmed.

Acknowledgments

The authors would like to thank Vidya B. Pai, MD, for assistance with proofreading.

References

1. Bejanyan N, Weisdorf DJ, Logan BR, et al. Survival of patients with acute myeloid leukemia relapsing after allogeneic hematopoietic cell transplantation: a center for international blood and marrow transplant research study. Biol Blood Marrow Transplant. 2015;21(3):454-459.
2. D'Souza A, Fretham C. Current Uses and Outcomes of Hematopoietic Cell Transplantation (HCT): CIBMTR Summary Slides, 2018.
3. Ciurea SO, Labopin M, Socie G, et al. Relapse and survival after transplantation for complex karyotype acute myeloid leukemia: A report from the Acute Leukemia Working Party of the European Society for Blood and Marrow Transplantation and the University of Texas MD Anderson Cancer Center. Cancer. 2018;124(10):2134-2141.
4. Kolb HJ, Mittermuller J, Clemm C, et al. Donor leukocyte transfusions for treatment of recurrent chronic myelogenous leukemia in marrow transplant patients. Blood. 1990;76(12):2462-2465.
5. Pati AR, Godder K, Lamb L, et al. Immunotherapy with donor leukocyte infusions for patients with relapsed acute myeloid leukemia following partially mismatched related donor bone marrow transplantation. Bone Marrow Transplant. 1995; 15(6):979-981.
6. Sica S, Di Mario A, Salutari P, et al. Chemotherapy and recombinant human granulocyte colony-stimulating factor primed donor leukocyte infusion for treatment of relapse after allogeneic bone marrow transplantation. Bone Marrow Transplant. 1995;16(3):483-485.
7. Deol A, Lum LG. Role of donor lymphocyte infusions in relapsed hematological malignancies after stem cell transplantation revisited. Cancer Treat Rev. 2010;36(7):528-538.
8. Chalandon Y, Passweg JR, Schmid C, et al. Outcome of patients developing GVHD after DLI given to treat CML relapse: a study by the Chronic Leukemia Working Party of the EBMT. Bone Marrow Transplant. 2010;45(3):558-564.
9. Takami A, Yano S, Yokoyama H, et al. Donor lymphocyte infusion for the treatment of relapsed acute myeloid leukemia after allogeneic hematopoietic stem cell transplantation: a retrospective analysis by the Adult Acute Myeloid Leukemia Working Group of the Japan Society for Hematopoietic Cell Transplantation. Biol Blood Marrow Transplant. 2014;20(11): 1785-1790.
10. Schmid C, Labopin M, Nagler A, et al. Donor lymphocyte infusion in the treatment of first hematological relapse after allogeneic stem-cell transplantation in adults with acute myeloid leukemia: a retrospective risk factors analysis and comparison with other strategies by the EBMT Acute Leukemia Working Party. J Clin Oncol. 2007;25(31): 4938-4945.
11. Jedlickova Z, Schmid C, Koenecke C, et al. Long-term results of adjuvant donor lymphocyte transfusion in AML after allogeneic stem cell transplantation. Bone Marrow Transplant. 2016;51(5):663-667.
12. Haines HL, Bleesing JJ, Davies SM, et al. Outcomes of donor lymphocyte infusion for treatment of mixed donor chimerism after a reduced-intensity preparative regimen for pediatric patients with nonmalignant diseases. Biol Blood Marrow Transplant. 2015;21(2):288-292.
13. Liga M, Triantafyllou E, Tiniakou M, et al. High alloreactivity of low-dose prophylactic donor lymphocyte infusion in patients with acute leukemia undergoing allogeneic hematopoietic cell transplantation with an alemtuzumab-containing conditioning regimen. Biol Blood Marrow Transplant. 2013;19(1):75-81.
14. Passweg JR, Baldomero H, Bader P, et al. Hematopoietic stem cell transplantation in Europe 2014: more than 40 000 transplants annually. Bone Marrow Transplant. 2016;51(6):786-792.
15. Kanakry CG, Fuchs EJ, Luznik L. Modern approaches to HLA-haploidentical blood or marrow transplantation. Nat Rev Clin Oncol. 2016;13(1):10-24.
16. Huang XJ, Liu DH, Liu KY, et al. Haploidentical hematopoietic stem cell transplantation without in vitro T-cell depletion for the treatment of hematological malignancies. Bone Marrow Transplant. 2006;38(4):291-297.
17. Ciceri F, Labopin M, Aversa F, et al. A survey of fully haploidentical hematopoietic stem cell transplantation in adults with high-risk acute leukemia: a risk factor analysis of outcomes for patients in remission at transplantation. Blood. 2008;112(9):3574-3581.
18. Locatelli F, Merli P, Pagliara D, et al. Outcome of children with acute leukemia given HLA-haploidentical HSCT after alpha-beta T-cell and B-cell depletion. Blood. 2017;130(5):677-685.
19. Lang PJ, Schlegel PG, Meisel R, et al. Safety and Efficacy of Tcralpha/Beta and CD19 Depleted Haploidentical Stem Cell Transplantation Following Reduced Intensity Conditioning in Children: Results of a Prospective Multicenter Phase I/II Clinical Trial. Blood. 2017;130(Suppl 1):214.
20. Roy DC, Lachance S, Cohen S, et al. Allodepleted T-cell immunotherapy after haploidentical haematopoietic stem cell transplantation without severe acute graft-versus-host disease (GVHD) in the absence of GVHD prophylaxis. Br J Haematol. 2019;186(5):754-766.
21. Ciceri F, Bonini C, Stanghellini MT, et al. Infusion of suicide-gene-engineered donor lymphocytes after family haploidentical haemopoietic stem-cell transplantation for leukaemia (the TK007 trial): a non-randomised phase I-II study. Lancet Oncol. 2009;10(5):489-500.
22. Zhou X, Dotti G, Krance RA, et al. Inducible caspase-9 suicide gene controls adverse effects from alloreplete T cells after haploidentical stem cell transplantation. Blood. 2015;125(26):4103-4113.
23. Ciurea SO, Zhang MJ, Bacigalupo AA, et al. Haploidentical transplant with posttransplant cyclophosphamide vs matched unrelated donor transplant for acute myeloid leukemia. Blood. 2015;126(8):1033-1040.
24. Bashey A, Zhang X, Jackson K, et al. Comparison of Outcomes of Hematopoietic Cell Transplants from T-Replete Haploidentical Donors Using Post-Transplantation Cyclophosphamide with 10 of 10 HLA-A, -B, -C, -DRB1, and -DQB1 Allele-Matched Unrelated Donors and HLA-Identical Sibling Donors: A Multivariable Analysis Including Disease Risk Index. Biol Blood Marrow Transplant. 2016;22(1):125-133.
25. McCurdy SR, Kasamon YL, Kanakry CG, et al. Comparable composite endpoints after HLA-matched and HLA-haploidentical transplantation with post-transplantation cyclophosphamide. Haematologica. 2017; 102(2):391-400.
26. Solomon SR, Sizemore CA, Zhang X, et al. Impact of Donor Type on Outcome after Allogeneic Hematopoietic Cell Transplantation for Acute Leukemia. Biol Blood Marrow Transplant. 2016;22(10): 1816-1822.
27. Wang Y, Liu DH, Xu LP, et al. Superior graft-versus-leukemia effect associated with transplantation of haploidentical compared with HLA-identical sibling donor grafts for high-risk acute leukemia: an historic comparison. Biol Blood Marrow Transplant. 2011;17(6):821-830.
28. Zeidan AM, Forde PM, Symons H, et al. HLA-haploidentical donor lymphocyte infusions for patients with relapsed hematologic malignancies after related HLA-haploidentical bone marrow transplantation. Biol Blood Marrow Transplant. 2014;20(3):314-318.
29. Ghiso A, Raiola AM, Gualandi F, et al. DLI after haploidentical BMT with post-transplant CY. Bone Marrow Transplant. 2015;50(1):56-61.
30. Goldsmith SR, Slade M, DiPersio JF, et al. Donor-lymphocyte infusion following haploidentical hematopoietic cell transplanta-

tion with peripheral blood stem cell grafts and PTCy. Bone Marrow Transplant. 2017;52(12):1623-1628.
31. Yan CH, Liu DH, Liu KY, et al. Risk stratification-directed donor lymphocyte infusion could reduce relapse of standard-risk acute leukemia patients after allogeneic hematopoietic stem cell transplantation. Blood. 2012;119(14):3256-3262.
32. Yan CH, Liu QF, Wu DP, et al. Prophylactic Donor Lymphocyte Infusion (DLI) Followed by Minimal Residual Disease and Graft-versus-Host Disease-Guided Multiple DLIs Could Improve Outcomes after Allogeneic Hematopoietic Stem Cell Transplantation in Patients with Refractory/Relapsed Acute Leukemia. Biol Blood Marrow Transplant. 22017;23(8):1311-1319.
33. Yan CH, Wang JZ, Liu DH, et al. Chemotherapy followed by modified donor lymphocyte infusion as a treatment for relapsed acute leukemia after haploidentical hematopoietic stem cell transplantation without in vitro T-cell depletion: superior outcomes compared with chemotherapy alone and an analysis of prognostic factors. Eur J Haematol. 2013;91(4):304-314.
34. Ma YR, Xu LP, Zhang XH, et al. Comparable post-relapse outcomes between haploidentical and matched related donor allogeneic stem cell transplantation. Bone Marrow Transplant. 2017;52(3):409-414.
35. Mo XD, Zhang XH, Xu LP, et al. Comparison of outcomes after donor lymphocyte infusion with or without prior chemotherapy for minimal residual disease in acute leukemia/myelodysplastic syndrome after allogeneic hematopoietic stem cell transplantation. Ann Hematol. 2017;96(5):829-838.
36. Mo XD, Zhang XH, Xu LP, et al. Salvage chemotherapy followed by granulocyte colony-stimulating factor-primed donor leukocyte infusion with graft-vs.-host disease control for minimal residual disease in acute leukemia/myelodysplastic syndrome after allogeneic hematopoietic stem cell transplantation: prognostic factors and clinical outcomes. Eur J Haematol. 2016;96(3):297-308.
37. Mo XD, Qin YZ, Zhang XH, et al. Minimal residual disease monitoring and preemptive immunotherapy in myelodysplastic syndrome after allogeneic hematopoietic stem cell transplantation. Ann Hematol. 2016;95(8):1233-1240.
38. Huang XJ, Liu DH, Liu KY, et al. Donor lymphocyte infusion for the treatment of leukemia relapse after HLA-mismatched/haploidentical T-cell-replete hematopoietic stem cell transplantation. Haematologica. 2007;92(3):414-417.
39. Yan CH, Xu LP, Liu DH, et al. Low-dose methotrexate may preserve a stronger antileukemic effect than that of cyclosporine after modified donor lymphocyte infusion in unmanipulated haploidentical HSCT. Clin Transplant. 2015;29(7):594-605.
40. Buckley SA, Wood BL, Othus M, et al. Minimal residual disease prior to allogeneic hematopoietic cell transplantation in acute myeloid leukemia: a meta-analysis, Haematologica. 2017;102(5):865-873.
41. Shen Z, Gu X, Mao W, et al. Influence of pre-transplant minimal residual disease on prognosis after Allo-SCT for patients with acute lymphoblastic leukemia: systematic review and meta-analysis. BMC Cancer. 2018;18(1):755.
42. Canaani J, Labopin M, Huang XJ, et al. Minimal residual disease status predicts outcome of acute myeloid leukaemia patients undergoing T-cell replete haploidentical transplantation. An analysis from the Acute Leukaemia Working Party (ALWP) of the European Society for Blood and Marrow Transplantation (EBMT). Br J Haematol. 2018;183(3):411-420.
43. Lee HC, Saliba RM, Rondon G, et al. Mixed T Lymphocyte Chimerism after Allogeneic Hematopoietic Transplantation Is Predictive for Relapse of Acute Myeloid Leukemia and Myelodysplastic Syndromes. Biol Blood Marrow Transplant. 2015;21(11):1948-1954.
44. Koreth J, Kim HT, Nikiforow S, et al. Donor chimerism early after reduced-intensity conditioning hematopoietic stem cell transplantation predicts relapse and survival. Biol Blood Marrow Transplant. 22014;20(10):1516-1521.
45. Solomon SR, Sizemore CA, Zhang X, et al. Preemptive DLI without withdrawal of immunosuppression to promote complete donor T-cell chimerism results in favorable outcomes for high-risk older recipients of alemtuzumab-containing reduced-intensity unrelated donor allogeneic transplant: a prospective phase II trial. Bone Marrow Transplant. 2014;49(5):616-621.
46. Di Grazia C, Pozzi S, Geroldi S, et al. Wilms Tumor 1 Expression and Pre-emptive Immunotherapy in Patients with Acute Myeloid Leukemia Undergoing an Allogeneic Hemopoietic Stem Cell Transplantation. Biol Blood Marrow Transplant. 2016;22(7):1242-1246.
47. Tan Y, Du K, Luo Y, et al. Superiority of preemptive donor lymphocyte infusion based on minimal residual disease in acute leukemia patients after allogeneic hematopoietic stem cell transplantation. Transfusion. 2014;54(6):1493-1500.
48. Shah MV, Jorgensen JL, Saliba RM, et al. Early Post-Transplant Minimal Residual Disease Assessment Improves Risk Stratification in Acute Myeloid Leukemia. Biol Blood Marrow Transplant. 2018;24(7):1514-1520.
49. Keil F, Haas OA, Fritsch G, et al. Donor leukocyte infusion for leukemic relapse after allogeneic marrow transplantation: lack of residual donor hematopoiesis predicts aplasia. Blood. 1997;89(9):3113-3117.
50. Schmid C, Schleuning M, Ledderose G, et al. Sequential regimen of chemotherapy, reduced-intensity conditioning for allogeneic stem-cell transplantation, and prophylactic donor lymphocyte transfusion in high-risk acute myeloid leukemia and myelodysplastic syndrome. J Clin Oncol. 2005;23(24):5675-5687.
51. Tsirigotis P, Liga M, Gkirkas K, et al. Low-dose alemtuzumab for GvHD prevention followed by prophylactic donor lymphocyte infusions in high-risk leukemia. Bone Marrow Transplant. 2017;52(3):445-451.
52. Maschan M, Blagov S, Shelikhova L, et al. Low-dose donor memory T-cell infusion after TCR alpha/beta depleted unrelated and haploidentical transplantation: results of a pilot trial. Bone Marrow Transplant. 2018;53(3):264-273.
53. Schmid C, Labopin M, Schaap N, et al. Prophylactic donor lymphocyte infusion after allogeneic stem cell transplantation in acute leukaemia - a matched pair analysis by the Acute Leukaemia Working Party of EBMT. Br J Haematol. 2018;184(5):782-787.
54. Gao XN, Lin J, Wang SH, et al. Donor lymphocyte infusion for prevention of relapse after unmanipulated haploidentical PBSCT for very high-risk hematologic malignancies. Ann Hematol. 2018;98(1):185-193.
55. Jaiswal SR, Zaman S, Nedunchezhian M, et al. CD56-enriched donor cell infusion after post-transplantation cyclophosphamide for haploidentical transplantation of advanced myeloid malignancies is associated with prompt reconstitution of mature natural killer cells and regulatory T cells with reduced incidence of acute graft versus host disease: A pilot study. Cytotherapy. 2017;19(4):531-542.
56. Jaiswal SR, Zaman S, Chakrabarti A, et al. Improved Outcome of Refractory/Relapsed Acute Myeloid Leukemia after Post-Transplantation Cyclophosphamide-Based Haploidentical Transplantation with Myeloablative Conditioning and Early Prophylactic Granulocyte Colony-Stimulating Factor-Mobilized Donor Lymphocyte Infusions. Biol Blood Marrow Transplant. 2016;22(10):1867-1873.
57. Yan CH, Wang Y, Wang JZ, et al. Minimal residual disease- and graft-vs.-host disease-guided multiple consolidation chemotherapy and donor lymphocyte infusion prevent second acute leukemia relapse after allotransplant. J Hematol Oncol. 2016;9(1):87.
58. Nagler A, Ackerstein A, Or R, et al. Adoptive immunotherapy with haploidentical allogeneic peripheral blood lymphocytes following autologous bone marrow transplantation. Exp Hematol. 2000;28(11):1225-1231.
59. Call SK, Kasow KA, Barfield R, et al. Total and active rabbit antithymocyte globulin (rATG;Thymoglobulin) pharmacokinetics in pediatric patients undergoing unrelated donor bone marrow transplantation. Biol Blood Marrow Transplant. 2009;15(2):274-278.
60. Gilman AL, Leung W, Cowan MJ, et al. Donor lymphocyte infusion and methotrexate for immune recovery after T-cell depleted haploidentical transplantation. Am J Hematol. 2018;93(2):169-178.
61. Martelli MF, Di Ianni M, Ruggeri L, et al. HLA-haploidentical transplantation with regulatory and conventional T-cell adoptive immunotherapy prevents acute leukemia relapse. Blood. 2014;124(4):638-644.
62. Dodero A, Carniti C, Raganato A, et al. Haploidentical stem cell transplantation after a reduced-intensity conditioning regimen for the treatment of advanced hematologic malignancies: posttransplantation CD8-depleted donor lymphocyte infusions contribute to improve T-cell recovery. Blood. 2009;113(19):4771-4779.
63. Perruccio K, Tosti A, Burchielli E, et al. Transferring functional immune responses to pathogens after haploidentical hematopoietic transplantation. Blood. 2005;106(13):4397-4406.
64. Edinger M, Hoffmann P, Ermann J, et al. CD4+CD25+ regulatory T cells preserve graft-versus-tumor activity while inhibiting graft-versus-host disease after bone marrow transplantation. Nat Med. 2003;9(9):1144-1150.
65. Lewalle P, Triffet A, Delforge A, et al. Donor lymphocyte infusions in adult haploidentical transplant: a dose finding study. Bone Marrow Transplant. 2003;31(1):39-44.
66. Wang Y, Liu DH, Xu LP, et al. Prevention of relapse using granulocyte CSF-primed PBPCs following HLA-mismatched/haploidentical, T-cell-replete hematopoietic SCT in patients with advanced-stage acute leukemia: a retrospective risk-factor analysis. Bone Marrow Transplant. 2012;47(8):1099-1104.

67. Cauchois R, Castagna L, Pagliardini T, et al. Prophylactic donor lymphocyte infusions after haploidentical haematopoietic stem cell transplantation for high risk haematological malignancies: a retrospective bicentric analysis of serial infusions of increasing doses of CD3(+) cells. Br J Haematol. 2019;185(3):570-573.
68. Dazzi F, Szydlo RM, Cross NC, et al. Durability of responses following donor lymphocyte infusions for patients who relapse after allogeneic stem cell transplantation for chronic myeloid leukemia. Blood. 2000;96(8):2712-2716.
69. Yan CH, Liu DH, Xu LP, et al. Modified donor lymphocyte infusion-associated acute graft-versus-host disease after haploidentical T-cell-replete hematopoietic stem cell transplantation: incidence and risk factors. Clin Transplant. 2012;26(6):868-876.
70. Jun HX, Jun CY, Yu ZX. In vivo induction of T-cell hyporesponsiveness and alteration of immunological cells of bone marrow grafts using granulocyte colony-stimulating factor. Haematologica. 2004;89(12):1517-1524.
71. Wen Q, Kong Y, Zhao HY, et al. G-CSF-induced macrophage polarization and mobilization may prevent acute graft-versus-host disease after allogeneic hematopoietic stem cell transplantation. Bone Marrow Transplant. 2019;54(9):1419-1433.
72. Chen SH, Li X, Huang XJ. Effect of recombinant human granulocyte colony-stimulating factor on T-lymphocyte function and the mechanism of this effect. Int J Hematol. 2004;79(2):178-184.
73. Huang XJ, Chang YJ, Zhao XY. Maintaining hyporesponsiveness and polarization potential of T cells after in vitro mixture of G-CSF mobilized peripheral blood grafts and G-CSF primed bone marrow grafts in different proportions. Transpl Immunol. 2007;17(3):193-197.
74. Gómez-De León A, Colunga Pedraza PR, Garcia-Camarillo DE, et al. Donor Lymphocyte Infusion from G-CSF-Primed, Unmanipulated Whole Blood Is Safe and Improves Chimerism in HLA-Matched and Haploidentical Transplantation. Blood. 2018;132(Suppl 1):4602.
75. Bracci L, Moschella F, Sestili P, et al. Cyclophosphamide enhances the antitumor efficacy of adoptively transferred immune cells through the induction of cytokine expression, B-cell and T-cell homeostatic proliferation, and specific tumor infiltration. Clin Cancer Res. 2007;13(2 Pt 1):644-653.
76. He F, Warlick E, Miller JS, et al. Lymphodepleting chemotherapy with donor lymphocyte infusion post-allogeneic HCT for hematological malignancies is associated with severe, but therapy-responsive aGvHD. Bone Marrow Transplant. 2016;51(8): 1107-1112.
77. Goodyear O, Agathanggelou A, Novitzky-Basso I, et al. Induction of a CD8+ T-cell response to the MAGE cancer testis antigen by combined treatment with azacitidine and sodium valproate in patients with acute myeloid leukemia and myelodysplasia. Blood. 2010;116(11):1908-1918.
78. Guillaume T, Yakoub-Agha I, Tabrizi R, et al. Prospective Phase II Study of Prophylactic Azacitidine and Donor Lymphocyte Infusions Following Allogeneic Hematopoietic Stem Cell Transplantation for High Risk Acute Myeloid Leukemia and Myelodysplastic Syndrome. Blood. 2016;128(22):1162.
79. Schroeder T, Rautenberg C, Haas R, Kobbe G. Hypomethylating agents after allogeneic blood stem cell transplantation. Stem Cell Investig. 2016;3:84.
80. Schroeder T, Czibere A, Platzbecker U, et al. Azacitidine and donor lymphocyte infusions as first salvage therapy for relapse of AML or MDS after allogeneic stem cell transplantation. Leukemia. 2013;27(6):1229-1235.
81. Schroeder T, Rautenberg C, Kruger W, et al. Treatment of relapsed AML and MDS after allogeneic stem cell transplantation with decitabine and DLI-a retrospective multicenter analysis on behalf of the German Cooperative Transplant Study Group. Ann Hematol. 2018;97(2):335-342.
82. Bazarbachi A, Labopin M, Battipaglia G, et al. Allogeneic Stem Cell Transplantation for FLT3-Mutated Acute Myeloid Leukemia: In vivo T-Cell Depletion and Posttransplant Sorafenib Maintenance Improve Survival. A Retrospective Acute Leukemia Working Party-European Society for Blood and Marrow Transplant Study. Clin Hematol Int. 2019;1(1):58-74.
83. Canaani J. Management of AML Beyond "3 + 7" in 2019. Clin Hematol Int. 2019;1:10-18.
84. Schmidt SA, Holter Chakrabarty J, Liu Y, et al. Tyrosine Kinase Inhibitors with or without Donor Lymphocyte Infusion Continue to Provide Long-Term Survival after Relapse of Chronic Myeloid Leukemia Following Hematopoietic Cell Transplantation. Blood. 2018;132(Suppl 1):704.
85. Vago L, Perna SK, Zanussi M, et al. Loss of mismatched HLA in leukemia after stem-cell transplantation. N Engl J Med. 2009;361(5):478-488.
86. Crucitti L, Crocchiolo R, Toffalori C, et al. Incidence, risk factors and clinical outcome of leukemia relapses with loss of the mismatched HLA after partially incompatible hematopoietic stem cell transplantation. Leukemia. 2015;29(5):1143-1152.
87. Imus PH, Blackford AL, Bettinotti M, et al. Major Histocompatibility Mismatch and Donor Choice for Second Allogeneic Bone Marrow Transplantation. Biol Blood Marrow Transplant. 2017;23(11):1887-1894.
88. McCurdy SR, Iglehart BS, Batista DA, et al. Loss of the Mismatched Human Leukocyte Antigen Haplotype in Two Acute Myelogenous Leukemia Relapses after Haploidentical Bone Marrow Transplantation with Posttransplantation Cyclophosphamide. Leukemia. 2016;30(10):2102-2106.
89. Russo A, Oliveira G, Berglund S, et al. NK cell recovery after haploidentical HSCT with posttransplant cyclophosphamide: dynamics and clinical implications. Blood. 2018;131(2):247-262.
90. Jaiswal SR, Bhakuni P, Bharadwaj P, et al. CTLA4Ig Primed Donor Lymphocyte Infusions (DLI): A Novel Approach to Natural Killer Cell Immunotherapy Following Haploidentical PBSC Transplantation for Advanced Hematological Malignancies. Blood. 2017;130(Suppl 1):4468.
91. Ciurea SO, Schafer JR, Bassett R, et al. Phase 1 clinical trial using mbIL21 ex vivo-expanded donor-derived NK cells after haploidentical transplantation. Blood. 2017;130(16):1857-1868.
92. Szczepanski MJ, Szajnik M, Welsh A, et al. Interleukin-15 enhances natural killer cell cytotoxicity in patients with acute myeloid leukemia by upregulating the activating NK cell receptors. Cancer Immunol Immunother. 2010;59(1):73-79.
93. Romee R, Rosario M, Berrien-Elliott MM, et al. Cytokine-induced memory-like natural killer cells exhibit enhanced responses against myeloid leukemia. Sci Transl Med. 2016;8(357):357ra123.
94. Langenkamp U, Siegler U, Jorger S, et al. Human acute myeloid leukemia CD34+CD38- stem cells are susceptible to allorecognition and lysis by single KIR-expressing natural killer cells. Haematologica. 2009;94(11):1590-1594.
95. Roy D-C, Walker I, Maertens J, et al. Efficacy and Safety of a Single Dose of Donor Lymphocytes Depleted of Alloreactive T-Cells (ATIR101) Following T-Cell-Depleted Haploidentical HSCT: A Pooled Analysis of Two Phase II Studies. Blood. 2018;132(Suppl 1):120.
96. Davies JK, Brennan LL, Wingard JR, et al. Infusion of Alloanergized Donor Lymphocytes after CD34-selected Haploidentical Myeloablative Hematopoietic Stem Cell Transplantation. Clin Cancer Res. 2018;24(17):4098-4109.
97. Di Stasi A, Tey SK, Dotti G, et al. Inducible apoptosis as a safety switch for adoptive cell therapy. N Engl J Med. 2011;365(18):1673-1683.
98. Merli P, Bertaina V, Galaverna F, et al. Donor T Cells Genetically Modified with a Novel Suicide Gene (inducible Caspase 9, iC9) Expand and Persist over Time after Post-Allograft Infusion in Patients Given αβ T-Cell and B-Cell Depleted HLA-Haploidentical Allogeneic Stem Cell Transplantation (αβ haplo-HSCT) Contributing to Accelerate Immune Recovery. Blood. 2017;130(Suppl 1):211.
99. Research CfDEa. Approved Drugs - FDA approves tisagenlecleucel for B-cell ALL and tocilizumab for cytokine release syndrome. 2018.
100. Neelapu SS, Locke FL, Bartlett NL, et al. Axicabtagene Ciloleucel CAR T-Cell Therapy in Refractory Large B-Cell Lymphoma. N Engl J Med. 2017;377(26):2531-2544.
101. Kebriaei P, Ciurea SO, Huls MH, et al. Pre-Emptive Donor Lymphocyte Infusion with CD19-Directed, CAR-Modified T Cells Infused after Allogeneic Hematopoietic Cell Transplantation for Patients with Advanced CD19⁺ Malignancies. Blood. 2015;126(23):862.
102. Liu J, Zhong JF, Zhang X, et al. Allogeneic CD19-CAR-T cell infusion after allogeneic hematopoietic stem cell transplantation in B cell malignancies. J Hematol Oncol. 2017;10(1):35.
103. Radestad E, Wikell H, Engstrom M, et al. Alpha/beta T-cell depleted grafts as an immunological booster to treat graft failure after hematopoietic stem cell transplantation with HLA-matched related and unrelated donors. J Immunol Res. 2014;2014:578741.
104. Durer C, Durer S, Shafqat M, et al. Concomitant Use of Blinatumomab and Donor Lymphocyte Infusion for Post-Transplant Relapsed CD19 Positive Acute Lymphoblastic Leukemia. Syst Rev. 2018;132:5742
105. Christopher MJ, Petti AA, Rettig MP, et al Immune Escape of Relapsed AML Cells after Allogeneic Transplantation. N Engl J Med. 2018;379(24):2330-2341.
106. Or R, Hadar E, Bitan M, et al. Safety and efficacy of donor lymphocyte infusions following mismatched stem cell transplantation. Biol Blood Marrow Transplant. 2006;12(12):1295-1301.

ARTICLE

Ttc7a regulates hematopoietic stem cell functions while controlling the stress-induced response

Claire Leveau,[1,2] Tania Gajardo,[1,2] Marie-Thérèse El-Daher,[1,2] Nicolas Cagnard,[2,3,4] Alain Fischer,[2,5,6,7] Geneviève de Saint Basile[1,2,8,*] and Fernando E. Sepulveda[1,2,9,*]

[1]Laboratory of Normal and Pathological Homeostasis of the Immune System, INSERM UMR 1163, Imagine Institute, Paris; [2]Université Paris Descartes -Sorbonne Paris Cité, Imagine Institute, Paris; [3]Bioinformatic Platform, INSERM UMR 1163, Université Paris Descartes-Sorbonne Paris Cité, Imagine Institute, Paris; [4]Structure Fédérative de Recherche (SFR) Necker, INSERM US24/CNRS UMS 3633, Paris; [5]Assistance Publique-Hôpitaux de Paris, Hôpital Necker-Enfants Malades Immunology and Pediatric Hematology Department, Paris; [6]Collège de France, Paris, France; [7]INSERM UMR1163, Paris; [8]Assistance Publique-Hôpitaux de Paris, Hôpital Necker-Enfants Malades, Centre d'Etudes des Déficits Immunitaires, Paris and [9]Centre National de la Recherche Scientifique – CNRS, Paris, France

** These authors contributed equally to this work*

Ferrata Storti Foundation

Haematologica 2020
Volume 105(1):59-70

ABSTRACT

The molecular machinery that regulates the balance between self-renewal and differentiation properties of hematopoietic stem cells (HSC) has yet to be characterized in detail. Here we found that the tetratricopeptide repeat domain 7 A (Ttc7a) protein, a putative scaffold protein expressed by HSC, acts as an intrinsic regulator of the proliferative response and the self-renewal potential of murine HSC *in vivo*. Loss of Ttc7a consistently enhanced the competitive repopulating ability of HSC and their intrinsic capacity to replenish the hematopoietic system after serial cell transplantations, relative to wildtype cells. Ttc7a-deficient HSC exhibit a different transcriptomic profile for a set of genes controlling the cellular response to stress, which was associated with increased proliferation in response to chemically induced stress *in vitro* and myeloablative stress *in vivo*. Our results therefore revealed a previously unrecognized role of Ttc7a as a critical regulator of HSC stemness. This role is related, at least in part, to regulation of the endoplasmic reticulum stress response.

Introduction

In flaky skin (*fsn*) mice, the spontaneous insertion of early transposon into the gene for tetratricopeptide repeat domain 7 A (*Ttc7a*) is known to impair Ttc7a protein expression.[1,2] Consequently, *fsn* mice develop a proliferative lymphoid and myeloid disorder, with hyperplasia of the spleen and lymph nodes, elevated monocyte, granulocyte and lymphoid cell counts,[3-6] and severe anemia.[7] Moreover, *fsn* mice have a reduced lifespan and changes in the skin (epidermal hyperplasia and inflammation)[8,9] and the intestinal tract (gastric papillomas).[10] The marked phenotypic alterations in *fsn* mice suggest that Ttc7a protein has one or more major regulatory roles in the hematopoietic system, and, potentially, in other tissues of epithelial origin.

Ttc7a is a putative scaffolding protein as it contains nine tetratricopeptide repeats (TPR) domains that are predicted to interact with proteins containing their own TPR or other motifs.[11] These TPR-containing proteins are involved in a variety of biological processes, including cell cycle control, protein trafficking, secretion and protein quality control. Indeed, TPR-containing proteins have been shown to bind chaperones such as Hsp90 and Hsp70, controlling their activity.[12-14] Thus, Ttc7a is likely to be involved in a broad range of protein complexes and hence functions. *In vitro* studies have shown that the loss of Ttc7a causes inappropriate activation of RhoA-dependent effectors and thus disrupts cytoskeletal dynamics.[15,16]

Correspondence:

GENEVIÈVE DE SAINT BASILE
genevieve.de-saint-basile@inserm.fr

FERNANDO E. SEPULVEDA
fernando.sepulveda@inserm.fr

Received: September 18, 2018.

Accepted: April 17, 2019.

Pre-published: April 19, 2019.

doi:10.3324/haematol.2018.207100

Check the online version for the most updated information on this article, online supplements, and information on authorship & disclosures: www.haematologica.org/content/105/1/59

Furthermore, TTC7A reportedly interacts with EFR3 homolog B and phosphatidylinositol 4-kinase alpha, which is known to catalyze the production of phosphatidylinositol 4-phosphate at the plasma membrane in yeast and human cells.[17,18] This observation emphasizes the conservation, at least in part, of the functions of Ttc7a during evolution. However, data on TTC7A's biological function(s) are still scarce.

Inadequate proliferation of peripheral hematopoietic lineages has been reported in several modified murine models; this impairment is ultimately associated with the exhaustion of the hematopoietic stem cell (HSC) pool.[19] Indeed, the production of blood cells requires HSC to leave their quiescent state and differentiate into functional progeny. An excessive requirement for hematopoietic cell production biases HSC function toward differentiation, at the expense of self-renewal.[20] Various intrinsic and extrinsic factors influence HSC fate, i.e. quiescence or proliferation. Endoplasmic reticulum (ER) stress has recently been highlighted as an important regulator of HSC function.[21] This stress is triggered by various stimuli and leads to the accumulation of unfolded proteins in the lumen of the ER, and induction of the unfolded protein response (UPR). The chaperone BIP (Hspa5/GRP78) is the main inducer of the UPR.[22] This response results in enhanced expression of chaperone proteins (heat shock proteins, Hsp), phosphodiesterase (Pdi), and other proteins such as calreticulin that, together with BIP, boost protein folding capacities. Depending on the intensity of the ER stress, UPR activation can lead to apoptosis or survival.[23]

In the present study, we found that Ttc7a regulates murine HSC self-renewal and hematopoietic reconstitution potential and controls the sensitivity of these cells to stress. Loss of Ttc7a consistently enhanced HSC stemness, since Ttc7a-deficient HSC displayed a greater proliferation capacity than control counterparts in response to ER stress *in vitro*, and after myeloablative stress *in vivo*. Hence, our results reveal a new role for Ttc7a as a regulator of self-renewal and response to stress in HSC.

Methods

Mice

Heterozygous Balb/cByJ *fsn* (CByJ.A-Ttc7fsn/J) mice and Balb/cByJ CD45.1 (CByJ.SJL(B6)-Ptprca/J) mice were obtained from the Jackson Laboratory. All mice were maintained in specific pathogen-free conditions and handled according to national and institutional guidelines.

Repopulations assays

Bone marrow (BM) cells were transferred into CD45.1$^+$ control recipient mice upon irradiation and then 30,000 Lin$^-$ Sca1$^+$ cKit$^+$ (LSK) donor cells were injected into the irradiated recipient mice. For serial transplantations, recipients were reconstituted with 10^7 BM cells. To perform competitive repopulation assays, 1,000 LSK cells were injected with 2 x 10^6 unfractionated CD45.1$^+$ BM cells. Twelve weeks after transfer, mice were treated with a single dose of 5-fluorouracil (5-FU, 150 mg/kg).

Flow cytometry and isolation of hematopoietic stem cells

Splenocytes and peripheral blood cells were incubated with conjugated antibodies and viability exclusion dyes. The antibodies used are listed in *Online Supplementary Table S2*. Stained cells were quantified using a Gallios flow cytometer (Beckman Coulter), and analyzed with FlowJo software (Treestar). HSC and LSK cells were isolated by depleting Lin$^+$ cells using the Lineage Cell Depletion Kit according to the manufacturer's protocol (Miltenyi Biotec), stained with a Lin$^-$ antibody cocktail, and antibodies against CD117, Sca-1, CD150 and CD48, and sorted with FACS Aria™ (BD Biosciences).

Cell culture

Lin$^-$ cells were cultured in StemSpan medium (StemCell Technologies) supplemented with 5% fetal bovine serum, 1% penicillin/streptomycin, recombinant human thrombopoietin (100 μg/mL), recombinant murine stem cell factor (100 μg/mL) and recombinant murine FLT3 ligand (100 μg/mL). Tunicamycin (Cayman Chemical) was added (0.6 or 1.2 μg/mL) for 24 or 48 h.

RNA-sequencing

RNA was extracted using the ZR-RNA MicroPrep™ isolation kit (Proteinegene). cDNA libraries were generated using the Ovation SoLo RNA-seq system (NuGEN). The libraries were controlled with a High Sensitivity DNA Analysis Kit and Bioanalyzer (Agilent). NextSeq 500 (Illumina) was used for sequencing. FASTQ files were mapped to the ENSEMBL MM38 reference using Hisat2 and counts were produced with feature Counts. Read count normalization and group comparisons were performed by DESeq2, edgeR, and LimmaVoom. Heatmaps were made with R and imaged by Java Treeview software. Differentially expressed genes were examined with gene set enrichment analysis (GSEA) for functional enrichment in gene ontology (GO) terms using normalized expression values of LimmaVoom.

Western blot

Lin$^-$ cells were cultured for 3 days and HSC were sorted directly into 10% trichloroacetic acid. Proteins were extracted and solubilized as previously described.[24]

Statistical analysis

Data were analyzed with GraphPad Prism 6 software. Statistical analyses were performed using two-tailed Student t-test. Differences were considered to be statistically significant when $P<0.05$ (indicated as $^*P<0.05$, $^{**}P<0.01$, $^{***}P<0.001$ and $^{****}P<0.0001$).

Data availability

The data are available at the Sequence Read Analysis (SRA) database under accession number SRA139913.

Results

Ttc7a is required for the maintenance of immune homeostasis

It has previously been shown that adult Ttc7a-deficient (*fsn*) mice (aged 8 to 10 weeks) develop an imbalance in hematopoiesis, characterized by leukocytosis and anemia.[7] To gain insight into the change over time in the *fsn* mice's pathology, we analyzed the different hematopoietic lineages in the blood and the spleen at 3, 6 and 12 weeks of age. *Fsn* mice had a considerably higher circulating leukocyte count than control littermates (*ctrl*) at all time points (Figure 1A). The spleen was much larger in *fsn* mice than in *ctrl* mice, twice as large at 3 weeks and ten times larger at 12 weeks (Figure 1B). The splenic architecture in *fsn* mice became increasingly disorganized, with an age-related expansion of red and white pulp (Figure 1C).

Furthermore, histological assessment of splenic sections revealed extramedullary hematopoiesis as evidenced by elevated counts of megakaryocytes (Figure 1C) and of hematopoietic stem and progenitor cells (HSPC) (*Online Supplementary Figure S1*). Relative to *ctrl* mice, the absolute splenic T-cell count in *fsn* mice was slightly lower at 3 weeks of age but higher at 6 and 12 weeks of age (Figure 1D). A large proportion of Ttc7a-deficient T lymphocytes had an effector memory phenotype ($CD44^+$ $CD62L^-$) (Figure 1E). Splenic B-cell counts were slightly elevated, and B cells presented the impaired maturation phenotype previously described in *fsn* mice[6] (Figure 1F). The lymphoid alterations were accompanied by massive myeloproliferation, with an increase over time in the numbers of splenic granulocytes (both neutrophils and eosinophils) and resident and inflammatory monocytes (Figure 1G, H). Thus, Ttc7a-deficient mice displayed a number of persistent hematopoietic alterations (i.e., leukocytosis, T-lymphocyte activation and anemia) at a very early age, whereas other manifestations appeared later in life and/or were exacerbated with age (i.e., myeloproliferation and elevated T-cell counts).

Since all the peripheral hematopoietic lineages were affected in *fsn* mice, we next looked at whether the HSPC compartment was also altered. BM cellularity in *fsn* mice, in contrast to *ctrl* mice, increased between 3 and 12 weeks of age (Figure 2A). The LSK stem cell population was slightly higher in *fsn* mice than in *ctrl* mice at all the time

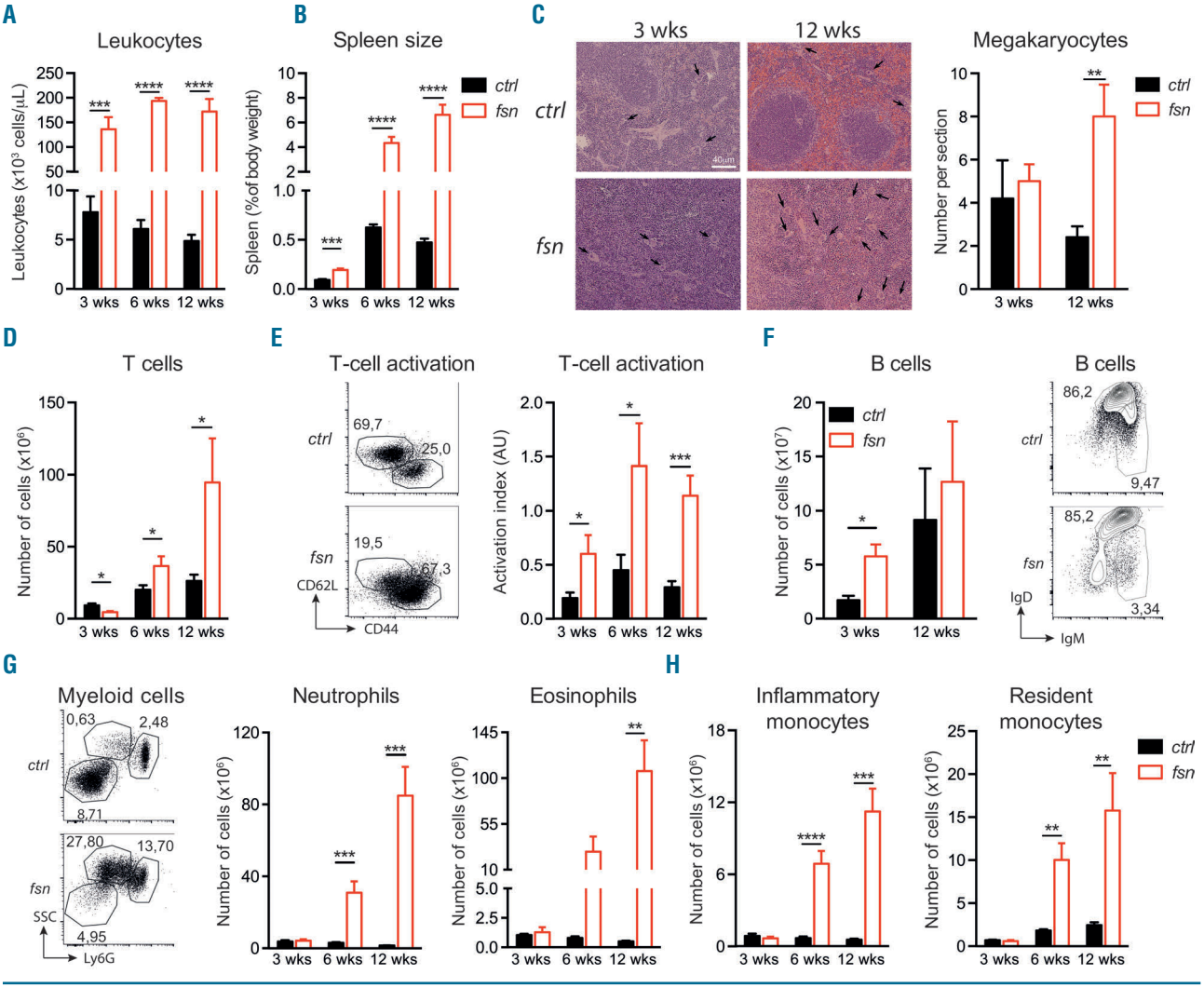

Figure 1. Ttc7a-deficiency perturbs homeostasis of all immune populations. Control littermates (*ctrl* – black bars) and Ttc7a-deficient (*fsn* – red bars) mice were analyzed at 3, 6 and 12 weeks of age (mean ± standard error of mean) **P*<0.05; ***P*<0.01; ****P*<0.001; *****P*<0.0001 (two-tailed *t*-test). (A) White blood cell count (n≥6). (B) Spleen size determined as percent of body weight (n≥6). (C) Histological sections of spleen stained with hematoxylin and eosin showing megakaryocytes (black arrow) (left panel) and quantification of spleen megakaryocytes (right panel). (D) Total number of T cells in the spleen (n≥7). (E) Flow cytometry representative of T-cell activation (according to CD44 and CD62L expression) at 12 weeks (left panel), and activation index of T cells [ratio of effector memory T cells ($CD44^+$ $CD62L^-$) to naïve T cells ($CD44^-$ $CD62L^+$)] (right panel) of *fsn* and *ctrl* mice (n≥7). Numbers adjacent to the outlined areas indicate percent cells in the parent gate (mean). (F) Total number of B cells in the spleen (n=4) (left panel) and flow cytometry representative of B-cell maturation (according to IgM and IgD expression) (right panel). (G) Representative flow cytometry at 12 weeks (left panel) and total number of neutrophils ($CD11b^+$ $Ly6G^{hi}$) and eosinophils ($CD11b^+$ $Ly6G^{int}$ SSC^{hi}). (H) Total number of inflammatory ($CD11b^+$ $Ly6G^-$ $Ly6C^+$) and resident monocytes ($CD11b^+$ $Ly6G^-$ $Ly6C^-$) (n≥6). Numbers adjacent to the outlined areas indicate percent cells among leukocytes in the spleen (mean).

points analyzed (*Online Supplementary Figure S2A*). The proportion of HSC (Lin$^-$ Sca1$^+$ cKit$^+$ CD150$^+$ CD48$^-$)[25] was decreased in *fsn* mice, whereas the proportion of more mature hematopoietic progenitor cells (HPC-1: Lin$^-$ Sca1$^+$ cKit$^+$ CD150$^-$ CD48$^+$) was increased, compared to the proportions in *ctrl* mice (Figure 2B and *Online Supplementary Figure S2B*). At 12 weeks of age, the HSC progenitor count was significantly lower in *fsn* mice than in *ctrl* mice, while the numbers of multipotent progenitors (MPP: Lin$^-$ Sca1$^+$ cKit$^+$ CD150$^-$ CD48$^+$) were unchanged and those of HPC-2 (Lin$^-$ Sca1$^+$ cKit$^+$ CD150$^+$ CD48$^+$) and HPC-1 were slightly higher (Figure 2C). Within the committed progenitor compartment, the numbers of common myeloid progenitors (CMP: Lin$^-$ Sca1$^-$ cKit$^+$ CD34$^+$ CD16/32^{low}) and granulocyte-monocyte progenitors (GMP: Lin$^-$ Sca1$^-$ cKit$^+$ CD34$^+$ CD16/32$^+$) were lower than *ctrl* values at 3 weeks of age, although the differences disappeared with time (Figure 2D, E). There were no significant differences in *fsn vs. ctrl* values in the numbers of common lymphoid progenitors (CLP: Lin$^-$ Sca1$^-$ cKit^{int}) or megakaryocyte-erythrocyte progenitors (MEP: Lin$^-$ Sca1$^-$ cKit$^+$ CD34$^-$ CD16/32$^-$) (Figure 2D, E). We confirmed previous reports that the profound anemia observed in *fsn* mice (*Online Supplementary Figure S3A*) is peripheral in nature and does not result from a decreased number of early erythroid progenitors but rather from a defect in the last step of erythropoiesis (*Online Supplementary Figure S3B, C*).[7] Erythropoiesis and enucleation processes have been shown to involve chromatin compaction[26] and actin cytoskeleton dynamics.[27] Interestingly, we previously showed that Ttc7a plays a role in actin dynamics[15,16] as well as in chromatin compaction and genomic stability.[28] Hence, it is tempting to speculate that altered actin dynamics and chromatin organization, as a consequence of Ttc7a-deficiency, contribute to defective erythrocyte generation in *fsn* mice. A high splenic erythroblast count

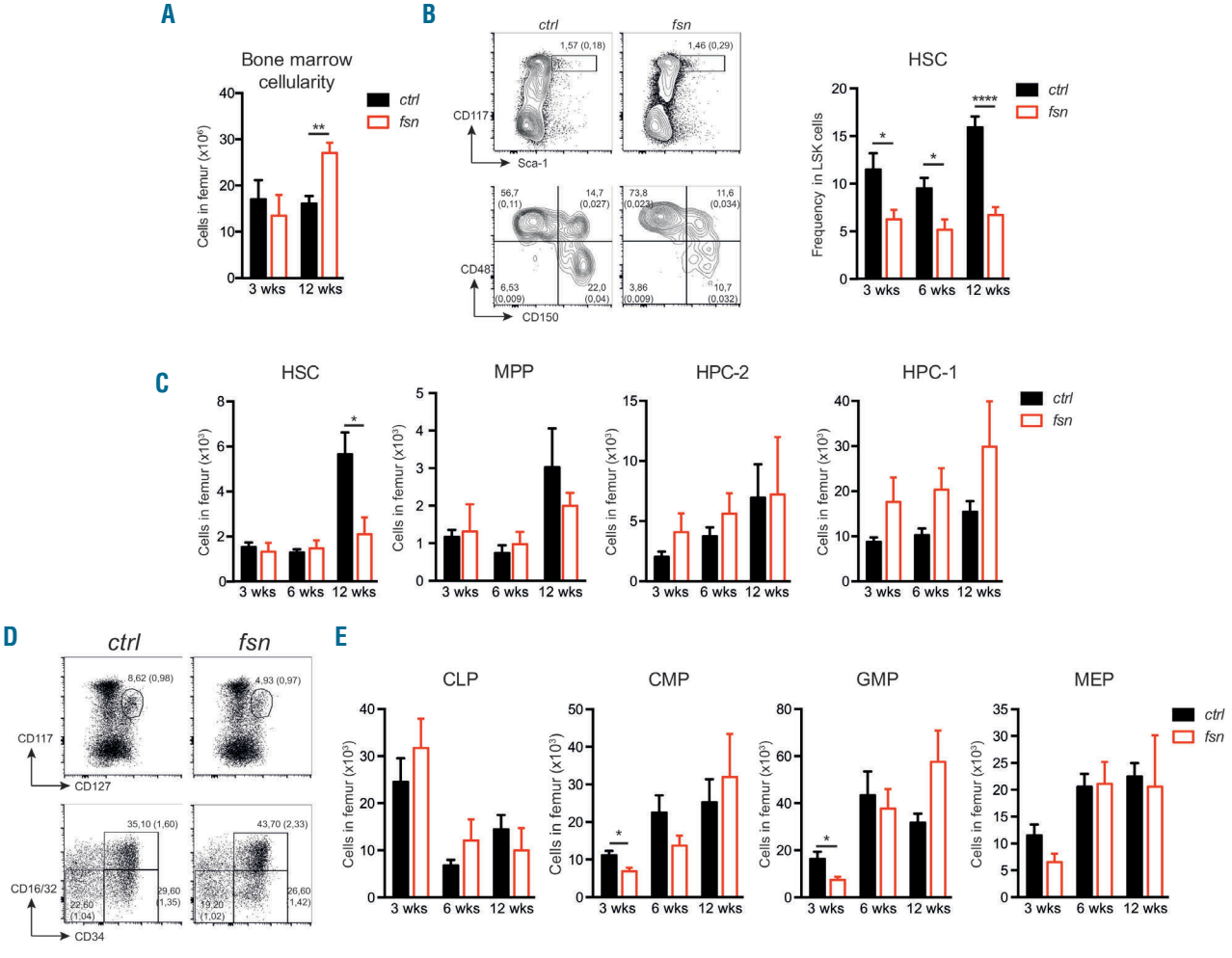

Figure 2. Ttc7a-deficiency alters the hematopoietic stem and progenitor cell compartment. The hematopoietic stem and progenitor cell compartment was analyzed in the bone marrow (BM) of 3-, 6-, and 12-week old control (*ctrl* - black bars) and Ttc7a-deficient (*fsn* - red bars) mice (mean ± standard error of mean) *P<0.05; **P<0.01; ****P<0.0001 (two-tailed *t*-test). (A) Quantification of total femoral BM cells (n≥6). (B) Representative flow cytometry at 12 weeks (left panel) and percentage of hematopoietic stem cells (HSC: Lin$^-$ Sca1$^+$ cKit$^+$ CD150$^+$ CD48$^-$) among LSK (Lin$^-$ Sca1$^+$ cKit$^+$) cells (right panel) (n≥7). (C) Quantification of LSK cell populations, HSC, multipotent progenitors (MPP: Lin$^-$ Sca1$^+$ cKit$^+$ CD150$^-$ CD48$^+$), HPC-2 (Lin$^-$ Sca1$^+$ cKit$^+$ CD150$^+$ CD48$^+$) and HPC-1 (Lin$^-$ Sca1$^+$ cKit$^+$ CD150$^-$ CD48$^+$). (D) Representative flow cytometry at 12 weeks and (E) quantification of common lymphoid progenitors (CLP: Lin$^-$ Sca1$^-$ cKit^{int} CD127$^+$), common myeloid progenitors (CMP: Lin$^-$ Sca1$^-$ cKit$^+$ CD34$^+$ CD16/32$^-$), granulocyte-monocyte progenitors (GMP: Lin$^-$ Sca1$^-$ cKit$^+$ CD34+ CD16/32$^+$) and megakaryocyte-erythroid progenitors (MEP: Lin$^-$ Sca1$^-$ cKit$^+$ CD34$^-$ CD16/32$^-$) (n≥7). (B-D) Numbers adjacent to outlined areas indicate percent cells in the parent gate (mean). Numbers in parentheses indicate percentage among leukocytes in the BM (mean).

suggested the presence of stress erythropoiesis as a possible attempt to compensate for the peripheral anemia (*Online Supplementary Figure S3B*).

Thus, our present results show that the absence of Ttc7a in *fsn* mice is associated with deregulation of the homeostatic balance between hematopoietic lineages, from the HSC stage onwards, and a tendency of all leukocyte subsets to expand over time.

Ttc7a has an intrinsic role in the fate of progenitor cells

Since Ttc7a is broadly expressed, it was not possible to distinguish the respective involvements of hematopoietic factors (i.e., HSC) and non-hematopoietic factors (e.g., BM niches and the thymic epithelium) in the generation of the *fsn* phenotype. In a previous study we found that the skin barrier is impaired in *fsn* mice;[9] this defect may enhance antigen sensitization and thus induce immune system activation. Therefore, in order to determine the Ttc7a-deficient hematopoietic cells' intrinsic contribution to *fsn*-associated hematologic manifestations, we generated chimeric mice by reconstituting lethally irradiated control recipients with LSK cells purified from either *ctrl* or *fsn* mice. Hereafter, these chimeric mice are respectively referred to as Ctrl^{ctrl} and Ctrl^{fsn}. Three-week old mice were chosen as donors so that we could use a similar LSK graft inoculum in both control and *fsn* samples, and thus minimize the potential immune consequences caused by the altered *fsn* skin barrier. We monitored the hematologic reconstitution over time by collecting blood samples from the recipient mice every 2 weeks. As observed in native *fsn* mice, white blood cell counts were higher in Ctrl^{fsn} mice than in Ctrl^{ctrl} mice, and a difference was observed as early as 4 weeks after transplantation (Figure 3A). The Ctrl^{fsn} mice were also anemic (Figure 3B) and developed splenomegaly (Figure 3C), although the latter was less pronounced than in native *fsn* mice (Figure 1B). The total body weight of Ctrl^{ctrl} and Ctrl^{fsn} mice was not different. The distribution of the splenic myeloid, T- and B-cell populations was the same as in *ctrl* mice (Figure 3D). As observed in *fsn* mice, BM cellularity was higher in Ctrl^{fsn} mice than in Ctrl^{ctrl} mice (Figure 3E), whereas the LSK counts were slightly increased (Figure 3F). The distribution of the HSC, MPP, HPC-2 and HPC-1 populations was similar in Ctrl^{fsn} and Ctrl^{ctrl} mice, suggesting that the low HSC count observed in 12-week old native *fsn* mice (Figure 2C) is primarily caused by external (i.e., non-hematopoietic) factors. Taken as a whole, these data suggest that Ttc7a has an intrinsic role in hematopoietic cells; the absence of Ttc7a in hematopoietic progenitors results in the over-proliferation of the various cell lineages as seen in native *fsn* mice.

Loss of Ttc7a enhances the reconstitution potential of hematopoietic stem cells

Next, we sought to determine the impact of Ttc7a loss on the reconstitution potential of HSC in a controlled *in vivo* environment. Using lethally irradiated congenic recipients, we transferred equal numbers of LSK cells purified from 3-week old *ctrl* (LSK^{ctrl})- or *fsn* (LSK^{fsn})-(CD45.2^{+}) mice together with competitor wildtype-(CD45.1^{+}) BM cells (i.e., Ctrl-LSK^{ctrl} or Ctrl-LSK^{fsn}). We then assessed the

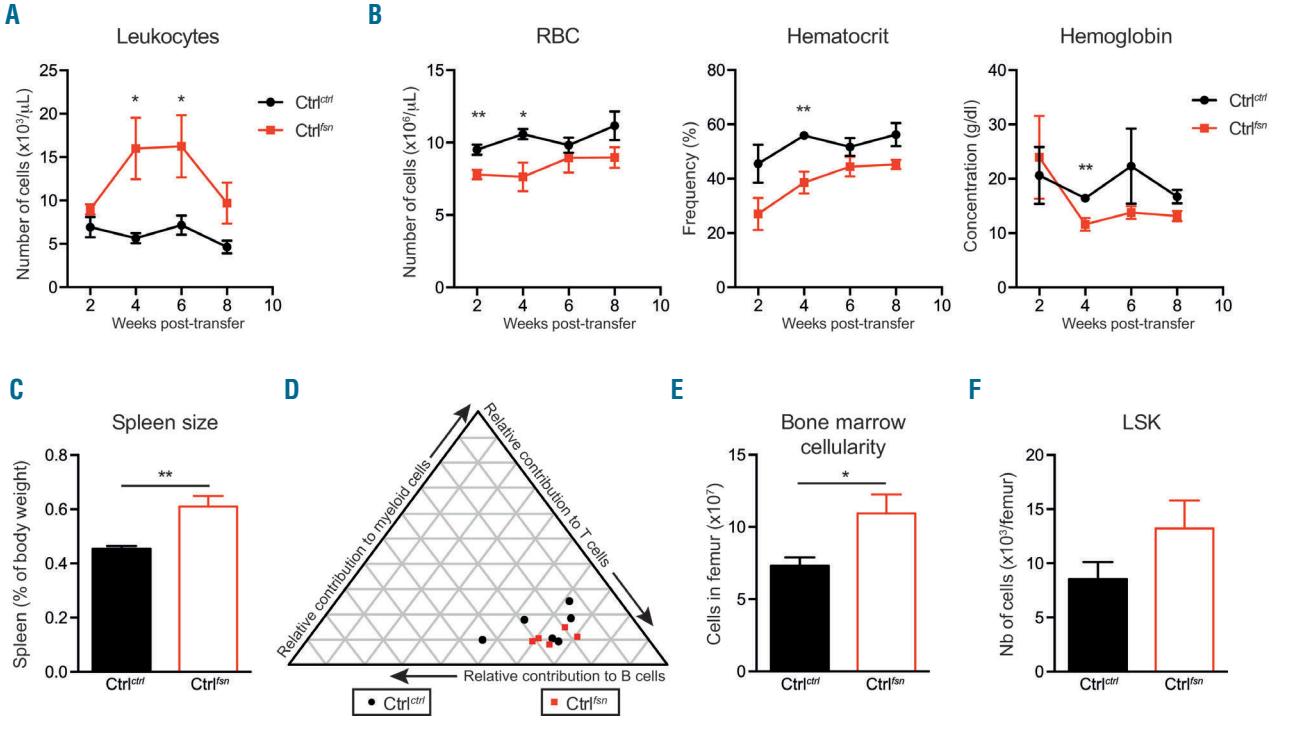

Figure 3. Transferred Ttc7a-deficient LSK cells reproduce fsn manifestations in a control environment. Control irradiated mice were transferred with LSK cells purified from 3-week old *ctrl* (Ctrl^{ctrl} – black bars) or Ttc7a-deficient mice (Ctrl^{fsn} – red bars). (mean ± standard error of mean) *P<0.05; **P<0.01 (two-tailed t-test). (A, B) Monitoring of the number of leukocytes (A) and red blood cells, hematocrit and hemoglobin (B) during hematopoietic reconstitution. (C) Spleen size determined as percent of body weight 10 weeks after bone marrow (BM) transfer. (D) Relative contribution of myeloid compared to T cells and B cells in the spleen. (E, F) BM cellularity (E) and absolute number of LSK cells (F) 10 weeks after BM transfer. RBC: red blood cells.

respective contributions of cells originating from *ctrl* or *fsn* LSK donors during hematopoietic reconstitution. As early as 2 weeks after transfer, the proportion of LSK^{fsn} donor-derived leukocytes in the recipients' blood was higher than that of LSK^{ctrl}. These differences persisted 14 weeks after transfer (Figure 4A). The proportions of cells originating from donor LSK in the recipients' organs, particularly the thymus and BM, were higher in Ctrl-LSK^{fsn} mice than in Ctrl-LSK^{ctrl} mice (Figure 4B). In the spleen, the reconstitution advantage of LSK^{fsn} donor-derived cells led to the expansion of neutrophil, eosinophil and monocyte lineages and to a lesser extent, T-cell lineages (Figure 4C). To further evaluate the effect of Ttc7a loss on long-term reconstitution, total BM cells from primary recipient mice were transplanted into secondary recipients. The competitive advantage of Ttc7a-deficient LSK donor cells with regards to reconstitution was maintained and even enhanced upon secondary and tertiary transplantation (Figure 4D). Thus, our results show that a defect in Ttc7a improves the competitive fitness of HSC following transplantation.

Loss of Ttc7a increases the long-term self-renewal potential of hematopoietic stem cells

In view of the elevated proliferative capacity of Ttc7a-deficient hematopoietic cells, we next sought to assess the properties of HSC that could modify their reconstitution potential (i.e., quiescence and self-renewal capacity). To evaluate the impact of Ttc7a loss on the quiescence of reconstituting HSC, we measured bromodeoxyuridine (BrdU) incorporation in control and Ttc7a-deficient HSPC before and after BM transplantation. Upon 24 h of BrdU treatment, we observed similar percentages of BrdU-positive (BrdU^{+}) HSC, HPC-1 and HPC-2 cells purified from control and *fsn* mice (*Online Supplementary Figure S4A*). Similar results were obtained when comparing cell cycle progression in control and Ttc7a-deficient HSC upon transplantation of irradiated recipients (*Online Supplementary Figure S4B, C*). Altogether, these results suggest that the increased repopulation capacity of *fsn* HSC was not caused by a disturbed quiescent state.

We then looked at whether the long-term self-renewal ability of HSC was altered in this context. We therefore performed serial BM transplants from irradiated mice having received whole BM from 3-week old *ctrl* or *fsn* mice. Unexpectedly, Ttc7a-deficient cells successfully sustained BM reconstitution longer than *ctrl* cells did. The *ctrl* HSC sustained six rounds of transplantation (Figure 5A) but all the Ctrl^{ctrl} mice died during the seventh round of BM transfer (Figure 5A, B). In contrast, most Ctrl^{fsn} mice survived 6 weeks after the seventh round and were able to undergo

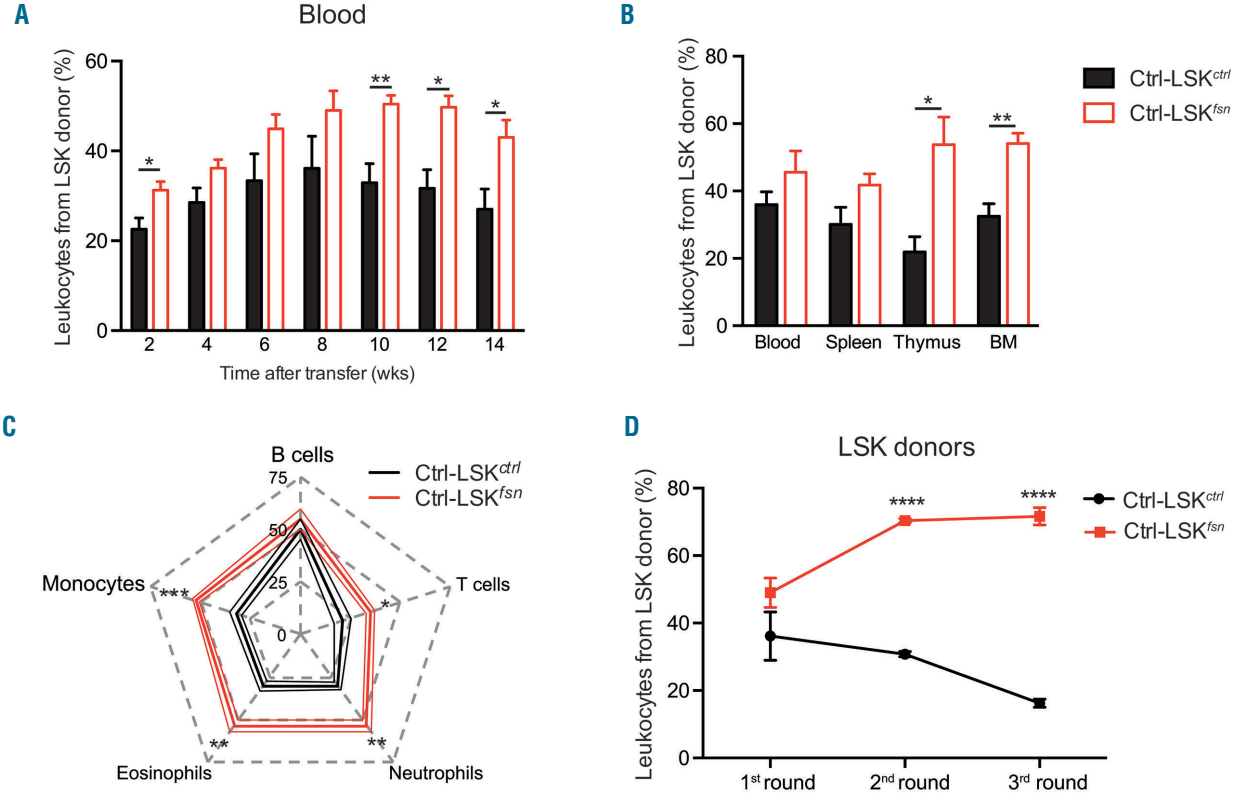

Figure 4. Ttc7a-deficient hematopoietic stem cells have a higher repopulation capacity. (A-C) Lethally irradiated CD45.1 mice were reconstituted with a mix of control whole bone marrow (BM) and sorted LSK cells purified from *ctrl* (Ctrl-LSK^{ctrl} – black bars and lines) or Ttc7a-deficient mice (Ctrl-LSK^{fsn} – red bars and lines) (mean ± standard error of mean) *P<0.05; **P<0.01; ***P<0.001; ****P<0.0001 (two-tailed t-test). These data are representative of three independent experiments. Proportion of LSK donor-derived leukocytes in the blood over time (A), in lymphoid organs (15 weeks after transfer) (B) and in the spleen for the different types of leukocytes (C) (n=8). (D) BM cells from first and then second round recipient mice of each group were pulled and transplanted to secondary and tertiary *ctrl* CD45.1 recipients, respectively. The proportions of LSK donor-derived leukocytes of Ctrl-LSK^{ctrl} and Ctrl-LSK^{fsn} mice were determined in each round (n=14 for control and n=16 for Ttc7a-reconstituted mice).

an additional round of transplantation before dying after the eighth round (Figure 5A, B). Similar results were obtained in experiments with 12-week old donors (*Online Supplementary Figure S5A, B*). We next determined the ability of *ctrl* and Ttc7a-deficient BM cells from 3-week old mice to properly reconstitute hematopoiesis over the different rounds of transplantation. During the first five rounds, the same phenotype was always observed. Ctrl^{fsn} mice displayed anemia (Figure 5C), together with an elevated leukocyte count up until the third round (Figure 5D). The spleen was larger in Ctrl^{fsn} mice than in Ctrl^{ctrl} mice until the fifth round (Figure 5E). However, differences between Ctrl^{fsn} and Ctrl^{ctrl} mice were no longer observed in the sixth round; this was probably caused by exhausted donor cells that failed to properly reconstitute recipient mice at the end of the reconstitution process (Figure 5C-E). Interestingly, the distribution of splenic leukocyte subsets in the Ctrl^{fsn} mice was progressively biased toward myeloid populations at the expense of B cells, and to a lesser extent, T cells, as notably observed for the fifth round (Figure 5F). In Ctrl^{fsn} mice, this bias became detectable in the third round and persisted until the seventh round (*Online Supplementary Figure S5C*). In summary, these data show that Ttc7a-deficient HSC have a greater ability to self-renew and to induce myeloid cell expansion.

Ttc7a-deficiency perturbs the transcriptomic profile of the endoplasmic reticulum stress response in hematopoietic stem cells

In order to gain further mechanistic insight into the Ttc7a-related regulation of HSC homeostasis, we carried out a transcriptomic analysis of HSC isolated from Ttc7a-deficient and control BM (from 4-week old mice). A two-way hierarchical clustering analysis of differentially expressed genes (P value ≤0.05, fold change ≥1.2) revealed a clear-cut separation between Ttc7a-deficient and control HSC samples (Figure 6A). We found that 1,103 genes were significantly upregulated and 928 significantly downregulated in Ttc7a-deficient HSC relative to the expression levels in control HSC (Figure 6B). Among the differentially

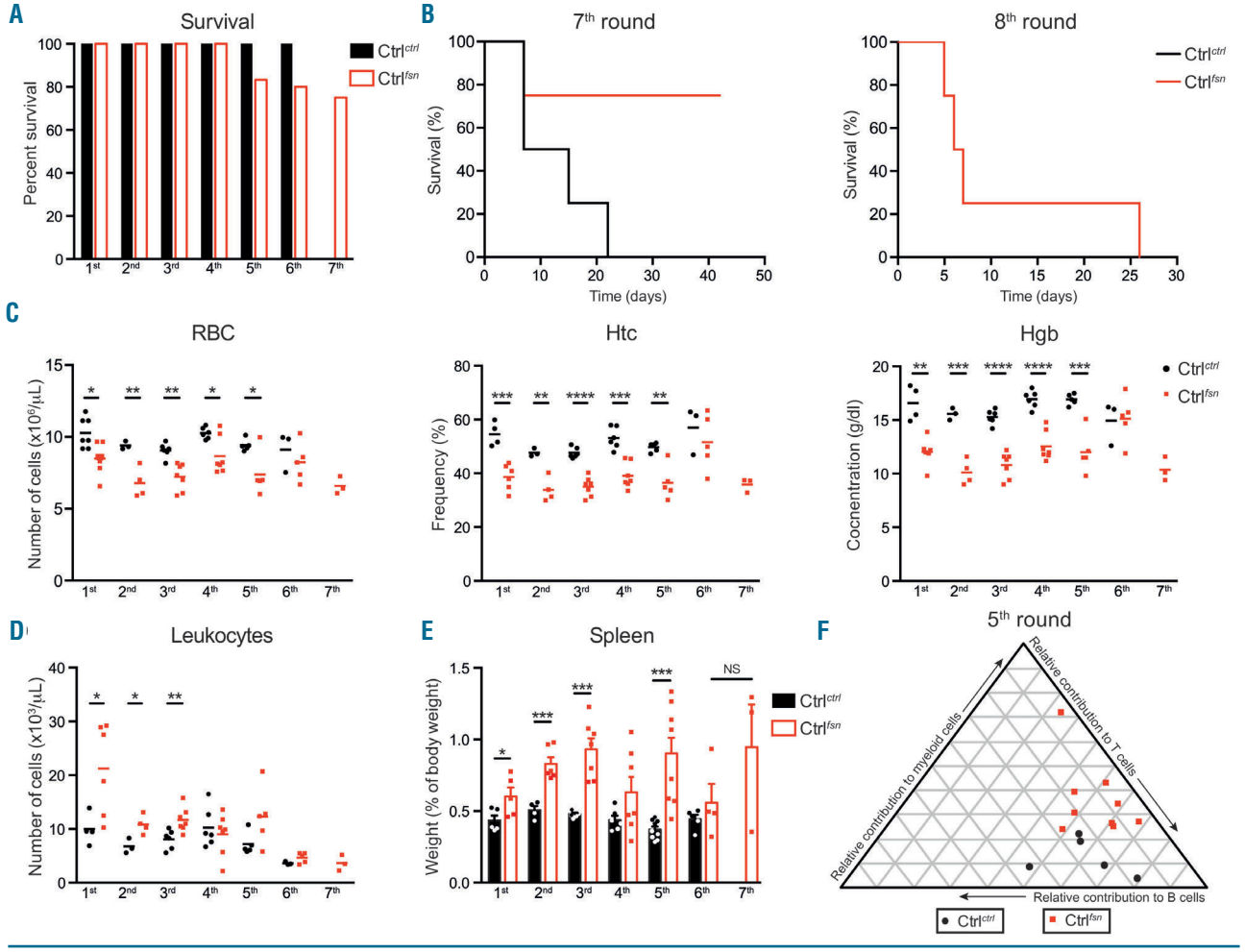

Figure 5. Ttc7a-deficiency promotes self-renewal ability of hematopoietic stem cells. Lethally irradiated mice were serially transplanted with 3-week old *ctrl* (Ctrl^{ctrl} – black bars, dots and lines) or Ttc7a-deficient (Ctrl^{fsn} – red bars, dots and lines) donor bone marrow (BM) cells (mean ± standard error of mean) *P<0.05; **P<0.01; ***P<0.001; ****P<0.0001 (two-tailed t-test). These data are representative of four independent experiments with at least four mice in each round of transplantation. (A) Percent survival of recipient mice across the seven transplantation cycles. (B) Survival of Ctrl^{ctrl} and Ctrl^{fsn} mice during the seventh round and Ctrl^{fsn} mice during the eighth over time (n=4 for control- and n=10 for Ttc7a-reconstituted mice). (C-F) Red blood cell count, hematocrit, and hemoglobin level (C), leukocytes count (D) and spleen weight (E) across the transplantation cycles. (F) Relative contribution of myeloid compared to T- and B-lymphoid cells in the spleen of mice transplanted with BM cells that had undergone five transplantation cycles. RBC: red blood cells; Htc: hematocrit; Hgb: hemoglobin.

expressed genes, the most statistically significant differences were observed in the group of downregulated genes (Figure 6B). To determine the functional profile of the differentially expressed genes, we performed GSEA for genes with a fold change ≥1.5. GO analysis of the identified gene signature revealed a significant enrichment of genes in three main categories. Two categories are related to chromatin organization/modification and DNA damage repair; this observation fits with our recent finding that Ttc7a is a chromatin-binding nuclear factor involved in chromatin compaction and nuclear organization[28] (Figure 6C, D). Another category corresponds to genes involved

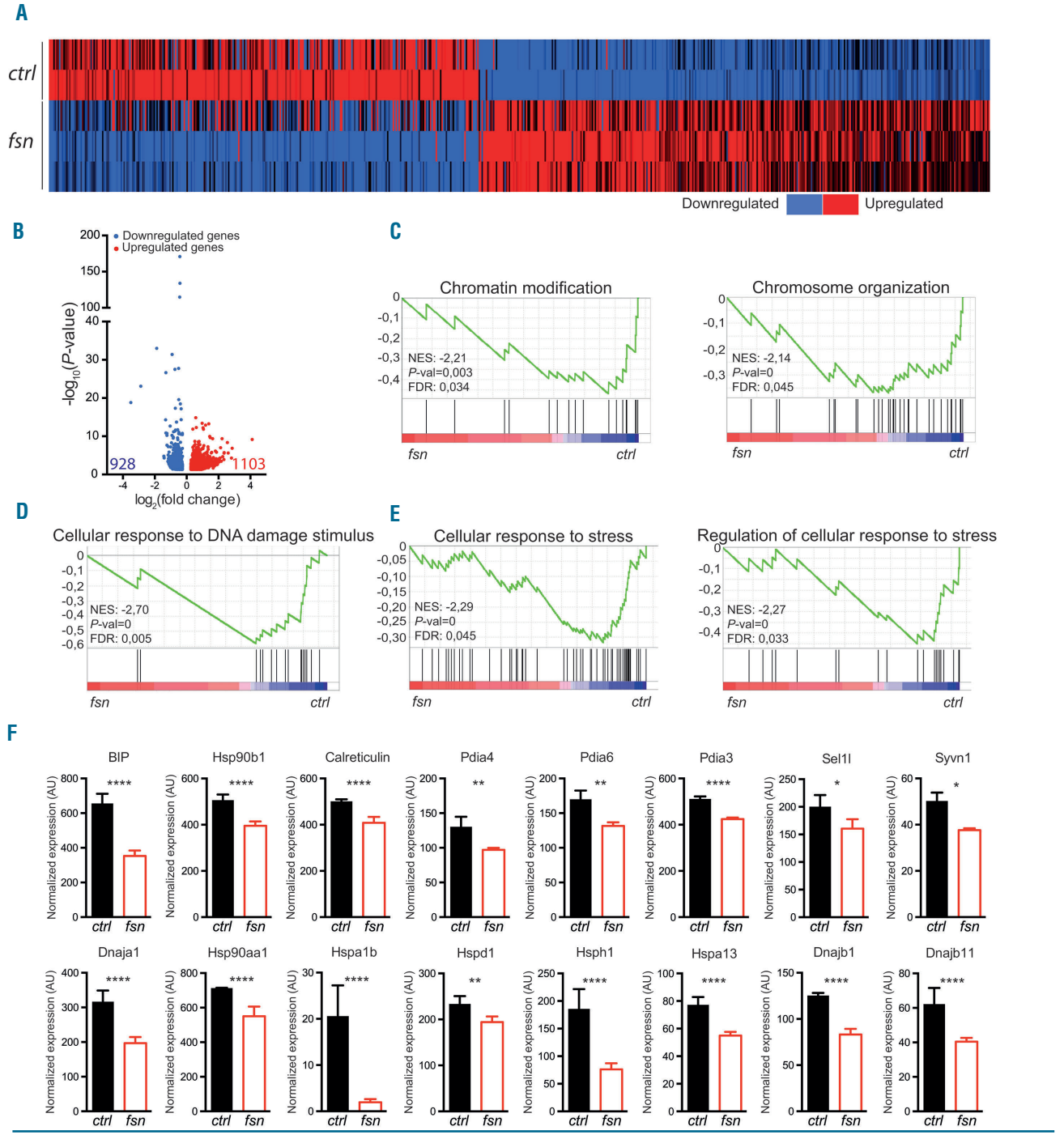

Figure 6. Ttc7a deficiency results in reduced expression of endoplasmic reticulum stress response genes in hematopoietic stem cells. RNA sequencing was performed on 3-week old control (*ctrl* – black bars) and Ttc7a-deficient (*fsn* – red bars) hematopoietic stem cell (HSC) transcripts. (A) Heatmap of relative expression of differentially expressed genes (fold change ≥1.2) in Ttc7a-deficient HSC compared to control. (B) Volcano plot of differentially expressed genes (fold change ≥1.2) in Ttc7a-deficient HSC compared to control HSC showing the adjusted *P*-value ($-\log_{10}$) *vs.* fold change ($\log_2$). Upregulated and downregulated genes are shown in red and blue, respectively. Total numbers in each group are indicated in red and blue, respectively. (C-E) Enriched gene sets in Ttc7a-deficient HSC compared to control HSC, as determined by gene set enrichment analysis of differentially expressed genes (fold change ≥1.5). (F) Normalized expression of endoplasmic reticulum stress response genes downregulated in Ttc7a-deficient HSC (fold change ≥1,2) **P*<0.05; ***P*<0.01; *****P*<0.0001 (LimmaVoom analysis). NES: normalized enrichment score; FDR: false discovery rate; AU: arbitrary units.

in cellular response to stress (Figure 6E). Our transcriptomic analysis also highlighted high expression levels of Ttc7a in HSC (*Online Supplementary Figure S6*). A growing body of evidence suggests that ER stress regulates the function of the HSC pool.[21] In particular, a recent study highlighted a link between ER stress perturbation in HSC and an elevated reconstitution capacity following BM transplantation.[29] Accordingly, we found that several effectors of the ER stress response were significantly downregulated in Ttc7a-deficient HSC, including the UPR master regulator Bip (Hspa5/GRP78), calreticulin, Pdia3, Pdia4, Pdia6, several Hsp, as well as Sel1l and Syvn1 which have been shown to regulate an ER-associated protein degradation (ERAD) pathway[30,31] (Figure 6F and *Online Supplementary Table S1*). Overall, our data suggest that Ttc7a loss affects the cellular response to ER stress in HSC.

Ttc7a controls the response to stress in hematopoietic stem cells

ER stress is mainly triggered in response to altered protein homeostasis leading to pro-apoptotic or pro-survival responses. Notably, Ttc7a-deficient HSC had reduced lev-

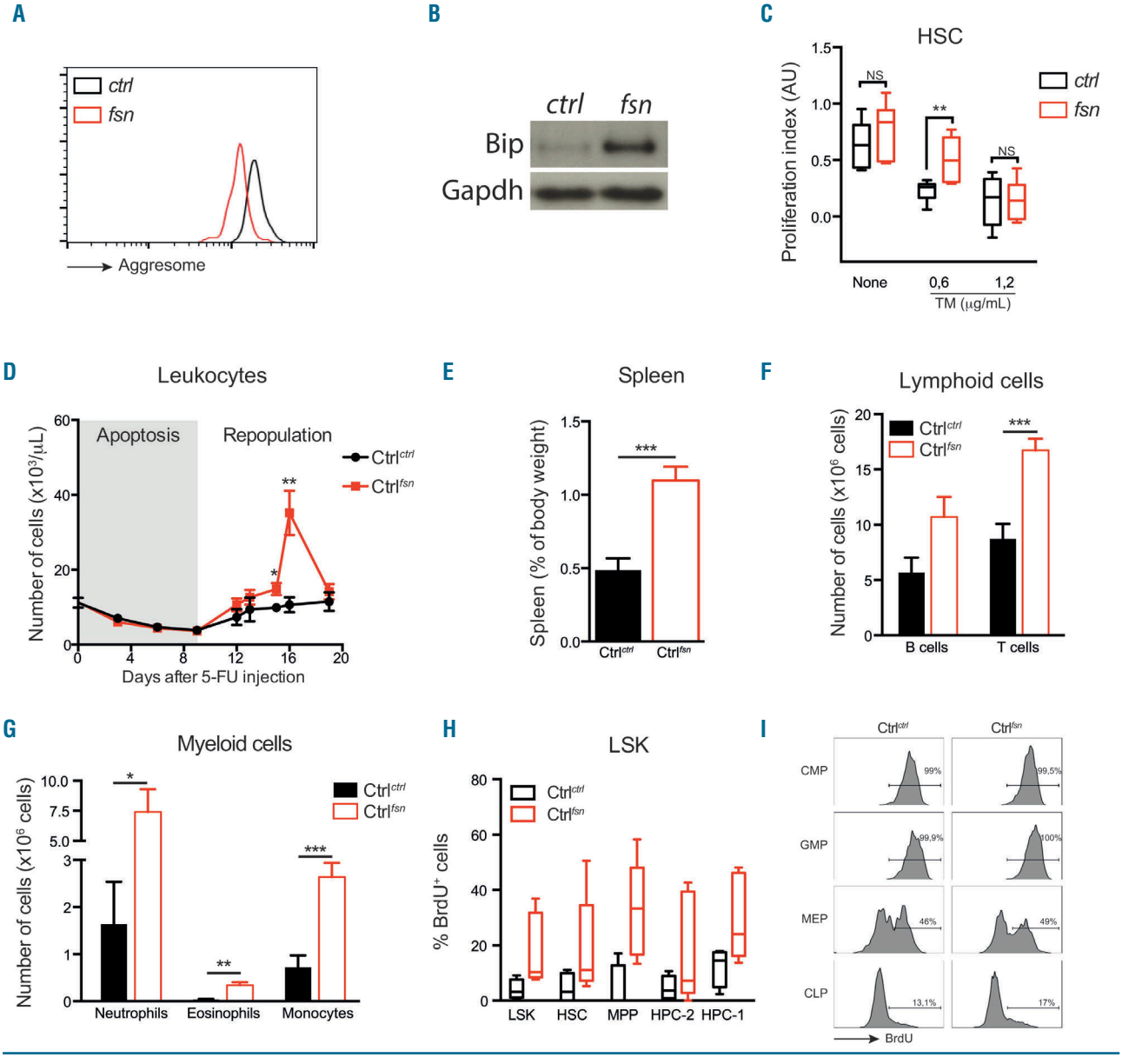

Figure 7. Ttc7a controls the response to stress in hematopoietic stem cells. (A) Representative histograms of protein aggregation level of 3-week old *ctrl* (black line) and *fsn* (red line) hematopoietic stem cells (HSC). (B) Protein expression of Bip in *ctrl* and *fsn* HSC after 3 days of *in vitro* expansion. (C) Proliferation index (calculated as the ratio between the number of cells at 48 h and 24 h) of HSC after Lin⁻ cells were sorted from *ctrl* (black bars) and Ttc7a-deficient (*fsn* – red bars) mice and cultured for 2 days with or without tunicamycin. $^{**}P<0.01$ (two-tailed *t*-test). (D-I) Ctrl^{ctrl} (black line and bars) and Ctrl^{fsn} (red line and bars) mice were analyzed after they had received a single intraperitoneal injection of 150 mg/Kg of 5-fluorouracil (5-FU), 12 weeks after bone marrow transfer. White blood cell count over time (D). Spleen size (E) and absolute number of lymphoid (F) and myeloid (G) cells in the spleen 15 days after 5-FU injection (n=9). Percentage bromodeoxyuridine (BrdU) incorporation in LSK subpopulations (H) and representative flow cytometry histograms of BrdU incorporation in LK (Lin⁻ Kit⁺) populations (I) 7 days after 5-FU injection. (n=10 for control- and n=12 for Ttc7a-reconstituted mice) $^{*}P<0.05$; $^{**}P<0.01$; $^{***}P<0.001$ (two-tailed t-test). AU: arbitrary units; LSK: Lin⁻ Sca1⁺ cKit⁺ cells; MPP: multipotent progenitors; HPC: hematopoietic progenitor cells; CMP: common myeloid progenitors; GMP: granulocyte-monocyte progenitors; MEP: megakaryocyte-erythroid progenitors; CLP: common lymphoid progenitors.

els of protein aggregation compared to control HSC (Figure 7A). In keeping with this, *in vitro*-expanded *fsn* HSC had an elevated level of BIP protein (Figure 7B). These results suggest that Ttc7a loss could modify HSC susceptibility to ER stress. Therefore, to determine the impact of Ttc7a loss in the response of HSC to ER stress, we analyzed the proliferative capacity of Ttc7a-deficient HSC and progenitor cells (i.e., HSC, MPP, HPC-2 and HPC-1) upon chemical induction of ER stress *in vitro*. To do so, lineage-negative cells from 4-week old *fsn* and *ctrl* mice were cultured for 48 h in the presence or absence of tunicamycin, which blocks the synthesis of N-linked glycoproteins, leading to an accumulation of unfolded proteins and the induction of ER stress.[32] As expected, on day 2, tunicamycin treatment reduced the proliferation ability of control cells in a dose-dependent manner (Figure 7C). In contrast, at a low dose of tunicamycin, the proliferative capacity of Ttc7a-deficient HSC was significantly greater than that of control HSC (Figure 7C). These differences were particular to HSC, as Ttc7a-deficient MPP, HPC-2 and HPC-1 subsets had a similar response to tunicamycin as their control counterparts (*Online Supplementary Figure S7A*). The alterations in the ER stress response in Ttc7a-deficient HSC were not due to protein aggregation (Figure 7A and *Online Supplementary Figure S7B*), nor to low expression of the ER stress sensors and effectors (Ire1α, Perk, Atf6, etc.), as no differences were observed in our transcriptomic analysis (*Online Supplementary Figure S7C* and *Online Supplementary Table S1*). Surprisingly, the reduction in cell proliferation of *ctrl* HSC in response to tunicamycin was independent of apoptosis, in contrast to that of other progenitor cells. Apoptosis of Ttc7a-deficient HSC was reduced compared to that of unstimulated *ctrl* cells, and remained unchanged upon tunicamycin treatment (*Online Supplementary Figure S7D*). No differences were observed in other progenitor populations (*Online Supplementary Figure S7D*). Altogether, these data suggest that *ex vivo* purified Ttc7a-deficient HSC had a higher level of ER stress compared to their control counterparts.

Interestingly, we observed that the expression of Hsp70, a chaperone protein associated with broad cellular stresses, was also higher in *fsn* HSC than in controls (*Online Supplementary Figure S7E*). In order to determine whether Ttc7a regulates the cellular response to stress *in vivo*, we monitored the proliferative response of Ttc7a-deficient cells following the induction of stress by 5-FU. The depletion of cycling cells by 5-FU stimulates HSC to replenish peripheral leukocytes,[33,34] inducing a broad stress response in HSC, not limited to ER stress (e.g., oxidative stress, proliferative stress). We injected 5-FU into Ctrl^{fsn} and Ctrl^{ctrl} mice 3 months after BM transplantation and monitored the replenishment of peripheral leukocytes for 19 days. The Ttc7a-deficient and *ctrl* leukocyte counts fell until day 9 post-injection, and then increased. On day 15, Ttc7a-deficient leukocytes were growing significantly more strongly than *ctrl* cells, with a peak on day 16 (Figure 7D). Interestingly, the spleen of Ctrl^{fsn} mice enlarged further after 5-FU treatment (Figure 7E, compared with Figure 3D), with higher lymphoid and myeloid counts (Figure 7F-G). To assess the proliferative response of Ttc7a-deficient HSC following stress injury, we assayed BrdU uptake by LSK subsets between day 6 and day 7 after 5-FU injection. The greater BrdU uptake in Ttc7a-deficient HSC, MPP, HPC-2 and HPC-1 (Figure 7H), suggested that Ttc7a controls the cell cycle progression of HSC under stress conditions. Strikingly, BrdU uptake did not differ in committed progenitors, CLP, CMP, GMP and MEP (Figure 7I). These results suggest that Ttc7a is involved in the regulation of the proliferative response of HSC under stress conditions but not in that of committed progenitor cells.

Discussion

The present study revealed a previously unrecognized role for Ttc7a in the negative regulation of HSC function. Using murine transplantation models and Ttc7a-deficient HSC, we found that Ttc7a intrinsically regulates the maintenance and proliferation of HSC *in vivo*, and the subsequent homeostasis of downstream cell populations. We also found that *Ttc7a* expression in HSC is closely associated with the transcriptional response to ER stress.

HSC are the only cells capable of self-renewing and differentiating into all mature blood lineages. The quiescence of HSC must be tightly regulated in order to control proliferation, maintain normal homeostasis, and prevent stem cell exhaustion[35,36] Various intrinsic and cell-extrinsic regulatory factors of the HSC cell cycle have been described, such as phosphatase and tensin homologue (Pten) signaling, Wnt signaling and cytokine signaling.[37] Indeed, in mice that lack growth factor independent 1 (Gfi1),[38] Pten, forkhead box proteins 1, 3, 4, or M1[39] or other proteins,[20,36] excessive HSC proliferation is associated with stem cell exhaustion and the loss of self-renewal. In contrast, we found that mice reconstituted with Ttc7a-deficient progenitors exhibit a characteristic phenotype with enhanced HSC function, higher HSC-derived peripheral blood cell counts and no evidence of stem cell exhaustion when compared with Ttc7a-proficient HSC. Indeed, Ttc7a-deficient HSC were able to repopulate the hematopoietic system better in serial transplantation experiments, indicating that the self-renewal of Ttc7a-deficient HSC is not compromised by repeated rounds of proliferation. Although this situation clearly differs from the above-mentioned knock-out mice, a few similar observations have been reported after the deletion of the cyclin-dependent kinase 4 inhibitor C (CDKN2C),[40] the ubiquitin-mediated protein degradation Cbl[41] and Itch,[41] and the transcription factors Hif1a[42] and Egr1.[43] The loss of these proteins enabled the maintenance of HSC, despite an increase in the cells' proliferative capacity. However, the specific mechanisms by which these proteins regulate HSC function remain largely unknown.

Our findings support a role for the ER stress response in the enhanced function of Ttc7a-deficient HSC. Since long-lived HSC are particularly sensitive to stress stimuli, their response must be tightly controlled in order to prevent either a loss of function or the clonal persistence of oncogenic mutations. It has been shown that HSC are enriched in components of the UPR pathway. Upon exposure to acute stress *in vitro*, HSC are more prone to apoptosis, via upregulation of the canonical UPR genes, than related progenitors that have lost their self-renewal capacity.[21,44] Along these lines, the ectopic expression of developmental pluripotency-associated 5 (Dppa5) was associated with enhanced HSC function, via suppression of the ER stress response (by downregulating the expression of ER stress chaperones) and the subsequent apoptotic signals.[29] However, UPR activation can also have an anti-apoptotic outcome in HSC. It has been shown that stimulation of

estrogen receptor α (ERα) confers HSC resistance to proteotoxic stress by activating the Ire1α-Xbp1 branch of the UPR and promoting the cells' reconstituting potential.[24] In Ttc7a deficient HSC, expression levels of ER stress response genes were abnormally low, whereas the level of the Bip chaperone protein was increased. Furthermore, Ttc7a deficient HSC were less sensitive to stress induction than Ttc7a-proficient-HSC both *in vitro* and *in vivo*. A similar phenomenon was observed in mouse liver in which mild chronic ER stress decreases the mRNA level of Bip while maintaining its protein level. This response allows hepatocytes to avoid the overproduction of UPR effectors that could lead to apoptosis.[45] It is, therefore, tempting to speculate that Ttc7a deficiency could be associated with mild chronic stress. In this context, the increased resistance of *fsn* HSC to tunicamycin could be caused by a cellular adaptive response aiming to increase the threshold of ER stress sensitivity, and ensure cell survival. Interestingly, HSC exposed to other sources of persistent cellular stress develop mechanisms of stress resistance resulting in increased self-renewal capacity and reconstitution potential.[46] Knowing that TTC7A stabilizes several interacting proteins, the role of additional components, altered as a consequence of Ttc7a deficiency, cannot be excluded. Ttc7a could represent a pivotal connection between ER stress regulation and the maintenance of HSC functions.

Along with an abnormally proliferative hematopoietic system, fsn mice develop hyperplasia of the epidermis and the gastric epithelium. Notably, stem cells from other tissues can similarly sense ER stress and activate the UPR pathway to control self-renewal and differentiation. This has been shown for the intestinal epithelium in particular, and several lines of evidences support the concept whereby ER stress and UPR activity regulate the differentiation of intestinal stem cells.[47] An attractive hypothesis would be that the other phenotypic manifestations that characterized Ttc7a deficiency might be due to perturbation of the ER stress response.

In summary, our results show that Ttc7a has a critical but previously unrecognized role as a regulator of HSC homeostasis and function through the regulation of the ER stress response.

Acknowledgments

We thank Gaël Ménasché, Annarita Miccio and Isabelle Andre-Schmutz for helpful comments and guidance; Olivier Pellé for help in cell sorting; the Necker histology and morphology facility [Structure Fédérative de Recherche (SFR) Necker] and the Cochin Genomic Platform for their services in histological and transcriptomic studies, respectively. This work was supported by The French National Institutes of Health and Medical Research (INSERM), state funding from the Agence Nationale de la Recherche "Investissements d'avenir" program, la Fondation pour la Recherche Médicale (FRM project DEQ20150734354), and the Imagine Foundation. CL was supported by a fellowship from the Ministry of Education and FRM and MTED by a fellowship from the ANR, the FRM and the European Research Council (ERC). TG is a fellow of the International PhD program of the Imagine Institute funded by the Bettencourt Schueller Foundation.

References

1. Helms C, Pelsue S, Cao L, et al. The tetratricopeptide repeat domain 7 gene is mutated in flaky skin mice: a model for psoriasis, autoimmunity, and anemia. Exp Biol Med (Maywood). 2005;230(9):659-667.
2. Lees JA, Zhang Y, Oh MS, et al. Architecture of the human PI4KIIIalpha lipid kinase complex. Proc Natl Acad Sci U S A. 2017;114(52):13720-13725.
3. Pelsue SC, Schweitzer PA, Schweitzer IB, et al. Lymphadenopathy, elevated serum IgE levels, autoimmunity, and mast cell accumulation in flaky skin mutant mice. Eur J Immunol. 1998;28(4):1379-1388.
4. Abernethy NJ, Hagan C, Tan PL, Birchall NM, Watson JD. The peripheral lymphoid compartment is disrupted in flaky skin mice. Immunol Cell Biol. 2000;78(1):5-12.
5. Abernethy NJ, Hagan C, Tan PL, Watson JD. Dysregulated expression of CD69 and IL-2 receptor alpha and beta chains on CD8+ T lymphocytes in flaky skin mice. Immunol Cell Biol. 2000;78(6):596-602.
6. Welner R, Hastings W, Hill BL, Pelsue SC. Hyperactivation and proliferation of lymphocytes from the spleens of flaky skin (fsn) mutant mice. Autoimmunity. 2004;37(3):227-235.
7. Beamer WG, Pelsue SC, Shultz LD, Sundberg JP, Barker JE. The flaky skin (fsn) mutation in mice: map location and description of the anemia. Blood. 1995;86(8):3220-3226.
8. Schon M, Denzer D, Kubitza RC, Ruzicka T, Schon MP. Critical role of neutrophils for the generation of psoriasiform skin lesions in flaky skin mice. J Invest Dermatol. 2000;114(5):976-983.
9. Leclerc-Mercier S, Lemoine R, Bigorgne AE, et al. Ichthyosis as the dermatological phenotype associated with TTC7A mutations. Br J Dermatol. 2016;175(5):1061-1064.
10. Sundberg JP, Kenty GA, Beamer WG, Adkison DL. Forestomach papillomas in flaky skin and steel-Dickie mutant mice. J Vet Diagn Invest. 1992;4(3):312-317.
11. Scheufler C, Brinker A, Bourenkov G, et al. Structure of TPR domain-peptide complexes: critical elements in the assembly of the Hsp70-Hsp90 multichaperone machine. Cell. 2000;101(2):199-210.
12. D'Andrea LD, Regan L. TPR proteins: the versatile helix. Trends Biochem Sci. 2003;28(12):655-662.
13. Assimon VA, Southworth DR, Gestwicki JE. Specific binding of tetratricopeptide repeat proteins to heat shock protein 70 (Hsp70) and heat shock protein 90 (Hsp90) is regulated by affinity and phosphorylation. Biochemistry. 2015;54(48):7120-7131.
14. Taipale M, Tucker G, Peng J, et al. A quantitative chaperone interaction network reveals the architecture of cellular protein homeostasis pathways. Cell. 2014;158(2):434-448.
15. Bigorgne AE, Farin HF, Lemoine R, et al. TTC7A mutations disrupt intestinal epithelial apicobasal polarity. J Clin Invest. 2014;124(1):328-337.
16. Lemoine R, Pachlopnik-Schmid J, Farin HF, et al. Immune deficiency-related enteropathy-lymphocytopenia-alopecia syndrome results from tetratricopeptide repeat domain 7A deficiency. J Allergy Clin Immunol. 2014;134(6):1354-1364 e1356.
17. Avitzur Y, Guo C, Mastropaolo LA, et al. Mutations in tetratricopeptide repeat domain 7A result in a severe form of very early onset inflammatory bowel disease. Gastroenterology. 2014;146(4):1028-1039.
18. Baird D, Stefan C, Audhya A, Weys S, Emr SD. Assembly of the PtdIns 4-kinase Stt4 complex at the plasma membrane requires Ypp1 and Efr3. J Cell Biol. 2008;183(6):1061-1074.
19. Rossi L, Lin KK, Boles NC, et al. Less is more: unveiling the functional core of hematopoietic stem cells through knockout mice. Cell Stem Cell. 2012;11(3):302-317.
20. Orford KW, Scadden DT. Deconstructing stem cell self-renewal: genetic insights into cell-cycle regulation. Nat Rev Genet. 2008;9(2):115-128.
21. van Galen P, Kreso A, Mbong N, et al. The unfolded protein response governs integrity of the haematopoietic stem-cell pool during stress. Nature. 2014;510(7504):268-272.
22. Rutkowski DT, Kaufman RJ. A trip to the ER: coping with stress. Trends Cell Biol. 2004;14(1):20-28.
23. Grootjans J, Kaser A, Kaufman RJ, Blumberg RS. The unfolded protein response in immunity and inflammation. Nat Rev Immunol. 2016;16(8):469-484.

24. Chapple RH, Hu T, Tseng YJ, et al. ERalpha promotes murine hematopoietic regeneration through the Ire1alpha-mediated unfolded protein response. Elife. 2018;7:e31159
25. Oguro H, Ding L, Morrison SJ. SLAM family markers resolve functionally distinct subpopulations of hematopoietic stem cells and multipotent progenitors. Cell Stem Cell. 2013;13(1):102-116.
26. Zhao B, Yang J, Ji P. Chromatin condensation during terminal erythropoiesis. Nucleus. 2016;7(5):425-429.
27. Konstantinidis DG, Pushkaran S, Johnson JF, et al. Signaling and cytoskeletal requirements in erythroblast enucleation. Blood. 2012;119(25):6118-6127.
28. El-Daher MT, Cagnard N, Gil M, et al. Tetratricopeptide repeat domain 7A is a nuclear factor that modulates transcription and chromatin structure. Cell Discov. 2018;4:61.
29. Miharada K, Sigurdsson V, Karlsson S. Dppa5 improves hematopoietic stem cell activity by reducing endoplasmic reticulum stress. Cell Rep. 2014;7(5):1381-1392.
30. Kikkert M, Doolman R, Dai M, et al. Human HRD1 is an E3 ubiquitin ligase involved in degradation of proteins from the endoplasmic reticulum. J Biol Chem. 2004;279(5):3525-3534.
31. Sun S, Shi G, Han X, et al. Sel1L is indispensable for mammalian endoplasmic reticulum-associated degradation, endoplasmic reticulum homeostasis, and survival. Proc Natl Acad Sci U S A. 2014;111(5):E582-591.
32. DuRose JB, Tam AB, Niwa M. Intrinsic capacities of molecular sensors of the unfolded protein response to sense alternate forms of endoplasmic reticulum stress. Mol Biol Cell. 2006;17(7):3095-3107.
33. Randall TD, Weissman IL. Phenotypic and functional changes induced at the clonal level in hematopoietic stem cells after 5-fluorouracil treatment. Blood. 1997;89(10):3596-3606.
34. Venezia TA, Merchant AA, Ramos CA, et al. Molecular signatures of proliferation and quiescence in hematopoietic stem cells. PLoS Biol. 2004;2(10):e301.
35. Wilson A, Laurenti E, Oser G, et al. Hematopoietic stem cells reversibly switch from dormancy to self-renewal during homeostasis and repair. Cell. 2008;135(6):1118-1129.
36. Trumpp A, Essers M, Wilson A. Awakening dormant haematopoietic stem cells. Nat Rev Immunol. 2010;10(3):201-209.
37. Walasek MA, van Os R, de Haan G. Hematopoietic stem cell expansion: challenges and opportunities. Ann N Y Acad Sci. 2012;1266:138-150.
38. Hock H, Hamblen MJ, Rooke HM, et al. Gfi-1 restricts proliferation and preserves functional integrity of haematopoietic stem cells. Nature. 2004;431(7011):1002-1007.
39. Hou Y, Li W, Sheng Y, et al. The transcription factor Foxm1 is essential for the quiescence and maintenance of hematopoietic stem cells. Nat Immunol. 2015;16(8):810-818.
40. Yuan Y, Shen H, Franklin DS, Scadden DT, Cheng T. In vivo self-renewing divisions of haematopoietic stem cells are increased in the absence of the early G1-phase inhibitor, p18INK4C. Nat Cell Biol. 2004;6(5):436-442.
41. Rathinam C, Matesic LE, Flavell RA. The E3 ligase Itch is a negative regulator of the homeostasis and function of hematopoietic stem cells. Nat Immunol. 2011;12(5):399-407.
42. Takubo K, Goda N, Yamada W, et al. Regulation of the HIF-1alpha level is essential for hematopoietic stem cells. Cell Stem Cell. 2010;7(3):391-402.
43. Min IM, Pietramaggiori G, Kim FS, Passegue E, Stevenson KE, Wagers AJ. The transcription factor EGR1 controls both the proliferation and localization of hematopoietic stem cells. Cell Stem Cell. 2008;2(4):380-391.
44. Laurenti E, Doulatov S, Zandi S, et al. The transcriptional architecture of early human hematopoiesis identifies multilevel control of lymphoid commitment. Nat Immunol. 2013;14(7):756-763.
45. Gomez JA, Rutkowski DT. Experimental reconstitution of chronic ER stress in the liver reveals feedback suppression of BiP mRNA expression. Elife. 2016;5:e20390
46. Cheng CW, Adams GB, Perin L, et al. Prolonged fasting reduces IGF-1/PKA to promote hematopoietic-stem-cell-based regeneration and reverse immunosuppression. Cell Stem Cell. 2014;14(6):810-823.
47. Heijmans J, van Lidth de Jeude JF, Koo BK, et al. ER stress causes rapid loss of intestinal epithelial stemness through activation of the unfolded protein response. Cell Rep. 2013;3(4):1128-1139.

ARTICLE

CD27, CD201, FLT3, CD48, and CD150 cell surface staining identifies long-term mouse hematopoietic stem cells in immunodeficient non-obese diabetic severe combined immune deficient-derived strains

Bianca Nowlan,[1,2,3,4,5] Elizabeth D. Williams,[2,4,5] Michael R. Doran,[1,2,3,4,5,6,*] and Jean-Pierre Levesque[3,5,*]

[1]Stem Cell Therapies Laboratory, School of Biomedical Science, Faculty of Health, Queensland University of Technology (QUT), Brisbane; [2]School of Biomedical Science, Faculty of Health, Institute of Health and Biomedical Innovation, QUT, Kelvin Grove, Queensland; [3]Mater Research Institute – The University of Queensland, Woolloongabba; [4]Australian Prostate Cancer Research Centre - Queensland, Brisbane, Queensland; [5]Translational Research Institute, Woolloongabba, Queensland and [6]Australian National Centre for the Public Awareness of Science, Australian National University, Canberra, Australian Capital Territory, Australia

** MRD and JPL contributed equally to this work.*

Ferrata Storti Foundation

Haematologica 2020
Volume 105(1):71-82

ABSTRACT

Staining for CD27 and CD201 (endothelial protein C receptor) has been recently suggested as an alternative to stem cell antigen–1 (Sca1) to identify hematopoietic stem cells in inbred mouse strains with low or nil expression of SCA1. However, whether staining for CD27 and CD201 is compatible with low fms-like tyrosine kinase 3 (FLT3) expression and the "SLAM" code defined by CD48 and CD150 to identify mouse long-term reconstituting hematopoietic stem cells has not been established. We compared the C57BL/6 strain, which expresses a high level of SCA1 on hematopoietic stem cells to non-obese diabetic severe combined immune deficient NOD.CB17-*prkdc*^{scid}/Sz (NOD-*scid*) mice and NOD.CB17-*prkdc*^{scid} *il2rg*^{tm1Wjl}/Sz (NSG) mice which both express low to negative levels of SCA1 on hematopoietic stem cells. We demonstrate that hematopoietic stem cells are enriched within the linage-negative C-KIT$^+$ CD27$^+$ CD201$^+$ FLT3$^-$ CD48$^-$ CD150$^+$ population in serial dilution long-term competitive transplantation assays. We also make the novel observation that CD48 expression is up-regulated in Lin$^-$ KIT$^+$ progenitors from NOD-*scid* and NSG strains, which otherwise have very few cells expressing the CD48 ligand CD244. Finally, we report that unlike hematopoietic stem cells, SCA1 expression is similar on bone marrow endothelial and mesenchymal progenitor cells in C57BL/6, NOD-*scid* and NSG mice. In conclusion, we propose that the combination of Lineage, KIT, CD27, CD201, FLT3, CD48, and CD150 antigens can be used to identify long-term reconstituting hematopoietic stem cells from mouse strains expressing low levels of SCA1 on hematopoietic cells.

Introduction

Blood myeloid and erythroid lineages are short-lived and require continuous replacement from hematopoietic stem cells (HSC) in the bone marrow (BM).[1-6] HSC are defined by their capacity to clonally reconstitute the hematopoietic system in lethally irradiated mice upon transplantation. Using cell surface markers, mouse HSC are comprised within the LSK population of cells, i.e., cells negative for B, T, myeloid and erythroid lineages (Lin$^-$), positive for c-KIT/CD117 and positive for stem cell antigen-1 (SCA1 or LY6A/E). Multipotent long-term reconstituting HSC (LT-HSC) are LSK cells that are negative for fms-like tyrosine kinase 3 (FLT3)/CD135 and CD48 and positive for signaling lymphocytic activation molecule (SLAMF1/CD150).[4,5] When transplanted, these HSC can clonally and serially reconstitute hematopoiesis in lethally irradiated mice.[5]

Correspondence:

JEAN-PIERRE LEVESQUE
jp.levesque@mater.uq.edu.au

MICHAEL DORAN
mike@mikedoranlab.com

Received: November 22, 2018.

Accepted: May 2, 2019.

Pre-published: May 9, 2019.

doi:10.3324/haematol.2018.212910

Check the online version for the most updated information on this article, online supplements, and information on authorship & disclosures: www.haematologica.org/content/105/1/71

Identifying HSC in inbred mouse strains that either do not or poorly express SCA1, such as BALB/c or non-obese diabetic (NOD) mice,[7,8] or when treatments affect SCA1 expression is challenging. The SCA1 antibody detects LY6A and LY6E, which are two similar proteins of the LY6 phosphatidylinositol-anchored membrane proteins antigen family encoded by two different genes.[9] LY6E is expressed by 10-15% of blood leukocytes, whereas LY6A is expressed by 50-70% of leukocytes.[8] Inbred strains with the LY6.1 haplotype (e.g., BALB/c, C3H, DBA/1, CBA, FVB/N) do not express LY6A. This causes reduced SCA1 expression, thus compromising the classical method of identifying the HSC population based on the LSK phenotype.[3,8] Furthermore, even though the NOD strain and other immunodeficient strains on the NOD background are from the LY6.2 haplotype, they also express low levels of SCA1.[10] In addition, SCA1 expression can be affected by treatments such as irradiation, bacterial infections, and interferons which cause a transient increase in SCA1 expression in Lin^- KIT^+ (LK) cells in C57BL/6 mice[11,12] further questioning the suitability of SCA1 antigen to characterize HSC in challenged mice.

The combination of CD27 and CD201 (endothelial protein C receptor – EPCR) has been proposed as an alternative to SCA1/c-kit staining for HSC identification in mouse strains with low expression of SCA1 or following irradiation.[13] It was demonstrated that Lin^- $CD27^+$ $CD201^+$ cells contained all HSC activity tested in a long-term competitive repopulation assay in lethally irradiated recipient mice and this HSC phenotype remained consistent in several mouse strains, including BALB/c and NOD, or following irradiation.[13]

Several reports suggest that mouse HSC express both CD27 and CD201.[14,15] CD27 is a member of the tumor necrosis factor receptor family expressed on T, B, and natural killer (NK) cells, involved in proliferation, differentiation, and IgG production. CD27 was detected on 90% of LSK cells in C57BL/6 mice.[15] Likewise, high expression of CD201 was also observed on 90% of LSK cells.[14] $CD201^+$ cells are multipotent in both colony assays and mouse transplant reconstitution. CD201 and CD150 are co-expressed in the embryonic mouse hematopoietic development of a long-term reconstituting population of HSC throughout life.[16,17] In addition, CD201 is also expressed on multipotent human $CD34^+$ HSC,[18] showing that the pattern of CD201 expression is conserved between human and mouse HSC, unlike that of the CD34 antigen.[6] As few HSC markers are shared between both species, this is becoming a significant cross-species HSC marker.

Recently, the use of NOD.CB17-*prkdc*^{scid} *il2rg*^{tm1Wjl}/Sz (NSG) mice for human xenografts has increased[19-21] relative to the parental (NOD.CB17-*prkdc*^{scid}/Sz, NOD-*scid*) mice. NSG mice do not express functional interleukin-2 receptor and therefore lack NK cells in addition to their lack of B and T cells from the parental NOD-*scid* strain, resulting in more profound immunosuppression and making the animals more amenable to human xenograft engraftment.[21]

Metastatic cancer cells and human HSC can hijack the mouse BM HSC niche,[22] thus any treatments affecting xenografts should also be examined for the drugs' effects on the host mouse HSC content in order to detect potential adverse effects of the drugs. However, there are no reliable flow cytometry methods to assess the impact of human xenografts or prototype anti-cancer therapies on the host mouse HSC in these strains.

In this study, we examined CD27 and CD201 expression on BM cells in NOD-*scid* and NSG mice. We demonstrate that staining protocols using CD27 and CD201 with FLT3, CD48, and CD150 are complementary to enrich functional HSC in these strains. These antibodies could be combined to prospectively enrich HSC as validated by serial dilution transplantations in recipient mice. We also investigated the overexpression of CD48 in NOD-*scid* and NSG mice. Furthermore, we identified that low SCA1 expression was limited to hematopoietic cells, whereas BM mesenchymal stromal cells (MSC) and endothelial cells expressed SCA1 at levels similar to those in C57BL/6 mice.

Methods

Mice

Mouse experiments were approved by both the University of Queensland and Queensland University of Technology Animal Ethics Committees. C57BL/6 and NOD-*scid* mice were purchased from the Australian Resource Centre (Cannin Vale, WA, Australia). NSG mice (Jackson Laboratories, Bar Harbor, ME, USA), were bred at the Translational Research Institute Biological Research Facility (Brisbane, Australia). Mice were 7-8 weeks old at the time of the experiments.

Sample isolation

BM was flushed from femurs using phosphate-buffered saline (PBS) containing 2% fetal bovine serum (FBS). Spleens were harvested from mice and processed in PBS and 2% FBS using the Miltenyi gentleMACS and a C-type tube (Bergisch Gladbach, Germany). Blood was collected via cardiac puncture into 3.2% sodium citrate. Each fraction was counted using a Coulter AcT Diff Analyzer (Beckman Coulter).

To isolate BM stromal/endothelial cells, bones were harvested from NSG and C57BL/6 mice. BM was flushed and discarded and the bones were treated with 1 mg/mL collagenase type-1 (Worthington) as previously described.[23] Blood cells were depleted using the EasySep™ Mouse Mesenchymal Stem/Progenitor Cell Enrichment Kit (Cat. n. 19771 StemCell Technologies) following the manufacturer's protocol.

BM-MSC were isolated from NSG femurs using a modification of a previously described protocol[24] (see *Online Supplementary Methods*).

Flow cytometry

All antibodies and stains used are described in *Online Supplementary Table S1*.

HSC stains were applied to $5x10^6$ BM cells, while lineage stains were applied to 10^6 BM or spleen cells. Cells were stained in PBS and 2% FBS containing 0.1 μg/mL purified rat anti-CD16/CD32 (Fc Block) (BD Bioscience), with the appropriate antibody cocktail. The cells were then washed and resuspended in PBS plus 2% FBS containing 2 μg/mL dead cell discriminator dye 7-amino-actinomycin D (7-AAD) (Invitrogen) and analyzed on a CyAn flow cytometer (Beckman Coulter).

Stromal and endothelial cells were stained with an "endosteal" stain (*Online Supplementary Methods* and *Online Supplementary Table S1*). Samples were analyzed on a Fortessa flow cytometer (BD Bioscience).

Flow cytometry data were analyzed with FlowJo v10 software (FlowJo LLC, Ashland, OR, USA).

Transplantations

Male donor BM cells were enriched for c-KIT by magnetic-acti-

vated cell sorting. LK CD27$^+$CD201$^+$FLT3$^-$CD48$^-$CD150$^+$ and LK CD27$^+$CD201$^+$FLT3$^-$CD48$^+$CD150$^-$ (NOT GATE) were sorted on a FACS Aria Fusion sorter (BD Bioscience). Sorted cells were washed, counted and defined cell doses were resuspended in saline with 2% heat-inactivated FBS containing 100,000 irradiated (15 Gy) BM carrier cells. Grafts were then injected retro-orbitally into female recipients 24 h after 2.5 Gy total-body γ irradiation (^{137}Cs, Gammacell 40 Exactor, Best Theratronics, Ontario, Canada).

Engraftment was monitored with regular bleeds. At 18 weeks after transplantation, BM, spleen, and blood were harvested. Chimerism by donor male cells was determined by Y-chromosome polymerase chain reaction analysis based on previous protocols,[6,25] as outlined in the *Online Supplementary Methods*. Engraftment was considered positive when female recipients had >1% male DNA in the blood

Results

Comparison of SCA1, CD48 and CD150 expression in LK CD27$^+$ CD201$^+$ cells in C57BL/6, NOD-*scid* and NSG mice

BM cells from C57BL/6, NOD-*scid*, and NSG mice were stained with a cocktail of antibodies combining the traditional markers (Lin, c-KIT, SCA1, FLT3, CD48, CD150)[26] together with more recently proposed markers CD27 and CD201.[13] After gating live cells, LK cells were examined for CD27 and CD201 expression (see gating strategy in *Online Supplementary Figure S1*). LK cells had a similar profile for CD27 and CD201 expression as previously reported for C57BL/6 and NOD strains[13] (Figure 1A-C). The LK CD27$^+$ CD201$^+$ population labeled 0.019% ± 0.007% (mean ± standard deviation) of live BM nucleated cells in C57BL/6 mice, 0.100% ± 0.012% in NOD-*scid* mice and 0.041% ± 0.014% in NSG mice (Figure 1D). When calculated as cells per femur, NOD-scid mice had significantly more LK CD27$^+$ CD201$^+$ cells than had C57BL/6 and NSG mice (*Online Supplementary Table S2* and Figure 1E). When the LK CD27$^+$ CD201$^+$ were back-gated for SCA1 and c-KIT expression, SCA1 staining was lower in NOD-*scid* and NSG mice than in C57BL/6 mice, which were predominantly SCA1$^+$ (Figure 1F-I). This resulted in a large proportion of the phenotypic HSC defined by the LK CD27$^+$ CD201$^+$ phenotype[13] in NOD-scid and NSG mice falling in the SCA1$^-$ gate compared to the proportion from C57BL/6 mice (Figure 1J). Consequently, any calculation of phenotypic HSC numbers using the classic LSK phenotype may underestimate the actual number of HSC in NOD-*scid* and NSG mice when calculated as cells per femur (Figure 1K).

Next, we investigated whether CD27 and CD201 staining was compatible or complementary with FLT3$^-$, CD48$^-$ and CD150$^+$ staining to phenotypically identify LT-HSC. Live LK CD27$^+$ CD201$^+$ cells were gated for FLT3$^-$, CD150, and CD48 expression analyzed for each mouse strain (Figure 2A-C). A similar CD150$^+$ and CD48$^-$ LT-HSC profile was observed in the three strains. The frequency of LK CD27$^+$ CD201$^+$ FLT3$^-$ CD48$^-$ CD150$^+$ cells among live BM nucleated cells was similar in C57BL/6 and NOD-*scid* mice but reduced in NSG mice (*Online Supplementary Table S2* and Figure 2D). When calculated as cells per femur, C57BL/6 and NOD-*scid* mice had similar levels of phenotypic LT-HSC per femur, whereas NSG had a significantly lower number of phenotypic LT-HSC cells per femur (*Online Supplementary Table S2* and Figure 2E).

As it has been proposed that in the absence of SCA1 staining, the LK FLT3$^-$ CD48$^-$ CD150$^+$ phenotype is sufficient to quantify mouse HSC,[27] we further examined the expression of CD27 and CD201 in this population. In C57BL/6 mice, only 17.6% of LK FLT3$^-$ CD48$^-$ CD150$^+$ cells were positive for both CD27 and CD201 (*Online Supplementary Figure S2*). As it has been previously reported that all HSC reconstitution activity is within the Lin$^-$ CD27$^+$ CD201$^+$ population,[13] this suggests that it is necessary to add CD27 and CD201 stains in order to further enrich HSC within the Lin$^-$ CD117$^+$ FLT3$^-$ CD48$^-$ CD150$^+$ population. Likewise, in NOD-*scid* and NSG mice, only 28.6-32.9% of LK FLT3$^-$ CD48$^-$ CD150$^+$ cells were positive for both CD27 and CD201.

High expression of CD48 in NOD-*scid* and NSG mice

In this analysis of CD48 and CD150 HSC detection (Figure 2A-C), we noticed that CD48 was more highly expressed in NOD-*scid* and NSG mice than in C57BL/6 mice as revealed by CD48 expression overlays of LK CD27$^+$ CD201$^+$ FLT3$^-$ cells from the different mouse strains (Figure 2F). In addition, the CD48 mean fluorescence intensity for the whole LK CD27$^+$ CD201$^+$ FLT3$^-$ population was significantly reduced in C57BL/6 mice compared to that in the other mouse strains (Figure 2G).

The ligand for CD48 is CD244[28] and is expressed by NK cells, some T cells, and monocytes.[29] As the NOD-*scid* and NSG mice are devoid of functionally mature B and T cells, and NSG lack NK cells (*Online Supplementary Figures S3* and *S4*) we speculated that CD48 upregulation in NSG and NOD-*scid* mice may be due to low expression of the ligand CD244. To assess this, we performed a lineage and CD244 stain on BM and spleen cells (Figures 3 and 4) to measure CD244 expression on each cell subset defined in *Online Supplementary Figures S3* and *S4*. In C57BL/6 mice, subsets of CD244$^+$ cells were observed on all BM lineages (Figure 3C, F) but predominantly on NK cells (*Online Supplementary Table S3* and Figure 3F). Within the C57BL/6 spleen (Figure 4), CD244 was highly expressed on a subset of NK cells as well as on monocytes, macrophages, and neutrophil/myeloid progenitors. In NOD-*scid* and NSG mice, the frequency of CD244$^+$ was less than 1% of all lineages examined (Figures 3 and 4).

We detected some lymphocyte-type cells that were B220$^+$ in BM and spleen in both NOD-*scid* and NSG mouse BM (*Online Supplementary Figures S3* and *S4*). In addition, NSG mice had rare NK1.1$^+$ cells whereas both NSG and NOD-*scid* had few CD3ε$^+$ cells.

Long-term hematopoietic stem cells are enriched in the Lin$^-$ KIT$^+$ CD27$^+$ CD201$^+$ FLT3$^-$ CD48$^-$ CD150$^+$ subset in NSG mice

Finally, we tested whether the combination of CD27 and CD201 with FLT3, CD48, and CD150 markers could identify functional LT-HSC in NSG mice by serial dilution transplantation assay into non-lethally irradiated syngeneic recipients (Figure 5). As it has been previously shown that the whole competitive repopulation unit (CRU) activity is contained within the Lin$^-$ CD27$^+$ CD201$^+$ fraction of the BM in NOD mice,[13] we further characterized the functional properties of these cells stained additionally with FLT3, CD48, and CD150 antibodies. We sorted two subsets of the LK CD27$^+$ CD201$^+$ population from the BM of male NSG mice, namely (i) LK CD27$^+$ CD201$^+$ FLT3$^-$ CD48$^-$ CD150$^+$ cells (CD48$^-$CD150$^+$ gate) and (ii) LK

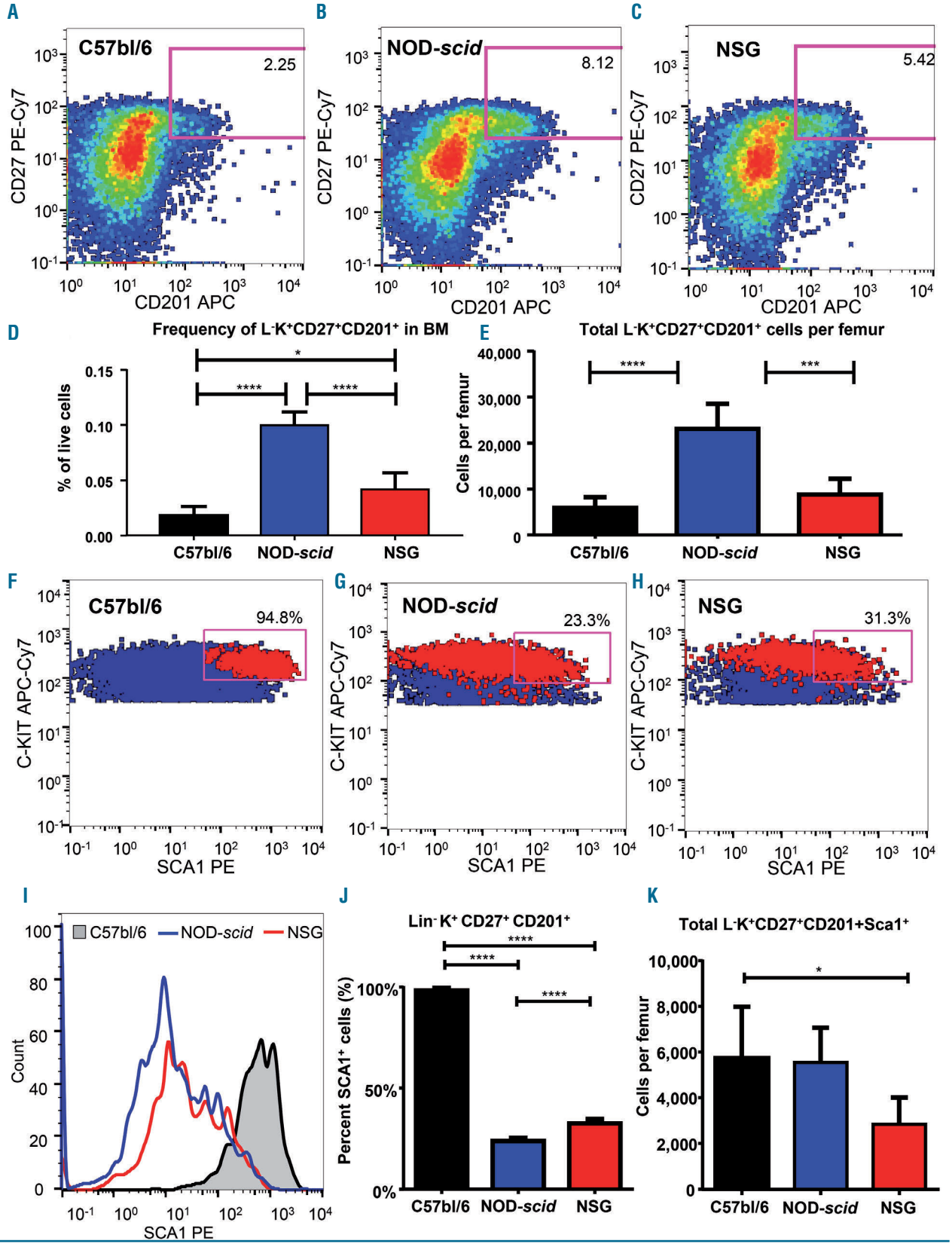

Figure 1. CD27 and CD201 expression in Lin⁻ KIT⁺ bone marrow hematopoietic stem and progenitor cells from different NOD-*scid*-derived mouse strains. (A-C) Expression of CD27 and CD201 in viable Lin⁻ KIT⁺ bone marrow (BM) hematopoietic stem and progenitor cells from C57BL/6 (A), NOD-*scid* (B) and NSG (C) mice. (D) Frequency of Lin⁻ KIT⁺ CD27⁺ CD201⁺ cells within BM leukocytes of the three mouse strains. (E) Absolute number of Lin⁻ KIT⁺ CD27⁺ CD201⁺ cells per femur in the three strains. (F-H) Comparison of SCA1 and KIT expression in Lin⁻ KIT⁺ CD27⁺ CD201⁺ cells (red overlay) compared to Lin⁻ KIT⁺ CD27⁺ CD201⁻ cells (blue overlay) in C57BL/6 (F), NOD-*scid* (G) and NSG (H) mice. (I) Overlay of SCA1 expression in Lin⁻ KIT⁺ CD27⁺ CD201⁺ cells from C57BL/6 (black), NOD-*scid* (blue) and NSG (red) mice. (J) Percentage of Lin⁻ KIT⁺ CD27⁺ CD201⁺ cells that are SCA1⁺. (K) Number of Lin⁻ CD27⁺ CD201⁺ cells that are SCA1⁺ per femur. Data are the mean ± standard deviation of five mice per group. *P* values were calculated by analysis of variance with Tukey corrections, **P*≤0.05, ***P*≤0.01, ****P*≤0.001, *****P*≤0.0001.

CD27$^+$ CD201$^+$ FLT3$^-$ cells that were not in the CD48$^-$ CD150$^+$ gate (NOT GATE) (Figure 5H, isotype controls in *Online Supplementary Figure S5*). We transplanted serial dilutions of these two populations (Figure 5H) into sub-lethally irradiated (2.5 Gy) female NSG recipient mice together with 100,000 lethally irradiated whole BM as carrier cells. At 8, 12, and 16 weeks a small amount of blood was lysed for longitudinal analysis of donor engraftment by genomic quantitative polymerase chain reaction using primers specific for the Y chromosome *Sry* gene compared to biallelic mouse *Il6* gene. In preliminary experiments, we validated this method of quantifying relative male cell number by mixing a known amount of male *vs.* female cells to demonstrate that the assay readout reflected the linear dilution series (*Online Supplementary Figure S6*). A level of >1% donor male cells at the 18-week harvest point was considered to be a successful reconstitution of the host (*Online Supplementary Table S4*).

In transplanted recipients, we measured chimerism between 8 and 18 weeks. There was robust long-term male donor chimerism in recipients that received 50 or 150 CD48$^-$ CD150$^+$ gated cells whereas there was a very "low" frequency of long-term chimerism in recipients of NOT GATE cells (Figure 5I, J). Poisson distribution analysis

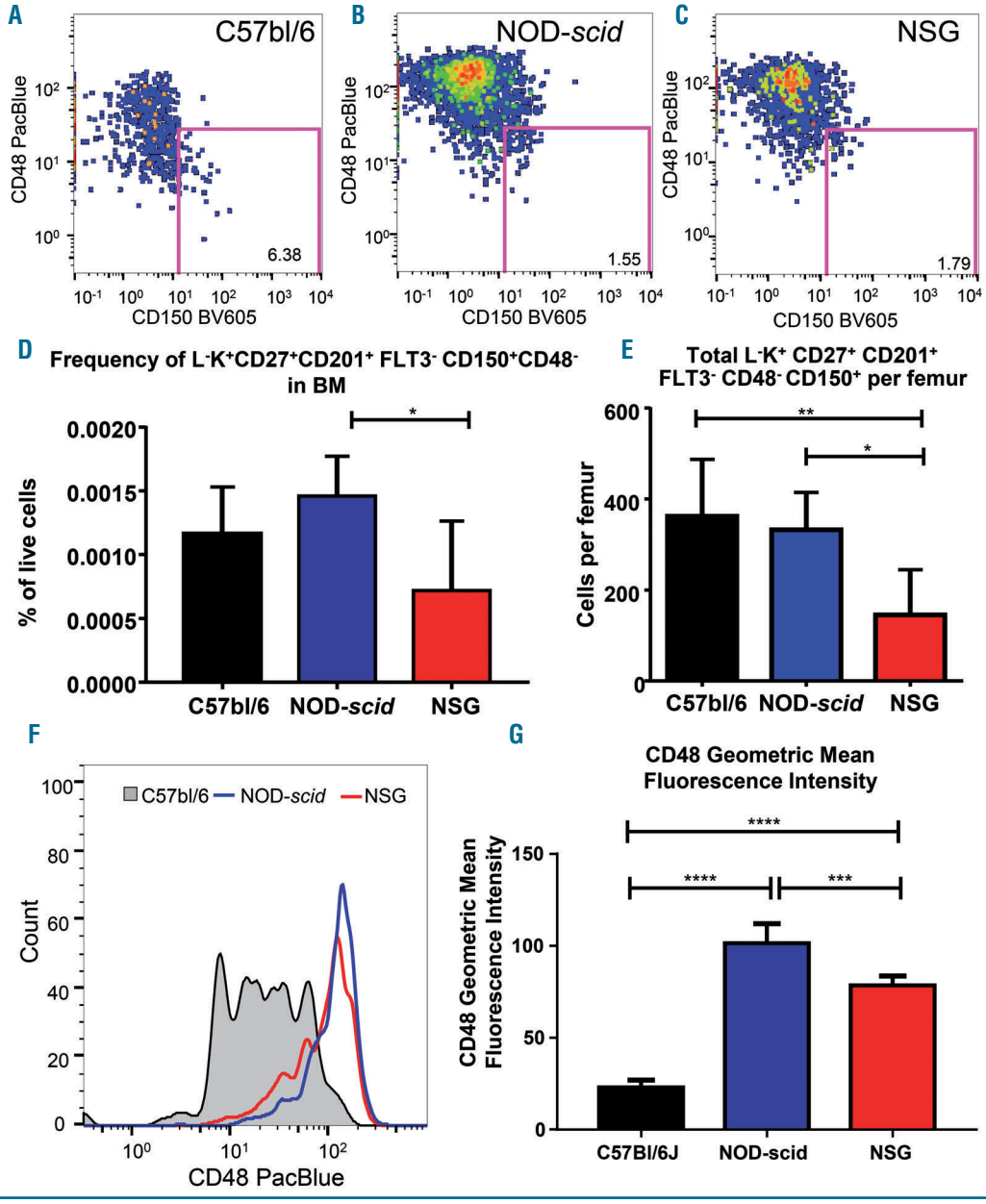

Figure 2. Complementarity of CD27 and CD201 with FLT3, CD48 and CD150 staining in different mouse strains. The gating strategy is shown in *Online Supplementary Figure S1*. (A-C) Lin$^-$ KIT$^+$ CD27$^+$ CD201$^+$ FLT3$^-$ bone marrow (BM) cells were gated and analyzed for CD150 and CD48 expression in C57BL/6 (A), NOD-*scid* (B) and NSG (C) mice. (D, E) Frequency (D) and total number (E) of Lin$^-$ KIT$^+$ CD27$^+$ CD201$^+$ FLT3$^-$ CD48$^-$ CD150$^+$ cells per femur in each strain. (F) Overlay of CD48 expression in Lin$^-$ KIT$^+$ CD27$^+$ CD201$^+$ FLT3$^-$ BM cells from C57BL/6 (grey shaded), NOD-*scid* (blue) and NSG (red) mice. (G) Geometric mean fluorescence intensity of CD48 on Lin$^-$ KIT$^+$ CD27$^+$ CD201$^+$ FLT3$^-$ cells in the three mouse strains. Data are the mean ± standard deviation of five mice per group. *P* values were calculated by analysis of variance with Tukey corrections for multiple comparisons, **P*≤0.05, ***P*≤0.01, ****P*≤0.001, *****P*≤0.0001.

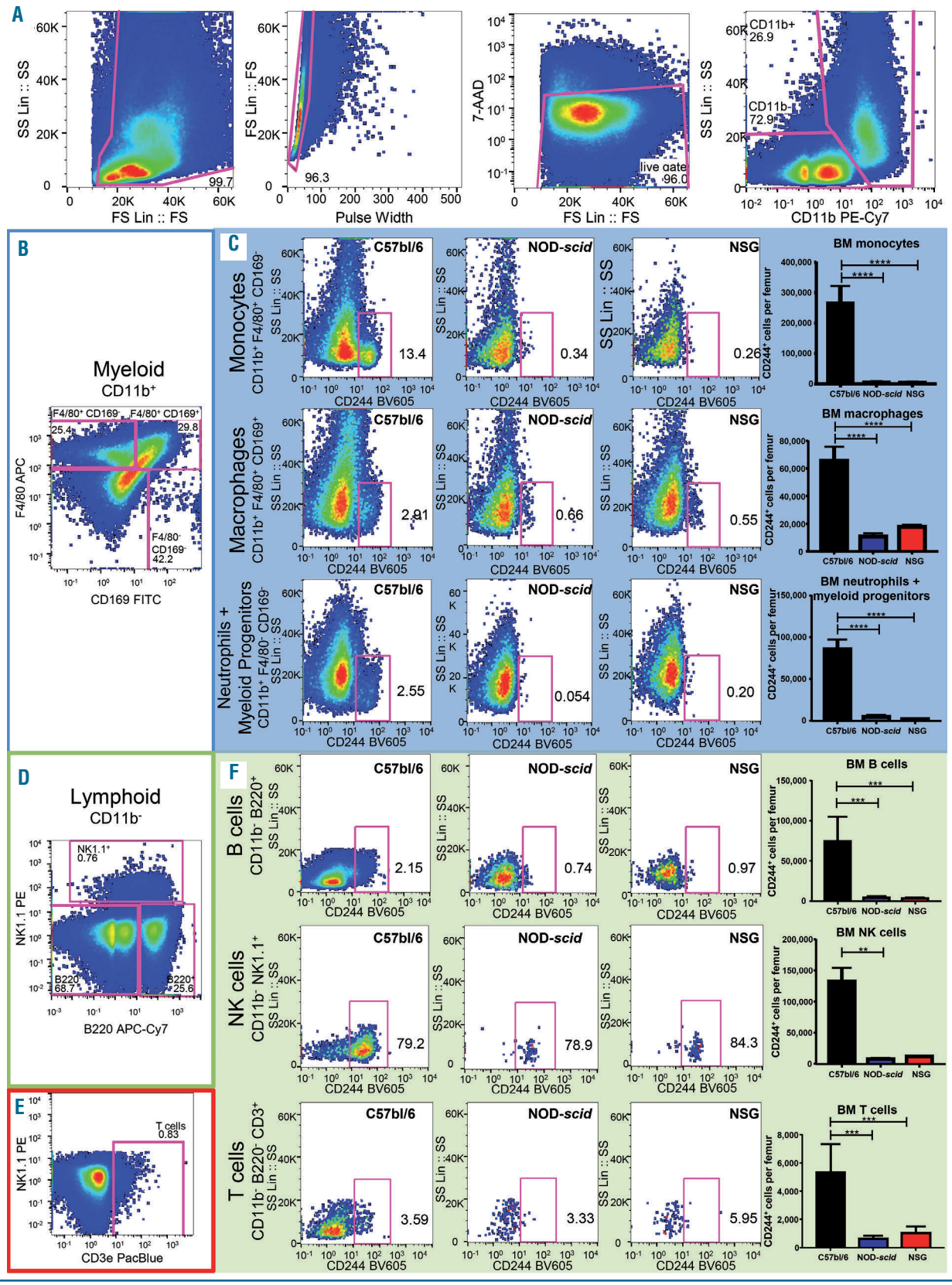

Figure 3. CD48 ligand CD244 is poorly expressed in the bone marrow of NOD-*scid* and NSG mice. (A) Viable single cells were gated into lymphoid (CD11b$^-$ low side scatter) and myeloid (CD11b$^+$) cells. (B) Myeloid cells were further separated using CD169 and F4/80 antigens. Monocytes were CD11b$^+$ F4/80$^+$ CD169$^-$; macrophages CD11b$^+$ F4/80$^+$ CD169$^+$; and neutrophils and remaining myeloid progenitors were CD11b$^+$ F4/80$^-$ CD169$^-$. (C) CD244 expression was measured in each subset in each mouse strain and plotted as numbers of CD244$^+$ cells per femur. (D) Lymphoid cells were separated using B220 and NK1.1 antigens to identify B cells (CD11b$^-$ B220$^+$ NK1.1$^-$) and natural killer (NK) cells (CD11b$^-$ NK1.1$^+$). (E) The B220$^-$ NK1.1$^-$ gate was then plotted for CD3ε expression to identify T cells (CD11b$^-$ B220$^-$ NK1.1$^-$ CD3ε$^+$). (F) CD244 expression on lymphoid subsets in each mouse strain. Numbers of CD244$^+$ cells in each subset per femur. Data are mean ± standard deviation of five mice per group. *P* values were calculated by analysis of variance with Tukey corrections for multiple comparisons: ***P*≤0.01, ****P*≤0.001, ****P≤0.0001.

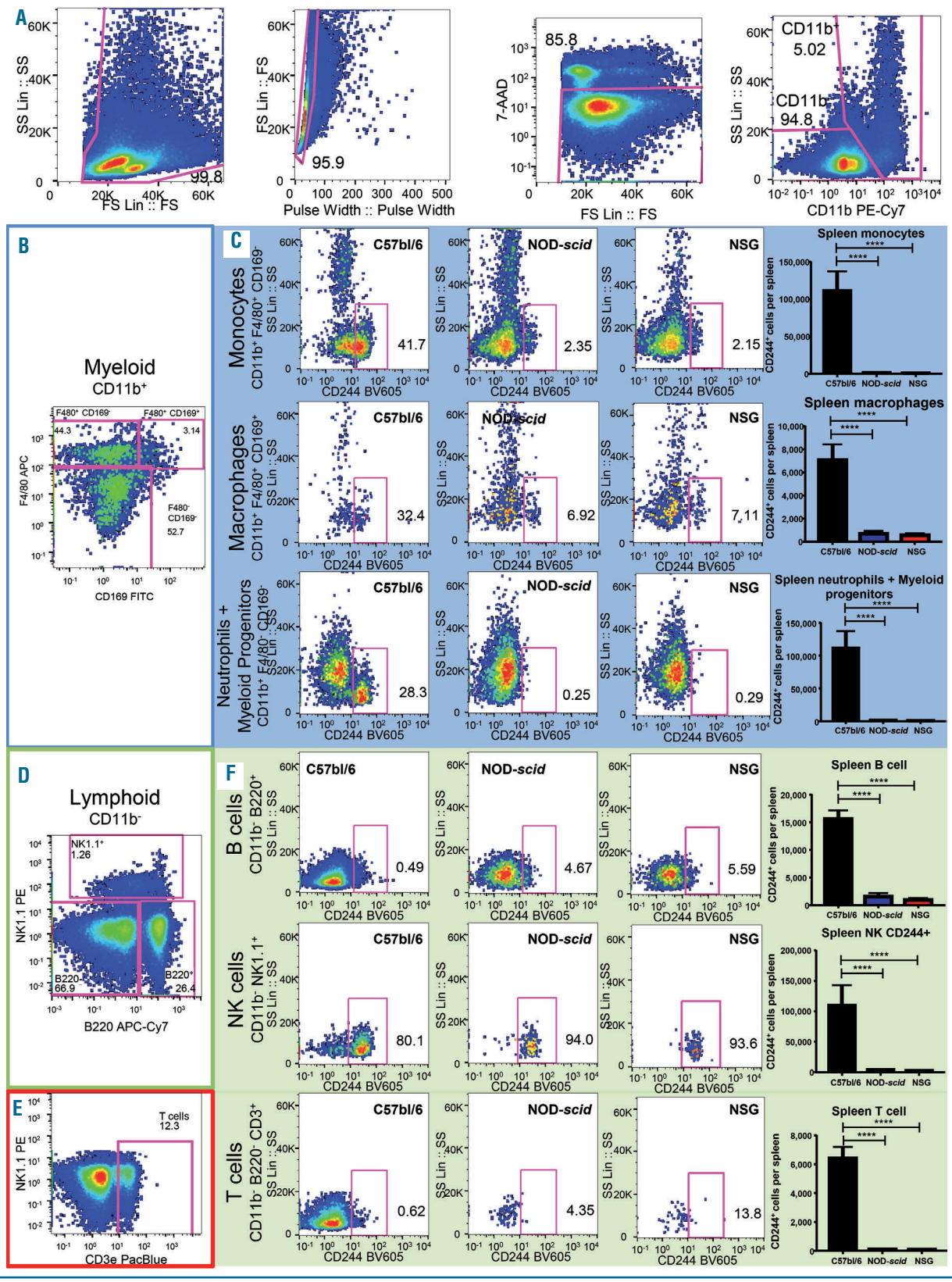

Figure 4. CD48 ligand CD244 is poorly expressed in the spleen of NOD-*scid* and NSG mice. (A) Viable single cells were gated with CD11b into lymphoid cells (CD11b$^-$ low side scatter) and myeloid cells (CD11b$^+$). (B) Myeloid cells were further separated using CD169 and F4/80 antigens. Monocytes were CD11b$^+$ F4/80$^+$ CD169$^-$; macrophages CD11b$^+$ F4/80$^+$ CD169$^+$; and neutrophils and remaining myeloid progenitors were in the CD11b$^+$ F4/80$^-$ CD169$^-$ gate . (C) CD244 expression was measured in each subset in each mouse strain and plotted as numbers of CD244$^+$ cells per femur. (D) Lymphoid cells were separated using B220 and NK1.1 antigens to identify B cells (CD11b$^-$ B220$^+$ NK1.1$^-$) and natural killer (NK) cells (CD11b$^-$ NK1.1$^+$). (E) The B220$^-$ NK1.1$^-$ gate was then plotted for CD3ε expression to identify T cells (CD11b$^-$ B220$^-$ NK1.1$^-$ CD3ε$^+$). (F) CD244 expression on lymphoid subsets in each mouse strain. Numbers of CD244$^+$ cells in each subset per femur. Data are average ± standard deviation of five mice per group. *P*-values were calculated by analysis of variance with Tukey corrections for multiple comparisons, *P≤0.05, **P≤0.01, ***P≤0.001, ****P≤0.0001.

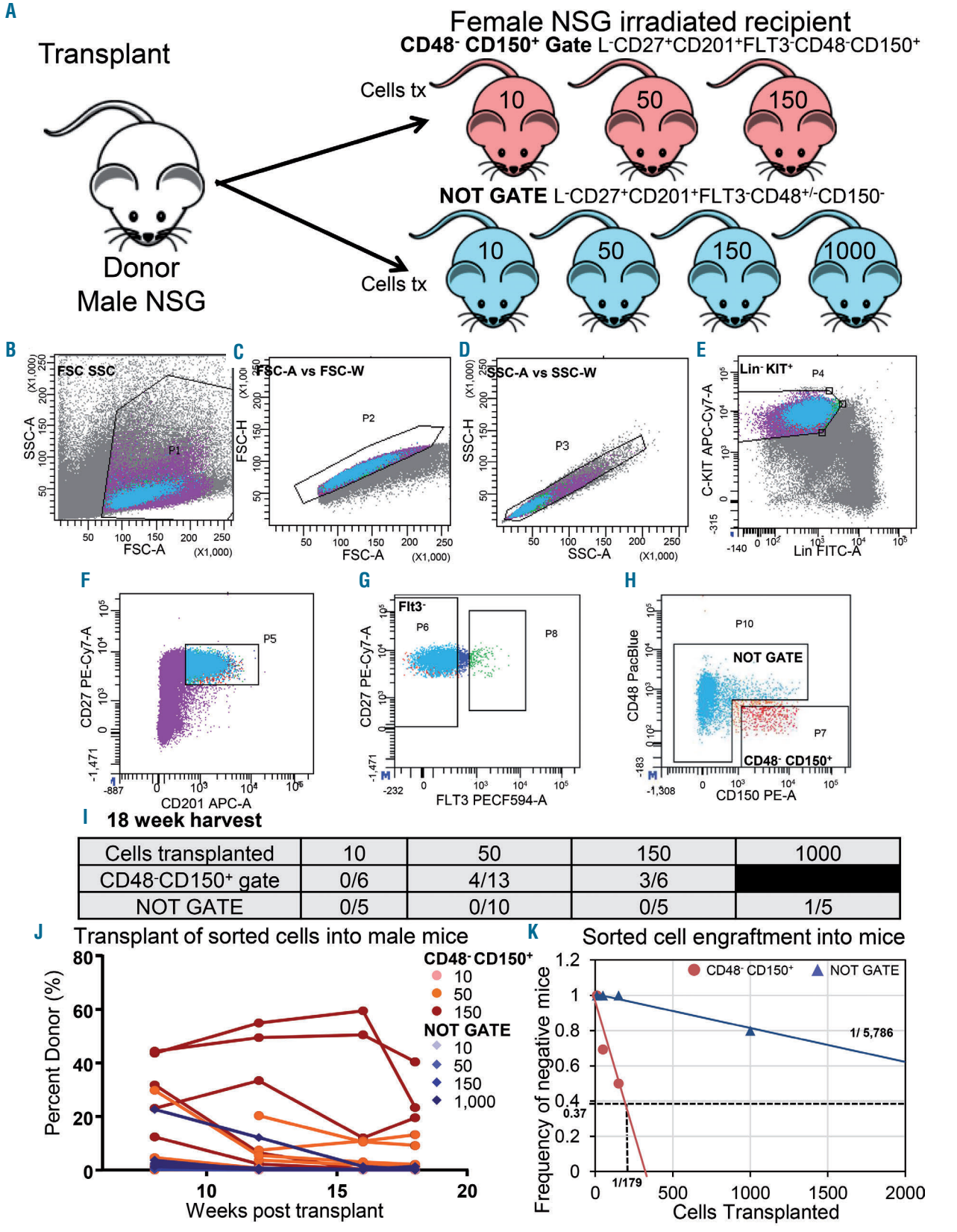

Cells transplanted	10	50	150	1000
CD48-CD150+ gate	0/6	4/13	3/6	
NOT GATE	0/5	0/10	0/5	1/5

Figure 5. Competitive repopulation unit cells are enriched in the Lin- KIT+ CD27+ CD201+ FLT3- CD48- CD150+ population in NSG mice. (A) Transplantation outline using sorted male donor cells transplanted into sublethally irradiated (2.5 Gy) female NSG mice to test competitive repopulation unit (CRU) activity. (B-H) Sorting profile from donor male c-KIT enriched bone marrow into either the Lin- KIT+ CD27+ CD201+ FLT3- CD48- CD150+ gate or the Lin- KIT+ CD27+ CD201+ FLT3- NOT GATE. (I) Frequencies of donor engraftment in blood at 18 weeks. (J) Time-course of male donor cell engraftment in each transplanted mouse. Warm colors are for dilutions of sorted Lin- KIT+ CD27+ CD201+ FLT3- CD48- CD150+ cells, cold colors are dilutions of Lin- KIT+ CD27+ CD201+ FLT3- NOT GATE sorted cells. (J) Frequency of donor engraftment at 18 weeks post-transplantation and Poisson distribution of donor hematopoietic stem cells. tx: transplant.

(Figure 5K) showed a 32-fold enrichment (P=1.86 x 10^{-5}) in CRU frequency in the CD48$^-$ CD150$^+$ gate (1 in 179 cells) compared to the NOT GATE cells (1 in 5,786 cells) confirming that the FLT3$^-$ CD48$^-$ CD150$^+$ phenotype complements the CD27$^+$ CD201$^+$ phenotype for further enrichment in functional LT-HSC. It is also important to note that the 1/5,786 CRU frequency found in the NOT GATE was due to a single recipient of the highest donor cell dose which had a very low level of engraftment (less than 3%) compared to recipients of CD48$^-$ CD150$^+$ cells (*Online Supplementary Table S4*). Therefore the CRU frequency in the NOT GATE could be overestimated. Nevertheless, by multiplying the CRU frequency obtained from each gate by the number of cells in each gate, we found that 70% of the CRU contained within LK CD27$^+$ CD201$^+$ FLT3$^-$ cells were within the CD48$^-$ CD150$^+$ subset (*Online Supplementary Table S5*).

SCA1 expression in unaltered in bone marrow endothelial and mesenchymal cells in NSG mice

As NSG mice and NOD-*scid* mice blood cells have low SCA1 expression in hematopoietic stem and progenitor cells (HSPC) (Figure 1I), we compared SCA1 expression in BM endothelial cells and MSC from C57BL/6 mice and NSG mice (Figure 6). Endosteal cells were collected from collagenase-treated femurs, magnetically enriched in non-hematopoietic cells, and stained against CD45, Lin, CD31, CD51, SCA1, and PDGFRα antibodies (gating strategy in Figure 6A-D). CD45$^-$ Ter119$^-$ CD31$^+$ BM endothelial cells (Figure 6E, F) expressed equivalent levels of SCA1 in C57BL/6 and NSG mice (Figure 6E, F, I). Likewise, BM MSC, defined as CD45$^-$ Ter119$^-$ CD31$^-$ CD51$^+$ cells (Figure 6G, H), expressed similar levels of SCA1 in the PDGFRα$^+$ subset which defines the PαS cells[30] (Figure 6J).

Finally, we found that plastic-adherent BM MSC derived from NSG mice also expressed high levels of SCA1 (Figure 6K).

Discussion

Considering that all the LT-HSC reconstituting activity resides within the Lin$^-$ CD27$^+$ CD201$^+$ population,[13] we sought to determine the expression profile of these cells for FLT3, CD48 and CD150 antigens, which are classically used to identified LT-HSC and various subsets of multipotent progenitors.[4,5,26] We found that in all three strains, irrespective of SCA1 expression levels, only a small subset of LK CD27$^+$ CD201$^+$ cells was also FLT3$^-$ CD48$^-$ CD150$^+$, a phenotype that defines LT-HSC when used in combination with SCA1 positivity.[26] Conversely, only a minority of LK FLT3$^-$ CD48$^-$ CD150$^+$ cells were double-positive for CD27 and CD201. Using a stringent serial dilution long-term transplantation assay, we demonstrated that CRU were 32-fold enriched in the small FLT3$^-$ CD48$^-$ CD150$^+$ subset of the LK CD27$^+$ CD201$^+$ population from NSG mice despite negative to low levels of SCA1 expression. This demonstrates that CD27 and CD201 positivity is complementary to the FLT3$^-$ CD48$^-$ CD150$^+$ phenotype to identify functional LT-HSC and can be used to replace SCA1. This is particularly advantageous in strains that express low levels of SCA1 in hematopoietic cells such as NOD-*scid* and NSG strains, or because of treatments that increase or decrease SCA1 expression, such as irradiation and lipopolysaccharide administration.[13,27] We also noted a lower CRU frequency compared to the reported 50% CRU frequency in LK CD48$^-$CD150$^+$ cells sorted from C57BL/6 mice.[6] Competitive assays in lethally irradiated recipient mice with congenic whole BM cells as a source of competing HSC were used in these studies[6] whereas in the present study, we sublethally irradiated our recipient mice (2.5 Gy) without exogenous competing HSC. This irradiation dose depresses circulating granulocytes and monocytes for only 8 days without transplantation *(data not shown*) and therefore spares an unknown number of host HSC. Consequently, this sublethal irradiation of the hosts creates a competitive assay between the residual female host HSC and the transplanted male HSC. This could in part explain the relatively low frequency of reconstituting cells that we measured in LK CD27$^+$ CD201$^+$ FLT3$^-$ CD48$^-$ CD150$^+$ cells from NSG mice. An additional factor to consider regarding this relatively low frequency of reconstituting cells in the LK CD27$^+$ CD201$^+$ FLT3$^-$ CD48$^-$ CD150$^+$ fraction from NSG mice is the known engraftment defect of HSC caused by the *scid* mutation, which would consequently reduce the reconstitution potential of the sorted cell populations.[31,32]

Our flow cytometry data revealed that the expression of CD48 was unusually higher in LK CD27$^+$ CD201$^+$ FLT3$^-$ cells from the NOD-*scid* and NSG mice compared to C57BL/6 mice. We found that the expression of CD244, the physiological ligand of CD48, was dramatically reduced in myeloid cells and lymphocytes from NOD-*scid* and NSG BM and spleen. Although NOD-*scid* and NSG mice have very low frequencies of T and NK cells that would express CD244, expression of CD244 in all myeloid lineages was also markedly reduced in the BM and spleen of NOD-*scid* and NSG mice. It is, therefore, tempting to speculate that CD48 upregulation in NOD-*scid*-derived strains is caused by the low expression of its ligand CD244. However, this potential mechanism will need to be confirmed in C57BL/6 mice with CD244 gene deficiency.

Interestingly, NOD-*scid* mice still contain a NK-cell population[33] but we did not detect higher numbers of NK1.1$^+$ cells compared to the numbers in NSG mice. As we did not perform functional assays, we cannot conclude from our experiments that NSG mice had less functional NK cells compared to the NOD-*scid* mice. The literature indicates that CD3$^+$ and primitive B cells are present in these mice but do not develop into mature functional lymphocytes.[33] The *scid* mutation is known to eliminate B and T cells at the education stage of development during VDJ recombination.[34] This means that the BM will develop immature B and T precursors, which migrate into the circulation but cannot fully mature into functional lymphocytes. With age, NOD-*scid* mice are known to have some 'leakiness' and develop functional B and T cells while NSG do not.[33] Previous studies on these mice have focused on the spleen and/or blood,[20,33] which are locations of mature B and T cells, and did not examine the BM in which these cells develop initially. As we used 8-week old mice, this small percentage of CD3ε$^+$ and B220$^+$ cells may represent immature lymphoid cells. The use of markers of more mature B cells, such as CD19 and surface IgM (sIgM), could have confirmed the absence of mature CD19$^+$ sIgM$^+$ B cells in these mice.[33,35]

Beside hematopoietic cells, SCA1 is expressed by various cell types such as mesenchymal and endothelial cells and is considered a progenitor/stem cell marker in many

adult mouse tissues.[36] In particular, SCA1 is known to be expressed by immature MSC in the BM and skeletal muscle, as well as by BM endothelial cells.[30,37,38] The literature is conflicting as to whether SCA1 expression on stromal cells is dependent on the mouse strain. For instance, some groups have identified that cultured plastic-adherent MSC derived from BALB/c mice[39,40] and CBA mice[40] are SCA1$^+$ (both haplotype LY6.1 mice). In contrast, other groups reported that the SCA1 staining on MSC was restricted to plastic-adherent cultured MSC from the C57BL/6 and FVB/N strains whereas DBA1-derived MSC

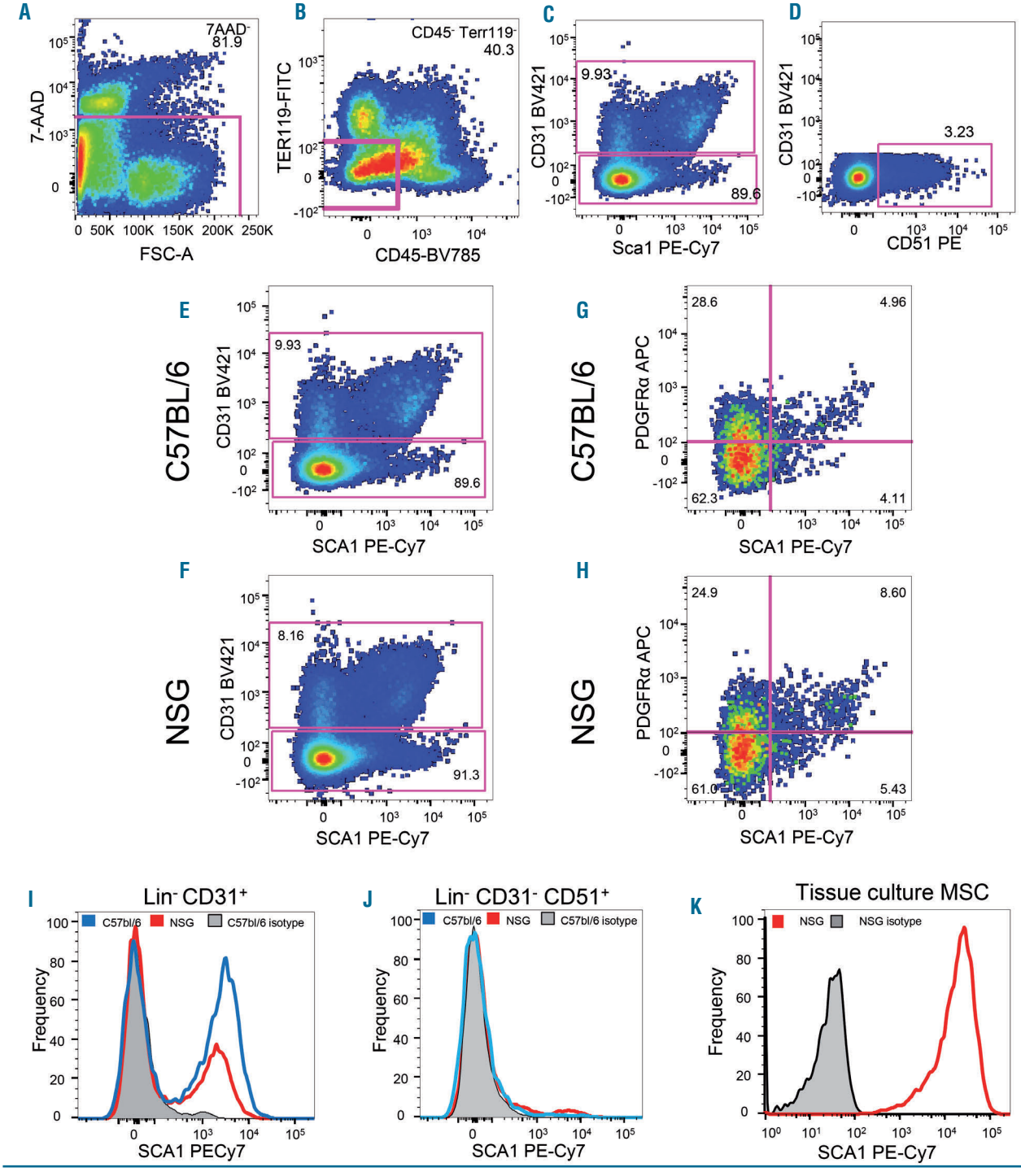

Figure 6. Comparative SCA1 expression in bone marrow endothelial and mesenchymal cells from C57BL/6 and NSG mice. (A-D) Live single cells (A) were gated for non-hematopoietic CD45$^-$ Ter119$^-$ cells (B). From these CD45$^-$ Ter119$^-$ cells, endothelial cells were gated as CD31$^+$ (C). The remaining CD31$^-$ non-endothelial cells were gated for CD51$^+$ mesenchymal cells (D). (E, F, I) SCA1 expression in bone marrow endothelial cells was similar in C57BL/6 (E) and NSG (F) mice as seen in the overlay histogram (I). (G, H, J) CD45$^-$ Ter119$^-$ CD31$^-$ CD51$^+$ mesenchymal cells were further gated for PDGFRα and SCA1 expression. SCA1 expression in mesenchymal cells was comparable in C57BL/6 (G) and NSG (H) mice in dot-plots and the overlay histograms (J). (K) SCA1 expression in mesenchymal stromal cells (MSC) cultured from NSG mice. These plots represent data from four separate mice for each strain.

expressed low levels and BALB/c-derived MSC were negative.[41] As SCA1 has been recently described as an activation marker facilitating cell cycling[8,42] and mesenchymal progenitor cell self-renewal *in vivo*,[43] culturing these cells *in vitro* could activate SCA1 expression and may explain this discordance. In our experiments, we found that low SCA1 expression is restricted to HSPC in NSG mice. Both freshly isolated BM endothelial cells (Figure 5G) and primitive mesenchymal progenitor cells (Figure 5H) from NSG mice expressed high levels of SCA1 similar to C57BL/6 mice as previously reported.[44,45] The high expression level of SCA1 on mesenchymal cells from NOD-*scid* and NSG mice is consistent with the absence of the osteoporotic phenotype that is observed in SCA1 knockout mice.[43] Our results therefore suggest that lower SCA1 expression may be limited to hematopoietic cells in NSG mice and may be a result of the original source of the *scid* mutation that was derived from the BALB/c background, a LY6.1 haplotype mouse or from the NOD background.[20,46]

In conclusion, co-staining for CD27 and CD201 can be used in place of SCA1 to identify HSC in NOD-*scid* and NSG mice in circumstances that SCA1 expression is weak. However, when the Lin$^-$ CD27$^+$ and CD201$^+$ phenotype is combined with the FLT3$^-$ CD48$^-$ CD150$^+$ phenotype, HSC with long-term engraftment potential are further enriched in NOD-*scid* and NSG mice. Compared to recent studies that focused only on Lin$^-$ CD27$^+$ CD201$^+$ cells,[32,47] we show that within this population the small subset that is FLT3$^-$, CD48$^-$ and CD150$^+$ is enriched in LT-HSC activity in NSG mice in a rigorous serial dilution long-term competitive transplantation assay. This alleviates the need to stain for SCA1, which is expressed at very low levels in these mice. In addition, we identified a non-reported upregulation of CD48 in NOD-*scid* and NSG mice possibly due to the low expression of its ligand CD244. Finally, the low SCA1 expression in NSG mice seems limited to the hematopoietic compartment as SCA1 expression remains high in primary BM endothelial and mesenchymal cells. Overall, our new strategy may provide a more accurate method to quantify murine HSC within xenograft models using NOD-*scid*-derived strains. For instance, in previous work[48,49] humanized scaffolds seeded with human MSC were transplanted into NOD-*scid* mice and once humanized ectopic bone organoid had been established, were injected with human BM or cord blood CD34$^+$ cells. The relative quantification of the seeding of humanised ectopic bone scaffolds by human *vs.* murine HSC was difficult due to low SCA1 expression by NOD-*scid* and NSG HSC. Likewise, in a common xenotransplanted model of NSG mice engrafted with human cold blood CD34$^+$ HSC, we were able to demonstrate that hypoxia-inducible factor prolyl hydroxylase inhibitor can rescue a human HSPC mobilization defect in NSG mice but we were unable to show a similar effect on murine HSC due to their low SCA1 expression.[50] Therefore, this new staining strategy identifying Lin$^-$ KIT$^+$ CD27$^+$ CD201$^+$ FLT3$^-$ CD48$^-$ CD150$^+$ cells as mouse HSC in NOD-*scid*-derived strains will enable a more accurate measurement of the relative colonization or distribution of mouse bones or ectopic bone organoids by endogenous mouse HSC *vs.* xenotransplanted human HSC.

Acknowledgments

The authors acknowledge the Translational Research Institute (TRI) for providing an excellent research environment and core facilities that enabled this research. We particularly thank the Flow Cytometry and the Biological Resources Core Facilities. BN was supported by an Australian Government Research Training Program Scholarship during her PhD studies. JPL is funded by Research Fellowship APP1136130 from the National Health and Medical Research Council of Australia (NHMRC). MRD is funded by a Career Development Fellowship APP1130013 and Project Grant APP1108043 from the NHMRC. EDW is supported by funding from the Movember Foundation and the Prostate Cancer Foundation of Australia through a Movember Revolutionary Team Award. The APCRC-Q is supported by funding from the Australian Government Department of Health. The TRI is supported by Therapeutic Innovation Australia (TIA). TIA is supported by the Australian Government through the National Collaborative Research Infrastructure Strategy (NCRIS) program.

References

1. Uchida N, Aguila HL, Fleming WH, Jerabek L, Weissman IL. Rapid and sustained hematopoietic recovery in lethally irradiated mice transplanted with purified Thy-1.1lo Lin-Sca-1+ hematopoietic stem cells. Blood. 1994;83(12):3758-3779.
2. Ikuta K, Weissman IL. Evidence that hematopoietic stem cells express mouse c-kit but do not depend on steel factor for their generation. Proc Natl Acad Sci U S A. 1992;89(4):1502-1506.
3. Spangrude GJ, Heimfeld S, Weissman IL. Purification and characterization of mouse hematopoietic stem cells. Science. 1988;241(4861):58-62.
4. Boles NC, Lin KK, Lukov GL, et al. CD48 on hematopoietic progenitors regulates stem cells and suppresses tumor formation. Blood. 2011;118(1):80-87.
5. Oguro H, Ding L, Morrison SJ. SLAM family markers resolve functionally distinct subpopulations of hematopoietic stem cells and multipotent progenitors. Cell Stem Cell. 2013;13(1):102-116.
6. Kiel MJ, Yilmaz OH, Iwashita T, et al. SLAM family receptors distinguish hematopoietic stem and progenitor cells and reveal endothelial niches for stem cells. Cell. 2005;121(7):1109-1121.
7. Jurecic R, Van NT, Belmont JW. Enrichment and functional characterization of Sca-1+WGA+, Lin-WGA+, Lin-Sca-1+, and Lin-Sca-1+WGA+ bone marrow cells from mice with an Ly-6a haplotype. Blood. 1993;82(9):2673-2683.
8. Spangrude GJ, Brooks DM. Mouse strain variability in the expression of the hematopoietic stem cell antigen Ly-6A/E by bone marrow cells. Blood. 1993;82(11):3327-3332.
9. Lee PY, Wang JX, Parisini E, Dascher CC, Nigrovic PA. Ly6 family proteins in neutrophil biology. J Leukoc Biol. 2013;94(4):585-594.
10. Chilton PM, Rezzoug F, Ratajczak MZ, et al. Hematopoietic stem cells from NOD mice exhibit autonomous behavior and a competitive advantage in allogeneic recipients. Blood. 2005;105(5):2189-2197.
11. Simonnet AJ, Nehme J, Vaigot P, et al. Phenotypic and functional changes induced in hematopoietic stem/progenitor cells after gamma-ray radiation exposure. Stem Cells. 2009;27(6):1400-1409.
12. Baldridge MT, King KY, Boles NC, Weksberg DC, Goodell MA. Quiescent haematopoietic stem cells are activated by IFN-gamma in response to chronic infection. Nature. 2010;465(7299):793-797.
13. Vazquez SE, Inlay MA, Serwold T. CD201 and CD27 identify hematopoietic stem and progenitor cells across multiple murine strains independently of Kit and Sca-1. Exp Hematol. 2015;43(7):578-585.
14. Balazs AB, Fabian AJ, Esmon CT, Mulligan RC. Endothelial protein C receptor (CD201) explicitly identifies hematopoietic stem cells in murine bone marrow. Blood. 2006;107(6):2317-2321.
15. Wiesmann A, Phillips RL, Mojica M, et al.

Expression of CD27 on murine hematopoietic stem and progenitor cells. Immunity. 2000;12(2):193-199.
16. Benz C, Copley MR, Kent DG, et al. Hematopoietic stem cell subtypes expand differentially during development and display distinct lymphopoietic programs. Cell Stem Cell. 2012;10(3):273-283.
17. Kent DG, Copley MR, Benz C, et al. Prospective isolation and molecular characterization of hematopoietic stem cells with durable self-renewal potential. Blood. 2009;113(25):6342-6350.
18. Fares I, Chagraoui J, Lehnertz B, et al. EPCR expression marks UM171-expanded CD34(+) cord blood stem cells. Blood. 2017;129(25):3344-3351.
19. Maykel J, Liu JH, Li H, et al. NOD-scidIl2rg (tm1Wjl) and NOD-Rag1 (null) Il2rg (tm1Wjl): a model for stromal cell-tumor cell interaction for human colon cancer. Dig Dis Sci. 2014;59(6):1169-1179.
20. Shultz LD, Lyons BL, Burzenski LM, et al. Human lymphoid and myeloid cell development in NOD/LtSz-scid IL2R gamma null mice engrafted with mobilized human hemopoietic stem cells. J Immunol. 2005;174(10):6477-6489.
21. Holzapfel BM, Wagner F, Thibaudeau L, Levesque JP, Hutmacher DW. Concise review: humanized models of tumor immunology in the 21st century: convergence of cancer research and tissue engineering. Stem Cells. 2015;33(6):1696-1704.
22. Ren G, Esposito M, Kang Y. Bone metastasis and the metastatic niche. J Mol Med (Berl). 2015;93(11):1203-1212.
23. Winkler IG, Barbier V, Nowlan B, et al. Vascular niche E-selectin regulates hematopoietic stem cell dormancy, self renewal and chemoresistance. Nat Med. 2012;18(11):1651-1657.
24. Cook MM, Futrega K, Osiecki M, et al. Micromarrows--three-dimensional coculture of hematopoietic stem cells and mesenchymal stromal cells. Tissue Eng Part C Methods. 2012;18(5):319-328.
25. Franco C, Britto K, Wong E, et al. Discoidin domain receptor 1 on bone marrow–derived cells promotes macrophage accumulation during atherogenesis. Circ Res. 2009;105 (11):1141-1148.
26. Pietras EM, Reynaud D, Kang YA, et al. Functionally distinct subsets of lineage-biased multipotent progenitors control blood production in normal and regenerative conditions. Cell Stem Cell. 2015;17(1):35-46.
27. Knudsen KJ, Rehn M, Hasemann MS, et al. ERG promotes the maintenance of hematopoietic stem cells by restricting their differentiation. Genes Dev. 2015;29(18): 1915-1929.
28. Boles KS, Stepp SE, Bennett M, Kumar V, Mathew PA. 2B4 (CD244) and CS1: novel members of the CD2 subset of the immunoglobulin superfamily molecules expressed on natural killer cells and other leukocytes. Immunol Rev. 2001;181:234-249.
29. Vaidya SV, Mathew PA. Of mice and men: different functions of the murine and human 2B4 (CD244) receptor on NK cells. Immunol Lett. 2006;105(2):180-184.
30. Pinho S, Lacombe J, Hanoun M, et al. PDGFRalpha and CD51 mark human nestin+ sphere-forming mesenchymal stem cells capable of hematopoietic progenitor cell expansion. J Exp Med. 2013;210(7):1351-1367.
31. Qing Y, Lin Y, Gerson SL. An intrinsic BM hematopoietic niche occupancy defect of HSC in scid mice facilitates exogenous HSC engraftment. Blood. 2012;119(7): 1768-1771.
32. Verbiest T, Finnon R, Brown N, et al. NOD Scid gamma mice are permissive to allogeneic HSC transplantation without prior conditioning. Int J Mol Sci. 2016; 17(11).
33. Katano I, Ito R, Eto T, Aiso S, Ito M. Immunodeficient NOD-scid IL-2Rgamma(null) mice do not display T and B cell leakiness. Exp Anim. 2011;60(2):181-186.
34. Bosma MJ, Carroll AM. The SCID mouse mutant: definition, characterization, and potential uses. Annu Rev Immunol. 1991;9:323-350.
35. Winkler IG, Bendall LJ, Forristal CE, et al. B-lymphopoiesis is stopped by mobilizing doses of G-CSF and is rescued by overexpression of the anti-apoptotic protein Bcl2. Haematologica. 2013;98(3):325-333.
36. Holmes C, Stanford WL. Concise review: stem cell antigen-1: expression, function, and enigma. Stem Cells. 2007;25(6):1339-1347.
37. Morikawa S, Mabuchi Y, Kubota Y, et al. Prospective identification, isolation, and systemic transplantation of multipotent mesenchymal stem cells in murine bone marrow. J Exp Med. 2009;206(11):2483-2496.
38. Xiao Q, Zeng L, Zhang Z, et al. Sca-1+ progenitors derived from embryonic stem cells differentiate into endothelial cells capable of vascular repair after arterial injury. Arterioscler Thromb Vasc Biol. 2006;26 (10):2244-2251.
39. Cahill EF, Tobin LM, Carty F, Mahon BP, English K. Jagged-1 is required for the expansion of CD4+ CD25+ FoxP3+ regulatory T cells and tolerogenic dendritic cells by murine mesenchymal stromal cells. Stem Cell Res Ther. 2015;6(1):19.
40. Ooi YY, Rahmat Z, Jose S, Ramasamy R, Vidyadaran S. Immunophenotype and differentiation capacity of bone marrow-derived mesenchymal stem cells from CBA/Ca, ICR and Balb/c mice. World J Stem Cells. 2013;5(1):34-42.
41. Peister A, Mellad JA, Larson BL, et al. Adult stem cells from bone marrow (MSCs) isolated from different strains of inbred mice vary in surface epitopes, rates of proliferation, and differentiation potential. Blood. 2004;103(5):1662-1668.
42. Morcos MNF, Schoedel KB, Hoppe A, et al. SCA-1 expression level identifies quiescent hematopoietic stem and progenitor cells. Stem Cell Reports. 2017;8(6):1472-1478.
43. Bonyadi M, Waldman SD, Liu D, et al. Mesenchymal progenitor self-renewal deficiency leads to age-dependent osteoporosis in Sca-1/Ly-6A null mice. Proc Natl Acad Sci U S A. 2003;100(10):5840-5845.
44. Xiao P, Sandhow L, Heshmati Y, et al. Distinct roles of mesenchymal stem and progenitor cells during the development of acute myeloid leukemia in mice. Blood Adv. 2018;2(12):1480-1494.
45. Passaro D, Di Tullio A, Abarrategi A, et al. Increased vascular permeability in the bone marrow microenvironment contributes to disease progression and drug response in acute myeloid leukemia. Cancer Cell. 2017;32(3):324-341.e6.
46. Coughlan AM, Harmon C, Whelan S, et al. Myeloid engraftment in humanized mice: impact of granulocyte-colony stimulating factor treatment and transgenic mouse strain. Stem Cells Dev. 2016;25(7):530-541.
47. Karimzadeh A, Scarfone VM, Varady E, et al. The CD11a and endothelial protein C receptor marker combination simplifies and improves the purification of mouse hematopoietic stem cells. Stem Cells Transl Med. 2018;7(6):468-476.
48. Holzapfel BM, Hutmacher DW, Nowlan B, et al. Tissue engineered humanized bone supports human hematopoiesis in vivo. Biomaterials. 2015;61:103-114.
49. Martine LC, Holzapfel BM, McGovern JA, et al. Engineering a humanized bone organ model in mice to study bone metastases. Nat Protoc. 2017;12(4):639-663.
50. Nowlan B, Futrega K, Brunck ME, et al. HIF-1alpha-stabilizing agent FG-4497 rescues human CD34+ cell mobilization in response to G-CSF in immunodeficient mice. Exp Hematol. 2017;52:50-55.e56.

ARTICLE

Mental stress causes vasoconstriction in subjects with sickle cell disease and in normal controls

Payal Shah,[1] Maha Khaleel,[1] Wanwara Thuptimdang,[2] John Sunwoo,[2] Saranya Veluswamy,[1] Patjanaporn Chalacheva,[2] Roberta M. Kato,[3] Jon Detterich,[4] John C. Wood,[2,4] Lonnie Zeltzer,[5] Richard Sposto,[6] Michael C.K. Khoo[2] and Thomas D. Coates[1]

[1]Division of Hematology, Children's Center for Cancer and Blood Diseases, Children's Hospital Los Angeles, Keck School of Medicine, University of Southern California, Los Angeles; [2]Biomedical Engineering, Viterbi School of Engineering, University of Southern California, Los Angeles; [3]Division of Pulmonology, Children's Hospital Los Angeles, Keck School of Medicine, University of Southern California, Los Angeles; [4]Division of Cardiology, Children's Hospital Los Angeles, Keck School of Medicine, University of Southern California, Los Angeles; [5]Pediatric Pain Program, David Geffen School of Medicine at UCLA, University of California, Los Angeles and [6]Department of Preventive Medicine, Keck School of Medicine, University of Southern California, Los Angeles, CA, USA

Ferrata Storti Foundation

Haematologica 2020
Volume 105(1):83-90

ABSTRACT

Vaso-occlusive crisis (VOC) is a hallmark of sickle cell disease (SCD) and occurs when deoxygenated sickled red blood cells occlude the microvasculature. Any stimulus, such as mental stress, which decreases microvascular blood flow will increase the likelihood of red cell entrapment resulting in local vaso-occlusion and progression to VOC. Neurally mediated vasoconstriction might be the physiological link between crisis triggers and vaso-occlusion. In this study, we determined the effect of mental stress on microvascular blood flow and autonomic nervous system reactivity. Sickle cell patients and controls performed mentally stressful tasks, including a memory task, conflict test and pain anticipation test. Blood flow was measured using photoplethysmography, autonomic reactivity was derived from electrocardiography and perceived stress was measured by the State-Trait Anxiety Inventory questionnaire. Stress tasks induced a significant decrease in microvascular blood flow, parasympathetic withdrawal and sympathetic activation in all subjects. Of the various tests, pain anticipation caused the highest degree of vasoconstriction. The magnitude of vasoconstriction, sympathetic activation and perceived stress was greater during the Stroop conflict test than during the N-back memory test, indicating the relationship between magnitude of experimental stress and degree of regional vasoconstriction. Baseline anxiety had a significant effect on the vasoconstrictive response in sickle cell subjects but not in controls. In conclusion, mental stress caused vasoconstriction and autonomic nervous system reactivity in all subjects. Although the pattern of responses was not significantly different between the two groups, the consequences of vasoconstriction can be quite significant in SCD because of the resultant entrapment of sickle cells in the microvasculature. This suggests that mental stress can precipitate a VOC in SCD by causing neural-mediated vasoconstriction.

Introduction

Sickle cell disease (SCD) is a genetic disorder in which polymerization of deoxygenated sickle hemoglobin (HbS) leads to decreased deformability of the normally flexible erythrocytes. These rigid sickle-shaped red blood cells (RBC) can occlude the microvasculature leading to the sudden onset of painful vaso-occlusive episodes (VOC).[1,2] After HbS deoxygenates in the capillaries, it takes some time (seconds) for

Correspondence:

THOMAS D. COATES
tcoates@chla.usc.edu

Received: December 6, 2018.

Accepted: April 5, 2019.

Pre-published: April 11, 2019.

doi:10.3324/haematol.2018.211391

Check the online version for the most updated information on this article, online supplements, and information on authorship & disclosures: www.haematologica.org/content/105/1/83

HbS polymerization and the subsequent flexible-to-rigid transformation. If the transit time of RBC through the microvasculature is longer than the polymerization time, sickled RBC will lodge in the microvasculature.[3] Any trigger that decreases microvascular blood flow will prolong the transit time, promoting the entrapment of sickled RBC, resulting in vaso-occlusion. This physiology of SCD, described decades ago,[4,5] is fundamental to understanding the triggering of VOC. Patients report that stress, cold, and pain itself can trigger the onset of VOC[6] but the frequency of VOC is highly variable. To date, the mechanism of how such events might trigger regional vaso-occlusion has not been fully elucidated.

Psychological stress is an exacerbating factor in many chronic illnesses, such as SCD,[7–10] coronary artery disease and myocardial ischemia.[11,12] Stress is significantly associated with increased pain intensity, reductions in social and physical activities and greater health care utilization.[8,13,14] Day-to-day stressors have been associated with onset of pain and the course of VOC in SCD.[9,10] Stress is well-known to modulate autonomic nervous system (ANS) activity which in turn plays a major role in the regulation of regional blood flow.[15] Interestingly, SCD children with greater mental-stress-induced autonomic reactivity had more severe clinical disease.[16,17] SCD subjects also have augmented ANS-mediated vasoconstriction in response to sighing, hypoxia, and pain.[18-20] Therefore, autonomic dysregulation in SCD represents a plausible physiological link between mental stress and sickle RBC retention in the microvasculature.[16,18–21] Further understanding of this proposed mechanism of VOC triggering would not only help to predict disease manifestations, but would also open up opportunities for therapeutic intervention in disorders such as SCD in which preservation of microvascular blood flow is important.[22]

To address the role of mental stress in the physiology of SCD, we objectively quantified microvascular blood flow, measured by photoplethysmography, in response to standardized mental stress tasks in subjects with SCD and in controls. We also assessed cardiac ANS balance by analysis of heart rate variability in response to mental stress. We correlated photoplethysmogram-derived physiological indices with subjective indices of perceived stress assessed from standardized anxiety questionnaires. The aim of this study was to determine the relationship of peripheral and cardiac ANS responses with mental stress in SCD.

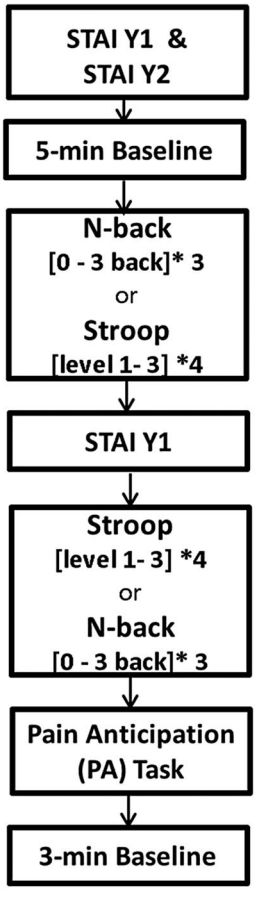

Figure 1. Time sequence of the study protocol. The subjects were randomly assigned to perform the N-back or Stroop test first. STAI: State-Trait Anxiety Inventory; Y-1: Sate questionnaire; Y-2 Trait questionnaire.

Methods

The study was conducted under an institutional review board-approved protocol at the Children's Hospital Los Angeles with approved consent/assent. Twenty SCD subjects with Hb SS, S-β^0, S-β^+ or SC genotype and 16 age- and race-matched controls from the patients' family and friends were recruited.

Experimental setup and study protocol

All studies were performed in an ANS laboratory under strictly controlled settings.[18] Neuropsychological stress was assessed at baseline using the State-Trait Anxiety Inventory (STAI) questionnaire.[23] The STAI Y-1 and Y-2 evaluate "anxiety at this moment, aka *state anxiety*" and "how people generally feel, aka *trait anxiety*", respectively.

Following 5 minutes of baseline recording, the stress induction protocol was presented through psychological software (E-prime 2.0, Psychology Software Tools, USA). The protocol consisted of a memory task (N-back)[24] and a conflict test (Stroop),[25,26] presented in a randomized order, followed by a pain anticipation (PA) test (Figure 1). During the N-back task, the subjects were asked to respond when the current letter matched the letter from n steps (n=zero, one, two, or three back) earlier in the sequence. During the Stroop task, the participants were asked to identify the font color of a word, not the written name of the word. We measured state anxiety between tasks. During the PA task, subjects read the following sentence on their computer screen: "You will receive a maximum pain stimulus in one minute. When you cannot tolerate the pain any longer, say STOP and the device will cool down to normal level immediately". However, no pain stimulus was actually applied.

Physiological measurements and analysis parameters

All the physiological monitoring sensors were attached to the subjects' left arm. Microvascular blood flow was measured using photoplethysmography (Nonin Medical Inc., USA) and laser Doppler flowmetry (Perimed, Sweden). Respiration (thoracic and abdominal bands, zRip DuraBelt, Philips), the electrocardiogram and continuous blood pressure (Nexfin, Amsterdam) were recorded.

Recorded data from all devices were exported for processing and analysis in MATLAB. The photoplethysmogram amplitude was normalized to its own 95th percentile value during the full study. The average microvascular blood flow was calculated over the 5 min baseline period, the N-back, Stroop and PA tasks. The percent decrease in the amplitude of the photoplethysmogram or microvascular perfusion waveforms (Figure 2; 2nd and 3rd signals,

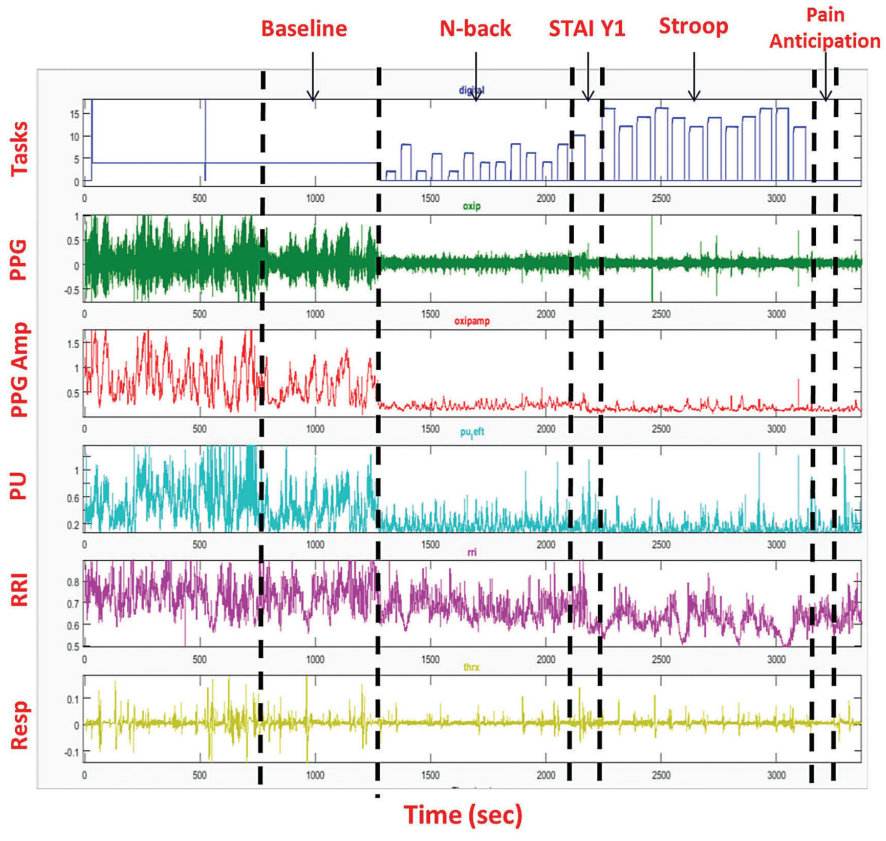

Figure 2. Raw waveform and wave amplitude signal output from the Biopac System. Example of a recording from a single subject. The top panel (Tasks) is the output of the E-prime software where the height of the bars represents the difficulty of the task. The second and third panels are the photoplethysmography (PPG) signal and PPG amplitude (PPG Amp), respectively. The fourth panel is microvascular perfusion (PU) determinecd by laser-Doppler. Panel five is the R-to-R interval from the electrocardiogram and panel six is the respiratory signal.

respectively) from the baseline mean was interpreted as a vasoconstriction response.[18,27]

Cardiac autonomic balance was assessed by analysis of the R-to-R interval and heart rate variability[19,28,29] during baseline and mental stress tasks. The following power spectral indices were calculated: low frequency power, reflecting a combination of cardiac sympathetic and parasympathetic activity; high frequency power, reflecting parasympathetic activity;[29,30] and the ratio of low frequency power to high frequency power, reflecting sympathovagal balance.[30]

Percent changes in mean microvascular blood flow and mean spectral indices from baseline to tasks were calculated. The Student *t*-test (or Wilcoxon sign rank) or χ^2 test was used to test baseline group differences and task differences. Robust regression was used to correlate vasoconstriction response and state anxiety during the PA task. Repeated measures analysis of variance was used to test differences in N-back and Stroop sublevels and accuracy scores. All statistical analyses were performed using STATA/IC 14.1 (StataCorp LP, TX, USA) with nominal significance set at $P \leq 0.05$.

The methods are described in detail in the *Online Supplementary Methods S1* .

Table 1. Population characteristics.

	Total N=36	SCD N=20	Controls N=16	*P*-value
Age in years	20 (0.94)	21 (1.40)	20 (1.24)	0.5¶
Gender, n (%)				
Male	19 (47)	11 (55)	8 (50)	0.77β
Female	17 (53)	9 (45)	8 (50)	
Hemoglobin g/dL	11.4 (0.36)	10.02 (0.37)	13.13(0.32)	<0.0001*¶
Hemoglobin S%§	56.58(5.98)	56.58(5.98)	--	--
State anxiety$^{\Delta}$	28.11(1.18)	28.95(1.61)	27.06(1.75)	0.36 ¶
Trait anxiety$^{\Delta}$	33.78(1.51)	35.55(2.40)	31.56(1.52)	0.30 ¶
Immediate anxiety after first task◊	33.97(1.91)	34.9 (2.99)	32.81(2.19)	0.96¶

¶*P*-value from the Student *t*-test. Continuous variables are listed as mean ± standard error. β *P*-value from the χ^2 test. Δ State anxiety was assessed by the State-Trait Anxiety Inventory (STAI) Y-1 questionnaire and Trait anxiety by the STAI Y-2 questionnaire at the beginning of the experiment. ◊ Immediate anxiety was assessed by STAI Y-1 after completion of the first task. § Hemoglobin S% is the percentage of hemoglobin S, which can contribute to sickling under normal physiological conditions. *Statistically significant difference ($P<0.05$).

Results

Data from a total of 20 SCD patients and 16 controls were analyzed. Transfused and non-transfused subjects with SCD were grouped together and healthy and sickle cell trait subjects (controls) were combined after it had been demonstrated that these factors were not statistically significant in the analyses. The percentage of HbS (HbS%) was considered to be zero in patients with sickle cell trait as the cellular distribution of HbS differs in sickle cell trait and does not contribute to sickling under the conditions of the experiments in this study, making the HbS% in sickle cell trait not comparable to that in transfused or non-trait sickle phenotypes. The subjects' characteristics are summarized in Table 1. Nine (45%) SCD subjects were on chronic transfusion, nine (45%) were being treated with hydroxyurea and two (10%) were not receiving either treatment. The characteristics of both groups were balanced except for hemoglobin concentration on the study

day. Sixty-one percent of subjects had a level of education equivalent to high school or superior. Seventy-two percent reported that they had a high level of competitiveness on the visit screening questionnaire.

Vasoconstriction due to mental stress

As determined from the photoplethysmogram, there was a significant drop in microvascular blood flow during both cognitive tasks (N-back and Stroop, $P<0.0001$) and the PA task ($P<0.0001$) (Figure 3). Figure 2 (signal 2) shows a typical response of vasoconstriction in one subject. The drop in microvascular blood flow from baseline was greater during the PA task than during the cognitive tasks. A similar vasoconstriction response was observed when the microvascular blood flow was assessed by laser-Doppler flowmetry. Subjects had higher anxiety scores immediately after completing the tasks than at baseline (STAI Y-1, mean difference=6; $P=0.0007$). Eighty-five percent of patients with SCD and 75% of controls showed vasoconstriction compared to baseline during at least one cognitive task. Eighty-five percent of SCD patients and 87.5% of controls had decreases in mean blood flow during the PA task. There was no difference in the magnitude of responses between individuals with SCD and controls. Demographic variables such as age, gender, race, number of days from last menstruation, and laboratory values were not associated with the magnitude of the vasoconstriction response.

The Stroop test caused greater vasoconstriction than the N-back task, irrespective of the order in which the tests were presented ($P=0.019$) (Figure 3). Subjects who were randomized to perform the Stroop task first had greater

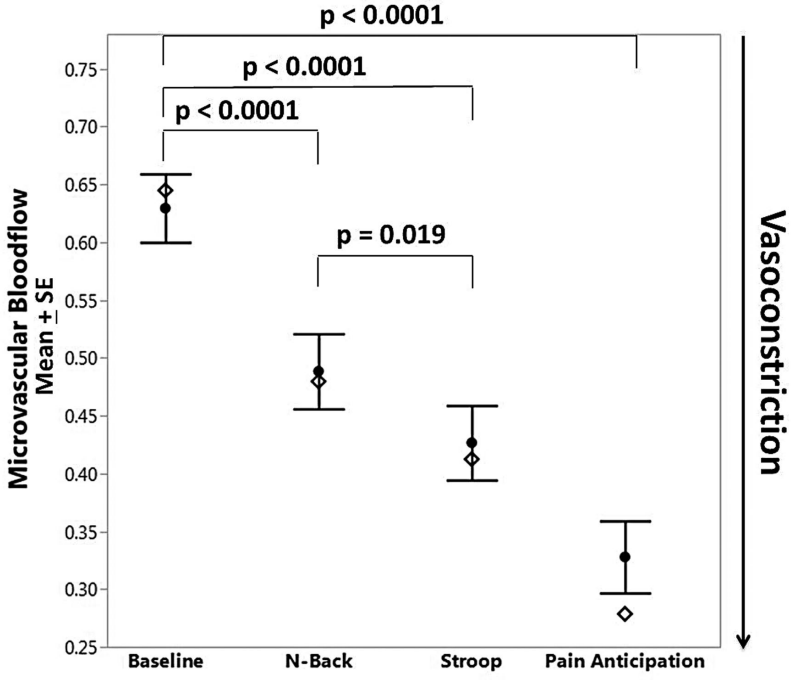

Figure 3. Microvascular blood flow under mental stress in all subjects. Significant vasoconstriction occurred during all mental stress tasks compared to baseline. Open diamonds represent group median values. SE: standard error of mean.

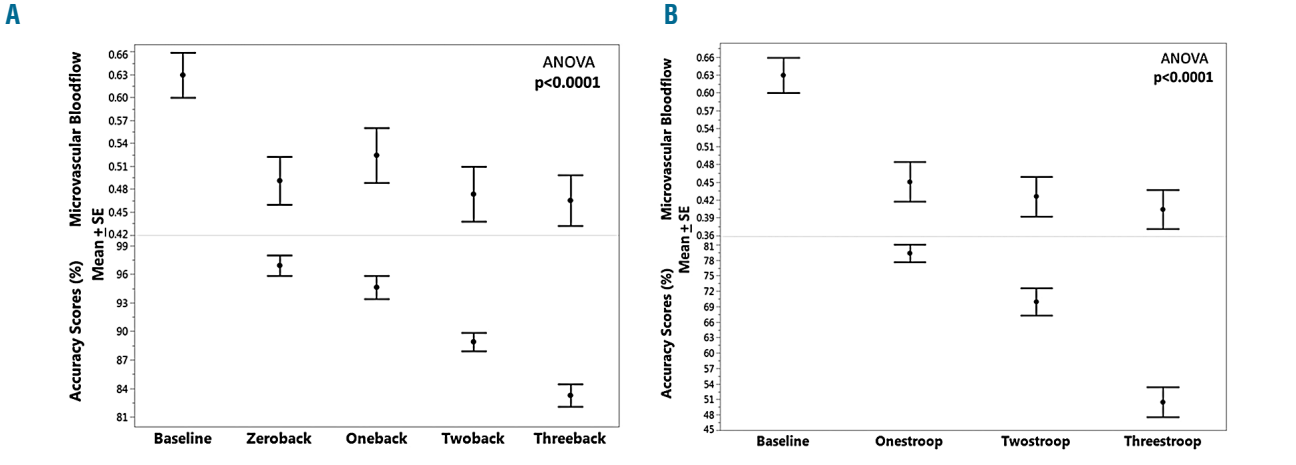

Figure 4. Effect of error rate during mental stress tasks on blood flow. (A, B) Mean ± standard error (SE) of microvascular blood flow and accuracy scores in sublevels of the N-Back (zeroback, oneback, twoback and threeback) task (A) and Stroop (onestroop, twostroop and threestroop) (B).

anxiety responses than did the subjects who performed the N-back task first (mean difference=10; P=0.03). Overall the accuracy score was significantly lower for the Stroop task than for the N-back task in all subjects (mean score difference=25, P<0.001).

The accuracy score for the Stroop and N-back tasks decreased as the difficulty increased from zero-back to three-back in the N-back task and from level one to level three in the Stroop task (P<0.0001) (Figure 4) but there was no further change in blood flow with increasing difficulty. Once the subjects manifested vasoconstriction, in comparison with baseline vascular tone, the vasoconstriction remained throughout the whole task regardless of the difficulty of the tasks.

Vasoconstriction response to perceived anxiety during pain anticipation

On robust regression, the effect of state anxiety on blood flow response was greater in SCD patients than in controls (P=0.03 for the interaction), suggesting that higher anxiety at baseline (STAI Y-1) in SCD subjects is associated with less change in blood flow (coefficient = -1.85, P=0.002) in response to pain anticipation (Figure 5). State anxiety had no effect on change in blood flow in control subjects. To understand why SCD subjects would have less response with high anxiety, we looked at the baseline blood flow. We found that highly anxious subjects tended to have a lower mean baseline blood flow (*Online Supplementary Figure S1*), meaning they were already vasoconstricted at baseline, limiting them from further vasoconstriction. This trend was not seen among controls. (*Online Supplementary Figure S2A, B*: high-anxiety SCD responder and low-anxiety SCD responder).

Cardiac autonomic response

Since the ANS regulates blood flow and SCD subjects have dysautonomia,[15,28,31,32] we explored the effect of mental stress responses on cardiac autonomic balance. In comparison to the value at baseline, there was a significant decrease in R-to-R interval, signifying an increase in heart rate, during all tasks (P<0.0001) (Figure 6A). As for the microvascular blood flow response, the R-to-R interval was less during the Stroop task than during the N-back task (P=0.002).

There was significant parasympathetic withdrawal during the N-back and Stroop tasks as reflected by the drop in high frequency power (P=0.002 and P<0.0001, respectively) (Figure 6B) The Stroop task caused stronger parasympathetic withdrawal than the N-back task (P<0.0001). There was more sympathetic activation during the Stroop test (low-to-high power ratio: P=0.03), but not during the N-back task. We did not analyze autonomic reactivity during the PA task because the 1-minute test period was not long enough to derive spectral indices.[29]

Discussion

VOC is a significant complication of SCD and a major cause of morbidity and mortality.[33] The frequency of VOC is related in part to hemoglobin-F content, white blood cell count, inflammatory status and other factors.[34-36] However, there is still significant variability in crisis frequency among SCD subjects with otherwise similar hematologic status. Pain crises can be promoted by preceding dehydration, infection, injury, exposure to cold or emotional stress.[37,38] Much of the research in past decades has focused on adhesion and processes attributed to occlusion in the post-capillary venule, and to decreased flow due to nitric oxide depletion.[39] While stress and cold are often mentioned, very little attention has been paid to decreased flow due to neurally induced vasoconstriction.[32,40] SCD patients undergo a tremendous amount of stress not only due to environmental challenges but also the illness-related stress of painful episodes, repeated medical procedures and life-threatening complications. Stress causes ANS

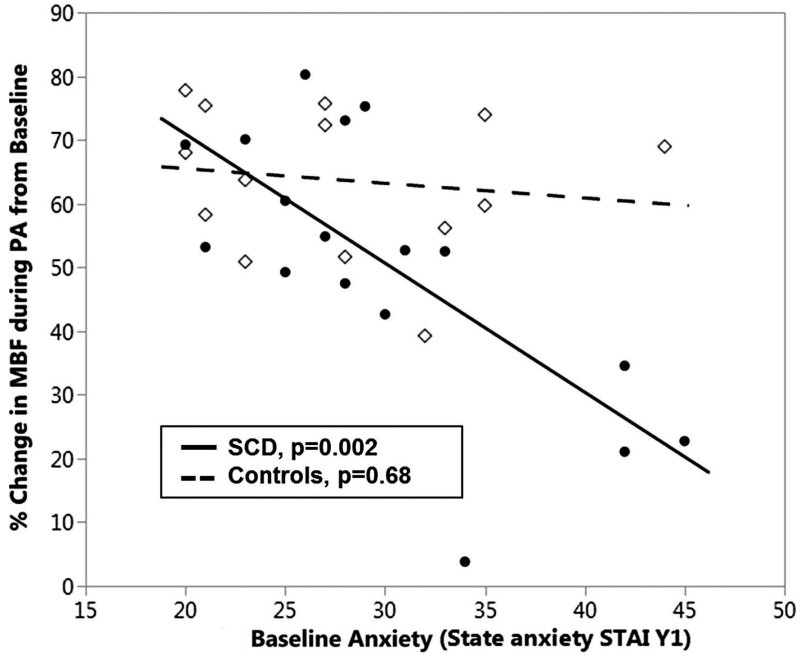

Figure 5. Relation between vasoconstriction during pain anticipation and perceived stress (state anxiety) in sickle cell disease subjects and controls. State anxiety was determined at baseline by the State-Trait Anxiety Inventory Y-1 questionnaire (STAI Y-1) and assessed in response to change in microvascular blood-flow during pain anticipation (PA) in sickle cell disease (SCD) subjects (closed circles, —) and controls (open diamonds, - - -). SCD subjects who were highly anxious at baseline had a smaller vasoconstriction response during the PA task than the SCD subjects who were less anxious (P=0.002); this effect was not seen among controls. MBF: microvascular blood flow.

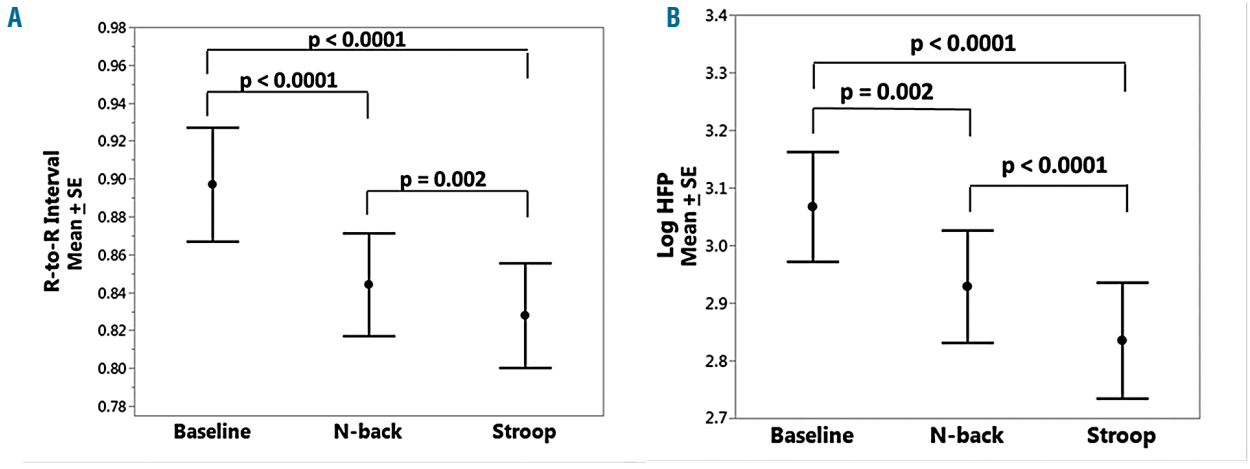

Figure 6. Autonomic nervous system responses to mental stress. (A) R-to-R interval (sec) and (B) high frequency power (sec^2/Hz, shown on a log scale) in response to the N-Back and Stroop tasks in all subjects. There is a significant decrease in R-to-R interval and parasympathetic withdrawal during mental stress tasks compared to baseline. SE: standard error of mean; HFP: high frequency power.

hyperreactivity by enhancing the sympathetic nervous system and dampening the parasympathetic system in SCD subjects compared to non-SCD individuals.[16,17] Sympathetic and parasympathetic responses have been related to clinical vaso-occlusion in SCD, through ANS modulation of regional blood flow.[15,17] SCD is probably the best example of a disorder in which decreased microvascular perfusion can be directly related to the pathology of the disorder, because the increase in transit time from decreased blood flow promotes entrapment of rigid red cells in small vessels.[3,5] To our knowledge, this is the first study to quantify regional blood flow modulated by ANS reactivity under mental stress in SCD.

Our data show that experimental mental stress caused a decrease in regional blood flow in all participants. While we thought that SCD subjects would exhibit stronger vasoconstriction because of their hyperresponsiveness to sympathetically induced stimuli, such as sighing,[28] we did not detect a difference in stress-induced vasoconstriction between SCD patients and controls. We did find a significantly higher anxiety response score (P=0.03) in subjects who were exposed to the more difficult mental stress test first (Stroop). We also found that the degree of vasoconstriction was proportional to the magnitude of the stress. Subjects reported that overall the Stroop task was more stressful: accuracy scores were lower and there was also a greater decrease in blood flow with this cognitive stressor task. However, different sublevels of difficulty within a task type did not correlate with levels of vasoconstriction. This finding suggests that consecutive stressful events could make SCD patients more vulnerable to vaso-occlusion. We think that variability in the vasoconstriction response to stress may account in part for differences in clinical severity among SCD patients who have the same hemoglobin phenotype. The frequency of VOC and intensity of pain are higher among patients found to have high anxiety and stress scores on standard psychological assessments.[8,41,42] We tried to correlate the vasoconstrictive response with clinical severity. As our SCD patients were either on chronic transfusion or hydroxyurea, the number of VOC was too low to detect differences in this current relatively small sample.

Along with a strong vasoconstriction response, significant autonomic reactivity was seen in all subjects. The Stroop test was consistently more stressful, and induced greater vasoconstriction as well as greater autonomic reactivity. There was both sympathetic activation as well as parasympathetic withdrawal during this cognitive task. Mental stressors are known to influence autonomic function by sympathetic or parasympathetic tone alterations. Higher anxiety induces atherosclerosis via enhanced sympathetic modulation, increasing the risk of cardiovascular disease.[43] In addition, mental stress and anxiety have been linked to impaired endothelial function via autonomic dysfunction.[43–45] Endothelial function, quantified by flow mediated dilation, decreases as a result of mental stress tasks.[46] Similarly, in SCD, a synergistic interaction between impaired local vascular function and the exaggerated neurally mediated vasoconstrictive response could further reduce peripheral blood flow, setting the stage for VOC.

Consistent with the findings of our previous study,[18] anticipation of pain caused significant vasoconstriction and this response was quantitatively greater than that of the calibrated experimental stress tasks (Figure 3). We do not have strong evidence to conclude that the presence of SCD alone influences mental stress-induced vasoconstriction but anxiety seems to be a modifying factor. Interestingly unlike control subjects, SCD subjects who were highly anxious had less vasoconstriction during the PA task and *vice versa*. We think that this pattern of response occurred because highly anxious subjects were already vasoconstricted at baseline and this limited the magnitude of further vasoconstriction. So the fact that SCD subjects have less change in the vasoconstriction response to the stressors than controls actually reflects their chronically vasoconstricted state. Although not statistically significant, the trend of lower baseline blood flow with high anxiety in SCD can be seen in *Online Supplementary Figure S1*, which also shows the significant variability in baseline measures. Photoplethysmogram and microvascular perfusion signals from Perimed do not have absolute units, so measurements made as percent changes from baseline are more reliable, basically correct-

ing for baseline variability and allowing detection of the differences seen in Figure 5. These findings may be related to pain catastrophization and increased psychophysical pain sensitivity due to frequent pain episodes.[7,47,48] Over the years, pain catastrophization may increase the frequency of pain and severity of pain crises.[47,49] From a standpoint of neural physiology, repeated acute pain creates a central neural pathological pain connectome[50] that leads to baseline chronic pain and chronic vasoconstriction. Although baseline blood flow was not statistically significantly lower, probably due to insufficient study power, we suspect that the above-described phenomenon is the explanation for our findings and warrants further study.

We showed that neurally mediated vasoconstriction is a biophysical marker of mental stress in SCD patients and controls. Mental stress has been identified as a trigger for pain crises in SCD and its connection with a decrease in microvascular perfusion seems to make a causal link to VOC. The probability of vaso-occlusion is predicted to be related to the relation between time to polymerization of deoxy HbS and microvascular flow.[3,5] Obviously, HbS is the major pathology in SCD. However, neurally mediated changes in microvascular flow certainly play a significant and unappreciated role. Individual variation in patterns of vasoconstriction with different ANS reactivity may offer a possible biological explanation for the variability in the frequency of VOC in SCD patients with similar hemoglobin phenotype. Identifying the high-risk individuals who show a phenotype of chronic vasoconstriction and repeated pain crises, and targeting them with neuro-modulatory cognitive-based therapies may improve vascular and neural physiology in SCD. In the primary stage of a crisis, implementing these learned cognitive-based therapies or distraction and relaxation techniques will help to improve the prognosis during acute pain. Microvascular flow in response to stress may also serve as an important surrogate endpoint for therapy in SCD and other diseases in which small vessel blood flow and reactivity are important.

Some limitations of this study should be acknowledged. One limitation was that the small sample size did not allow us to detect a difference in the magnitude of vasoconstriction between groups and correlate it with a clinical outcome such as VOC. Since the concept that mental stress causes vasoconstriction has not been studied in SCD, prior effect size was not known to permit sample size calculation. Another reason for lack of difference between groups is that over 90% of our patients are on hydroxyurea or chronic transfusion and thus clinical crises are relatively uncommon. Any real magnitude differences would be more likely to emerge in studies with larger samples and untreated patients. However, the primary aim of this study was to understand the changes in peripheral and cardiac responses to mental stress. The fundamental study design presented here was able to detect changes in physiological signals with millisecond accuracy and clearly showed vasoconstriction responses and ANS reactivity due to mental stress in all subjects. We think that the consequences of these findings are mechanistically related to the pathophysiology of sickle cell vaso-occlusion.

Acknowledgments

This work was supported by grants from the National Institutes of Health National Heart, Lung, and Blood Institute (U01 HL117718). The authors thank Justin Abbott for his contribution to the data collection.

References

1. Rees DC, Williams TN, Gladwin MT. Sickle-cell disease. Lancet. 2010;376(9757):2018-2031.
2. Kassim AA, DeBaun MR. Sickle cell disease, vasculopathy, and therapeutics. Annu Rev Med. 2013;64(1):451-466.
3. Christoph GW, Hofrichter J, Eaton WA. Understanding the shape of sickled red cells. Biophys J. 2005;88(2):1371-1376.
4. Eaton WA, Hofrichter J. Sickle cell hemoglobin polymerization. In: Advances in Protein Chemistry. Elsevier; p63-279.
5. Eaton WA, Hofrichter J, Ross PD. Editorial: Delay time of gelation: a possible determinant of clinical severity in sickle cell disease. Blood. 1976;47(4):621-627.
6. Murray N, May A. Painful crises in sickle cell disease--patients' perspectives. BMJ. 1988;297(6646):452-454.
7. Bhatt RR, Martin SR, Evans S, et al. The effect of hypnosis on pain and peripheral blood flow in sickle-cell disease: a pilot study. J Pain Res. 2017;10:1635-1644.
8. Gil KM, Carson JW, Porter LS, et al. Daily stress and mood and their association with pain, health-care use, and school activity in adolescents with sickle cell disease. J Pediatr Psychol. 2003;28(5):363-373.
9. Levenson JL, McClish DK, Dahman BA, et al. Depression and anxiety in adults with sickle cell disease: the PiSCES project. Psychosom Med. 2008;70(2):192-196.
10. Thomas LS, Stephenson N, Swanson M, Jesse DE, Brown S. A pilot study: the effect of healing touch on anxiety, stress, pain, pain medication usage, and physiological measures in hospitalized sickle cell disease adults experiencing a vaso-occlusive pain episode. J Holist Nurs. 2013;31(4):234-247.
11. Jain D. Mental stress, a powerful provocateur of myocardial ischemia: Diagnostic, prognostic, and therapeutic implications. J Nucl Cardiol. 2008;15(4):491-493.
12. Wei J, Rooks C, Ramadan R, et al. Meta-analysis of mental stress-induced myocardial ischemia and subsequent cardiac events in patients with coronary artery disease.. Am J Cardiol. 2014;114(2):187-192.
13. Porter LS, Gil KM, Sedway JA, Ready J, Workman E, Thompson RJ. Pain and stress in sickle cell disease: an analysis of daily pain records. Int J Behav Med. 1998;5(3):185–203.
14. Porter LS, Gil KM, Carson JW, Anthony KK, Ready J. The role of stress and mood in sickle cell disease pain: an analysis of daily diary data. J Health Psychol. 2000;5(1):53-63.
15. Connes P, Coates TD. Autonomic nervous system dysfunction: implication in sickle cell disease. C R Biol. 2013;336(3):142–147.
16. Pearson SR, Alkon A, Treadwell M, Wolff B, Quirolo K, Boyce WT. Autonomic reactivity and clinical severity in children with sickle cell disease. Clin Auton Res. 2005;15(6):400-407.
17. Treadwell MJ, Alkon A, Styles L, Boyce WT. Autonomic nervous system reactivity: children with and without sickle cell disease. Nurs Res. 2011;60(3):197-207.
18. Khaleel M, Puliyel M, Shah P, et al. Individuals with sickle cell disease have a significantly greater vasoconstriction response to thermal pain than controls and have significant vasoconstriction in response to anticipation of pain. Am J Hematol. 2017;92(11):1137-1145.
19. Sangkatumvong S, Khoo MCK, Kato R, et al. Peripheral vasoconstriction and abnormal parasympathetic response to sighs and transient hypoxia in sickle cell disease. Am J Respir Crit Care Med. 2011;184(4):474-481.
20. Chalacheva P, Khaleel M, Sunwoo J, et al. Biophysical markers of the peripheral vasoconstriction response to pain in sickle cell disease. PLoS One. 2017;12(5):e0178353.
21. Connes P. Altered autonomic nervous system function in sickle cell disease. Am J Respir Crit Care Med. 2011;184(4):398-400.
22. Goor DA, Sheffy J, Schnall RP, et al. Peripheral arterial tonometry: a diagnostic method for detection of myocardial ischemia induced during mental stress tests: a pilot study. Clin Cardiol. 2004;27(3):137-141.
23. The State-Trait Anxiety Inventory (STAI).

http://www.apa.org. http://www.apa.org/pi/about/publications/caregivers/practice-settings/assessment/tools/trait-state.aspx (accessed June 4, 2018).
24. Smith KE, Schatz J. Working memory in children with neurocognitive effects from sickle cell disease: contributions of the central executive and processing speed. Dev Neuropsychol. 2016;41(4):231-244.
25. Hoshikawa Y, Yamamoto Y. Effects of Stroop color-word conflict test on the autonomic nervous system responses. Am J Physiol. 1997;272(3 Pt 2):H1113-1121.
26. Callister R, Suwarno NO, Seals DR. Sympathetic activity is influenced by task difficulty and stress perception during mental challenge in humans. J Physiol. 1992;454:373-387.
27. Sunwoo J, Chalacheva P, Khaleel M, et al. A novel cross-correlation methodology for assessing biophysical responses associated with pain. J Pain Res. 2018;11:2207-2219.
28. Sangkatumvong S, Khoo MCK, Coates TD. Abnormal cardiac autonomic control in sickle cell disease following transient hypoxia. Conf Proc IEEE Eng Med Biol Soc. 2008;2008:1996-1999.
29. [No authors listed]. Heart rate variability: standards of measurement, physiological interpretation and clinical use. Task Force of the European Society of Cardiology and the North American Society of Pacing and Electrophysiology. Circulation. 1996;93(5):1043-1065.
30. Eckberg DL. Sympathovagal balance: a critical appraisal. Circulation. 1997;96(9):3224-3232.
31. Chalacheva P, Kato RM, Sangkatumvong S, et al. Autonomic responses to cold face stimulation in sickle cell disease: a time-varying model analysis. Physiol Rep. 2015;3(7).
32. Coates TD, Chalacheva P, Zeltzer L, Khoo MCK. Autonomic nervous system involvement in sickle cell disease. Clin Hemorheol Microcirc. 2018;68(2–3):251-262.
33. Platt OS, Thorington BD, Brambilla DJ, et al. Pain in sickle cell disease. N Engl J Med. 1991;325(1):11-16.
34. Hofstra TC, Kalra VK, Meiselman HJ, Coates TD. Sickle erythrocytes adhere to polymorphonuclear neutrophils and activate the neutrophil respiratory burst. Blood. 1996;87(10):4440-4447.
35. Turhan A, Weiss LA, Mohandas N, Coller BS, Frenette PS. Primary role for adherent leukocytes in sickle cell vascular occlusion: A new paradigm. Proc Natl Acad Sci U S A. 2002;99(5):3047-3051.
36. Hebbel RP, Boogaerts MAB, Eaton JW, Steinberg MH. Erythrocyte adherence to endothelium in sickle-cell anemia. N Engl J Med. 1980;302(18):992-995.
37. Rees DC, Olujohungbe AD, Parker NE, Stephens AD, Telfer P, Wright J. Guidelines for the management of the acute painful crisis in sickle cell disease. Br J Haematol. 2003;120(5):744-752.
38. Diggs LW. Sickle cell crises: Ward Burdick Award contribution. Am J Clin Pathol. 1965;44(1):1-19.
39. [No authors listed]. Sickle cell disease. Nat Rev Dis Primers. 2018;4:18011.
40. Serjeant GR, Chalmers RM. Current concerns in haematology. 1. Is the painful crisis of sickle cell disease a "steal" syndrome? J Clin Pathol. 1990;43(10):789-791.
41. Mahdi N, Al-ola K, Khalek NA, Almawi WY. Depression, anxiety, and stress comorbidities in sickle cell anemia patients with vaso-occlusive crisis. J Pediatr Hematol Oncol. 2010;32(5):345-349.
42. Gil KM, Abrams MR, Phillips G, Keefe FJ. Sickle cell disease pain: relation of coping strategies to adjustment. J Consult Clin Psychol. 1989;57(6):725-731.
43. Narita K, Murata T, Hamada T, et al. Interactions among higher trait anxiety, sympathetic activity, and endothelial function in the elderly. J Psychiatr Res. 2007;41(5):418-427.
44. Amiya E, Watanabe M, Komuro I. The relationship between vascular function and the autonomic nervous system. Ann Vasc Dis. 2014;7(2):109-119.
45. Toda N, Nakanishi-Toda M. How mental stress affects endothelial function. Pflugers Arch. 2011;462(6):779-794.
46. Ghiadoni L, Donald AE, Cropley M, et al. Mental stress induces ttransient endothelial dysfunction in humans. Circulation. 2000;102(20):2473-2478.
47. Mathur VA, Kiley KB, Carroll CP, et al. Disease related, non-disease related, and situational catastrophizing in sickle cell disease and its relationship with pain. J Pain. 2016;17(11):1227-1236.
48. Quartana PJ, Campbell CM, Edwards RR. Pain catastrophizing: a critical review. Expert Rev Neurother. 2009;9(5):745-758.
49. Campbell CM, Moscou-Jackson G, Carroll CP, et al. An evaluation of central sensitization in patients with sickle cell disease. J Pain. 2016;17(5):617-627.
50. Mansour AR, Baliki MN, Huang L, et al. Brain white matter structural properties predict transition to chronic pain. Pain. 2013;154(10):2160-2168.

ARTICLE

Long-term event-free survival, chimerism and fertility outcomes in 234 patients with sickle-cell anemia younger than 30 years after myeloablative conditioning and matched-sibling transplantation in France

Françoise Bernaudin,[1,2] Jean-Hugues Dalle,[3] Dominique Bories,[4] Regis Peffault de Latour,[2] Marie Robin,[2] Yves Bertrand,[5] Corinne Pondarre,[1,5] Jean-Pierre Vannier,[6] Benedicte Neven,[7] Mathieu Kuentz,[8] Sébastien Maury,[8] Patrick Lutz,[9] Catherine Paillard,[9] Karima Yakouben,[3] Isabelle Thuret,[10] Claire Galambrun,[10] Nathalie Dhedin,[2,11] Charlotte Jubert,[12] Pierre Rohrlich,[13] Jacques-Olivier Bay,[14] Felipe Suarez,[15] Nicole Raus,[16] Jean-Paul Vernant,[11] Eliane Gluckman,[2,17] Catherine Poirot[18] and Gérard Socié[2] for the Société Française de Greffe de Moelle et de Thérapie Cellulaire

[1]Referral Center for Sickle Cell Disease, Centre Hospitalier Intercommunal Créteil (CHIC), Université Paris XII, France; [2]Hematology, Transplantation, AP-HP Hôpital Saint Louis, Paris, France; [3]Pediatric Hematology, Hôpital Robert Debré, Paris, France; [4]Molecular Biochemistry, Hôpital Henri Mondor, Creteil, Université Paris XII, Paris, France; [5]Institute of Pediatric Hematology and Oncology, Hospices Civils, Lyon, France; [6]Pediatric Hematology, Centre Hospitalo-Universitaire Charles Nicolle, Rouen, France; [7]Pediatric Immuno-Hematology, Hôpital Necker, Paris, France; [8]Hematology, Hôpital Henri Mondor, Université Paris XII, Créteil, France; [9]Department of Pediatric Hematology-Oncology, University Hospital Hautepierre, Strasbourg, France; [10]Hemato-Pediatrics, La Timone, Marseille, France; [11]Hematology, Hôpital la Pitié, Paris, France; [12]Hemato-Pediatrics, Hôpital de Bordeaux, France; [13]Hematology, Hôpital de Besançon, Besançon, France; [14]Hematology, Limoges, France; [15]Hematology, Hôpital Necker, Paris, France; [16]Data Manager, SFGM-TC; [17]Eurocord/Monacord, Hôpital Saint-Louis, Paris, France and Centre Scientifique de Monaco, Monaco and [18]Reproductive Biology Hôpital Saint-Louis, Sorbonne University, Paris

Ferrata Storti Foundation

Haematologica 2020
Volume 105(1):91-101

ABSTRACT

Allogeneic stem cell transplantation remains the only curative treatment for sickle cell anemia (SCA), but the place of myeloablative conditioning in the procedure remains to be defined. The aim of the present study was to analyze long-term outcomes, including chimerism, SCA-related events and biological data (hemoglobin, reticulocytes, HbS%), and fertility in a French series of 234 SCA patients under 30 years of age who, from 1988 to 2012, received a matched-sibling-donor stem cell transplantation following standardized myeloablative conditioning [busulfan, cyclophosphamide and rabbit anti-thymocyte globulin (ATG)]. Since the first report of the series (1988-2004), 151 new consecutive patients with SCA have been similarly transplanted. Considering death, non-engraftment or rejection (donor cells <5%) as events, the 5-year event-free survival was 97.9% (95% confidence interval: 95.5-100%), confirming, since the year 2000, an at least 95% chance of cure. In the overall cohort (n=234, median follow up 7.9 years), event-free survival was not associated with age, but chronic-graft-*versus*-host disease (cGvHD) was independently associated with recipient's age >15 years (hazard ratio=4.37; *P*=0.002) and lower (5-15 *vs.* 20 mg/kg) ATG dose (hazard ratio=4.55; *P*=0.001). At one year, 44% of patients had mixed chimerism (5-95% donor cells), but those prepared with ATG had no graft rejection. No events related to SCA occurred in patients with mixed chimerism, even those with 15-20% donor cells, but hemolytic anemia stigmata were observed with donor cells <50%. Myeloablative transplantation with matched-sibling donor currently has a higher event-free survival (98%) in patients under 30 years of age than that reported for non-myeloablative conditioning (88%). Nevertheless, the risk of cGvHD in older patients and the need to preserve fertility might be indications for a non-myeloablative conditioning.

Correspondence:

FRANÇOISE BERNAUDIN
francoise.bernaudin@chicreteil.fr

Received: December 3, 2018.

Accepted: May 15, 2019.

Pre-published: May 16, 2019.

doi:10.3324/haematol.2018.213207

Check the online version for the most updated information on this article, online supplements, and information on authorship & disclosures: www.haematologica.org/content/105/1/91

Introduction

Sickle cell anemia (SCA) represents a growing global health problem. Over 300,000 children are born each year with SCA worldwide, with 85% of these births occurring in sub-Saharan Africa.[1] SCA is a severe recessive genetic disorder, resulting from a single nucleotide substitution in codon 6 of the beta-globin gene, producing abnormal hemoglobin (HbS) that is prone to polymer formation under deoxygenated conditions. Polymerized HbS leads to decreased red blood cell deformability and sickling within end arterioles, resulting in vaso-occlusive crisis and pain.

Despite significant progress in the management of SCA, such as the prevention of pneumococcal infection,[2,3] the introduction of hydroxyurea therapy (HU),[4-10] and early detection of cerebral vasculopathy with transcranial Doppler,[11,12] followed by rapid establishment of transfusion programs for patients at risk of stroke,[13,14] SCA remains a disease with a high risk of morbidity and early death.[15-18]

Allogeneic hematopoietic stem cell transplantation (SCT) is the only curative therapy for SCD[19-26] as it can prevent SCA-related organ damage if the erythroid compartment is adequately replaced by donor erythropoiesis. However, barriers to SCT use include the risks of rejection, transplant-related mortality (TRM), chronic graft-*versus*-host disease (cGvHD), infertility, and the lack of matched-sibling donors (MSD). While at least 1,000 MSD-SCT have been performed so far worldwide, the number of transplanted SCA patients remains very low,[23] especially in developing countries that have a large SCA population. We have previously reported studies in 87 consecutive myeloablative MSD-SCT for SCA patients performed in France between 1988 and December 2004.[22] We showed that the addition of antithymocyte globulin (ATG) to the conditioning regimen (CR) allowed a significant reduction in the risk of rejection despite a higher prevalence of mixed chimerism. The myeloablative CR (MAC), consisting of busulfan, cyclophosphamide and rabbit ATG was well tolerated by these young patients (aged 2.2-22 years), as only one death occurred during aplasia and limited early toxicity was noted. Moreover, the outcome significantly improved with time, as event-free survival (EFS) was 95.3% at five years for the 44 patients transplanted between January 2000 and December 2004.[22] These results led us to use the same MAC in SCA adults under the age of 30 years without major organ dysfunction and children with less severe cerebral vasculopathy.

Since that initial report, extremely interesting results have been obtained in adults using non-myeloablative (NMA) CR, resulting in 87% EFS with 13% rejection risk, but with preserved fertility and no GvHD with mixed chimerism.[27-29] It is thus timely and warranted to report the long-term outcome of chimerism, cGvHD and fertility after MAC-MSD-SCT in order to provide evidence for making an informed decision about the use of MAC or NMA CR for SCA children and young adults. For this reason, we analyzed the results of MAC-MSD-SCT performed in France between 1988 and December 2012 in 234 SCA patients, ranging in age from 2.2 to 28.9 years with a minimum 5-year follow up for surviving patients, to evaluate long-term outcomes, especially in the context of incidence of cGvHD and chimerism.

Methods

Considering the better cure rate observed with MSD-SCT after MAC for SCA patients transplanted after 2000 (95.3%), the Société Française de Greffe de Moelle et de Thérapie Cellulaire (SFGM-TC) decided to continue the previously described protocol,[22] and 151 new consecutive patients were transplanted between January 2005 and December 2012 for severe SCA. Thus, a total of 234 SCA patients had received MSD-SCT following MAC between November 1988 and December 2012. Informed consent was obtained from recipients, donors and their parents or guardians before transplantation. The data were obtained in the context of consensual treatment guidelines among French transplant centers in accordance with the Declaration of Helsinki, and the French laws and regulations protecting human subjects. To complement the data from the European Group for Blood and Marrow Transplantation (EBMT) registry, clinical and biological data including chimerism, eventual carcinogenic issues and fertility were recorded in a French database, and its use for this project was approved by the Créteil Institutional Review Board.

Patients' characteristics are presented in Table 1. The overall median age at transplant was 8.4 years (range: 2.2-28.9) with 32 patients (13.7%) older than 15 years (Figure 1A). All donors were MSD and genotype, available in 208 of 234 patients, was heterozygous AS (n=127), AThal (n=2), AC (n=1), A/DPunjab (n=1), and homozygous AA (n=77). Median age of donors was 9.6 years (range 0-33.7), counting the donor's age for isolated CBT as 0. The stem cell sources are shown in Table 2. All 234 consecutive patients were transplanted with an MSD following myeloablative CR using busulfan, cyclophosphamide at 200 mg/kg and rabbit ATG at different doses (Table 2 and Figure 1B).

Chimerism was studied by analyzing various polymorphisms after polymerase chain reaction (PCR) amplification of DNA obtained from whole blood at 1, 3, 6, 9 and 12 months after transplantation and every year thereafter. Real-time (RT) quantitative PCR of insertion/deletion polymorphisms was used when the minority chimeric fraction was below 10% and short-tandem-repeat (STR)-PCR was performed when the minority fraction was over 10%. In both cases, analyses were performed according to the kit manufacturer's recommendations (Promega; PowerPlex 16S assay for STR-PCR) and GenDex for Indel RT-PCR (KMRDX Chimerism Assay). When possible, peripheral-blood $CD3^+$ T cells and $CD3^-$ cells were selected for analysis.

Exact Fisher tests were used to compare proportions and Wilcoxon rank sum tests for continuous distributions. Patients were censored on the date of death or last visit for Kaplan-Meier (KM) estimates of survival and on the date of event (death, non-engraftment or rejection) or last visit for KM estimates of EFS. Cumulative incidences of rejections, deaths, acute GvHD (aGvHD) grade ≥II and cGvHD were also estimated by the KM method because of the small number of deaths and rejections. Failure time data curves were compared by the Log rank test. Risk factors for EFS, acGvHD and cGvHD, were analyzed by Cox regression with estimated hazards ratio (HR) and 95% Confidence Interval (CI). Type 1 error was fixed at the 5% level. All tests were two-tailed. Univariate models were fitted and all variables associated with the outcome at the 10% level were retained for introduction into a multivariate model. Statistical analyses were performed on SPSS version 22, and MedCalc (Belgium).

Results

The median (range) follow up was of 7.9 years (0.1-27.6

Table 1. Characteristics of sickle cell anemia patients transplanted in France with matched-sibling donors and myeloablative conditioning regimen.

Period	Nov 1988-Dec 2004 Blood Paper 2007	Jan 2005- Dec 2012 New cohort	Nov 1988-Dec 2012 Overall cohort
PATIENTS' CHARACTERISTICS			
Number	83	151	234
Phenotype, n	81 SS, 2 Sb0	147 SS, 2 Sb0, 2 SDPunjab	228 SS, 4 Sb0, 2 SDPunjab
Sex (F/M)	37/46	73/78	109/125
Median age (range) years	8.8 (2.2-22)	8.1y (3-28.9)	8.4y (2.2-28.9)
Age > 15 years, n (%)	9 (10.8%)	23 (15.2%)	32 (13.7%)
Transfusion number: median (range)	15 (2-119)	16.5 (2-108)	16 (2-61)
Ferritin: median (range) ng/ml	462 (13-3820)	970 (8-6208)	804 (8-6208)
Pre-transplant SCA-complications			
Stroke + TIA, n (%)	30 + 3 (39.8%)	20 + 3 (15.2%)	50 + 6 (23.9%)
Ischemic lesions, n (%)	48 (57.8%)	57 (37.7%)	105 (44.9%)
Silent infarcts , n (%)	16 (19.3%)	34 (22.5%)	50 (21.4%)
Stenoses, n (%)	30 (36.1%)	44 (29.1%)	74 (31.6%)
Moya, n (%)	9 (10.8%)	7 (4.6%)	16 (6.8%)
History of abnormal TCD, n (%)	8 (9.6%)	57 (37.7%)	65 (27.8%)
Abnormal TCD at transplant, n (%)	10 (12.0%)	8 (5.3%)	18 (7.7%)
≥ 3 VOC per year, n (%)	28 (33.7%)	46 (30.5%)	74 (31.6%)
≥ 2 ACS, n (%)	13 (15.7%)	36 (23.8%)	49 (20.9%)
Multiple osteonecroses, n (%)	13 (15.7%)	5 (3.3%)	18 (7.7%)
Red cell alloimmunization (≥ 2), n (%)	2 (2.4%)	5 (3.3%)	7 (3.0%)
Rare erythroid group, n (%)	3 (3.6%)	3 (2.0%)	6 (2.6%)
TRJV >= 2.7m/s, n (%)	0 (0%)	5 (3.3%)	5 (2.1%)
Severe anemia, n (%)	10 (12.0%)	7 (4.6%)	17 (7.3%)
Priapism, n (%)		5 (3.3%)	5 (2.1%)
Splenectomized total/partial, n (%)	4 (4.8%)/0	12 (7.6%%)/ 6 (4.0%)	16 (6.8%) /6 (2.6%)
Seizures, n (%)	7 (8.4%)	4 (2.6%)	11 (4.7%)

Cytomegalovirus status in recipient at transplant was available in 219 of these patients and was positive in 167 (76%). Exclusion criteria were not defined in the protocol, but patients were always discussed in multidisciplinary meetings, and the final decision was left to the physician in charge of the patient. Patients with severe sequelae post-stroke were excluded, but several patients, for example those with hemiparesis, were transplanted. The main issue was to evaluate if the child could withstand the 4-6 weeks hospitalization in the transplant unit.

years). All survivors had at least five years of follow up and results are presented in Table 2.

Engraftment

Two non-engraftments were observed, with rapid autologous reconstitution, in two patients transplanted with cord blood (CB) (Table 3). The first one, a patient who was transplanted 20 years ago, has not experienced any further SCA-related crisis since transplant, but still has 21% fetal Hb (HbF) (*vs.* <2% before SCT) and was still anemic (Hb 7 g/dL) at last visit. The second one, transplanted 12 years ago, is currently on HU therapy because of recurrent crises. For the other 232 patients, the time to absolute neutrophil count >0.5x10^9/L was significantly shorter after bone marrow transplantation (BMT) compared to CB transplantation (CBT) [mean±Standard Deviation (SD); 20.7±5.7 *vs.* 32.0±10.0, respectively; *P*<0.001]. Similarly, platelets reached 50x10^9/L sooner after BMT (day 26.5±12.2) than after CBT (day 44.6±18.3; *P*=0.001).

Rejection

Rejection was defined as donor chimerism <5%. Despite initial successful donor engraftment, six rejections were observed 0.5, 0.9, 1.2, 2.0, 2.3 and 9-years post transplant in patients transplanted before year 2005, as previously reported.[22] Five of them did not receive ATG as part of the preparative CR, and only one rejection occurred despite CR including ATG. Taking into account the two patients with non-engraftment and the six patients with rejection, the cumulative incidence of rejection for the overall cohort was 3.1% (95%CI: 0.7-5.5%) at five years; this was 20.0% (95%CI: 3.0-37.0%) in patients not prepared with ATG *versus* only 1.4% (95%CI: 0.0-3.0%) in those who received ATG (*P*<0.001). However, the ATG dose had no impact on the rejection risk (Figure 2A).

Transplant-related mortality

Seven deaths occurred after MSD-SCT. Five occurred in patients transplanted before year 2005, as previously reported.[22] Two deaths occurred at 0.5 and 2.5 years post transplant in the second cohort, because of adenoviral encephalitis[30] and GvHD-related obliterans bronchiolitis, respectively. The cumulative incidence of TRM at five years was 3.0% (95%CI: 0.8-5.2%) and significantly decreased with time from 6.0% (95%CI: 0.8-11.2%) before January 2005 to only 1.4% (95%CI: 0-3.4%) for the 151 patients transplanted since January 2005 (*P*=0.045).

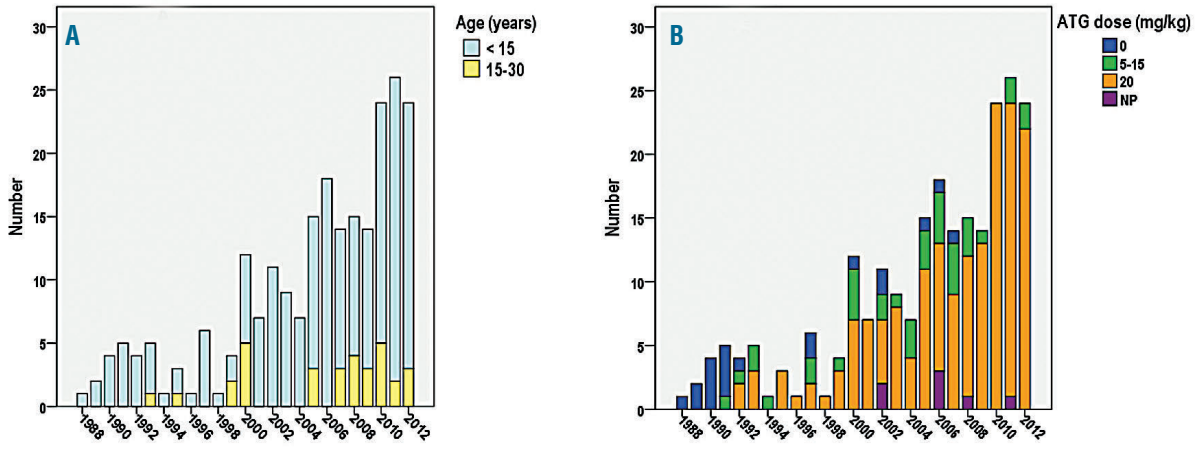

Figure 1. Matched-sibling donor hematopoietic stem cell transplantation (MSD-SCT) performed in France (1988-2012) after myeloablative conditioning regimen (n=234). Only 2% of patients were not prepared with anti-thymocyte globulin (ATG) in the second cohort *versus* 20.5% in the first cohort. The transplantation procedure and prophylaxis for graft-*versus*-host disease (GvHD) were as previously reported,[22] except that busulfan has been administered intravenously since year 2001 (Busilvex® Pierre Fabre Médicaments, Boulogne-Billancourt, France) from day –10 to day –7 at the total dose of 12.8 mg/kg for patients weighing >34 kg, 15.2 mg/kg for patients weighing 23-34 kg, 17.6 mg/kg for patients weighing 16-23 kg, or 19.2 mg/kg for patients weighing 9-16 kg. Busulfan pharmacokinetics were not performed for the majority of patients (n=202). In addition, cyclosporine was replaced by mycophenolate mofetil after 2002 in case of GvHD requiring steroid therapy. (A) Proportion of patients younger or older than 15 years. (B) ATG doses. NP: not precise; these patients received ATG, but the exact dose was not recorded.

There was no significant difference in TRM (P=0.490) between those prepared with 5-15 mg/kg ATG (5.5%; 95%CI: 0-13.1%) and those prepared with 20 mg/kg ATG (3.0%; 95%CI: 0.4-5.6%).

Event-free survival

Considering deaths (n=7), non-engraftments (n=2), and rejections (n=5) as events, the overall 5-year EFS was 93.9% (95%CI: 90.7-97.1%), but EFS strongly improved with time since it was 97.9% (95%CI: 95.5-100%) in the 151 patients of the second cohort *versus* 86.9% (79.5-94.3%) in the 83 patients of the first series (Figure 2B). Among the 190 patients transplanted after year 2000 and prepared with ATG, 5-year EFS was 97.8% (95%CI: 95.6-100%). EFS was similar in patients prepared with 5-15 mg/kg or with 20 mg/kg ATG (Figure 2C), in patients younger or older than 15 years (Figure 2D), and in patients transplanted from CB alone *versus* BM (Table 3). Cox regression analysis showed that EFS was not associated with the recipient's or donor's age or with the cell source, but was significantly associated (P<0.001) with the period of transplant (i.e. before or after year 2000) (HR=11.3; 95%CI: 3.9-33.4).

Graft-*versus*-host disease

Acute GvHD was assessable in the 232 successfully engrafted patients. The overall cumulative incidence of aGvHD ≥II at day 100 was 20.1% (95%CI: 14.9-25.3%). The multivariate Cox regression analysis retained sex mismatch (HR=2.12, 95%CI: 1.15-3.90; P=0.016) and donor's cytomegalovirus (CMV) positive status (HR=5.10, 95%CI: 2.15-12.05; P<0.001) as significant and independent risk factors for aGvHD ≥II (Figure 3A).

Chronic GvHD was assessable in 228 patients, and occurred in 24 patients. It was mostly mild in 18 patients, but extensive in six. Organ involvement included resolutive cutaneo-digestive (n=2), and obliterans bronchiolitis (n=4) which was responsible for death in two patients. The cumulative incidence of cGVHD at five years was 10.5% (95%CI: 6.5-14.5%), and was significantly lower (5.4%, 95%CI: 1.8-9.0%) in patients who received the highest ATG dose (20 mg/kg) than in those prepared without ATG (25%, 95%CI: 5.6-44.4%) and receiving lower doses (5-15 mg/kg) (27.0%, 95%CI: 12.4-41.6%) (Log Rank P<0.001). Moreover, 5-year chronic GvHD in children under 15 years of age was 7.6% (95%CI: 3.8-11.4%) *versus* 29.7% (95%CI: 13.1-46.3%) in those over 15 years of age. Multivariate Cox regression analysis retained only the recipient's age (HR=1.098 per 1 year increase, 95%CI: 1.033-1.168; P=0.003) and the ATG dose (HR=0.91 per mg/kg increase, 95%CI: 0.86-0.96; P=0.001) as independent risk factors.

Other post-transplant complications

The number of seizures, hemorrhagic cystitis, and veno-occlusive disease are shown in Table 2. The proportion of patients experiencing seizures and/or posterior reversible leukoencephalopathy was significantly reduced in the second cohort (5.3% *vs.* 18.1%; P=0.002). CMV replication occurred in 23.9% of patients. No CMV-related disease occurred with pre-emptive therapy. Epstein-Barr virus (EBV) asymptomatic viral replications had not been systematically assessed in the first cohort, and were observed in 15 patients (6%) in the second cohort. Six of them required anti-CD20 treatment, but none developed post-transplant lymphoproliferative disease. Among the 234 patients, B-lymphoma occurred six years post transplant in one patient who had received long-term immunosuppressive therapy, but no other secondary malignancies were observed.

Gonadal function

All females who were post-pubertal at the time of transplantation (n=14) developed amenorrhea with low serum estradiol and elevated LH and FSH levels during the year following transplant, necessitating hormone replacement

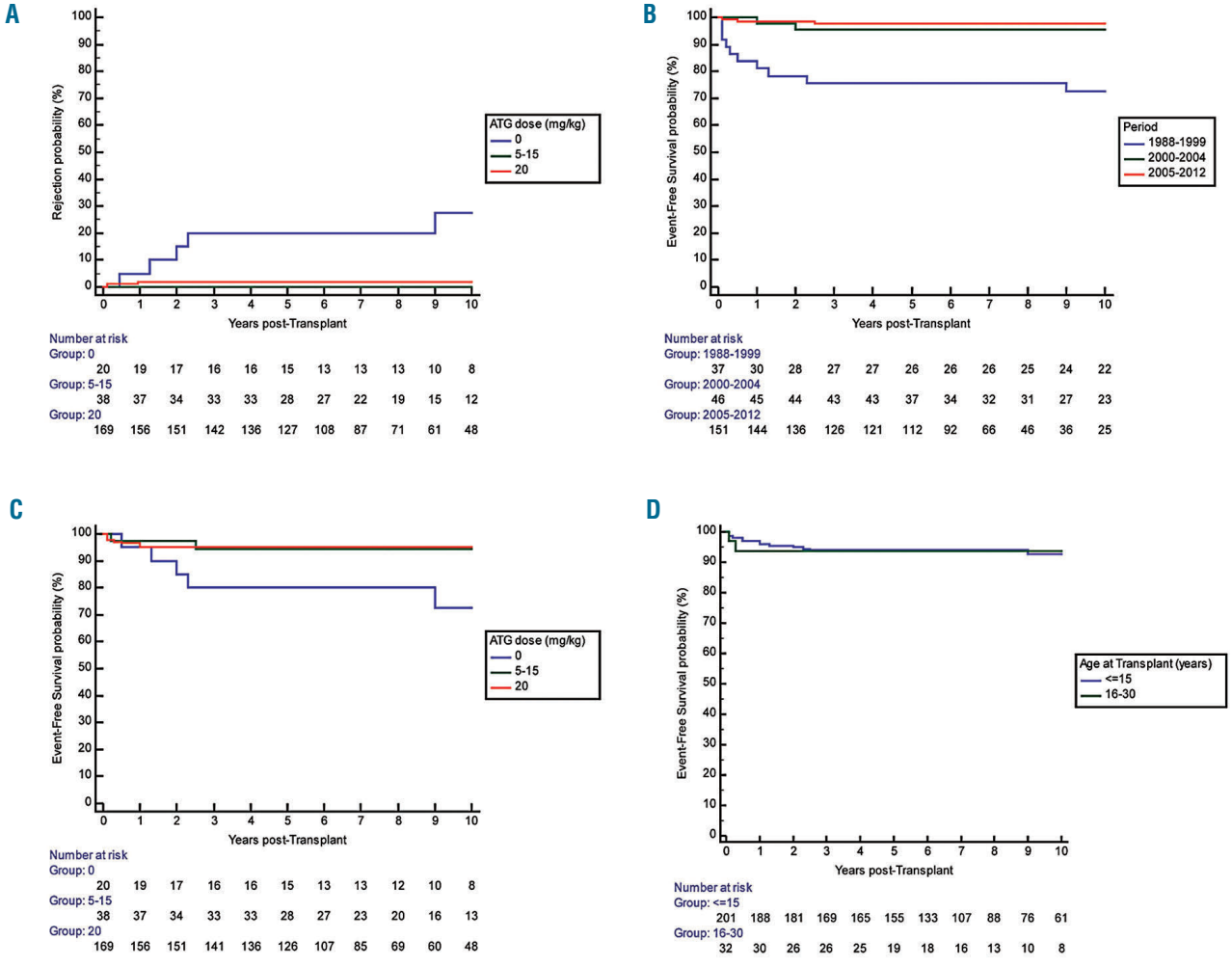

Figure 2. Rejection probability and event-free-survival (EFS) in sickle cell anemia (SCA) patients transplanted with matched-sibling donor (MSD) after myeloablative conditioning regimen. (A) Probability of rejection according to the anti-thymocyte globulin (ATG) dose. Overall cumulative incidence of rejection at five years was 20.0% (95%CI: 3.0-37.0%) in patients prepared without ATG and only 1.4% (95%CI: 0.0-3.0%) (P<0.001) in those prepared with ATG. However, the risk of rejection was not associated with the ATG dose (5-15 mg/kg *vs.* 20 mg/kg). (B) EFS according to the ATG dose. EFS was similar after bone marrow transplantation (BMT) and cord blood transplantation (CBT), and in patients prepared with 5-15 mg/kg ATG than in those prepared with 20 mg/kg. (C) EFS in 234 patients depending on the period of transplant. EFS improved strongly as it was only 73.3% (95%CI: 58.7-87.9%) among the 38 patients transplanted before year 2000 and 97.4% (95%CI: 95.0 -99.8%) in the 196 patients transplanted after year 2000. (D) EFS according to age over or under 15 years. EFS was similar in patients younger or older than 15 at transplant.

therapy. Thirty-two girls were pre-pubertal at transplantation, and most required hormonal therapy to develop secondary sexual characteristics at the bone age of 13 years. However, 9 of 32 of the pre-pubertal girls at SCT, who had reported to have spontaneously undergone normal puberty at the last visit, were significantly younger at transplant than those who required hormonal substitution for puberty induction [mean (SD) age 5.9 (2.6) *vs.* 10.1 (2.1); P=0.002]. At last visit, 20 females were older than 25, and four of them, who had been transplanted between 1988 and 1998 at 5.8, 6.1, 6.6 and 7.7 years of age, respectively, had had six spontaneous pregnancies and five children at approximately 20 years after SCT. Pre-transplant ovarian tissue cryopreservation has been systematically performed since year 1998. Unilateral oophorectomy was performed by laparoscopy under general anesthesia and ovarian cortical fragments were cryopreserved at a median age of 8.0 years (range: 3.0-26.4). Among the 93 girls transplanted since 1998, 11 were older than 25 years at the last visit; two wanted to become pregnant and requested autograft of ovarian fragments. The first of these was transplanted at 20 years of age and had received hormone replacement therapy because of post-transplant ovarian failure. Orthotopic ovarian fragment autograft was performed by laparoscopy 29 months after SCT, and the first signs of recovery of ovarian function were observed nine weeks after ovarian graft. Hormone replacement therapy was stopped at four months and the patient became pregnant six months after ovarian autograft, delivering a healthy girl at 38 weeks of gestation. She had another child three years later without requiring a new graft of ovarian fragments.[31] In the second patient, transplanted at 22 years of age, autograft of ovarian fragments was performed 12 years post SCT, and recovery of ovarian function was observed after four months, but unfortunately no pregnancy occurred thereafter.

Table 2. Matched-sibling donor hematopoietic stem cell transplantation (MSD-SCT) procedure and outcome in sickle cell anemia patients transplanted in France.

Period	Nov 1988-Dec 2004 Blood Paper 2007	Jan 2005- Dec 2012 New cohort	Nov 1988-Dec 2012 Overall cohort
Number of Patients	83	151	234
Conditioning regimen	Busulfan/Cyclophosphamide		
ATG dose	Rabbit ATG		
0 mg/kg, n (%)	17 (20.5%)	3 (2.0%)	20 (8.5%)
5-15 mg/kg, n (%)	18 (21.7%)	18 (11.9%)	36 (15.4%)
20 mg/kg, n (%)	40 (48.2%)	124 (82.1%)	164 (70.1%)
not recorded, n (%)	8 (9.6%)	6 (4.0%)	14 (6.0%)
Stem cell source			
Bone Marrow (BM), n (%)	70 (84.3%)	125 (82.8%)	195 (83.3%)
Cord Blood (CB), n (%)	11 (13.3%)	19 (12.6%)	30 (12.8%)
CB+BM, n (%)	1 (1.2%)	7 (4.6%)	8 (3.4%)
PBC, n (%)	1 (1.2%)	0 (0%)	1 (0.4%)
Outcome			
Median Follow-up (range)	13.8 years (0.1-27.6)	6.8 years (0.4-13.2)	7.9 years (0.1-27.6)
Non-Engraftment, n (%)	1 (1.2%)	1 (0.7%)	2 (0.9%)
Rejection, n (%)	6 (7.2%)	0 (0%)	6 (2.6%)
Deaths, n (%)	5 (6.0%)	2 (1.3%)	7 (3.0%)
Acute GvHD, grade (n)	II (n=11), III (n=4), IV (n=2)	II (n=24), III (n=5), IV (n=1)	II (n=35), III (n=9), IV (n=3)
Chronic GvHD,	mild (n=7), extensive (n=2)	mild (n=11), extensive (n=4)	mild (n=18), extensive (n=6)
Cumulative Incidences (95%CI)			
Non-Engraftment/Rejection at 5 years	7.5% (1.5-13.5%)	0.7% (0-2.1%)	3.1% (0.7-5.5%)
Transplant Related Mortality at 5 years	6.0% (0.8-11.2%)	1.4% (0-3.4%)	3.0% (0.8-5.2%)
Event-Free Survival at 5 years	86.9% (79.5-94.3%)	97.9% (95.5-100%)	93.9% (90.7-97.1%)
Acute GVHD ≥ II at Day 100	20.4% (11.6-29.2%)	20.0% (13.4-26.6%)	20.1% (14.9-25.3%)
Chronic GVHD at 5 years	11.2% (4.2-18.2%)	10.1% (5.1-15.1%)	10.5% (6.5-14.5%)
Other post-SCT complications			
Seizures, n (%)	15 (18.1%)	1 (0.7%)	16 (6.8%)
Hemorrhagic cystitis, n (%)	6 (7.2%)	8 (5.3%)	14 (6.0%)
Veno-occlusive disease, n (%)	0 (0%)	2 (1.3%)	2 (0.9%)
CMV replication	18 (21.7%)	38 (25.2%)	56 (23.9%)

Cytomegalovirus (CMV) donor status, available in 217, was positive in 133 patients (61%). ABO compatibility was available in 212 donor-recipient couples, and major and minor incompatibility was present in 34 (16%) and 36 patients (17%), respectively. There was donor/recipient sex mismatch in 120 cases (FM: 61; MF 59).

All the boys who were pre-pubertal at transplant and of pubertal age at the last visit developed normal puberty with normal testosterone, FSH and LH levels, in keeping with their bone age and pubertal status. At last visit, 19 males were over 25 years of age. Three of them who had been transplanted 11, 12 and 20 years ago fathered spontaneously. Pre-transplant sperm cryopreservation was performed in all pubertal males and pre-transplant testicular tissue cryopreservation has been systematically performed since year 2010 in prepubertal boys (n=25) (median age: 7.5 years; range: 3.4-10.2). However, so far, no patient has requested testicular fragment autografting (median age at last visit: 13.7 years; range: 5.8-21.2).

Chimerism studies

Chimerism was assessable in 208 patients and was categorized as full donor chimerism (>95% donor cells), rejection (<5% donor cells), and low (5-50% donor cells) or high (50-95% donor cells) mixed chimerism. At one year, full donor chimerism was present in 112 patients (54%), while 92 patients (44%) had mixed chimerism (83 high, and 9 low), and 4 (2%) had <5% donor cells (the 2 patients with no-engraftment and 2 who rejected the graft at 0.5 and 0.9 years).

Multivariate logistic regression analysis showed that the ATG dose (OR=1.06 per 1 mg/kg increase, 95%CI:1.01-1.12; P=0.017) and recipient's age (OR=0.94 per year increase, 95%CI: 0.88-0.99; P=0.041) were independently inversely associated with the presence of mixed chimerism at one year. Moreover, cGvHD was significantly more frequent (P=0.018) in patients with full donor chimerism (18 of 112; 16.1%) than in those with mixed chimerism (5 of 92; 5.5%), These five patients all had donor cell% >75%. No significant association was found between ABO compatibility and chimerism.

Chimerism on separated populations ($CD3^+$ and $CD3^-$) was assessed in 103 patients. Whole blood donor cell chimerism was more significantly correlated with the $CD3^-$ (r=0.917, $P<1x10^{-128}$) than with the $CD3^+$ (r=0.418, $P<1x10^{-15}$) population. During the first two years post

transplant, $CD3^+$ chimerism was significantly lower than $CD3^-$ and whole blood donor cell chimerism, but was similar thereafter.

Long-term outcome of chimerism

One-hundred and twelve patients remained stable with donor chimerism >70% at last visit. However, one girl with a rare erythroid group (U-), transplanted in 2000 from her brother's CB (U+), had full donor chimerism at one and two years that remained stable for five years, but decreased thereafter with the appearance of hemolytic anemia. The patient was given donor lymphocyte infusions (DLI), which allowed the reversion to full donor chimerism along with anemia and hemolysis correction, but it induced cGvHD which was responsible for chronic pulmonary disease (currently well under control).

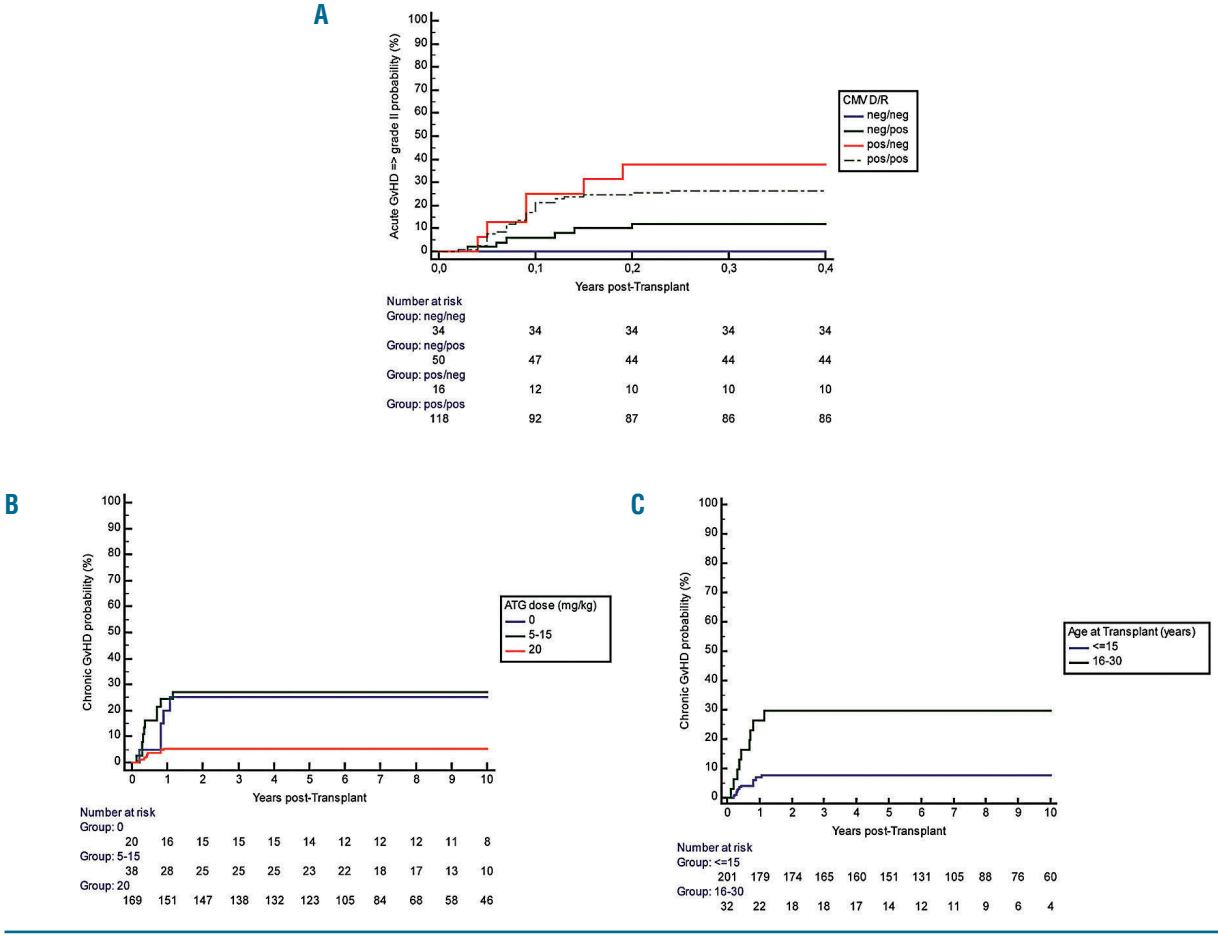

Figure 3. Relationship of graft-*versus*-host disease (GvHD) and donor/recipient (D/R) cytomegalovirus (CMV) status, anti-thymocyte globulin (ATG) dose and recipient age. (A) Acute GvHD according to the D/R CMV status. Cumulative incidence of acute-GvHD at day 100 according to the D/R CMV status. (B) Chronic GvHD according to the ATG dose. Cumulative incidence of chronic GvHD at five years was significantly lower in the patients having received the high dose of ATG (20 mg/kg) (5.4%, 95%CI: 1.8-9.0%) *versus* those not prepared with ATG (25%, 95%CI: 5.6-44.4%) and those having received lower doses (5-15 mg/kg): 27.0%, 95%CI: 12.4-41.6%) (Log Rank *P*<0.001). (C) Chronic graft-*versus*-host disease (GvHD) according to recipient age at transplant. Cumulative incidence of chronic GvHD in children under 15 years of age was 7.6% (95%CI: 3.8-11.4%) *versus* 29.7% (95%CI: 13.1-46.3%) in those older than 15.

Table 3. Rejection, transplant-related mortality, event-free survival as a function of the cell source, bone marrow (BM) *versus* cord blood (CB) alone.

	CB alone (n=30)	BM (n=195)	*P*
Non-engraftment (n)	2	0	0.017
Late rejection	0	6	NS
Cumulative Incidence of rejection at 5 years (including non-engraftment)	6.7% ± 9.2%	2.7% ± 2.4%	NS
Deaths	0	7	NS
Events	2	13	NS
EFS at 5 years	93.3% ± 9.2%	93.7% ± 3.6%	NS
Cumulative Incidence of acute GVHD ≥ grade II	13.3% ± 12.4%	21.1% ± 5.8%	NS
Cumulative Incidence of chronic-GVHD	3.3% ± 6.6%	11% ± 4.6%	NS
EFS chronic-GVHD free at 5 years	90.0% ± 10.1%	84.5% ± 5.2%	NS

Among the 92 patients with mixed chimerism at one year, four rejected the graft (4.3%) at 1.5, 2, 2.3 and 9 years post transplant, but none had been prepared with ATG. Among the other 88 patients, none had rejected the graft at last visit, nine had switched to full donor chimerism, and 69 had high and 10 low mixed chimerism (Table 4). None of those with low mixed chimerism experienced SCA-related vaso-occlusive crisis (VOC) or acute-chest-syndrome (ACS), but five had hemoglobin <100 g/L or reticulocytes >150x10^9/L, considered as SCA-related symptoms. Thus, despite the absence of rejection and the absence of VOC or ACS occurrence, these patients were deemed as having SCA recurrence, resulting in an overall disease-free survival (DFS) of 95.5% at five years (95%CI: 92.7-98.3%). Three of the patients with low mixed chimerism and hemolytic anemia stigmata received DLI, which did not induce GvHD, but did not offer improvement of anemia and hemolysis. Figure 4 reports all biological data recorded at the same time as chimerism during the entire follow up. It can be seen that as long as donor chimerism remains higher than 50%, Hb and reticulocytes remain normal, resulting in no anemia, no hemolysis and similar HbS% as donor.

Discussion

In this report, we confirm that SCA children and young adults transplanted after year 2000 (n=197) with an MSD and prepared with myeloablative-CR associating busulfan, cyclophosphamide and ATG have at least a 95% chance of cure. These results compare favorably with other published series using myeloablative[19-26] and non-myeloablative[27-29] CR.

The TRM < 2% in this series must be interpreted in the context of mortality risk related to the SCA disease itself, which was reported to be 6.1% before the age of 18 years in the Dallas cohort,16 and 1% in the London[17] and 2.5% in the Créteil[14] newborn cohorts. Thus, MSD-SCT does not expose children to a higher risk of death than SCA itself, but offers improved quality of life. Moreover, it is important to remember that transition to adulthood carries a high risk of death,[32] and that mortality in adults[18] has increased during the last few years, whereas it has significantly decreased for children.

Except for frequent high fever during ATG infusion, myeloablative conditioning was well tolerated in the 234 young patients, with only one death during aplasia and two mild veno-occlusive diseases. High doses of ATG are known to increase the risk of viral complications. The occurrence of EBV reactivation, however well controlled with anti-CD20 treatment, and the case of fatal adenoviral meningoencephalitis[30] are of concern, but the risk benefits between viral infections, which are manageable, and cGvHD, which is more difficult to control, need to be taken into account. Seizures and posterior reversible encephalopathy syndromes (PRES), which were highly frequent (16 of 83; 19%) before year 2005,[22] despite preventive measures such as anticonvulsant prophylaxis with clonazepam during busulfan administration and cyclosporine therapy, strict control of arterial hypertension, prompt correction of magnesium deficiency, maintenance of the Hb concentration above 9 g/dL and platelet count above 50x10^9/L,[33] were significantly (P=0.002) less frequent after 2005 (8 of 151; 5%), following the SFGM-TC recommendation to promptly replace cyclosporine with mycophenolate mofetil in case of GvHD requiring steroid therapy.[22] However, the risk of seizures and PRES remains an adverse effect of cyclosporine and steroid therapy,[34] and may warrant substituting cyclosporine for

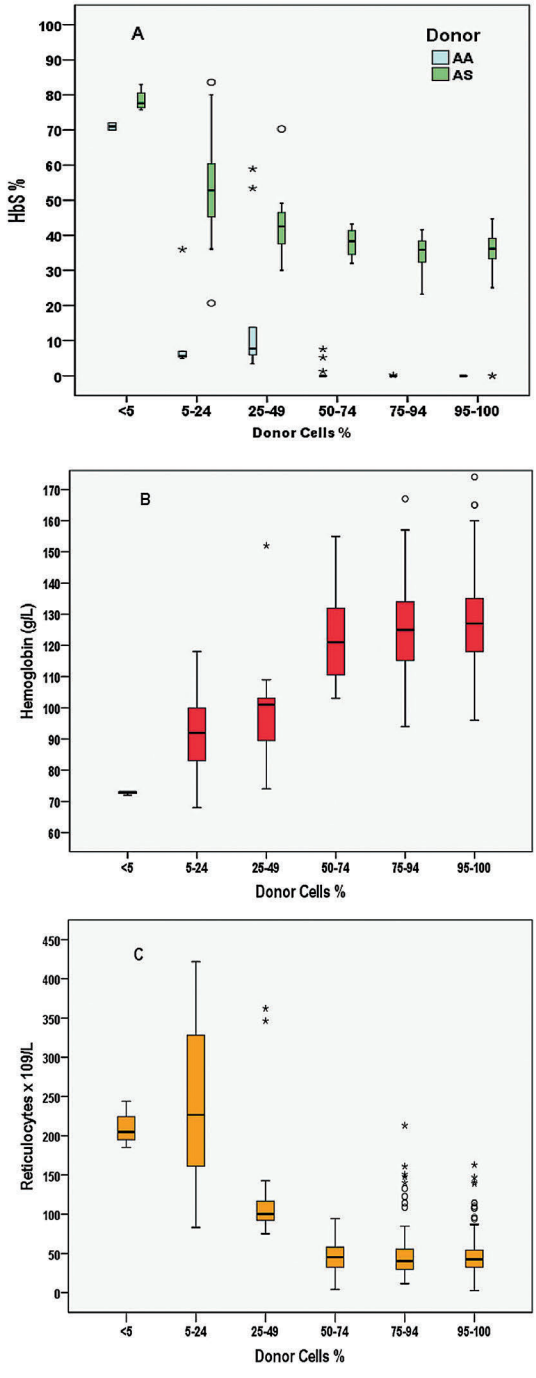

Figure 4. Relationship between % donor cells and hemoglobin S percentage (HbS%), hemoglobin (Hb) level, and reticulocyte count. All biological data (HbS%, Hb and reticulocytes) recorded at the same time as the chimerism during the overall follow up were used for these box-plots. (A) Box-plot of HbS% according to the donor cell% category. This graph shows that HbS% is similar to that of the donor (AA or AS) as long as donor cell% is higher than 50%. (B) Box plot of Hb level according to donor cell% category. Hb level remains higher than 100g/L as long as donor cell% is higher than 50%. (C) Box plot of reticulocyte count according to % donor cells. Reticulocyte count remains lower than 100x10^9/L as long as % donor cells is higher than 50%.

sirolimus[27,28] that is less neurotoxic and induces good tolerance.[35] Hemorrhagic cystitis occurred in 21 of 234 patients (9%) and was particularly severe in two patients. Cyclophosphamide is generally considered to be the most important predisposing factor for occurrence of hemorrhagic cystitis.[36,37] Despite the absence of prospective randomized trials comparing busulfan-fludarabine to busulfan-cyclophosphamide, several reports mention a lower risk of hemorrhagic cystitis with fludarabine.[38,39] This complication may suggest replacing cyclophosphamide with fludarabine, as only a 2% risk of hemorrhagic cystitis was reported in children transplanted for non-malignant disease following busulfan-fludarabine *versus* 9% with busulfan-cyclophosphamide CR.[39]

The major long-term concern with busulfan is the ovarian failure observed in post-pubertal females and infertility risk in both genders.[40,41] Despite the occurrence of spontaneous puberty in girls transplanted at a younger age and the birth without treatment of several babies from females transplanted 20-25 years ago during infancy, demonstrating some reversibility of ovarian dysfunction, it remains crucial to maximize the chances of fertility and to recommend pre-transplant cryopreservation of ovarian[42-44] and testis[45] tissues before SCT with myeloablative CR. In France, systematic ovarian and testicular tissue cryopreservation has been established since 1998 and 2010, respectively, and is free of charge. However, CR preserving fertility such as the one proposed by the National Institutes of Health (NIH) protocol using 3Gy total body irradiation with testis shielding in males and alemtuzumab[27-29] should be preferred when gonadal cryopreservation is not easily accessible and for adults. It is also important to keep in mind that fertility is also compromised by SCA itself,[46] and that this risk is lower when SCT is performed at a younger age.

Event-free survival in this series was similar for patients younger and older than 15 years, but the risk of cGvHD, not acceptable in this non-malignant disease, was much more frequent in older patients. We show that the high dose of ATG (20 mg/kg) significantly reduced the risk of cGvHD independently of the age at transplant by favoring mixed chimerism occurrence. In the 20 of 234 patients not prepared with ATG, mixed chimerism was unstable, and secondary graft failed in 5 of 20. In contrast, only one secondary rejection was observed before year-1 among the 214 patients prepared with ATG.

Mixed chimerism was present in 44% of patients at one year in this series. None of the patients prepared with ATG rejected the graft and none experienced VOC or acute chest syndrome. The absence of SCA-related symptoms in patients with mixed chimerism has been reported in other series.[22,47-50] Low levels of donor erythroid engraftment were shown to result in donor cell predominance among erythroblasts and erythrocytes.[48] This stimulated the development of non-myeloablative CR in order to reduce TRM and preserve fertility, and resulted in the recommendation of HSCT to older adult patients with organ dysfunction. While the first results after non-myeloablative SCT have been disappointing, very encouraging results were obtained by the NIH team in adults (17-64 years of age)[27,28] using as stem cell source granulocyte-colony stimulating factor (G-CSF)-stimulated peripheral blood progenitors from HLA-matched sibling donors and sirolimus for GvHD prophylaxis, which was stopped after one year in those with >50% donor T-cell chimerism. The mean duration of immunosuppression was 2.1 years (range: 1.0-8.4). Among 30 patients transplanted, four experienced rejection (13%), which was responsible for one death in a patient with Moya Moya, but no TRM and no GvHD were observed. Mean donor T cell was 48%, mean myeloid chimerism was 86%, and 15 patients had stable chimerism despite sirolimus withdrawal. These results were reproduced in 13 adult patients by another team in Chicago.[29] Thus, among the 43 patients reported in both series, 88% were alive, free of SCA and without GvHD. However, the limitations of the protocol are the long-term immunosuppression and the 300 cGy TBI that could favor a secondary malignancy. Other non-myeloablative or reduced intensity CR have been reported by several teams and fully described in a review,[50] but the most successful results were obtained with the NIH protocol described above.

It is to be noted that the excellent results reported here mostly concern young patients and are less applicable to older patients with higher morbidities. Moreover, outcomes of cognitive performances, quality of life, costs and organ functioning are not reported here. This is an important limitation of our study but only prospective trials comparing MSD-SCT to standard-care would be able to define the true risk benefit balance for each procedure.

Table 4. Biological data in patients with low mixed chimerism (5-49% donor cells) at last visit.

Donor genotype	Years post-HSCT	Donor cells % at 1 year	at last visit	HbS %	Hb g/L at last visit	Retic x10^9/L
AS	15.5	24	19	51	103	226
AS	5.1	60	20	60	83	230
AS	7.1	35	21	70	69	422
AS	14.1	46	22	63	87	360
AS	15.4	73	42	44	151	79
AA	12.1	20	12	36	73	138
AA	9.5	30	20	30	130	nd
AA	10.2	32	22	5	118	83
AA	6.2	61	30	10	100	101
AA	5.9	57	38	8	103	75

HSCT: hematopoietic stem cell transplantation; HbS: sickle hemoglobin; Retic: reticulocytes.

Furthermore, this study does not allow the chances of fertility after ovarian or testicular reimplantation to be estimated. However, the present study is the first to report the very long-term outcome in patients with mixed chimerism and to show that the correction of hemolytic anemia requires a higher donor cell% than the prevention of SCA-related crises.

The issue now is to determine whether a protocol offering an EFS at 87% with no TRM and no GvHD should also be favored for children. In France, the myeloablative CR with 98% EFS with a very low risk of cGvHD is still currently used in children under 15 years of age, but we recommend the NIH protocol for patients older than 15. However, we recognize that this is still a matter of debate and additional prospective studies may result in a change in course depending on the long-term results of MSD-SCT with non-myeloablative CR.

Acknowledgments

The authors would like to thank all the patients and their families for their participation in this study, all the nurses on the various transplantation units and outpatient clinics for their dedicated work and the doctors who referred patients for transplantation. We also thank Dr. Martine Torres for her critical reading and editing of the manuscript which was supported through an unrestricted grant from bluebird bio.

References

1. Piel FB, Hay SI, Gupta S, Weatherall DJ, Williams TN. Global burden of sickle cell anaemia in children under five, 2010-2050: modelling based on demographics, excess mortality, and interventions. PLoS Med. 2013;10(7):e1001484.
2. Gaston MH, Verter JI, Woods G, et al. Prophylaxis with oral penicillin in children with sickle cell anemia. N Engl J Med. 1986;314(25):1593-1599.
3. Adamkiewicz TV, Silk BJ, Howgate J, et al. Effectiveness of the 7-valent pneumococcal conjugate vaccine in children with sickle cell disease in the first decade of life. Pediatrics. 2008;121(3):562-569.
4. Charache S, Terrin ML, Moore RD, et al . Effect of hydroxyurea on the frequency of painful crisis in sickle cell anemia. N Engl J Med. 1995;332(20):1317-1322.
5. Ferster A, Vermylen C, Cornu G, et al. Hydroxyurea for treatment of severe sickle cell anemia: a pediatric clinical trial. Blood. 1996;88(6):1960-1964.
6. de Montalembert M, Belloy M, Bernaudin F, et al Three-year follow-up of hydroxyurea treatment in severely ill children with sickle cell disease. The French Study Group on Sickle Cell Disease. J Pediatr Hematol/Oncol. 1997;19(4):313-318.
7. Ware RE, Davis BR, Schultz WH, et al. Hydroxycarbamide versus chronic transfusion for maintenance of transcranial doppler flow velocities in children with sickle cell anaemia-TCD With Transfusions Changing to Hydroxyurea (TWiTCH): a multicentre, open-label, phase 3, non-inferiority trial. Lancet. 2016;387(10019):661-670.
8. Thornburg CD, Files BA, Luo Z, et al; BABY HUG Investigators. Impact of hydroxyurea on clinical events in the BABY HUG trial. Blood. 2012;120(22): 4304-4310.
9. Steinberg MH, Barton F, Castro O, et al. Effect of hydroxyurea on mortality and morbidity in adult sickle cell anemia: risks and benefits up to 9 years of treatment. JAMA. 2003;289(13):1645-1651.
10. Wang WC, Ware RE, Miller ST, et al. BABY HUG investigators. Hydroxycarbamide in very young children with sickle-cell anaemia: a multicentre, randomised, controlled trial (BABY HUG). Lancet. 2011; 377(9778):1663-1672.
11. Adams RJ, McKie V, Nichols F, et al. The use of transcranial ultrasonography to predict stroke in sickle cell disease. N Engl J Med. 1992;326(9):605-610.
12. Verlhac S, Bernaudin F, Tortrat D, et al. Detection of cerebrovascular disease in sickle cell disease children by transcranial Doppler sonography. Correlation with MRI and MRA and conventionnal angiography. Pediatr Radiol. 1995;25 Suppl 1:S14-S19.
13. Adams RJ, McKie VC, Hsu L, et al. Prevention of a first stroke by transfusions in children with sickle cell anemia and abnormal results on transcranial Doppler ultrasonography. N Engl J Med. 1998; 339(1):5-11.
14. Bernaudin F, Verlhac S, Arnaud C, et al. Impact of early transcranial Doppler screening and intensive therapy on cerebral vasculopathy outcome in a newborn sickle cell anemia cohort. Blood. 2011; 117(4):1130-1140; quiz 1436.
15. Platt OS, Brambilla DJ, Rosse WF, et al. Mortality in sickle cell disease: life expectancy and risk factors for early death. N Engl J Med. 1994;330(23):1639-1644.
16. Quinn CT, Rogers ZR, Buchanan GR. Survival of children with sickle cell disease. Blood. 2004;103(11): 4023-4027.
17. Telfer P, Coen P, Chakravorty S, et al. Clinical outcomes in children with sickle cell disease living in England: a neonatal cohort in East London. Haematologica. 2007;92(7):905-912.
18. Lanzkron S, Carroll CP, Haywood C Jr. Mortality rates and age at death from sickle cell disease: U.S., 1979-2005. Public Health Rep. 2013;128(2):110-116.
19. Vermylen C, Fernandez Robles E, Ninane J, Cornu G. Bone marrow transplantation in five children with sickle cell anaemia. Lancet. 1988;1(8600):1427-1428.
20. Bernaudin F, Souillet G, Vannier JP, et al. Bone marrow transplantation (BMT) in 14 children with severe sickle cell disease (SCD): the French experience. GEGMO. Bone Marrow Transplant. 1993;12 Suppl 1:118-121.
21. Walters MC, Patience M, Leisenring W, et al. Bone marrow transplantation for sickle cell disease. N Engl J Med. 1996;335 (6):369-376.
22. Bernaudin F, Socie G, Kuentz M, et al. SFGM-TC. Long-term results of related myeloablative stem-cell transplantation to cure sickle cell disease. Blood. 2007; 110(7):2749-2756.
23. Gluckman E, Cappelli B, Bernaudin F, et al. Sickle cell disease: an international survey of results of HLA-identical sibling hematopoietic stem cell transplantation. Blood. 2017;129(11):1548-1556.
24. Vermylen C, Cornu G, Ferster A, et al. Haematopoietic stem cell transplantation for sickle cell anaemia: the first 50 patients transplanted in Belgium. Bone Marrow Transplant. 1998;22(1):1-6.
25. Walters MC, Storb R, Patience M, et al. Impact of bone marrow transplantation for symptomatic sickle cell disease: an interim report. Multicenter investigation of bone marrow transplantation for sickle cell disease. Blood. 2000;95(6):1918-1924.
26. Kuentz M, Robin M, Dhedin N, et al. Is there still a place for myeloablative regimen to transplant young adults with sickle cell disease? Blood. 2011;118(16):4491-4492; author reply 4492-4493.
27. Hsieh MM, Kang EM, Fitzhugh CD, et al. Allogeneic hematopoietic stem-cell transplantation for sickle cell disease. N Engl J Med. 2009;361(24):2309-2317.
28. Hsieh MM, Fitzhugh CD, Weitzel RP, et al. Nonmyeloablative HLA-matched sibling allogeneic hematopoietic stem cell transplantation for severe sickle cell phenotype. JAMA. 2014;312(1):48-56.
29. Saraf SL, Oh AL, Patel PR, et al. Nonmyeloablative Stem Cell Transplantation with Alemtuzumab/Low-Dose Irradiation to Cure and Improve the Quality of Life of Adults with Sickle Cell Disease. Biol Blood Marrow Transplant. 2016;22(3):441-448.
30. Frange P, Peffault de Latour R, Arnaud C, et al. Adenoviral infection presenting as an isolated central nervous system disease without detectable viremia in two children after stem cell transplantation. J Clin Microbiol. 2011;49(6):2361-2364.
31. Roux C, Amiot C, Agnani G, Aubard Y, Rohrlich PS, Piver P. Live birth after ovarian tissue autograft in a patient with sickle cell disease treated by allogeneic bone marrow transplantation. Fertil Steril. 2010; 93(7):2413.e15-19.
32. Quinn CT, Rogers ZR, McCavit TL, Buchanan GR. Improved survival of children and adolescents with sickle cell disease. Blood. 2010;115(17):3447-3452.
33. Walters MC, Sullivan KM, Bernaudin F, et al. Neurologic complications after allogeneic marrow transplantation for sickle cell anemia. Blood. 1995;85(4):879-884.
34. Gaziev J, Marziali S, Paciaroni K, et al. Posterior Reversible Encephalopathy Syndrome after Hematopoietic Cell

Transplantation in Children with Hemoglobinopathies. Biol Blood Marrow Transplant. 2017;23(9):1531-1540.
35. Powell JD, Lerner CG, Schwartz RH.Inhibition of cell cycle progression by rapamycin induces T cell clonal anergy even in the presence of costimulation. J Immunol. 1999;162(5):2775-2784.
36. Brugieres L, Hartmann O, Travagli JP, et al. Hemorrhagic Cystitis Following High-Dose Chemotherapy and Bone-Marrow Transplantation in Children with Malignancies - Incidence, Clinical Course, and Outcome. J Clin Oncol. 1989;7(2):194-199.
37. Lunde LE, Dasaraju S, Cao Q, et al. Hemorrhagic cystitis after allogeneic hematopoietic cell transplantation: risk factors, graft source and survival. Bone Marrow Transplant. 2015;50(11):1432-1437.
38. Bartelink IH, van Reij EM, Gerhardt CE, et al. Fludarabine and exposure-targeted busulfan compares favorably with busulfan/cyclophosphamide-based regimens in pediatric hematopoietic cell transplantation: maintaining efficacy with less toxicity. Biol Blood Marrow Transplant. 2014; 20(3):345-353.
39. Harris AC, Boelens JJ, Ahn KW, et al. Comparison of pediatric allogeneic transplant outcomes using myeloablative busulfan with cyclophosphamide or fludarabine. Blood Adv. 2018;2(11):1198-1206.
40. Sanders JE, Hawley J, Levy W, et al. Pregnancies following high-dose cyclophosphamide with or without high-dose busulfan or total-body irradiation and bone marrow transplantation. Blood. 1996; 87(7):3045-3052.
41. Vatanen A, Wilhelmsson M, Borgström B, et al. Ovarian function after allogeneic hematopoietic stem cell transplantation in childhood and adolescence. Eur J Endocrinol. 2013;170(2):211-218.
42. Poirot C, Abirached F, Prades M, Coussieu C, Bernaudin F, Piver P. Induction of puberty by autograft of cryopreserved ovarian tissue. Lancet. 2012;379(9815):588.
43. Donnez J, Dolmans MM, Demylle D, et al. A. Livebirth after orthotopic transplantation of cryopreserved ovarian tissue. Lancet. 2004;364(9443):1405-1410. Erratum in: Lancet. 2004;364(9450):2020.
44. Baert Y, Van Saen D, Haentjens P, In't Veld P, Tournaye H, Goossens E. What is the best cryopreservation protocol for human testicular tissue banking? Hum Reprod. 2013;28(7):1816-1826.
45. Smith-Whitley K. Reproductive issues in sickle cell disease. Blood. 2014; 124(24): 3538-3543.
46. Walters MC, Patience M, Leisenring, et al. Stable mixed hematopoietic chimerism after bone marrow transplantation for sickle cell anemia. Biol Blood Marrow Transplant. 2001;7(12):665-673.
47. Hsieh MM, Wu CJ, Tisdale JF. In mixed hematopoietic chimerism, the donor red cells win. Haematologica. 2011;96(1):13-15.
48. Fitzhugh CD, Cordes S, Taylor T, et al. At least 20% donor myeloid chimerism is necessary to reverse the sickle phenotype after allogeneic HSCT. Blood. 2017;130(17):1946-1948.
49. Abraham A, Hsieh M, Eapen M, et al. Relationship between Mixed Donor-Recipient Chimerism and Disease Recurrence after Hematopoietic Cell Transplantation for Sickle Cell Disease. Biol Blood Marrow Transplant. 2017;23(12):2178-2183.
50. Bernaudin F, Pondarré C, Galambrun C, Thuret I. Allogeneic/Matched Related Transplantation for β-Thalassemia and Sickle Cell Anemia. Adv Exp Med Biol. 2017;1013:89-122.

Ferrata Storti Foundation

Haematologica 2020
Volume 105(1):102-111

Use of immunosuppressive therapy for management of myelodysplastic syndromes: a systematic review and meta-analysis

Maximilian Stahl,[1] Jan Philipp Bewersdorf,[2] Smith Giri,[2] Rong Wang[3,4] and Amer M. Zeidan[2,3]

[1]Leukemia Service, Memorial Sloan Kettering Cancer Center, New York, NY; [2]Department of Internal Medicine, Section of Hematology, Yale School of Medicine, New Haven, CT; [3]Cancer Outcomes, Public Policy, and Effectiveness Research (COPPER) Center, Yale University, New Haven, CT and [4]Department of Chronic Disease Epidemiology, School of Public Health, Yale University, New Haven, CT, USA

ABSTRACT

Immunosuppressive therapy (IST) is one therapy option for treatment of patients with lower-risk myelodysplastic syndromes (MDS). However, the use of several different immunosuppressive regimens, the lack of high-quality studies, and the absence of validated predictive biomarkers pose important challenges. We conducted a systematic review and meta-analysis according to the Meta-Analysis of Observational Studies in Epidemiology (MOOSE) guidelines and searched MEDLINE *via* PubMed, Ovid EMBASE, COCHRANE registry of clinical trials (CENTRAL), and the Web of Science without language restriction from inception through September 2018, as well as relevant conference proceedings and abstracts, for prospective cohort studies or clinical trials investigating IST in MDS. Fixed and Random-effects models were used to pool response rates. We identified nine prospective cohort studies and 13 clinical trials with a total of 570 patients. Overall response rate was 42.5% [95% confidence interval (CI): 36.1-49.2%] including a complete remission rate of 12.5% (95%CI: 9.3-16.6%) and red blood cell transfusion independence rate of 33.4% (95% CI: 25.1–42.9%). The most commonly used forms of IST were anti-thymocyte globulin alone or in combination with cyclosporin A with a trend towards higher response rates with combination therapy. Progression rate to acute myeloid leukemia was 8.6% per patient year (95%CI: 3.3-13.9%). Overall survival and adverse events were only inconsistently reported. We were unable to validate any biomarkers predictive of a therapeutic response to IST. IST for treatment of lower-risk MDS patients can be successful to alleviate transfusion burden and associated sequelae.

Correspondence:

AMER.ZEIDAN
amer.zeidan@yale.edu

Received: February 12, 2019.

Accepted: April 15, 2019.

Pre-published: April 19, 2019.

doi:10.3324/haematol.2019.219345

Check the online version for the most updated information on this article, online supplements, and information on authorship & disclosures: www.haematologica.org/content/105/1/102

Introduction

Myelodysplastic syndromes (MDS) comprise a spectrum of clonal hematopoietic stem cell disorders that are characterized by peripheral blood cytopenias and dysplastic changes due to ineffective hematopoiesis, recurrent cytogenetic abnormalities, and an increased risk of progression to acute myeloid leukemia (AML).[1,2] As a heterogenous group of diseases, treatment regimens for MDS patients need to be individualized and mainly based on the extent of MDS-associated symptoms and the risk of progression to AML, as assessed by various risk stratification tools such as the International Prognostic Scoring System (IPSS) and its revised version (IPSS-R).[3-5] For patients with lower-risk MDS (which is usually defined as patients with very low, low or intermediate-1 risk based on IPSS and IPSS-R) several treatment options including lenalidomide, erythropoiesis-stimulating agents, immunosuppressive therapy (IST), and hypomethylating agents are available.[3,5-7] The rationale for the use of IST in MDS is based on studies showing that up to 48% of patients with MDS had evidence of autoimmune disease, but the impact of this finding on prognosis is controversial.[8,9] Additionally, dysregulation of T-cell function has been linked to impaired hematopoiesis in patients with both aplastic anemia and lower-

risk MDS and can potentially be restored by IST.[9-11] Several forms of IST have been tested in MDS treatment with varying degrees of success. Previous studies have reported durable objective responses and transfusion independence ranging up to 55% and 27%, respectively.[12,13] Consensus guidelines recommend consideration of IST in patients with low or intermediate-1 risk, non-del(5q-) MDS patients.[3,6,14] The most commonly used of these are anti-thymocyte globulin (ATG), cyclosporine A (CsA), and monoclonal antibodies (etanercept, alemtuzumab) which can be used either as monotherapy or in combination.[13,15-20] Although IST has been used for over two decades in MDS treatment, response rates are highly heterogeneous between various patient subpopulations and studies. While several predictive response markers such as age, HLA-DR15 positivity, bone marrow cellularity, and disease duration have been identified in some studies, these findings could not be reproduced in others.[12,16,21-23]

Given this large heterogeneity among published studies, we performed a systematic literature review and meta-analysis on several forms of IST in MDS to objectively assess overall response rates (ORR), rates of achieving a complete remission (CR), erythroid hematologic improvement (HI-E), and red blood cell transfusion independence (TI) as well as the rate of AML progression per patient-year for patients receiving IST.

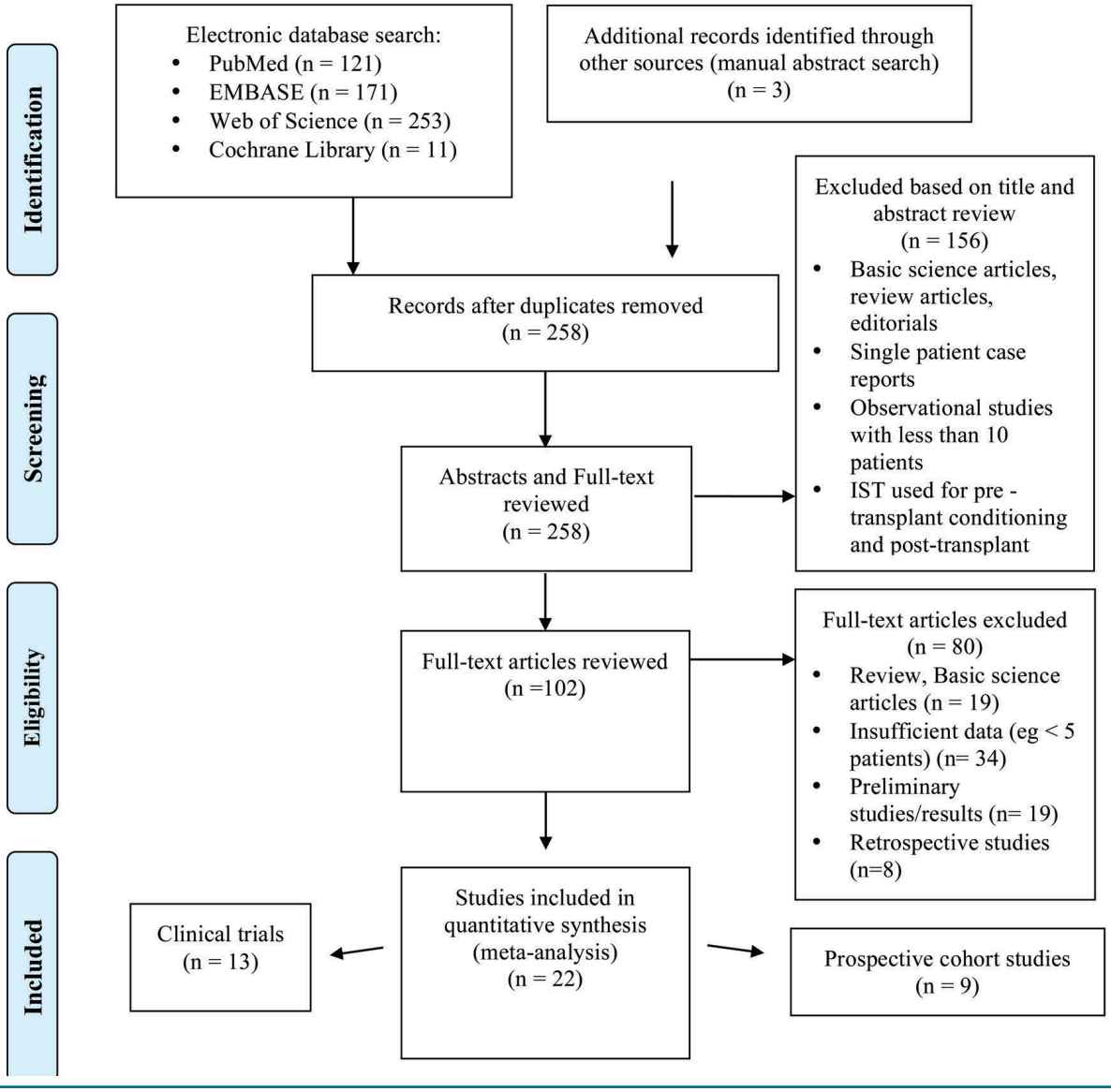

Figure 1. Flow chart showing study selection as per the MOOSE guidelines. The search strategy and stepwise process of study selection used in this meta-analysis. MEDLINE *via* PubMed, Ovid EMBASE, the COHRANE registry of clinical trials (CENTRAL), and the Web of Science electronic databases were searched with no language restriction from inception through September 2018, using the following combination of free-text terms linked by Boolean operators: ("MDS" OR "myelodysplasia" OR "myelodysplastic syndrome") AND ("IST" OR "immunosuppressive therapy" OR "immunosuppression" OR "ATG" OR "anti-thymocyte globulin" OR "tacrolimus" OR "cyclosporine" OR "sirolimus" OR "prednisone" OR "prednisolone" OR "steroids" OR "etanercept" OR "alemtuzumab"). Two authors (MS and JPB) independently screened the titles and abstracts of all retrieved studies for eligibility and removed any duplicate records. In a second step, full texts of the potentially eligible studies were reviewed for the final eligibility. Review, basic science articles and articles with insufficient patient number (< 5 patients) as well as preliminary studies and retrospective studies were excluded.

Table 1. ATG.

Author	Year	Treatment and treatment schedule	N	IPSS risk category	FAB/WHO classification	Outcomes	Adverse events	Ref.
Molldrem JJ *et al.*	2002	ATG 40mg/kg/d for 4 doses	61	Low: 18% Intermediate-1: 67% Intermediate 2: 5% High: 10%	RA: 61% RARS: 16% RAEB: 23%	No CRs or PR HI-E: 34% TI: 34%	Every patient with serum sickness; no CTCAE grading provided	(28)
Steensma DP *et al.*	2003	r-ATG 40mg/kg/d for 4 doses	8	Intermediate-1: 63% Intermediate-2: 37%	RA: 25% RAEB-I: 75%	No responses	20 AE, no CTCAE grading provided	(33)
Killick S. *et al.*	2003	Lymphoglobuline 15mg/kg/d for 5 doses	30	Not reported	RA: 43% RARS: 10% RCMD: 33% RAEB-I: 14%	CR: 5% PR: 45% HI-E: 45%	46 AE, no grading provided	(34)
Stadler *et al.*	2004	r-ATG 3.75 mg/kg/d h-ATG: 15 mg/kg/d for 5 doses	35	Low: 14% Intermediate-1: 57% Intermediate-2: 26% High: 3%	RA: 37% RCMD: 37% CMML: 3% RAEB-I: 17% RAEB-II: 11%	CR: 11% PR: 17% HI-E: 26% TI: 20%	AE ≥ grade 3: 66%	(35)
Komrokji R. *et al.*	2014	r-ATG 10mg/kg/d for 4 doses	27	Low: 30% Intermediate-1: 56% Intermediate 2: 14%	RA: 7% RCMD: 30% MDS-U: 19% MDS/MPN: 4% RAEB: 19%	No CR or PR HI-E: 39%	70 AE 9 AE ≥ grade 3 (4 infectious)	(16)
Yazji S. *et al.*	2003	ATG 40mg/d for 4 doses + CsA titrated to 200-400mg/dl for 6 months + methylprednisolone 1mg/kg for 4 days followed by oral taper over 1 month	31	Not reported	RA/RARS: 58% CMML: 3% RAEB-I/II: 39%	CR: 13% PR: 3% TI: 19%	65 AE in 31 patients; 7 AEs ≥ grade 3 (0 infectious)	(30)
Saunthararajah Y *et al.*	2003	ATG 40mg/kg/d for 4 doses + CsA 5-12mg/kg/d for 6 months	23	Not reported	RA: 74% RARS: 9% RAEB-I/II: 17%	HI-E: 30% TI: 30%	Not reported	(21)
Broliden PA *et al*	2006	ATG 10-20mg/kg/d for 3 doses; CsA 200ng/ml for 32 weeks	25	Low: 72% Intermediate-1: 28%	RA: 80% RAEB-I: 20%	CR: 15% PR: 15%	6 patients off trial due to AE	(36)
Garg R. *et al.*	2009	rATG 3.5 mg/kg/d for 5 doses + Methylprednisolone 1 mg/kg/day IV for 5 doses with PO prednisone taper over 3 weeks + CsA 5 mg/kg/d ≥6 months for trough of 200 and 400 mg/dl + G-CSF 5 µg/kg/d s.c. daily for 3 months	15	Not reported	Not reported PR: 20%	CR: 7%	79 AE in 15 patients of which 35 AE ≥grade 3 (6 infectious)	(37)
Xiao, L *et al.*	2012	CsA 3-5mg/kg/d for 6 months +/- ATG 4mg/kg/d for 4 doses	71	Low: 100%	RA: 4% RCMD: 92% MDS-U: 4%	CR: 16% HI-E: 77% TI: 64%	Not reported	(13)
Passweg JR *et al.*	2011	h-ATG 15mg/kg/d for 5 doses + CsA for 6 months	45	Low: 18% Intermediate-I: 53% Intermediate-II: 16% High: 2%	RA: 47% RARS: 13% RAEB-I: 20% Hypoplastic MDS: 20%	CR: 7% PR: 24%	16 patients with SAE (4 infectious)	(18)
Kadia TM *et al.*	2012	ATG (3.5 mg/kg/day × 5 days + CsA 5 mg/kg/d × 6 months + methylprednisolone 1 mg/kg/d with 1month taper of prednisone	24	Not reported	Not reported	CR: 8% HI-E: 17% TI: 8%	Not reported for MDS cohort independently	(17)

continued on the next page

continued from the previous page

Deeg, HJ *et al.*	2004	ATG 40 mg/kg/d for four doses + etanercept 25 mg s.c. twice a week for 8 weeks. If no hematologic by week 8, etanercept three times per week for additional 8 weeks.	14	Low: 7% Intermediate-1: 71% Intermediate-2: 21%	RA: 64% RARS: 7% RAEB-I: 7% RAEB-II: 21%	CR: 15% HI-E: 39% TI: 39%	Not reported	(31)
Scott BL *et al.*	2010	ATG 40 mg/kg/d for 4 doses + etanercept 25 mg s.c. twice a week for 2 weeks, every month for 4 months	25	Low: 44% Intermediate-1: 56%	RA: 16% RARS: 8% RCMD: 72% RAEB-I: 4%	CR: 4% HI-E: 62%	Not reported	(38)

AE: adverse events; ATG: anti-thymocyte globulin; h-ATG: horse anti-thymocyte globulin, r-ATG: rabbit anti-thymocyte globulin, AZA: azacitidine, CMML: chronic myelomonocytic leukemia; CR: complete remission; CTCAE: Common Terminology Criteria for Adverse Events; HI-E: hematologic improvement-erythroid; IPSS: International Prognostic Scoring System; MDS-U: unclassifiable myelodysplastic syndrome; PR: partial remission; RA: refractory anemia; RARS: refractory anemia with ringed sideroblasts; RAEB: refractory anemia with excess blasts; RCMD: Refractory cytopenia with multilineage dysplasia; TI: transfusion independence.

Methods

Date sources and search strategy

This systematic review and meta-analysis was conducted according to the Preferred Reporting Items for Systematic Reviews and Meta-Analysis (PRISMA) and Meta-Analysis of Observational Studies in Epidemiology (MOOSE) guidelines.[24] MEDLINE *via* PubMed, Ovid EMBASE, the COHRANE registry of clinical trials (CENTRAL), and the Web of Science electronic databases were searched without language restriction from inception through September 2018, using the following combination of free-text terms linked by Boolean operators: ("MDS" OR "myelodysplasia" OR "myelodysplastic syndrome") AND ("IST" OR "immunosuppressive therapy" OR "immunosuppression" OR "ATG" OR "anti-thymocyte globulin" OR "tacrolimus" OR "cyclosporine" OR "sirolimus" OR "prednisone" OR "prednisolone" OR "steroids" OR "etanercept" OR "alemtuzumbab").

We performed a gray literature search through: 1) manual search of bibliographies of all identified studies; and 2) conference proceedings and abstracts of the following annual meetings: American Society of Hematology, American Society of Clinical Oncology, European Hematology Association, and European Society of Medical Oncology.

Study selection and endpoints

Two reviewers (MS and JPB) independently screened the titles and abstracts of all retrieved studies for eligibility and removed duplicates. Subsequently, full texts of the potentially eligible studies were reviewed for eligibility. We excluded studies that: 1) lack information on either ORR or CR rate; 2) review articles, editorials, and correspondence letters that did not report independent data; 3) case series and studies reporting outcomes on fewer than five patients; and 4) retrospective studies. There was no disagreement among the two reviewers regarding the inclusion of any study. The study selection process is illustrated in a flow diagram (Figure 1).

Prospective cohort studies or clinical trials investigating the use of IST for the treatment of MDS were included. IST was defined as receipt of one or a combination of the following drugs: rabbit and horse ATG, CsA, sirolimus, mycophenolate mofetil and monoclonal antibodies (etanercept, alemtuzumab).

The primary outcomes were ORR and CR rate. Secondary outcomes included rates of HI-E, TI, and AML progression. ORR was defined based on the 2006 modified International Working Group (IWG) response criteria for MDS.[25]

Data extraction

Two investigators (MS and JPB) extracted data using a standardized data-extraction form, and a third investigator (SG) performed a cross-check for data accuracy. A more detailed description of the extracted information is provided in the *Online Supplementary Methods*.

Quality assessment

The quality of each study was assessed by two authors (MS and JPB) using the modified Down and Black checklist.[26] Quality assessments for individual studies are provided in *Online Supplementary Table S1*.

Statistical analysis

Random-effects models were used to pool ORR, rates of CR, HI-E, TI, and progression to AML. All effect sizes underwent logarithmic transformation prior to pooling using an inverse variance weighting approach. Heterogeneity of studies was determined using Cochran Q and I^2 indices and significant heterogeneity (defined as I2 > 60%) was further explored with sensitivity analyses.[27] Subgroup analyses were planned based on the type of IST used. All analyses were performed with Comprehensive Meta-Analysis (CMA 2.2, Biostat).

Results

Description of included studies

The flow diagram of study selection based on the MOOSE guidelines is shown in Figure 1. An electronic search of PubMed, EMBASE, the Cochrane Library, and the Web of Science plus a manual search retrieved a total of 258 publications after removal of duplicates. Of the 258 articles reviewed, 156 articles were excluded on the basis of the title and abstract review if the article was clearly labeled as a review article, editorial, correspondence letter, case series or retrospective study in the title or abstract. A total of 102 articles were reviewed in full text. Of these, 80 articles were excluded because they were reviews, basic science articles, presented insufficient data (<5 patients), only showed preliminary results, or were retrospective in nature. Of the 22 studies included, there were 9 prospective cohort studies[13,21,28-32] and 13 clinical trials.[16-20,33-40] Patients were treated with ATG , ATG + CsA , ATG + Etanercept (Table 1), CsA (Table 2), and other IST regimens (Table 3).

There was a total of 570 patients in the 22 included studies. The average median age was 62.0 years (range 12-87 years). Among the studies that reported IPSS scores, 360 (80.9%) patients had IPSS scores of low- or intermediate-1, while 71 patients (16.0%) had intermediate-2 and high IPSS scores. The median duration of follow up of individual studies, where reported, was 16.4 months (range 0-60 months).

Assessment of study quality

Except for three studies,[18,29,35] all studies included in this meta-analysis used a single-arm design. Study quality was assessed using the Downs and Black checklist. Assessments for individual studies are provided in *Online Supplementary Table S1.*

Rates of overall response and complete remission

The ORR was reported by all 22 studies (Figure 2A). Overall, the ORR was 42.5% (95%CI: 36.1-49.2%). There was a significant heterogeneity among the various studies, with a Cochran's Q statistic of 80% (P<0.001) and an I^2 statistic of 74%.

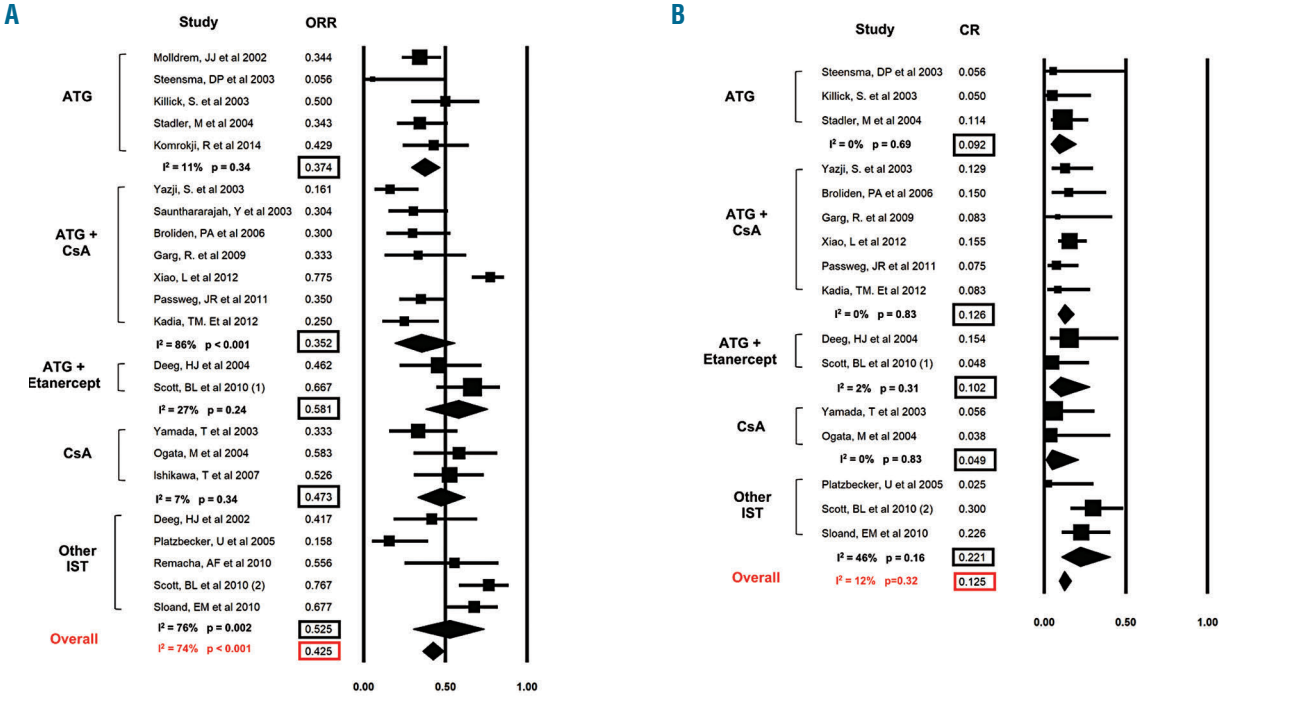

Figure 2. Overall and complete response rates to various forms of immunosuppressive therapy (IST). Forest plots of odds ratios (squares, proportional to study weights used in meta-analysis, 95% confidence intervals) for various forms of IST with the summary measures (center line of diamond) and associated confidence intervals (lateral tips of diamond) for overall response rate (ORR) and complete response (CR) rate are shown in panel (A) and (B), respectively.

Table 2. Cyclosporine A.

Author	Year	Treatment and treatment schedule	N	IPSS risk category	FAB/WHO classification	Outcomes	Adverse events	Ref.
Yamada T *et al.*	2003	Methylprednisolone 1000mg for 3 doses followed by oral taper +/- CsA 4-5mg/kg for trough of 100-200 ng/ml	18	Intermediate-1: 72% Intermediate 2: 6%	RA: 56% CMML: 11% RAEB-I: 33%	CR: 6% PR: 11% TI: 18%	Not reported	(29)
Ogata M *et al.*	2004	CsA 1.1-6.0 mg/kg until disease progression or intolerable side effects	12	Not reported	RA: 92% RAEB-I: 8%	No CRs or PRs HI-E: 58% TI: 64%	Not reported	(52)
Ishikawa T *et al.*	2007	CsA titrated to trough 150-200ng/ml for 32 weeks	20	Low: 10% Intermediate-1: 90%	RA: 40% RARS: 5% RCMD: 45% RAEB-I: 10%	No CRs or PRs HI-E: 42% TI: 40%	51 AEs in 19 patients, AEs ≥ grade 3 in 4 patients (2 infectious)	(41)

AE: adverse events; ATG: anti-thymocyte globulin; AZA: azacitidine; CMML: chronic myelomonocytic leukemia; CR: complete remission; CTCAE: Common Terminology Criteria for Adverse Events; HI-E: hematologic improvement-erythroid; IPSS: International Prognostic Scoring System; PR: partial remission; RA: refractory anemia; RARS: refractory anemia with ringed sideroblasts; RAEB: refractory anemia with excess blasts; RCMD: refractory cytopenia with multilineage dysplasia; TI: transfusion independence.

A pre-specified subgroup analysis showed that the ORR was highest with ATG + Etanercept at 58.1% (95%CI: 37.8-75.9%; I^2=27%), followed by other IST at 52.5% (95%CI: 30.4-73.7%; I^2=76%), CsA at 47.3% (95%CI: 33-62%; I^2=7%), ATG at 37.4% (95%CI: 29.1-46.6%; I^2=11%), and ATG + CsA at 35.2% (95%CI: 18.9-55.9%; I^2=86%), respectively (Figure 2A).

Complete remission rates were reported by 16 studies (Figure 2B). Overall, the CR rate was 12.5% (95%CI: 9.3-16.6%). Heterogeneity among the various studies was low, with a Cochran's Q statistic of 17 (P=0.32) and an I^2 statistic of 12%.

A pre-specified subgroup analysis for patients, who received ATG, ATG + CsA, ATG + Etanercept, CsA and other IST, showed that the CR was 9.2% (95%CI: 4.0-19.6%; I^2=0%), 12.6% (95%CI: 8.6-18.1%; I^2=0%), 10.2% (95%CI: 3.3-27.8%; I^2=2%), 4.9% (95%CI: 1.0-21.1%; I^2=0) and 22.1% (95%CI: 10.6-40.4%; I^2=46%), respectively (Figure 2B).

Hematologic improvement and transfusion independence

Erythroid hematologic improvement rates were reported by 16 studies (Figure 3A). Overall, the HI-E rate was 41.8% (95%CI: 33.3-50.8%). Heterogeneity among the various studies was high, with a Cochran's Q statistic of 53.1 (P<0.001) and an I^2 statistic of 72%.

A pre-specified subgroup analysis showed that the HI-E rate was highest with ATG + Etanercept at 51.8% (95%CI: 29.8-73.1%; I^2=42%), followed by CsA at 50% (95%CI: 32.7-67.3%; I^2=0), ATG + CsA at 44.8% (95%CI: 14.3-79.8%; I^2=92%), other IST agents at 43.1% (95%CI: 24.0-64.4%; I^2=70%), and ATG at 31.7% (95%CI: 20.3-45.8%; I^2=29%), respectively (Figure 3A).

The rates of TI were reported by 14 studies (Figure 3B). Overall, the TI was 33.4% (95%CI: 25.1-42.9%). There was a significant heterogeneity among the various studies, with a Cochran's Q statistic of 35.1 (P=0.001) and an I^2 statistic of 63%.

A pre-specified subgroup analysis showed that the TI rate was highest with CsA at 44.8% (95%CI: 28.8-61.9%; I^2=9%) followed by ATG + Etanercept at 38.5% (95%CI: 17-65.6%; I^2=0%), ATG at 25.2% (95%CI: 13.3-42.5%; I^2=50%), ATG + CsA at 28.4% (95%CI: 10.0-58.6%; I^2=86%), and other IST at 25.9% (95%CI: 11.7-48.0; I^2=27%), respectively (Figure 3B).

Acute myeloid leukemia progression rate and adverse events

The rates of progression to AML were reported by 11 studies (Figure 4). Overall, the AML progression rate per person year of follow up was low (8.6%; 95%CI: 3.3-13.9%). There was a significant heterogeneity among the various studies, with a Cochran's Q statistic of 45.2 (P<0.001) and an I^2 statistic of 78%. Pre-specified subgroup analysis showed an AML transformation rate per patient year of 13.7% (95%CI: 1.4-25.9%; I^2=73%), 13.5% (95%CI: 0-31.3; I^2=91%), 7.0% (95%CI: 0-22.4%; I^2=71%), and 6.7% (95%CI: 0-13.5%; I^2=0%) for patients who received ATG, ATG + CsA, CsA and other IST, respectively.

Only 10 of the 22 studies reported grade 3/4 side effects.[16,18,19,30,32,35,37,39-41] The data included in these papers were insufficient to conduct any further meta-analysis on the safety of IST in LR-MDS.

Sensitivity analysis

Separate sensitivity analyses for ORR, HI, TI and AML progression rate showed that exclusion of any one study did not change the overall effect direction but did change

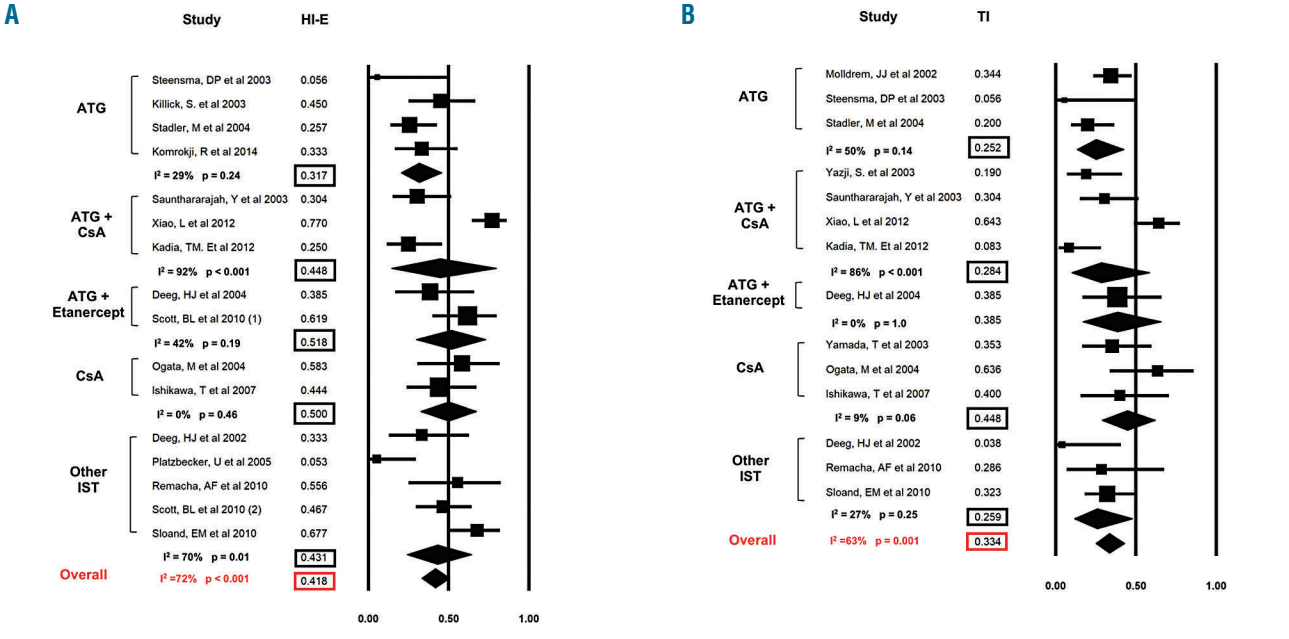

Figure 3. Rate of hematologic improvement in the erythroid lineage (HI-E) and red blood cell transfusion independence. Forest plots of odds ratios (squares, proportional to study weights used in meta-analysis, 95% confidence intervals) for various forms of immunosuppressive therapy (IST), with the summary measure (center line of diamond) and associated confidence intervals (lateral tips of diamond) for hematologic improvement in the erythroid lineage (HI-E) and achievement of red blood cell transfusion independence (TI) are shown in panel (A) and (B), respectively.

the effect size in subgroup analysis, and led to a reduction in heterogeneity.

For ORR, HI-E and TI, the study with the largest influence on the heterogeneity of these outcomes was the study by Xiao *et al.* examining the use of ATG + CsA.13 Removal of this study changed the ORR by 5.1% (from 42.5% to 37.4%) in the overall analysis and by 6.5% (from 35.2% to 28.7%) in the subgroup analysis of studies examining ATG + CsA. In addition, removal of this study led to a loss of heterogeneity in the overall analysis (I^2=62%, Cochran's Q statistic = 52.1, *P*=0.001) and in the subgroup analysis of studies examining ATG + CsA (I^2= 0%, Cochran's Q statistic = 3.4, *P*=0.64). Removal of the study by Xiao *et al.* also changed the HI-E by 3.9% (from 41.8% to 37.9%) in the overall analysis and 17.1% (from 44.8% to 27.7) in the subgroup analysis of studies examining ATG + CsA. This led to a loss of heterogeneity in the overall analysis (I2 = 55%, Cochran's Q statistic = 31.1, *P*=0.005) and in the subgroup analysis of studies examining ATG + CsA (I2 = 0%, Cochran's Q statistic = 0.17, *P*=0.68). For TI, removal of this study changed the outcome by 2.8% (from 33.4% to 30.6%) in the overall analysis and by 8.8% (from 28.4% to 19.6%) in the subgroup analysis of studies examining ATG + CsA. This also led to a loss of heterogeneity in the overall analysis (I^2=35%, Cochran's Q statistic = 18.6, *P*=0.1) and in the subgroup analysis of studies examining ATG + CsA (I^2=40.6, Cochran's Q statistic = 3.4, *P*=0.19).

The study with the largest influence on the AML progression rate was that reported by Passweg *et al.*,[18] the removal of which changed the AML progression rate by 0.5% (from 8.6% to 8.1%). In addition, removal of this study led to a loss of heterogeneity (I2 = 67%, Cochran's Q statistic = 27.6, *P*=0.001).

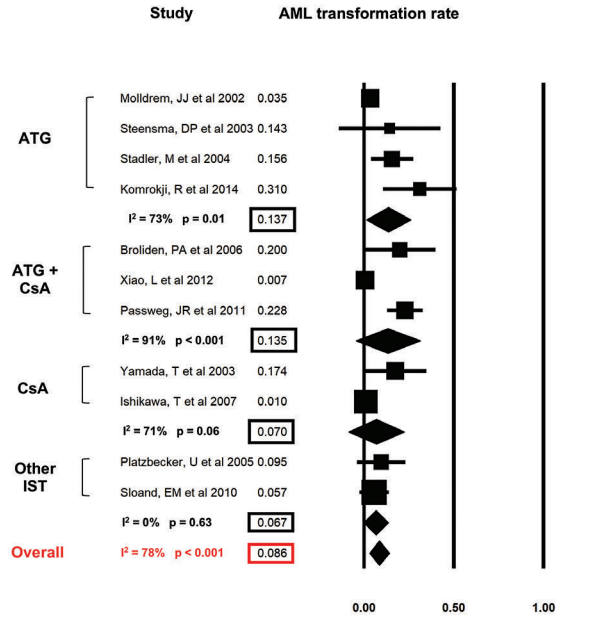

Figure 4. Rate of acute myeloid leukemia (AML) progression during study duration. Forest plots of odds ratios (squares, proportional to study weights used in meta-analysis, 95% confidence intervals) for various forms of immunosuppressive therapy (IST), with the summary measure (center line of diamond) and associated confidence intervals (lateral tips of diamond) for rate of transformation to AML during the study period.

Discussion

To our knowledge, this is the first systematic review and meta-analysis on IST in MDS, and included a total of nine prospective cohort studies and 13 clinical trials. The meta-analysis of these studies demonstrated an ORR of 42.5% (with a CR rate of 12.5%) and achievement of red blood cell transfusion independence in one-third of the patients.

Previous retrospective studies reported similar ORR and TI rates among MDS patients with IST. A recent uncontrolled large international retrospective study in MDS patients treated with various different IST regimens demonstrated results very similar to our meta-analysis, with an ORR and TI rate of 48% (with 11.2% achieving a CR) and 30% of patients, respectively. In other large retrospective studies, the ORR and TI rates ranged from 30% to 42% and from 31% to 41%, respectively.[22,23,42] In our meta-analysis, ATG +/- CsA was the most commonly used IST regimen, similar to the finding in a recent large retrospective study.[12] Importantly, while the National Comprehensive Cancer Network (NCCN; Version 2.2019) guidelines suggest the use of ATG +/- CsA as a treatment option for certain types of MDS,[14] they do not suggest other IST regimens. However, in our meta-analysis, multiple different IST regimens other than ATG +/- CsA were included, among them ATG + etanercept, CsA and several "other IST" regimens including etanercept +/- azacitidine, sirolimus, mycophenolate mofetil and alemtuzumab. It is important to point out that these other IST regimens do not have completely overlapping mechanisms of action, tolerability, and expected response rates compared to ATG and CsA. Acknowledging these differences, we included these IST regimens in our analysis as they all provide an element of immunosuppression regardless of their specific mechanism of action.

While the identification of clinical and molecular markers to predict response to IST would be of clinical importance to optimize treatment of individual patients, data for several of these co-variates that had been proposed, such as younger age, shorter disease duration, hypocellular bone marrow, or the presence of HLA DR15 and PNH clones, are controversial.[12,21-23,42,43] Given the heterogeneity of the studies included in this meta-analysis, we were unable to address the utility of predictive biomarkers as they were only reported by a minority of studies. However, several studies, including the largest study to date by Stahl *et al.*, were unable to validate any predictive biomarkers except of bone marrow hypocellularity.[42-44]

Based on available prospective data, the current National Comprehensive Cancer Network guidelines suggest IST with ATG +/- CsA as a treatment option for symptomatic anemia in low-risk, non-del(5q) MDS especially for patients younger than 60 years of age, ≤5% blasts in the bone marrow, or with a hypocellular bone marrow, PNH clone positivity, or STAT-3 mutant cytotoxic T-cell clones.[14] However, further prospective studies are warranted to verify these predictive markers. It also remains to be shown how the wider availability of genetic testing, for example, by next generation sequencing, will impact individualized treatment decisions for MDS patients. Supporting a potential role in guiding manage-

Table 3. Other immunosuppressive therapy regimens.

Author	Year	Treatment and treatment schedule	N	IPSS risk category	FAB/WHO classification	Outcomes	Adverse events	Ref.
Deeg HJ *et al.*	2002	Etanercept, 25 mg, 2x/ week s.c. for 16 weeks (increased to 3x/week if no response at 8 weeks).	14	Low: 29% Intermediate-1: 36% Intermediate-2: 29% High: 7%	RA: 43% RARS: 14% CMML: 14% RAEB-I/II: 29%	No CR or PR HI-E: 33% TI: 0%	4 infectious AE (2 ≥ grade 3)	(20)
Platzbecker U *et al.*	2005	Sirolimus PO 6 mg loading dose followed by 2 mg once daily adjusted to target blood concentration of 3–12 ng/ml for ≥ 3 months	19	Low: 11% Intermediate-1: 68% Intermediate-2: 21%	RA: 5% RARS: 11% RCMD: 53% RAEB-I: 26% RAEB-II: 5%	PR: 5% HI-E: 5%	10 AE in 8 patients; 1 case of grade IV thrombocytopenia	(39)
Remacha AF *et al.*	2010	Mycophenolate mofetil 1 g twice a day PO + prednisone 0.5 mg/Kg/d PO tapering to 10 mg/d for 12 weeks	10	Not reported	RARS: 60% RCMD: 40%	No CRs or PRs HI-E: 56% TI: 33%	5 AE in 10 patients (1 infectious ≥ grade 3)	(40)
Scott BL *et al.*	2010	AZA 75 mg/m2 on days 1-7 every 28 days + Etanercept 25 mg s.c. on days 8, 11, 15, and 18	20	Low: 9% Intermediate-1: 38% Intermediate-2: 31% High: 22%	RA: 6% RARS: 3% CMML: 9% RCMD: 16% RAEB-I: 31% RAEB-II: 34%	CR: 28% PR: 6% HI-E: 44%	37 AE ≥ grade 3 in 32 patients (3 infectious)	(32)
Sloand, EM et al.	2010	Alemtuzumab 10 mg/d IV for 10 days	31	Low: 7% Intermediate-1: 71% Intermediate-2: 23%	Not reported	CR: 23% PR: 3% HI (any cell line): 39% TI: 32%	84 AE in 31 patients of which 28 ≥grade 3 (13 patients with ≥grade 3 infectious AE)	(19)

AE: adverse events; ATG: anti-thymocyte globulin; AZA: azacitidine; CMML: chronic myelomonocytic leukemia; CR: complete remission; CTCAE: Common Terminology Criteria for Adverse Events; HI-E: hematologic improvement-erythroid; IPSS: International Prognostic Scoring System; PR: partial remission; RA: refractory anemia; RARS: refractory anemia with ringed sideroblasts; RAEB: refractory anemia with excess blasts; RCMD: refractory cytopenia with multilineage dysplasia; TI: transfusion independence.

ment decisions, two recent phase II clinical trials on the transforming growth factor (TGF)-β pathway inhibitors luspatercept and sotatercept have shown that the presence of ≥15% ringed sideroblasts or of a *SF3B1* mutation was predictive of a higher rate of treatment response.[45-47]

Given the small sample sizes of most studies, the different treatment regimens used, and the various diagnostic techniques employed, there was a high degree of heterogeneity among included studies. However, sensitivity analyses accounting for the type of IST as well as a 'one-study removed' analysis, found no significant impact of this heterogeneity on the overall results of the meta-analysis. The study by Xiao *et al.*[13] demonstrated a significantly higher ORR and rate of HI-E and TI compared to other studies studying the application of ATG + CsA. This can be explained by the fact that in the study by Xiao *et al.*[13] patients were strictly selected to have a high chance of responding to IST. Patients were required to have low risk MDS (IPSS score equal or less 1.0) and either expression of the HLA-DR15 allele or a BM cellularity of less than 30%, or an abnormal immune index of BM T lymphocytes. Furthermore, patients were excluded if they had >5% marrow myeloblasts or a poor risk karyotype or a diagnosis of concurrent non-hematologic malignancy. By excluding the study by Xiao *et al.*,[13] from the analysis, heterogeneity in the subgroup analysis of studies examining ATG + CsA decreased significantly. This demonstrates that by strict selection of MDS patients, who are predicted to benefit from IST, the response to IST can be significantly increased.

While a randomized, placebo-controlled, double-blinded design is the gold standard of clinical studies, the heterogenous patient population in terms of demographic, clinical (e.g. prior treatments), and molecular co-factors makes such a trial design challenging. As expected, this systematic review and meta-analysis confirmed the lack of published prospective, randomized controlled trials of IST in MDS. In this meta-analysis, 20 out of 22 included studies were single arm clinical trials or prospective cohort studies. As the Downs and Black checklist had been originally developed for the evaluation of multi-arm studies, several of its quality criteria such as randomization, equal distribution of confounding variables among study groups, and blinding were not applicable to the majority of the studies in our meta-analysis. However, when eliminating items from the modified Downs and Black check-

list that are only applicable to multi-arm studies, 12 out of 22 studies scored at least 15 out of the remaining 20 points. A notable exception in terms of methodological quality was the phase III trial by Passweg *et al*. comparing ATG + CsA to best supportive care.[18] Importantly, treatment with ATG + CsA resulted in a hematologic response in 31% of patients in this trial which is comparable to the 33.7% for ATG + CsA in our meta-analysis. Although the limitations in terms of study quality must be kept in mind, the overall comparable results among different studies suggest that our meta-analysis provides robust evidence on the effect of IST in the treatment of MDS.

Previous studies have suggested that IST may contribute to the risk of progression to AML because of a suppression of immune surveillance. However, this seems to be more relevant in high-risk MDS subtypes rather than the lower risk MDS forms that constitute the patients primarily treated with IST.[48,49] In our meta-analysis, we found a rate of progression to AML of 8.6% per patient year (95%CI: 3.3-13.9%). The risk of progression to AML varies substantially based on the IPSS risk category as well as the presence of certain cytogenetic abnormalities.[50] The majority of patients in our meta-analysis had either low (32.8%) or intermediate-1 (49.2%) risk disease by IPSS (Tables 1-3). In previous studies, the time of progression to AML in the absence of treatment for 25% of patients with IPSS-low and intermediate-1 MDS patients was reported at 10.8 and 3.2 years, respectively.[51] Although comparison of our data with these historical results is limited, our meta-analysis does not show a significantly higher AML transformation rate than expected for IPSS lower and intermediate-1 risk MDS patients in general.

Our study has several limitations. In many of these studies, the patients included were selected and judged by the investigators to potentially benefit from IST. Therefore, the efficacy results might be inflated and not necessarily apply to all lower-risk MDS patients. In addition to the heterogeneity of studies and the overall low methodological quality, there were insufficient data to assess adverse events in our meta-analysis. While at least a minimum amount of information on treatment-associated adverse events was provided in 17 out of 22 studies, only 5 studies provided CTCAE grading of adverse events and reported those on a patient level.[18,35,39-41] Given the heterogeneity of adverse event reporting, we were unable to conduct a meta-analysis on the side effect profile of IST in MDS. As IST is most commonly used for lower-risk MDS patients to alleviate symptom burden resulting from red blood cell transfusion dependence and to limit the detrimental sequelae of resulting iron overload rather than modifying AML transformation risk, information on treatment-associated adverse events is essential for physicians to appropriately counsel patients. We were not able to analyze the effect of IST on platelet transfusion independence as it was reported in only the minority of studies. Lastly, publication bias could not be assessed in this meta-analysis because of the lack of a comparative treatment arm in the majority of the studies.

Given that the median overall survival rate among untreated patients with lower-risk MDS is 5.3 years, a long duration of follow up would be required to detect any survival benefit from IST and data on overall survival were provided in 5 out of 23 studies only. Therefore, we were unable to assess whether IST provides an actual survival benefit in MDS.

Conclusions

In summary, our data showed an ORR of 42.5% and a TI rate of 33.4% for IST in MDS, with ATG-based treatment regimens being the most commonly used option. Response rates tended to be higher for combination therapy of ATG in conjunction with mostly CsA compared to ATG monotherapy. While we were unable to assess the utility of various biomarkers in predicting response to IST, current guidelines recommend considering IST for symptomatic treatment of lower-risk MDS patients to alleviate transfusion burden and associated sequelae. However, given the lack of prospective, randomized, controlled studies, it is difficult to definitively determine the impact of IST on response and survival in patients with MDS, and randomized trials of IST are warranted to confirm our results.

Funding

Amer Zeidan is a Leukemia and Lymphoma Society Scholar in Clinical Research and is also supported by a National Cancer Institute (NCI) Cancer Clinical Investigator Team Leadership Award (CCITLA). Research reported in this publication was supported by the NCI of the National Institutes of Health under Award Number P30 CA016359. The content is solely the responsibility of the authors and does not necessarily represent the official views of the National Institutes of Health.

References

1. Arber DA, Orazi A, Hasserjian R, et al. The 2016 revision to the World Health Organization classification of myeloid neoplasms and acute leukemia. Blood. 2016;127(20):2391-2405.
2. Swerdlow SH CE, Harris NL, Jaffe ES, et al. WHO Classification of Tumours of Haematopoietic and Lymphoid Tissues. WHO Classification of Tumours, Revised 4th Edition. 2017;Volume 2.
3. Steensma DP. Myelodysplastic syndromes current treatment algorithm 2018. Blood Cancer J. 2018;8(5):47.
4. Montalban-Bravo G, Takahashi K, Patel K, et al. Impact of the number of mutations in survival and response outcomes to hypomethylating agents in patients with myelodysplastic syndromes or myelodysplastic/myeloproliferative neoplasms. Oncotarget. 2018;9(11):9714-9727.
5. Greenberg PL, Stone RM, Al-Kali A, et al. Myelodysplastic Syndromes, Version 2.2017, NCCN Clinical Practice Guidelines in Oncology. J Natl Compr Canc Netw. 2017;15(1):60-87.
6. Fenaux P, Ades L. How we treat lower-risk myelodysplastic syndromes. Blood. 2013; 121(21):4280-4286.
7. Stahl M, Zeidan AM. Lenalidomide use in myelodysplastic syndromes: Insights into the biologic mechanisms and clinical applications. Cancer. 2017;123(10):1703-1713.
8. Montoro J, Gallur L, Merchan B, et al. Autoimmune disorders are common in myelodysplastic syndrome patients and confer an adverse impact on outcomes. Ann Hematol. 2018;97(8):1349-1356.
9. Komrokji RS, Kulasekararaj A, Al Ali NH, et al. Autoimmune diseases and myelodysplastic syndromes. Am J Hematol. 2016; 91(5):E280-E283.
10. Young NS. Aplastic Anemia. N Engl J Med. 2018;379(17):1643-1656.
11. Olnes MJ, Sloand EM. Targeting immune dysregulation in myelodysplastic syn-

dromes. JAMA. 2011;305(8):814-819.
12. Stahl M, DeVeaux M, de Witte T, Neukirchen J, et al. The use of immunosuppressive therapy in MDS: clinical outcomes and their predictors in a large international patient cohort. Blood Adv. 2018;2(14):1765-1772.
13. Xiao L, Qi Z, Qiusheng C, et al . The use of selective immunosuppressive therapy on myelodysplastic syndromes in targeted populations results in good response rates and avoids treatment-related disease progression. Am J Hematol. 2012;87(1):26-31.
14. National Comprehensive Cancer Network. NCCN Guidelines Version 2.2019: Myelodysplastic syndromes. 2019 [cited 2018 20.12.2018]; Available from: https://www.nccn.org/store/login/login.aspx?ReturnURL=https%3a%2f%2fwww.nccn.org%2fprofessionals%2fphysician_gls%2fPDF%2fmds.pdf
15. Molldrem JJ, Caples M, Mavroudis D, et al. Antithymocyte globulin for patients with myelodysplastic syndrome. Br J Haematol. 1997;99(3):699-705.
16. Komrokji RS, Mailloux AW, Chen DT, et al. A phase II multicenter rabbit anti-thymocyte globulin trial in patients with myelodysplastic syndromes identifying a novel model for response prediction. Haematologica. 2014;99(7):1176-1183.
17. Kadia TM, Borthakur G, Garcia-Manero G, et al. Final results of the phase II study of rabbit anti-thymocyte globulin, ciclosporin, methylprednisone, and granulocyte colony-stimulating factor in patients with aplastic anaemia and myelodysplastic syndrome. Br J Haematol. 2012;157(3):312-320.
18. Passweg JR, Giagounidis AA, Simcock M, et al. Immunosuppressive therapy for patients with myelodysplastic syndrome: a prospective randomized multicenter phase III trial comparing antithymocyte globulin plus cyclosporine with best supportive care--SAKK 33/99. J Clin Oncol. 2011;29(3):303-309.
19. Sloand EM, Olnes MJ, Shenoy A, et al. Alemtuzumab treatment of intermediate-1 myelodysplasia patients is associated with sustained improvement in blood counts and cytogenetic remissions. J Clin Oncol. 2010;28(35):5166-5173.
20. Deeg HJ, Gotlib J, Beckham C, et al. Soluble TNF receptor fusion protein (etanercept) for the treatment of myelodysplastic syndrome: a pilot study. Leukemia. 2002;16(2):162-164.
21. Sauntharajah Y, Nakamura R, Wesley R, et al. A simple method to predict response to immunosuppressive therapy in patients with myelodysplastic syndrome. Blood. 2003;102(8):3025-3027.
22. Lim ZY, Killick S, Germing U, et al. Low IPSS score and bone marrow hypocellularity in MDS patients predict hematological responses to antithymocyte globulin. Leukemia. 2007;21(7):1436-1441.
23. Sloand EM, Wu CO, Greenberg P, et al. Factors affecting response and survival in patients with myelodysplasia treated with immunosuppressive therapy. J Clin Oncol. 2008;26(15):2505-2511.
24. Stroup DF, Berlin JA, Morton SC, et al. Meta-analysis of observational studies in epidemiology: a proposal for reporting. Meta-analysis Of Observational Studies in Epidemiology (MOOSE) group. JAMA. 2000;283(15):2008-2012.
25. Cheson BD, Greenberg PL, Bennett JM, et al. Clinical application and proposal for modification of the International Working Group (IWG) response criteria in myelodysplasia. Blood. 2006;108(2):419-425.
26. Downs SH, Black N. The feasibility of creating a checklist for the assessment of the methodological quality both of randomised and non-randomised studies of health care interventions. J Epidemiol Community Health. 1998;52(6):377-384.
27. Collaboration TC. The Cochrane Collaboration. Cochrane Handbook for Systematic Reviews of Interventions Version 5.1.02011. 2011.
28. Molldrem JJ, Leifer E, Bahceci E, et al. Antithymocyte globulin for treatment of the bone marrow failure associated with myelodysplastic syndromes. Ann Intern Med. 2002;137(3):156-163.
29. Yamada T, Tsurumi H, Kasahara S, et al. Immunosuppressive therapy for myelodysplastic syndrome: efficacy of methylprednisolone pulse therapy with or without cyclosporin A. J Cancer Res Clin Oncol. 2003;129(8):485-491.
30. Yazji S, Giles FJ, Tsimberidou AM, et al. Antithymocyte globulin (ATG)-based therapy in patients with myelodysplastic syndromes. Leukemia. 2003;17(11):2101-2106.
31. Deeg HJ, Jiang PY, Holmberg LA, et al. Hematologic responses of patients with MDS to antithymocyte globulin plus etanercept correlate with improved flow scores of marrow cells. Leuk Res. 2004;28(11):1177-1180.
32. Scott BL, Ramakrishnan A, Storer B, et al. Prolonged responses in patients with MDS and CMML treated with azacitidine and etanercept. Br J Haematol. 2010;148(6):944-947.
33. Steensma DP, Dispenzieri A, Moore SB, et al. Antithymocyte globulin has limited efficacy and substantial toxicity in unselected anemic patients with myelodysplastic syndrome. Blood. 2003;101(6):2156-2158.
34. Killick SB, Mufti G, Cavenagh JD, et al. A pilot study of antithymocyte globulin (ATG) in the treatment of patients with 'low-risk' myelodysplasia. Br J Haematol. 2003;120(4):679-684.
35. Stadler M, Germing U, Kliche KO, et al. A prospective, randomised, phase II study of horse antithymocyte globulin vs rabbit antithymocyte globulin as immune-modulating therapy in patients with low-risk myelodysplastic syndromes. Leukemia. 2004;18(3):460-465.
36. Broliden PA, Dahl IM, Hast R, et al. Antithymocyte globulin and cyclosporine A as combination therapy for low-risk non-sideroblastic myelodysplastic syndromes. Haematologica. 2006;91(5):667-670.
37. Garg R, Faderl S, Garcia-Manero G, et al. Phase II study of rabbit anti-thymocyte globulin, cyclosporine and granulocyte colony-stimulating factor in patients with aplastic anemia and myelodysplastic syndrome. Leukemia. 2009;23(7):1297-1302.
38. Scott BL, Ramakrishnan A, Fosdal M, et al. Anti-thymocyte globulin plus etanercept as therapy for myelodysplastic syndromes (MDS): a phase II study. Br J Haematol. 2010;149(5):706-710.
39. Platzbecker U, Haase M, Herbst R, et al. Activity of sirolimus in patients with myelodysplastic syndrome--results of a pilot study. Br J Haematol. 2005;128(5):625-630.
40. Remacha AF, Arrizabalaga B, Bueno J, et al. Treatment with mycophenolate mofetil followed by recombinant human erythropoietin in patients with low-risk myelodysplastic syndromes resistant to erythropoietin treatment. Haematologica. 2010; 95(2):339-340.
41. Ishikawa T, Tohyama K, Nakao S, et al. A prospective study of cyclosporine A treatment of patients with low-risk myelodysplastic syndrome: presence of CD55(-)CD59(-) blood cells predicts platelet response. Int J Hematol. 2007;86(2):150-157.
42. Haider M, Al Ali N, Padron E, et al. Immunosuppressive Therapy: Exploring an Underutilized Treatment Option for Myelodysplastic Syndrome. Clin Lymphoma Myeloma Leuk. 2016;16 Suppl:S44-S48.
43. Komrokji RS, Haider M, Al Ali NH, et al. Somatic Gene Mutations Serve As Molecular Biomarkers Predictive for Response to Immunosuppressive Therapy (IST) in Myelodysplastic Syndromes (MDS). Blood. 2015;126(23):1664.
44. Shallis RM, Chokr N, Stahl M, et al. Immunosuppressive therapy in myelodysplastic syndromes: a borrowed therapy in search of the right place. Expert Rev Hematol. 2018;11(9):715-726.
45. Fenaux P, Platzbecker U, Mufti GJ, et al. The Medalist Trial: Results of a Phase 3, Randomized, Double-Blind, Placebo-Controlled Study of Luspatercept to Treat Anemia in Patients with Very Low-, Low-, or Intermediate-Risk Myelodysplastic Syndromes (MDS) with Ring Sideroblasts (RS) Who Require Red Blood Cell (RBC) Transfusions. Blood. 2018;132(Suppl 1):1.
46. Platzbecker U, Germing U, Gotze KS, et al. Luspatercept for the treatment of anaemia in patients with lower-risk myelodysplastic syndromes (PACE-MDS): a multicentre, open-label phase 2 dose-finding study with long-term extension study. Lancet Oncol. 2017;18(10):1338-1347.
47. Komrokji R, Garcia-Manero G, Ades L, et al. Sotatercept with long-term extension for the treatment of anaemia in patients with lower-risk myelodysplastic syndromes: a phase 2, dose-ranging trial. Lancet Haematol. 2018;5(2):e63-e72.
48. Wang C, Yang Y, Gao S, et al. Immune dysregulation in myelodysplastic syndrome: Clinical features, pathogenesis and therapeutic strategies. Crit Rev Oncol Hematol. 2018;122:123-132.
49. Kojima S, Ohara A, Tsuchida M, et al. Risk factors for evolution of acquired aplastic anemia into myelodysplastic syndrome and acute myeloid leukemia after immunosuppressive therapy in children. Blood. 2002;100(3):786-790.
50. Santini V. Treatment of low-risk myelodysplastic syndromes. Hematology Am Soc Hematol Educ Program. 2016;2016(1):462-469.
51. Greenberg PL, Tuechler H, Schanz J, et al. Revised international prognostic scoring system for myelodysplastic syndromes. Blood. 2012;120(12):2454-2465.
52. Ogata M, Ohtsuka E, Imamura T, et al. Response to cyclosporine therapy in patients with myelodysplastic syndrome: a clinical study of 12 cases and literature review. Int J Hematol. 2004;80(1):35-42.

Ferrata Storti Foundation

Haematologica 2020
Volume 105(1):112-123

Multilayer intraclonal heterogeneity in chronic myelomonocytic leukemia

Allan Beke,[1,2,*] Lucie Laplane,[1,3,*] Julie Riviere,[1] Qin Yang,[4] Miguel Torres-Martin,[4] Thibault Dayris,[5] Philippe Rameau,[5] Veronique Saada,[6] Chrystèle Bilhou-Nabera,[7] Ana Hurtado,[8] Larissa Lordier,[1,5] William Vainchenker,[1] Maria E. Figueroa,[4,9] Nathalie Droin[1,2] and Eric Solary[1,2,10]

[1]INSERM U1170, Gustave Roussy Cancer Center, Villejuif, France; [2]Université Paris-Sud, Faculté de Médecine, Le Kremlin-Bicêtre, France; [3]CNRS UMR8590, IHPST, Université Paris 1 Panthéon-Sorbonne, Paris, France; [4]Human Genetics, University of Miami Miller School of Medicine, Miami, FL, USA; [5]CNRS 3655 & INSERM US23, AMMICa, Gustave Roussy Cancer Center, Villejuif, France; [6]Department of Biopathology, Gustave Roussy Cancer Center, Villejuif, France; [7]Service d'Hématologie Biologique, Hôpital Saint-Antoine, Paris, France; [8]Hematology and Medical Oncology Department, Hospital Morales Meseguer, IMIB, Murcia, Spain; [9]Sylvester Comprehensive Cancer Center, University of Miami Miller School of Medicine, Miami, FL, USA and [10]Department of Hematology, Gustave Roussy Cancer Center, Villejuif, France

**AB and LL contributed equally to this study*

ABSTRACT

The functional diversity of cells that compose myeloid malignancies, i.e., the respective roles of genetic and epigenetic heterogeneity in this diversity, remains poorly understood. This question is addressed in chronic myelomonocytic leukemia, a myeloid neoplasm in which clinical diversity contrasts with limited genetic heterogeneity. To generate induced pluripotent stem cell clones, we reprogrammed CD34$^+$ cells collected from a patient with a chronic myelomonocytic leukemia in which whole exome sequencing of peripheral blood monocyte DNA had identified 12 gene mutations, including a mutation in *KDM6A* and two heterozygous mutations in *TET2* in the founding clone and a secondary *KRAS*(G12D) mutation. CD34$^+$ cells from an age-matched healthy donor were also reprogrammed. We captured a part of the genetic heterogeneity observed in the patient, i.e. we analyzed five clones with two genetic backgrounds, without and with the *KRAS*(G12D) mutation. Hematopoietic differentiation of these clones recapitulated the main features of the patient's disease, including overproduction of granulomonocytes and dysmegakaryopoiesis. These analyses also disclosed significant discrepancies in the behavior of hematopoietic cells derived from induced pluripotent stem cell clones with similar genetic background, correlating with limited epigenetic changes. These analyses suggest that, beyond the coding mutations, several levels of intraclonal heterogeneity may participate in the yet unexplained clinical heterogeneity of the disease.

Correspondence:

ERIC SOLARY
eric.solary@gustaveroussy.fr

Received: October 4, 2018.

Accepted: April 30, 2019.

Pre-published: May 2, 2019.

doi:10.3324/haematol.2018.208488

Check the online version for the most updated information on this article, online supplements, and information on authorship & disclosures: www.haematologica.org/content/105/1/112

Introduction

Intratumoral heterogeneity is a major tenet of cancer biology. A tumor clone emerges from a single cell that has acquired one or several somatic mutations. Additional driver events that occur in individual daughter cells generate tumor subclones, each being endowed with specific functional properties and fitness.[1] This intraclonal genetic heterogeneity may not explain all the functional heterogeneity among individual cells within a tumor clone. Epigenetic variation also contributes to the heterogeneity of cells that form a tumor.[2,3]

Chronic myelomonocytic leukemia (CMML) is a neoplastic disease whose limited genetic heterogeneity contrasts with its clinical diversity.[4] CMML is defined by a persistent clonal monocytosis, with or without dysplasia.[5] The mutational landscape contains a small number of somatic mutations in DNA methylation, histone

modifier, splicing factor and signaling genes.[6] Mapping of CMML clonal architecture identified early clonal dominance, intratumor heterogeneity in the hematopoietic stem and progenitor cell compartment in which mutations accumulate mostly linearly, and growth advantage to the most mutated cells.[7] Hypomethylating agents, which are commonly used in severe dysplastic forms of the disease, can restore a balanced hematopoiesis.[8] The response to these drugs, which correlates with DNA demethylation, can occur in the absence of any decrease in mutation allele burden measured in circulating monocytes,[6] arguing for a role of epigenetic alterations in disease expression and outcome.[9]

One of the main limitations in studying CMML pathophysiology is the lack of appropriate models, either patient-derived cell lines or genetically modified animals, which faithfully reproduce disease features. Currently, the best available CMML preclinical model is xenotransplantation of CMML cells in immunocompromised mice, especially those with transgenic expression of human cytokines including granulocyte-macrophage colony-stimulating factor.[10,11] The modeling of myeloid malignancies by generating patient-derived induced pluripotent stem cells (iPSC) recently appeared as another opportunity to model these diseases and, although challenging, capture their genetic heterogeneity.[12–15] In CMML, we previously demonstrated that intraclonal heterogeneity was rarely detected in mature cells of the clone as a consequence of a growth advantage to most mutated cells with differentiation but was preserved in stem and progenitor cells.[6,7] Therefore, we sorted CD34$^+$ cells from a CMML patient and reprogrammed these cells to capture some intraclonal genetic heterogeneity and characterize hematopoiesis derived from genetically close but distinct iPSC.

Methods

Generation, characterization and maintenance of induced pluripotent stem cells

CD34$^+$ cells collected from a healthy donor and a CMML patient, with informed consent and approval of the Ethics Committee (DC-2014-209), were infected with non-integrated Sendai virus encoding Klf4, Oct4, Sox2 and c-Myc to generate iPSC. An additional iPSC (Co6) was kindly provided by Dr Weiss.[16] iPSC were passaged once a week to yield a cell suspension of small colonies (3-10 cells). Intracellular and extracellular pluripotency markers were detected by flow cytometry and teratoma formation was evaluated by intramuscular injection of iPSC into *NOD/SCID/IL2rγ*$^{-/-}$ mice. Karyotyping and comparative genomic hybridization were performed. The procedures are detailed in the *Online Supplementary Material*.

Hematopoietic cell differentiation

A two-dimensional monolayer system was used to differentiate iPSC into CD34$^+$CD43$^+$ hematopoietic progenitor cells (HPC). Clonogenic assays were performed by mixing HPC in serum-free medium with MethoCult H4434 classic (Stem Cell Technologies, Grenoble, France) before plating the cell suspension in 35-mm dishes. Colonies were scored after 14 days and analyzed on a BD LSRFortessa X-20. HPC mixed with serum-free fibrin clots were seeded for 10 days in the presence of thrombopoietin and stem cell factor before measuring colony-forming unit-megakaryocyte (CFU-Mk) colonies. HPC were also suspended in serum-free liquid medium with growth factors for 10 days before flow analysis of cell surface markers and May-Grünwald-Giemsa staining of cytospins. More details are provided in the *Online Supplementary Material*.

Flow cytometry and cell sorting

The antibodies used are listed in *Online Supplementary Table S1*. Cells were analyzed using a BD LSRFortessa™ X-20 and Kaluza analysis software. HPC, monocytes and megakaryocytes were sorted on a BD Influx™ Cell sorter. Details are provided in the *Online Supplementary Material*.

Whole exome sequencing

We collected genomic DNA from sorted monocytes and CD3$^+$ T cells and iPSC to perform whole exome sequencing. Raw reads were aligned to the reference human genome hg19 (Genome Reference Consortium GRCh37) using BWA 0.5.9 (Burrows–Wheeler Aligner) backtrack algorithm with default parameters. A mutation was reported as present if the variant allele frequency was ≥4%. More details are provided in the *Online Supplementary Material*.

Genome-wide DNA methylation detected by enhanced reduced representation bisulfite sequencing

High-molecular weight DNA was sequenced on a HiSeq3000 Illumina sequencer and 50 bp reads were aligned against a bisulfite-converted human genome (hg19). Differentially methylated regions (DMR) identified an absolute methylation difference ≥40% with a false discovery rate <5% and were annotated using the ChIPenrich R package,[17] which was also used for gene ontology and pathway analysis. For correspondence analysis and hierarchical clustering, tiles with the highest standard deviation (SD >0.03) were used. More details are provided in the *Online Supplementary Material*.

Statistical analysis

Statistical analysis was performed with GraphPad Prism software, using an unpaired *t* test and Mann-Whitney test, depending on distribution, similarity of variance, and sample number. The Kruskal-Wallis test was used for multiple comparisons.

Data availability

Accession numbers for enhanced reduced representation bisulfite sequencing, whole exome sequencing and RNA sequencing data are GSE114115, E-MTAB-7917 and E-MTAB-7850, respectively.

Results

Reprogramming of CD34$^+$ cells from a patient with chronic monomyelocytic leukemia captures a part of the disease's genetic heterogeneity

We reprogrammed CD34$^+$ cells collected from a CMML patient whose monocyte DNA whole exome sequencing had identified 12 mutations, including two mutations in *TET2* (S1691fs and R1516X) and heterozygous mutations in *KRAS*(G12D) and *KDM6A*(R61X). The clinical and biological features of the patient's disease are depicted in the *Online Supplementary Material.* Reprogramming of CD34$^+$ cells collected from an age-matched healthy donor generated control clones (Figure 1A, B). We selected nine clones (5 from the patient; 4 from the healthy donor) demonstrating pluripotency features, including morphology (*Online Supplementary Figure S1A*), expression of markers (*Online Supplementary Figure S1B*) and formation of teratomas in

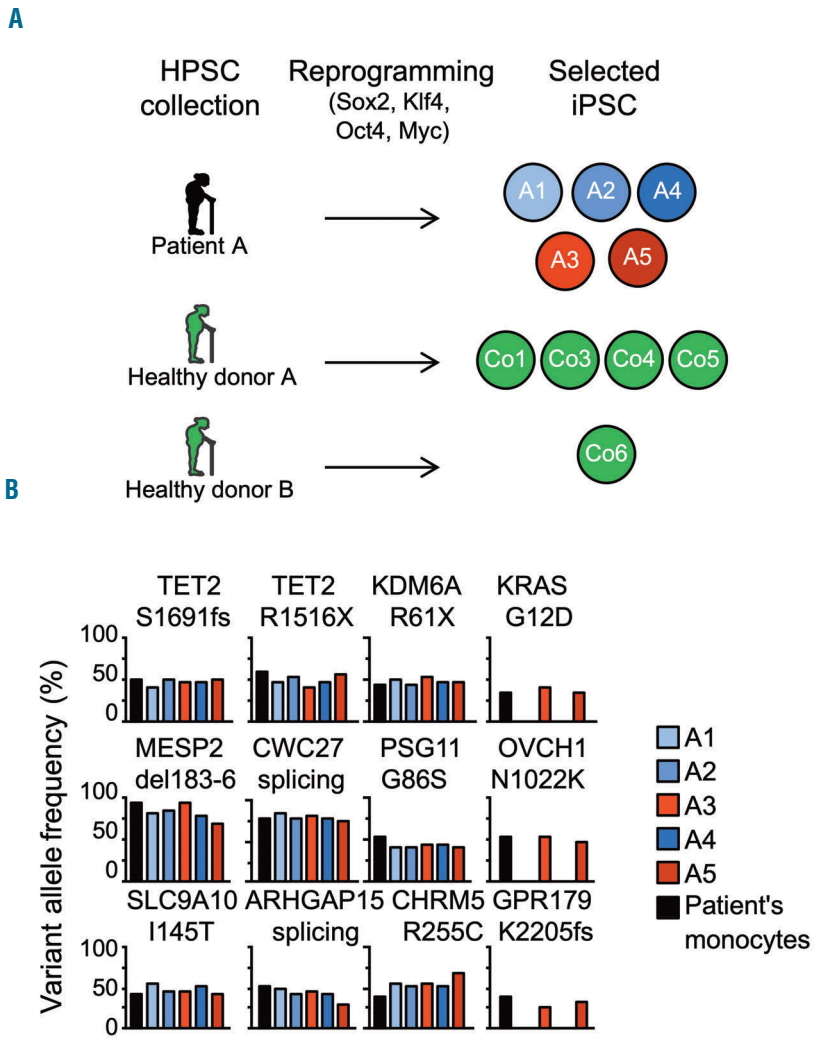

Figure 1. Generation and genetic characterization of chronic myelomonocytic leukemia- and control-induced pluripotent stem cells. (A) CD34$^+$ cells from a patient with chronic myelomonocytic leukemia and an age-matched healthy donor were reprogrammed through infection with Sendai virus encoding the transcription factors Sox2, Klf4, Oct4, and c-Myc (SKOM) before characterization and selection of indicated induced-pluripotent stem clones (iPSC). An additional control iPSC (Co6) was kindly provided by Dr. Weiss. (B) Whole exome sequencing of DNA collected from sorted peripheral blood monocytes (in black) and from five iPSC selected from patient A (each color indicates a specific clone), showing the detection of two genotypes with nine and 12 somatic variants, respectively.

immunodeficient mice (*Online Supplementary Figure S1C*), without reprogramming-induced cytogenetic abnormalities (*Online Supplementary Figure S1D*). We also used an additional, independently generated control clone (Figure 1A).[16] Whole exome sequencing and Sanger sequencing of patient-derived iPSC indicated that we had captured a part of the genetic heterogeneity of her leukemic clone, i.e., three clones (A1, A2, A4) recapitulated the founding clone while the other two (A3, A5) were reprogrammed from a *KRAS*(G12D) subclone (Figure 1A, B and *Online Supplementary Figure S1E*). In contrast with other studies,[18] we did not reprogram any wildtype CD34$^+$ cells, probably due to the early clonal dominance that characterizes CMML clonal architecture, with very few residual wildtype cells in the stem cell compartment.[7]

Hematopoietic cells derived from chronic myelomonocytic leukemia induced pluripotent stem cells recapitulate the disease features

iPSC were induced to differentiate into CD34$^+$CD43$^+$ hematopoietic progenitors (*Online Supplementary Figure S2A*), which were plated for 10 days in methylcellulose in the presence of stem cell factor, interleukin-3, erythropoietin, and granulocyte-macrophage colony-stimulating factor (Figure 2A). The total numbers of colonies generated by healthy donor- and CMML iPSC-derived hematopoietic progenitors were similar (Figure 2B and *Online Supplementary Figure S3A*). The fraction of clusters (colonies <50 cells) generated by *KRAS* wildtype CMML iPSC was significantly higher than that generated by *KRAS*(G12D)-mutated CMML iPSC and control clones (Figure 2C and *Online Supplementary Figure S3B, C*). *KRAS*(G12D) clones produced larger granulocyte-macrophage (CFU-GM) and macrophage (CFU-M) colonies (Figure 2D) as well as a higher proportion of CFU-M colonies (Figure 2E). Compared to control clones, CMML-derived clones generated fewer granulocytic and multipotent progenitor colonies (Figure 2E, F and *Online Supplementary Figure S3D*) and more granulocyte-macrophage colonies (Figure 2E) whereas the proportions of erythroid colonies were not significantly different (Figure 2F and *Online Supplementary Figure S3D*). Colonies derived from CMML iPSC also demonstrated an increased fraction of CD14$^+$ cells (Figure 2G) at the expense of CD33$^+$, CD123$^+$, CD235a$^+$ or CD41$^+$ populations (*Online Supplementary Figure S3E*, summary in Figure 2H).

Cells that formed CFU-M generated by CMML iPSC did not show the typical, fibroblast-like shape of macrophages generated by healthy donor-derived iPSC (Figure 3A, B) and expressed less CD16 and CD163 than

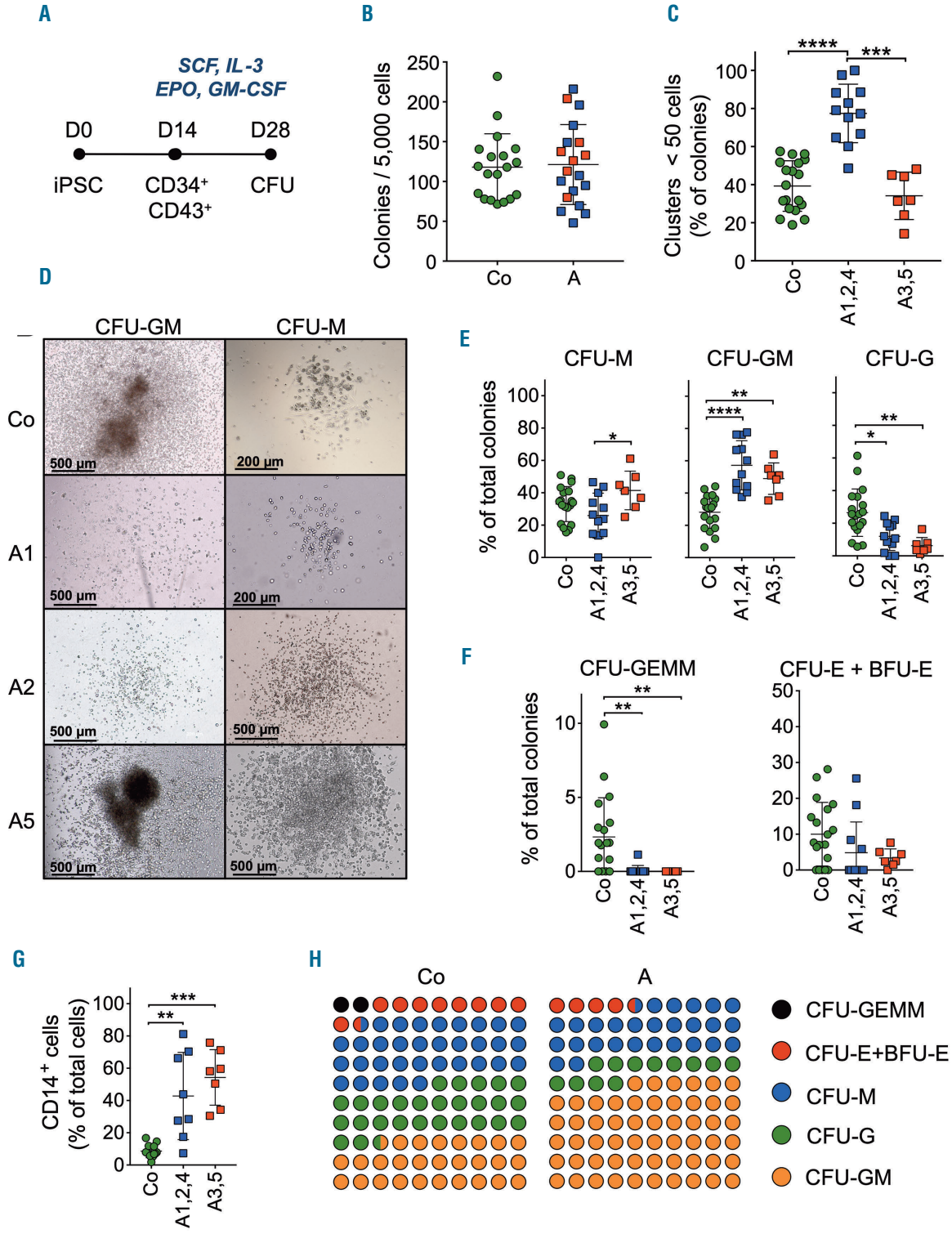

Figure 2. Hematopoietic cells derived from chronic myelomonocytic leukemia induced pluripotent stem cells are biased toward the monocytic lineage. (A) $CD34^+CD43^+$ hematopoietic stem cells derived from control and chronic myelomonocytic leukemia (CMML) induced pluripotent stem cells (iPSC) were sorted and plated for 14 days in methylcellulose in the presence of 50 ng/mL stem cell factor (SCF), 10 ng/mL interleukin-3 (IL-3), 1 U/mL erythropoietin (EPO), and 10 ng/mL granulocyte-macrophage colony-stimulating factor (GM-CSF) before analyzing the generated colonies (CFU). (B) Total number of colonies generated by plating 5,000 cells in methylcellulose for 14 days. Co and A represent the five control and five patient's clones respectively. (C) Fraction of clusters, as defined by colonies <50 cells, among total colonies, separating results obtained with *KRAS*v-wildtype (A1, A2, A4) and *KRAS*-mutated (A3, A5) iPSC; Kruskal-Wallis test. (D) Representative colony-forming unit – granulocyte-macrophage (CFU-GM) and colony-forming unit – macrophage (CFU-M) generated by the indicated clones and visualized by light microscopy. Scale bars indicate magnification. (E) Fractions of CFU-M, CFU-GM and colony-forming unit – granulocyte (CFU-G) among colonies; Kruskal-Wallis test. (F) Fractions of erythroid colonies (CFU-E: colony-forming unit - erythroid; BFU-E: burst-forming unit - erythroid) and CFU-GEMM (colony-forming unit - granulocyte-erythroid-monocyte-megakaryocyte) among colonies; Kruskal-Wallis test. (G) Flow cytometry analysis of $CD14^+$ cells in colonies generated by the indicated clones in methylcellulose; Kruskal-Wallis test. (H) Summary of the colonies generated by hematopoietic progenitors derived from five healthy donor and five CMML patient's iPSC. (B, C, E-G) Green dots, control iPSC; blue squares, *KRAS* wildtype CMML-iPSC; red squares, *KRAS*(G12D) CMML iPSC; bars, mean ± standard deviation. **P*<0.05; ***P*<0.01; ****P*<0,001 *****P*<0.0001.

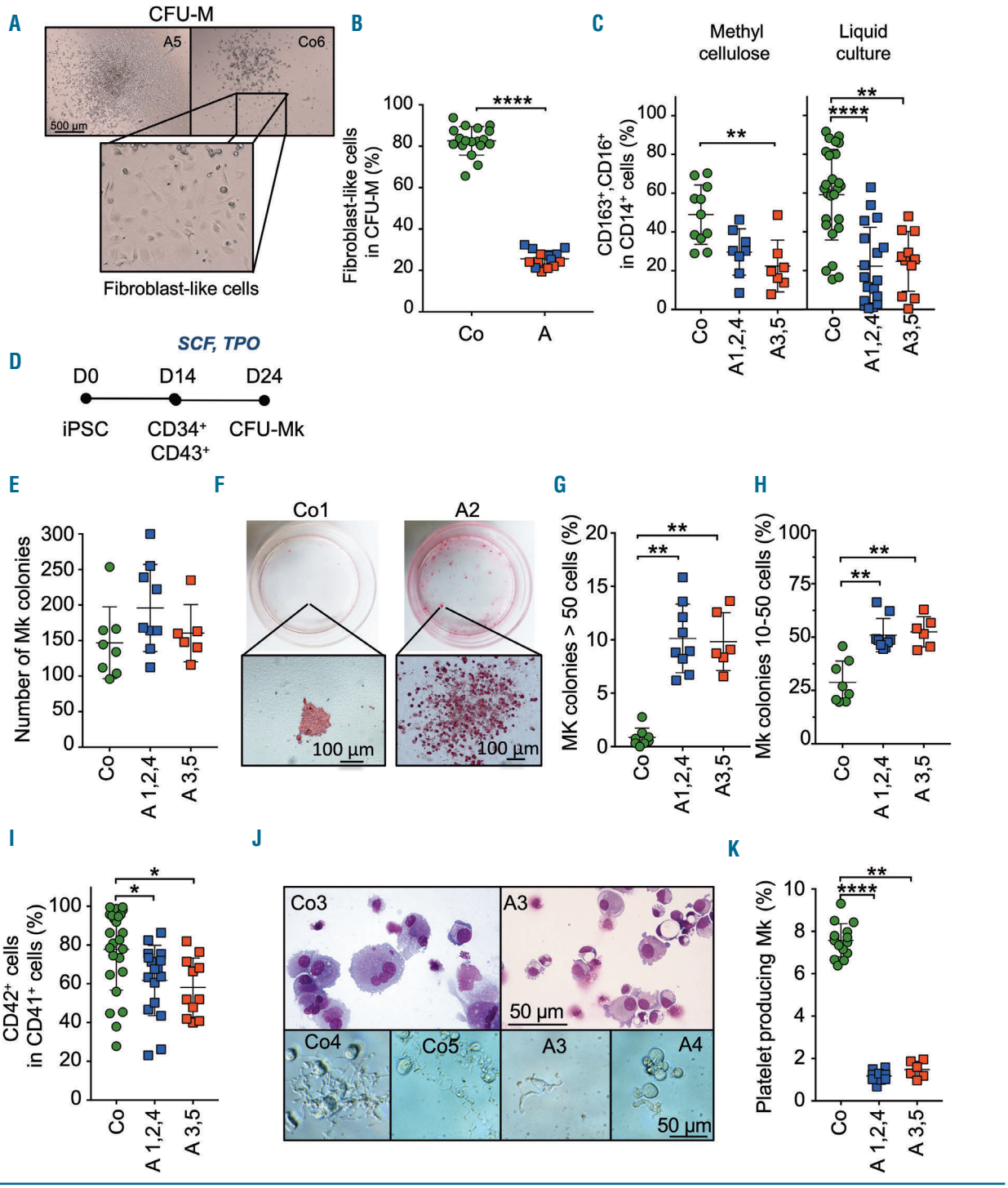

Figure 3. Defective maturation of chronic myelomonocytic leukemia induced pluripotent stem cell-derived hematopoietic cells into macrophages and platelet-forming megakaryocytes. (A) Representative morphology of colony-forming unit – macrophage (CFU-M) generated by hematopoietic cells derived from control (Co6) and chronic myelomonocytic leukemia (CMML) (clone A5) induced pluripotent stem cells (iPSC) cultured in methylcellulose as described in Figure 2A. Light microscopy visualization; scale bar indicates magnification. The rectangle is a zoom on the fibroblast-like shape of macrophages in the Co6 culture, which was not observed in A5 colonies. (B) Fraction of cells with a fibroblast-like shape in CFU-M generated from hematopoietic cells derived from four control and five CMML iPSC; unpaired *t* test. (C) Flow cytometry analysis of cells expressing both CD16 and CD163 in CD14$^+$ cells collected from colonies generated by the five control iPSC- and the five CMML iPSC-derived hematopoietic cells plated in methylcellulose or in liquid medium, Kruskal-Wallis test. (D) Control iPSC and CMML iPSC-derived CD34$^+$CD43$^+$ hematopoietic cells were sorted and plated in coagulum for 10 days in the presence of 50 ng/mL stem cell factor (SCF) and 10 ng/mL thrombopoietin (TPO) to generate colony-forming unit - megakaryocyte (CFU-Mk). (E) Total number of colonies generated by plating 1,500 hematopoietic cells derived from the indicated iPSC. (F) Representative experiments showing the differential morphology of CFU-Mk generated by plating healthy donor (Co1 clone) or CMML (A2 clone) iPSC-derived hematopoietic cells (scale bar, 100 µm). (G) Fractions of large colonies, >50 cells, among the total number of colonies shown in panel E; Kruskal-Wallis test. (H) Fractions of intermediate colonies, 10-50 cells, among the total number of colonies shown in panel E; Kruskal-Wallis test. (I) Fractions of CD41$^+$ megakaryocytes generated in liquid culture with all cytokines for 10 days and expressing the cell surface marker CD42, as detected by flow cytometry; Kruskal-Wallis test. (J) Upper panels show May-Grünwald-Giemsa-stained cytospins of CD41$^+$ cells generated in liquid culture, 5 days after cell sorting, with a normal (Co3) or dysplastic (A3) morphology. Lower panels: representative images of platelet-producing megakaryocytes generated by hematopoietic cells derived from indicated clones; scale bars, 50 µm. (K) Fractions of platelet-producing megakaryocytes in CD41$^+$ cells sorted from liquid culture of CD34$^+$CD43$^+$ cells with all cytokines for 10 days, then cultured for 6 days with SCF and TPO; Kruskal-Wallis test. Mk: megakaryocytes. Colors as in Figure 1. Bars: mean ± standard deviation. *P<0.05; **P<0.01; ****P<0.0001.

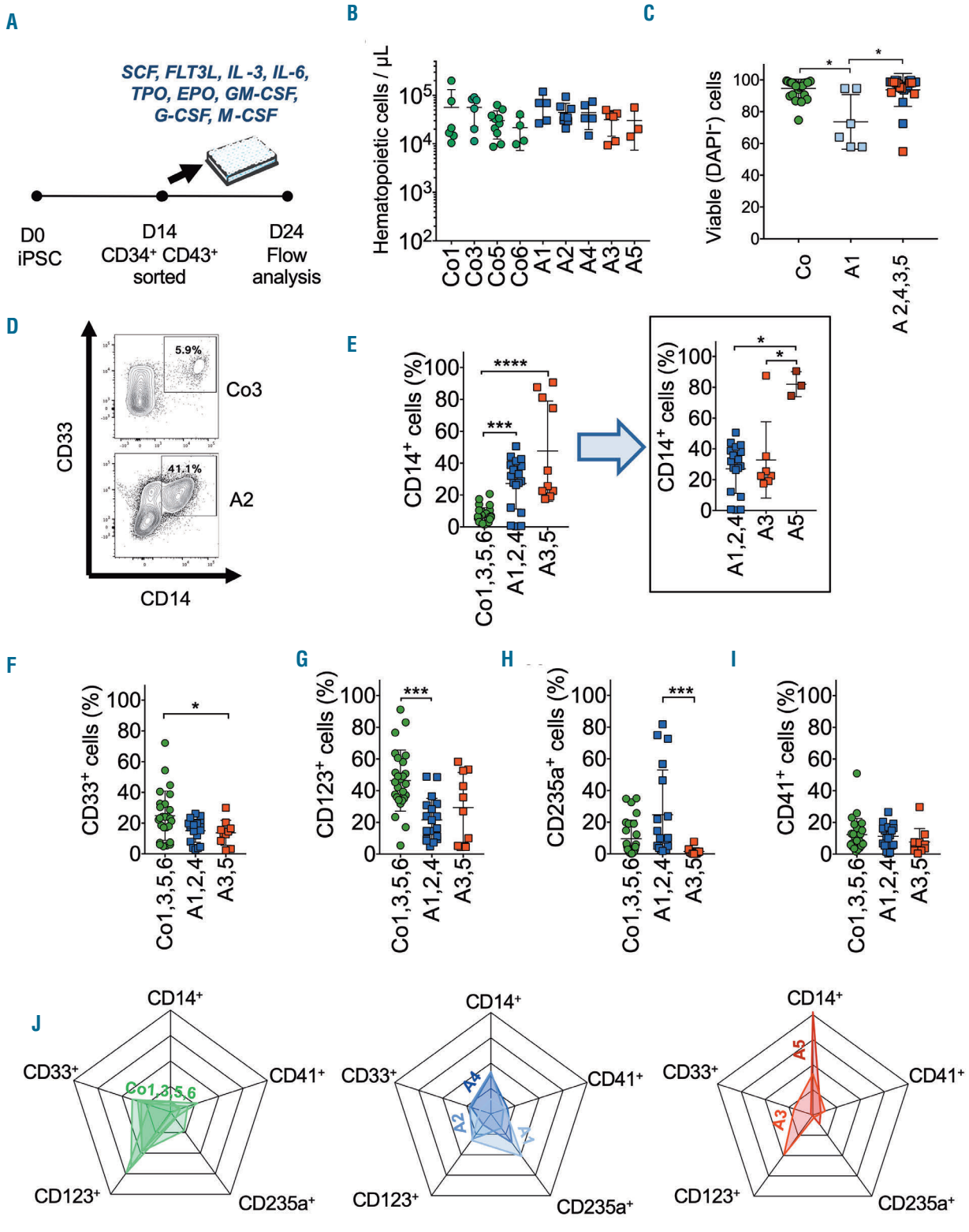

Figure 4. Functional heterogeneity of the patient's induced pluripotent stem cell-derived hematopoietic cells. (A) Control and chronic myelomonocytic leukemia (CMML) induced pluripotent stem cell (iPSC)-derived CD34$^+$CD43$^+$ cells were cultured in liquid medium for 10 days in the presence of 50 ng/mL stem cell factor (SCF), 10 ng/mL Fms-like tyrosine kinase 3 ligand (FLT3L), 10 ng/mL interleukin-3 (IL-3), 10 ng/mL interleukin-6 (IL-6), 50 ng/mL thrombopoietin (TPO), 1 U/mL erythropoietin (EPO), 10 ng/mL granulocyte-macrophage colony-stimulating factor (GM-CSF), 10 ng/mL granulocyte colony-stimulating factor (G-CSF), and 10 ng/mL monocyte colony-stimulating factor (M-CSF). (B) Total number of hematopoietic cells generated by 5,000 CD34$^+$CD43$^+$ cells cultured in liquid medium for 10 days. (C). Fractions of viable, DAPI-negative cells measured on day 10; Kruskal-Wallis test. (D) Representative flow cytometry analysis of CD33$^+$CD14$^+$ cells generated in liquid culture by the Co3 and A2 clones. (E-I) Fractions of CD33$^+$CD14$^+$ cells (E and insert), CD33$^+$CD14$^-$CD41$^-$ cells (F), CD123$^+$CD33$^-$CD235a$^-$CD14$^-$CD41$^-$ cells (G), CD235a$^+$CD14$^-$CD41$^-$ cells (H), and CD41$^+$CD14$^-$ cells (I) generated in liquid culture by the indicated clones; Kruskal-Wallis test. (J) Radar representation of the differentiation potential of CD34$^+$CD43$^+$ hematopoietic cells derived from control iPSC (green), *KRAS* wildtype CMML iPSC (blue) and *KRAS*(G12D) CMML iPSC (red). Bars: mean ± standard deviation. *P<0.05; ***P<0,001 ****P<0.0001

those from control iPSC-derived CFU-M (Figure 3C). A similar defect in the generation of CD14$^+$ cells expressing both CD16 and CD163 was detected when iPSC-derived hematopoietic cells were induced to differentiate in liquid culture (Figure 3C).

Since the patient demonstrated megakaryocytic hyperplasia and dysplasia, we performed coagulum assays in the presence of stem cell factor and thrombopoietin to analyze the generation of megakaryocytes and platelets (Figure 3D). All iPSC generated a similar number of colonies (Figure 3E) but those generated by CMML iPSC were much larger (Figure 3F-H). We observed a decrease in the fraction of CD42$^+$ cells among CD41$^+$ cells (Figure 3I) and the fraction of CMML iPSC-derived megakaryocytes that produced platelets was decreased (Figure 3J, K).

CD34$^+$CD43$^+$ cells generated from iPSC were also cultured in liquid medium in the presence of stem cell factor, interleukin-3, interleukin-6, erythropoietin, granulocyte-macrophage colony-stimulating factor, thrombopoietin, Fms-like tyrosine kinase 3 ligand, granulocyte colony-stimulating factor and monocyte colony-stimulating factor for 10 days (Figure 4A). The quantity of cells generated by each clone and the number of viable cells after 10 days were not significantly different, except for clone A1 that demonstrated more dead cells (Figure 4B, C). Multiparameter flow cytometry analysis was used to measure each cell population obtained in culture (*Online Supplementary Figure S2B*). CMML iPSC generated a majority (~40%) of CD14$^+$ cells (Figure 4D, E). Although they both had a *KRAS*(G12D) mutation, the A5 clone generated more CD14$^+$ cells (~80%) than the A3 clone. In fact, monocyte production by the A3 clone was not significantly different from that of *KRAS* wildtype clones (Figure 4E, insert). Compared to control clones, *KRAS*(G12D) CMML iPSC generated fewer CD33$^+$, CD14$^-$, CD41$^-$, CD235a$^-$ cells (Figure 4F) and *KRAS* wildtype CMML clones generated fewer CD123$^+$, CD14$^-$, CD41$^-$, CD235a$^-$ cells (Figure 4G). The generation of CD235a$^+$ erythroid cells was more heterogeneous and higher in *KRAS* wildtype compared to *KRAS*(G12D) CMML clones (Figure 4H). The generation of CD41$^+$ cells was not significantly different between control and patient-derived iPSC (Figure 4I). These liquid cultures also revealed the defective differentiation of monocytes into macrophages (Figure 3C) and the defective generation of platelets (Figure 3D).

As expected, patient-derived clones showed a bias in their differentiation towards monocyte production. However, hematopoietic differentiation of CMML iPSC also demonstrated significant intraclonal heterogeneity that could not be explained by the sole genetic alterations detected in coding regions. The A1, A2 and A4 clones, which have the same mutations in coding regions, showed heterogeneous differentiation into CD235a$^+$ and CD14$^+$ cells whereas A3 and A5, which are *KRAS*-mutated clones, showed a marked difference in their monocytic differentiation in liquid culture. A summary of this clonal heterogeneity is shown in Figure 4J.

While the viability of cells generated by control iPSC was high in all but one experiment, the viability of CMML iPSC, especially *KRAS* wildtype CMML iPSC, was much more heterogeneous than that of control clones, suggesting a higher sensitivity to small variations in culture conditions (Figure 5A). Of note, the number of generated cells (indicated by the diameter of the circles in Figure 5A) could remain high in cultures in which the cell death rate was elevated. In contrast, a decrease in cell viability was associated with an increase in the fraction of CD235a$^+$ cells and a decrease in the fraction of CD14$^+$ cells generated by *KRAS* wildtype CMML iPSC (Figure 5A). By eliminating this culture condition-related variability in cell production, using a cut-off of 90% viability, we observed a much more robust trend in the differentiation of A1, A2 and A4 clones (*Online Supplementary Figure S4*). In contrast, even with this cut-off on viability, the A5 clone consistently produced more CD14$^+$ cells than the A3 clone (Figure 5B).

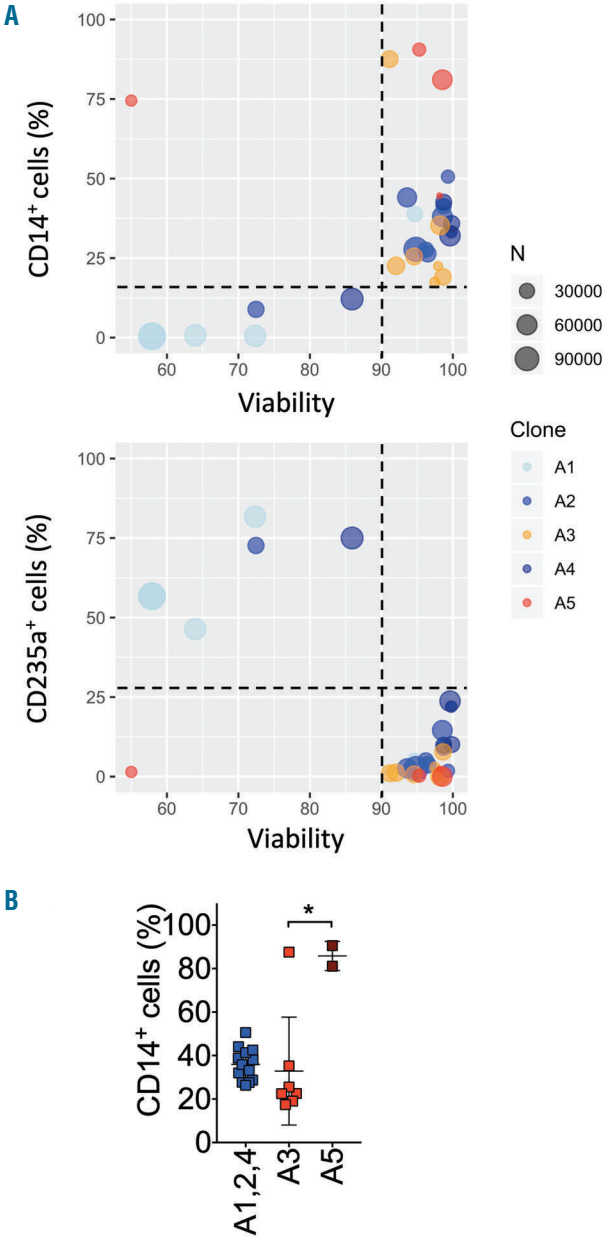

Figure 5. Impact of viability on differentiation pattern analysis. (A) Percentages of DAPI-negative viable cells (x axis) and numbers of hematopoietic cells generated (dots size) are plotted against the fraction of CD14$^+$ and CD235a$^+$ cells generated in liquid culture. The vertical hatched line is an arbitrary cut-off value established at 90% viable cells; the horizontal hatched line emphasizes the discrepancies between samples with <90% viable cells and the others. (B) Fractions of CD33$^+$CD14$^+$ cells for the indicated clones after removing experiments in which cell viability was below 90%; Kruskal-Wallis test. *P<0.05.

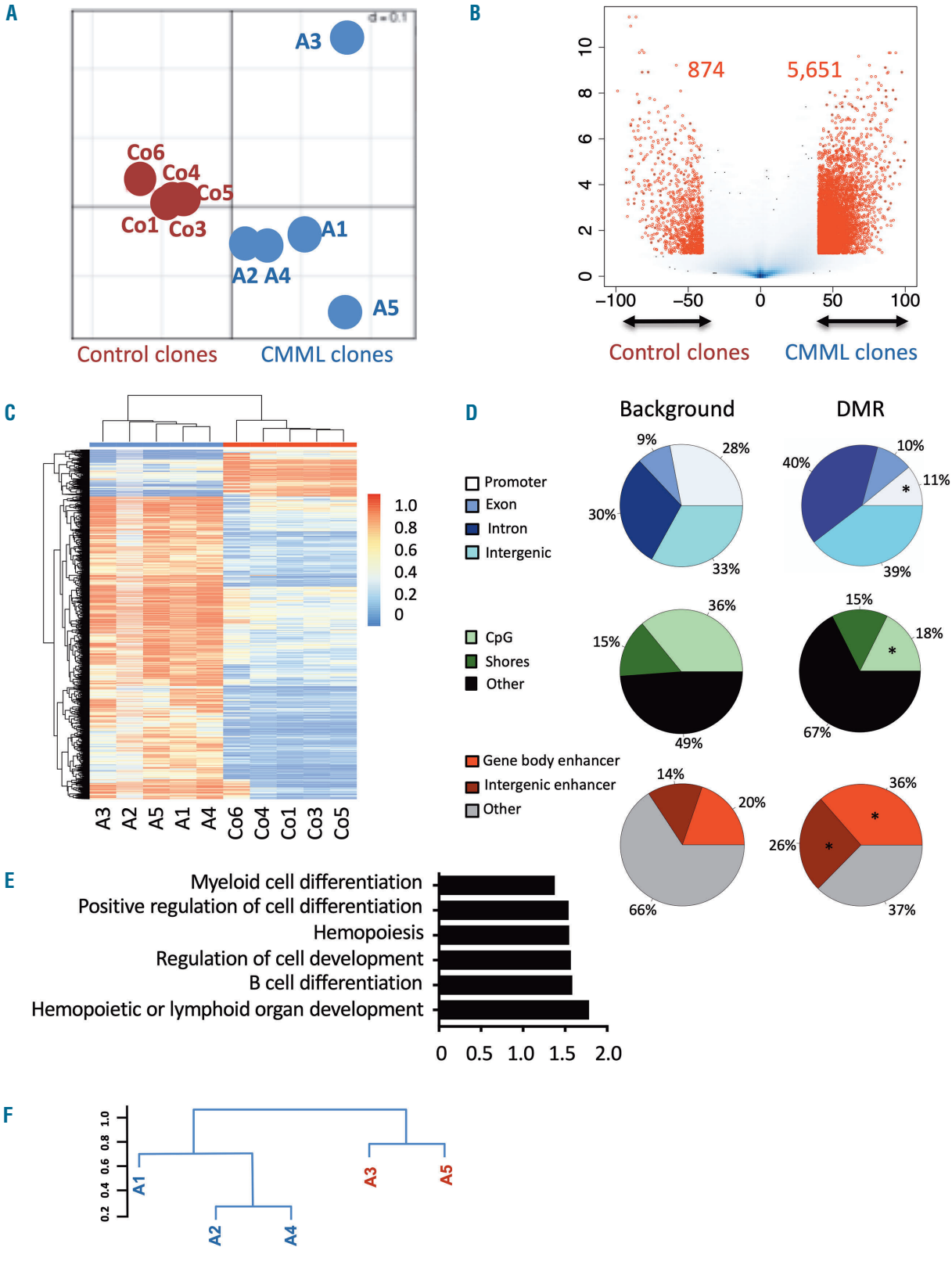

Figure 6. Methylation profile recapitulates features related to the biology of the chronic myelomonocytic leukemia clones. (A) Unsupervised clustering by correspondence analysis showing a clear separation between control, 'Co', and chronic myelomonocytic leukemia (CMML) clones 'A', using tiles with a standard deviation (SD)>0.03. (B) Supervised analysis (β binomial model) displayed a clear trend toward hypermethylation in CMML clones compared to Co clones. Arrows, percentage of methylation required to be considered as a differentially methylated region (DMR). Red dots, tiles that fulfill the criteria [absolute methylation difference ≥40% and false discovery rate (FDR) <5%]. (C) Heatmap of DMR based on the Euclidean distance matrix. Red, hypomethylation; blue, hypermethylation; gray, DMR that were not covered by enhanced reduced representation bisulfite sequencing in a specific tile. (D) Annotation to genomic regions of background of all tiles (left) and DMR (right). Asterisk, significance according to the binomial test (P<0.001). (E) Gene ontology of DMR methylated on CMML clones. Bar chart: processes related to hematopoiesis with a FDR <0.1. X-axis, -$\log_{10}$ of the FDR. (F) Hierarchical cluster of methylation tiles with the highest SD (SD>0.03). Y-axis, distance metric obtained from the Euclidean distance matrix.

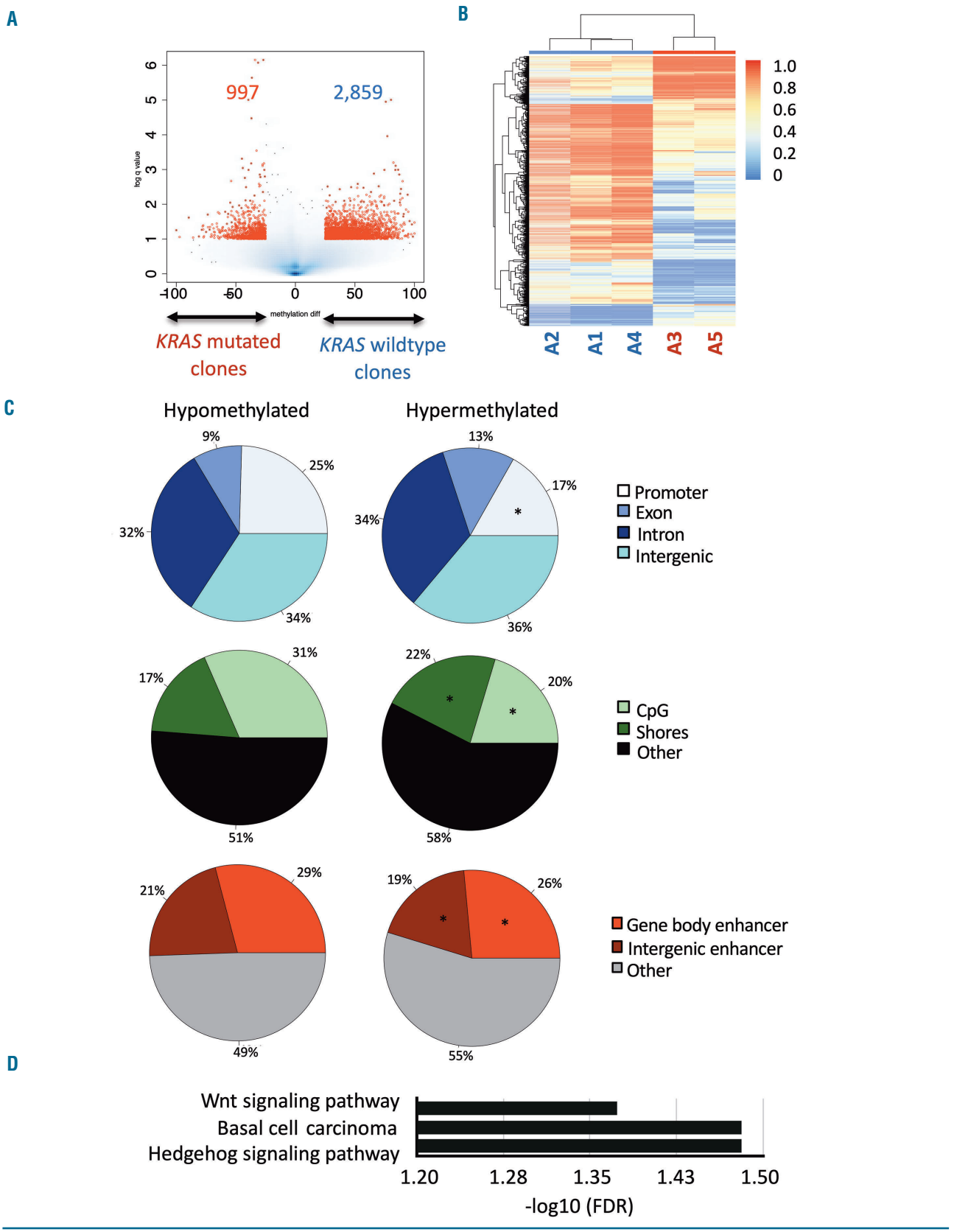

Figure 7. Differential methylation profile of *KRAS*-wildtype and *KRAS*-mutated chronic myelomonocytic leukemia clones. (A) Hypermethylated regions detected by enhanced reduced representation bisulfite sequencing in *KRAS* wildtype (A1, A2, A4) compared to *KRAS* mutated (A3, A5) chronic myelomonocytic leukemia (CMML)-derived induced pluripotent stem cells (iPSC). Arrows, percentage of methylation required to be considered as a differentially methylated region (DMR). Red dots, tiles that fulfill the criteria [absolute methylation difference ≥40% and false discovery rate (FDR) <5%]. (B) Heatmap of DMR based on the Euclidean distance matrix. Red, hypomethylation; blue, hypermethylation; (C) Repartition of DMR that are hypo- or hyper-methylated in *KRAS* wildtype compared to *KRAS*(G12D) clones. Asterisk, significance according to the binomial test (P<0.001). (D) Gene ontology of DMR methylated on *KRAS*(G12D) clones. Bar chart: processes related to hematopoiesis with a FDR <0.1. X-axis, -$\log_{10}$ of the FDR.

Epigenetic heterogeneity among induced pluripotent stem cell clones from the patient with chronic myelomonocytic leukemia

Epigenetic intraclonal heterogeneity has been reported in hematologic malignancies[2,19] as well as in solid tumors,[20] and co-dependency between epigenetic and genetic evolution has been questioned, e.g., in large B-cell lymphoma[21] and acute myeloid leukemia.[3] We performed DNA methylation analysis on $CD34^+CD43^+$ cells generated from iPSC to investigate their epigenetic state. Unsupervised analysis by correspondence analysis separated control- from CMML-derived cells. The latter showed a much greater diversity (Figure 6A). We then used a β binomial model implemented in methylSig[22] to perform a supervised analysis of differentially methylated regions (DMR). We identified 5,651 hypermethylated DMR in CMML-derived cells compared to controls. In contrast, only 874 DMR were identified as more methylated in control iPSC-derived cells (Figure 6B, C). Genomic annotation revealed that, in CMML samples, DMR were depleted at promoter regions and CpG islands while being enriched at gene body and intergenic enhancers (P<0.001 in all cases) (Figure 6D). DMR detected at CpG islands, gene body enhancers and intergenic enhancers were significantly more often hypermethylated regions (P<0.001) (*Online Supplementary Figure S5A*). In accordance with changes in DNA methylation affecting enhancers, we observed significant enrichment of DMR within enhancers[23] compared to background (36.8% at total DMR *vs*. 15.2% background, P-value $<2.2\times10^{-16}$). Motif enrichment analysis suggested that the main sequences targeted by DMR were motifs recognized by transcription factors of the ETS family (*Online Supplementary Figure S5B*). Gene ontology analysis of biological processes of DMR hypermethylated in CMML-derived cells showed enrichment of differentiation and hematopoietic development categories (Figure 6E), suggesting that DNA methylation differences between CMML- and control-derived cells may capture an epigenetic memory related to the biology of the disease, still present after having been reprogrammed. Finally, focusing on CMML iPSC-derived hematopoietic cells, unsupervised hierarchical clustering based on their DNA methylation profiles revealed high concordance with their phylogenetic background (Figure 6F).

In order to correlate changes in DNA methylation with those seen at the expression level, we first looked at the expression status of genes closest to DMR using a nearest gene annotation approach. Using this approach, only 114 genes showed overlapping changes in expression and DNA methylation. However, since focusing on DMR-nearest gene correlations may not correctly capture the three-dimensional nature of gene regulation, we next explored the role of DMR within specific topologically associated domains (TAD) identified using publicly available coordinates. We thus localized each DMR into a given TAD. For every gene within a TAD, we correlated gene expression and methylation levels across the samples using Pearson correlation. With this method, of 196 DMR identified in 66 TAD, we detected changes in gene expression in 72 genes (*Online Supplementary Table S2*).

To further explore the epigenetic differences between subclones of the original disease and the potential contribution of specific mutations to the epigenetic programming, we also compared DNA methylation profiles in *KRAS* wildtype (A1, A2, A4) and *KRAS*(G12D) (A3, A5) clones (Figure 7). Globally, clones that had acquired *KRAS*(G12D) seemed to be relatively hypomethylated compared to the *KRAS* wildtype clones (Figure 7A, B). Acquisition of *KRAS*(G12D) correlated with a new repartition of DMR, including a significant decrease in methylation at intronic regions (P<0.001), CpG shores (P<0.001),

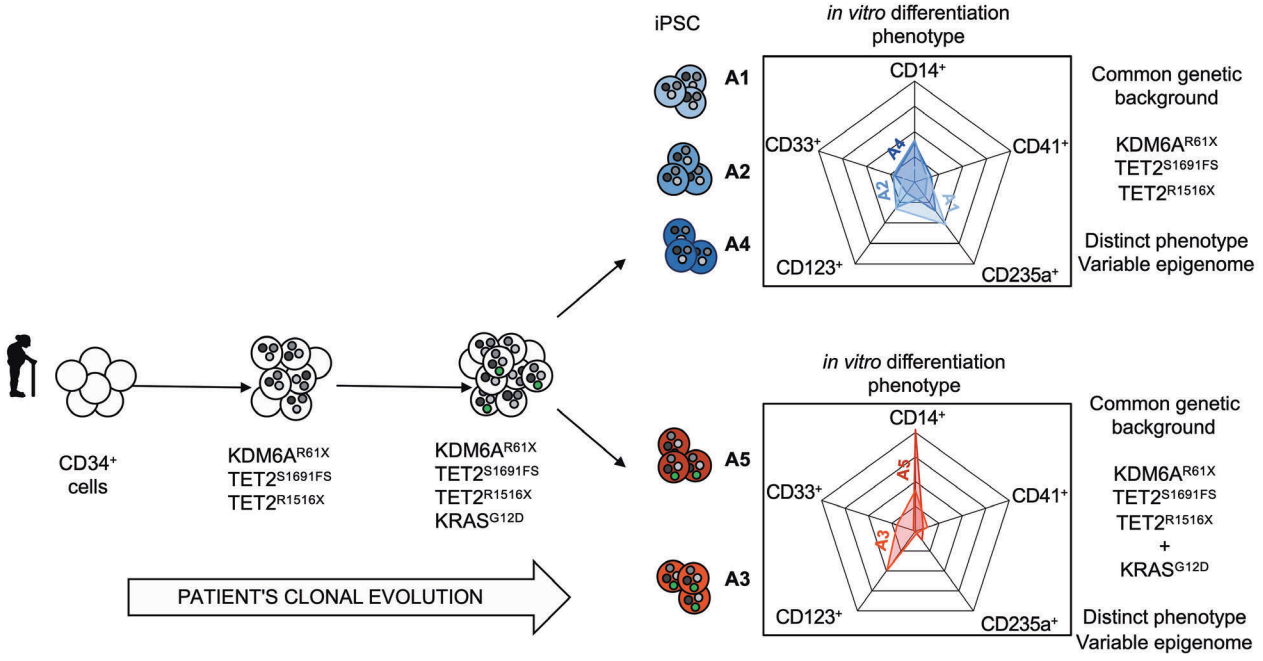

Figure 8. Graphical summary of intratumor heterogeneity layers detected by analysis of five patient-derived induced pluripotent stem cells.

gene body ($P<2.2\ 10^{-16}$) and intergenic enhancers ($P<0.001$) and a significant increase in methylation at promoter regions ($P<0.001$) and CpG islands ($P<0.001$) (Figure 7C). Importantly, using Kyoto Encyclopedia of Genes and Genomes (KEGG) pathway analysis, *KRAS*(G12D) acquisition was shown to induce significant changes in Wnt and Hedgehog signaling pathways, which may indicate a differential role for these pathways in the malignant transformation of the different clones (Figure 7D).

Discussion

The reprogramming of CD34$^+$ cells from a CMML patient generated iPSC whose hematopoietic differentiation recapitulated the main features of the disease while demonstrating functional heterogeneity between clones (see graphical abstract in Figure 8).

Discrepancies between the functional properties of clones sharing a similar genetic background have been reported in organoids derived from colorectal cancer cells.[24] We cannot exclude an effect of recurrent somatic mutations in non-coding regions, as described in some solid tumors,[25] but such events have not been identified yet in CMML cells.[6] A role for cell reprogramming[26,27] in this heterogeneity is also unlikely as control iPSC established independently from two healthy donors had a similar and reproducible behavior, in contrast to the differences observed between genetically identical CMML iPSC (Figure 4J). In addition differences sometimes observed between individual clones derived from the same genotype were shown to pre-exist in the tissue of origin rather than being induced by reprogramming.[28,29] The distinct behavior of CMML-derived iPSC could also reflect intrinsic heterogeneity in CD34$^+$ cell-priming for differentiation.[30,31] If such an intrinsic heterogeneity of CD34$^+$ cell-priming is a general property of CD34$^+$ cells, discrepancies should also have been observed between control iPSC. An alternative explanation is that heterogeneous priming is a specific feature of CMML progenitor cells, which could be related to intraclonal epigenetic heterogeneity. Our epigenetic analyses indicate that, in patient-derived clones, the global pattern of DNA methylation correlates with genetic alterations. However, limited differences in their methylation profiles could possibly account for their functional heterogeneity.

iPSC allow the combined investigation of all levels of intratumoral heterogeneity, from genetic, to epigenetic, to phenotypic and functional properties associated with the disease, offering unique opportunities to study diseases in which functional heterogeneity exceeds genetic heterogeneity, such as CMML.[4] These benefits do, however, come at a cost. As recently reviewed,[15] the derivation of iPSC from patients with a myeloid malignancy to model their disease has to face the relative refractoriness of malignant progenitors to reprogramming, which is in part related to their genetic background and could preclude the capture of intraclonal heterogeneity as some subclones may be reprogrammed more easily than others. The dysplastic nature of these cells, which often correlates with an increased sensitivity to apoptosis, is another challenge to overcome. Lastly, in the patients, the heterogeneous behavior of individual cells may be further influenced by clonal interference and non-cell-autonomous factors,[32] contributing to the diversity of CMML phenotypic traits, and accounting for the current failure of treatments aiming at eradicating the malignant clone.

Acknowledgments

The authors would like to thank Dr Weiss for kindly providing a control iPSC clone. This work was supported by grants from the Ligue Nationale Contre le Cancer (équipe labelisée), Institut National du Cancer (INCA_8073; PRT-K 16-047), Fondation ARC (to AB), Cancéropole Ile de France (emergence program to LL), Siric SOCRATE (INCa-DGOS-INSERM_12551), Molecular Medicine in Oncology program (Agence Nationale de la Recherche), Gustave Roussy Cancer Center (taxe d'apprentissage), the University of Miami Sylvester Comprehensive Cancer Center, the Sylvester Comprehensive Cancer Center Onco-Genomics Shared resource, and the John P. Hussman Institute for Human Genomics, Center for Genome Technology at the University of Miami Miller School of Medicine.

References

1. McGranahan N, Swanton C. Clonal heterogeneity and tumor evolution: past, present, and the future. Cell. 2017;168(4): 613-628.
2. Landau DA, Clement K, Ziller MJ, et al. Locally disordered methylation forms the basis of intratumor methylome variation in chronic lymphocytic leukemia. Cancer Cell. 2014;26(6):813-825.
3. Li S, Garrett-Bakelman FE, Chung SS, et al. Distinct evolution and dynamics of epigenetic and genetic heterogeneity in acute myeloid leukemia. Nat Med. 2016;22 (7):792-799.
4. Ball M, List AF, Padron E. When clinical heterogeneity exceeds genetic heterogeneity: thinking outside the genomic box in chronic myelomonocytic leukemia. Blood. 2016;128 (20):2381-2387.
5. Deininger MWN, Tyner JW, Solary E. Turning the tide in myelodysplastic/myeloproliferative neoplasms. Nat Rev Cancer. 2017;17(7):425-440.
6. Merlevede J, Droin N, Qin T, et al. Mutation allele burden remains unchanged in chronic myelomonocytic leukaemia responding to hypomethylating agents. Nat Commun. 2016;7:10767.
7. Itzykson R, Kosmider O, Renneville A, et al. Clonal architecture of chronic myelomonocytic leukemias. Blood. 2013;121(12):2186-2198.
8. Solary E, Itzykson R. How I treat chronic myelomonocytic leukemia. Blood. 2017;130 (2):126-133.
9. Meldi K, Qin T, Buchi F, et al. Specific molecular signatures predict decitabine response in chronic myelomonocytic leukemia. J Clin Invest. 2015;125(5):1857-1872.
10. Zhang Y, He L, Selimoglu-Buet D, et al. Engraftment of chronic myelomonocytic leukemia cells in immunocompromised mice supports disease dependency on cytokines. Blood Adv. 2017;1(14):972-979.
11. Yoshimi A, Balasis ME, Vedder A, et al. Robust patient-derived xenografts of MDS/MPN overlap syndromes capture the unique characteristics of CMML and JMML. Blood. 2017;130(4):397-407.
12. Chao MP, Gentles AJ, Chatterjee S, et al. Human AML-iPSCs reacquire leukemic properties after differentiation and model clonal variation of disease. Cell Stem Cell. 2017;20(3):329-344.e7.
13. Kotini AG, Chang CJ, Chow A, et al. Stage-specific human induced pluripotent stem cells map the progression of myeloid transformation to transplantable leukemia. Cell Stem Cell. 2017;20(3):315-328.e7.
14. Taoka K, Arai S, Kataoka K, et al. Using patient-derived iPSCs to develop humanized mouse models for chronic myelomonocytic leukemia and therapeutic drug identification, including liposomal clodronate. Sci Rep. 2018;8(1):15855.
15. Papapetrou EP. Modeling myeloid malignancies with patient-derived iPSCs. Exp Hematol. 2019;71:77-84.
16. Mills JA, Wang K, Paluru P, et al. Clonal genetic and hematopoietic heterogeneity

among human induced pluripotent stem cell lines. Blood. 2013;122(12):2047-2052.
17. Welch RP, Lee C, Imbriano PM, et al. ChIP-Enrich: gene set enrichment testing for ChIP-seq data. Nucleic Acids Res. 2014;42(13):e105-e105.
18. Chang CJ, Kotini AG, Olszewska M, et al. Dissecting the contributions of cooperating gene mutations to cancer phenotypes and drug responses with patient-derived iPSCs. Stem Cell Reports. 2018;10(5):1610-1624.
19. Oakes CC, Claus R, Gu L, et al. Evolution of DNA methylation is linked to genetic aberrations in chronic lymphocytic leukemia. Cancer Discov. 2014;4(3):348-361.
20. Mazor T, Pankov A, Song JS, Costello JF. Intratumoral heterogeneity of the epigenome. Cancer Cell. 2016;29(4):440-451.
21. Pan H, Jiang Y, Boi M, et al. Epigenomic evolution in diffuse large B-cell lymphomas. Nat Commun. 2015;6(1):6921.
22. Park Y, Figueroa ME, Rozek LS, Sartor MA. MethylSig: a whole genome DNA methylation analysis pipeline. Bioinformatics. 2014;30(17):2414-2422.
23. Akalin A, Garrett-Bakelman FE, Kormaksson M, et al. Base-pair resolution DNA methylation sequencing reveals profoundly divergent epigenetic landscapes in acute myeloid leukemia. PLoS Genet. 2012;8(6):e1002781.
24. Roerink SF, Sasaki N, Lee-Six H, et al. Intra-tumour diversification in colorectal cancer at the single-cell level. Nature. 2018;556(7702):457-462.
25. Nault JC, Mallet M, Pilati C, et al. High frequency of telomerase reverse-transcriptase promoter somatic mutations in hepatocellular carcinoma and preneoplastic lesions. Nat Commun. 2013;4(1):2218.
26. Cahan P, Daley GQ. Origins and implications of pluripotent stem cell variability and heterogeneity. Nat Rev Mol Cell Biol. 2013;14(6):357-368.
27. Nishizawa M, Chonabayashi K, Nomura M, et al. Epigenetic variation between human induced pluripotent stem cell lines is an indicator of differentiation capacity. Cell Stem Cell. 2016;19(3):341-354.
28. Kwon EM, Connelly JP, Hansen NF, et al. iPSCs and fibroblast subclones from the same fibroblast population contain comparable levels of sequence variations. Proc Natl Acad Sci U S A. 2017;114(8):1964-1969.
29. Yoshizato T, Dumitriu B, Hosokawa K, et al. Somatic mutations and clonal hematopoiesis in aplastic anemia. N Engl J Med. 2015;373(1):35-47.
30. Naik SH, Perie L, Swart E, et al. Diverse and heritable lineage imprinting of early haematopoietic progenitors. Nature. 2013;496(7444):229-232.
31. Velten L, Haas SF, Raffel S, et al. Human haematopoietic stem cell lineage commitment is a continuous process. Nat Cell Biol. 2017;19(4):271-281.
32. Marusyk A, Tabassum DP, Altrock PM, Almendro V, Michor F, Polyak K. Non-cell-autonomous driving of tumour growth supports sub-clonal heterogeneity. Nature. 2014;514(7520):54-58.

Ferrata Storti Foundation

Oncogenic D816V-KIT signaling in mast cells causes persistent IL-6 production

Araceli Tobío,[1] Geethani Bandara,[1] Denise A. Morris,[1] Do-Kyun Kim,[1] Michael P. O'Connell,[2] Hirsh D. Komarow,[1] Melody C. Carter,[1] Daniel Smrz,[1] Dean D. Metcalfe[1*] and Ana Olivera[1*]

[1]Mast Cell Biology Section and [2]Genetics and Pathogenesis of Allergy Section, Laboratory of Allergic Diseases, National Institute of Allergy and Infectious Diseases, National Institutes of Health, Bethesda, MD, USA

[*]*DDM and AO contributed equally to this work as senior co-authors*

Haematologica 2020
Volume 105(1):124-135

ABSTRACT

Persistent dysregulation of IL-6 production and signaling have been implicated in the pathology of various cancers. In systemic mastocytosis, increased serum levels of IL-6 associate with disease severity and progression, although the mechanisms involved are not well understood. Since systemic mastocytosis often associates with the presence in hematopoietic cells of a somatic gain-of-function variant in KIT, D816V-KIT, we examined its potential role in IL-6 upregulation. Bone marrow mononuclear cultures from patients with greater D816V allelic burden released increased amounts of IL-6 which correlated with the percentage of mast cells in the cultures. Intracellular IL-6 staining by flow cytometry and immunofluorescence was primarily associated with mast cells and suggested a higher percentage of IL-6 positive mast cells in patients with higher D816V allelic burden. Furthermore, mast cell lines expressing D816V-KIT, but not those expressing normal KIT or other KIT variants, produced constitutively high IL-6 amounts at the message and protein levels. We further demonstrate that aberrant KIT activity and signaling are critical for the induction of IL-6 and involve STAT5 and PI3K pathways but not STAT3 or STAT4. Activation of STAT5A and STAT5B downstream of D816V-KIT was mediated by JAK2 but also by MEK/ERK1/2, which not only promoted STAT5 phosphorylation but also its long-term transcription. Our study thus supports a role for mast cells and D816V-KIT activity in IL-6 dysregulation in mastocytosis and provides insights into the intracellular mechanisms. The findings contribute to a better understanding of the physiopathology of mastocytosis and suggest the importance of therapeutic targeting of these pathways.

Correspondence:

ANA OLIVERA
ana.olivera@nih.gov

Received: November 16, 2018.

Accepted: April 2, 2019.

Pre-published: April 4, 2019.

doi:10.3324/haematol.2018.212126

Check the online version for the most updated information on this article, online supplements, and information on authorship & disclosures: www.haematologica.org/content/105/1/124

Introduction

Mastocytosis defines a group of heterogeneous disorders characterized by the accumulation of neoplastic/clonal mast cells in the skin, bone marrow (BM) and other organs.[1] Mastocytosis is clinically subdivided into systemic (SM) and cutaneous (CM) mastocytosis, both of which are comprised of several variants defined in accordance with histological and clinical parameters and organ involvement.[1] Somatic variants in the receptor for stem cell factor (SCF), KIT, that render it constitutively active often associate with SM, particularly p.(D816V), a missense in the tyrosine kinase domain of KIT. D816V-KIT may be accompanied by variants in other genes that further contribute to the oncogenic expansion of mast cells.[2-4]

Interleukin-6 (IL-6) is a pleiotropic cytokine produced by several cell types including stromal, hematopoietic and tumor cells. In addition to its involvement in normal inflammatory processes and host immune defense mechanisms, IL-6 may contribute to malignancy in a range of cancers including multiple myeloma, B-cell and non-B-cell leukemias and lymphomas,[5,6] by modulating cellular development, growth, apoptosis, metastasis and/or cellular resistance to chemotherapy.[6] As elevated IL-6 levels in the serum of patients with such malignancies have been associ-

ated with poor clinical outcomes, blocking IL-6 or its synthesis in these patients is viewed as a potential therapeutic avenue.[7,8]

In SM, the levels of serum IL-6 are higher in patients with aggressive *versus* indolent variants of SM and have been associated with adverse clinical features of mastocytosis such as accumulation of mast cells in the BM, organomegaly, elevated tryptase levels,[9,10] osteoporosis and/or bone pain.[11] Although progression into more aggressive disease within patients with indolent SM (ISM) occurs only in a subset of patients, IL-6 plasma levels significantly correlate with disease progression and lower progression-free survival, suggesting that blockade of IL-6 synthesis or function may be beneficial in cases with aberrant IL-6 pathways.[10] Other studies have shown that IL-6 promotes the differentiation, growth and degranulation of normal mast cells,[12] and induces the production of reactive oxygen species by malignant mast cells and their accumulation in tissues in a model of mastocytosis.[13] Despite the potential implications for disease pathology, the cell types and the mechanisms that may contribute to the constitutively elevated IL-6 levels in mastocytosis are not known.

In this study, we test the hypothesis that cells expressing gain of function variants of KIT, particularly D816V-KIT, confer the ability to constitutively produce IL-6. As will be shown, *ex vivo* BM mast cells from patients with SM release IL-6 in correlation with the allelic frequency of D816V-KIT. We further demonstrate that expression of D816V-KIT causes persistent IL-6 induction by mechanisms independent of autocrine feed-forward loops involving IL-6 and signal transducer and activator of transcription 3 (STAT3) described in other malignant cells, but dependent on oncogenic KIT-derived signals. These signals include phosphatidylinositide 3-kinase (PI3K) pathways and oncogenic STAT5 activation by both janus kinase 2 (JAK2) and, unexpectedly, by the mitogen-activated protein kinase MEK/ERK1/2 pathways. These data expand our understanding of the potential mechanisms initiating enhanced IL-6 production in mastocytosis and emphasize targets for therapeutic intervention in cases of high IL-6 profiles and suspected disease progression.

Methods

A detailed description of the methods used in this study can be found in *Online Supplementary Appendix*.

Study patients

Bone marrow samples were obtained when clinically indicated from patients with SM classified according to the World Health Organization (WHO) guidelines[1,3,14] (*Online Supplementary Table S1*). All human samples were obtained after informed consent, on clinical protocols approved by the Institutional Review Board of the National Institute of Allergy and Infectious Diseases (02-I-0277 and 08-I-0184) in agreement with the Declaration of Helsinki. D816V-KIT mutation analysis and its allele burden in the BM (D816V-KIT frequency) were determined by allele-specific polymerase chain reaction (PCR) from patient blood and BM genomic DNA.[15]

Cell lysates

Cell lines were cultured as described in the *Online Supplementary Appendix*. To obtain lysates for western blots, $3x10^6$ cells were plated in 6-well plates and incubated with or without the indicated inhibitors for 2 hours (h) in serum-free media. Cells were lysed as previously described.[16]

IL-6 measurements

Cells ($3x10^6$) were plated in 6-well plates for 2 h to overnight in 6 mL of serum-free media to exclude the possibility that any extrinsic stimulant present in the serum would influence the results. IL-6 released into the media was measured by ELISA (R&D Systems). Human colorectal carcinoma HCT116 cells were stimulated with 20 ng/mL PMA plus 1 μM ionomycin overnight and the supernatants then collected for IL-6 measurements.

Mononuclear cells in BM aspirates from patients were cultured in StemPro-34 medium with human recombinant SCF (100 ng/mL) for 2-4 days. IL-6 released into the media was determined by ELISA. Alternatively, IL-6 expression in single cells was determined by flow cytometry using a LSRII flow cytometer. BM cells were incubated with Brefeldin A for 4 h and stained with an antibody cocktail containing anti-CD3-QDOT605, anti-CD34-APC, anti-KIT-BV605 and anti-FcεRI-FITC, for 30 minutes (min). Cells were fixed, permeabilized and stained with anti-IL-6-PE for 30 min. Expression of IL-6 in mast cells ($CD3^-/CD34^-/KIT+/Fc\varepsilon RI^+$) was analyzed using FlowJo software.

Quantitative real-time polymerase chain reaction

HMC-1.2 cells ($3x10^6$) were plated in 6-well plates in 6 mL and incubated for 2 h in serum-free media. Cellular RNA was extracted and reverse-transcribed into cDNA. cDNA was then amplified using TaqMan® Gene Expression Master Mix and Taqman® Gene Expression Assays for IL-6, STAT3, STAT4, STAT5A, STAT5B or GAPDH as described in the *Online Supplementary Appendix*.

Knockdown of STAT transcription factors

Knockdown of STAT3 and STAT4 was performed by lentiviral-mediated transduction of small hairpin RNA (sh-RNA) (Sigma-Aldrich, St. Louis, MO, USA) as previously described.[17] STAT5 mRNA was silenced by a small interference-RNA (si-RNA) "ON-TARGET" pool from Dharmacon (Lafayette, CO, USA), introduced into cells by electroporation.

Statistical analysis

Data were expressed as mean±Standard Error of Mean (SEM). Values were from at least three independent experiments, each performed at least in duplicate. Statistically significant differences were calculated by using the Student *t*-test (unpaired). Statistical significance was indicated as follows: $^*P<0.01$; $^{**}P<0.01$; $^{***}P<0.001$; $^{****}P<0.0001$.

Results

Release of IL-6 from patient's bone marrow cells and its association with D816V-KIT and mast cell frequencies

The levels of IL-6 in serum[9] as well as the allelic frequency of D816V-KIT[18] correlate with the levels of tryptase, a surrogate marker of mast cell burden. As mast cells often accumulate in the BM in SM, we tested the ability of BM cells to produce IL-6 in short-term cultures. BM mononuclear cells isolated from patients with SM showed varied ability to release IL-6 into the culture media after 2-4 days, with more release observed in cells from patients with a higher BM D816V-KIT allelic frequency (Figure 1A). Although cells other than mature mast cells may express D816V-KIT,[18] the release of IL-6 into the media correlated with the percentage of mast cells within BM live cells

(Figure 1B), suggesting a contributory role for mast cells in IL-6 production. In addition, we analyzed intracellular IL-6 staining in single BM mast cells by flow cytometry from three separate patients (see *Online Supplementary Table S1* for patients' characteristics). Patient 1 had idiopathic anaphylaxis and did not meet criteria for SM and thus was used as a control. This patient had no detectable D816V-KIT, 0.098% of BM cells were $CD3^-/CD34^-/KIT^+/Fc\varepsilon RI^+$ (mast cells) and a minor percentage of these were IL-6 positive (0.063%) (Figure 1C, left panel). However, $CD3^-/CD34^-/KIT^+/Fc\varepsilon RI^+$ cells from Patients 2 and 3, with BM D816V frequencies of 2.7% and 5.5%, were 77% and 99% positive for IL-6, respectively (Figure 1C, middle and right panels, respectively). In this *ex vivo* experiment, where BM cells were cultured up to 4 days (d) in the presence of SCF, cell lineages other than mast cells ($KIT^+/Fc\varepsilon RI^-$, $KIT^-/Fc\varepsilon RI^+$ and $KIT^-/Fc\varepsilon RI^-$) also showed positive intracellular IL-6 staining (*Online Supplementary Table S2*). However, the highest IL-6 mean fluorescence intensity (MFI) was associated with KIT^+ cells. As SCF in the media may induce IL-6 directly or through autocrine/paracrine signals in clonal and non-clonal cells in these cultures, we examined the expression of IL-6 in BM biopsies by immunofluorescence (IF). IF images of BM of patients with SM indicated that IL-6 intracellular content was mostly associated with mast cells (*Online Supplementary Figure S1*). Thus, the combination of *ex vivo* and *in situ* experiments suggests mast cells as the predominant producers of IL-6, with variable participation of other cell lineages. Data are also consistent with an association between increased IL-6 expression by BM mast cells and D816V-KIT frequency.

Expression of D816V-KIT causes IL-6 upregulation and secretion

Given these associations and that mast cells and their progenitors often carry somatic D816V-KIT variants in SM, we investigated the hypothesis that D816V-KIT

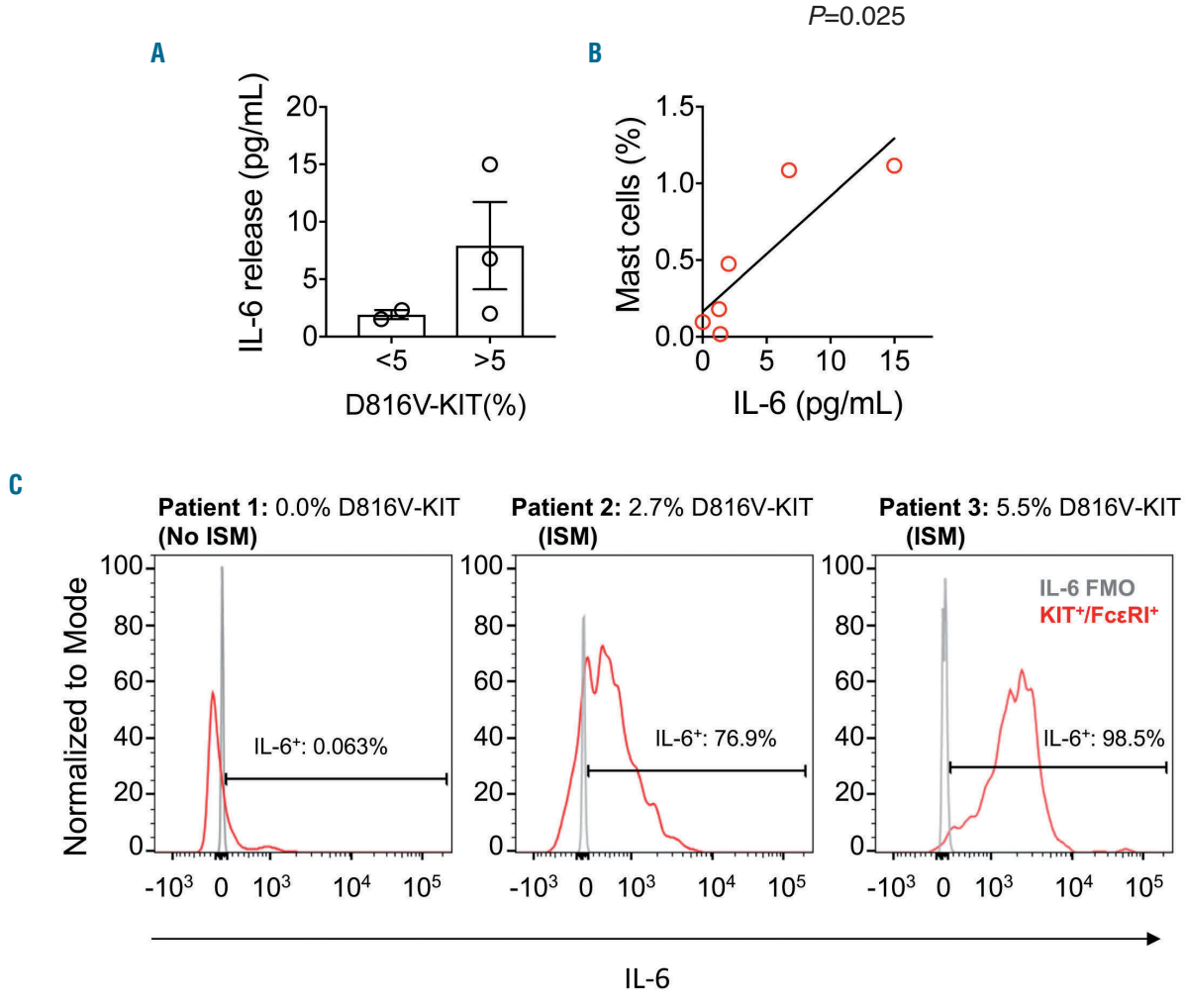

Figure 1. Production of IL-6 by bone marrow cells and mast cells is enhanced in patients with systemic mastocytosis (SM) in association with the D816V-KIT allelic burden. (A) IL-6 release from bone marrow mononuclear cells isolated from five patients with SM with D816V-KIT bone marrow allelic frequencies of <5 (Patients 4 and 5 in *Online Supplementary Table S1*) or >5 (Patients 6, 7, and 10). BM aspirates were cultured for 2-4 days and IL-6 released into the culture media was measured by ELISA. Data are the mean±Standard Error of Mean (SEM). (B) Correlation between IL-6 released into the media by BM cells and the percentage of mast cells in those cultures which was determined by flow cytometry. (C) Flow cytometry histograms showing intracellular IL-6 staining in BM mast cells. Mast cells were gated as $CD3^-/CD34^-/KIT^+/Fc\varepsilon RI^+$ within the BM cells of three patients (Patients 1-3 in *Online Supplementary Table S1*), with D816V-KIT allelic frequencies in the bone marrow also indicated in the figure. Patient 1 had idiopathic anaphylaxis and did not meet criteria for SM but was used as a control. The percentage of IL-6 positive cells within the mast cell population is indicated in the histograms. ISM: indolent SM.

expression intrinsically promotes IL-6 production. Thus, we analyzed the production of IL-6 at the protein and message levels in various cell lines expressing or not D816V-KIT. In agreement with our previous observations, the HMC-1.2 mastocytosis mast cell line which harbors KIT with D816V plus another missense variant in the juxta membrane domain of KIT (V560G), showed markedly higher IL-6 mRNA synthesis[13] (Figure 2A, left panel) and IL-6 release than HMC-1.1 cells, which express only the monoallelic V560G-KIT variant (Figure 2A, right panel).

The mastocytoma mouse mast cell line P815 carrying the homolog to the D816V-KIT variant (D814Y-KIT), also released significantly more IL-6 than primary mouse BMMC (Figure 2B). Furthermore, expression of human D816V-KIT in an immortalized mouse mast cell line that lacks KIT,[13,19] unlike cells expressing normal KIT or vector alone, released significant amounts of IL-6 into the media (Figure 2C). In aggregate, the results using the various mast cell lines demonstrate an association between expression of D816V-KIT in mast cells and persistent transcription and release of IL-6. This may not be restricted to mast cells, since introduction of D816V-KIT by CRISPR in the colorectal carcinoma cell line HCT116 also promoted IL-6 transcription and release (Figure 2D, left and right panels, respectively) when cells were stimulated with PMA and ionomycin, indicating that in these cells D816V-KIT primes HCT116 cells for more robust IL-6 production.

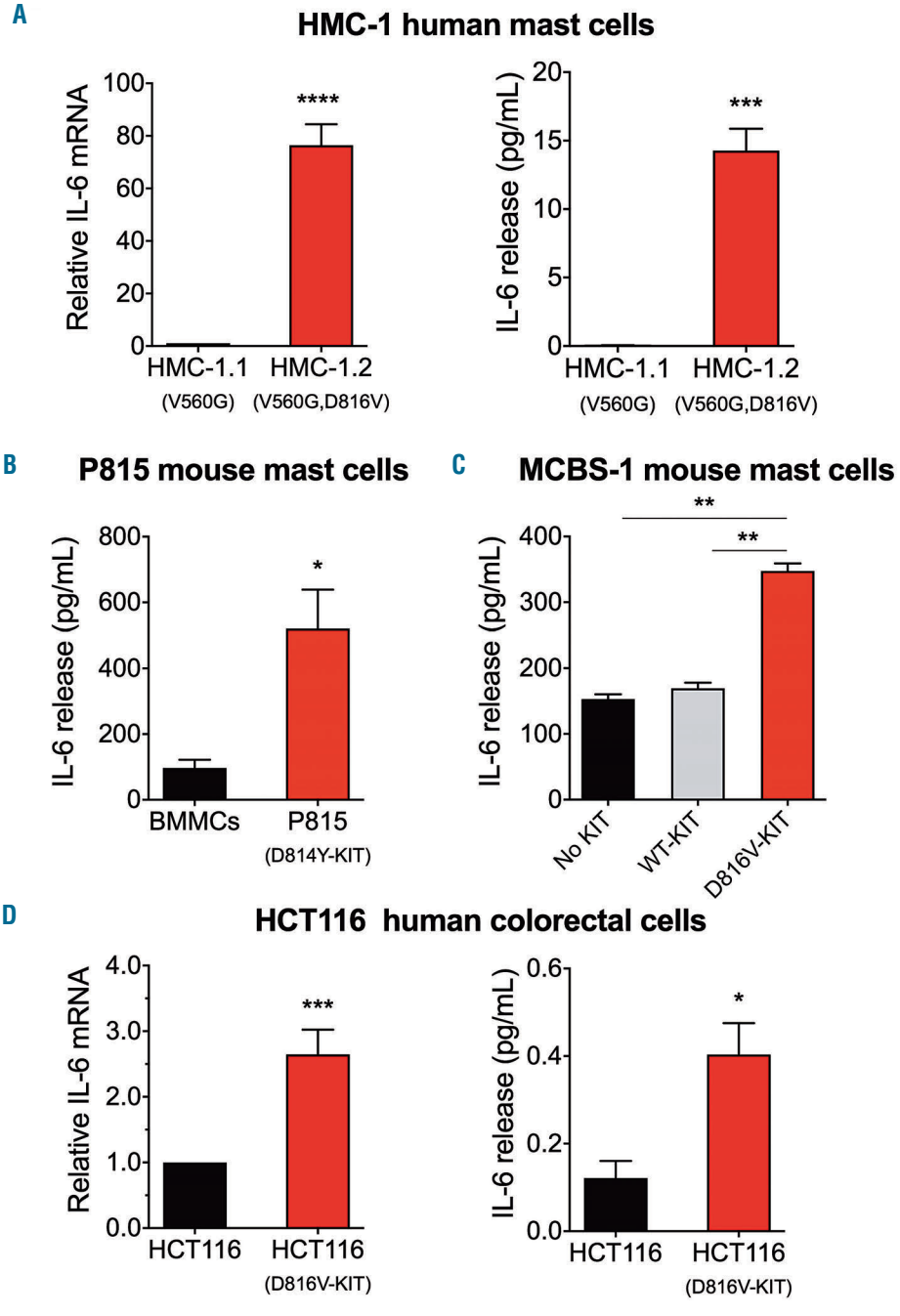

Figure 2. Cells with D816V-KIT constitutively express and release IL-6. (A) IL-6 mRNA expression (left) and IL-6 released into the media (right) by the mastocytosis cell lines HMC-1.1 (with V560G) and HMC-1.2 (with V560G and D816V) after 2 hours (h) in serum-free media. (B and C) Comparison of IL-6 released into the media by the mouse P815 mastocytoma mast cell line (with D814Y-KIT) compared to normal murine bone marrow mononuclear cells (BMMC) (B), and by the murine mast cell line MCBS-1 (which lacks c-Kit) transfected with human *KIT* or D816V-*KIT* compared to MCBS-1 transfected with vector alone (C). (D) Comparison of IL-6 mRNA expression (left) and IL-6 released into the media (right) by the human colorectal carcinoma cell line HCT116 expressing or not D816V-KIT. HCT116 cells were stimulated with phorbol 12-myristate 13-acetate (PMA) and ionomycin overnight. IL-6 mRNA expression was determined by quantitative-real-time polymerase chain reaction (q-RT-PCR) and relative expression was calculated in relationship to the expression of GAPDH using the ΔCt method and expressed as fold change compared to HMC-1.1 (A, left), or the HCT116 parental cell line (D). All data (A-D) are the results of three independent experiments done in triplicates. **P*=0.01; ***P*<0.01; ****P*<0.001 and *****P*<0.0001.

KIT tyrosine kinase activity is required for IL-6 production in mast cells

Ligand-activated KIT signaling induces IL-6 production in mast cells and enhances IgE-receptor-driven IL-6 production.[20] Indeed, stimulation of KIT by SCF in the LAD2 cell line, which expresses normal KIT, induced IL-6 release, albeit the amounts were quantitatively limited (Figure 3A). HMC-1.1 showed higher production of IL-6 than LAD2 cells, particularly when stimulated with SCF (Figure 3A). However, not only was IL-6 production approximately 100-fold higher in unstimulated HMC-1.2 than in LAD2 or HMC-1.1 cells, but ligand-induced stimulation of KIT did not cause any further IL-6 secretion by HMC-1.2 cells (Figure 3A). These data are consistent with the conclusion that ligand-independent signals induced by oncogenic KIT activity, particularly those from D816V-KIT, are more effective in inducing IL-6 secretion than ligand-activated KIT signals.

We next blocked D816V-KIT activity in HMC-1.2 cells with dasatinib, a tyrosine kinase inhibitor that effectively suppresses the activity of the active, open conformation of D816V-KIT. Dasatinib markedly reduced IL-6 mRNA levels (Figure 3B) and IL-6 secretion (Figure 3C), while concentrations of the tyrosine kinase inhibitor imatinib that are ineffective in blocking D816V-KIT, did not alter IL-6 mRNA levels (Figure 3B), further suggesting an involvement of D816V-KIT signaling. Inhibition by gefitinib of the epidermal growth factor receptor (EGFR), a tyrosine kinase receptor that can drive IL-6 production in transformed cells,[21] had no significant effects on IL-6 mRNA levels in HMC-1.2 cells (Figure 3B). Similar to HMC-1.2 cells, dasatinib effectively inhibited IL-6 release in P815 murine mastocytoma cells (Figure 3D). In contrast, persistent IL-6 production in HMC-1.2 cells did not appear to be mediated *via* feed-forward loops of activation by other receptors as those reported for the IL-6 receptor (IL-6R),[22] sphingosine-1-phosphate receptors[23] or the TGFβ receptor[24] in other neoplastic cells, since it was not altered by specific blockage of these receptors (*Online Supplementary Figure S2A-C*). Overall, these data suggest that signals

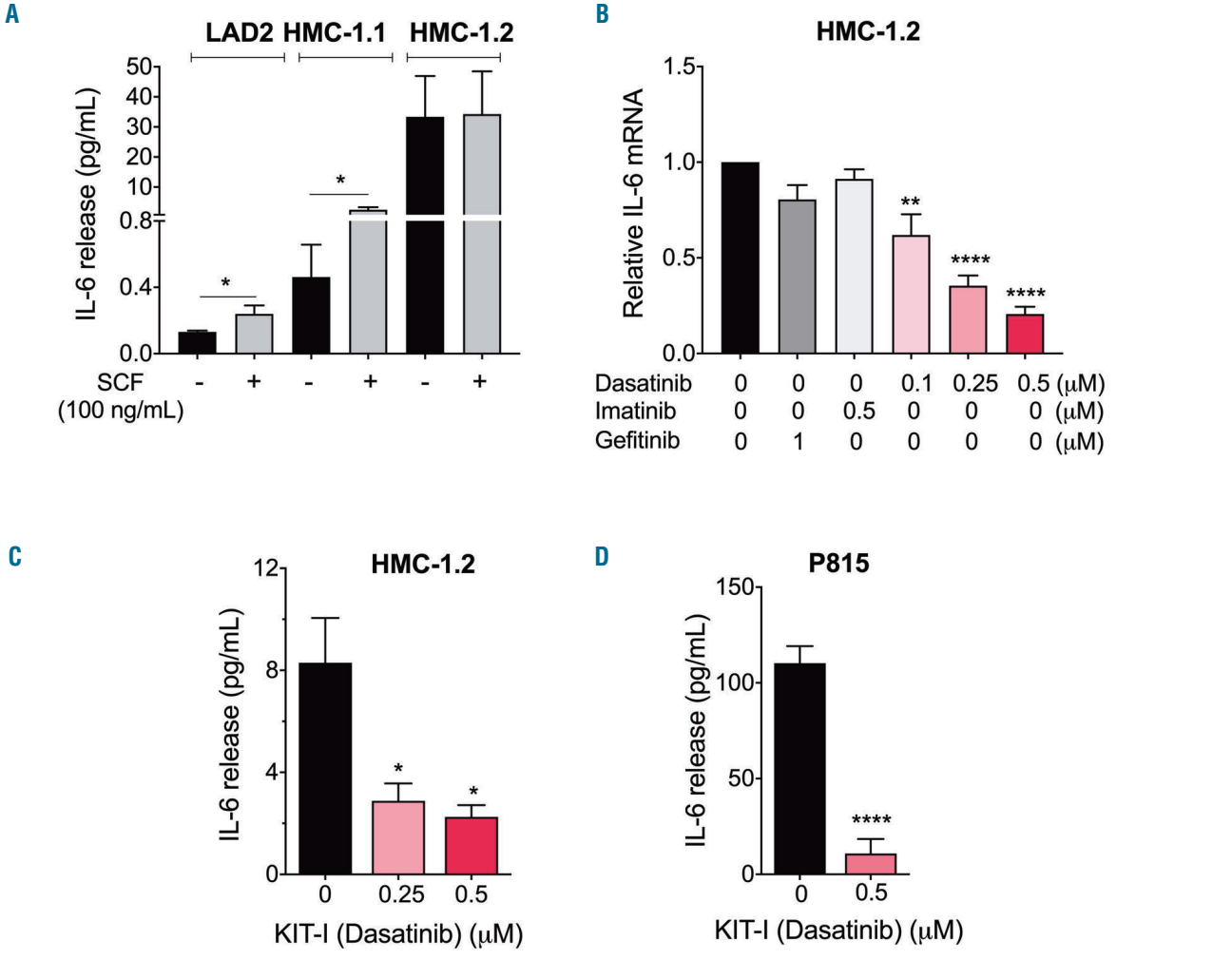

Figure 3. D816V-KIT oncogenic activity drives ligand-independent IL-6 induction. (A) IL-6 released to the extracellular media was measured in LAD2, HMC-1.1 and HMC-1.2 cells incubated for 48 hours (h) (37C, 5%CO_2) in serum-free medium in the presence or absence of 100 ng/mL stem cell factor (SCF). (B) IL-6 mRNA levels were measured in HMC-1.2 after 2 h incubation in serum-free medium in the presence or absence of the KIT inhibitors, dasatinib and imatinib, or the EGFR inhibitor gefitinib at the indicated concentrations. Relative expression of IL-6 mRNA was obtained by normalizing to the expression of GAPDH using the ΔCt method and the results are expressed as fold change compared to untreated cells. The effect of the KIT inhibitor dasatinib (0.5 μM) on the secretion of IL-6 by HMC-1.2 (C) or by P815 mast cells (D) was determined after 6 h incubation in serum free medium. All data are the mean±Standard Error of Mean of three independent experiments done in triplicates. SCF: stem cell factor. *P=0.01, **P<0.01 and ****P<0.0001.

from D816V-KIT can promote ligand-independent IL-6 production without involving some of the most common autocrine feed-forward loops described in malignant cells.

The constitutive release of IL-6 by unstimulated HMC-1.2 was enhanced by stimuli such as complement component 5a (C5a), IL-1b, 10% FBS and PMA/ionomycin (*Online Supplementary Figure S3A*, left panel) suggesting that the production and secretion of IL-6 due to D816V-KIT can synergize with other complementary signals or environmental cues. Of interest, the intracellular content of IL-6 protein was only approximately 10% of the total IL-6 released (*Online Supplementary Figure S3A*), and although dasatinib did not affect this percentage, it also reduced the total intracellular content. Thus, dasatinib inhibited the transcription, intracellular content and release of IL-6 (Figure 3B and C, and *Online Supplementary Figure S3A*, right panel), consistent with the conclusion that D816V-KIT signals cause constitutive *de novo* production and release of IL-6 without regulating storage. In addition, we demonstrate that IL-6 protein released by HMC-1.2 cells is biologically active since conditioned media of these cells caused IL-6R-mediated STAT3 phosphorylation in LAD2 cells which express and respond to IL-6R activation[12] (*Online Supplementary Figure S3B*).

D816V-KIT-induced IL-6 production is dependent on JAK2, ERK and PI3K pathways

Mitogen-activated protein kinase (ERK1/2 and p38) and PI3K pathways are part of the oncogenic signals derived from D816V-KIT activity.[2,25] Since these pathways may affect IL-6 expression,[26-28] we investigated their potential roles in D816V-KIT-induced IL-6 production. While inhibition of p38 with SB203580 had minor effects on IL-6 synthesis, inhibition of the ERK1/2 pathway using a MEK1/2 inhibitor (U0126) (Figure 4A) or inhibition of the PI3K pathway by the PI3Kα/δ/β inhibitor LY294002 (Figure 4B), caused a 50-60% reduction, respectively, in IL-6 production at the message (Figure 4B, left panel) and protein levels (Figure 4B, right panel).

The JAK/STAT axis is also known to be prominently upregulated by D816V-KIT activity.[29,30] JAK2 is activated by SCF[31] leading to STAT phosphorylation and translocation into the nucleus, where it exerts its transcriptional activity.[32] Inhibition of JAK2 by the JAK2 selective inhibitor fedratinib (TG101348) markedly blocked IL-6 constitutive transcription and cytokine release (Figure 4C, left and right panels, respectively). Ruxolitinib which inhibits JAK1 in addition to JAK2, similarly inhibited IL-6 expression, although at higher concentrations than fedratinib (Figure 4D). However, tofacitinib, a pan-JAK inhibitor preferential for JAK3 and to a lesser extent JAK1, was less effective (Figure 4D). Similar to HMC-1.2 cells, in mouse P815 cells inhibition of MEK/ERK1/2, PI3K or JAK2 pathways markedly reduced IL-6 release in mouse P815 cells (Figure 4E). The data thus implicate JAK2 in D816V-KIT induced IL-6 production.

Since JAK2 has also been reported in certain cells to activate PI3K or ERK,[32,33] we further investigated the potential inter-relationships between JAK2 and the ERK and PI3K pathways. While, as expected, inhibition of KIT by dasatinib blocked the phosphorylation of JAK2, AKT and ERK1/2 signaling pathways downstream of the receptor by 40-80% (Figure 4F), inhibitors of JAK2, PI3K/AKT or MEK1/2/ERK1/2 reduced phosphorylation of their respective targets but did not show significant effects on any of the others, suggesting that these signals are activated independently from each other.

D816V-KIT-induced IL-6 production is dependent on STAT5

JAK phosphorylates STAT, and STAT family members such as STAT3,[34,35] STAT4[36] and STAT5[37] have been implicated in the regulation of IL-6 transcription in various cells and conditions. As the levels of expression or phosphorylation of STAT3, STAT4 and STAT5 (*Online Supplementary Figure S4A-C*) are increased in HMC-1.2 and other cells with D816V-KIT[30] and STAT4 and STAT5 are up-regulated in BM mast cells from patients with SM,[29,38,39] we investigated their possible involvement in the induction of IL-6 transcription by silencing STAT3-5 expression using sh-RNA or si-RNA.

Sh-RNA-mediated STAT3 silencing resulted in >75% reduction in STAT3 at the messenger and protein levels (Figure 5A) but did not affect IL-6 production by HMC-1.2 (Figure 5A, red bar). Similarly, a selective small inhibitor molecule for STAT3, C188-9, at concentrations that caused >80% reduction in STAT3 phosphorylation (*Online Supplementary Figure S5A*, top panel) did not alter constitutive IL-6 production by these cells (*Online Supplementary Figure S5A*, bottom panel). Neutralizing antibodies for the IL-6R, which signals through STAT3, were also ineffective on IL-6 production (*Online Supplementary Figure S2A*). Reduction of STAT4 message and protein by >50% using sh-RNA knockdown was also inconsequential for IL-6 persistent production by these cells (Figure 5B).

However, specific reduction in the mRNA for STAT5A or STAT5B messages by >50% and in protein expression (Figure 5C) using STAT5-specific si-RNA pools, resulted in concomitant reductions in IL-6 transcription (Figure 5D). Simultaneous knockdown of STAT5A and B did not accomplish significantly greater effects on IL-6 expression than silencing each individually (Figure 5C and D), suggesting a redundant function for the two isoforms. The selective STAT5 inhibitor (CAS 285986-31-4), at a concentration that inhibited STAT5 phosphorylation by 50% (50 μM) (*Online Supplementary Figure S5B*, top panel) also significantly reduced IL-6 transcription and IL-6 protein synthesis by 50% (*Online Supplementary Figure S5B, bottom panel,* and *S5C*), a result that was also confirmed in P815 cells (*Online Supplementary Figure S5D*). As STAT5 is overexpressed and hyperactivated in cells carrying D816V (*Online Supplementary Figure S4C*)[29,38,39] and STAT5 mRNA was not depleted even when both STAT5A and B were silenced (Figure 5C), we treated STAT5-knockdown cells with the STAT5 inhibitor, which showed a reduction in IL-6 mRNA expression by 80% (*Online Supplementary Figure S5E*) consistent with the reduction observed by inhibition of JAK2. The results point towards JAK2/STAT5 as a major pathway leading to the constitutive expression of IL-6 in D816V-KIT expressing cells.

ERK contributes to STAT5 phosphorylation and expression while the effect of the PI3K pathway on IL-6 is STAT5-independent

As MAP kinases have been implicated in the phosphorylation and the activation of STAT family members,[40] we sought to determine whether ERK1/2 may contribute to the induction of IL-6 by enhancing STAT5 phosphorylation. While inhibition of ERK1/2 did not affect JAK2 phosphorylation (Figure 4F), it substantially inhibited STAT5

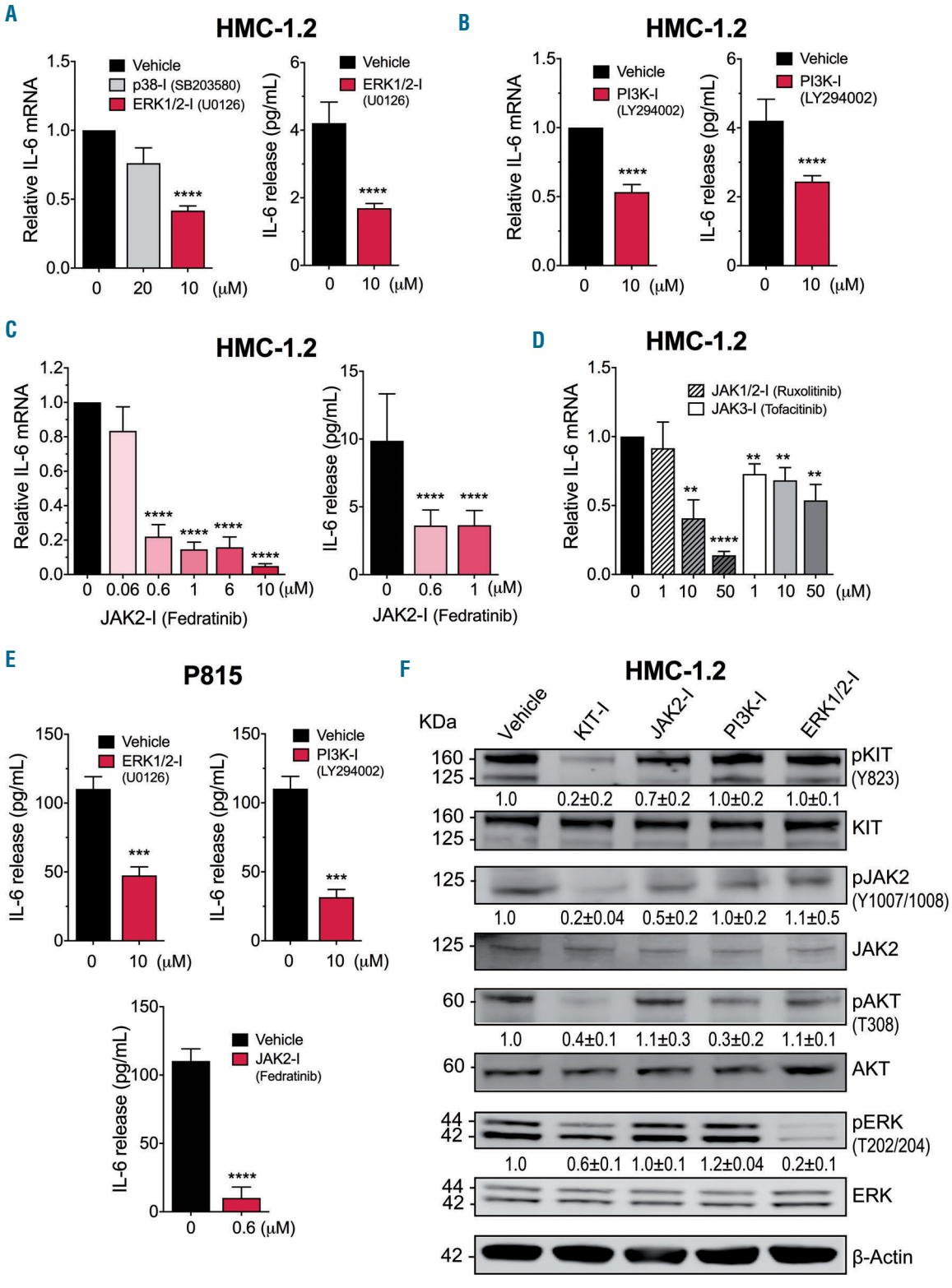

Figure 4. MEK/ERK-, PI3K- and JAK2-mediated pathways are independently activated by D816V-KIT and contribute to ligand-independent IL-6 induction. (A and B) Effect of inhibition of MEK/ERK1/2 (U0126), p38 (SB203580) (A) or PI3K pathways (LY294002) (B) on the expression of IL-6 mRNA (left) after treatment for 2 hours (h) and the release of IL-6 into the media (right) by HMC-1.2 cells for 16 h. (C) Effect of the JAK2 inhibitor fedratinib at the indicated concentrations on the expression of IL-6 mRNA (left) and the release of IL-6 into the media (right) by HMC-1.2 cells. (D) Effect of various concentrations of inhibitors for JAK1/2 (ruxolitinib) and JAK3 (tofacitinib) on the expression of IL-6 mRNA by HMC-1.2 cells. (E) Effect of inhibition of MEK/ERK1/2, PI3K or JAK2 on the production of IL-6 by mouse P815 cells after 6 h of incubation. (F) Effect of inhibitors for KIT (KIT-I: dasatinib; 0.5 μM), JAK2 (JAK2-I: fedratinib; 1 μM), PI3K (PI3K-I: LY294002; 10 μM) and MEK/ERK1/2 (ERK-I: U0126; 10 μM) on the phosphorylation of KIT, JAK2, AKT and ERK1/2 in the indicated amino acid residues. Inhibitors were incubated for 2 h in serum-free medium. Numbers under each phosphorylated band are Standard Error of Mean (SEM) of at least three experiments and represent fold changes in the relative band fluorescence (normalized to the corresponding total expression) compared to untreated cells. Relative expression of IL-6 mRNA was obtained by comparing to the expression of GAPDH using the ΔCt method and the results were expressed as fold change compared to untreated cells. Data represent the mean±SEM and are from three independent experiments. ***P*<0.01, ****P*<0.001 and *****P*<0.0001.

tyrosine phosphorylation (Figure 6A) and reduced STAT5 serine (Ser780) phosphorylation (Figure 6B), with the effects on STAT5 tyrosine phosphorylation being less pronounced than those of the JAK2 and STAT5 inhibitors (Figure 6A). Simultaneous inhibition of both JAK2 and ERK1/2 markedly blunted STAT5 phosphorylation (Figure 6B). In addition, inhibition of MEK/ERK also reduced STAT5A and STAT5B mRNA expression by 16 h, an effect that was not seen by 2 h (Figure 6C). The results implicate MEK/ERK1/2 as a dual regulator of STAT5 activity (*via* JAK2-independent phosphorylation) and STAT5 transcription. In contrast, inhibition of PI3K had no effect on STAT5 phosphorylation or transcription in HMC-1.2 cells (Figure 6A and C), indicating the PI3K pathway regulates IL-6 independently of STAT5.

Combination treatment of inhibitors for STAT5, ERK1/2 and PI3K markedly suppressed constitutive IL-6 expression (Figure 6D, left panel) and release (Figure 6D, right

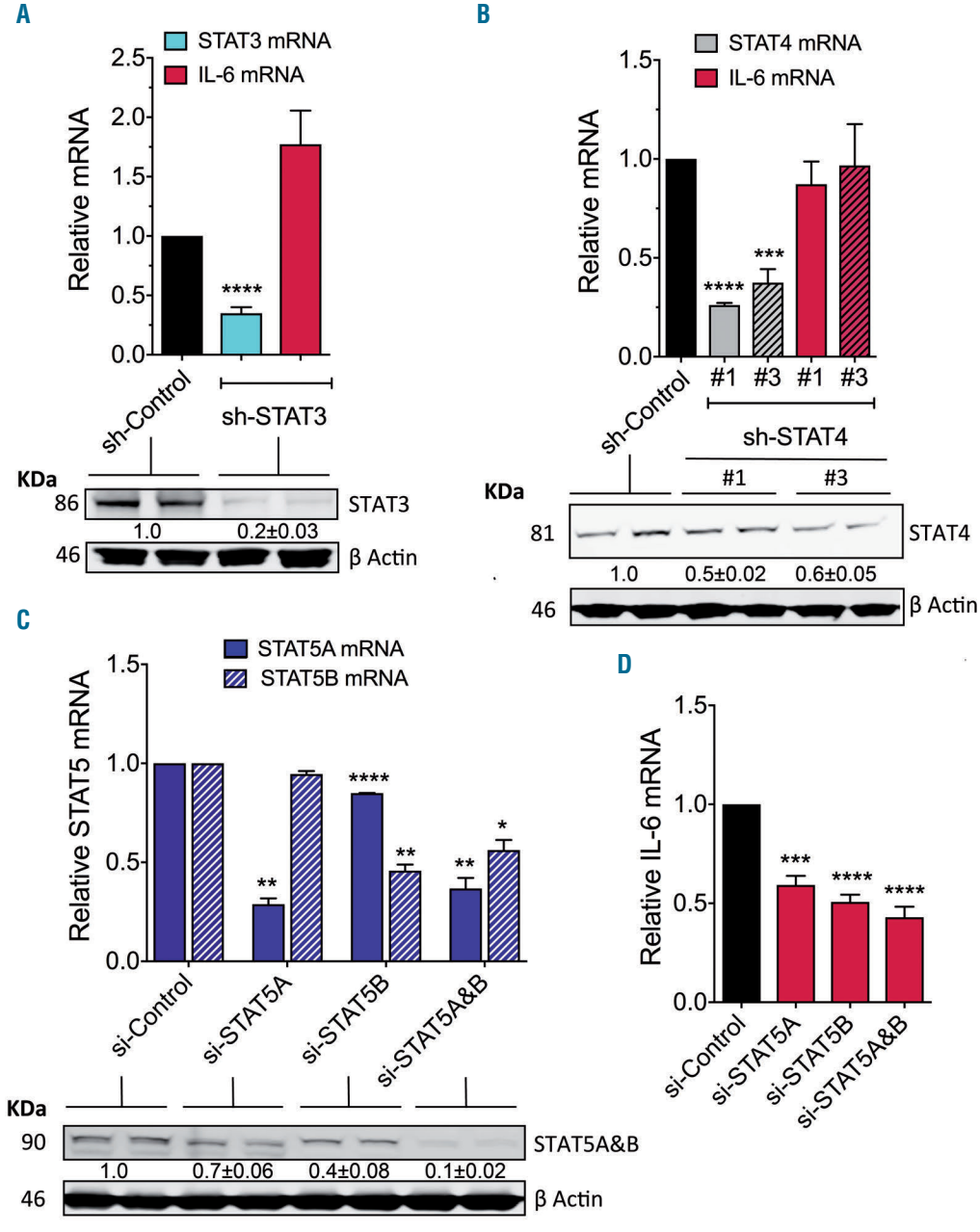

Figure 5. STAT5A and B are key in mediating D816V-KIT-induced persistent IL-6 production. Effect of STAT3 (A) and STAT4 (B) knockdown by lentiviral sh-RNA on their respective targets and on the expression of IL-6 mRNA by HMC-1.2 cells. For sh-STAT4, the effect of two different constructs are shown (#1 and #3). Western blot gels underneath the bar graphs represent the effect of sh-STAT3 (A) or sh-STAT4 (B) constructs on the protein levels of STAT3 and STAT4, respectively. Lysates from duplicate samples are shown. The numbers under each pair are mean±Standard Error of Mean (SEM) of at least three separate experiments and represent fold change in the relative band fluorescence compared to the sh-RNA non-target (control). Actin content was used as loading control. (C and D) Effect of silencing STAT5A, STAT5B or the combination of both STAT5A&B by si-RNA on the expression of STAT5A and STAT5B mRNA (C) and of IL-6 mRNA (D) in HMC-1.2. The blots under the bar graph in (C) show the effect of STAT5 silencing in the protein levels of STAT5A/B and the numbers under the blot, the fold change as in (A) and (B). Of note, the antibody used recognizes both STAT5A and B. **P*=0.01, ***P*<0.01, ****P*<0.001 and *****P*<0.0001.

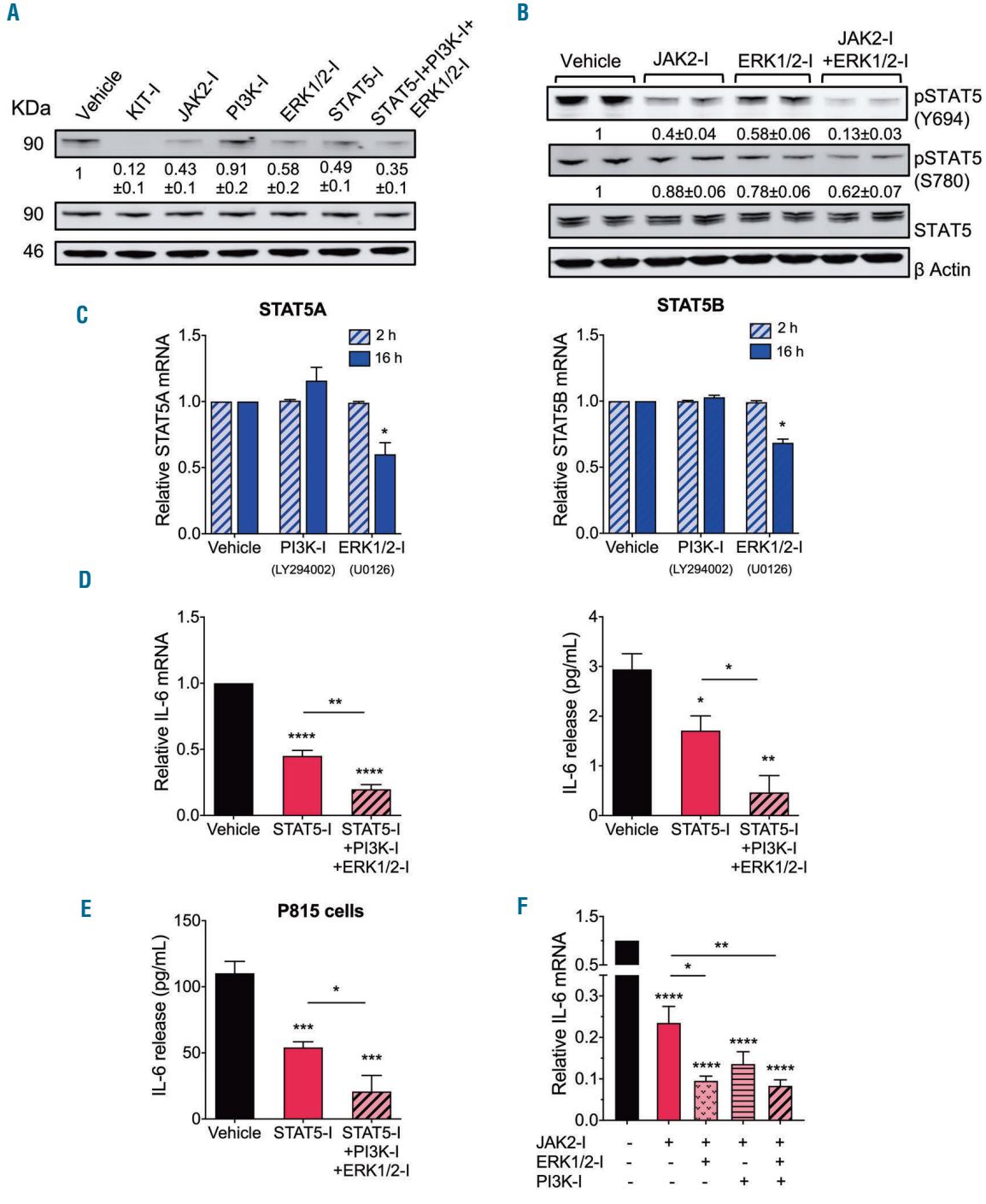

Figure 6. MEK/ERK signaling pathway co-operates with JAK2 in the regulation of STAT5 to induce IL-6 while PI3K regulates IL-6 independently of STAT5. (A) Effect of inhibitors for KIT (KIT-I: dasatinib; 0.5 μM), JAK2 (JAK2-I: fedratinib; 1 μM), PI3K (PI3K-I: LY294002; 10 μM), MEK/ERK1/2 (ERK-I: U0126; 10 μM), STAT5 (STAT5-I: CAS285986-31-4; 50 μM), or their combination on the protein and phosphorylation levels of STAT5 in HMC-1.2 cells. (B) Effect of inhibitors of JAK2 and ERK1/2 alone or in combination on STAT5 phosphorylation in HMC-1.2 cells. (A and B) Lysates were obtained after 2 hours (h) incubation with the indicated inhibitors in serum-free medium. Data under the blots are the mean±Standard Error of Mean (SEM) of three independent experiments carried out in duplicates, and represent fold change in the relative band fluorescence compared to the untreated. STAT5 content was used to normalize the data. (C) Inhibition of MEK/ERK1/2 reduces STAT5A and STAT5B expression ((left and right, respectively) after 16 h incubation. Relative expression of STAT5 mRNA was obtained by comparison with the expression of GAPDH using the DCt method and the results are expressed as fold change compared to untreated cells at each time (2 h or 16 h). (D and E) Inhibitors for STAT5, PI3K and MEK/ERK1/2 additively prevent IL-6 mRNA induction (D, left) and IL-6 release in HMC-1.2 cells (D, right) and P815 cells (E). The release of IL-6 into the media was determined after 6 h. (F) Inhibitors for JAK2, PI3K and MEK/ERK1/2 additively prevent IL-6 mRNA induction in HMC-1.2 cells. All data represent mean±Standard Error of Mean of at least three independent experiments. **P*=0.01, ***P*<0.01, ****P*<0.001 and *****P*<0.0001.

panel) in HMC-1.2 cells and in P815 cells (Figure 6E). Similarly, the JAK2 inhibitor fedratinib, currently in clinical trials, nearly ablated IL-6 production in HMC-1.2 cells when in combination with either (or both) PI3K and ERK1/2 inhibitors (Figure 6F), indicating the separate contributions of these pathways to persistent IL-6 induction.

Discussion

IL-6 plays important roles in host defense, but if produced in an uncontrolled or persistent manner it may be detrimental and contribute to the development of inflammatory diseases (e.g. rheumatoid arthritis and inflammatory bowel disease) and malignancies.[7,8,41] Although little is known about the exact role of IL-6 in mastocytosis and how it is dysregulated, the levels of IL-6 in circulation correlate with mast cell burden and tissue involvement, osteoporosis,[9,11] and risk of progression.[10] Our data suggest a contributory role for mast cells in IL-6 production in mastocytosis and implicate aberrant signaling of D816V-KIT as an initial event promoting persistent IL-6 transcription and consequent protein secretion. Among these aberrant signals, we identified increased JAK2 activity and MEK/ERK- and PI3K-derived signals as drivers of IL-6 transcription, the former two by regulating the activation/expression of STAT5. The study provides the first clues into mechanisms leading to persistent IL-6 production in mastocytosis and potential target molecules for therapeutic intervention.

Increased expression of IL-6 and its signaling through STAT3 in many malignancies can be driven by overexpression of IL-6R, co-receptors and regulators (such as JAK and STAT3), polymorphisms in the IL-6 promoter and/or oncogenic signaling from tyrosine kinase receptors such as EGFR/HER, and may occur when negative regulation is not fully effective.[34] Often, in malignant cells, production of IL-6 and constitutive STAT3 activation drive their own expression in feed-forward regulatory loops that are key for tumorigenesis.[22,23,34,41] Here, we show that upregulation of IL-6 in mast cells with the D816V-KIT missense variant does not involve the IL-6R and co-receptor gp130 (*Online Supplementary Figure S2A*) or feedback loops involving STAT3 (Figure 5). Moreover, STAT4, shown to enhance IL-6 transcription in human fibroblasts,[36] had no role in IL-6 upregulation in HMC-1.2 mast cells. Instead, we demonstrate that persistent IL-6 production was dependent on oncogenic D816V-KIT activity and aberrant STAT5 activation, as it was suppressed by tyrosine kinase inhibitors that effectively block D816V-KIT tyrosine kinase activity and by STAT5 silencing or inhibition. In addition, BM mast cells from patients with mastocytosis produced and released IL-6 *ex vivo* in correlation with D816V-KIT allelic burden (Figure 1). As STAT5 expression and phosphorylation are also up-regulated in BM mast cells of patients with SM,[29,38,39] our data suggest that oncogenic STAT5 activation may be a priming event contributing to the elevated serum IL-6 levels in mastocytosis. This does not exclude the involvement of other mechanisms such as IL-6-mediated feed-forward loops on other cell types in the surrounding tissue, which may drive IL-6 production further. In addition, it is important to note that, although most of the intracellular IL-6 staining was associated with mast cells in patient's BM biopsies (*Online Supplementary Figure S1*), enhanced production of IL-6 in SM may not be restricted to mast cells as the presence of D816V-KIT may also induce or promote IL-6 production in other clonal cells (Figure 2D and *Online Supplementary Table S2*). Furthermore, additional signals in the local environment could crosstalk with oncogenic KIT signals in mast cells or other hematopoietic clonal cells in SM with associated multilineage involvement, further contributing to IL-6 dysregulation.

Even though canonical binding sites for STAT3, but not STAT5, are recognized in the IL-6 promoter, stimulation of STAT5 by the IgE receptor in mast cells was reported to mediate IL-6 production[37] and constitutively active STAT5 mutants to induce IL-6 expression.[42] Whether active STAT5 in D816V-KIT mast cells binds directly to the IL-6 promoter driving transcription, or does so indirectly by binding other transcription factors[42] or by causing chromatin remodeling,[43] needs further evaluation. Regardless of this, as STAT5 hyperactivation is critical for neoplastic D816V-KIT mast cell growth and survival[39,44] and for normal mast cell development,[45] our description of a novel regulatory role for STAT5 on constitutive IL-6 expression supports targeting STAT5 for treatment of patients with mastocytosis and high IL-6 levels. This could also be a potential treatment for patients with other hematologic malignancies such as chronic myelogenous leukemia where serum IL-6 levels represent a predictor of outcome[46,47] and pathogenesis is in part driven by constitutive STAT5 activation.[48]

The activation of STAT5 by D816V-KIT was complex and involved an interplay of JAK2- and MEK/ERK1/2-mediated pathways. JAK2-selective inhibitors such as fedratinib markedly reduced constitutive IL-6 production, while the effectiveness of other pan-jakinib correlated with their relative selectivity for JAK2, suggesting that JAK1 and 3 have no significant role. The specific involvement of JAK2 agrees with the notion that STAT5 is a major target for JAK2 in hematopoietic cells[29] and that activation of KIT by SCF causes JAK2 phosphorylation.[31] Unlike the known effect on JAK2 inhibition, the effect of MEK/ERK1/2 inhibition on STAT5 activity and transcript abundance was unexpected. Phosphorylation in serine/threonine residues of STAT1/3/4 by MAPK was reported to affect STAT1/3/4 activity.[33,40] Although serine phosphorylation at the C-terminal tail of STAT5 proteins is essential for leukemogenesis[49] and for growth hormone-induced gene expression,[50] the serine/threonine kinases that mediate this type of phosphorylation or the exact functional implications are not well understood. Surprisingly, in cells with D816V-KIT, inhibition of MEK/ERK1/2 caused a more pronounced effect on STAT5 phosphorylation at tyrosine 694 (a target for JAK2) than at serine 780 (Figure 6), even though JAK2 activity was not affected by the ERK inhibitor (Figure 4). A similar JAK-independent role for ERK in STAT3 tyrosine phosphorylation was reported in plasma cells for IL-6,[27] but the mechanism for such regulation, and what potential kinases or phosphatase may be involved, need further evaluation.

We also found a role for PI3K/AKT-dependent pathways on IL-6 induction in D816V-KIT mast cells, but in a STAT5-independent manner, indicating that persistent IL-6 expression likely involves multiple transcription factors. Similar to STAT5,[39,44] oncogenic growth and survival of mast cells with D816V-KIT is also dependent on constitutive activation of AKT.[2,30] Thus, combined targeting

of STAT5 and PI3K/AKT pathways may be desirable to treat patients with mastocytosis and elevated IL-6, as was proposed for drug-resistant chronic myelogenous leukemia where both pathways are critical for disease evolution.[44] Alternatively, since small molecule inhibitors for JAK2 such as fedratinib and the dual JAK1/2 inhibitor ruxolitinib inhibit STAT5 activity and IL-6 upregulation in neoplastic mast cells (Figures 4 and 6), and both drugs are approved by the US Federal Drug Administration for various blood disorders, they are also feasible drug candidates alone or in combination with other therapies for increased therapeutic index.

The work presented here links expression of the D816V-KIT variant with IL-6 persistent activation in mast cells and sheds light into the molecular mechanisms driving dysregulated IL-6. Our data underscore a role for constitutive STAT5 activation, achieved by both JAK2 and ERK-mediated activities, and PI3K/AKT signals on IL-6 dysregulation. Together, our findings establish the groundwork for exploring new potential therapeutic combinations targeting the mentioned kinases in the treatment of patients with mastocytosis.

Acknowledgments

We thank Robin Eisch in her role as protocol study coordinator, Linda Scott, the nurse practitioner on the study protocols, Pahul Hanjra and Irina Maric for providing information on patients and Daly Cantave for arranging for patient bone marrow samples.

Funding

This work was supported by the Division of Intramural Research within the National Institute of Allergy and Infectious Diseases (NIAID), at the National Institutes of Health.

References

1. Valent P, Akin C, Hartmann K, et al. Advances in the Classification and Treatment of Mastocytosis: Current Status and Outlook toward the Future. Cancer Res. 2017;77(6):1261-1270.
2. Cruse G, Metcalfe DD, Olivera A. Functional deregulation of KIT: link to mast cell proliferative diseases and other neoplasms. Immunol Allergy Clin North Am. 2014;34(2):219-237.
3. Valent P, Akin C, Metcalfe DD. Mastocytosis: 2016 updated WHO classification and novel emerging treatment concepts. Blood. 2017;129(11):1420-1427.
4. Metcalfe DD, Mekori YA. Pathogenesis and Pathology of Mastocytosis. Annu Rev Pathol. 2017;12:487-514.
5. Burger R. Impact of Interleukin-6 in Hematological Malignancies. Transfus Med Hemoth. 2013;40(5):336-343.
6. Taniguchi K, Karin M. IL-6 and related cytokines as the critical lynchpins between inflammation and cancer. Semin Immunol. 2014;26(1):54-74.
7. Hong DS, Angelo LS, Kurzrock R. Interleukin-6 and its receptor in cancer: implications for translational therapeutics. Cancer. 2007;110(9):1911-1928.
8. Rossi JF, Lu ZY, Jourdan M, Klein B. Interleukin-6 as a therapeutic target. Clin Cancer Res. 2015;21(6):1248-1257.
9. Brockow K, Akin C, Huber M, Metcalfe DD. IL-6 levels predict disease variant and extent of organ involvement in patients with mastocytosis. Clin Immunol. 2005;115(2):216-223.
10. Mayado A, Teodosio C, Garcia-Montero AC, et al. Increased IL6 plasma levels in indolent systemic mastocytosis patients are associated with high risk of disease progression. Leukemia. 2016;30(1):124-130.
11. Theoharides TC, Boucher W, Spear K. Serum interleukin-6 reflects disease severity and osteoporosis in mastocytosis patients. Int Arch Allergy Immunol. 2002;128(4):344-350.
12. Desai A, Jung MY, Olivera A, et al. IL-6 promotes an increase in human mast cell numbers and reactivity through suppression of suppressor of cytokine signaling 3. J Allergy Clin Immunol. 2016;137(6):1863-1871 e1866.
13. Kim DK, Beaven MA, Kulinski JM, et al. Regulation of Reactive Oxygen Species and the Antioxidant Protein DJ-1 in Mastocytosis. PLoS One. 2016;11(9): e0162831.
14. Horny HP, Metcalfe DD, Akin C, et al. Mastocytosis. In: Swerdlow SH, Campo E, Harris NL, Jaffee ES, Pileri SA, Stein H, et al., eds. WHO classification of tumours of haematopoietic and lymphoid tissues. 2017 ed. Lyon, France: IARC Press, 2017:62-69.
15. Kristensen T, Vestergaard H, Moller MB. Improved detection of the KIT D816V mutation in patients with systemic mastocytosis using a quantitative and highly sensitive real-time qPCR assay. J Mol Diagn. 2011;13(2):180-188.
16. Kim DK, Beaven MA, Metcalfe DD, Olivera A. Interaction of DJ-1 with Lyn is essential for IgE-mediated stimulation of human mast cells. J Allergy Clin Immunol. 2017;142(1):195-206 e8.
17. Siegel AM, Stone KD, Cruse G, et al. Diminished allergic disease in patients with STAT3 mutations reveals a role for STAT3 signaling in mast cell degranulation. J Allergy Clin Immunol. 2013;132(6):1388-1396.
18. Kristensen T, Broesby-Olsen S, Vestergaard H, Bindslev-Jensen C, Moller MB, Mastocytosis Centre Odense University H. Serum tryptase correlates with the KIT D816V mutation burden in adults with indolent systemic mastocytosis. Eur J Haematol. 2013;91(2):106-111.
19. Smrz D, Bandara G, Zhang S, et al. A novel KIT-deficient mouse mast cell model for the examination of human KIT-mediated activation responses. J Immunol Methods. 2013;390(1-2):52-62.
20. Ito T, Smrz D, Jung MY, et al. Stem cell factor programs the mast cell activation phenotype. J Immunol. 2012;188(11):5428-5437.
21. Gao SP, Mark KG, Leslie K, et al. Mutations in the EGFR kinase domain mediate STAT3 activation via IL-6 production in human lung adenocarcinomas. J Clin Invest. 2007;117(12):3846-3856.
22. Grivennikov S, Karin M. Autocrine IL-6 signaling: a key event in tumorigenesis? Cancer Cell. 2008;13(1):7-9.
23. Lee H, Deng J, Kujawski M, et al. STAT3-induced S1PR1 expression is crucial for persistent STAT3 activation in tumors. Nat Med. 2010;16(12):1421-1428.
24. Yao Z, Fenoglio S, Gao DC, et al. TGF-beta IL-6 axis mediates selective and adaptive mechanisms of resistance to molecular targeted therapy in lung cancer. Proc Natl Acad Sci U S A. 2010;107(35):15535-15540.
25. Harir N, Boudot C, Friedbichler K, et al. Oncogenic Kit controls neoplastic mast cell growth through a Stat5/PI3-kinase signaling cascade. Blood. 2008;112(6):2463-2473.
26. Guo X, Gerl RE, Schrader JW. Defining the involvement of p38alpha MAPK in the production of anti- and proinflammatory cytokines using an SB 203580-resistant form of the kinase. J Biol Chem. 2003;278(25): 22237-22242.
27. Kopantzev Y, Heller M, Swaminathan N, Rudikoff S. IL-6 mediated activation of STAT3 bypasses Janus kinases in terminally differentiated B lineage cells. Oncogene. 2002;21(44):6791-6800.
28. Li J, Lan T, Zhang C, et al. Reciprocal activation between IL-6/STAT3 and NOX4/Akt signalings promotes proliferation and survival of non-small cell lung cancer cells. Oncotarget. 2015;6(2):1031-1048.
29. Grimwade LF, Happerfield L, Tristram C, et al. Phospho-STAT5 and phospho-Akt expression in chronic myeloproliferative neoplasms. Br J Haematol. 2009; 147(4):495-506.
30. Lasho T, Tefferi A, Pardanani A. Inhibition of JAK-STAT signaling by TG101348: a novel mechanism for inhibition of KITD816V-dependent growth in mast cell leukemia cells. Leukemia. 2010;24(7):1378-1380.
31. Morales JK, Falanga YT, Depcrynski A, Fernando J, Ryan JJ. Mast cell homeostasis and the JAK-STAT pathway. Genes Immun. 2010;11(8):599-608.
32. Rane SG, Reddy EP. Janus kinases: components of multiple signaling pathways. Oncogene. 2000;19(49):5662-5679.
33. Jain N, Zhang T, Fong SL, Lim CP, Cao X. Repression of Stat3 activity by activation of mitogen-activated protein kinase (MAPK). Oncogene. 1998;17(24):3157-3167.

34. Chang Q, Daly L, Bromberg J. The IL-6 feed-forward loop: a driver of tumorigenesis. Semin Immunol. 2014;26(1):48-53.
35. Yoon S, Woo SU, Kang JH, et al. NF-kappaB and STAT3 cooperatively induce IL6 in starved cancer cells. Oncogene. 2012; 31(29):3467-3481.
36. Nguyen HN, Noss EH, Mizoguchi F, et al. Autocrine Loop Involving IL-6 Family Member LIF, LIF Receptor, and STAT4 Drives Sustained Fibroblast Production of Inflammatory Mediators. Immunity. 2017; 46(2):220-232.
37. Barnstein BO, Li G, Wang Z, et al. Stat5 expression is required for IgE-mediated mast cell function. J Immunol. 2006; 177(5):3421-3426.
38. Teodosio C, Garcia-Montero AC, Jara-Acevedo M, et al. Gene expression profile of highly purified bone marrow mast cells in systemic mastocytosis. J Allergy Clin Immunol. 2013;131(4):1213-1224.
39. Baumgartner C, Cerny-Reiterer S, Sonneck K, et al. Expression of activated STAT5 in neoplastic mast cells in systemic mastocytosis: subcellular distribution and role of the transforming oncoprotein KIT D816V. Am J Pathol. 2009;175(6):2416-2429.
40. Decker T, Kovarik P. Serine phosphorylation of STATs. Oncogene. 2000; 19(21):2628-2637.
41. Bromberg J, Wang TC. Inflammation and cancer: IL-6 and STAT3 complete the link. Cancer Cell. 2009;15(2):79-80.
42. Kawashima T, Murata K, Akira S, et al. STAT5 induces macrophage differentiation of M1 leukemia cells through activation of IL-6 production mediated by NF-kappaB p65. J Immunol. 2001;167(7):3652-3660.
43. Xu R, Nelson CM, Muschler JL, Veiseh M, Vonderhaar BK, Bissell MJ. Sustained activation of STAT5 is essential for chromatin remodeling and maintenance of mammary-specific function. J Cell Biol. 2009;184(1): 57-66.
44. Bibi S, Arslanhan MD, Langenfeld F, et al. Co-operating STAT5 and AKT signaling pathways in chronic myeloid leukemia and mastocytosis: possible new targets of therapy. Haematologica. 2014;99(3):417-429.
45. Shelburne CP, McCoy ME, Piekorz R, et al. Stat5 expression is critical for mast cell development and survival. Blood. 2003; 102(4):1290-1297.
46. Nievergall E, Reynolds J, Kok CH, et al. TGF-alpha and IL-6 plasma levels selectively identify CML patients who fail to achieve an early molecular response or progress in the first year of therapy. Leukemia. 2016;30(6): 1263-1272.
47. Welner RS, Amabile G, Bararia D, et al. Treatment of chronic myelogenous leukemia by blocking cytokine alterations found in normal stem and progenitor cells. Cancer Cell. 2015;27(5):671-681.
48. Nelson EA, Walker SR, Weisberg E, et al. The STAT5 inhibitor pimozide decreases survival of chronic myelogenous leukemia cells resistant to kinase inhibitors. Blood. 2011;117(12):3421-3429.
49. Friedbichler K, Kerenyi MA, Kovacic B, et al. Stat5a serine 725 and 779 phosphorylation is a prerequisite for hematopoietic transformation. Blood. 2010;116(9):1548-1558.
50. Pircher TJ, Petersen H, Gustafsson JA, Haldosen LA. Extracellular signal-regulated kinase (ERK) interacts with signal transducer and activator of transcription (STAT) 5a. Mol Endocrinol. 1999;13(4):555-565.

Ferrata Storti Foundation

Haematologica 2020
Volume 105(1):136-147

The vascular bone marrow niche influences outcome in chronic myeloid leukemia *via* the E-selectin - SCL/TAL1 - CD44 axis

Parimala Sonika Godavarthy,[1] Rahul Kumar,[1] Stefanie C. Herkt,[2] Raquel S. Pereira,[1] Nina Hayduk,[1] Eva S. Weissenberger,[1] Djamel Aggoune,[1] Yosif Manavski,[3] Tina Lucas,[3] Kuan-Ting Pan,[4] Jenna M. Voutsinas,[5] Qian Wu,[5] Martin C. Müller,[6] Susanne Saussele,[7] Thomas Oellerich,[8,9] Vivian G. Oehler,[10] Joern Lausen[2] and Daniela S. Krause[1,9,11,12]

[1]Georg-Speyer-Haus, Institute for Tumor Biology and Experimental Therapy, Frankfurt am Main, Germany; [2]Institute for Transfusion Medicine DRK- Blutspendedienst Baden-Württemberg – Hessen, Frankfurt am Main, Germany; [3]Institute of Cardiovascular Regeneration, Center for Molecular Medicine, Goethe University Frankfurt, Frankfurt am Main, Germany; [4]Bioanalytical Mass Spectrometry Group, Max Planck Institute for Biophysical Chemistry, Göttingen, Germany; [5]Fred Hutchinson Cancer Research Center, Clinical Research Division, Biostatistics, Seattle, WA, USA; [6]Institute for Hematology and Oncology, Mannheim, Germany; [7]Department of Hematology and Oncology, University Hospital Mannheim, Heidelberg University, Mannheim, Germany; [8]Department of Internal Medicine, Hematology/Oncology, Goethe University, Frankfurt am Main, Germany; [9]German Cancer Research Center and German Cancer Consortium, Heidelberg, Germany; [10]Fred Hutchinson Cancer Research Center, Clinical Research Division, Division of Hematology, University of Washington Medical Center, Seattle, WA, USA; [11]Faculty of Medicine, Johann Wolfgang Goethe University, Frankfurt and [12]Frankfurt Cancer Institute, Frankfurt, Germany

ABSTRACT

The endosteal bone marrow niche and vascular endothelial cells provide sanctuaries for leukemic cells. In murine chronic myeloid leukemia (CML) CD44 on leukemia cells and E-selectin on bone marrow endothelium are essential mediators for the engraftment of leukemic stem cells. We hypothesized that non-adhesion of CML-initiating cells to E-selectin on the bone marrow endothelium may lead to superior eradication of leukemic stem cells in CML after treatment with imatinib than imatinib alone. Indeed, here we show that treatment with the E-selectin inhibitor GMI-1271 in combination with imatinib prolongs survival of mice with CML via decreased contact time of leukemia cells with bone marrow endothelium. Non-adhesion of BCR-ABL1$^+$ cells leads to an increase of cell cycle progression and an increase of expression of the hematopoietic transcription factor and proto-oncogene *Scl/Tal1* in leukemia-initiating cells. We implicate SCL/TAL1 as an indirect phosphorylation target of BCR-ABL1 and as a negative transcriptional regulator of CD44 expression. We show that increased *SCL/TAL1* expression is associated with improved outcome in human CML. These data demonstrate the BCR-ABL1-specific, cell-intrinsic pathways leading to altered interactions with the vascular niche via the modulation of adhesion molecules – which could be exploited therapeutically in the future.

Correspondence:

DANIELA S. KRAUSE
krause@gsh.uni-frankfurt.de

Received: November 26, 2018.

Accepted: April 23, 2019.

Pre-published: April 24, 2019.

doi:10.3324/haematol.2018.212365

Check the online version for the most updated information on this article, online supplements, and information on authorship & disclosures: www.haematologica.org/content/105/1/136

Introduction

The bone marrow (BM) microenvironment and in particular the endosteal BM niche,[1] vascular endothelial cells,[2] as well as secreted factors and mesenchymal stromal cells,[3,4] protect leukemic stem cells (LSC) from eradication by various therapies, thereby leading to treatment resistance, disease relapse and disease progression. E-selectin, an adhesion molecule exclusively expressed on endothelial cells and activated by cytokines, is an essential component of the vascular niche in the BM microenvironment, where it promotes the proliferation of normal hematopoietic stem cells (HSC).[5] E-selectin[6] and one of its ligands,[7] CD44,[8] have been shown to be

essential mediators of engraftment of chronic myeloid leukemia (CML)-initiating cells. However, the mechanism for overexpression of CD44 on leukemia-initiating cells (LIC) in CML mediating engraftment, as previously described by us,[8] has not been established. CD44, known to mediate the transport of acute myeloid leukemia cells to stem cell-supportive niches,[9] also acts as an E-selectin ligand on colon cancer[10] and breast cancer cells.[11]

GMI-1271 is a specific small molecule antagonist of E-selectin with a dissociation constant of 0.54 μM. Co-administration of GMI-1271 was recently demonstrated to overcome resistance to bortezomib in E-selectin ligand-enriched multiple myeloma cells,[12] and GMI-1271 is currently being tested in clinical trials in combination with chemotherapy in patients with acute myeloid leukemia. It is surmised that - similar to mobilization by granulocyte colony-stimulating factor[13,14] - GMI-1271-mediated mobilization of LSC may break LSC dormancy and, thereby, lead to improved eradication by tyrosine kinase inhibitors or chemotherapy. We had previously shown that targeting the osteolineage compartment of the BM microenvironment can lead to successful reduction of LSC in CML.[15] Imatinib, a tyrosine kinase inhibitor targeting BCR-ABL1, the oncoprotein causing CML, does not eradicate LSC.[16,17] We hypothesized that treatment with GMI-1271 may lead to non-adhesion of CML-initiating cells to the BM endothelium and in combination with imatinib may be better at eliminating LSC in CML than imatinib alone.

Indeed, in this study we show that inhibition of E-selectin leads to a dissociation of BCR-ABL1$^+$ cells from the endothelium. Concomitantly, this leads to increased leukemic cell proliferation and upregulation of the hematopoietic transcription factor and proto-oncogene *Scl/Tal1*, whose overexpression is frequently found in T-cell acute lymphoblastic leukemia.[18] SCL/TAL1, itself phosphorylated by pAKT downstream of BCR-ABL1, is demonstrated to be a negative transcriptional regulator of CD44. Collectively, these data illustrate the reciprocal link between external cues from the BM microenvironment and LSC-intrinsic effects which, in turn, can influence LSC expression of adhesion molecules essential for interaction with the BM microenvironment and, thereby, modify therapy response. This is a concept which could influence future treatment strategies.

Methods

Additional methods are described in the *Online Supplementary Material*.

Mice

BALB/c or FVB mice were purchased from Charles River Laboratories (Wilmington, MA, USA). Rag-2$^{-/-}$ CD47$^{-/-}$ IL-2 receptor γ$^{-/-}$ (C57/Bl6 background) and Tie2-GFP mice (FVB background) were bred in our institute. All murine studies were approved by the local animal care committee (Regierungspräsidium Darmstadt).

Statistical analysis

Statistical significance between different treatment groups was assessed by the Student *t*-test or analysis of variance (ANOVA) test (with a Tukey test as a post-hoc test) using Prism Version 6 software (GraphPad, La Jolla, CA, USA). Differences in survival were assessed by Kaplan-Meier nonparametric tests (log-rank or Wilcoxon tests). Data are presented as the mean ± standard deviation and differences are considered statistically significant when $P \leq 0.05$.

Results

GMI-1271 decreases the contact time of human chronic myeloid leukemia cells with bone marrow endothelium

In order to test whether inhibition of E-selectin by GMI-1271 decreases adhesion of human CML cells to BM endothelium, we injected leukocytes from five different human CML patients into Rag-2$^{-/-}$CD47$^{-/-}$IL-2 receptor γ$^{-/-}$ mice[19] treated with vehicle or GMI-1271 and imaged the calvarium of the injected mice by *in vivo* microscopy (Figure 1A and *Online Supplementary Movie*). This revealed a significantly reduced contact time of leukemia cells from four out of five patients with BM endothelium in mice treated with GMI-1271 ($P<0.0001$, Figure 1B and *Online Supplementary Figure S1A-D*). As anticipated, this result suggested that GMI-1271 leads to non-adhesion of human cells to the BM endothelium. Furthermore, in an *in vitro* adhesion assay of human CML cells plated on E-selectin, a smaller number of human CML cells adhered to E-selectin in the presence of GMI-1271 than in the presence of vehicle ($P=0.0013$) (Figure 1C).

Inhibition of E-selectin affects survival in mice with chronic myeloid leukemia

Next, we tested the effect of inhibition of E-selectin in combination with imatinib mesylate, considered the standard of care for CML, on the survival of mice with CML. Treatment of murine recipients of BCR-ABL1-transduced BM in the retroviral transduction/ transplantation model of CML-like myeloproliferative neoplasia[15,20] with vehicle, imatinib, GMI-1271 or a combination of imatinib and GMI-1271 (*Online Supplementary Figure S2A*) revealed a modest, but significant prolongation of survival in mice that received the combination therapy compared to mice that received imatinib alone ($P=0.028$) (Figure 1D) with all mice succumbing to BCR-ABL1$^+$ leukemia and pulmonary infiltration by mature neutrophils, as described elsewhere.[8,15] Leukocyte counts ($P=0.0008$) (*Online Supplementary Figure S2B*), BCR-ABL1$^+$ (GFP$^+$) CD11b$^+$ myeloid cells ($P=0.031$) (*Online Supplementary Figure S2C*) and spleen weights ($P=0.024$) (*Online Supplementary Figure S2D*) were significantly reduced in mice with CML treated with imatinib plus GMI-1271, when compared to vehicle-treated mice. However, the direct comparison of treatment with imatinib plus GMI-1271 *vs*. imatinib alone did not reveal a statistically significant difference. A significant reduction of GFP (BCR-ABL1)$^+$ Lin$^-$ c-Kit$^+$ (LK) cells, which harbor the LSC fraction in this model,[21] was observed in mice treated with imatinib and GMI-1271, when compared to vehicle-treated mice ($P=0.001$) (*Online Supplementary Figure S2E*). Lin$^-$ GFP$^+$ (BCR-ABL1$^+$) cells from CML mice ($P=0.001$) (Figure 1E) or BCR-ABL1$^+$ BaF3 cells ($P=0.002$) (*Online Supplementary Figure S2F*) injected into Tie2-GFP mice, which express green fluorescent protein (GFP) under the TEK receptor tyrosine kinase (*Tie2*)-promoter, were found significantly further away from the endothelium, but not the bone (*Online Supplementary Figure S2G-H*), when mice had been treated with GMI-

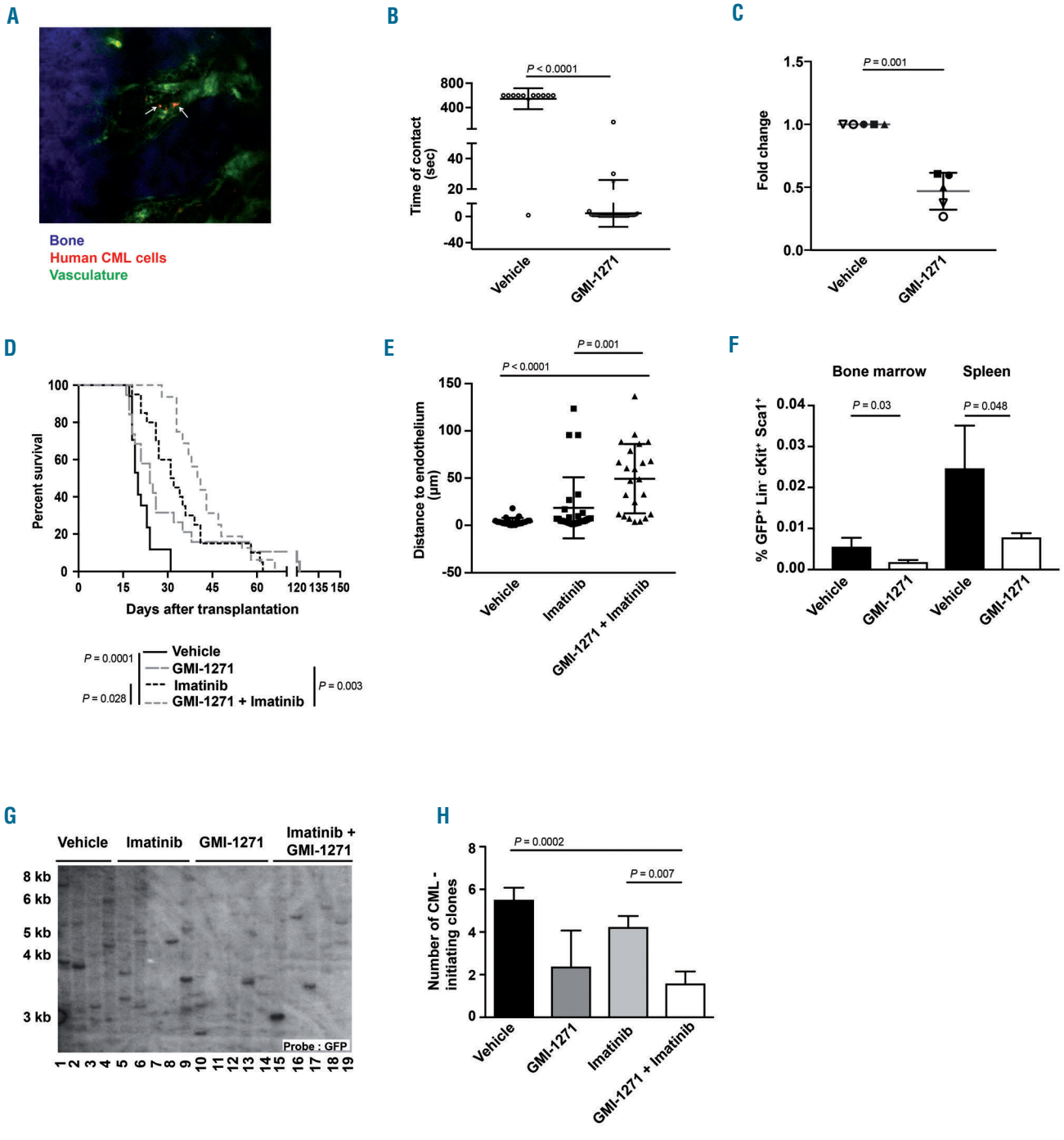

Figure 1. Inhibition of E-selectin affects survival in mice with chronic myeloid leukemia. (A) Representative two-photon *in vivo* microscopy image of the bone marrow (BM) calvarium of an unirradiated Rag-2$^{-/-}$CD47$^{-/-}$IL-2 receptor $\gamma^{-/-}$ mouse injected with 200,000-500,000 unsorted human chronic myeloid leukemia (CML) cells [from peripheral blood (PB) or BM], labeled with CMTMR (orange; white arrows), 2 h prior to *in vivo* microscopy. Vessels were visualized via the injection of dextran-FITC (1 mg per injection), while bones were visualized in blue due to second harmonic generation. The scale bar represents 50 µm. (B) Time of contact (seconds), determined by *in vivo* microscopy, between the calvarial endothelium and human unsorted CML cells from the PB of one patient labeled with CMTMR and injected into vehicle- or GMI-1271 (20 mg/kg/dose)-treated unirradiated Rag-2$^{-/-}$CD47$^{-/-}$IL-2 receptor $\gamma^{-/-}$ mice (P<0.0001, *t*-test). The mice had been treated with vehicle or GMI-1271 2 h before transplantation. (C) Adhesion (presented as fold change) of unsorted human CML cells from PB or BM to E-selectin-coated wells (50,000 CML cells/well) in the presence of vehicle *vs.* GMI-1271 (P=0.001, *t*-test) (n=5) after incubation for 6 h. Different symbols signify individual patients. The experiment was performed in duplicate. (D) Kaplan-Meier-style survival curve for Balb/c recipients of BCR-ABL1-transduced BM treated with vehicle (black solid line), 20 mg/kg/dose GMI-1271 intraperitoneally (long gray dashes), 100 mg/kg imatinib orally (black dots) and the combination of both imatinib and GMI-1271 (short gray dashes) beginning on day 9 after transplantation. Vehicle and imatinib were administered daily, while GMI-1271 was given twice daily. The difference in survival between mice treated with imatinib or imatinib plus GMI-1271 was statistically significant (P=0.028, log-rank test, n=15). (E) Distance (in µm) from endothelium of CMTMR-labeled GFP$^+$ (BCR-ABL1$^+$) Lin$^-$ cells (200,000) from FVB mice with established CML-like disease transplanted by intravenous injection into Tie2-GFP mice (FVB background) and imaged by *in vivo* microscopy 19 h after injection [P=0.001, analysis of variance /(ANOVA); Tukey test]. The imaging analysis was performed by ImageJ. (F) Percentage of GFP$^+$ (BCR-ABL1$^+$) Lin$^-$ c-Kit$^+$ Sca-1$^+$ cells of total leukocytes which homed to the BM (P=0.03, *t*-test) or spleen (P=0.048, *t*-test) of vehicle (black)- or GMI-1271 (white)-treated mice 18 h after transplantation (n=4). A total of 2.5 × 10^6 unsorted, BCR-ABL1-transduced cells had been injected. (G, H) Southern blot showing distinct proviral integration sites and, consequently, disease clonality in spleens (taken at the time of death, as shown in Figure 1D) of Balb/c recipients of BCR-ABL1-transduced BM treated with vehicle (lanes 1-4), imatinib (lanes 5-9), GMI-1271 (lanes 10-14) or imatinib plus GMI-1271 (lanes 15-19) (G) and disease clonality (H). The difference in disease clonality between imatinib- and imatinib plus GMI-1271-treated recipients as a measure of engraftment of leukemia-initiating clones is statistically significant (P=0.007, ANOVA; Tukey test). Data are expressed as mean ± standard deviation.

1271 and imatinib than when they had been treated with vehicle or imatinib alone. Short-term homing of CML-initiating cells to BM (P=0.03) (Figure 1F) and spleen (P=0.048) (Figure 1F) of GMI-1271-treated recipients was impaired compared to that of vehicle-treated recipients. Long-term engraftment of CML-initiating clones, as measured by the enumeration of distinct proviral integration events in splenic tissue of diseased mice by Southern blotting, was significantly reduced in primary mice treated with imatinib plus GMI-1271 compared to those treated with imatinib alone (P=0.007) (Figure 1G, H).

In summary, these data suggest that in comparison to monotherapy with imatinib, inhibition of E-selectin in combination with imatinib mildly prolongs survival in mice with a CML-like myeloproliferative neoplasia via a reduction of homing and long-term engraftment of CML-initiating clones. Inhibition of E-selectin also reduces the number of human CML cells adhering to E-selectin.

Inhibition of E-selectin leads to an increase of *Scl/Tal1* in BCR-ABL1$^+$ leukemia-initiating cells

In order to explain the prolonged survival of mice treated with imatinib and GMI-1271, we tested the adhesion and gene expression of cell cycle-relevant genes and transcription factors in LIC in the presence of GMI-1271. To do so, we plated BCR-ABL1$^+$ Lin$^-$ c-Kit$^+$ BM cells from mice with CML on E-selectin-coated plates in the presence of vehicle, GMI-1271,[22] imatinib[23,24] or the combination of GMI-1271 plus imatinib (Figure 2A). As expected, this revealed that treatment with GMI-1271 (P=0.02) or GMI-1271 plus imatinib (P=0.029) significantly reduced the number of adherent cells (Figure 2B). In a competitive inhibition assay we plated BCR-ABL1$^+$ BaF3 cells, which were used because sufficient numbers of LIC can only be retrieved from a large number of diseased mice, on plates pre-coated with E-selectin, while adding soluble E-selectin to the BCR-ABL1$^+$ BaF3 cells treated with GMI-1271. This reversed the decreased adhesion of leukemia cells in the presence of GMI-1271 (P=0.021) (*Online Supplementary Figure S3A*) suggesting a specific role of E-selectin in this process. Furthermore, non-adhesion of primary murine BCR-ABL1$^+$ LIC (P=0.017) (Figure 2C) or K562 cells (P=0.007) (*Online Supplementary Figure S3B*), which were tested in order to show the validity also in a human cell line, to E-selectin in the presence of GMI-1271 led to an increase of the transcription factor and cell cycle regulator[25] stem cell leukemia/T-cell acute lymphocytic leukemia protein 1 (*Scl/Tal1*). Other transcription factors, however, did not significantly change in K562 cells (*Online Supplementary Figure S3C-G, Online Supplementary Table S1*). Conversely, addition of soluble E-selectin to BCR-ABL1$^+$ BaF3 cells plated on E-selectin in the presence of GMI-1271 (as in *Online Supplementary Figure S3A*) decreased the expression of *Scl/Tal1* (P=0.028) (*Online Supplementary Figure S4A*). In summary, these data suggest that E-selectin is involved in adhesion of CML cells and that non-adhesion leads to increased expression of *Scl/Tal1*.

Scl/Tal1 regulates CD44 expression

As SCL/TAL1 is a known transcriptional regulator involved in various hematologic malignancies and cell cycle progression,[25] we performed a gene expression screen after knockdown of *SCL/TAL1* in K562 cells (data deposited in the GEO-Expression database, GSE92251). This revealed that knockdown of *SCL/TAL1* led to an upregulation of CD44[26] (Figure 3A). As we had previously shown CD44[8] and its receptor E-selectin[6,7] to be important mediators of the engraftment of LIC in CML, we hypothesized that SCL/TAL1 may regulate the expression of CD44 on CML cells, where CD44 is known to be overexpressed[8] – albeit through an unknown mechanism.

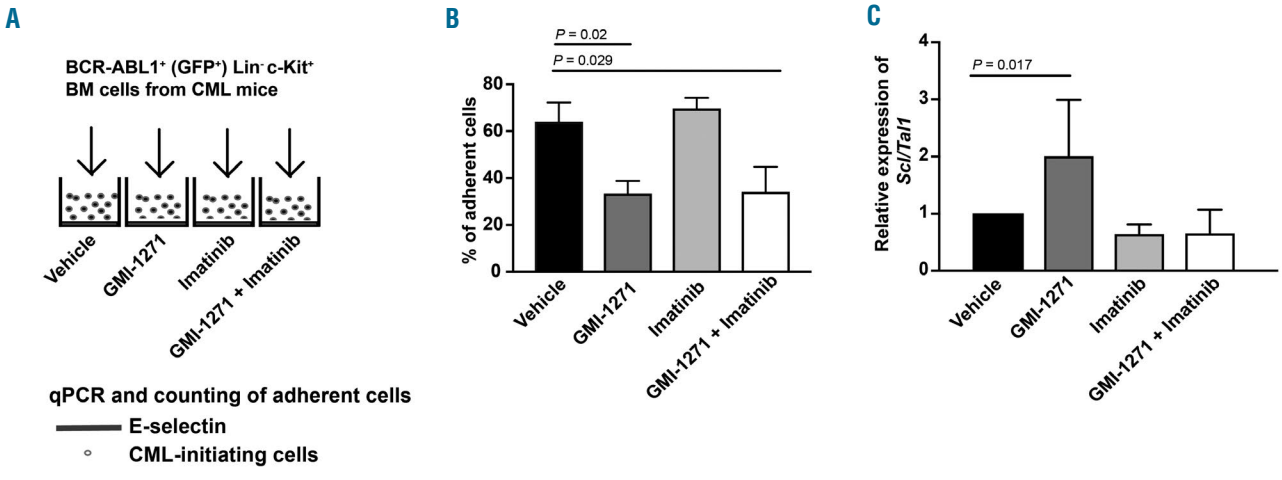

Figure 2. Inhibition of E-selectin leads to an increase of *Scl/Tal1* in BCR-ABL1$^+$ leukemia-initiating cells. (A) Schematic of an *in vitro* adhesion assay, in which 20,000 GFP$^+$ (BCR-ABL1$^+$) Lin$^-$ c-Kit$^+$ bone marrow cells from mice with chronic myeloid leukemia treated with vehicle, GMI-1271, imatinib or the combination of GMI-1271 plus imatinib were plated on recombinant E-selectin in the presence of the respective drugs for 6 h. (B) Percentage of adherent GFP$^+$ (BCR-ABL1$^+$) Lin$^-$ c-Kit$^+$ of total cells after 6 h of incubation on recombinant E-selectin in the presence of vehicle (black), 20 μM GMI-1271 (dark gray), 10 μM imatinib (light gray) or imatinib plus GMI-1271 (white) and several washing steps, normalized by the number of live cells. Twenty thousand cells per well were plated in triplicate. The percentage of adherent cells was reduced by treatment with GMI-1271 or imatinib plus GMI-1271 compared to vehicle [P=0.02 or P=0.029, respectively, analysis of variance (ANOVA); Tukey test, n=4]. (C) Relative expression of *Scl/Tal1* in all GFP$^+$ (BCR-ABL1$^+$) Lin$^-$ c-Kit$^+$ cells plated on recombinant E-selectin as in (A) and (B) in the presence of vehicle (black), GMI-1271 (dark gray), imatinib (light gray) or imatinib plus GMI-1271 (white). The expression of *Scl/Tal1* in GMI-1271-treated cells was significantly increased compared to that of vehicle-treated cells (P=0.017, ANOVA; Tukey test, n=3). BM: bone marrow; CML: chronic myeloid leukemia; qPCR: real-time polymerase chain reaction.

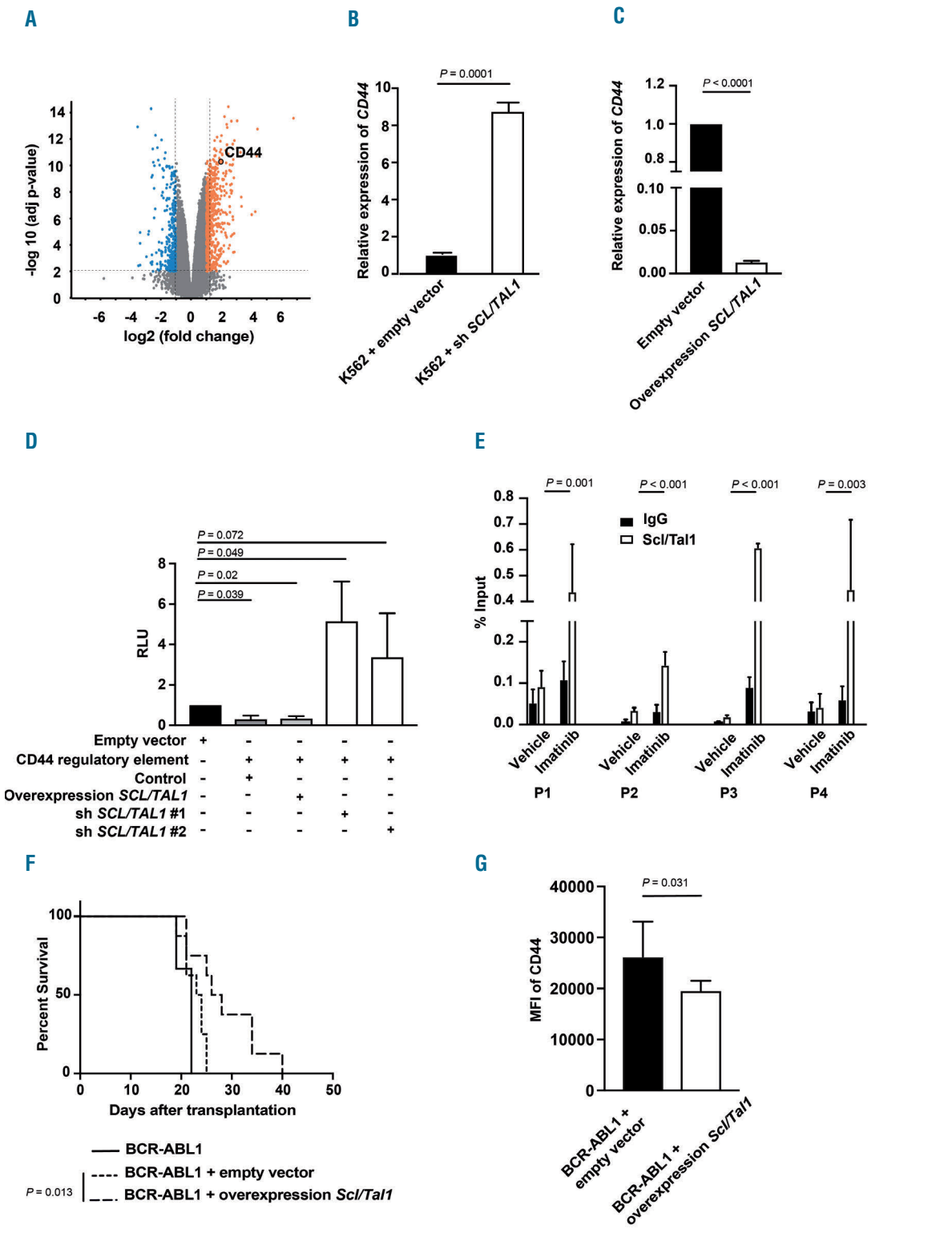

Figure 3. Scl/Tal1 regulates CD44 expression. (A) Volcano plot showing up- or down-regulated genes in K562 cells after knockdown of *SCL/TAL1* relative to knockdown of lacZ as a control. The x-axis indicates the fold change and the y-axis indicates the $-\log_{10}$ *P* value. The orange and blue highlighted regions show 2-fold up- and down-regulated genes, respectively, with a *P* value ≤0.05. CD44 has been circled. (B, C) Relative expression of *CD44* in K562 cells after infection with a *SCL/TAL1* shRNA-expressing or empty vector control (*P*=0.0001, *t*-test) (B) or an empty vector control- or a *SCL/TAL1*-overexpressing lentivirus (*P*<0.0001, *t*-test) (C). (D) Relative luminescence units (RLU) in a luciferase assay of K562 cells transfected with empty vector (control, black) or a plasmid expressing the *CD44* regulatory element alone [*P*=0.039, analysis of variance (ANOVA); Tukey test], or the same *CD44*-regulatory element-transfected K562 cells transduced with a *SCL/TAL1*-overexpressing lentivirus (*P*=0.02, ANOVA; Tukey test) or transduced with two different sh*SCL/TAL1*-expressing lentiviruses (*P*=0.049 and *P*=0.072, ANOVA; Tukey test, n=4). (E) Binding of SCL/TAL1 to the *CD44* regulatory element in K562 cells treated with vehicle or imatinib as measured by a chromatin immunoprecipitation assay using an anti-SCL/TAL1 (white) or a control IgG (black) antibody and four different *CD44* primer pairs (P1-P4). (F) Kaplan-Meier-style survival curve for Balb/c recipients of BCR-ABL1-transduced bone marrow (BM) (solid line) or BCR-ABL1-transduced BM cotransduced with empty vector (dotted line) or cotransduced with an *Scl/Tal1*-overexpressing lentivirus (dashed line) (*P*=0.013, log-rank test, n=8). (G) Median fluorescence intensity (MFI) of CD44 on BCR-ABL1$^+$ CD11b$^+$ myeloid cells from recipients of BCR-ABL1-transduced BM (black) or BCR-ABL1-transduced BM cotransduced with empty vector (black) or cotransduced with a *Scl/Tal1*-overexpressing vector (white) as in (F) (*P*=0.031, *t*-test, n=6).

Indeed, specific knockdown of *SCL/TAL1* in K562 cells led to upregulation of CD44 (P=0.0001) (Figure 3B and *Online Supplementary Figure S5A*) and, conversely, overexpression of *SCL/TAL1* in K562 (P<0.0001) (Figure 3C and *Online Supplementary Figure S5B, C*) or in human CD34$^+$ cells (P=0.0001) (*Online Supplementary Figure S5D*) led to decreased expression of *CD44*. We performed luciferase assays on K562 cells transfected with a control plasmid or a CD44 regulatory element with SCL/TAL1-binding sites and transduced with *SCL/TAL1* shRNA- or *SCL/TAL1*-overexpressing lentivirus, in order to test activity of the CD44 regulatory element (*Online Supplementary Figure S5E*). This revealed decreased activity of the CD44 regulatory element when *SCL/TAL1* was overexpressed (P=0.02) (Figure 3D and *Online Supplementary Figure S5B, C*) and increased activity when *SCL/TAL1* was knocked down (P=0.049) (Figure 3D and *Online Supplementary Figure S5A*). Having shown the influence of SCL/TAL1 on the activity of the *CD44* regulatory element, we tested the dependence of this on BCR-ABL1 in a chromatin immunoprecipitation assay using K562 cells treated with vehicle or imatinib. This revealed that imatinib treatment significantly increased the binding of SCL/TAL1 to the *CD44* regulatory element (Figure 3E and *Online Supplementary Figure S6A*), but not to a control region (*Online Supplementary Figure S6B*). Furthermore, overexpression of *SCL/TAL1* (*Online Supplementary Figure S7A*) in BCR-ABL1$^+$ LIC *in vivo* significantly prolonged survival (P=0.013) (Figure 3F), led to decreased median fluorescence intensity of CD44 on BCR-ABL1$^+$ CD11b$^+$ myeloid cells (P=0.031) (Figure 3G) and a trend towards decreased disease clonality (*Online Supplementary Figure S7B*) in murine recipients in our CML model. This resembled what we had observed when using CD44-deficient BCR-ABL1$^+$ donor BM,[8] although the effect was not as pronounced. Overexpression of *SCL/TAL1* in K562 cells (*Online Supplementary Figure S5B*) also decreased the median fluorescence intensity of CD44 (P=0.019) (*Online Supplementary Figure S5C*). Taken together, these data suggest that SCL/TAL1 negatively regulates the expression of CD44 and that overexpression of *SCL/TAL1* on LIC leads to prolongation of survival in CML, similar to the effect of CD44 deficiency on CML-initiating cells.[8]

Binding of CD44 to E-selectin influences the cell cycle of BCR-ABL1$^+$ cells

In order to test the nature of the interaction between CD44 and the BM endothelium directly, we performed *in vivo* imaging of the murine calvarium of live anesthetized mice as shown in Figure 1A, B and *Online Supplementary Figure S1A-D*. Indeed, *in vivo* imaging of CD44-overexpressing BCR-ABL1$^+$ or BCR-ABL1$^+$ BaF3 cells injected into Tie2-GFP mice revealed an increased contact time with the endothelium by CD44-overexpressing BCR-ABL1$^+$ compared to BCR-ABL1$^+$ BaF3 cells (P<0.001) (Figure 4A, B). In recapitulation of our findings with human CML cells (Figure 1B) treatment of mice with GMI-1271 decreased the contact time of BCR-ABL1$^+$ BaF3 cells with BM endothelium (P=0.05) (*Online Supplementary Figure S7C*). Testing a possible influence of CD44, a marker for cancer stem cells,[27] and SCL/TAL1[25] on cell cycle progression via binding to E-selectin, we plated BaF3 cells coexpressing BCR-ABL1 and CD44 on E-selectin in the presence of the four drugs or their combination. This demonstrated that GMI-1271 (with or without imatinib) did not alter the cell cycle of the non-adherent fraction, either when the cells were plated on E-selectin (Figure 4C and *Online Supplementary Figure S8A*), or on bovine serum albumin (*Online Supplementary Figure S8B*). In contrast, cell cycle analysis of the non-adherent fraction of BCR-ABL1$^+$ BaF3 cells plated on E-selectin showed an increase of cells in the G2-S-M phase and a decrease in the G0 phase of the cell cycle in the presence of GMI-1271 (P=0.03 and P=0.01, respectively) (Figure 4D and, *Online Supplementary Figure S8A*) or GMI-1271 plus imatinib (P=0.02) (Figure 4D). No such differences were observed in the adherent fraction (Figure 4E and *Online Supplementary Figure S8A*) or when the BCR-ABL1$^+$ BaF3 cells were plated on bovine serum albumin (*Online Supplementary Figure S8C*). BCR-ABL1$^+$ BaF3 cells plated on E-selectin in the presence of GMI-1271 also exhibited increased expression of the cell cycle promoter cyclin dependent kinase (CDK) 6 (P<0.0001) (Figure 4F), a possible trend towards increased nuclear CDK4 (*Online Supplementary Figure S8D, E*), which has been associated with cell cycle progression, and decreased expression of the cell cycle inhibitor p16 (or cyclin dependent kinase inhibitor 2A) (P<0.0001) (Figure 4G). Consistently, GFP$^+$ (BCR-ABL1$^+$) Lin$^-$ c-Kit$^+$ cells from mice with CML treated with GMI-1271 or GMI-1271 and imatinib had increased proportions of cells in the G2-S-M phase of the cell cycle compared to those treated with vehicle (P=0.01) or imatinib alone (P<0.0001) (Figure 4H). GFP$^+$ (BCR-ABL1$^+$) Lin$^-$ cells also expressed higher levels of SCL/TAL1 (P=0.04) (*Online Supplementary Figure S8F*) and lower levels of p16 (P=0.002) (*Online Supplementary Figure S8G*) when derived from CML mice treated with GMI-1271 compared to vehicle-treated animals. CD44 was significantly more highly expressed on most GFP$^+$ (BCR-ABL1$^+$) progenitor fractions or CD11b$^+$ cells compared to GFP$^-$ (BCR-ABL1$^-$) cells (*Online Supplementary Figure S8H*), in line with our previous results.[8] Taken together, these data suggest that CD44 is involved in mediating contact with BM endothelium. Treatment with GMI-1271 leads to non-adhesion of BCR-ABL1$^+$ cells to E-selectin, an increase in cell cycle and a concomitant increase of *Scl/Tal1* in BCR-ABL1$^+$ cells, which leads to downregulation of CD44. These data suggest a possible role for CD44 in cell cycle regulation of BCR-ABL1$^+$ cells.

Expression of CD44 is synergistically influenced by SCL/TAL1 and BCR-ABL1

In order to test whether the expression of CD44 and/or SCL/TAL1 may be BCR-ABL1-dependent, we treated BaF3 cells transduced with empty vector or BCR-ABL1 with imatinib.[23,24] This led to a significant decrease of the median fluorescence intensity of CD44, specifically on BCR-ABL1$^+$ compared to empty vector-transduced BaF3 cells (P=0.05) (Figure 5A and *Online Supplementary Figure S9A, B*). Furthermore, in the non-adherent, but not the adherent fraction, of BCR-ABL1$^+$ BaF3 cells plated on E-selectin the median fluorescence intensity of CD44 was synergistically reduced by combined treatment with GMI-1271 and imatinib compared to imatinib alone (P=0.05) (Figure 5B). Consistently, in non-adherent, but not adherent, BCR-ABL1$^+$ BaF3 cells plated on E-selectin, expression of SCL/TAL1 and pSCL/TAL1 was significantly higher upon treatment with GMI-1271 or GMI-1271 and imatinib (*Online Supplementary Figure S9C*). These results suggest that the expression of CD44 is BCR-ABL1-dependent and that reduction of CD44 expression by GMI-1271 (via

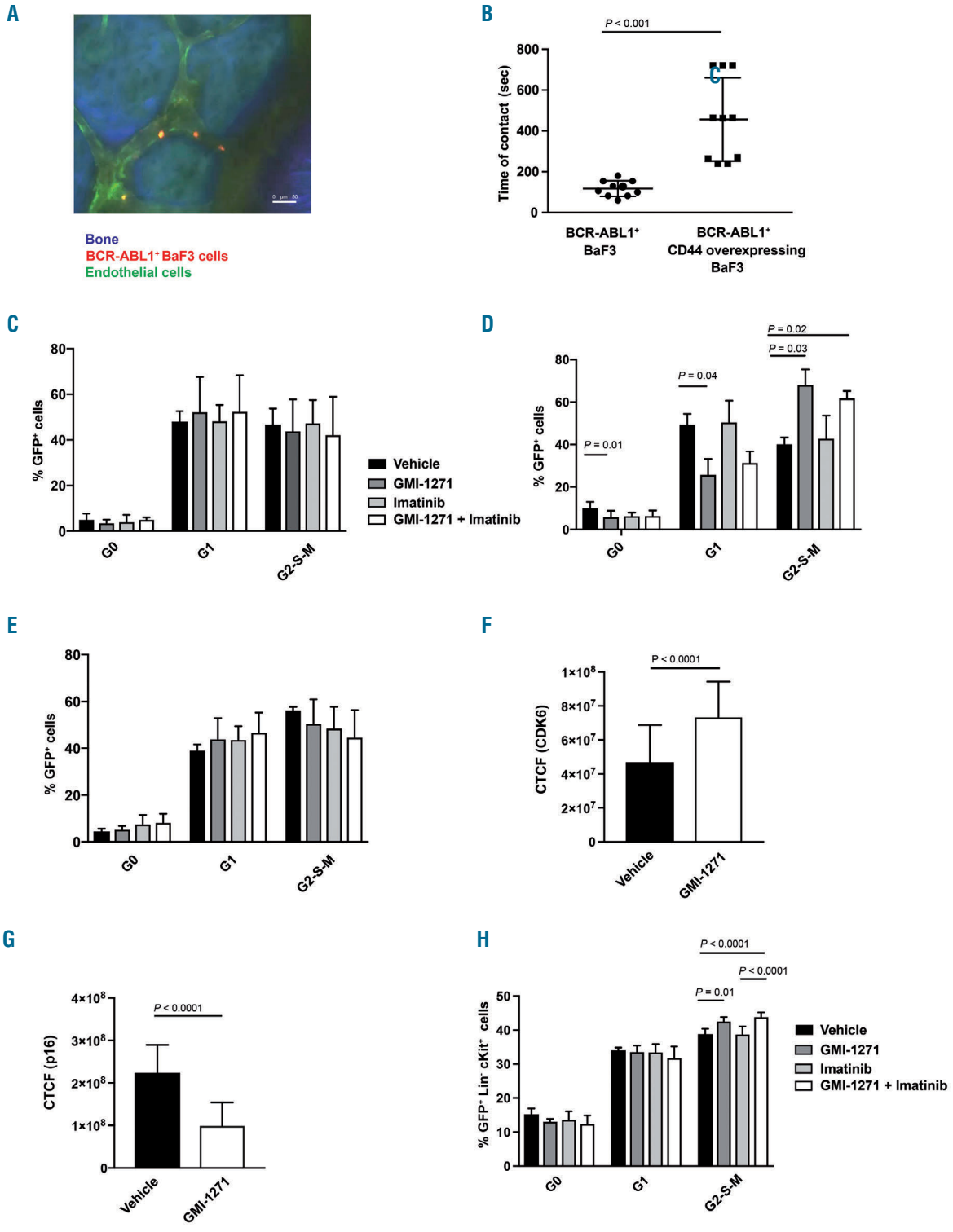

Figure 4. Binding of CD44 to E-selectin influences the cell cycle of BCR-ABL1⁺ cells. (A) Representative two-photon *in vivo* microscopy image of the calvarial bone marrow of an unirradiated Tie2-GFP mouse injected with 1×10⁶ sorted BCR-ABL1⁺ BaF3 cells, labeled with CMTMR (orange), 2 h prior to *in vivo* microscopy. Bones were visualized in blue due to second harmonic generation. The scale bar represents 50 μm. (B) Time of contact (seconds), determined by *in vivo* microscopy as in (A) between the calvarial endothelium and BCR-ABL1⁺ or BCR-ABL1⁺ CD44 overexpressing BaF3 cells labeled with CMTMR and injected into unirradiated Tie2-GFP mice ($P<0.001$, *t*-test, n=3). (C) Cell cycle analysis by Ki67-staining of serum-starved BaF3 cells coexpressing BCR-ABL1 and CD44 plated on E-selectin-coated plates and treated with vehicle, GMI-1271, imatinib or the combination of GMI-1271 plus imatinib. The percentages of GFP⁺ (BCR-ABL1⁺) cells of total in the G0, G1 or G2-S-M phases of the cell cycle are shown. The differences are not statistically significant. (D, E) Cell cycle analysis by Ki67-staining of serum-starved non-adherent (D) or adherent (E) BCR-ABL1⁺ BaF3 cells plated on E-selectin-coated plates and treated with vehicle, GMI-1271, imatinib or the combination of GMI-1271 plus imatinib. The percentages of GFP⁺ (BCR-ABL1⁺) cells of total in the different phases of the cell cycle are shown. Seventy thousand cells were plated and allowed to adhere for 6 h (n=3). (F, G) Corrected total cell fluorescence (CTCF) for CDK6 (F) and p16 (G) in BCR-ABL1⁺ BaF3 cells plated on E-selectin in the adhesion assay, performed in the presence of vehicle or GMI-1271. Seventy thousand cells were plated (n=3). (H) Cell cycle analysis by Ki67-staining of GFP⁺ (BCR-ABL1⁺) Lin⁻ c-Kit⁺ cells from Balb/c mice with established chronic myeloid leukemia treated with vehicle, GMI-1271, imatinib or the combination of GMI-1271 plus imatinib on day 14 after transplantation. The percentages of GFP⁺ (BCR-ABL1⁺) Lin⁻ c-Kit⁺ cells of total in the G0, G1 or G2-S-M phases of the cell cycle are shown (*P* values as indicated, analysis of variance; Tukey test, n=5).

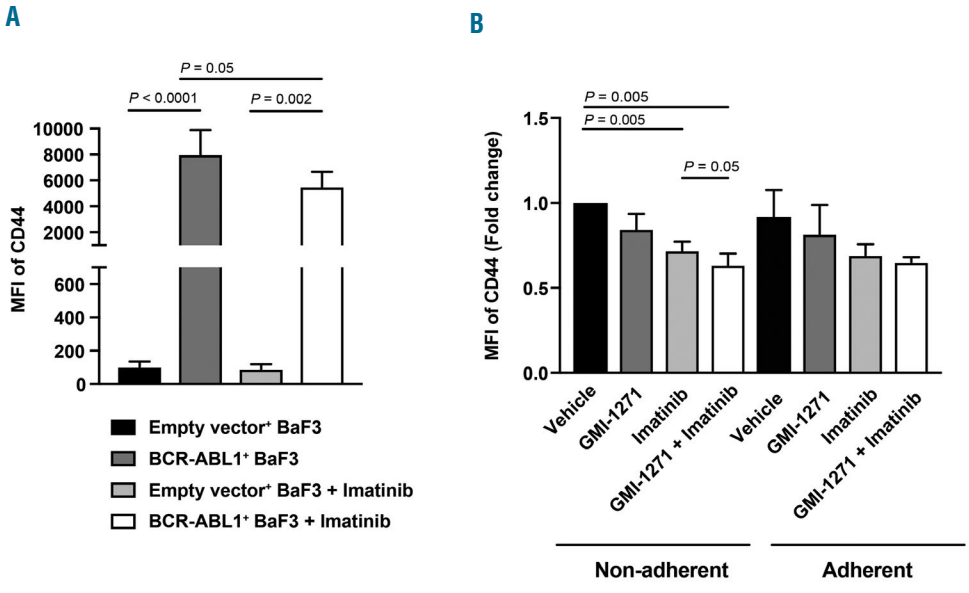

Figure 5. Expression of CD44 is influenced by BCR-ABL1. (A) Median fluorescence intensity (MFI) of CD44 on BaF3 cells transduced with empty vector or BCR-ABL1 plated on E-selectin after treatment with vehicle or 10 μM imatinib [*P* values as indicated, analysis of variance (ANOVA); Tukey test, n=3]. (B) MFI of CD44 (fold change) on the non-adherent and adherent fractions of BCR-ABL1$^+$ BaF3 cells after treatment with vehicle, GMI-1271, imatinib or GMI-1271 and imatinib, normalized to vehicle (*P*=0.005 for vehicle *vs.* GMI-1271 plus imatinib, ANOVA; Tukey test, n=4).

an increase in SCL/TAL1) is synergistically enhanced by cotreatment with imatinib.

CD44 expression influences adhesion and cell cycle status in imatinib-resistant chronic myeloid leukemia

Imatinib-resistance due to the point mutation BCR-ABL1^{T315I} in CML is associated with worse clinical outcome[28,29] and is due to altered interactions between BCR-ABL1^{T315I+} cells and the BM microenvironment.[30] In support of this, the expression of CD44 was higher in BCR-ABL1^{T315I+} than in BCR-ABL1$^+$ BaF3 cells (*Online Supplementary Figure S10A, B*) and also higher than in cells resistant to imatinib due to other point mutations (*P*=0.034) (*Online Supplementary Figure S10B*). Consistently, adhesion of BCR-ABL1^{T315I+} BaF3 cells to E-selectin was increased compared to that of BCR-ABL1$^+$ cells (*P*=0.011) (*Online Supplementary Figure S10C*) and a larger percentage of adherent, but not non-adherent, BCR-ABL1^{T315I+} BaF3 cells were found in the G_0 phase of the cell cycle (*P*=0.042) (*Online Supplementary Figure S10D*). These data support our findings on the role of CD44 in influencing the cell cycle in BCR-ABL1$^+$ cells and suggest that increased CD44 expression and increased binding to E-selectin by BCR-ABL1^{T315I+} cells may contribute to dormancy and imatinib resistance.

BCR-ABL1 modulates SCL/TAL1-binding to the CD44 regulatory element via pAKT

As SCL/TAL1 activity is regulated by phosphorylation at S122 and T90, we hypothesized that a kinase downstream of BCR-ABL1, such as AKT, may be phosphorylating SCL/TAL1.[31] In confirmation of this, we demonstrated that treatment of K562 cells with imatinib, the phosphoinositide-3-kinase (PI3K) inhibitor wortmannin, and in particular the AKT inhibitor MK-2206 reduced the expression of pTal1S122 and pTal1T90 (Figure 6A). Furthermore, quantitative mass spectrometry, performed using triple stable isotope labeling with amino acids in cell culture (SILAC)-labeling of K562 cells treated with vehicle, imatinib or MK-2206, demonstrated the mass increments resulting from medium (+6 Da) or heavy (+10 Da) SILAC-labeling on arginine on the pS122-bearing peptide "oxMVQLpSPPALAAPAAPGR" of SCL/TAL1 in AKT-inhibited cells (Figure 6B and *Online Supplementary Figure S11A*). More precise quantitative measurements by comparing the areas under the extracted ion chromatograms of individual SILAC triplets revealed the decrease of pTal1 S122 both 2 and 4 h after inhibition with imatinib (Figure 6C) or MK-2206 (Figure 6D). Taken together, these data suggest that SCL/TAL1 regulates the expression of CD44 via binding to the *CD44* regulatory element in a BCR-ABL1- and AKT-dependent manner. BCR-ABL1 is known to activate AKT (Figure 6A),[32,33] which phosphorylates SCL/TAL1 at S122 and T90, which in turn regulates the activity of the *CD44* regulatory element by acting as a transcriptional repressor. Binding of SCL/TAL1 leads to decreased expression of CD44, decreased adhesion to the vascular niche in CML and an increase in cell cycling.

SCL/TAL1 influences outcome in human chronic myeloid leukemia

Given our observations in murine models and murine or human CML cells, we correlated levels of *CD44* and *SCL/TAL1* in leukocytes from healthy individuals and patients with CML. This revealed lower delta cycle threshold values for *SCL/TAL1* and higher delta cycle threshold values for *CD44* in healthy individuals (*P*<0.0001) (Figure 7A), while this relationship was reversed in human CML samples (*P*<0.0001) (Figure 7B), suggesting that *SCL/TAL1* also acts as a transcriptional regulator in human CML cells. In order to test the significance of *SCL/TAL1* and/or *CD44* for phase of CML and disease course, we examined published datasets of *SCL/TAL1* and *CD44* gene expression in human CML samples[34,35] and identified that *SCL/TAL1* levels in patients in chronic phase (*P*=0.042) (Figure 7C) and – as a trend - accelerated phase were lower than in normal human CD34$^+$ cells, as expected. *CD44* expression increased with progression of CML from chronic to advanced phase CML with the highest *CD44* expression found in samples from patients in blast crisis (*P*<0.0001) (Figure 7D).

As we did not establish a clear inverse relationship between *SCL/TAL1* and *CD44* expression in samples from individual patients from this dataset, we examined expres-

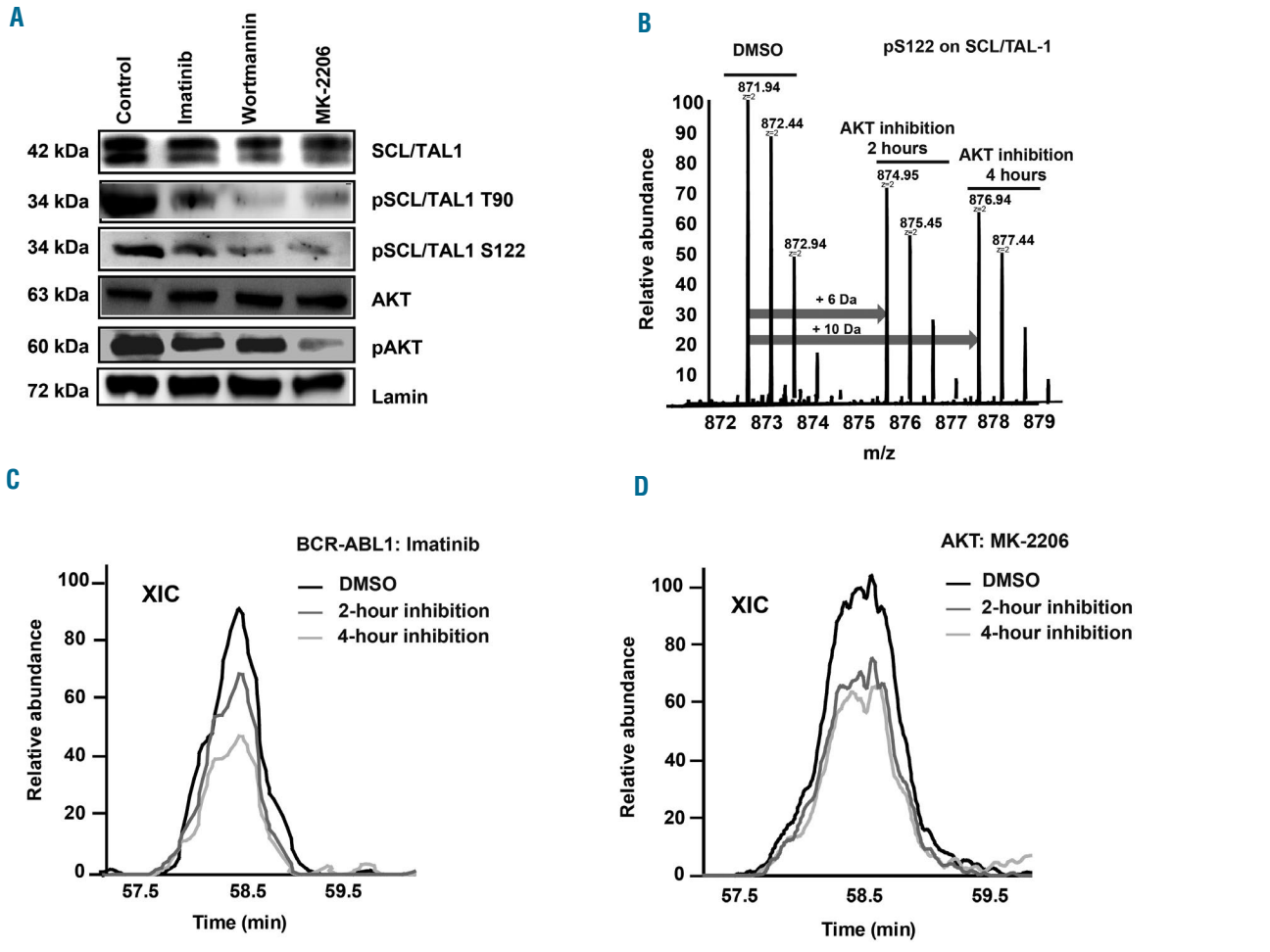

Figure 6. BCR-ABL1 modulates SCL/TAL1-binding to the CD44 regulatory element via pAKT. (A) Immunoblot of lysates of K562 cells treated with vehicle, imatinib (10 μM), the PI3-kinase inhibitor wortmannin (20 μM) or the AKT-inhibitor MK-2206 (20 μM) and probed with antibodies to SCL/TAL1, pSCL/TAL1 T90, pSCL/TAL1S122, AKT, pAKT and lamin. Molecular weights are as indicated. The immunoblot is representative of three independent experiments. (B-D) Quantitative mass spectrometry (MS) of K562 cells treated with vehicle (dimethylsulfoxide, DMSO), imatinib or the AKT inhibitor MK-2206 for 0, 2 or 4 h using triple stable isotope labeling with amino acids in cell culture (SILAC) and light-, medium- or heavy-labeled cells. After treatment, differently labeled cells were mixed and followed by MS analysis. (B) An averaged MS1 spectrum showing the SILAC triplets of the pS122-bearing peptide "oxMVQLpSPPALAAPAAPGR" on SCL/TAL1 in AKT-inhibited cells. The arrows indicate the mass increments resulting from the medium (+6 Da) or heavy (+10 Da) SILAC-labeling on arginine. The relative intensities of the SILAC triplets revealed the changes of phosphorylation level on the peptide during the course of AKT inhibition. (C, D) Areas under the extracted ion chromatogram (XIC) after MS by triple SILAC labeling of the cells in (B) showing the relative abundance of pSCL/TAL1 S122 after inhibition with imatinib (10 μM) (C) and the AKT inhibitor MK-2206 (20 μM) (D).

sion of *SCL/TAL1* and *CD44* in CD34⁺-sorted samples from chronic phase CML patients (n=59). We observed a statistically significant negative correlation (P=0.002, correlation coefficient -0.40) between *SCL/TAL1* and *CD44* expression in these samples (Figure 7E). Lastly, we examined the association between *SCL/TAL1* expression and outcomes after allogeneic transplantation in chronic phase CML patients (n=37),[35] although this procedure is no longer the standard of care in CML. When dichotomizing *SCL/TAL1* into high and low expression groups at the third quartile, we found that low *SCL/TAL1* expression was statistically significantly associated with increased risk of relapse (P=0.033) (Figure 7F) and inferior relapse-free survival (P=0.024) (Figure 7G). In summary, these data suggest that expression of *SCL/TAL1* (and, therefore, converse expression of *CD44*) may correlate with disease stage and survival in human CML patients, although larger cohorts would be needed to prove this definitively.

Discussion

In this study we show that inhibition of binding of BCR-ABL1⁺ cells to E-selectin in the vascular niche increases cell cycle progression and response to imatinib therapy. Furthermore, our data also imply that SCL/TAL1 is a regulator of the expression of CD44, whereby SCL/TAL1 is activated by AKT downstream of BCR-ABL1 (*Online Supplementary Figure S12*). In turn, CD44 influences the cell cycle of BCR-ABL1⁺ cells via its binding to E-selectin. The data connect the previously unknown mechanism of increased expression of CD44, a ligand for E-selectin and cancer stem cell marker, on BCR-ABL1⁺ cells with transcriptional regulation by SCL/TAL1, E-selectin in the vascular niche, engraftment in the BM microenvironment, cell cycle progression and response to therapy.

Our data on CML LSC contrast with findings in the normal HSC niche, in which a prominent role for E-

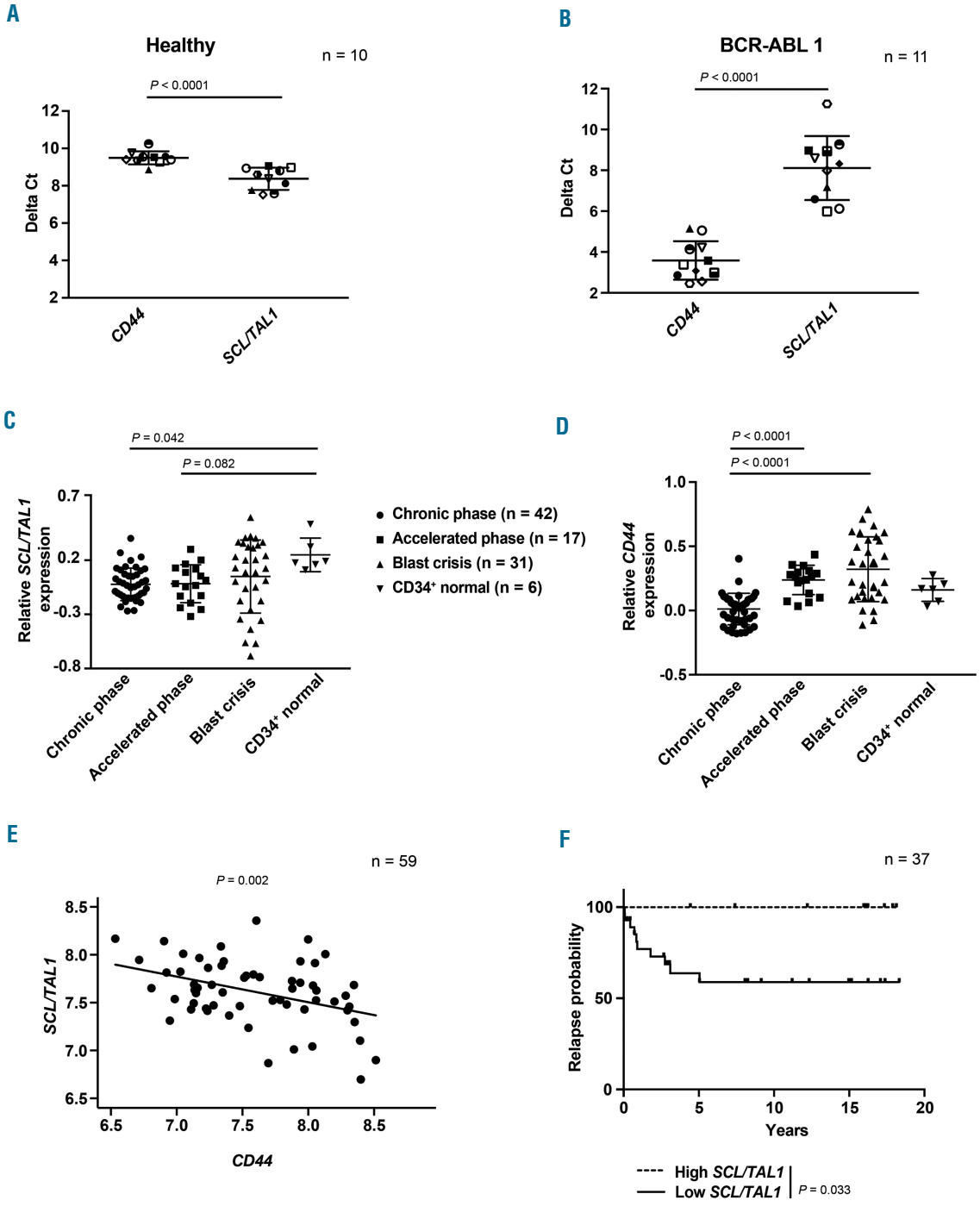

Figure 7. SCL/TAL1 influences outcome in human chronic myeloid leukemia. (A, B) Delta Ct values for *CD44* and *SCL/TAL1* in peripheral blood leukocytes of healthy individuals (n=10) (A) or patients with chronic myeloid leukemia (CML) (n=11) (B). (C, D) Relative *SCL/TAL1* (C) and *CD44* (D) expression in unsorted bone marrow cells of patients in chronic phase (CP) (circles), accelerated phase (AP) (squares) or blast crisis (BC) (triangles) of CML *vs.* normal human CD34$^+$ cells (upside down triangles). Gene expression for each individual sample is normalized to mean expression in CP samples and is shown on a $\log_{10}$ scale. The expression of *SCL/TAL1* in CP CML is significantly lower than that in human CD34$^+$ cells from healthy individuals [*P*=0.042, analysis of variance (ANOVA); Tukey test]. (C) and the expression of *CD44* is significantly higher in BC than in CP CML (*P*<0.0001, ANOVA; Tukey test. CP, n=42; AP, n=17; BC, n=31; normal CD34$^+$ cells, n=6) (D). (E) Negative correlation between *SCL/TAL1* and *CD44* expression in CD34$^+$ sorted samples from CP CML patients (n=59) from the study by McWeeney *et al.*[34] (*P*=0.002, correlation coefficient -0.40). Normalized $\log_2$-transformed expression is shown. (F, G) Kaplan-Meier-style curve of the probability of relapse (*P*=0.033, log-rank test) (F) or relapse-free survival (*P*=0.024, log-rank test) (G) of CP CML patients grouped by low or high expression of *SCL/TAL1* (n=37).

selectin in promoting HSC proliferation has been described.[5] This could be explained by our previous work demonstrating that interactions with the BM microenvironment differ drastically between normal HSC[8] and LSC and even between oncogenes.[15] However, in their study, Winkler *et al.* used GMI-1070, a pan-selectin antagonist and precursor to GMI-1271.[5] In addition, a role for SCL/TAL1 in impeding the transition of HSC from G0 to G1 has been demonstrated,[36] which may support the pro-proliferative effects of E-selectin on normal HSC.[5] Additionally, similar to our findings, CD44 inhibited cell cycle progression of vascular smooth muscle cells in response to binding of high molecular weight hyaluronan,[37] another CD44 ligand in the extracellular matrix, and modulated the ERK and AKT pathways upon cell adhesion via CD44.[38] In the present study, it cannot be excluded that the SCL/TAL1-mediated reduction of CD44 expression may also have led to decreased binding to hyaluronan and osteopontin, another extracellular matrix protein known to bind CD44.[39] However, CML induction did not differ significantly between wildtype and osteopontin-knockout mice (*unpublished data,* DSK), suggesting that, unlike E-selectin, osteopontin is not essential for the engraftment of LIC in CML.

In agreement with our work it was demonstrated that inhibition of E- and P-selectin led to reduced rolling of neutrophils on endothelium, lowering the risk of neutrophil-mediated endothelial injury after xenotransplantation.[40] Furthermore, in CML, we previously showed that deficiency of E-selectin in BM endothelium or deficiency of L-selectin, P-selectin glycoprotein ligand (PSGL)-1, enzymes involved in the synthesis of selectin ligands[6] or CD44[8] on LIC were required for efficient engraftment of LIC, whereas P-selectin in the BM was not required.[6] Therefore, emphasis in this work was laid on E-selectin and its ligands. Treatment with GMI-1271 also reverted the insensitivity of multiple myeloma cells overexpressing E-selectin ligands to bortezomib.[12]

Normal hematopoietic cells predominantly express the standard isoform of CD44 (CD44s).[41] However, variant isoforms of CD44 (CD44v) are generated in cancers, including solid tumors[42] and acute myeloid leukemia,[43] but both forms, CD44s and CD44v, are cancer stem cell markers and both influence cancer cell stemness.[42,44] In CML we found that the CD44s isoform has a role in homing and engraftment of LIC,[8] while CD44v3 enhanced the replating capacity of CML progenitors.[45]

In summary, regulation of CD44 expression via SCL/TAL1, the AKT pathway and an oncogene, as well as the mechanism of cell cycle regulation of LSC upon non-adhesion to the niche, suggest a concept of how dislocation from the niche may alter LSC proliferation and response to therapy. This has, similarly, been hypothesized in the case of the concomitant use of granulocyte colony-stimulating factor[46,47] or C-X-C motif chemokine receptor (CXCR) 4 inhibitors plus tyrosine kinase inhibitors or chemotherapy in leukemia,[48] suggesting that these therapeutic strategies may be further exploitable in the future.

Acknowledgments

The authors thank M. Zörnig for helpful discussions and Glycomimetics Inc., in particular J. Magnani and W. Fogler, for provision of drugs and initial funding of this work. The authors also thank Stefanie Dimmeler for use of the in vivo microscope. This work was supported by the LOEWE Center for Cell and Gene Therapy Frankfurt (CGT) and institutional funds of the Georg-Speyer-Haus to DSK. The Georg-Speyer-Haus is funded jointly by the German Federal Ministry of Health (BMG) and the Ministry of Higher Education, Research and the Arts of the State of Hessen (HMWK). The LOEWE Center for Cell and Gene Therapy Frankfurt is funded by HMWK, reference number: III L 4-518/17.004 (2010). The project was also partly supported by Deutsche Krebshilfe (SyTASC / 70111969).

References

1. Ishikawa F, Yoshida S, Saito Y, et al. Chemotherapy-resistant human AML stem cells home to and engraft within the bone-marrow endosteal region. Nat Biotechnol. 2007;25(11):1315-1321.
2. Pitt LA, Tikhonova AN, Hu H, et al. CXCL12-producing vascular endothelial niches control acute T cell leukemia Maintenance. Cancer Cell. 2015;27(6):755-768.
3. Zhang B, Li M, McDonald T, et al. Microenvironmental protection of CML stem and progenitor cells from tyrosine kinase inhibitors through N-cadherin and Wnt-beta-catenin signaling. Blood. 2013;121 (10):1824-1838.
4. Yamamoto-Sugitani M, Kuroda J, Ashihara E, et al. Galectin-3 (Gal-3) induced by leukemia microenvironment promotes drug resistance and bone marrow lodgement in chronic myelogenous leukemia. Proc Natl Acad Sci U S A. 2011;108(42): 17468-17473.
5. Winkler IG, Barbier V, Nowlan B, et al. Vascular niche E-selectin regulates hematopoietic stem cell dormancy, self renewal and chemoresistance. Nat Med. 2012;18(11):1651-1657.
6. Krause DS, Lazarides K, Lewis JB, von Andrian UH, Van Etten RA. Selectins and their ligands are required for homing and engraftment of BCR-ABL1+ leukemic stem cells in the bone marrow niche. Blood. 2014;123(9):1361-1371.
7. Dimitroff CJ, Lee JY, Rafii S, Fuhlbrigge RC, Sackstein R. CD44 is a major E-selectin ligand on human hematopoietic progenitor cells. J Cell Biol. 2001;153:1277-1286.
8. Krause DS, Lazarides K, von Andrian UH, Van Etten RA. Requirement for CD44 in homing and engraftment of BCR-ABL-expressing leukemic stem cells. Nat Med. 2006;12(10):1175-1180.
9. Jin L, Hope KJ, Zhai Q, Smadja-Joffe F, Dick JE. Targeting of CD44 eradicates human acute myeloid leukemic stem cells. Nat Med. 2006;12(10):1167-1174.
10. Thomas SN, Zhu F, Schnaar RL, Alves CS, Konstantopoulos K. Carcinoembryonic antigen and CD44 variant isoforms cooperate to mediate colon carcinoma cell adhesion to E- and L-selectin in shear flow. J Biol Chem. 2008;283(23):15647-15655.
11. Shirure VS, Liu T, Delgadillo LF, et al. CD44 variant isoforms expressed by breast cancer cells are functional E-selectin ligands under flow conditions. Am J Physiol Cell Physiol. 2015;308(1):C68-78.
12. Natoni A, Smith TAG, Keane N, et al. E-selectin ligands recognised by HECA452 induce drug resistance in myeloma, which is overcome by the E-selectin antagonist, GMI-1271. Leukemia. 2017;31(12):2642-2651.
13. Saito Y, Uchida N, Tanaka S, et al. Induction of cell cycle entry eliminates human leukemia stem cells in a mouse model of AML. Nat Biotechnol. 2010;28(3):275-280.
14. Drummond MW, Heaney N, Kaeda J, et al. A pilot study of continuous imatinib vs pulsed imatinib with or without G-CSF in CML patients who have achieved a complete cytogenetic response. Leukemia. 2009;23(6):1199-1201.
15. Krause DS, Fulzele K, Catic A, et al. Differential regulation of myeloid leukemias by the bone marrow microenvironment. Nat Med. 2013;19(11):1513-1517.
16. Graham SM, Jorgensen HG, Allan E, et al. Primitive, quiescent, Philadelphia-positive stem cells from patients with chronic myeloid leukemia are insensitive to STI571 in vitro. Blood. 2002;99(1):319-325.
17. Bhatia R, Holtz M, Niu N, et al. Persistence of malignant hematopoietic progenitors in chronic myelogenous leukemia patients in

complete cytogenetic remission following imatinib mesylate treatment. Blood. 2003;101(12):4701-4707.
18. Chen B, Jiang L, Zhong ML, et al. Identification of fusion genes and characterization of transcriptome features in T-cell acute lymphoblastic leukemia. Proc Natl Acad Sci U S A. 2018;115(2):373-378.
19. Lavender KJ, Pang WW, Messer RJ, et al. BLT-humanized C57BL/6 Rag2-/-γc-/-CD47-/- mice are resistant to GVHD and develop B- and T-cell immunity to HIV infection. Blood. 2013;122(25):4013-4020.
20. Li S, Ilaria RL, Million RP, Daley GQ, Van Etten RA. The P190, P210, and P230 forms of the BCR/ABL oncogene induce a similar chronic myeloid leukemia-like syndrome in mice but have different lymphoid leukemogenic activity. J Exp Med. 1999;189(9): 1399-1412.
21. Hu Y, Swerdlow S, Duffy TM, Weinmann R, Lee FY, Li S. Targeting multiple kinase pathways in leukemic progenitors and stem cells is essential for improved treatment of Ph+ leukemia in mice. Proc Natl Acad Sci U S A. 2006;103(45):16870-16875.
22. Chien S, Zhao X, Brown M, et al. A novel small molecule e-selectin inhibitor GMI-1271 blocks adhesion of AML blasts to e-selectin and mobilizes blood cells in nodscid IL2Rgc–/– mice engrafted with human AML. Blood. 2012;120(21):4092.
23. Copland M, Hamilton A, Elrick LJ, et al. Dasatinib (BMS-354825) targets an earlier progenitor population than imatinib in primary CML but does not eliminate the quiescent fraction. Blood. 2006;107(11):4532-4539.
24. Chu S, Xu H, Shah NP, et al. Detection of BCR-ABL kinase mutations in CD34+ cells from chronic myelogenous leukemia patients in complete cytogenetic remission on imatinib mesylate treatment. Blood. 2005;105(5):2093-2098.
25. Dey S, Curtis DJ, Jane SM, Brandt SJ. The TAL1/SCL transcription factor regulates cell cycle progression and proliferation in differentiating murine bone marrow monocyte precursors. Mol Cell Biol. 2010;30(9): 2181-2192.
26. Kolodziej S, Kuvardina ON, Oellerich T, et al. PADI4 acts as a coactivator of Tal1 by counteracting repressive histone arginine methylation. Nat Comm. 2014;5:3995.
27. Senbanjo LT, Chellaiah MA. CD44: a multifunctional cell surface adhesion receptor is a regulator of progression and metastasis of cancer cells. Front Cell Dev Biol. 2017;5:18.
28. Branford S, Melo JV, Hughes TP. Selecting optimal second-line tyrosine kinase inhibitor therapy for chronic myeloid leukemia patients after imatinib failure: does the BCR-ABL mutation status really matter? Blood. 2009;114(27):5426-5435.
29. Nicolini FE, Ibrahim AR, Soverini S, et al. The BCR-ABLT315I mutation compromises survival in chronic phase chronic myelogenous leukemia patients resistant to tyrosine kinase inhibitors, in a matched pair analysis. Haematologica. 2013;98(10): 1510-1516.
30. Kumar R, Merten M, Minciacchi V, et al. Specific and targetable interactions with the bone marrow microenvironment govern outcome in imatinib-resistant chronic myeloid leukemia. Blood. 2018;132(Suppl 1):936.
31. Palamarchuk A, Efanov A, Maximov V, Aqeilan RI, Croce CM, Pekarsky Y. Akt phosphorylates Tal1 oncoprotein and inhibits its repressor activity. Cancer Res. 2005;65(11):4515-4519.
32. Skorski T, Kanakaraj P, Nieborowska-Skorska M, et al. Phosphatidylinositol 3-kinase activity is regulated by BCR/ABL and is required for the growth of Philadelphia chromosome-positive cells. Blood. 1995;86 (2):726-736.
33. Atfi A, Abécassis L, Bourgeade MF. Bcr-Abl activates the AKT/Fox O3 signalling pathway to restrict transforming growth factor-beta-mediated cytostatic signals. EMBO Rep. 2005;6(10):985-991.
34. McWeeney SK, Pemberton LC, Loriaux MM, et al. A gene expression signature of CD34+ cells to predict major cytogenetic response in chronic-phase chronic myeloid leukemia patients treated with imatinib. Blood. 2010;115(2):315-325.
35. Radich JP, Dai H, Mao M, et al. Gene expression changes associated with progression and response in chronic myeloid leukemia. Proc Natl Acad Sci U S A. 2006;103(8):2794-2799.
36. Lacombe J, Herblot S, Rojas-Sutterlin S, et al. Scl regulates the quiescence and the long-term competence of hematopoietic stem cells. Blood. 2010;115(4):792-803.
37. Kothapalli D, Flowers J, Xu T, Puré E, Assoian RK. Differential activation of ERK and Rac mediates the proliferative and anti-proliferative effects of hyaluronan and CD44. J Biol Chem. 2008;283(46):31823-31829.
38. Yu S, Cai X, Wu C, et al. Adhesion glycoprotein CD44 functions as an upstream regulator of a network connecting ERK, AKT and Hippo-YAP pathways in cancer progression. Oncotarget. 2015;6(5):2951-2965.
39. Rangaswami H, Bulbule A, Kundu GC. Osteopontin: role in cell signaling and cancer progression. Trends Cell Biol. 2006;16: 79-87.
40. Laird CT, Hassanein W, O'Neill NA, et al. P- and E-selectin receptor antagonism prevents human leukocyte adhesion to activated porcine endothelial monolayers and attenuates porcine endothelial damage. Xenotransplantation. 2018;25(2):e12381.
41. Zöller M. CD44, hyaluronan, the hematopoietic stem cell, and leukemia-initiating cells. Front Immunol. 2015;6:235.
42. Yan Y, Zuo X, Wei D. Concise review: emerging role of CD44 in cancer stem cells: a promising biomarker and therapeutic target. Stem Cells Transl Med. 2015;4(9):1033-1043.
43. Bendall LJ, Bradstock KF, Gottlieb DJ. Expression of CD44 variant exons in acute myeloid leukemia is more common and more complex than that observed in normal blood, bone marrow or CD34+ cells. Leukemia. 2000;14(7):1239-1246.
44. Wang L, Zuo X, Xie K, Wei D. The role of CD44 and cancer stem cells. Methods Mol Biol. 2018;1692:31-42.
45. Holm F, Hellqvist E, Mason CN, et al. Reversion to an embryonic alternative splicing program enhances leukemia stem cell self-renewal. Proc Natl Acad Sci U S A. 2015;112(50):15444-15449.
46. Borthakur G, Kantarjian H, Wang X, et al. Treatment of core-binding-factor in acute myelogenous leukemia with fludarabine, cytarabine, and granulocyte colony-stimulating factor results in improved event-free survival. Cancer. 2008;113(11):3181-3185.
47. Holtz M, Forman SJ, Bhatia R. Growth factor stimulation reduces residual quiescent chronic myelogenous leukemia progenitors remaining after imatinib treatment. Cancer Res. 2007;67:1113-1120.
48. Uy GL, Rettig MP, Motabi IH, et al. A phase 1/2 study of chemosensitization with the CXCR4 antagonist plerixafor in relapsed or refractory acute myeloid leukemia. Blood. 2012;119(17):3917-3924.

Ferrata Storti Foundation

Haematologica 2020
Volume 105(1):148-160

Homoharringtonine exhibits potent anti-tumor effect and modulates DNA epigenome in acute myeloid leukemia by targeting SP1/TET1/5hmC

Chenying Li,[1,2,3,*] Lei Dong,[2,3,*] Rui Su,[2,3,*] Ying Bi,[4] Ying Qing,[2,3] Xiaolan Deng,[2,3,5] Yile Zhou,[1] Chao Hu,[1] Mengxia Yu,[1] Hao Huang,[6] Xi Jiang,[2,3,7] Xia Li,[1] Xiao He,[1] Dongling Zou,[2,3,8] Chao Shen,[2,3] Li Han,[2,5] Miao Sun,[9] Jennifer Skibbe,[2] Kyle Ferchen,[2] Xi Qin,[2,3] Hengyou Weng,[2,3] Huilin Huang,[2,3] Chunxiao Song,[4] Jianjun Chen[2,3] and Jie Jin[1]

[1]Department of Hematology, The First Affiliated Hospital, Zhejiang University College of Medicine, Hangzhou, China; Key Laboratory of Hematologic Malignancies, Diagnosis and Treatment, Zhejiang, China; [2]Department of Systems Biology & the Gehr Family Center for Leukemia Research, Beckman Research Institute of City of Hope, Monrovia, CA, USA; [3]Department of Cancer Biology, University of Cincinnati, Cincinnati, OH, USA; [4]Ludwig Institute for Cancer Research & Target Discovery Institute, Nuffield Department of Medicine, University of Oxford, Oxford, UK; [5]School of Pharmacy, China Medical University, Shenyang, Liaoning, China; [6]Division of Gynecologic Oncology, Feinberg School of Medicine, Northwestern University, Chicago, IL, USA; [7]Department of Pharmacology, and Bone Marrow Transplantation Center of the First Affiliated Hospital, Zhejiang University School of Medicine; Institute of Hematology, Zhejiang University & Zhejiang Engineering Laboratory for Stem Cell and Immunotherapy, Hangzhou, Zhejiang, China; [8]Department of Gynecologic Oncology, Chongqing University Cancer Hospital & Chongqing Cancer Institute & Chongqing Cancer Hospital, Chongqing, China; [9]Department of Pediatrics, University of Cincinnati College of Medicine; Division of Human Genetics, Cincinnati Children's Hospital Medical Center, Cincinnati, OH, USA

**CL, LD and RS contributed equally to this work.*

Correspondence:

JIE JIN
jiej0503@zju.edu.cn

JIANJUN CHEN
jianchen@coh.org

Received: October 8, 2018.

Accepted: April 9, 2019.

Pre-published: April 11, 2019.

doi:10.3324/haematol.2018.208835

Check the online version for the most updated information on this article, online supplements, and information on authorship & disclosures: www.haematologica.org/content/105/1/148

ABSTRACT

Homoharringtonine, a plant alkaloid, has been reported to suppress protein synthesis and has been approved by the US Food and Drug Administration for the treatment of chronic myeloid leukemia. Here we show that in acute myeloid leukemia (AML), homoharringtonine potently inhibits cell growth/viability and induces cell cycle arrest and apoptosis, significantly inhibits disease progression *in vivo*, and substantially prolongs survival of mice bearing murine or human AML. Strikingly, homoharringtonine treatment dramatically decreases global DNA 5-hydroxymethylcytosine abundance through targeting the SP1/TET1 axis, and *TET1* depletion mimics homoharringtonine's therapeutic effects in AML. Our further 5hmC-seq and RNA-seq analyses, followed by a series of validation and functional studies, suggest that FLT3 is a critical down-stream target of homoharringtonine/SP1/TET1/5hmC signaling, and suppression of FLT3 and its downstream targets (e.g. *MYC*) contributes to the high sensitivity of *FLT3*-mutated AML cells to homoharringtonine. Collectively, our studies uncover a previously unappreciated DNA epigenome-related mechanism underlying the potent antileukemic effect of homoharringtonine, which involves suppression of the SP1/TET1/5hmC/FLT3/MYC signaling pathways in AML. Our work also highlights the particular promise of clinical application of homoharringtonine to treat human AML with FLT3 mutations, which accounts for more than 30% of total cases of AML.

Introduction

Homoharringtonine (HHT, also known as omacetaxine mepesuccinate) is a cytotoxic alkaloid originally isolated from the cephalotaxus hainanensis.[1] It has been approved by the US Food and Drug Administration (FDA) for treatment of chronic myeloid leukemia (CML) with resistance and/or intolerance to imatinib or other

tyrosine kinase inhibitors.[2] However, it is still awaiting approval for use in the treatment of acute myeloid leukemia (AML). In China, HHT has been used in the treatment of leukemia for more than 30 years due to its low price and high efficiency.[3] In a pilot clinical trial we launched in 2006 in Zhejiang Province, China, we used an HHT-based induction regimen, namely HAA (HHT 4 mg/m^2/day, days 1-3; cytarabine 150 mg/m^2/day, days 1-7; aclarubicin 12 mg/day, days 1-7) to treat *de novo* AML and achieved a complete remission rate of 83%.[4] Afterwards, a multi-center, open-label, randomized, controlled phase III trial was carried out in China and confirmed modified HAA regimen (HHT 2 mg/m^2/day, days 1-7; cytarabine 100 mg/m^2/day, days 1-7; aclarubicin 20 mg/day, days 1-7) as an alternative therapeutic strategy in treating *de novo* AML, especially for those patients with favorable and intermediate prognosis.[5] A potential mechanism by which HHT exerts its biological function is through its binding to the A site of the ribosome, resulting in the inhibition of protein synthesis.[6] However, it is unclear whether there is any other mechanism(s) underlying antileukemic effect of HHT, in particular in AML.

Acute myeloid leukemia is one of the most common and fatal forms of hematopoietic malignancies, characterized by blockage of myeloid differentiation and malignant proliferation of immature myeloid blasts.[7] With contemporary therapies, the vast majority (over 70%) of patients with AML cannot survive over five years. Despite the common myeloid background, molecular and cytogenetic alterations contribute to the heterogeneity of the disease and the variable responses to treatment. For instance, mutations in FLT3, including internal-tandem duplications (ITD) and tyrosine kinase domain (TKD) point mutations, occur in over 30% of AML cases and are often associated with poor prognosis.[7-9] Meanwhile, overexpression of *FLT3* has also been reported in more than 60% of AML with a variety of AML subtypes, such as AML carrying FLT3-ITD or t(11q23) [i.e. chromosome rearrangements involving the mixed lineage leukemia (*MLL*) gene].[9] *FLT3*-ITD activates multiple signaling pathways, leading to the aberrant overexpression of a set of oncogenes including *MYC*.[10] Despite extensive efforts in developing and testing various FLT3 tyrosine kinase inhibitors (TKI) in clinical trials, the long-term therapeutic effects are still not promising,[11,12] indicating that the development of more effective therapeutics to treat FLT3-mutated AML remains an unmet need.

The Ten-eleven translocation (TET) proteins (including TET1/2/3) are a family of methylcytosine dioxygenases that convert 5-methylcytosine (5mC) to 5-hydroxymethylcytosine (5hmC), leading to active or passive DNA demethylation.[13] *TET1*, the founding member of the TET family, was first identified as a fusion partner of the *MLL* gene associated with t(10;11)(q22;q23) in AML.[14,15] In contrast to the frequent loss-of-function mutations and tumor-suppressor role of TET2 observed in hematopoietic malignancies,[16] we reported recently that TET1 plays a critical oncogenic role in the pathogenesis of various subtypes of AML and represents a promising therapeutic target for AML treatment.[17-19] The oncogenic role of Tet1 in the development of myeloid malignancies was also observed by others.[20]

In the present study, we show that HHT exhibits potent anti-AML effects both *in vitro* and *in vivo*, and affects DNA epigenome by directly targeting SP1 and inhibiting SP1-mediated transcriptional regulation of *TET1* expression, thereby reducing global 5hmC levels. Moreover, we demonstrate that FLT3 is a direct target of the HHT–SP1/TET1/5hmC axis, and therefore HHT treatment substantially inhibits the FLT3/MYC pathways. Consistently, human primary FLT3-ITD AML cell samples display particularly high sensitivity to HHT treatment. Taken together, our studies reveal a previously unrecognized mechanism involving HHT-induced 5hmC reduction in treating AML, and suggest that HHT-based regimens hold great therapeutic potential for the treatment of AML, especially that carrying FLT3 mutations.

Methods

Cell lines and cell culture

MA9.3ITD (*MLL*-AF9 fusion gene plus FLT3-ITD mutation; MLL, also known as KMT2A) and MA9.3RAS (*MLL*-AF9 fusion gene plus NRAS^{G12D} mutation) were established by Dr. James Mulloy and cultured in IMDM supplemented with 20% FBS.[21] MONOMAC 6, MV4-11, MOLM13, Kasumi-1, THP-1, SKNO-1 and ML-2 are obtained and maintained as previously described.[22] Homoharringtonine purchased from Sigma-Aldrich was used in this study.

Mouse model

B6.SJL-Ptprc (CD45.1) mice and NOD/LtSz-scid IL2RG-SGM3 (NSGS) mice were obtained from the Jackson Lab (Bar Harbor, ME, USA), and bone marrow transplantation (BMT) or xenotransplantation assays were carried out as previously described.[17,19,22,23] All mice were maintained in the animal core facility of the University of Cincinnati. All experiments were conducted according to our research protocol which was approved by the Institutional Animal Care and Use Committee. In all mouse models, HHT (1 mg/kg body weight) or phosphate-buffered saline (PBS) was intraperitoneally injected daily for ten consecutive days from day 11. The mice were euthanized by CO_2 inhalation once typical leukemic symptoms, i.e. paralysis, hunched posture, labored breathing and decreased activity, had been observed. The peripheral blood (PB), bone marrow (BM), spleen and liver samples were harvested for further analysis.

Patients' samples

Bone marrow aspirates and PB samples were obtained from AML patients with their written informed consent. Mononuclear cells (MNC) were isolated and used for subsequent experiments. The genetic mutations were tested by the First Affiliated Hospital, Zhejiang University College of Medicine. The study was approved by the Ethics Committee of the First Affiliated Hospital, Zhejiang University College of Medicine.

DNA 5hmC sequencing

DNA samples were collected and sent for 5hmC sequencing. 5hmC library construction and sequencing were performed by Dr. Chunxiao Song's lab as previously reported.[24] The identification of 5hmC peaks in each sample was performed using MACS2,[25] gene expression was analyzed by RSEM,[26] 5hmC and expression target analysis was performed by BETA.[27] 5hmC sequencing data have been deposited in the Gene Expression Omnibus (GEO) repository with the accession number GSE103144.

RNA sequencing and RNA-sequencing analysis

RNA sequencing was performed with total RNA samples isolated from MA9.3RAS and MA9.3ITD AML cells with or without

HHT treatment (5 or 10 ng/mL for 48 hours) by The Genomics, Epigenomics and Sequencing Core of the University of Cincinnati. The Gene Set Enrichment Analysis (GSEA)[28] was used to analyze the enriched signaling pathway in PBS or HHT treated cell samples. The RNA sequencing data have been deposited in the GEO repository with the accession number GSE103143.

Statistical analysis

Data were analyzed with GraphPad Prism 6 and were presented as mean±Standard Deviation as indicated. Two-tailed Student *t*-test was used to compare means between groups as indicated. $P<0.05$ was considered significant. The Kaplan-Meier survival curves were produced with GraphPad Prism 6 and *P*-values were calculated using the log rank test. The densitometric analysis of the bands from Western blot or dots from dot blot were performed with Gel-Pro analyzer and normalized to the loading controls.

A detailed description of all materials and methods is available in the *Online Supplementary Appendix*.

Results

Homoharringtonine potently inhibits cell growth and viability and promotes cell cycle arrest, apoptosis and differentiation in human acute myeloid leukemia

To systematically investigate the therapeutic potential of HHT in AML, we first analyzed the responses of human AML cells to HHT *in vitro*. Three AML cell lines with various backgrounds, including MONOMAC 6, MA9.3ITD and MA9.3RAS, were included for the analyses (Figure 1A). Remarkably, we found that all three AML cell lines were highly sensitive to HHT treatment, with very low IC_{50} values (5~20 ng/mL; or 9.2~36.7 nM) (Figure 1A), and HHT significantly inhibited their growth and viability in a dose- and time-dependent manner (Figure 1B and *Online Supplementary Figure S1A*). HHT dramatically induced apoptosis (Figure 1C and D, and *Online Supplementary Figure S1B and C*) and cell cycle arrest in G0/G1 phase (Figure 1E and F, *Online Supplementary Figure S1D and E*) in AML cells. Furthermore, we also assessed the potential effect of HHT on myeloid differentiation of MONOMAC 6 and NB4 (carrying t(15;17)/PML-RARA) AML cells. Notably, HHT also significantly promoted myeloid differentiation of AML cell as detected by both flow cytometry and qualitative polymerase chain reaction (qPCR) (Figure 1G and H, *Online Supplementary Figure S1F and G*), including PMA-induced monocytic differentiation and ATRA-induced granulocytic differentiation. Thus, HHT exhibits a broad-spectrum antileukemic activity involving the inhibition of AML cell growth/viability and the promotion of apoptosis, cell cycle arrest, and myeloid differentiation.

Homoharringtonine substantially inhibits murine and human acute myeloid leukemia progression *in vivo*

We next examined the effect of HHT on survival and proliferation of primary mouse AML cells *via* colony forming assays. Leukemic BM blast cells collected from primary BMT recipient mice carrying MLL-AF9- or NRAS+AE9a (*AML1-ETO9a* fusion gene[29] plus $NRAS^{G12D}$)-induced full-blown AML were seeded into semi-solid medium containing PBS or HHT (5 ng/mL or 10 ng/mL) for serial plating. After three rounds of plating, HHT significantly suppressed colony-forming activity and decreased cell proliferation of primary AML cells in a dose-dependent manner (Figure 2A). HHT treatment also markedly reduced the colony size (Figure 2B).

We then utilized leukemic mouse BMT model to assess the effect of HHT on AML progression *in vivo*. Briefly, primary mouse MLL-AF9 AML cells (CD45.2) were injected *via* tail vein (i.v.) into semi-lethally irradiated recipient mice (CD45.1). Ten days post transplantation, the recipients were treated with either HHT (1 mg/kg body weight) or PBS once daily for ten consecutive days (Figure 2C). As expected, HHT treatment significantly inhibited AML progression and substantially prolonged survival in the AML mice (102 days *vs.* 63 days; $P=0.0007$) (Figure 2D). Compared to the PBS-treated control group, HHT treatment dramatically reduced leukemic burden in PB, BM, spleen and liver in mice (Figure 2E-G and *Online Supplementary Figure S2A and B*).

We also employed "human-in-mouse" xenograft models to further evaluate the effect of HHT on human AML progression *in vivo*. Human MA9.3ITD AML cells were i.v. injected into NSGS mice and ten days post xenotransplantation, the mice were treated with PBS or HHT (1 mg/kg body weight) for ten days (Figure 2H). HHT substantially delayed leukemia progression and prolonged survival of treated mice, associated with significantly inhibited engraftment of human AML cells and remarkably reduced leukemia burden in recipient mice (Figure 2I and *Online Supplementary Figure S2C-F*). Pathological morphologies also identified a significant decrease of leukemia blasts in PB, BM, liver, and spleen tissues in HHT-treated group compared with the control group (Figure 2J). Similar effects of HHT treatment were also observed in NSGS mice xeno-transplanted with human MONOMAC 6 AML cells (*Online Supplementary Figure S2G-I*). Collectively, HHT treatment can substantially inhibit leukemia progression and prolong survival of mice carrying human or murine AML, demonstrating the potent therapeutic efficacy of HHT in treating AML.

Homoharringtonine down-regulates global 5hmC level by targeting SP1/TET1 in acute myeloid leukemia cells

Altered epigenetic modification at DNA levels is a well-known feature of AML and displays critical effects during AML initiation, progression, and prognosis.[30,31] Strikingly, we found that HHT treatment significantly reduced global 5hmC level, but not 5mC level, both in MA9.3RAS and MA9.3ITD AML cells (Figure 3A and B). Notably, amongst the genes encoding methylcytosine dioxygenase TET proteins (including TET1, TET2, and TET3) that convert 5mC to 5hmC,[13] we found that only *TET1*, but not *TET2* or *TET3*, was significantly down-regulated upon HHT treatment (in a dose-dependent manner) in AML cells as detected by qPCR (*Online Supplementary Figure S3A*). Furthermore, we also confirmed HHT-induced suppression of TET1 expression through our RNA-seq data analysis and Western blotting assay (Figure 3C). Notably, our qPCR results indicated that the significant downregulation of *TET1* started as early as at 18 hours and continued afterwards in MA9.3ITD upon HHT treatment (Figure 3E). Thus, HHT-induced decrease of 5hmC level is owing to the downregulation of TET1. To further determine whether HHT-mediated TET1 inhibition is due to transcriptional inhibition, we employed nuclear run-on assay,[32] with biotin-labeled uridine 5'-triphosphate (UTP) (*Online Supplementary Figure S3B*) and showed that HHT

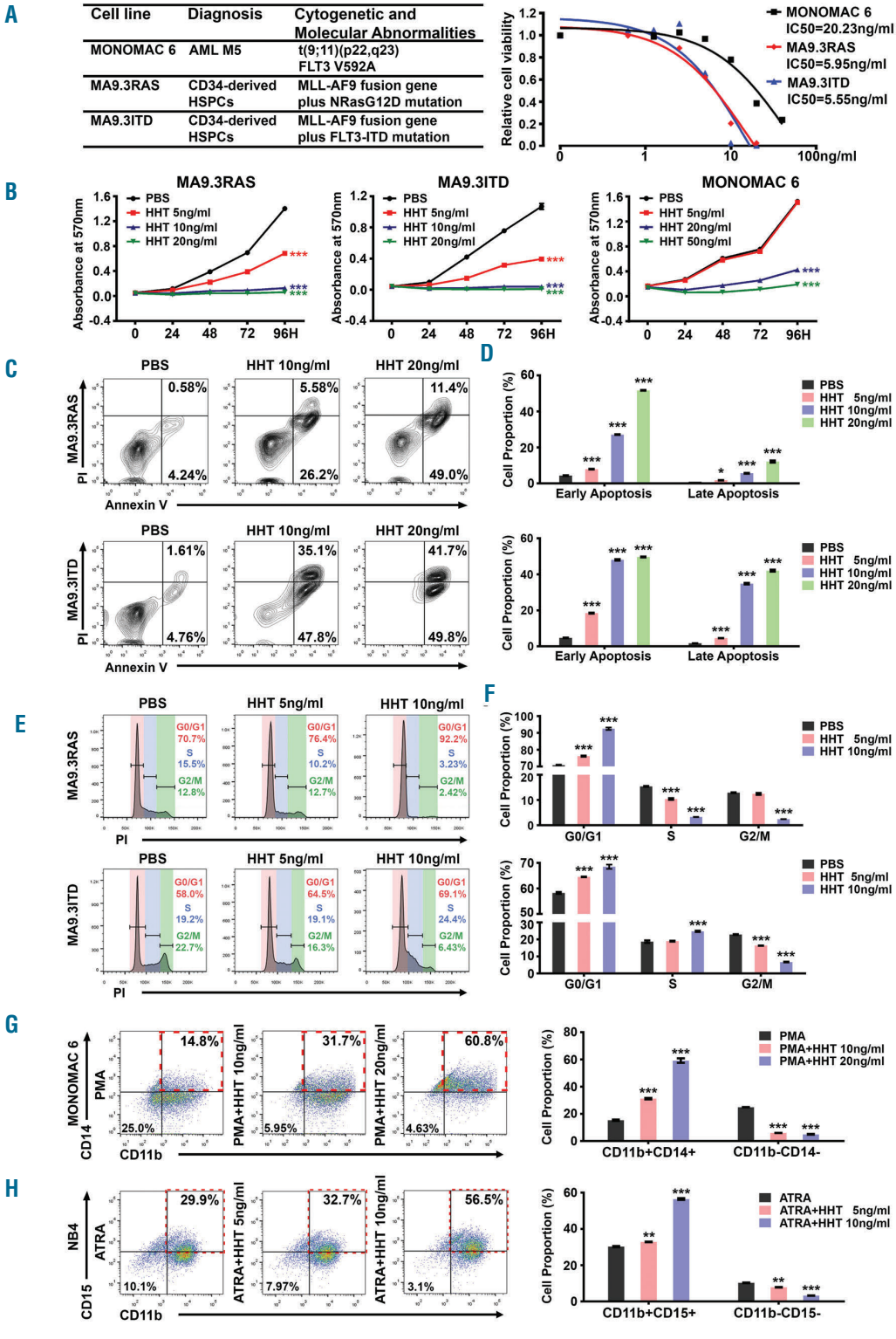

Figure 1. Acute myeloid leukemia (AML) cells display high sensitivity to homoharringtonine (HHT) treatment *in vitro*. (A) (Left) Genetic information of MA9.3RAS, MA9.3ITD and MONOMAC 6 and (right) the inhibitory concentration of 50% (IC_{50}) values with HHT treatment at 48 hours (h) for these three AML cell lines. (B) Effects of HHT treatment on cell growth/proliferation in MA9.3RAS, MA9.3ITD and MONOMAC 6 at different time points (0, 24, 48, 72 and 96 h). The colors represent different HHT concentrations (0, 5, 10, 20 ng/mL; or, 0, 9.2, 18.3, 36.7 nM). (C) Effect of HHT on apoptosis in AML cells. All the cells were treated with HHT for 48 h and representative flow cytometric plots and percentages of cell apoptosis are shown. (D) Statistical apoptosis analysis from three independent experiments determined by flow cytometry. (E) Function of HHT on cell cycle arrest in AML cells. All the cells were treated with HHT for 48 h and representative flow cytometric percentages of cell cycle phases are shown. (F) Statistical analysis of cell cycle assays from three independent experiments determined by flow cytometry. (G) Staining of CD11b and CD14 in MONOMAC 6 cells upon HHT treatment for 96 h during PMA-induced monocytic differentiation (left panel), along with statistical analysis of cell proportions of $CD11b^+CD14^+$ and $CD11b^-CD14^-$ in MONOMAC 6 (right panel). (H) Staining of CD11b and CD15 in NB4 cells [carrying t(15;17)/PML-RARA; AML-M3] upon treatment with HHT for 96 h during ATRA-induced granulocytic differentiation (left panel), along with statistical analysis of cell proportions of $CD11b^+CD15^+$ and $CD11b^-CD15^-$ in NB4 (right panel). Red boxes in (G) and (H) represent the differentiated cell population with double positive markers. **P*<0.05; ***P*<0.01; ****P*<0.001; *t*-test. Error bar, mean±Standard Deviation.

treatment significantly decreased the transcriptional rate of *TET1* (Figure 3D), suggesting transcriptional inhibition largely contributes to HHT-induced downregulation of *TET1*. To elucidate the molecular mechanism by which HHT inhibits the transcription of *TET1*, we examined the potential binding of transcription factors (TF) on the promoter region of *TET1* (-530 to +10 bp) and identified multiple putative binding sites of SP1 (Figure 3F, top panel, and *Online Supplementary Figure S3C*). SP1 is an important TF in AML and mediates drug resistance to chemotherapy.[33,34] Our ChIP-qPCR confirmed the direct binding of SP1 on *TET1* promoter region and such binding was remarkably decreased upon HHT treatment in AML cells (Figure 3F, bottom panel). Furthermore, we conducted drug affinity

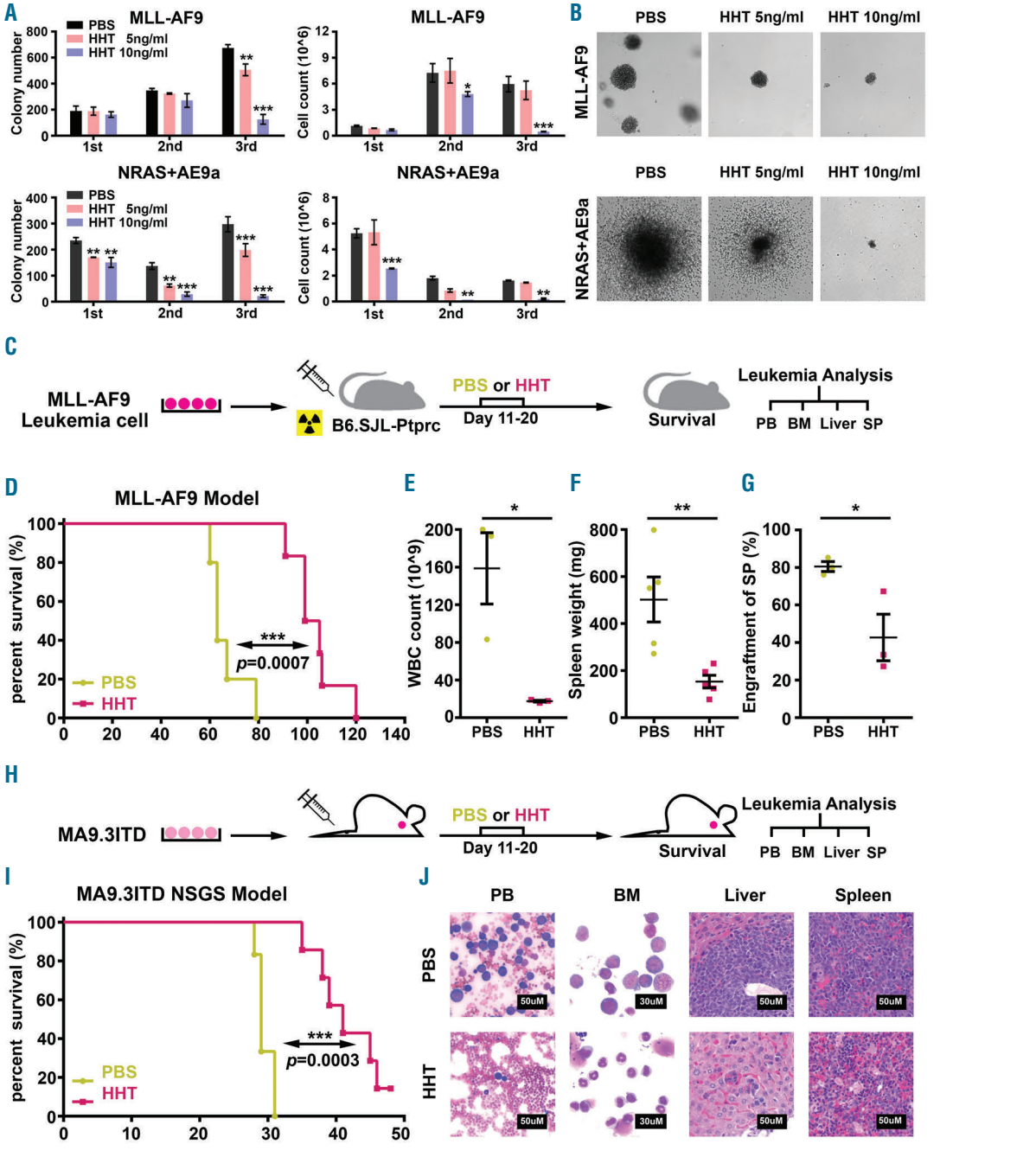

Figure 2. Homoharringtonine (HHT) inhibits the progression of acute myeloid leukemia (AML) *in vivo*. (A) Effects of HHT on colony forming activity of mouse hematopoietic stem/progenitor cells (HSPC) transformed by *MLL-AF9* or *NRAS* plus *AML-ETO9a* (AE9a). Colony numbers (left panel) and cell counts (right panel) from colony forming assay (CFA) were displayed. (B) Representative images of the 3rd generation of colonies under treatment with different HHT concentrations (0, 5 and 10 ng/mL) (5× microscope). (C) Schematic illustration of secondary *MLL-AF9* AML transplantation mouse model coupled with HHT or phosphate-buffered saline (PBS) treatment. (D) Kaplan-Meier curves of PBS- and HHT-treated mice that were transplanted with mouse *MLL-AF9* AML cells. (E-G) White blood cell (WBC) count (E), spleen (SP) weight (F), and the engraftment ratio of leukemic cells into SP (G) at the end point of the PBS- or HHT-treated *MLL-AF9* AML mice. (H) Schematic illustration of the MA9.3ITD AML xenograft NOD/LtSz-scid IL2RG-SGM3 (NSGS) model coupled with HHT or PBS treatment. (I) Kaplan-Meier curves of PBS- and HHT-treated NSGS mice that were xenotransplanted with human MA9.3ITD AML cells. (J) Wright-Giemsa staining of mouse peripheral blood (PB) and bone marrow (BM), and Hematoxylin and Eosin (H&E) staining of liver and spleen (SP) from PBS- or HHT-treated MA9.3ITD leukemic mice. Bars represent 50 μM for PB, SP and liver; 30 μM for BM. *P<0.05; **P<0.01; ***P<0.001; *t*-test. Error bar, mean±Standard Deviation. For Kaplan-Meier curve, *P*-values were calculated by log-rank test.

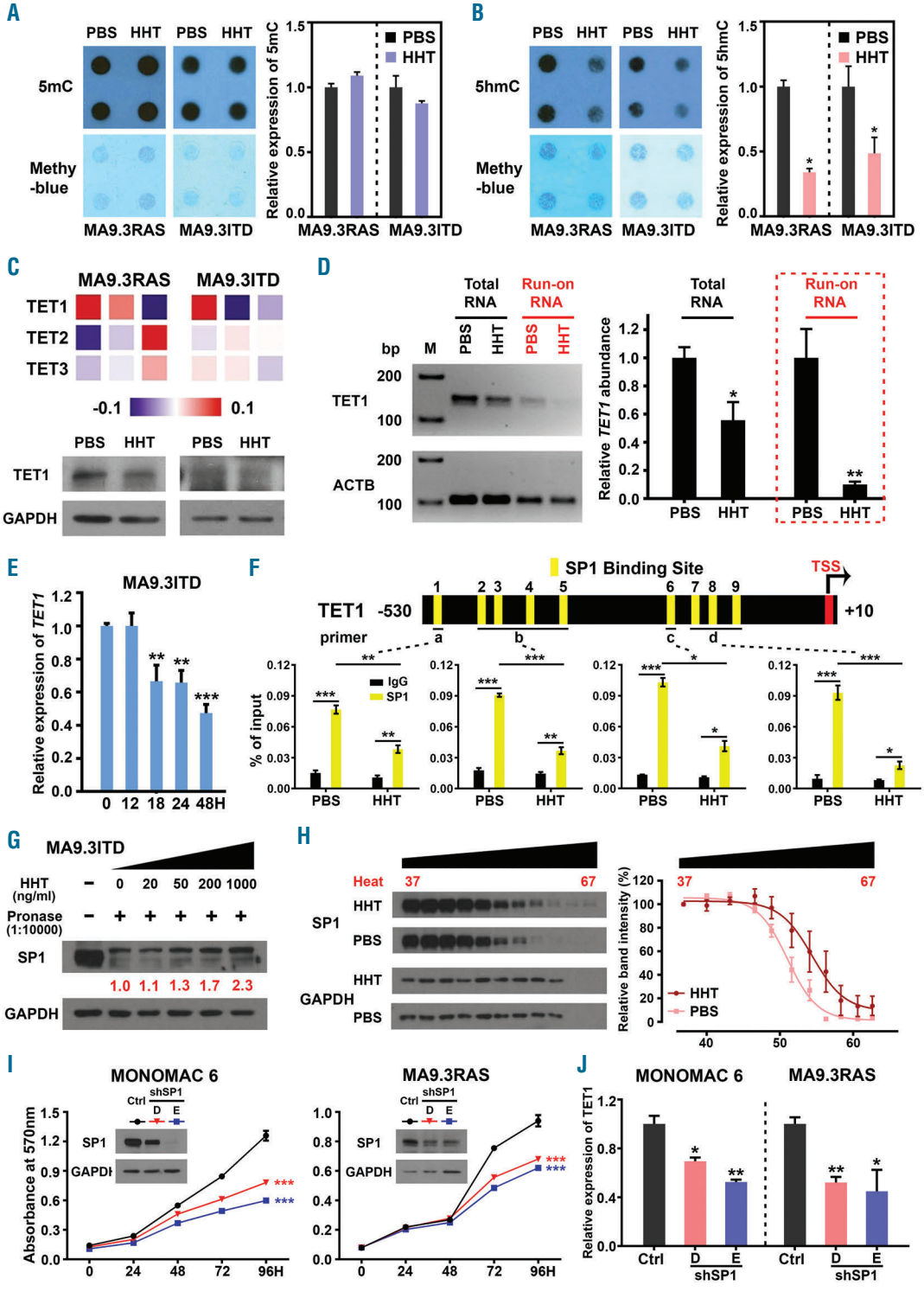

Figure 3. Homoharringtonine (HHT) substantially reduces global 5hmC abundance *via* targeting SP1/TET1 in acute myeloid leukemia (AML). (A and B) Effects of HHT on global 5mC (A) and 5hmC (B) abundance in MA9.3RAS and MA9.3ITD AML cells upon treatment with 5 ng/mL HHT for 48 hours (h). (C) Relative expression of TET1 in HHT-treated MA9.3ITD at different time points, including 0, 12, 18, 24 and 48 h. (D) Heat map showing gene expression of the individual TET family members in MA9.3RAS and MA9.3ITD AML cells treated with phosphate-buffered saline (PBS) or HHT (5 or 10 ng/mL) for 48 h as detected by RNA-sequencing (RNA-seq) (top panel), along with western blotting result of TET1 in MA9.3RAS and MA9.3ITD AML cells treated with PBS or HHT (5 ng/mL) for 48 h (bottom panel). (E) RNA levels of *TET1* and *ACTB* in Total RNA (in black) and Run-on RNA (in red) were determined by reverse transcription polymerase chain reaction (RT-PCR) (left panel, M, Marker). Qualitative PCR (qPCR) analysis of relative *TET1* abundance in Total RNA and Run-on RNA isolated from PBS- or HHT-treated MA9.3ITD cells (right panel). (F) Schematic presentation of SP1 binding sites within the promoter region of TET1 (top panel). Chromatin immune-precipitation (ChIP)-qPCR assay was used to determine the binding of SP1 to the *TET1* promoter in MA9.3ITD treated with PBS or 5 ng/mL HHT for 48 h. IgG was used as a negative control. (G) Identification of direct binding between HHT and SP1 *via* DARTS assay in MA9.3ITD cells. Western blot analysis of the DARTS samples. (H) Identification of direct binding between HHT and SP1 *via* CETSA assay in MA9.3ITD cells. Western blot analysis of the CETSA samples. (I) Western blotting analysis of SP1 knockdown efficacy and effects of *SP1* knockdown on the growth/proliferation of MA9.3RAS and MONOMAC 6 AML cells. (J) Relative expression of *TET1* in MA9.3RAS and MONOMAC 6 AML cells with or without *SP1* knockdown. **P*<0.05; ***P*<0.01; ****P*<0.001; *t*-test. Error bar, mean±Standard Deviation.

responsive target stability (DARTS) assay and cellular thermal shift assay (CETSA) to clarify whether SP1 is a potential direct binding target of HHT.[35,36] Indeed, the DARTS result suggests that HHT directly binds with SP1 protein and confers drug-induced pronase-resistance for SP1 (Figure 3G). Moreover, the CETSA result confirms the direct association of HHT to SP1 and leads to the shift thermal stability of SP1 protein (Figure 3H). Finally, we showed that depletion of SP1 expression significantly inhibited AML cell growth and suppressed *TET1* expression (Figure 3I and J), recapitulating the effects of HHT treatment (Figures 1B and 3C, and *Online Supplementary Figure S3A*). Thus, by inhibiting the binding of SP1 on *TET1* promoter, HHT negatively regulates transcription of

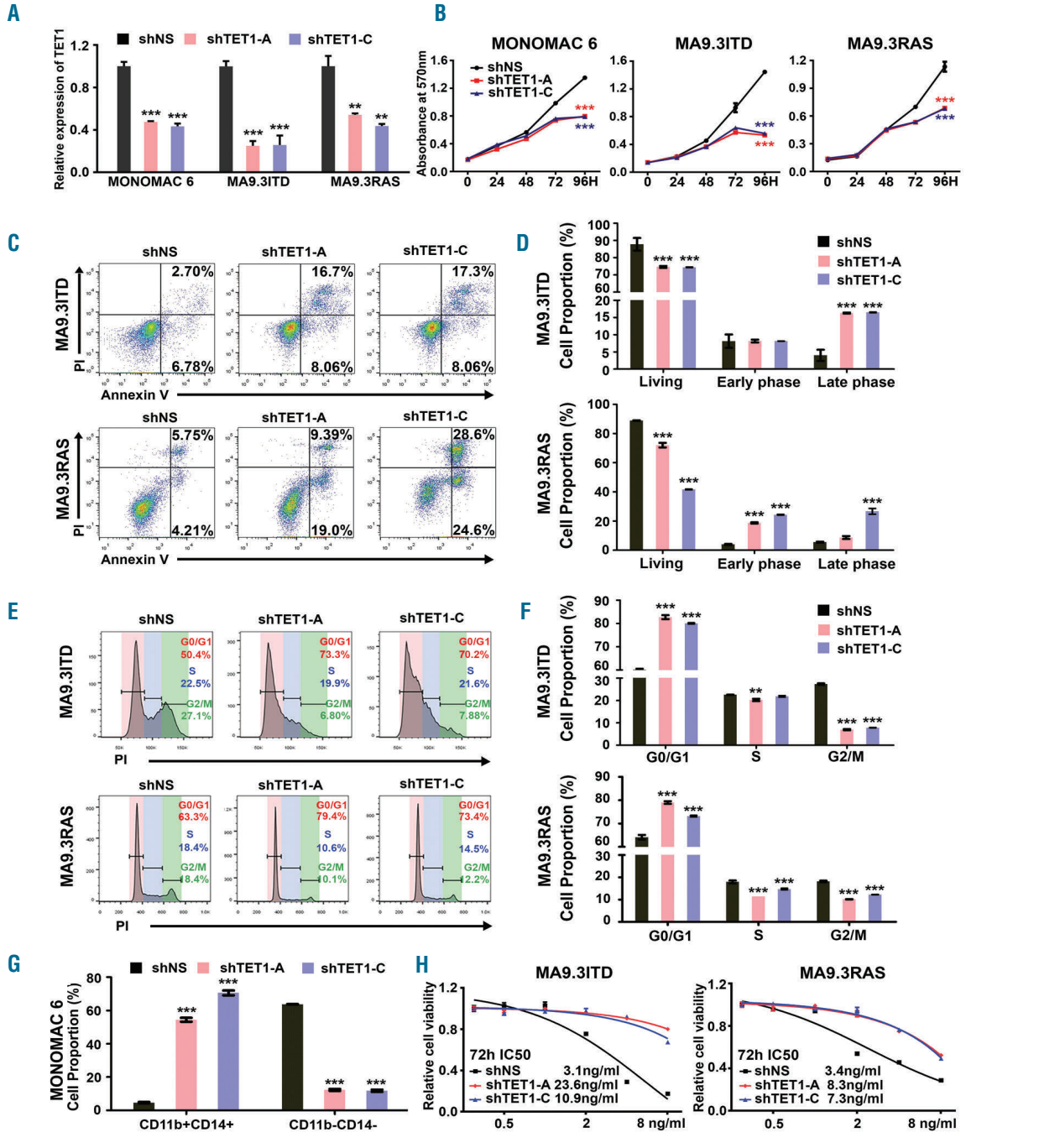

Figure 4. Knockdown of *TET1* expression recapitulates effects of homoharringtonine (HHT) treatment in acute myeloid leukemia (AML) cells. (A) Qualitative polymerase chain reaction (qPCR) analysis of *TET1* knockdown efficacy in MONOMAC 6, MA9.3ITD and MA9.3RAS cells. (B) Effects of *TET1* knockdown on cell growth/proliferation of these three AML cell lines at different time points [0, 24, 48, 72 and 96 hours (h)]. (C) Effects of *TET1* knockdown on apoptosis in MA9.3ITD and MA9.3RAS AML cells. (D) Statistical analysis of apoptosis assay in AML cells from three independent experiments determined by flow cytometry. (E) Effects of *TET1* knockdown on cell cycle arrest in AML cells. (F) Statistical analysis of cell cycle assays from three independent experiments determined by flow cytometry. (G) Statistical analysis of cell proportions of $CD11b^{+}CD14^{+}$ and $CD11b^{-}CD14^{-}$ in TET1 knockdown or control MONOMAC 6 cells. (H) HHT IC_{50} in MA9.3ITD and MA9.3RAS cells with or without TET1 knockdown. These cells were exposed to HHT for 72 h. **P*<0.05; ***P*<0.01; ****P*<0.001; *t*-test. Error bar, mean±Standard Deviation.

TET1. Collectively, our data reveal a previously unrecognized signal pathway involving HHT, SP1 and TET1, and identify a novel mechanism by which HHT inhibits TET1 expression and thereby reduces global 5hmC modification in AML cells.

TET1 is a functionally important target of homoharringtonine that mediates homoharringtonine effects in acute myeloid leukemia

We next investigated whether knockdown of *TET1* can mimic the effects of HHT (TET1 inhibition) and whether the treatment efficacy of HHT is dependent on its inhibition on *TET1* expression in AML. As expected, depletion of *TET1* expression by shRNA (Figure 4A) could largely mimic the effects of HHT treatment in AML cells, including inhibiting cell growth, inducing apoptosis, blocking cell cycle, and promoting myeloid differentiation (Figure 4B-G, and *Online Supplementary Figure S4A-C*). Furthermore, knockdown of *TET1* dramatically reduced the sensitivity of AML cells to HHT treatment, with IC_{50} values increased to more than 2-fold (Figure 4H), suggesting that TET1 is a critical target of HHT that mediates the effects of HHT treatment in AML cells. Together, our data indicate that HHT induced cell growth inhibition, cell apoptosis, cell cycle arrest, and cell differentiation largely owing to its inhibition on TET1 expression/function in AML.

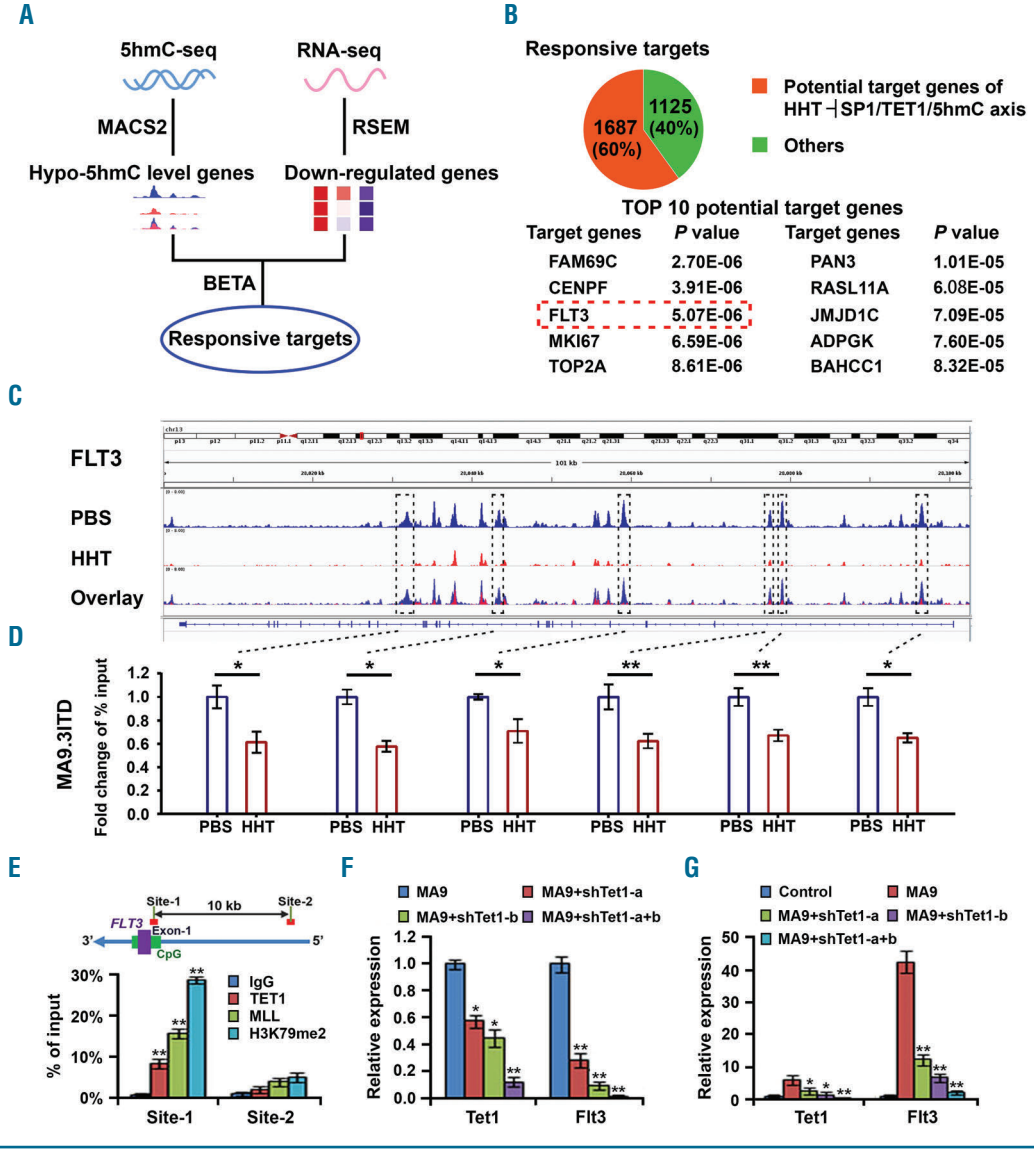

Figure 5. *FLT3* is a critical target of the homoharringtonine (HHT) SP1/TET1/5hmC axis. (A) Scheme of identification of response targets of the HHT⊣SP1/TET1/5hmC axis by 5hmC-sequencing (5hmC-seq) and RNA-seq of MA9.3 RAS and MA9.3ITD acute myeloid leukemia (AML) cells treated with phosphate-buffered saline (PBS) or HHT (10 ng/mL for 5hmC-seq samples) for 48 hours (h). Responsive targets refer to genes with downregulation in both 5hmC abundance and RNA level upon HHT treatment. (B) Potential HHT⊣SP1/TET1/5hmC targets found by overlap analysis of the responsive targets and putative TET1 targets (top panel). Top ten target genes were shown (bottom panel). (C) The view of 5hmC abundance across *FLT3* genomic locus in MA9.3ITD cells with PBS or HHT (10 ng/mL) treatment. (D) The verification of decreased 5hmC abundance on FLT3 *via* Chromatin immune-precipitation (ChIP)-qPCR analysis with different primers covering corresponding 5hmC peaks shown in boxes in (C). (E) ChIP-qPCR analysis of the binding of TET1, as well as MLL-fusion proteins, to the loci of *FLT3* in MONOMAC 6 cells. Green bar represents the CpG island and purple bar represents exons of FLT3. Both MLL and H3K79me2 were used as positive controls. (F and G) The effects of knockdown of *Tet1* on expression of *Flt3* in MLL-AF9 transformed colony cells (F) and in leukemic bone marrow (BM) blast cells of bone marrow transplantation (BMT) recipient mice that developed MLL-AF9-induced AML (G). **P*<0.05; ***P*<0.01; ****P*<0.001; *t*-test. Error bar, mean±Standard Deviation.

FLT3 is a direct target of TET1 and is suppressed by the homoharringtonine ⊣TET1/5hmC/ axis

We next performed 5hmC-seq and RNA-seq of AML cells with or without HHT treatment to identify downstream targets that are regulated by the HHT⊣TET1/5hmC axis. As TET1 has been reported to positively regulate expression of many target genes through a 5hmC-dependent mechanism,[17,37] we sought to identify responsive targets that exhibit reduced 5hmC level and downregulation in expression upon HHT treatment (Figure 5A). By overlapping such responsive targets with the list of TET1 potential direct targets as detected by ChIP-on-chip or ChIP-seq in the mammalian genome,[37-39] we identified 1,687 potential TET1 targets that showed significant decreases in 5hmC level and significant downregulation in expression (Figure 5B, top

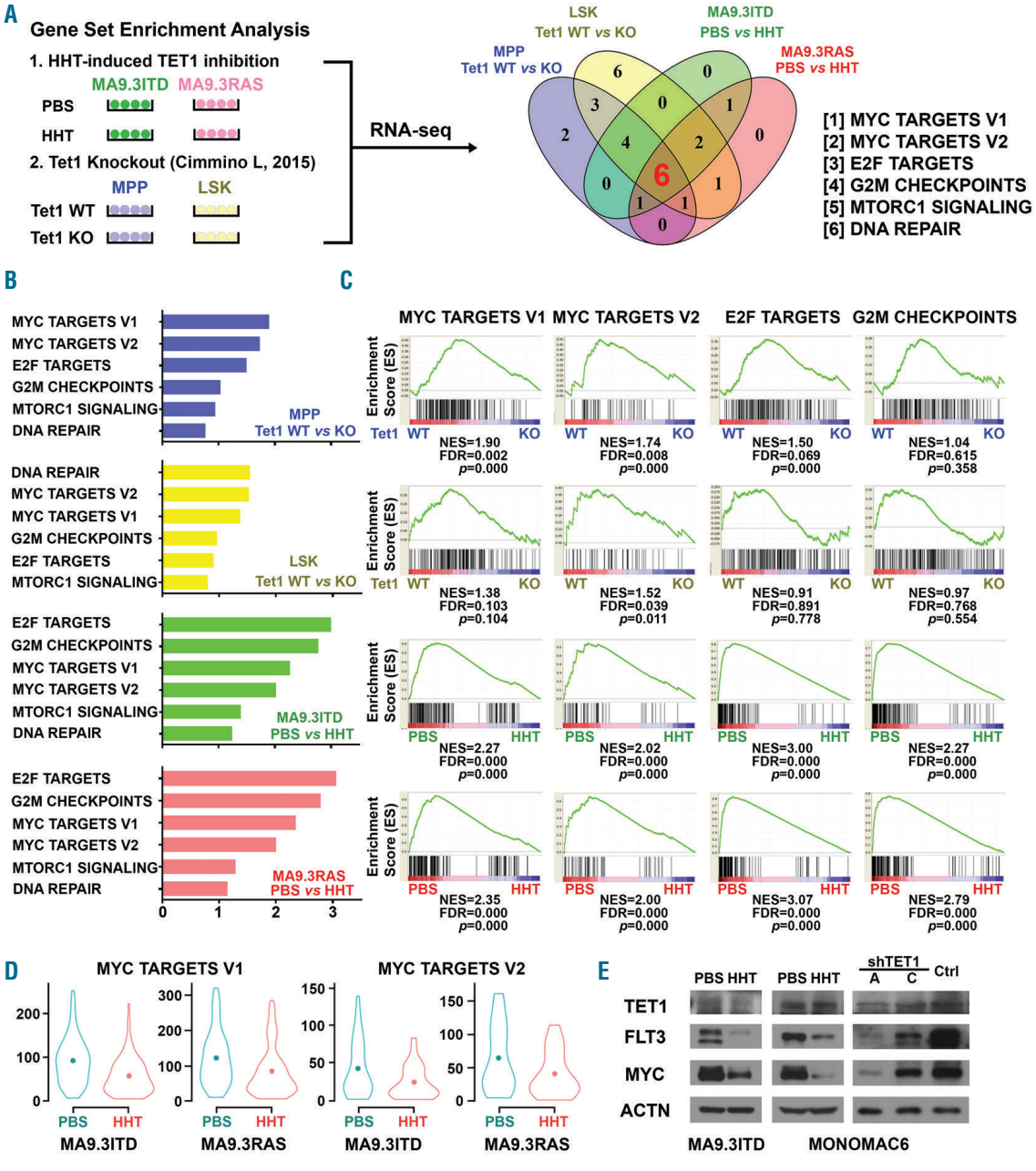

Figure 6. Pathways affected by the homoharringtonine (HHT)-SP1/TET1/5hmC axis. (A) Integrative analysis of our HHT-treatment RNA-sequencing (RNA-seq) data with published *Tet1* knockout RNA-seq data[42] to identify pathways or gene sets that were commonly affected by both HHT treatment and Tet1 knockout. RNA-seq data from MA9.3RAS and MA9.3ITD AML cells treated with phosphate-buffered saline (PBS) or HHT (10 ng/mL) for 48 hours (h), along with RNA-seq data from mouse BM Lin$^-$/c-Kit$^+$/Sca1$^+$ (LSK) and multipotent progenitor (MPP) cells with or without Tet1 knockout,[42] were used in the analysis. Six gene sets were identified to be affected by both HHT treatment and Tet1 knockout in all four conditions. (B) Normalized enrichment score (NES) of the six gene sets. (C) Among the six signaling pathways, MYC targets V1, *MYC* targets V2, E2F targets, and G2M checkpoints gene sets were significantly suppressed upon both HHT treatment and Tet1 knockout. (D) Decreased relative expression levels of genes of the MYC targets V1/V2 gene sets in MA9.3ITD and MA9.3RAS upon HHT treatment. The dot inside represents the median expression levels of the gene sets. (E) Western blot analysis of TET1, FLT3, and MYC in PBS- or HHT-treated MA9.3ITD and MONOMAC-6 cells and in MONOMAC-6 cells with or without *TET1* knockdown. ACTIN was used as an endogenous control.

panel, and *Online Supplementary Table S3*). Across the genomic locus of these potential targets, the top ten targeted genes with the most significant decreases in 5hmC levels were listed (Figure 5B, bottom panel). Notably, *FLT3*, a well-recognized oncogene related to leukemogenesis,[7,9] is in the top list, associated with substantially decreased 5hmC abundance and significant downregulation in expression after HHT treatment (Figure 5C and *Online Supplementary Figure S5A*). Our ChIP-qPCR further confirmed the decreased 5hmC abundance on FLT3 gene locus upon HHT treatment in AML cells (Figure 5D).

The ChIP-seq data reported previously[38] showed that *Flt3* is a direct target gene of Tet1 in mouse embryonic stem cells (*Online Supplementary Figure S5B*). To validate whether *FLT3* is also a direct target of TET1 in human AML cells, we performed ChIP-qPCR in MONOMAC 6 cells and showed that TET1 was especially enriched at the CpG area (Site 1) rather than the distal upstream area (Site 2) of *FLT3* (in Figure 5E MLL and H3K79me2 are included as positive controls). Moreover, we showed that knockdown of *Tet1* resulted in decreased expression of *Flt3* in MLL-AF9 transformed colony cells (Figure 5F) and in BM cells of MLL-AF9 leukemia mice (Figure 5G). Conversely, forced expression of wild-type Tet1 (but not catalytically inactive mutant Tet1) in non-*MLL* rearranged human AML cells, such as Kasumi-1 cells (carrying t(8;21)/*AML1-ETO*), results in a significantly elevated expression of *FLT3* (*Online Supplementary Figure S5C*). Similarly, in human CD34$^+$ hematopoietic stem/progenitor cells (HSPC), we observed a strong positive correlation between *FLT3* and *TET1* in expression during both granulocytic and monocytic differentiation models (*Online Supplementary Figure S5D*). Furthermore, both HHT treatment and TET1 knockdown suppressed *FLT3* expression in human AML cells (*Online Supplementary Figure S5E*). Taken together, our results suggest that *FLT3* is a direct target of TET1 and HHT treatment-induced TET1 inhibition or knockdown of TET1 suppresses *FLT3* expression through a 5hmC-related mechanism.

We previously reported that *HOXA9* and *MEIS1* were directly targeted by TET1 in AML cells.[17] Consistently, here we showed that HHT treatment could also decrease expression of HOXA9 and MEIS1 in human AML cells (*Online Supplementary Figure S5F*). Interestingly, we and others have also reported previously that HOXA9/MEIS1 and FLT3 may each positively regulate the expression of the other.[23,40,41] Indeed, here we showed that forced expression of either wild-type *FLT3* or *FLT3*-ITD could significantly up-regulate expression of HOXA9 and MEIS1 in human 293T cells (*Online Supplementary Figure S5G*) in a manner similar to *FLT3*-ITD-mediated upregulation of HOXA9 and MEIS1 in human MONOMAC 6 AML cells, as we had reported previously.[23] Conversely, we also showed that forced expression of *HOXA9* and *MEIS1* could substantially increase FLT3 level in mouse bone marrow progenitor cells (*Online Supplementary Figure S6A*). Thus, there may be a reciprocal positive regulatory loop between TET1 targets, such as *FLT3* and *HOXA9/MEIS1*.

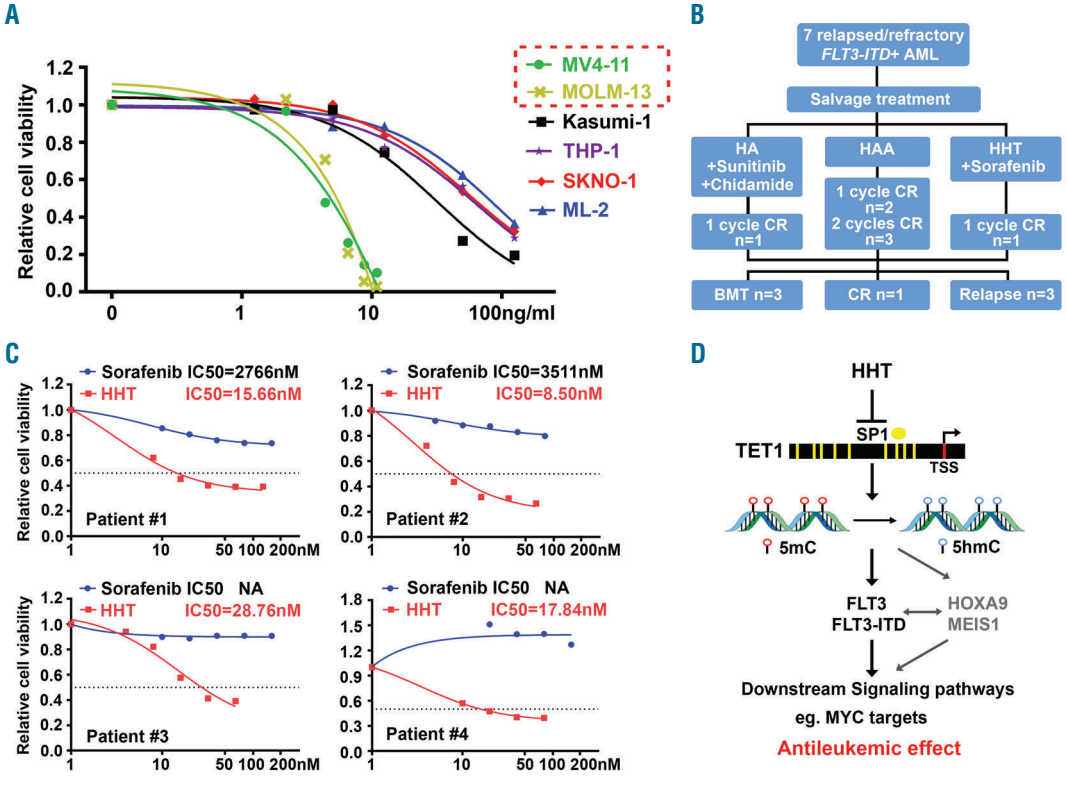

Figure 7. Acute myeloid leukemia (AML) with FLT3 mutations are highly sensitive to homoharringtonine (HHT) treatment. (A) The sensitivity of AML cells with and without FLT3 mutations to HHT treatment. The AML cells were treated with a series of concentrations of HHT for 48 hours. (B) The HHT-based treatment regimen used for seven relapsed/refractory FLT3-ITD AML patients in clinic. HA: HHT plus cytarabine; HAA: HHT plus cytarabine and aclarubicin. (C) The IC_{50} values of HHT and sorafenib in primary FLT3-ITD AML patients' samples.(C) The HHT-based treatment regimen used for seven relapsed/refractory *FLT3*-ITD AML patients in clinic. HA: HHT plus cytarabine; HAA: HHT plus cytarabine and aclarubicin. (D) Schematic illustration of the molecular mechanism underlying the anti-tumor effects of HHT mainly through suppression of the SP1/TET1/5hmC/FLT3-HOXA9-MEIS1/MYC axis.

Notably, MA9.3ITD cell line was established from human cord blood CD34$^+$ cells virally transduced with *MLL-AF9* and *FLT3*-ITD.[21] Thus, one may expect that ectopic expression of *FLT3*-ITD in this cell line would not be suppressed by HHT/TET1 and thereby should show resistance to HHT, which is somewhat opposite to what we observed (e.g. Figure 1A and B). We presumed that such a discrepancy might be due to the possibility that virally transduced *FLT3*-ITD in MA9.3ITD cells was by chance integrated to a locus that is also under control of TET1. Actually, there are a total of 11,632 genes that are associated with Tet1 enrichment in their promoter regions [-2kb to +2kb relative to annotated transcription start sites (TSS)] as detected by at least 2 out of 3 genome-wide ChIP-on-chip or ChIP-seq analyses in mouse embryonic stem cells (mESC).[37-39] Therefore, although many of such putative targets identified from mESC might not be genuine targets of TET1 in human AML cells, there is still a good chance that the virally transduced *FLT3*-ITD in MA9.3ITD cell line was integrated, by chance, to a locus that is also under control of TET1. Indeed, HHT treatment could dramatically decrease the overall FLT3 (including *FLT3*-ITD) protein level, suggesting that is highly likely that *FLT3*-ITD expression in MA9.3ITD cell line is also under control of HHT/TET1 (Figure 6E). To determine whether non-TET1-controlled ectopic expression of *FLT3* or *FLT3*-ITD can cause resistance to HHT in transduced AML cells, we virally transduced human Kasumi-1 AML cells with a high titer of *FLT3* or *FLT3*-ITD viruses. In this way, each transduced cell had multiple copies of *FLT3* or *FLT3*-ITD, and thus there would be a good chance that at least one copy was integrated into a locus not controlled by TET1. We sorted transduction-positive cells (i.e. RFP$^+$ cells) 48 hours post transduction and then treated the cells with HHT or PBS for 24 hours. Forced expression of *FLT3* or *FLT3*-ITD conferred at least partial resistance in transduced Kasumi-1 cells to HHT, while TET1 expression was still suppressed by HHT (*Online Supplementary Figure 5H-J*). Taken together, our data suggest that *FLT3* is a downstream target of HHT/TET1 and mediates the sensitivity of AML cells to HHT.

MYC signaling is a major downstream pathway affected by the homoharringtonine ⊣ SP1/TET1/5hmC axis

To further identify downstream pathways affected by the HHT ⊣ TET1/5hmC axis, we conducted an integrative analysis of our RNA-seq data of HHT-induced TET1 inhibition in AML cells and RNA-seq data of Tet1 knockout in mouse HSPCs [Lin$^-$/c-Kit$^+$/Sca1$^+$ (LSK) and multipotent progenitor (MPP) cells] reported by Cimmino *et al.*[42] Through gene set enrichment analysis (GSEA), we identified six gene sets strongly enriched in both HHT-induced *TET1* inhibition and *Tet1* knockout, including MYC targets V1, MYC targets V2, E2F targets, G2M checkpoints, MTORC1 signaling, and DNA repair (Figure 6A). The normalized enrichment score (NES) of the six co-enriched signaling pathways in all four pairs of samples are shown in Figure 6B. Among the six gene sets, MYC targets V1, MYC targets V2, E2F targets, and G2M checkpoints were significantly suppressed upon HHT treatment and *Tet1* knockout (Figure 6C). The violin plots showed the down-regulated expression of the clustering genes in MYC targets V1 and MYC targets V2 after HHT treatment in AML cell lines (Figure 6D). Among these suppressed signal pathways, MYC functions as universal transcriptional amplifier and directly and indirectly regulates expression of multiple core enriched genes.[43] More interestingly, MYC was reported as a downstream target of FLT3, and was significantly enriched in FLT3 constitutively activated cells and largely suppressed with the treatment of FLT3 inhibitor.[10,12] Indeed, we showed that forced expression of either FLT3 or FLT3-ITD can substantially increase expression of MYC (*Online Supplementary Figure S6B*). In addition, consistent with previous studies showing that HOXA9/MEIS1 can up-regulate expression of *MYC*,[44] we found that forced expression of HOXA9 and MEIS1 could also substantially increase MYC level (*Online Supplementary Figure S6A*). Our Western blot results also confirmed the decreased expression of TET1, FLT3 and MYC in HHT-treated or *TET1*-knockdown human *MLL*-rearranged or non-MLL-rearranged AML cells (Figure 6E and *Online Supplementary Figure S6C*). These findings suggest that *MYC* is an essential downstream target of the HHT ⊣ SP1/TET1/5hmC/FLT3-HOXA9-MEIS1 axis and MYC signaling is a major pathway inhibited by HHT treatment in AML.

Homoharringtonine treatment represents a promising therapeutic strategy for the treatment of acute myeloid leukemia with FLT3 mutations

In line with the above discoveries, we found that human AML cell lines with FLT3 mutations are indeed much more sensitive to HHT than those without (Figure 7A). Next, we collected four primary AML samples from *de novo* or relapse/refractory patients with *FLT3*-ITD mutation (*Online Supplementary Table S4*). Notably, all the primary AML samples are highly sensitive to HHT treatment, with IC_{50} values < 30 nM; in contrast, these AML samples are relatively resistant to sorafenib, a tyrosine kinase inhibitor that was usually recommended to patients with FLT3-ITD mutation in clinic,[45] with IC_{50} values >2.7 μM (Figure 7C). The superior effect of HHT, relative to sorafenib, might be owing to the fact that HHT can suppress expression of not only *FLT3* but also other critical oncogenic targets of TET1 (e.g. *HOXA9* and *MEIS1*), as mentioned above. Furthermore, we have successfully applied the HHT-based salvage chemotherapy in treating relapse/refractory patients in Zhejiang, China, and some of them were successfully bridged to BMT (Figure 7B and Jie *et al., unpublished data*). Together with our mechanistic studies described above, our data suggest that the high sensitivity of HHT in AML with *FLT3* mutations is largely attributed to the HHT-induced inhibition of *FLT3/HOXA9/MEIS1* expression/function through the HHT ⊣ SP1/TET1/5hmC axis (Figure 7D).

Discussion

Previous studies have reported that HHT-based chemotherapy exhibited a high efficiency in treating *de novo* AML patients,[4,5] but the underlying mechanism has not been well elucidated. In the present study, we showed that HHT treatment alone caused potent inhibition of AML cell growth/survival *in vitro* and substantial suppression of AML progression *in vivo*, and such inhibitory effects are likely attributed to HHT-induced cell cycle blockage and apoptosis, as well as enhanced myeloid differentiation. Mechanistically, we showed that, by target-

ing SP1/TET1, HHT treatment causes a substantial decrease in global 5hmC abundance and thereby markedly changes DNA epigenome and reprograms the downstream pathways. We demonstrated that SP1 is a direct drug target of HHT and a positive transcriptional regulator of *TET1*, and HHT competitively inhibits the binding of SP1 to the promoter region of *TET1* and thereby suppresses SP1-mediated *TET1* transcription; knockdown of either *SP1* or *TET1* can largely recapitulate the effects of HHT in AML. In addition, we have previously showed that depletion or suppression of *TET1* expression dramatically inhibited AML progression and substantially prolonged survival in AML mice,[17-19] recapitulating the potent *in vivo* anti-AML effect of HHT. Moreover, depletion of *TET1* expression could make AML cells much less sensitive to HHT, further suggesting that the anti-AML activity of HHT relies on the suppression of the SP1/TET1/5hmC axis. However, further systematical studies are warranted to determine which particular sites/domains of SP1 are bound by HHT; such information would help us better understand how HHT disrupts the transcription-factor activity of SP1. Interestingly, SP1 has also been reported to positively regulate expression of BCR-ABL in chronic myeloid leukemia (CML) cells.[46] Thus, the antileukemic effect of HHT in CML might not be solely due to its binding to ribosome,[6] but likely also through targeting SP1 directly and thereby suppressing SP1-mediated activation of the BCR-ABL and *TET1* signaling pathways.

Furthermore, our 5hmC-seq and RNA-seq analyses identified FLT3 as a critical target of the HHT ⊣ SP1/TET1/5hmC axis; HHT treatment or *TET1* knockdown markedly reduced 5hmC abundance on *FLT3* locus and decreased *FLT3* expression in AML cells, and our ChIP-qPCR assay confirmed that FLT3 is a direct target of *TET1*. Interestingly, consistent with previous reports,[23,40,41] here we showed that FLT3 exhibits a positive reciprocal regulation relationship with HOXA9/MEIS1, two known targets of TET1.[17] Thus, our data suggest that, by suppression of *TET1* expression, HHT simultaneously inhibits expression of multiple target genes of TET1 (which may form a reciprocal positive regulatory loop) in AML cells and thereby displays a potent antileukemic effect.

FLT3 encodes a class III receptor tyrosine kinase that regulates hematopoiesis and the mutation of FLT3 is the most common driven mutation found in more than 30% of AML patients.[47] Both ITD and tyrosine kinase domain mutation of FLT3 result in its constitutive activation and thus lead to leukemogenesis by promoting expression of a number of critical oncogenic downstream targets such as *MYC*.[10-12,48] Despite the extensive efforts in developing and testing FLT3 inhibitors in the clinic, AML patients with high allelic ratio FLT3-ITD are still classified as adverse risk category in 2017 European LeukemiaNet recommendation due to the high relapse rate and poor overall survival.[7,11,12] Thus, the development of improved therapeutics for treating *FLT3*-ITD AML is still an unmet need.

Here we also showed that primary AML patients with *FLT3* mutations, including both newly diagnosed and relapsed patients, exhibit a high sensitivity to HHT treatment (with IC_{50} <30 nM). Consistent with our findings, another group also reported recently that HHT exhibited preferential antileukemic effect against AML carrying *FLT3*-ITD as detected by an *in vitro* drug screening on patients' samples.[49] In addition, they conducted a phase II clinical trial in relapsed/refractory *FLT3*-ITD AML patients, in which 20 out of 24 patients achieved complete remission with sorafenib and HHT combination treatment (median leukemia-free survival and overall survival: 12 and 33 weeks, respectively).[49] While they showed sorafenib alone reduced the amount of pFLT3 protein, and HHT alone reduced the amount of both FLT3 and pFLT3 protein in *FLT3*-ITD AML cell lines, no further mechanistic studies were carried out.[49] Our studies elucidated the molecular mechanism underlying the high sensitivity of *FLT3*-mutated AML to HHT treatment. This mechanism involves HHT-induced reprogramming of DNA epigenome by targeting the SP1/TET1/5hmC axis and thereby inhibition of transcription of a set of critical oncogenic targets, especially *FLT3*, which in turn leads to the suppression of FLT3 downstream pathways, such as MYC signaling. Notably, it is well known that *FLT3*-ITD mutation patients under therapy often develop secondary FLT3 mutations which result in drug resistance. Interestingly, we found that MONOMAC 6, which carries the *FLT3* V592A mutation,[50] was also sensitive to HHT. Moreover, the relapsed/refractory *FLT3*-ITD AML patient also showed sensitivity to HHT treatment and could be bridged to transplantation in subsequent treatment[49] (Figure 7B). Therefore, HHT-based therapeutics (i.e. HHT plus other therapeutic agents such as FLT3 inhibitors and/or standard chemotherapy) represent effective novel treatments for *de novo* or relapsed/refractory *FLT3*-mutated AML patients.

In summary, here we show that HHT, approved by the FDA for CML treatment, also exhibits potent therapeutic efficacy in AML and decreases global 5hmC abundance by targeting the SP1/TET1/5hmC axis. Although other mechanisms, such as inhibition of protein synthesis,[6] may also contribute to the overall antileukemic effects of HHT in AML, which warrant further systematical studies in the future, our work reveals a novel mechanism involving suppression of the SP1/TET1/5hmC/FLT3-HOXA9-MEIS1/MYC signaling through which HHT exhibits potent therapeutic activity in treating AML. Since AML is characterized by cytogenetic and molecular heterogeneity, targeted therapy is a growing trend for selected subtypes of AML, especially for those with adverse prognosis. Here we provide compelling functional and mechanistic data suggesting that an HHT-based therapeutic approach represents effective target therapeutics to treat AML carrying FLT3 mutations and/or with overexpression of endogenous *TET1/FLT3/HOXA9/MEIS1*, which accounts for more than 40% of total human AML cases.[7]

Acknowledgments

The authors would also like to thank Dr. James Mulloy for the generous gift of MA9.3ITD and MA9.3RAS cell lines, and Dr. Ravi Bahtia for the kind gift of MV4-11 and MOLM-13 cell lines.

Funding

The work was supported in part by the National Institutes of Health (NIH) R01 Grants CA214965 (JC), CA211614 (JC), CA178454 (JC), CA182528 (JC), and CA236399 (JC) and a R56 grant DK120282 (JC), as well as grants from National Natural Science Foundation of China 81820108004 (JJ) and 81900154 (CL). JC is a Leukemia & Lymphoma Society (LLS) Scholar.

References

1. Powell RG, Weisleder D, Smith CR Jr. Antitumor alkaloids for Cephalataxus harringtonia: structure and activity. J Pharm Sci. 1972;61(8):1227-1230.
2. Nazha A, Kantarjian H, Cortes J, Quintas-Cardama A. Omacetaxine mepesuccinate (synribo) - newly launched in chronic myeloid leukemia. Expert Opin Pharmacother. 2013;14(14):1977-1986.
3. Cephalotaxine esters in the treatment of acute leukemia. A preliminary clinical assessment. Chin Med J (Engl). 1976; 2(4):263-272.
4. Jin J, Jiang DZ, Mai WY, et al. Homoharringtonine in combination with cytarabine and aclarubicin resulted in high complete remission rate after the first induction therapy in patients with de novo acute myeloid leukemia. Leukemia. 2006; 20(8):1361-1367.
5. Jin J, Wang JX, Chen FF, et al. Homoharringtonine-based induction regimens for patients with de-novo acute myeloid leukaemia: a multicentre, open-label, randomised, controlled phase 3 trial. Lancet Oncol. 2013;14(7):599-608.
6. Gurel G, Blaha G, Moore PB, Steitz TA. U2504 determines the species specificity of the A-site cleft antibiotics: the structures of tiamulin, homoharringtonine, and bruceantin bound to the ribosome. J Mol Biol. 2009;389(1):146-156.
7. Dohner H, Estey E, Grimwade D, et al. Diagnosis and management of AML in adults: 2017 ELN recommendations from an international expert panel. Blood. 2017;129(4):424-447.
8. Patel JP, Gonen M, Figueroa ME, et al. Prognostic relevance of integrated genetic profiling in acute myeloid leukemia. N Engl J Med. 2012;366(12):1079-1089.
9. Jiang X, Bugno J, Hu C, et al. Eradication of Acute Myeloid Leukemia with FLT3 Ligand-Targeted miR-150 Nanoparticles. Cancer Res. 2016;76(15):4470-4480.
10. Kim KT, Baird K, Davis S, et al. Constitutive Fms-like tyrosine kinase 3 activation results in specific changes in gene expression in myeloid leukaemic cells. Br J Haematol. 2007;138(5):603-615.
11. Leung AY, Man CH, Kwong YL. FLT3 inhibition: a moving and evolving target in acute myeloid leukaemia. Leukemia. 2013;27(2):260-268.
12. Konig H, Levis M. Targeting FLT3 to treat leukemia. Expert Opin Ther Targets. 2015;19(1):37-54.
13. Tahiliani M, Koh KP, Shen Y, et al. Conversion of 5-methylcytosine to 5-hydroxymethylcytosine in mammalian DNA by MLL partner TET1. Science. 2009;324(5929):930-935.
14. Ono R, Taki T, Taketani T, Taniwaki M, Kobayashi H, Hayashi Y. LCX, leukemia-associated protein with a CXXC domain, is fused to MLL in acute myeloid leukemia with trilineage dysplasia having t(10;11)(q22;q23). Cancer Res. 2002; 62(14):4075-4080.
15. Lorsbach RB, Moore J, Mathew S, Raimondi SC, Mukatira ST, Downing JR. TET1, a member of a novel protein family, is fused to MLL in acute myeloid leukemia containing the t(10;11)(q22;q23). Leukemia. 2003;17(3):637-641.
16. Moran-Crusio K, Reavie L, Shih A, et al. Tet2 loss leads to increased hematopoietic stem cell self-renewal and myeloid transformation. Cancer Cell. 2011;20(1):11-24.
17. Huang H, Jiang X, Li Z, et al. TET1 plays an essential oncogenic role in MLL-rearranged leukemia. Proc Natl Acad Sci USA. 2013;110(29):11994-11999.
18. Jiang X, Hu C, Arnovitz S, et al. miR-22 has a potent anti-tumour role with therapeutic potential in acute myeloid leukaemia. Nat Commun. 2016;7:11452.
19. Jiang X, Hu C, Ferchen K, et al. Targeted inhibition of STAT/TET1 axis as a therapeutic strategy for acute myeloid leukemia. Nat Commun. 2017;8(1):2099.
20. Zhao Z, Chen L, Dawlaty MM, et al. Combined Loss of Tet1 and Tet2 Promotes B Cell, but Not Myeloid Malignancies, in Mice. Cell Rep. 2015;13(8):1692-1704.
21. Wunderlich M, Mizukawa B, Chou FS, et al. AML cells are differentially sensitive to chemotherapy treatment in a human xenograft model. Blood. 2013;121(12):e90-97.
22. Su R, Dong L, Li C, et al. R-2HG Exhibits Anti-tumor Activity by Targeting FTO/m(6)A/MYC/CEBPA Signaling. Cell. 2018;172(1-2):90-105 e123.
23. Jiang X, Huang H, Li Z, et al. Blockade of miR-150 maturation by MLL-fusion/MYC/LIN-28 is required for MLL-associated leukemia. Cancer Cell. 2012; 22(4):524-535.
24. Song CX, Szulwach KE, Fu Y, et al. Selective chemical labeling reveals the genome-wide distribution of 5-hydroxymethylcytosine. Nat Biotechnol. 2011; 29(1):68-72.
25. Zhang Y, Liu T, Meyer CA, et al. Model-based analysis of ChIP-Seq (MACS). Genome Biol. 2008;9(9):R137.
26. Li B, Dewey CN. RSEM: accurate transcript quantification from RNA-Seq data with or without a reference genome. BMC Bioinformatics. 2011;12:323.
27. Wang S, Sun H, Ma J, et al. Target analysis by integration of transcriptome and ChIP-seq data with BETA. Nat Protoc. 2013; 8(12):2502-2515.
28. Subramanian A, Tamayo P, Mootha VK, et al. Gene set enrichment analysis: a knowledge-based approach for interpreting genome-wide expression profiles. Proc Natl Acad Sci U S A. 2005;102(43):15545-15550.
29. Yan M, Kanbe E, Peterson LF, et al. A previously unidentified alternatively spliced isoform of t(8;21) transcript promotes leukemogenesis. Nat Med. 2006;12(8):945-949.
30. Conway O'Brien E, Prideaux S, Chevassut T. The epigenetic landscape of acute myeloid leukemia. Adv Hematol. 2014; 2014:103175.
31. Eriksson A, Lennartsson A, Lehmann S. Epigenetic aberrations in acute myeloid leukemia: Early key events during leukemogenesis. Exp Hematol. 2015;43(8):609-624.
32. Smale ST. Nuclear run-on assay. Cold Spring Harb Protoc. 2009; 2009(11):pdb.prot5329.
33. Liu S, Wu LC, Pang J, et al. Sp1/NFkappaB/HDAC/miR-29b regulatory network in KIT-driven myeloid leukemia. Cancer Cell. 2010;17(4):333-347.
34. Zhang Y, Chen HX, Zhou SY, et al. Sp1 and c-Myc modulate drug resistance of leukemia stem cells by regulating survivin expression through the ERK-MSK MAPK signaling pathway. Mol Cancer. 2015; 14:56.
35. Lomenick B, Jung G, Wohlschlegel JA, Huang J. Target identification using drug affinity responsive target stability (DARTS). Curr Protoc Chem Biol. 2011; 3(4):163-180.
36. Jafari R, Almqvist H, Axelsson H, et al. The cellular thermal shift assay for evaluating drug target interactions in cells. Nat Protoc. 2014;9(9):2100-2122.
37. Xu Y, Wu F, Tan L, et al. Genome-wide regulation of 5hmC, 5mC, and gene expression by Tet1 hydroxylase in mouse embryonic stem cells. Mol Cell. 2011;42(4):451-464.
38. Williams K, Christensen J, Pedersen MT, et al. TET1 and hydroxymethylcytosine in transcription and DNA methylation fidelity. Nature. 2011;473(7347):343-348.
39. Wu H, D'Alessio AC, Ito S, et al. Dual functions of Tet1 in transcriptional regulation in mouse embryonic stem cells. Nature. 2011; 473(7347):389-393.
40. Wang GG, Pasillas MP, Kamps MP. Meis1 programs transcription of FLT3 and cancer stem cell character, using a mechanism that requires interaction with Pbx and a novel function of the Meis1 C-terminus. Blood. 2005;106(1):254-264.
41. Burillo-Sanz S, Morales-Camacho RM, Caballero-Velazquez T, et al. NUP98-HOXA9 bearing therapy-related myeloid neoplasm involves myeloid-committed cell and induces HOXA5, EVI1, FLT3, and MEIS1 expression. Int J Lab Hematol. 2016; 38(1):64-71.
42. Cimmino L, Dawlaty MM, Ndiaye-Lobry D, et al. TET1 is a tumor suppressor of hematopoietic malignancy. Nat Immunol. 2015;16(6):653-662.
43. Nie Z, Hu G, Wei G, et al. c-Myc is a universal amplifier of expressed genes in lymphocytes and embryonic stem cells. Cell. 2012;151(1):68-79.
44. Bessa J, Tavares MJ, Santos J, et al. meis1 regulates cyclin D1 and c-myc expression, and controls the proliferation of the multipotent cells in the early developing zebrafish eye. Development. 2008; 135(5):799-803.
45. Rollig C, Serve H, Huttmann A, et al. Addition of sorafenib versus placebo to standard therapy in patients aged 60 years or younger with newly diagnosed acute myeloid leukaemia (SORAML): a multicentre, phase 2, randomised controlled trial. Lancet Oncol. 2015;16(16):1691-1699.
46. Jin B, Wang C, Shen Y, Pan J. Anthelmintic niclosamide suppresses transcription of BCR-ABL fusion oncogene via disabling Sp1 and induces apoptosis in imatinib-resistant CML cells harboring T315I mutant. Cell Death Dis. 2018;9(2):68.
47. Papaemmanuil E, Gerstung M, Bullinger L, et al. Genomic Classification and Prognosis in Acute Myeloid Leukemia. N Engl J Med. 2016;374(23):2209-2221.
48. Brondfield S, Umesh S, Corella A, et al. Direct and indirect targeting of MYC to treat acute myeloid leukemia. Cancer Chemother Pharmacol. 2015;76(1):35-46.
49. Lam SS, Ho ES, He BL, et al. Homoharringtonine (omacetaxine mepesuccinate) as an adjunct for FLT3-ITD acute myeloid leukemia. Sci Transl Med. 2016; 8(359):359ra129.
50. Spiekermann K, Dirschinger RJ, Schwab R, et al. The protein tyrosine kinase inhibitor SU5614 inhibits FLT3 and induces growth arrest and apoptosis in AML-derived cell lines expressing a constitutively activated FLT3. Blood. 2003;101(4):1494-1504.

ARTICLE

Allogeneic hematopoietic cell transplantation improves outcome of adults with t(6;9) acute myeloid leukemia: results from an international collaborative study

Sabine Kayser,[1,2] Robert K. Hills,[3] Marlise R. Luskin,[4] Andrew M. Brunner,[5] Christine Terré,[6] Jörg Westermann,[7] Kamal Menghrajani,[8] Carole Shaw,[9,10] Maria R. Baer,[11,12] Michelle A. Elliott,[13] Alexander E. Perl,[14] Zdeněk Ráčil,[15] Jiri Mayer,[15] Pavel Zak,[16] Tomas Szotkowski,[17] Stéphane de Botton,[18] David Grimwade,[19*] Karin Mayer,[20] Roland B. Walter,[9,10,21] Alwin Krämer,[1,2] Alan K. Burnett,[3] Anthony D. Ho,[1] Uwe Platzbecker,[22] Christian Thiede,[23] Gerhard Ehninger,[23] Richard M. Stone,[4] Christoph Röllig,[23] Martin S. Tallman,[8] Elihu H. Estey,[9,10] Carsten Müller-Tidow,[1] Nigel H. Russell,[24] Richard F. Schlenk[25] and Mark J. Levis[26]

[1]Department of Internal Medicine V, University Hospital of Heidelberg, Heidelberg, Germany; [2]German Cancer Research Center (DKFZ) and Department of Internal Medicine V, University of Heidelberg, Heidelberg, Germany; [3]Cardiff University School of Medicine, Cardiff, UK; [4]Department of Medical Oncology, Dana-Farber Cancer Institute, Boston, MA, USA; [5]Massachusetts General Hospital, Boston, MA, USA; [6]Laboratory of Hematology, André Mignot Hospital, Le Chesnay, France; [7]Department of Hematology, Oncology and Tumor Immunology, Charité-University Medical Center, Campus Virchow Clinic, Berlin, Germany; [8]Leukemia Service, Department of Medicine, Memorial Sloan Kettering Cancer Center, Weill Cornell Medical College, New York, NY, USA; [9]Clinical Research Division, Fred Hutchinson Cancer Research Center, Seattle, WA, USA; [10]Division of Hematology/Department of Medicine, University of Washington, Seattle, WA, USA; [11]University of Maryland Greenebaum Comprehensive Cancer Center, Baltimore, MD, USA; [12]Department of Medicine, University of Maryland School of Medicine, Baltimore, MD, USA; [13]Division of Hematology, Department of Internal Medicine, Mayo Clinic, Rochester, MN, USA; [14]Division of Hematology and Oncology, Abramson Cancer Center, Perelman School of Medicine at the University of Pennsylvania, Philadelphia, PA, USA; [15]Department of Internal Medicine, Hematology and Oncology, Masaryk University and University Hospital Brno, Brno, Czech Republic; [16]4th Department of Internal Medicine-Hematology, Faculty of Medicine, Charles University and University Hospital Hradec Králové, Hradec Králové, Czech Republic; [17]Department of Hemato-Oncology, Faculty of Medicine and Dentistry, Palacky University Olomouc and University Hospital Olomouc, Olomouc, Czech Republic; [18]Université Paris-Saclay, Gustave Roussy Villejuif, France; [19]Department of Medical & Molecular Genetics, King's College London, Faculty of Life Sciences and Medicine, London, UK; [20]Medical Clinic III for Oncology, Hematology and Rheumatology, University Hospital Bonn, Bonn, Germany; [21]Department of Epidemiology, University of Washington, Seattle, WA, USA; [22]Medical Clinic and Policlinic I, Hematology and Cellular Therapy, University Hospital Leipzig, Leipzig, Germany; [23]Department of Internal Medicine I, University Hospital Carl-Gustav-Carus, Dresden, Germany; [24]Department of Haematology, Nottingham University Hospitals NHS Trust, Nottingham, UK; [25]NCT Trial Center, National Center for Tumor Diseases, Heidelberg, Germany and [26]Sidney Kimmel Comprehensive Cancer Center, Johns Hopkins University, Baltimore, MD, USA

Ferrata Storti Foundation

Haematologica 2020
Volume 105(1):161-169

Correspondence:

SABINE KAYSER
s.kayser@dkfz-heidelberg.de

Received: January 21, 2019.

Accepted: April 15, 2019.

Pre-published: April 19, 2019.

doi:10.3324/haematol.2018.208678

Check the online version for the most updated information on this article, online supplements, and information on authorship & disclosures: www.haematologica.org/content/105/1/161

ABSTRACT

Acute myeloid leukemia (AML) with t(6;9)(p22;q34) is a distinct entity accounting for 1-2% of AML cases. A substantial proportion of these patients have a concomitant *FLT3*-ITD. While outcomes are dismal with intensive chemotherapy, limited evidence suggests allogeneic hematopoietic cell transplantation (allo-HCT) may improve survival if performed early during first complete remission. We report on a cohort of 178 patients with t(6;9)(p22;q34) within an international, multicenter collaboration. Median age was 46 years (range: 16-76), AML was *de novo* in 88%, *FLT3*-ITD was present in 62%, and additional cytogenetic abnormalities in 21%. Complete remission was achieved in 81% (n=144), including 14 patients who received high-dose cytarabine after initial induction failure. With a median follow up of 5.43 years, estimated overall survival at five years was 38% (95%CI: 31-47%). Allo-HCT was performed in 117 (66%) patients, including 89 in first complete remission. Allo-HCT in first com-

plete remission was associated with higher 5-year relapse-free and overall survival as compared to consolidation chemotherapy: 45% (95%CI: 35-59%) and 53% (95%CI: 42-66%) *versus* 7% (95%CI: 3-19%) and 23% (95%CI: 13-38%), respectively. For patients undergoing allo-HCT, there was no difference in overall survival rates at five years according to whether it was performed in first [53% (95%CI: 42-66%)], or second [58% (95%CI: 31-100%); n=10] complete remission or with active disease/relapse [54% (95%CI: 34-84%); n=18] (*P*=0.67). Neither *FLT3*-ITD nor additional chromosomal abnormalities impacted survival. In conclusion, outcomes of t(6;9)(p22;q34) AML are poor with chemotherapy, and can be substantially improved with allo-HCT.

Introduction

Acute myeloid leukemia (AML) with t(6;9)(p22;q34) has been listed as a distinct entity in the World Health Organization classification since 2008 and accounts for a small group (1-2%) of AML patients.[1,2] The translocation t(6;9), first described in AML in 1976,[3] results in formation of the *DEK-NUP214* chimeric fusion gene, where DEK at 6p22[3] is fused to *NUP214* (formerly known as CAN), located at 9q34.[4] This fusion gene acts as an aberrant transcription factor and alters nuclear transport by binding soluble transport factors.[5] In addition, *DEK-NUP214* has been reported to enhance protein synthesis in myeloid cells.[6,7] In a murine model, *DEK-NUP214* induced leukemia when transduced to long-term repopulating stem cells.[8]

Acute myeloid leukemia with t(6;9) occurs in children and adults, as reported in a retrospective cohort analysis of 69 patients (31 children and 38 adults) with a median age of 23 years, most of whom presented with *de novo* AML.[2] Of note, 42-69% of pediatric and 73-90% of adult AML patients with t(6;9) are described to harbor a concomitant internal tandem duplication of the *FLT3* gene (*FLT3*-ITD),[2,9-13] while secondary cytogenetic abnormalities are observed in 12-19% of pediatric and adult patients.[2,13]

Clinically, t(6;9) AML has been associated with a poor prognosis in children and adults,[2,12-15] with reported 5-year overall survival (OS) rates of 28% and 9%, respectively.[2] With this, adult patients with this translocation are categorized into the adverse risk group according to the National Comprehensive Cancer Network guidelines.[16] Allogeneic hematopoietic cell transplantation (allo-HCT) may improve survival if performed during first complete remission (CR1).[2,17] However, the results were hampered by the small number of patients. Even results derived from a large registry data base were inconclusive on this issue due to missing data on allo-HCT.[15] Additionally, results on AML patients with t(6;9)(p22;q34) are rarely reported, although these patients were included in a recent large randomized trial.[18] Thus, international multicenter cohort studies are the only opportunity to better describe characteristics and evaluate outcome according to treatment strategies.

The objectives of our study were to characterize a large cohort of AML patients with t(6;9)(p22;q34) in an international, multicenter cohort and to evaluate outcomes according to treatment.

Methods

Patients and treatment

Information on 178 patients with AML and t(6;9)(p22;q34) diagnosed between 1989 and 2016 was collected from fourteen study groups/institutions in the US and Europe. Participating centers were chosen upon network relationships of the first and last author. Detailed case report forms (including information on baseline characteristics, chemotherapy, allo-HCT, response, and survival) were collected from all participating centers. Inclusion criteria were adult patients with t(6;9)(p22;q34), eligible for intensive therapy (ECOG 0-2), including (but not limited to) allo-HCT. All patients who fulfilled these criteria were included by the participating groups/institutions, respectively. Diagnosis of AML was based on French-American-British Cooperative Group criteria[19] and, after 2003, on revised International Working Group criteria.[20] Chromosome banding was performed using standard techniques, and karyotypes were described according to the International System for Human Cytogenetic Nomenclature.[21] *FLT3* mutation screening for internal tandem duplications (ITD) and point mutations within the tyrosine kinase domain (TKD) was carried out at each institution per local practice.[10,22] Data collection and analysis were approved by the Institutional Review Boards of the participating centers.

Treatment

One-hundred and seventy-six of the 178 patients (99%) received intensive induction treatment either within clinical trials (n=116) or according to local institutional standards (n=62). Treatment protocols included the Study Alliance Leukemia (SAL) AML96[23] and AML2003[24] trials, the United Kingdom AML10,[15] AML11,[25] AML12,[15] AML14,[25] AML15,[15] AML16[26] and AML17[27] protocols, as well as the ALFA 9801,[28] 9802[29] and 0702[30] trials. Induction therapy according to local standard most frequently consisted of the 7+3 regimen of anthracycline plus cytarabine (n=53). Two patients (1%) received either azacitidine or decitabine as induction therapy and both went on to allo-HCT. Response was assessed according to International Working Group recommendations.[20] All studies were approved by the institutional review boards of the participating centers. All patients provided written informed consent for participation in one of the treatment trials or for therapy according to local standards.

Statistical analysis

Survival end points including OS, relapse-free survival (RFS), cumulative incidence of relapse (CIR), and cumulative incidence of death in CR (CID) were defined according to the revised recommendations of the International Working Group.[20] Comparisons of patients' characteristics were performed with the Kruskal-Wallis rank sum test for continuous variables and Fisher's exact test for categorical variables. The median follow-up time was computed using the reverse Kaplan-Meier estimate.[31] The Kaplan-Meier method was used to estimate the distribution of RFS and OS.[32] Confidence interval (CI) estimation for survival curves was based on the cumulative hazard function using Greenwood's formula for variance estimation. Log rank tests were employed to compare survival curves between groups. A Cox proportional hazards regression model was used to identify

prognostic variables for OS.[33] The following variables were included in the Cox models: age at diagnosis, gender, logarithm of white blood cells, platelet count, *FLT3*-ITD mutational status, and detection of additional cytogenetic abnormalities. The effect of allo-HCT on OS as a time-dependent intervening event was tested by using the Mantel-Byar method[34] for univariable and Andersen-Gill model for multivariable analyses.[35] The method of Simon and Makuch was used to estimate survival distributions with respect to time-dependent interventions.[36]

The individuals at risk were initially all represented in the chemotherapy group. If patients received an allo-HCT, they were censored at this time point in the chemotherapy group and further followed up within the allo-HCT group.

Cumulative incidence of relapse and CID and their standard errors were computed according to the method described by Gray[37] and included only patients attaining CR. Missing data were replaced by 50 imputations using multivariate imputations by chained equations applying predictive mean matching.[38] Backward selection applying a stopping rule based on *P*-values was used in multivariable regression models to exclude redundant or unnecessary variables. All statistical analyses were performed with the R statistical software environment, version 3.3.1, using the R packages prodlim, version 1.5.7, and survival, version 2.39-5.[39]

Results

Study cohort

Overall demographic and clinical data were collected from 178 patients (MRC, n=75; SAL, n=27; Fred Hutchinson Cancer Research Center, Seattle, n=12; ALFA, n=12; Dana-Faber Cancer Institute and Massachusetts General Hospital, Boston, n=12; Johns Hopkins University, Baltimore, n=8; Charité-University Medical Center Berlin, n=7; University of Maryland Greenebaum Comprehensive Cancer Center, n=6; Memorial Sloan Kettering Cancer Center, New York, n=6; Perelman School of Medicine at the University of Pennsylvania, n=4; Mayo Clinic Rochester, n=4; Czech Leukemia Centers, n=4; University Hospital Bonn, n=1) diagnosed with t(6;9)(p22;q34) AML between 1989 and 2016. Baseline characteristics are summarized in Table 1; median age was 46 years (range: 16-76) and 82 patients (46%) were female. Type of AML was *de novo* in 157 (88%), therapy-related in 4 (2%), and secondary after previous myelodysplastic syndrome (MDS)/myeloproliferative neoplasm in 12 (7%) patients. In addition, five (3%) patients with MDS treated intensively according to AML protocols were included in this analysis. Median white blood cell (WBC) count was $16.6x10^9$/L (range: 0.5-274) and was significantly higher in patients with, compared to without, *FLT3*-ITD (*P*=0.02).

Cytogenetic and molecular analyses

The balanced translocation t(6;9)(p22;q34) was the sole abnormality in 140 (79%) patients, while additional cytogenetic abnormalities were present in 38 (21%). Of note, trisomy 13 was present in ten patients, either as a sole additional abnormality (n=1), in combination with trisomy 8 (n=2) or with another balanced translocation (n=2), or within a complex karyotype characterized by gains only (n=5). *FLT3*-ITD molecular testing was available in 127 (71%) patients and 79 (62%) had *FLT3*-ITD. *FLT3*-TKD mutational status was available in 76 (43%) and 4 (5%) were mutated (Table 1).

Response to induction therapy

Data on response to induction therapy were available in all patients. Early death (ED) occurred in two (1%) patients. Overall, CR was achieved in 144 patients (81%). Thirty-five patients with initial induction failure received a salvage therapy [high-dose cytarabine (HiDAC-)-based, n=23; other intensive, n=3; not intensive, n=4; unknown, n=5)] and 23 of them achieved a CR (66%), including 14 after HiDAC. The CR rate in patients with *FLT3*-ITD was 81% (64 of 79 patients) as compared to 77% (37 of 48 patients) in patients without *FLT3*-ITD (*P*=0.65). No prognostic factors for CR achievement were identified within the available baseline characteristics. Two of five patients with MDS achieved a CR according to AML criteria. In six patients with *FLT3*-ITD treated on the AML15 (n=2) or AML17 (n=4) trials, lestaurtinib[40] was added to induction therapy and all patients achieved a CR.

Further therapy including intensive consolidation and allogeneic hematopoietic stem cell transplantation

Fifty-five (38%) of 144 patients in CR1 received intensive consolidation chemotherapy without transplantation, whereas 89 (62%) proceeded to allo-HCT. The majority of the patients (n=52 of 89, 58%) who went on to allo-HCT received a consolidation therapy prior to transplant.

Relapses occurred in 47 (85%) patients after consolidation chemotherapy and in 28 (31%) after allo-HCT in CR1. Relapsed patients without allo-HCT died after in median 5.4 months (range: 1-31.6 months). Twenty-one patients who relapsed after allo-HCT died.

Three patients died after consolidation chemotherapy and seventeen in CR after allo-HCT in CR1, mainly due to graft-*versus*-host disease (GvHD; n=5) or infections (n=4).

Tyrosine kinase inhibitors (TKI) were given after relapse in seven patients with *FLT3*-ITD, either as single agents (n=6) or in combination with chemotherapy (n=1) (post allo-HCT, n=4; post chemotherapy, n=3). A CR2 was achieved in one patient after treatment with gilteritinib[41] and a second patient achieved CR2 with incomplete hematologic recovery (CRi) after treatment with lestaurtinib in combination with mitoxantrone/etoposide/cytarabine. The first patient died in CR one month after initiation of gilteritinib due to a perforated intestine and sepsis. The second patient relapsed six months after achieving CR2 and received donor lymphocytes, but died six months later due to progressive disease. Another patient was salvaged with quizartinib and achieved a partial remission (9% blast cells in bone marrow). The patient then went on to allo-HCT, but died one month later due to GvHD. Treatment with either gilteritinib or sorafenib was not successful in the other four patients.

Allogeneic hematopoietic stem cell transplantation in second complete remission

Among patients not proceeding to allo-HCT in CR1, ten patients were transplanted in CR2. Of those, six have died at a median of 16.5 months after allo-HCT. Causes of death in CR were infection (n=2), graft failure (n=1), multi-organ failure (n=1), and unknown (n=1). One patient relapsed and died due to AML.

Allogeneic hematopoietic stem cell transplantation with residual disease

In 34 patients not achieving a CR after intensive induction therapy, 15 (44%) proceeded to allo-HCT with active

disease. Of those, six patients are still in CR after a median follow up of 66.5 months (range: 11.8-110.8 months) and two patients achieved CR2 after relapse and are still in CR, whereas seven patients died (transplant-related mortality, n=4; refractory AML after relapse, n=2; pulmonary embolism 7.9 years after transplant, n=1).

Allogeneic hematopoietic stem cell transplantation after relapse

Three patients proceeded to allo-HCT with active disease after relapse and all of these patients died. Causes of death included infection after 56 days in one and GvHD 15 days after transplant in another patient. One patient died due to refractory AML after relapse.

Characteristics of patients undergoing allogeneic hematopoietic stem cell transplantation

Overall, an allo-HCT was performed in 117 of the 178 patients (66%), either in CR1 (n=89) or CR2 (n=10), with refractory disease (n=15) or after relapse (n=3) with no differences in baseline characteristics between groups (Table 1).

The majority of patients (n=76) received myeloablative conditioning, including total body irradiation (TBI) in 39

Table 1. Baseline characteristics of patients with acute myeloid leukemia and t(6;9)(p22;q34).

	All patients (n=178)	Subset of patients undergoing allo-HCT in CR (n=99)	Subset of patients undergoing allo-HCT with active disease/ relapse (n=18)
Median age (years) (Range)	46 (16-76)	43 (16-71)	46 (19-69)
Male gender, n (%)	96 (54)	57 (58)	9 (50)
Median WBC, x10^9/L (Range)	16.6 (0.5-274)	13.1 (0.5-274)	16.3 (1.5-200.4)
Missing	12	8	1
Median hemoglobin, g/dL (Range)	8.6 (3.2-14.2)	8.6 (3.2-14.2)	9 (4.6-13.1)
Missing	29	18	2
Median platelets, x10^9/L (Range)	53 (7-451)	53 (7-451)	59 (10-229)
Missing	21	13	2
Median BM blasts, % (Range)	60 (7-100)	55 (10-100)	60 (7-90)
Missing	22	12	1
Cytogenetics, n (%)			
As sole aberration	140 (79)	79 (80)	14 (78)
Including +13*	10 (6)	6 (6)	–
Sole +13	1	–	–
+ 8, +13	2	1	–
Other complex**	11 (6)	6 (6)	1 (6)
Nullisomy X/Y	4 (2)	–	2 (11)
Other$^+$	13 (7)	7 (7)	1 (6)
Disease type, n (%)			
De novo AML	157 (88)	88 (89)	15 (83)
s-AML	12 (7)	7 (7)	1 (6)
t-AML	4 (2)	3 (3)	–
MDS	5 (3)	1 (1)	2 (11)
***FLT3*-ITD**			
n (%)	79 (62)	43 (57)	9 (60)
Missing	51	25	3
***FLT3*-TKD**			
n (%)	4 (5)	4 (8)	–
Missing	102	48	9

allo; allogeneic; AML: acute myeloid leukemia; BM: bone marrow; CR: complete remission; FLT3: fms-related tyrosine kinase 3; HCT: hematopoietic cell transplantation; ITD: internal tandem duplication; s-AML: AML after previous myelodysplastic syndrome / myeloproliferative neoplasm; t-AML: therapy-related AML; TKD: tyrosine kinase domain; WBC: white blood cell count. *Within a complex karyotype characterized by gains only (n=5). **Within a complex karyotype characterized by losses and unbalanced translocations. $^+$Other than +8/+13/nullisomy X/Y. Results may not add-up to 100 due to rounding.

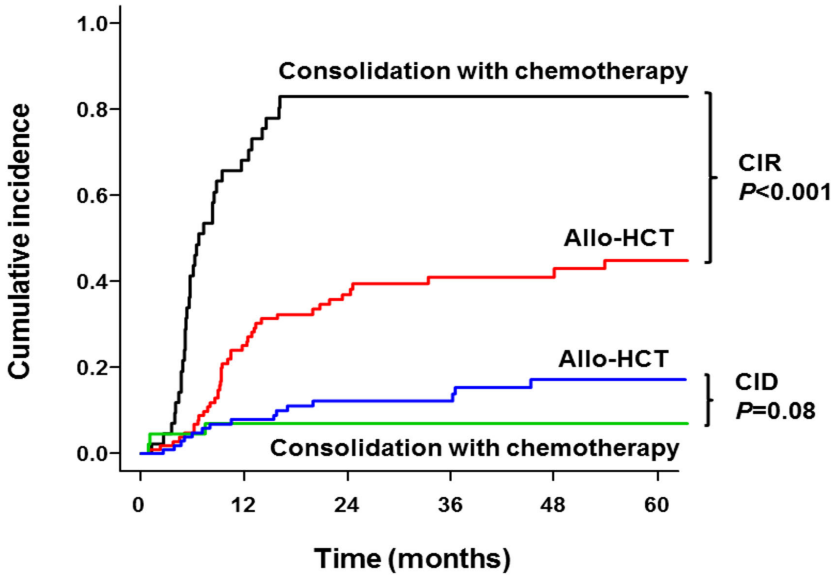

Figure 1. Cumulative incidence of relapse (CIR) and cumulative incidence of death (CID) according to treatment strategy. CIR and CID included only patients achieving complete remission.

Table 2. Relapse-free and overall survival according to treatment strategy in first complete remission.

	5-years RFS %	95%-CI	5-year OS %	95%-CI
Allo-HCT (n=89)	45	35-59	53	42-66
Consolidation chemotherapy (n=55)	7	3-19	23	13-38

allo-HCT: allogeneic hematopoietic cell transplantation; CI: confidence interval; OS: overall survival; RFS: relapse-free survival. Median follow up was 5.43 years (95%CI: 3.93-6.53 years).

patients. Forty-one patients received reduced-intensity conditioning. Source of donor was matched related in 46, matched unrelated in 54, haplo-identical in 11, cord blood in five, and unknown in one of the 117 patients.

Cumulative incidence of relapse, cumulative incidence of death in complete remission and survival

The median follow up of the entire cohort was 5.43 years (95%CI: 3.93-6.53 years). Median and 5-year OS of the entire cohort were 2.25 years (95%CI: 1.56-3.70 years) and 38% (95%CI: 31-47%). Five-year RFS and OS were 45% (95%CI: 35-59%) and 53% (95%CI: 42-66%) in patients proceeding to allo-HCT in CR1 after induction therapy (n=89), as compared to 7% (95%CI: 3-19%;) and 23% (95%CI: 13-38%), respectively, in those who received consolidation chemotherapy alone (n=55) (Table 2). In subgroup analysis, presence of *FLT3*-ITD had no prognostic impact on OS, either in the total analyzed cohort (P=0.093), or in those patients proceeding to allo-HCT (P=0.39). Similarly, additional chromosomal abnormalities had no prognostic impact on OS in the mentioned cohorts (P=0.49; P=0.86; respectively). A Cox regression analysis revealed, after limited backward selection, higher WBC [hazard ratio (HR) for log10, 1.62; 95%CI: 1.12-2.29; P=0.005] and age (HR for a difference of 10 years, 1.29; 95%CI: 1.12-1.50; P=0.001) as unfavorable variables, whereas platelet count, type of AML (*de novo vs.* therapy-related/secondary after previous MDS/myeloproliferative neoplasm), presence of *FLT3*-ITD, and additional cytogenetic aberrations had no impact on prognosis.

In 144 patients achieving CR1, CIR was significantly lower in patients proceeding to allo-HCT (n=89) as compared to those who were treated with consolidation chemotherapy (n=55; P<0.001). As expected, CID tended to be higher in patients proceeding to allo-HCT as compared to those receiving consolidation chemotherapy (P=0.08) (Figure 1).

One hundred and seventeen patients proceeded to allo-HCT in CR1 (n=89) or CR2 (n=10), or with refractory (n=15) or relapsed (n=3) disease. The influence of allo-HCT assessed as a time-dependent co-variable as post remission therapy on OS is illustrated by a Simon Makuch plot (Figure 2). In addition, Figure 3 shows a Kaplan Meier plot illustrating the influence of allo-HCT performed in CR1 on RFS. The Mantel-Byar tests revealed a significantly better OS (P=0.001) and RFS (P<0.0001) for patients proceeding to allo-HCT in CR1 as compared to consolidation with chemotherapy only. Neither type of conditioning (P=0.90) nor donor type (matched related donor *versus* matched unrelated/haploidentical/cord blood donor; P=0.30) had an impact on outcome. There was no difference in OS measured from date of transplant in patients transplanted in CR1 or CR2 as compared to those with active disease (P=0.66) (Figure 4). An Andersen-Gill model including allo-HCT as a time-dependent variable revealed higher WBC and older age as unfavorable variables, whereas allo-HCT performed either in CR or with active disease was associated with a favorable prognosis. Decade of treatment, additional chromosomal abnormalities or *FLT3*-ITD had no prognostic impact (Table 3).

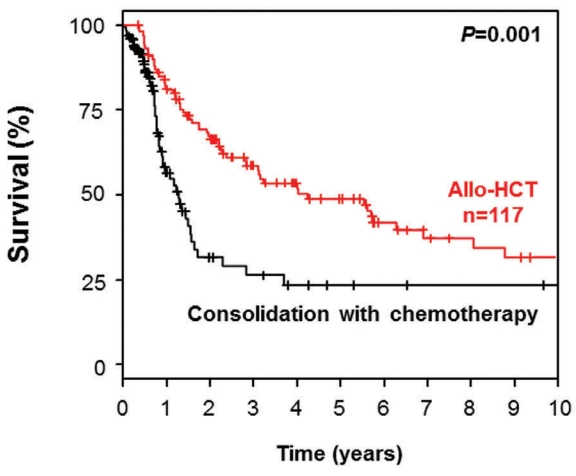

Figure 2. Simon Makuch plot evaluating the impact of allogeneic hematopoietic cell transplantation (allo-HCT) assessed as a time-dependent co-variable in comparison with chemotherapy consolidation on overall survival.

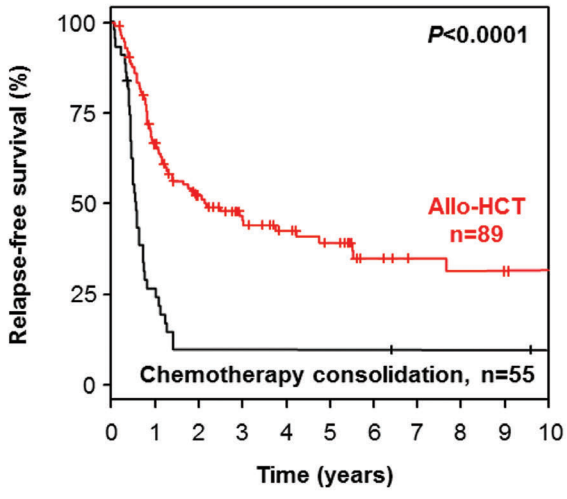

Figure 3. Kaplan Meier plot illustrating the influence of allogeneic hematopoietic cell transplantation (allo-HCT) performed in first complete remission on relapse-free survival.

Discussion

The focus of our study was to characterize adult AML patients with t(6;9) in an international cohort study and compare outcomes according to treatment strategies, with a specific focus on the impact of *FLT3* mutations as well as the impact of allo-HCT as compared to conventional chemotherapy on survival.

We studied 178 patients (AML, n=173; MDS, n=5), all harboring the balanced translocation t(6;9)(p22;q34). A concomitant *FLT3*-ITD has been described in 42-69% of pediatric and 62-90% of adult AML patients with t(6;9),[2,9-13,42] but these reports were hampered by the availability of mutational status in only a subset of patients[2,9,42] and/or analysis of a low patient number.[9-12] In our large cohort, with available mutational status in 71% of patients, a concomitant *FLT3*-ITD was detected in 62% and was significantly associated with higher WBC at diagnosis, which adds to previously published data.[2,9-13,42] Preliminary data suggest that *FLT3*-ITD promotes leukemia induction by *DEK-NUP214* in a murine model.[43] However, a synergistic effect to explain the high coincidence of the two mutations has yet to be demonstrated. In contrast, *FLT3*-TKD mutations were uncommon in our cohort and were slightly less frequent than those reported in AML with normal cytogenetics.[44] In addition, secondary cytogenetic abnormalities were present in 21% of our patients, most commonly including trisomy 13, and/or trisomy 8, or a complex karyotype. To date, there are still conflicting data regarding the impact of *FLT3*-ITD on outcome in AML patients with t(6;9).[13,14,45] While results of a meta-analysis in 50 adult patients indicated an association between *FLT3*-ITD mutations and an inferior outcome in t(6;9) AML,[45] others were inconclusive due to the low number of patients without *FLT3*-ITD,[2] or did not find a significant adverse impact in pediatric AML patients,[13,14] which may be due to an already very dismal prognosis.[14] In our large cohort, neither a concurrent *FLT3*-ITD nor the presence of additional cytogenetic abnormalities had an impact on the achievement of CR or OS, which adds to the recent evaluation by the European Society for Blood and Marrow Transplantation (EBMT).[42]

Table 3. Multivariable Andersen-Gill model on overall survival.

	HR (95%-CI)	P
FLT3-ITD*	1.35 (0.80-2.27)	0.26
Log10(WBC)*	1.69 (1.14-2.51)	0.009
Platelets ($10x10^9$/L difference)	1.00 (0.95-1.04)	0.92
Female gender	1.43 (0.96-2.13)	0.08
Age (10 years difference)	1.22 (1.05-1.42)	0.01
Type of AML#	0.83 (0.44-1.56)	0.55
Additional abnormalities	1.09 (0.67-1.77)	0.74
Decade**	0.81 (0.58-1.13)	0.22
Transplant status	0.55 (0.33-0.90)	0.02

AML: acute myeloid leukemia; CI: confidence interval; HR: hazard ratio; ITD: internal tandem duplication; OS: overall survival; WBC: white blood cell count. *Sensitivity analysis revealed no significant interaction between transplant status and *FLT3*-ITD (P=0.44) or WBC (P=0.12) **Decade, 1989-1999, 2000-2009, 2010-2016. #Type of AML denotes: *de novo versus* therapy-related/secondary after previous myelodysplastic syndrome/myeloproliferative neoplasm.

Previous publications in adult AML patients with t(6;9) reported a fairly low CR rate of 33-58% in adult patients.[2,46] In contrast to these reports, we observed a high CR rate of 81%. The favorable CR rate in our cohort after intensive chemotherapy was in part due to a high response rate of 66% after intensive salvage chemotherapy in patients with failure after standard induction therapy. Intensive combination chemotherapy that incorporates higher doses of cytarabine is frequently used in patients with relapsed/refractory AML, but no specific salvage regimen has emerged as standard. While CR/CRi rates with intensive combination chemotherapy were overall below 40% and nearly similar in refractory (36%) and relapsed AML (36.8%),[47,48] the observed CR rate of 66% in our cohort points to a high sensitivity towards higher doses of cytarabine in patients with initial induction failure. Particularly patients with adverse-risk cytogenetics or *FLT3*-ITD were shown to benefit from HiDAC

therapy.[49] Therefore, the HiDAC approach might be beneficial in patients with t(6;9) and should be addressed further.

In addition, anthracycline dose intensification during induction therapy with daunorubicin at 90 mg/m² has been shown to have a beneficial impact,[27] not only in patients with core-binding factor leukemia,[50] but also in patients with *FLT3*-ITD.[27,51] Although our analysis included patients from the AML17 trial (n=22), which studied high-dose daunorubicin, no meaningful analysis could be made due to the low number of patients.

In our analysis, we found that allo-HCT resulted in an excellent RFS and OS, which is in line with the data of Ishiyama *et al*.[17] In a matched-pair analysis of *de novo* AML using data from the Japanese allo-HCT data registry, they compared outcome of 57 patients with t(6;9) to that of 171 patients with normal karyotype.[17] All patients received an allo-HCT between 1996 and 2007, either in CR1 or CR2 (n=116), or with active disease (n=112). In patients with t(6;9), the 5-year OS (45% *vs.* 40%), disease-free survival (42% *vs.* 33%), CIR (42 *vs.* 45%), and non-relapse mortality (16 *vs.* 22%) did not differ from those observed in AML with normal karyotype.[17] Nevertheless, the results were hampered by a lack of molecular profile in the group of AML with normal karyotype, as well as lack of data on *FLT3*-ITD mutational status in AML with t(6;9). Our data are particularly impressive when compared to the dismal survival of patients with t(6;9) disease treated with chemotherapy alone. Thus, allo-HCT seems to ameliorate outcome in patients with t(6;9), with outcomes comparable to those of patients with intermediate-risk cytogenetics.[52] As expected, CIR was significantly reduced in our cohort after allo-HCT performed in CR1 as compared to intensive consolidation chemotherapy.

Since supportive care might have impacted outcome, we have included the decade of treatment in multivariable analysis. However, this had no impact on overall survival. In addition, neither type of conditioning nor donor type had any impact on outcome. Outcome after allo-HCT was also favorable if performed in CR2, or even with active disease. Overall, this suggests the existence of a specific and very strong graft-*versus*-leukemia effect in this molecular context. Of note, recently presented data by Beya *et al*. on behalf of the EBMT demonstrated similar efficacy of allo-HCT in AML with t(6;9) transplanted in CR2 or active (relapsed/refractory) disease.[42] Although this partly supports the finding from our cohort, we would like to emphasize that retrospectively collected data have serious limitations since the factors for allocating patients to allo-HCT, such as co-morbidities, individual assessment of the treating physician, choice of conditioning, and availability of a donor, remain unknown, and this needs to be taken into account when evaluating the value of allo-HCT in our series.

Despite the large number of patients with *FLT3*-ITD, only thirteen patients were treated with TKI, either front-line with lestaurtinib (n=6) in combination with intensive induction chemotherapy,[40] or after relapse either with single-agent gilteritinib[41] or sorafenib (n=6), or with lestaurtinib in combination with intensive chemotherapy (n=1). Interestingly, all six patients who received front-line lestaurtinib + chemotherapy achieved a CR, whereas TKI treatment ± chemotherapy in relapsed patients showed limited efficacy, with only two patients achieving CR2. Currently, midostaurin is the only approved TKI in *de novo* AML with *FLT3* mutations, based on the positive results from the large, international randomized phase III trial.[18] The combination of midostaurin with intensive chemotherapy significantly improved OS in younger adults with *FLT3*-mutated AML, as compared to the placebo arm. In that study, patients receiving an allo-HCT in CR1 had a better outcome if they were treated with midostaurin during induction therapy, suggesting that the optimal treatment strategy in *FLT3*-mutated AML would be to move on to allo-HCT early in CR1.[18] Unfortunately, no data were presented either in the manuscript or in the supplement for the small subgroup of patients characterized by t(6;9).[18] Thus, the impact of adding TKI to induction chemotherapy in t(6;9) AML is currently unknown.

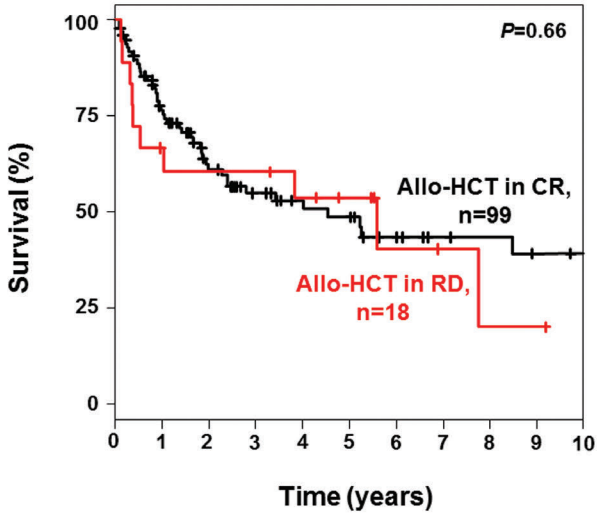

Figure 4. Overall survival after allogeneic hematopoietic cell transplantation according to remission status.

Conclusions

Our cohort of AML patients with t(6;9)(p22;q34) showed a high CR rate after intensive induction therapy, suggesting that these patients should be candidates for intensive induction therapy whenever possible. Despite the initial high chemo-sensitivity of the disease, treatment with consolidation chemotherapy alone resulted in dismal survival outcomes. Thus, based on our encouraging results with allo-HCT, this should be standard of care whenever possible for these patients.

Funding

SK gratefully acknowledges to be supported by the Olympia-Morata fellowship program from the Medical Faculty of the Heidelberg University as well as financial support by Deutsche Forschungsgemeinschaft within the funding program Open Access Publishing, by the Baden-Württemberg Ministry of Science, Research and the Arts and by Ruprecht-Karls-Universität Heidelberg. MJL is supported by a grant from the NCI (NCI Leukemia SPORE P50 CA100632). RBW is a Leukemia & Lymphoma Society Scholar in Clinical Research. ZR, JM, PZ and TS were supported by the Ministry of the Czech Republic, grant No. 15-25809A. Data from the AML10, AML11, AML12, AML14, AML15, AML16, and AML17 trials were supplied by Cardiff University HCTU on behalf of the NCRI AMLWG.

References

1. Swerdlow SH, Campo E, Harris NL, et al. WHO classification of tumours of haematopoietic and lymphoid tissues, revised 4th edition. WHO Press, Geneva, Switzerland, 2017.
2. Slovak ML, Gundacker H, Bloomfield CD, et al. A retrospective study of 69 patients with t(6;9)(p23;q34) AML emphasizes the need for a prospective, multicenter initiative for rare 'poor prognosis' myeloid malignancies. Leukemia. 2006;20(7):1295-1297.
3. Rowley JD and Potter D. Chromosomal banding patterns in acute nonlymphocytic leukemia. Blood.1976;47(5):705-721.
4. von Lindern M, Fornerod M, van Baal S, et al. The translocation (6;9), associated with a specific subtype of acute myeloid leukemia, results in the fusion of two genes, dek and can, and the expression of a chimeric, leukemia-specific dek-can mRNA. Mol Cell Biol. 1992;12(4):1687-1697.
5. Scandura JM, Boccuni P, Cammenga J, Nimer SD. Transcription factor fusions in acute leukemia: variations on a theme. Oncogene. 2002;21(21):3422-3444.
6. Ageberg M, Drott K, Olofsson T, et al. Identification of a novel and myeloid specific role of the leukemia-associated fusion protein DEK-NUP214 leading to increased protein synthesis. Genes Chromosomes Cancer. 2008;47(4):276-287.
7. Boer J, Bonten-Surtel J, Grosveld G. Overexpression of the nucleoporin CAN/NUP214 induces growth arrest, nucleocytoplasmic transport defects, and apoptosis. Mol Cell Biol. 1998;18(3):1236-1247.
8. Oancea C, Rüster B, Henschler R, et al. The t(6;9) associated DEK/CAN fusion protein targets a population of long-term repopulating hematopoietic stem cells for leukemogenic transformation. Leukemia. 2010; 24(11):1910-1919.
9. Oyarzo MP, Lin P, Glassman A, et al. Acute myelogenous leukemia with t(6;9)(p23;q34) is associated with dysplasia and a high frequency of FLT3 gene mutations. Am J Clin Pathol. 2004;122(3):348-358.
10. Thiede C, Steudel C, Mohr B, et al. Analysis of FLT3-activating mutations in 979 patients with acute myelogenous leukemia: association with FAB subtypes and identification of subgroups with poor prognosis. Blood. 2002;99(12):4326-4335.
11. Chi Y, Lindgren V, Quigley S, Gaitonde S. Acute myelogenous leukemia with t(6;9)(p23;q34) and marrow basophilia: an overview. Arch Pathol Lab Med. 2008;132(11):1835-1837.
12. Gupta M, Ashok Kumar J, Sitaram U, et al. The t(6;9)(p22;q34) in myeloid neoplasms: a retrospective study of 16 cases. Cancer Genet Cytogenet. 2010;203(2):297-302.
13. Sandahl JD, Coenen EA, Forestier E, et al. t(6;9)(p22;q34)/DEK-NUP214-rearranged pediatric myeloid leukemia: an international study of 62 patients. Haematologica. 2014;99(5):865-872.
14. Tarlock K, Alonzo TA, Moraleda PP, et al. Acute myeloid leukaemia (AML) with t(6;9)(p23;q34) is associated with poor outcome in childhood AML regardless of FLT3-ITD status: a report from the Children's Oncology Group. Br J Haematol. 2014;166(2):254-259.
15. Grimwade D, Hills RK, Moorman AV, et al. Refinement of cytogenetic classification in acute myeloid leukemia: determination of prognostic significance of rare recurring chromosomal abnormalities among 5876 younger adult patients treated in the United Kingdom Medical Research Council trials. Blood. 2010;116(3):354-365.
16. O'Donnell MR, Tallman MS, Abboud CN, et al. Acute Myeloid Leukemia, Version 3.2017, NCCN Clinical Practice Guidelines in Oncology. J Natl Compr Canc Netw. 2017;15(7):926-957.
17. Ishiyama K, Takami A, Kanda Y, et al. Allogeneic hematopoietic stem cell transplantation for acute myeloid leukemia with t(6;9)(p23;q34) dramatically improves the patient prognosis: a matched-pair analysis. Leukemia. 2012;26(3):461-464.
18. Stone RM, Mandrekar SJ, Sanford BL, et al. Midostaurin plus Chemotherapy for Acute Myeloid Leukemia with a FLT3 Mutation. N Engl J Med. 2017;377(5):454-464.
19. Bennett JM, Catovsky D, Daniel MT, et al. Proposed revised criteria for the classification of acute myeloid leukemia. A report of the French-American-British Cooperative Group. Ann Intern Med. 1985;103(4):620-625.
20. Cheson BD, Bennett JM, Kopecky KJ, et al. Revised recommendations of the International Working Group for Diagnosis, Standardization of Response Criteria, Treatment Outcomes, and Reporting Standards for Therapeutic Trials in Acute Myeloid Leukemia. J Clin Oncol. 2003;21(24):4642-4649.
21. Mitelman F: ISCN: An International System for Human Cytogenetic Nomenclature. Basel, Switzerland: S. Karger; 1995.
22. Yokota S, Kiyoi H, Nakao M, et al. Internal tandem duplication of the FLT3 gene is preferentially seen in acute myeloid leukemia and myelodysplastic syndrome among various hematological malignancies. A study on a large series of patients and cell lines. Leukemia. 1997;11(10):1605-1609.
23. Schaich M, Röllig C, Soucek S, et al. Cytarabine dose of 36 g/m² compared with 12 g/m² within first consolidation in acute myeloid leukemia: results of patients enrolled onto the prospective randomized AML96 study. J Clin Oncol. 2011; 29(19):2696-2702.
24. Schaich M, Parmentier S, Kramer M, et al. High-dose cytarabine consolidation with or without additional amsacrine and mitoxantrone in acute myeloid leukemia: results of the prospective randomized AML2003 trial. J Clin Oncol. 2013;31(17):2094-2102.
25. Wheatley K, Brookes CL, Howman AJ, et al. Prognostic factor analysis of the survival of elderly patients with AML in the MRC AML11 and LRF AML14 trials. Br J Haematol. 2009;145(5):598-605.
26. Burnett AK, Russell NH, Culligan D, et al. The addition of the farnesyl transferase inhibitor, tipifarnib, to low dose cytarabine does not improve outcome for older patients with AML. Br J Haematol. 2012;158(4):519-522.
27. Burnett AK, Russell NH, Hills RK, et al. A randomized comparison of daunorubicin 90 mg/m2 vs 60 mg/m2 in AML induction: results from the UK NCRI AML17 trial in 1206 patients. Blood. 2015;125(25):3878-3885.
28. Pautas C, Merabet F, Thomas X, et al. Randomized study of intensified anthracycline doses for induction and recombinant interleukin-2 for maintenance in patients with acute myeloid leukemia age 50 to 70 years: results of the ALFA-9801 study. J Clin Oncol. 2010;28(5):808-814.
29. Thomas X, Elhamri M, Raffoux E, et al. Comparison of high-dose cytarabine and timed-sequential chemotherapy as consolidation for younger adults with AML in first remission: the ALFA-9802 study. Blood. 2011;118(7):1754-1762.
30. Thomas X, de Botton S, Chevret S, et al. Randomized phase II study of clofarabine-based consolidation for younger adults with acute myeloid leukemia in first remission. J Clin Oncol. 2017;35(11):1223-1230.
31. Schemper M, Smith TL. A note on quantifying follow-up in studies of failure time. Control Clin Trials. 1996;17(4):343-346.
32. Kaplan E, Meier P. Nonparametric estimation from incomplete observations. J Am Stat Assoc. 1958;53(282):457-481.
33. Cox DR. Regression models and life tables (with discussion). J R Stat Soc. 1972; 34(2):187-220.
34. Mantel N, Byar D. Evaluation of response-time data involving transient states: An illustration using heart transplant data. J Am Stat Assoc. 1974;69(345):81-86.
35. Andersen P, Gill RD. Cox's regression model for counting processes: A large sample study. Ann Stat. 1982;10(4):1100-1120.
36. Simon R, Makuch RW. A non-parametric graphical representation of the relationship between survival and the occurrence of an event: application to responder versus non-responder bias. Stat Med. 1984;3(1):35-44.
37. Gray RJ. A class of k-sample tests for comparing the cumulative incidence of a competing risk. Ann Stat. 1988;16(3):1141-1154.
38. Harrell FE. Regression Modeling Strategies: With Applications to Linear Models, Logistic Regression, and Survival Analysis. New York: Springer; 2001.
39. R Development Core Team. R: A language and environment for statistical computing. R Foundation for Statistical Computing. Vienna, Austria, 2014.
40. Knapper S, Russell N, Gilkes A, et al. A randomized assessment of adding the kinase inhibitor lestaurtinib to first-line chemotherapy for FLT3-mutated AML. Blood. 2017;129(9):1143-1154.
41. Perl AE, Altman JK, Cortes J, et al. Selective inhibition of FLT3 by gilteritinib in relapsed or refractory acute myeloid leukaemia: a multicentre, first-in-human, open-label, phase 1-2 study. Lancet Oncol. 2017; 18(8):1061-1075.
42. Beya MD, Labopin M, Maertens J, et al. Allogeneic stem cell transplantation in acute myeloid leukemia with t(6;9)(p23;q34);dek-NUP214 is followed by a low relapse risk and favorable outcome in early phase- a study from the Acute Leukemia Working Party (ALWP) of the European Society for Blood and Marrow Transplantation (EBMT). Blood. 2017; 130(Suppl 1):596.
43. Heinssmann M, Drangmeister L, Schmid K, et al. T(6;9)-DEK/CAN-positive leukemia: role of FLT3-ITD for the determination of the leukemic phenotype. Blood. 2012; 120(21):1316.
44. Kayser S and Levis MJ. FLT3 tyrosine kinase inhibitors in acute myeloid leukemia: clinical implications and limitations. Leuk Lymphoma. 2014;55(2):243-255.
45. Thiede C, Bloomfield CD, Lo Coco F, et al. The high prevalence of FLT3-ITD mutations is associated with the poor outcome in adult patients with t(6;9)(p23;q34) posi-

tive AML - results of an international meta-analysis. Blood. 2007;110(11):761.
46. Visconte V, Shetty S, Przychodzen B, et al. Clinicopathologic and molecular characterization of myeloid neoplasms with isolated t(6;9)(p23;q34). Int J Lab Hematol. 2017; 39(4):409-417.
47. Wattad M, Weber D, Döhner K, et al. Impact of salvage regimens on response and overall survival in acute myeloid leukemia with induction failure. Leukemia. 2017;31(6):1306-1313.
48. Schlenk RF, Frech P, Weber D, et al. Impact of pretreatment characteristics and salvage strategy on outcome in patients with relapsed acute myeloid leukemia. Leukemia. 2017;31(6):1306-1313.
49. Willemze R, Suciu S, Meloni G, et al. High-dose cytarabine in induction treatment improves the outcome of adult patients younger than age 46 years with acute myeloid leukemia: results of the EORTC-GIMEMA AML-12 trial. J Clin Oncol. 2014;32(3):219-228.
50. Prebet T, Bertoli S, Delaunay J, et al. Anthracycline dose intensification improves molecular response and outcome of patients treated for core binding factor acute myeloid leukemia. Haematologica. 2014;99(10):e185-e187.
51. Luskin MR, Lee JW, Fernandez HF, et al. Benefit of high-dose daunorubicin in AML induction extends across cytogenetic and molecular groups. Blood. 2016; 127(12): 1551-1558.
52. Röllig C, Bornhäuser M, Thiede C, et al. Long-term prognosis of acute myeloid leukemia according to the new genetic risk classification of the European LeukemiaNet recommendations: evaluation of the proposed reporting system. J Clin Oncol. 2011; 29(20):2758-2765.

Ferrata Storti Foundation

Therapeutic targeting of mutant p53 in pediatric acute lymphoblastic leukemia

Salih Demir,[1,2] Elena Boldrin,[1,2,3] Qian Sun,[1] Stephanie Hampp,[4] Eugen Tausch,[5] Cornelia Eckert,[6] Martin Ebinger,[7] Rupert Handgretinger,[7] Geertruy te Kronnie,[8] Lisa Wiesmüller,[4] Stephan Stilgenbauer,[5] Galina Selivanova,[9] Klaus-Michael Debatin[1] and Lüder Hinrich Meyer[1]

[1]Department of Pediatrics and Adolescent Medicine, Ulm University Medical Center, Ulm, Germany; [2]International Graduate School of Molecular Medicine, Ulm University, Ulm, Germany; [3]PhD Program in Biosciences, University of Padova, Padova, Italy; [4]Department of Obstetrics and Gynecology, Ulm University Medical Center, Ulm, Germany; [5]Department of Internal Medicine III, Ulm University Medical Center, Ulm, Germany; [6]Department of Pediatrics, Charité Center Gynecology, Perinatal, Pediatric and Adolescent Medicine, Berlin, Germany; [7]Department of General Pediatrics, Hematology and Oncology, Children's University Hospital Tübingen, Tübingen, Germany; [8]Department of Women's and Children's Health, University of Padova, Padova, Italy and [9]Department of Microbiology, Tumor and Cell Biology, Karolinska Institute, Stockholm, Sweden

Haematologica 2020
Volume 105(1):170-181

ABSTRACT

Alterations of the tumor suppressor gene *TP53* are found in different cancers, in particular in carcinomas of adults. In pediatric acute lymphoblastic leukemia (ALL), *TP53* mutations are infrequent but enriched at relapse. As in most cancers, mainly DNA-binding domain missense mutations are found, resulting in accumulation of mutant p53, poor therapy response, and inferior outcome. Different strategies to target mutant p53 have been developed including reactivation of p53's wildtype function by the small molecule APR-246. We investigated *TP53* mutations in cell lines and 62 B-cell precursor ALL samples and evaluated the activity of APR-246 in *TP53*-mutated or wildtype ALL. We identified cases with *TP53* missense mutations, high (mutant) p53 expression and insensitivity to the DNA-damaging agent doxorubicin. In *TP53*-mutated ALL, APR-246 induced apoptosis showing strong anti-leukemia activity. APR-246 restored mutant p53 to its wildtype conformation, leading to pathway activation with induction of transcriptional targets and re-sensitization to genotoxic therapy *in vitro* and *in vivo*. In addition, induction of oxidative stress contributed to APR-246-mediated cell death. In a preclinical model of patient-derived *TP53*-mutant ALL, APR-246 reduced leukemia burden and synergized strongly with the genotoxic agent doxorubicin, leading to superior leukemia-free survival *in vivo*. Thus, targeting mutant p53 by APR-246, restoring its tumor suppressive function, seems to be an effective therapeutic strategy for this high-risk group of *TP53*-mutant ALL.

Correspondence:

LÜDER HINRICH MEYER
lueder-hinrich.meyer@uniklinik-ulm.de

Received: June 25, 2018.

Accepted: May 2, 2019.

Pre-published: May 9, 2019.

doi:10.3324/haematol.2018.199364

Check the online version for the most updated information on this article, online supplements, and information on authorship & disclosures: www.haematologica.org/content/105/1/170

Introduction

Although most pediatric patients diagnosed with acute lymphoblastic leukemia (ALL) have a favorable prognosis, achievement of long-term survival remains a major clinical challenge, particularly at relapse.[1] Alterations of cell death programs cause treatment failure and resistance in many cancers including leukemia. The nuclear phosphoprotein p53 is a transcription factor that controls cellular responses to stress, including DNA damage. Originally identified more than three decades ago,[2,3] p53 was characterized as a tumor suppressor negatively regulating cell cycle and growth, inhibiting the cancer cell's oncogenic potential.[4,5] The gene coding for p53 (*TP53*) is localized on the short arm of chromosome 17 (17p13) and it is the most frequently mutated gene across different cancers.[6,7] Both deletions and point mutations have been described and mutations often co-occur with loss of the corresponding wildtype allele.[8,9] The majority are *TP53* missense mutations found within the DNA-binding domain coding region (codons 100-300, exons 5-8) and

affect the structural integrity and DNA-binding ability of p53, leading to accumulation of dysfunctional p53 protein and increased oncogenic potential.[10-13]

TP53 mutations are found frequently, in up to 95% of carcinomas, typically in older patients.[7,8] In ALL, recent studies identified alterations of *TP53* in subsets of up to 16%, with higher rates in T-ALL, at relapse, and in elderly patients.[14-18] Moreover, more than 90% of ALL cases with a low hypodiploid karyotype (including loss of chromosome 17) carry somatic *TP53* alterations[19,20] and *TP53* germline mutations confer a high risk for hypodiploid ALL.[21] In pediatric ALL, *TP53* alterations are associated with poor response to chemotherapy and an inferior outcome, particularly at relapse, identifying *TP53*-mutant B-cell precursor (BCP)-ALL patients as a high-risk subgroup with a particular need for alternative therapies.[14,16-18,22]

Different strategies to interfere with the p53 pathway have been evaluated. Inhibition of the interaction of p53 and its negative regulator, mouse double minute 2 (MDM2), leads to sustained p53 transcriptional activity, but requires the presence of wildtype p53.[23] Therefore, direct targeting of mutant p53 has been investigated, identifying small molecules that reactivate p53 function.[24] In line, anti-tumor activity has been observed in murine lymphoma and liver cancer models upon genetic restoration of p53, supporting the principle of p53 reactivation as a therapeutic strategy.[25,26] APR-246 (PRIMA-1^{Met}), the structural analog of PRIMA-1 (p53 reactivation and induction of massive apoptosis) is a small molecule, identified in a screen for mutant p53-dependent growth suppression in sarcoma cells, showing activity on both structural and DNA-binding mutants.[27] APR-246 is a prodrug that is converted into methylene quinuclidinone, which binds covalently to the core domain of mutant p53 interacting with thiol groups of cysteines, restoring p53 wildtype conformation and function.[28,29] In addition, induction of oxidative stress has been reported as a second activity of APR-246, deriving from glutathione depletion, thioredoxin reductase inhibition and other effects.[30-33]

APR-246 demonstrated preclinical antitumor activity and synergism with DNA-damaging drugs in different cancers[32,34-39] and showed very moderate side effect profiles in a first-in-human phase I/IIa clinical trial in patients with refractory prostate cancer, acute myeloid leukemia, chronic lymphocytic leukemia, multiple myeloma and lymphoma.[40] Accordingly, APR-246 is currently being investigated in ovarian and esophageal cancer, myeloid neoplasms and melanoma in phase II clinical trials (*ClinicalTrials.gov*).[41] However, mutant p53 has so far not been addressed as a target for therapeutic intervention in ALL.

In this study, we investigated a large cohort of patient-derived pediatric BCP-ALL primograft samples identifying *TP53*-mutated cases and analyzed the effects of APR-246 in *TP53*-mutated (*TP53*mut) and *TP53*-wildtype (*TP53*wt) BCP-ALL. We identified strong and selective antileukemia activity of APR-246 in *TP53*mut ALL providing the basis to develop personalized therapy regimens for this high-risk subgroup of ALL.

Methods

Additional detailed information is provided in the *Online Supplementary Data*.

Sixty-two patient-derived xenograft samples established by transplantation of patients' ALL cells onto NOD.CB17-Prkdcscid/J mice[42] and six BCP-ALL cell lines were studied. Leukemia samples were obtained from pediatric BCP-ALL patients at diagnosis or relapse upon informed consent from the children and/or their legal guardians in accordance with the institution's ethical review boards. All animal experiments were approved by the appropriate authority (Regierungspräsidium Tübingen) and carried out following the national animal welfare guidelines. *TP53* mutations were analyzed by denaturing high-performance liquid chromatography and confirmed by Sanger sequencing, 17p deletions were assessed by fluorescence *in situ* hybridization. Mutation information was matched to the IARC-*TP53* database.[43] The sensitivity of leukemia samples to doxorubicin, APR-246 (kindly provided by Aprea Therapeutics, Stockholm, Sweden) or the combination was assessed after incubation of ALL cells with increasing drug concentrations, analyzing cell death by flow-cytometry according to forward- and side-scatter criteria. Data from three independent experiments performed in triplicate (cell lines) or of one experiment performed in triplicate (primografts) were analyzed by *t*-test, and differences of half maximal inhibitory concentrations (IC_{50}) titrations by F-test. *P* values ≤0.05 were considered statistically significant. Synergies of drug combinations were assessed calculating combination indices (CI), indicating strong synergism (CI 0.1-0.3), synergism (CI <1), an additive effect (CI=1) or antagonism (CI>1). Apoptosis was analyzed assessing annexin-V-FLUOS positivity and caspase-3 activity. Proteins (p53, PUMA, p21, NOXA, GAPDH) were detected by western blot analysis using the respective antibodies. The wildtype conformation of p53 was detected by immunoprecipitation using a conformation-specific anti-p53 wildtype antibody (PAb1620) followed by western blot analysis with an anti-p53 (total) antibody (DO-7). An immunoglobulin light chain-specific peroxidase conjugated binding protein was used for western blot analyses carried out following immuno-precipitation. Depletion of p53 was achieved by lentiviral shRNA-mediated knockdown or siRNA-mediated downregulation in *TP53*mut or *TP53*wt ALL cells. For *in vivo* treatment, transplanted recipients showing >5% human ALL cells in peripheral blood were randomized and treated (for 3 weeks) with solvent, APR-246 (days 1-5), doxorubicin (day 1), or the combination (APR-246 days 1-5, doxorubicin day 5) and sacrificed at the end of treatment for analysis of leukemia loads. For survival analyses, recipients were followed up after treatment until onset of leukemia-related morbidity and sacrificed. High loads of human ALL cells were detected in bone marrow and spleen in all cases, confirming reoccurrence of manifest leukemia.

Results

Identification of *TP53* mutations in B-cell precursor acute lymphoblastic leukemia

We investigated 62 patient-derived pediatric BCP-ALL samples, which were established in our NOD/SCID/huALL xenograft model from patients at diagnosis (n=53) or relapse (n=9). *TP53*mut cases were identified by denaturing high-performance liquid chromatography and confirmed by Sanger sequencing (exons 4-10). Four *TP53*mut cases were found, one derived from a patient at second relapse (*TP53*mut-1) and three at diagnosis (*TP53*mut-2, -3, -4) (*Online Supplementary Table S1*). In parallel, we characterized six BCP-ALL cell lines and identified two *TP53*mut (RS4;11, KOPN-8) and four *TP53*wt (MUTZ-5, EU-3, UoCB-6 and NALM-6) lines. All samples carried missense mutations previously described (p53.iarc.fr),[15,43] localized

within the region encoding the DNA-binding domain, suggesting loss of p53's tumor suppressive function (Figure 1A, Table 1). In the *TP53*mut samples, the second allele carried a nonsense mutation (*TP53*mut-1), was absent (loss of 17p, *TP53*mut-2, -3), or carried the same missense mutation (*TP53*mut-4) (Table 1). Somatic and germline *TP53*mut are associated with (low) hypodiploid ALL.[15,19-21] One primograft sample (*TP53*mut-3) showed a hypodiploid karyotype with 44 chromosomes (Table 1). In line with disrupted degradation and accumulation of mutant p53 protein, *TP53*mut cases showed higher p53 protein levels compared to *TP53*wt leukemias (Figure 1B).

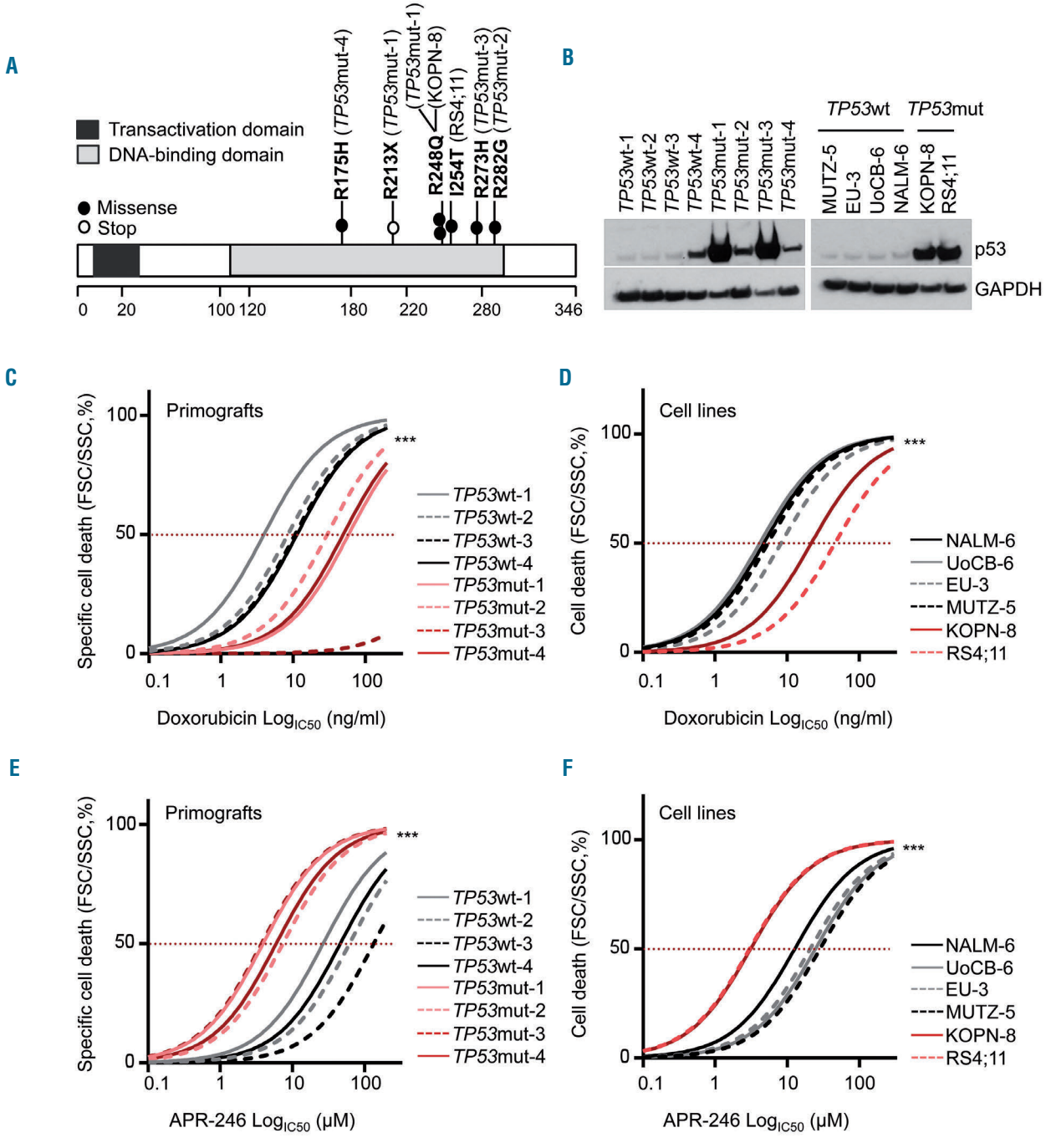

Figure 1. *TP53*-mutated acute lymphoblastic leukemias are DNA-damage resistant but sensitive to APR-246. (A) All *TP53*mut B-cell precursor (BCP) acute lymphoblastic leukemia (ALL) primograft and cell lines harbor missense mutations (filled circles) localized in the DNA-binding domain of *TP53*. The primograft sample *TP53*mut-1 carries an additional stop mutation (R213X, open circle). See also Table 1. (B) Increased p53 protein expression in *TP53*mut compared to *TP53*wt ALL in primograft (left) and cell line (right) leukemia samples. Western blot, anti-p53 antibody (total, clone DO-7) with GAPDH as a loading control. (C-F) Significantly higher half maximal inhibitory concentrations (IC_{50}) for doxorubicin in *TP53*mut (red curves) primograft (C) and cell line (D) BCP-ALL, and significantly lower IC_{50} values for APR-246 in *TP53*mut primograft (E) and cell line (F) samples, indicating insensitivity to the DNA-damaging agent doxorubicin but sensitivity to APR-246 in *TP53*mut BCP-ALL. Dose-response curves reflect cell death induction in response to increasing concentrations summarizing one (primografts, 24 h; C, E) or three (cell lines, 48 h; D, F) independent experiments, each performed in triplicate. Comparison of sensitivities of *TP53*wt and *TP53*mut leukemias, *F*-test, ***$P<0.001$. See also *Online Supplementary Table S2*.

TP53-mutated leukemias are sensitive to APR-246 but not to genotoxic therapy

In response to genotoxic agents and stress, wildtype p53 suppresses cellular viability and proliferation. However, dysfunctional, mutant p53 fails to mediate tumor-suppressive functions such as induction of cell death. Therefore, we analyzed cell death in *TP53*mut and *TP53*wt ALL primografts (*TP53*mut n=4, *TP53*wt n=4) and cell lines (*TP53*mut n=2, *TP53*wt n=4) in response to increasing concentrations of the DNA-damaging agent doxorubicin, a standard genotoxic drug regularly used in ALL treatment protocols, and to APR-246. All *TP53*mut primografts and cell lines showed, as expected, insensitivity to doxorubicin indicated by significantly higher IC_{50} values, in contrast to doxorubicin-sensitive *TP53*wt leukemias (Figure 1C, D; *Online Supplementary Table S2A, B*). An opposite effect was observed upon exposure to APR-246 with high sensitivity and cell death induction in all *TP53*mut leukemias, but low APR-246 sensitivity in *TP53*wt ALL (Figure 1E, F; *Online Supplementary Table S2C, D*). Interestingly, diagnosis- (*TP53*mut-2, -3, -4) or relapse-derived (*TP53*mut-1) primograft samples did not show differences in APR-246 or doxorubicin sensitivity.

Activation of the p53 pathway results in apoptosis induction. Along with cell death, APR-246 led to annexin-V/propidium iodide positivity and caspase-3 activation indicating apoptosis induction in *TP53*mut ALL. In contrast, apoptosis was induced by doxorubicin but not APR-246 in *TP53*wt cells (Figure 2 and *Online Supplementary Figure S1*).

Thus, all identified *TP53*mut leukemias carried missense mutations in the DNA-binding domain, showed accumulation of p53 indicative of dysfunctional mutant p53, resistance to the genotoxic agent doxorubicin, and were highly sensitive to APR-246-induced apoptosis.

APR-246 restores p53's wildtype conformation reactivating tumor suppressive functions

We further addressed the mode of action of APR-246 in *TP53*mut ALL and examined the conformation of p53 and activation of the pathway in response to APR-246. Using a p53 wildtype conformation-specific antibody (PAb1620), larger amounts of p53 with wildtype conformation were immunoprecipitated from lysates of *TP53*mut ALL cells exposed to APR-246, indicating reconstitution of p53 wildtype conformation in *TP53*mut ALL by APR-246 (Figure 3A). However, this effect was not observed in *TP53*wt leukemia cells (*Online Supplementary Figure S2*). Next, we assessed expression of the p53 transcriptional targets PUMA (P53-Upregulated Modulator of Apoptosis), p21 (Cyclin Dependent Kinase Inhibitor 1A, CDKN1), and NOXA upon APR-246 or doxorubicin treatment in *TP53*mut (KOPN-8, RS4;11) and *TP53*wt (NALM-6, UoCB-6) ALL lines. In *TP53*mut ALL, APR-246 led to induction of all p53 targets (Figure 3B, C and *Online Supplementary Figure S3*). In contrast, an opposite picture of activation of p53 transcriptional targets in *TP53*wt but not in *TP53*mut leukemias was observed upon incubation with doxorubicin (Figure 3D, E and *Online Supplementary Figure S3*). Thus, APR-246 induces restoration of mutant p53 to wildtype conformation, transcriptional target expression, and apoptosis in *TP53*mut ALL.

Induction of oxidative stress contributes to APR-246-mediated cellular death

Induction of oxidative stress has been described as a second activity of APR-246 in different cancers.[30-32] APR-246 was reported to interfere with different regulators of the cellular redox system, such as thioredoxin reductase, thioredoxin and glutathione, and with the transcription factor NRF2, leading to induction of reactive oxygen species (ROS).[28,30-33,44-47] Given the activity of APR-246 in *TP53*mut ALL, we addressed whether *TP53*mut and *TP53*wt ALL display distinct sensitivities in response to ROS generation. Upon treatment with 3-morpholinosydnonimine, a spontaneous generator of reactive oxygen and nitrogen species, and the oxidant tert-butyl hydroxyperoxide, increased ROS levels were observed in both

Table 1. ***TP53*** **mutations in acute lymphoblastic leukemia cell lines and primograft samples.**

Sample	Exon	Mut. (bp)	Mut. (aa)	Region	Mut. type	del (17p)	Genotype	Number of chr.s.
*TP53*mut-1	exon 6 exon 7	c.637C>T c.743G>A	p.R213X p.R248Q	DBD	stop missense	-	heterozygous	47
*TP53*mut-2	exon 8	c.844C>G	p.R282G	DBD	missense	del	hemizygous	47
*TP53*mut-3	exon 8	c.818G>A	p.R273H	DBD	missense	del	hemizygous	44
*TP53*mut-4	exon 5	c.524G>A	p.R175H	DBD	missense	-	homozygous	46
RS4;11	exon 7	c.761T>C	p.I254T	DBD	missense	-	heterozygous	47
KOPN-8	exon 7	c.743G>A	p.R248Q	DBD	missense	-	heterozygous	46

Mut: mutation; bp: base pair; aa: amino acid; del: deletion; DBD,: DNA-binding domain; Chr.s: chromosomes.

Table 2. ***TP53*** **mutations in primary samples from patients with acute lymphoblastic leukemia.**

Sample	Exon	Mut. (bp)	Mut. (aa)	Region	Mut. type	del (17p)	Genotype	Diploidy
Patient-1	exon 4	c.375G>A	p.T125T	DBD	splice site	del	hemizygous	diploid
Patient-2	exon 7	c.743G>A	p.R248Q	DBD	missense	-	heterozygous	diploid
Patient-3	exon 7	c.743G>A	p.R248Q	DBD	missense	-	heterozygous	diploid
Patient-4	exon 7	c.733G>C	p.G245R	DBD	missense	-	heterozygous	diploid

Mut: mutation; bp: base pair; aa,: amino acid; del: deletion; DBD: DNA-binding domain.

*TP53*mut and *TP53*wt ALL cells, leading to similar cell death rates (*Online Supplementary Figure S4*).

Next, we investigated whether induction of oxidative stress is involved in APR-246-mediated cell death in *TP53*mut ALL. Importantly, methyl quinuclidinone, the active drug spontaneously formed from APR-246, binds covalently to cysteine residues in the core domain of p53, but also to cysteines in the widely used antioxidant and ROS inhibitor N-acetylcysteine (NAC).[28,44] Thus, NAC directly blocks APR-246 activity and cannot be used to investigate the role of ROS in APR-246-mediated cell death. Therefore, the synthetic antioxidant compound and ROS inhibitor superoxide dismutase mimetic Mn (III) tetrakis (5, 10, 15, 20-benzoic acid) porphyrin (MnTBAP) was used. Cell death was analyzed together with ROS levels in *TP53*mut (KOPN-8 and RS4;11) and *TP53*wt (NALM-6 and UoCB6) leukemia cells exposed to APR-246 with or without NAC or MnTBAP. Similar ROS levels were observed upon APR-246 treatment in both *TP53*mut and *TP53*wt ALL (*Online Supplementary Figure S5A, C, E, G*), however induction of cell death was only seen in *TP53*mut cells (*Online Supplementary Figure S5F, H*) but not in *TP53*wt cells (*Online Supplementary Figure S5B, D*). Interestingly, ROS inhibition by MnTBAP partially inhibited APR-246-induced cell death in *TP53*mut ALL, indicating that ROS contribute to APR-246- induced cell death. It was also interesting that, even in the presence of MnTBAP, i.e. in the absence of ROS, APR-246 retained a statistically significant cytotoxic effect (*Online Supplementary Figure S5F, H*). In line with previous reports,[44] the activity of APR-246 was completely blocked by NAC.

Taken together, these data show that induction of oxidative stress might contribute to APR-246-mediated cell death in ALL, in line with previously reported data of a dual mode of action of APR-246 in other malignancies.[28,30-33,44-46]

APR-246 activity depends on mutant p53

Activity of APR-246 was observed in *TP53*mut but not *TP53*wt ALL. Therefore, we analyzed the effect of APR-246 in *TP53*mut and *TP53*wt cell lines upon lentiviral shRNA-mediated knockdown of p53 (Figure 4A-C). In both *TP53*mut lines (KOPN-8 and RS4;11) depletion of p53 led to APR-246 insensitivity and cell death resistance, in contrast to dose-dependent cell death induction in control-transduced cells (Figure 4D, E). However, *TP53*wt cells with p53 depletion were unresponsive to APR-246, like the corresponding control transduced cells (Figure 4F). A similar result was observed upon siRNA-mediated p53 downregulation with clearly lower cell death induction in

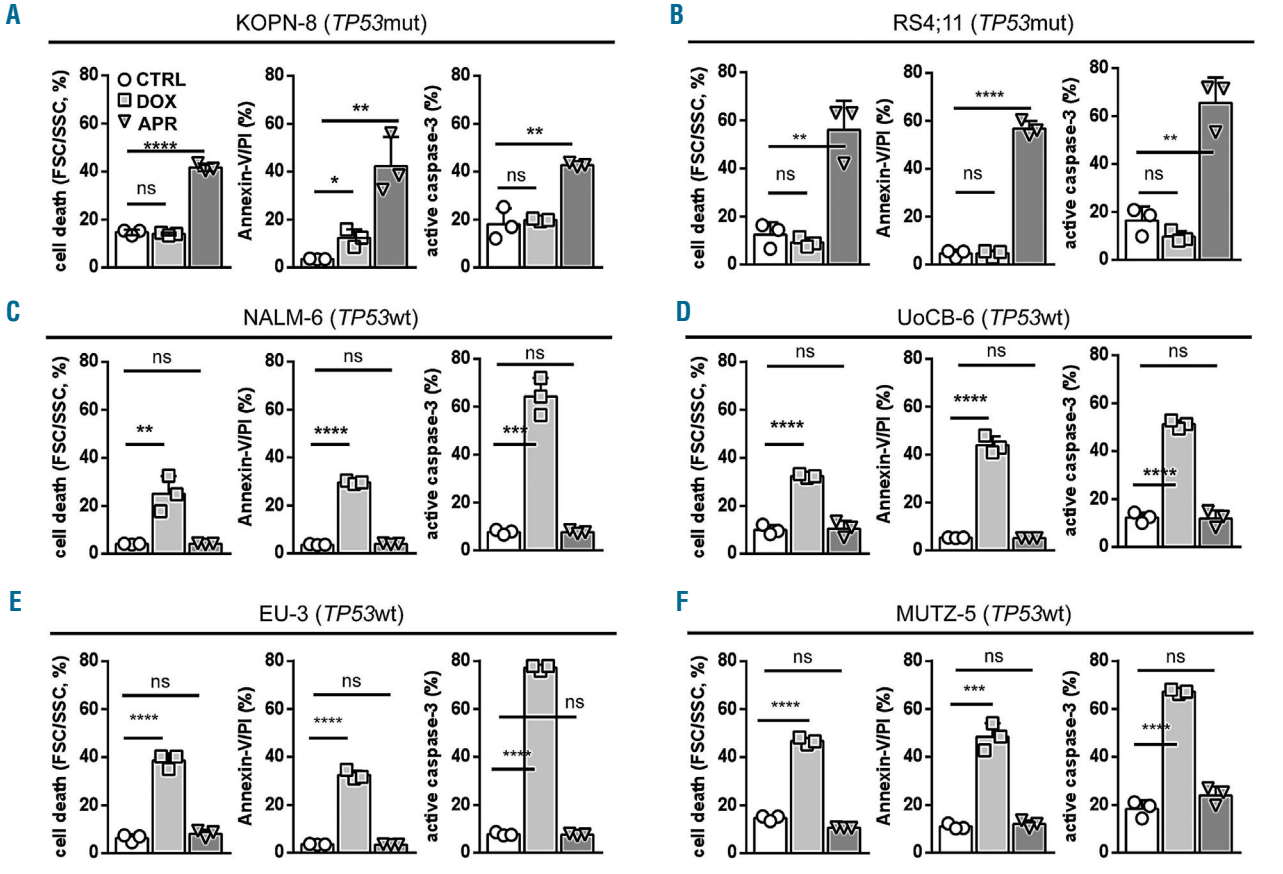

Figure 2. APR-246 induces apoptosis in *TP53*-mutated acute lymphoblastic leukemia. (A-F) Induction of cell death (left diagrams, forward/side scatter criteria, flow cytometry), annexin-V/propidium iodide (PI) positivity (middle diagrams) and caspase-3 activation (right diagrams) by APR-246 in *TP53*mut cell lines KOPN-8 (A) and RS4;11 (B), in contrast to cell death and apoptosis induction by doxorubicin in *TP53*wt lines NALM-6 (C), UoCB-6 (D), EU-3 (E), and MUTZ-5 (F). Proportions of cells after 48 h exposure to solvent (CTRL), APR-246 (APR, 5 μM), or doxorubicin (DOX, 15 ng/mL). Mean values ± standard deviation of three independent experiments, each performed in triplicate. Student *t*-test, ****P<0.0001; ***P<0.001; **P<0.01; *P<0.05; n.s., not significant.

*TP53*mut ALL but no effect in *TP53*wt cells (Figure 4G-J and *Online Supplementary Figure S6*). Together with our observations on APR-246 insensitivity in *TP53*wt ALL (Figure 1E, F) and the absence of p53 transcriptional target expression upon APR-246 treatment in *TP53*wt ALL (Figure 3D, E), these findings indicate that the activity of APR-246 is associated with the presence of mutant p53. Accordingly, distinct sensitivities to APR-246 were found in four primary ALL samples obtained from patients with therapy-resistant disease or relapse carrying different *TP53* mutations (Figure 4L, Table 2). Robust dose-dependent cell death induction was observed in leukemia cells from patients 2, 3, and 4 carrying missense mutations resulting in expression of mutant p53 (Figure 4L, N-P), whereas APR-246 did not induce cell death in ALL cells of patient 1 carrying a hemizygous splice site mutation without detectable expression of p53 protein (Figure 4L, M).

APR-246 re-sensitizes *TP53*-mutated acute lymphoblastic leukemia to doxorubicin

*TP53*mut cancer cells show resistance to DNA damage. Therefore, we analyzed whether reactivation of mutant

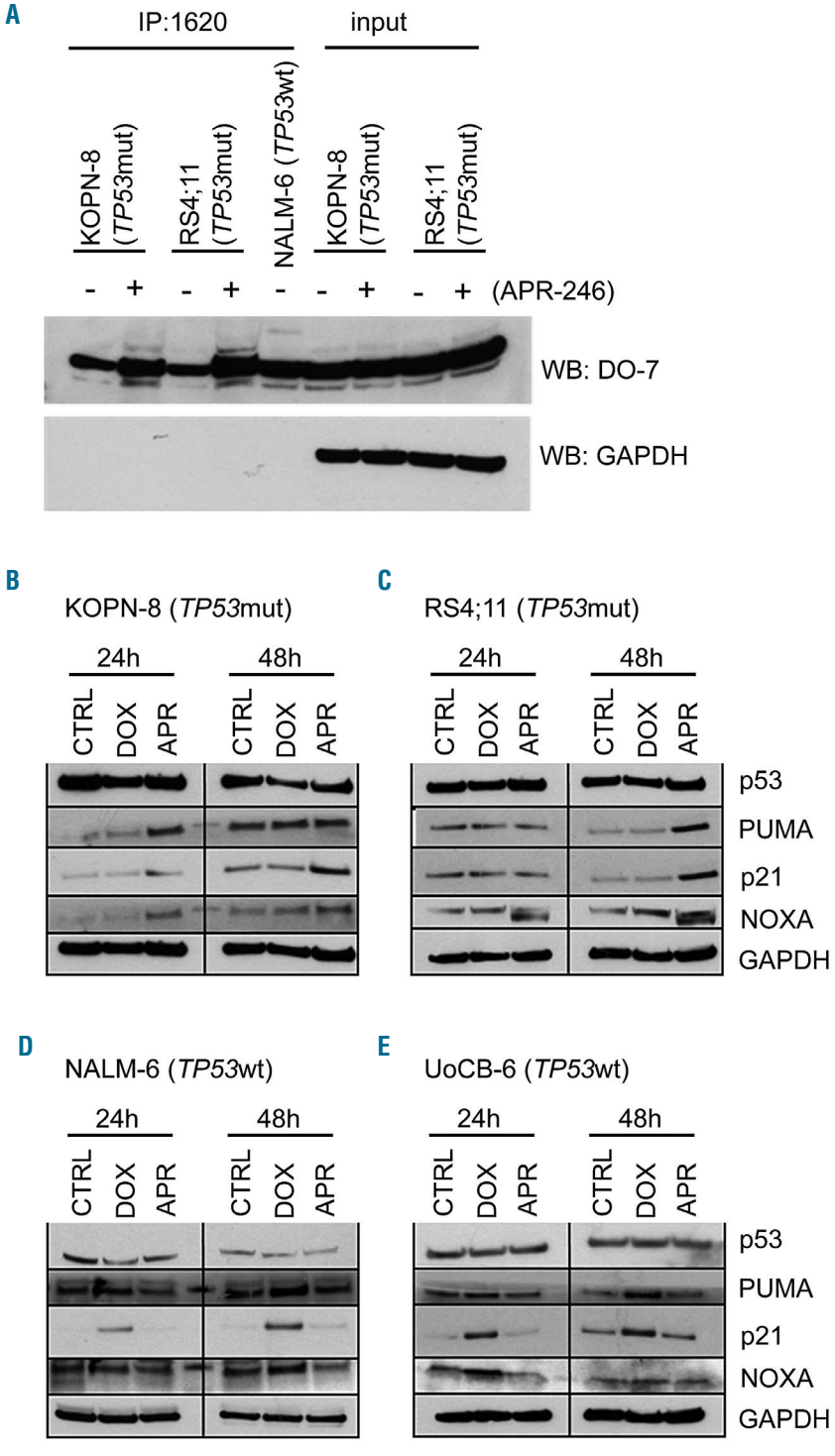

Figure 3. Conformational and functional restoration of mutant p53 by APR-246. (A) Increased levels of p53 with wildtype conformation in *TP53*mut ALL (KOPN-8, mutation R248Q; RS4;11, mutation I254T) upon exposure to APR-246 (5 μM, 24 h). Immunoprecipitation (IP, anti-wt p53 specific antibody PAb1620) and western blot analysis (WB, anti-p53 antibody DO-7, light chain-specific goat anti-mouse peroxidase conjugated binding protein), GAPDH expression in input lysates and absence in precipitates, NALM-6 serves as a wildtype p53 positive control. (B-E) Expression of p53 transcriptional targets PUMA, p21 and NOXA in (B, C) *TP53*mut ALL upon APR-246 treatment and in (D, E) *TP53*wt ALL upon doxorubicin treatment. Western blot, exposure to solvent (CTRL), doxorubicin (DOX, 15 ng/mL), or APR-246 (APR, 5 μM) for the indicated times, with GAPDH as a loading control. The results of one representative out of two independent experiments are shown. See also *Online Supplementary Figures S2 and S3*.

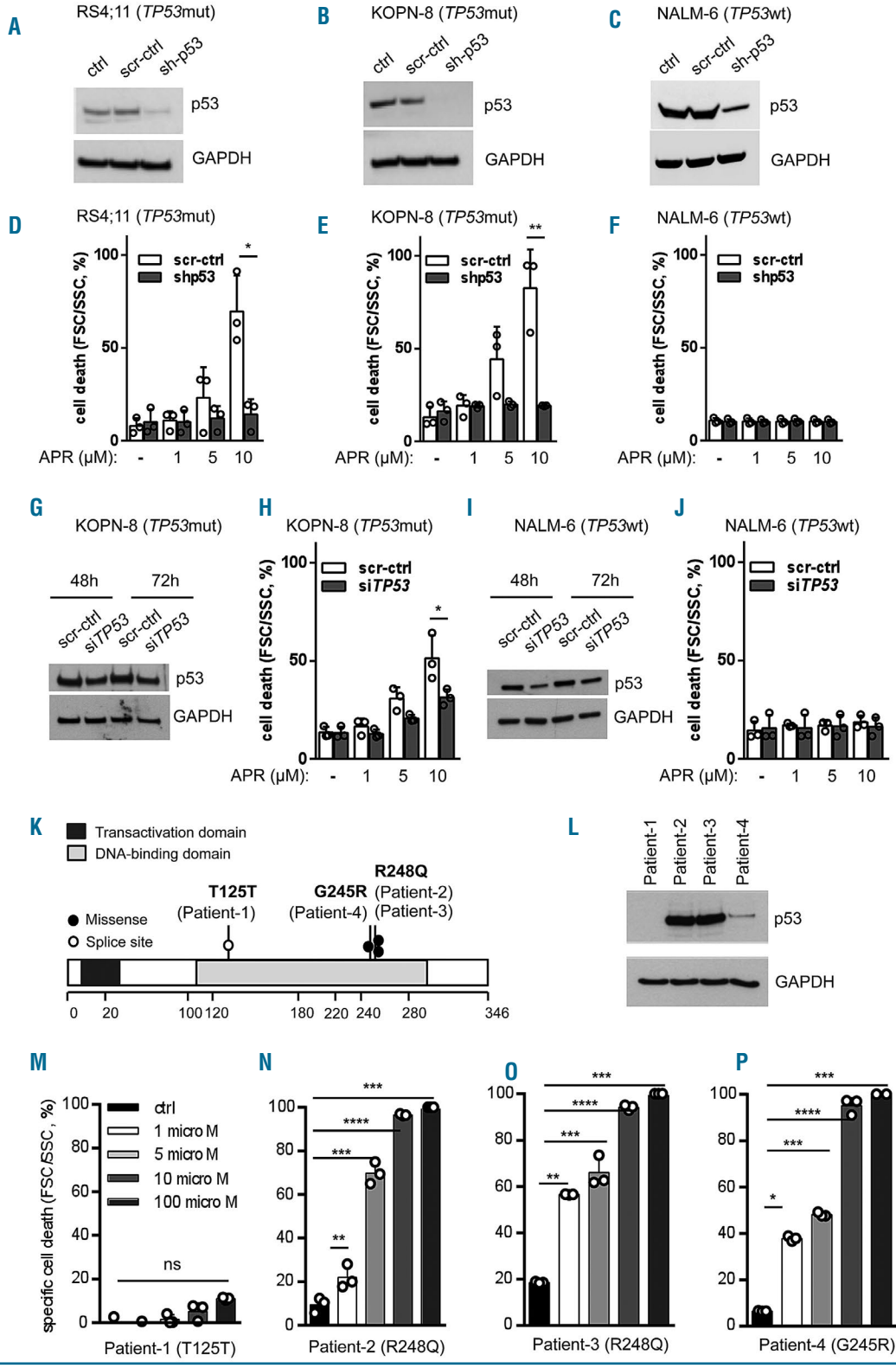

Figure 4. APR-246 activity depends on mutant p53. (A-C) Stable lentiviral shRNA-mediated p53 knockdown in *TP53*mut (RS4;11 and KOPN-8) and *TP53*wt (NALM-6) cell lines. Western blot, anti-p53 antibody DO-7, with GAPDH as a loading control, non-transduced cells (ctrl), cells transduced with scrambled control (scr-ctrl) and *TP53*-specific shRNA (sh-p53). (D-F) Increasing cell death (forward/side scatter criteria, flow cytometry) in control transduced cells and abrogated cell death induction upon p53 knockdown at increasing concentrations of APR-246 (APR, 48 h) in *TP53*mut but not *TP53*wt cells. Mean values ± standard deviation (SD) of three independent experiments, each performed in triplicate. Student t-test, **P*<0.05; ***P*<0.01. (G-J) si-RNA-mediated p53 downregulation in *TP53*mut (KOPN-8), (G) and *TP53*wt (NALM-6), (I) cells leading to clearly lower cell death induction upon p53 downregulation as compared to higher cell death in control cells (H), while p53 downregulation in *TP53*wt cells did not affect cell death induction upon APR-246 treatment (J). Mean values ± SD of three independent experiments. Student *t*-test, **P*<0.05; ***P*<0.01. (K) *TP53* mutations identified in primary samples from patients with acute lymphoblastic leukemia (ALL): the mutations were localized in the DNA-binding domain with one splice site mutation (open circle, Patient-1) and three missense mutations (filled circles, Patients -2, -3, -4). (L) No detectable p53 protein in ALL cells from Patient-1 (western blot, anti-p53 antibody DO-7, GAPDH as a loading control), and (M) no APR-246 activity in these cells (Patient-1), in contrast to cell death induction in cases carrying missense hot spot *TP53* mutations (N, O, P; Patients-2, -3, -4). Mean values ± SD, measurements performed in triplicate. Student *t*-test, *****P*<0.0001; ****P*<0.001; ***P*<0.01; **P*<0.05; n.s., not significant.

p53 re-sensitizes *TP53*mut ALL to the DNA-damaging agent doxorubicin, which is also used in treatment of pediatric ALL. *TP53*mut and *TP53*wt ALL cell lines and primograft samples were exposed to APR-246, doxorubicin, or to combinations of both at increasing concentrations. Strongly increased cell death rates were observed in all four *TP53*mut primografts and two cell lines upon combination treatment with APR-246, as compared to APR-246 or doxorubicin alone, indicating synergistic activity for APR-246 and doxorubicin in *TP53*mut ALL (Figure 5A-F, *Online Supplementary Table S3A)*. In *TP53*wt leukemias however, only doxorubicin showed cell death-inducing activity, which was not increased by adding APR-246 (Figure 5G-L, *Online Supplementary Table S3B*).

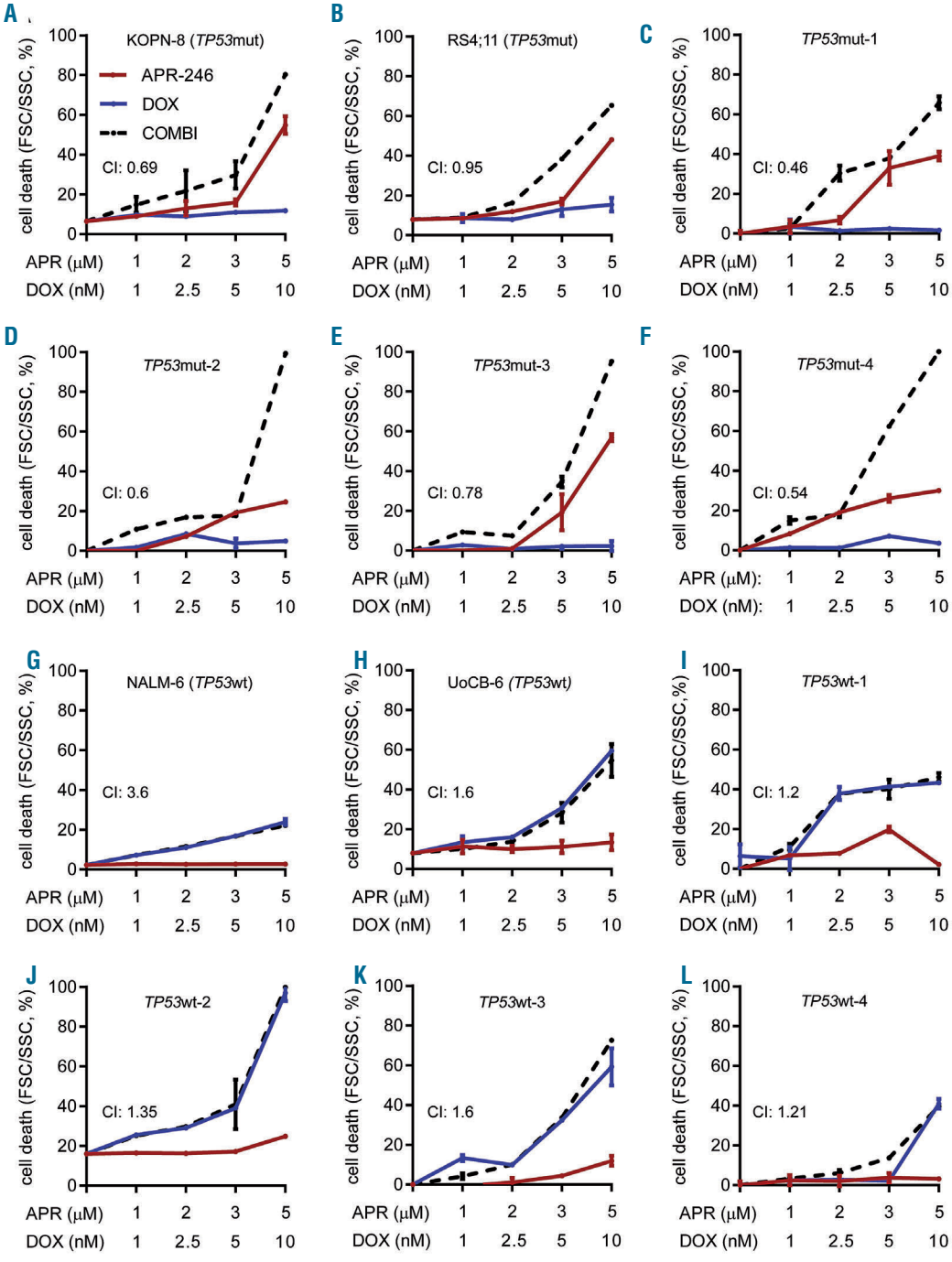

Figure 5. APR-246 synergizes with doxorubicin. Synergistic activity of APR-246 in combination with the DNA-damage-inducing agent doxorubicin in *TP53*mut B-cell precursor (BCP)-acute lymphoblastic leukemia (ALL) cell lines (A, B) and *TP53*mut primograft leukemias (C-F) leading to doxorubicin re-sensitization, in contrast to no increased activity compared to treatment with doxorubicin alone in *TP53*wt cell lines (G, H) and *TP53*wt primograft ALL (I-L). Cell death (forward/side scatter criteria, flow cytometry) after exposure (primografts 24 h, cell lines 48 h) at indicated concentrations of APR-246 (APR), doxorubicin (DOX) or the combination (COMBI, 3 h APR-246 pre-incubation). Mean values ± standard deviation (SD) of three independent experiments, each performed in triplicate (cell lines: A, B, G, H). Mean values ± SD, three measurements (primografts: C-F, I-L). Combination indices (CI) indicating a strong synergistic (CI 0.1-0.3), a synergistic (CI <1), an additive (CI=1) or an antagonistic effect (CI>1) upon combination.

We also addressed whether induction of oxidative stress would increase the antileukemia activity of APR-246. In contrast to clearly increased cell death upon treatment with APR-246 together with the DNA-damaging agent doxorubicin, combining APR-246 with the ROS inducers 3-morpholinosydnonimine and tert-butyl hydroxyperoxide did not lead to clearly increased cell death (*Online Supplementary Figure S7*). Thus, APR-246 effectively synergizes with doxorubicin and re-sensitizes *TP53*mut ALL to DNA-damage-induced cell death, while additional ROS induction did not increase APR-246-mediated leukemia cell death.

Preclinical antileukemia activity of APR-246 and *in vivo* synergy with genotoxic therapy

Based on our findings, we investigated the antileukemia activity of APR-246 in a preclinical setting *in vivo*. Mice were transplanted with the *TP53*mut primograft (*TP53*mut-4; R175H). Upon manifestation of leukemia, as indicated by 5% or more human CD19$^+$ ALL cells in the recipients' peripheral blood, mice were treated with APR-246 (25, 50 or 100 mg/kg) or vehicle until control-treated animals showed signs of leukemia-related morbidity (3 weeks, days 1-5) (Figure 6A). Upon APR-246 treatment, a clear dose-dependent reduction of leukemia loads was observed in all three organ compartments: spleen, bone marrow and central nervous system (Figure 6B-D). Moreover, in leukemia cells isolated from these APR-246-treated animals, dose-dependent increases in mutant p53 with wildtype conformation and expression of PUMA and p21 were detected (Figure 6E, F), indicating restoration of wildtype p53 conformation and function *in vivo*.

Furthermore, APR-246 demonstrated strong *in vivo* antileukemia activity in another *TP53*mut ALL primograft sample (*TP53*mut-1; R248Q/R213X) leading to significantly reduced leukemia loads in the spleen, bone marrow and central nervous system upon therapy of leukemia-bearing recipients (Figure 6G-I).

We also addressed the effects of APR-246 in combination with doxorubicin *in vivo*. Recipients with manifest ALL (*TP53*mut-1; R248Q/R213X; 5% or more human ALL cells in the peripheral blood) were treated with APR-246, doxorubicin, or the combination of both for 3 weeks. After treatment, the animals were followed up and the time until onset of ALL-related morbidity was analyzed for each animal (Figure 6J). Upon sacrifice, high loads of human ALL were detected in the spleen and bone marrow of all recipients, confirming recurrence of manifest leukemia at clinical onset. Importantly, in addition to clear antileukemia activity as a single agent, leading to increased post-treatment survival (P<0.0001), APR-246 synergized strongly with doxorubicin and re-sensitized *TP53*mut ALL to genotoxic therapy *in vivo*, resulting in significantly prolonged survival as compared to APR-246 alone (P=0.0005) (Figure 6K). In all treatment experiments, application of APR-246 was well tolerated and no side effects were observed in the recipients.

Taken together, our findings in ALL carrying *TP53* missense mutations in the DNA-binding domain, which lead to accumulation of dysfunctional p53, indicate that targeting mutant p53 with APR-246 results in refolding of mutant p53 into its native wildtype conformation, induction of p53 transcriptional targets, involvement of oxidative stress, induction of apoptosis, sensitization to DNA damage and, most importantly, preclinical antileukemia activity with significant reduction of leukemia loads, re-sensitization to genotoxic therapy and clearly prolonged survival *in vivo*. Thus, application of APR-246 can provide an effective strategy for directed therapeutic intervention in the high-risk subtype of *TP53*mut BCP-ALL.

Discussion

Investigating a large cohort of 62 patient-derived BCP-ALL samples, all identified *TP53*mut cases showed missense mutations leading to alterations in the DNA-binding domain of p53, high levels of p53 protein and insensitivity to doxorubicin. Interestingly, APR-246 demonstrated robust antileukemia activity in these cases, including induction of apoptosis, effective reduction of leukemia loads, and sensitization to doxorubicin in an *in vivo* model of *TP53*mut ALL. Both *in vitro* and *in vivo* experiments showed that treatment with APR-246 led to restored conformation and activation of mutant p53, and induction of transcriptional targets.

Alterations in *TP53* have been described in diverse cancers at high frequencies of up to 95%.[7] In our cohort, *TP53* mutations were identified in four out of 62 cases (6.5%), in line with reported rates in ALL of 6-16%.[14-16,18] All mutations identified in the primograft and cell line samples were missense mutations localized in the DNA-binding domain, with additional loss of the second allele in some of the cases, consistent with mutational patterns reported throughout different cancer types.[10,43] One *TP53*mut sample showed hypodiploidy, in line with reported associations of hypodiploidy with germline and somatic *TP53* mutations.[19-21]

Mutated dysfunctional p53 results in resistance to therapy-induced DNA damage[48] and poor patient outcome.[14,16-18,22] Correspondingly, increased numbers of *TP53* alterations are seen at ALL relapse[16] and all *TP53*mut leukemias were insensitive to the DNA-damaging agent doxorubicin. Importantly, these *TP53*mut leukemias were sensitive to APR-246, likely by reactivation of high levels of dysfunctional p53 accumulated in the cells. Most importantly, in line with reports in ovarian cancer,[32,39] APR-246 clearly synergized with doxorubicin *in vitro*, *ex vivo* and *in vivo*, re-sensitizing initially resistant *TP53*mut ALL to DNA damage. Therefore, combining functional p53 restoration with genotoxic therapies triggering the p53-mediated DNA-damage response would be the rationale to apply APR-246 together with doxorubicin, a classical DNA-damage-inducing agent used in ALL treatment regimens. Importantly, a favorable pharmacological profile and antitumor effects were observed upon first clinical use of APR-246 in patients with refractory cancers[40] and APR-246 is being tested in combination with anticancer agents, including doxorubicin, in ongoing phase II trials (*ClinicalTrials.gov*).[41]

We addressed the molecular mechanism of action of APR-246 and demonstrated restoration of p53 wildtype conformation, p53 pathway activation with induction of downstream transcriptional targets, and a contribution of oxidative stress leading to apoptosis of *TP53*mut BCP-ALL cells. Importantly, this antileukemia effect was also observed *in vivo* in *TP53*mut ALL, but not in *TP53*wt ALL, upon p53 knockdown or in a patient's sample with a splice site mutation and loss of p53 protein expression. High levels of misfolded mutant p53 were described to be

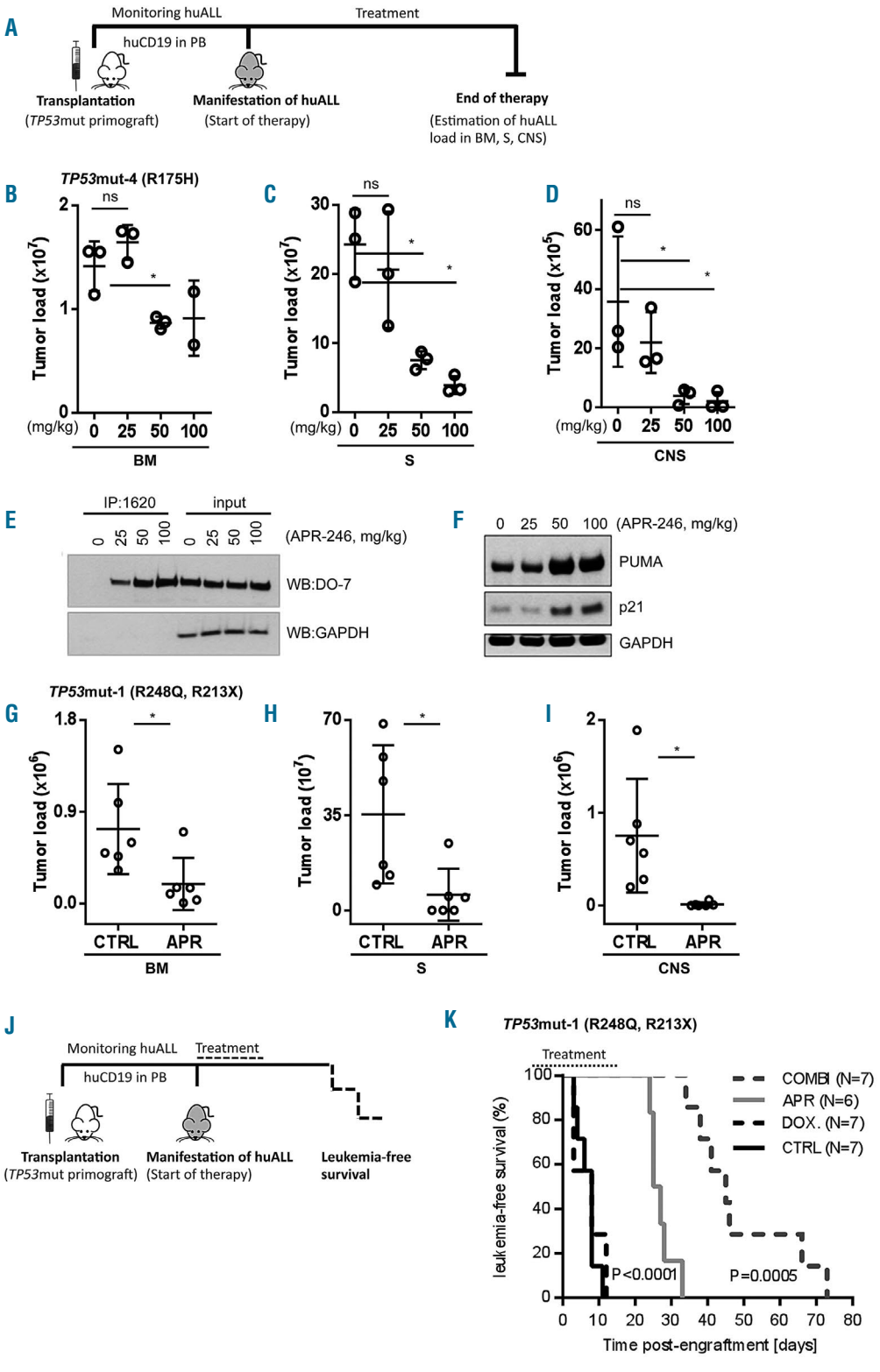

Figure 6. Anti-leukemia activity of APR-246 and synergy with genotoxic therapy in *TP53*-mutated acute lymphoblastic leukemia *in vivo*. (A) Schematic representation of the experimental procedure: endpoint analysis assessing leukemia loads in differently treated recipients. (B-D) Dose-dependent reduction of leukemia load in bone marrow (BM) (B), spleen (S) (C) and central nervous system (CNS) (D) upon treatment of mice bearing *TP53*mut-4 (mutation R175H) acute lymphoblastic leukemia (ALL) with solvent or increasing doses of APR-246 for 3 weeks as indicated (n=3 recipients per group, except n=2 for BM 100 mg/kg). Student t-test, **P*<0.05; n.s., not significant. (E) Restoration of p53 wildtype conformation upon *in vivo* APR-246 therapy, immunoprecipitation (IP: anti-wt p53 specific antibody PAb1620, western blot: anti-p53 antibody DO-7, light chain-specific goat anti-mouse peroxidase conjugated binding protein, GAPDH as a loading control), and (F) dose-dependent induction of p53 transcriptional targets PUMA and p21 (western blot, GAPDH as a loading control). (G-I) Significant reduction of leukemia load in bone marrow (BM) (G), spleen (S) (H) and central nervous system (CNS) (I) upon treatment of *TP53*mut-3 (mutations R248Q, R213X) ALL-bearing mice with APR-246 (APR, 100 mg/kg) or solvent (CTRL) for 3 weeks, n=6 mice per group, Student *t*-test, **P*<0.05. (J) Schematic representation of the experimental procedure: survival analysis. (K) Superior survival of animals treated with APR-246 (APR, 50 mg/kg, 3 weeks, days 1-5; n=6) as compared to doxorubicin (DOX, 2 mg/kg, 3 weeks, day 1; n=7) or vehicle (CTRL, 3 weeks, days 1-5; n=7) (*P*<0.0001); and synergy of the combination of APR-246 and doxorubicin (COMBI, APR-246, 50 mg/kg, days 1-5, and doxorubicin, 2 mg/kg, day 5; n=7) leading to increased survival as compared to APR-246 treatment alone (*P*=0.0005). Kaplan-Meier analysis, log-rank test.

associated with APR-246 sensitivity in cancer cell lines,[38,49,50] consistent with our observation of high APR-246 activity in *TP53*mut ALL with high p53 expression. However, evaluation of larger cohorts of patients together with outcome data would be required to explore the value of the level of expression of p53 as an indicator of APR-246 responsiveness in *TP53*mut ALL.

APR-246 activity has been reported to be mediated independently of p53 by induction of oxidative stress in other types of cancer, including acute myeloid leukemia and multiple myeloma.[30-33] However, we only observed cell death in *TP53*mut ALL, although *TP53*mut and *TP53*wt ALL showed no differences in induction of and sensitivity to oxidative stress. Interestingly, APR-246 activity in *TP53*mut ALL was partially inhibited by ROS neutralization. This suggests that induction of oxidative stress contributes to APR-246-mediated cell death in ALL, in line with reports on a dual mode of action of APR-246,[30-32] which might vary between tumor types and cellular context.

The presence of p53 in a mutated, dysfunctional form, as typically is the case for missense mutations in the DNA-binding core domain, enables binding of the active moiety of APR-246, leading to activity in BCP-ALL.[11,28] This is of clinical relevance, since the majority of *TP53* mutations in BCP-ALL are missense hot spot mutations in the DNA-binding domain[15,43] resulting in accumulation of misfolded p53 protein, which is targeted by APR-246. However, the precise mechanism of activity on DNA contact mutations is not yet known. Importantly, we and others [27] have demonstrated antitumor activity on structural and contact mutants including clear preclinical antileukemia activity on *TP53*mut ALL carrying either a structure (R175H) or contact (R248Q) mutation.

Taken together, our study shows that the small molecule APR-246 exhibits profound antileukemia activity in *TP53*mut BCP-ALL, targeting non-functional mutant p53 resulting from missense mutations in the DNA-binding domain of *TP53*, the most frequent mutation type reported throughout different malignancies. Mechanistically, we showed that APR-246 led to restoration of p53's wildtype conformation, pathway activation with expression of transcriptional targets and induction of apoptosis in *TP53*mut ALL. Moreover, we found a clear synergism between APR-246 and doxorubicin treatment, strongly suggesting that the combination of p53 reactivation and DNA-damage induction could be an effective antileukemia strategy for BCP-ALL patients with *TP53* missense mutations. Hence, targeting mutant p53 appears to be a promising, directed treatment for this high-risk subgroup of *TP53*mut ALL.

Acknowledgments

The authors would like to thank Aprea Therapeutics (Stockholm, Sweden) for kindly providing APR-246 for the study, S. Volk and S. Essig for excellent technical assistance, the Ulm University Sorting and Animal Facilities and Pharmacy of the Ulm University Medical Center, and the INFORM study group. The authors would also like to thank the International Graduate School in Molecular Medicine Ulm (SD, EB), Madeleine-Schickedanz-Stiftung and "Förderverein für Krebskranke Kinder Tübingen" (ME, RH), Swedish Research Council and Swedish Childhood Cancer Society (GS), EU COST Action CA16223 (GtK), the German Research Foundation, SFB 1074 B6 (LHM, KMD) and B1 (SS) for supporting the work.

References

1. Hunger SP, Mullighan CG. Acute lymphoblastic leukemia in children. N Engl J Med. 2015;373(16):1541-1552.
2. Lane DP, Crawford LV. T antigen is bound to a host protein in SV40-transformed cells. Nature. 1979;278(5701):261-263.
3. Linzer DI, Levine AJ. Characterization of a 54K dalton cellular SV40 tumor antigen present in SV40-transformed cells and uninfected embryonal carcinoma cells. Cell. 1979;17(1):43-52.
4. Finlay CA, Hinds PW, Levine AJ. The p53 proto-oncogene can act as a suppressor of transformation. Cell. 1989;57(7):1083-1093.
5. Chen PL, Chen YM, Bookstein R, Lee WH. Genetic mechanisms of tumor suppression by the human p53 gene. Science. 1990;250 (4987):1576-1580.
6. Isobe M, Emanuel BS, Givol D, Oren M, Croce CM. Localization of gene for human p53 tumour antigen to band 17p13. Nature. 1986;320(6057):84-85.
7. Kandoth C, McLellan MD, Vandin F, et al. Mutational landscape and significance across 12 major cancer types. Nature. 2013;502(7471):333-339.
8. Nigro JM, Baker SJ, Preisinger AC, et al. Mutations in the p53 gene occur in diverse human tumour types. Nature. 1989;342 (6250):705-708.
9. Baker SJ, Fearon ER, Nigro JM, et al. Chromosome 17 deletions and p53 gene mutations in colorectal carcinomas. Science. 1989;244(4901):217-221.
10. Hollstein M, Sidransky D, Vogelstein B, Harris CC. p53 mutations in human cancers. Science. 1991;253(5015):49-53.
11. Levine AJ. p53, the cellular gatekeeper for growth and division. Cell. 1997;88(3):323-331.
12. Cho Y, Gorina S, Jeffrey PD, Pavletich NP. Crystal structure of a p53 tumor suppressor-DNA complex: understanding tumorigenic mutations. Science. 1994;265(5170):346-355.
13. Kim MP, Zhang Y, Lozano G. Mutant p53: multiple mechanisms define biologic activity in cancer. Front Oncol. 2015;5:249.
14. Chiaretti S, Brugnoletti F, Tavolaro S, et al. TP53 mutations are frequent in adult acute lymphoblastic leukemia cases negative for recurrent fusion genes and correlate with poor response to induction therapy. Haematologica. 2013;98(5):e59-61.
15. Stengel A, Schnittger S, Weissmann S, et al. TP53 mutations occur in 15.7% of ALL and are associated with MYC-rearrangement, low hypodiploidy, and a poor prognosis. Blood. 2014;124(2):251-258.
16. Hof J, Krentz S, van Schewick C, et al. Mutations and deletions of the TP53 gene predict nonresponse to treatment and poor outcome in first relapse of childhood acute lymphoblastic leukemia. J Clin Oncol. 2011;29(23):3185-3193.
17. Richter-Pechanska P, Kunz JB, Hof J, et al. Identification of a genetically defined ultra-high-risk group in relapsed pediatric T-lymphoblastic leukemia. Blood Cancer J. 2017;7(2):e523.
18. Stengel A, Kern W, Haferlach T, Meggendorfer M, Fasan A, Haferlach C. The impact of TP53 mutations and TP53 deletions on survival varies between AML, ALL, MDS and CLL: an analysis of 3307 cases. Leukemia. 2017;31(3):705-711.
19. Muhlbacher V, Zenger M, Schnittger S, et al. Acute lymphoblastic leukemia with low hypodiploid/near triploid karyotype is a specific clinical entity and exhibits a very high TP53 mutation frequency of 93%. Genes Chromosomes Cancer. 2014;53(6): 524-536.
20. Holmfeldt L, Wei L, Diaz-Flores E, et al. The genomic landscape of hypodiploid acute lymphoblastic leukemia. Nat Genet. 2013;45(3):242-252.
21. Qian M, Cao X, Devidas M, et al. TP53 germline variations influence the predisposition and prognosis of B-cell acute lymphoblastic leukemia in children. J Clin Oncol. 2018;36(6):591-599.
22. Krentz S, Hof J, Mendioroz A, et al. Prognostic value of genetic alterations in children with first bone marrow relapse of childhood B-cell precursor acute lymphoblastic leukemia. Leukemia. 2013;27(2): 295-304.
23. Gu L, Zhu N, Findley HW, Zhou M. MDM2 antagonist nutlin-3 is a potent inducer of

apoptosis in pediatric acute lymphoblastic leukemia cells with wild-type p53 and overexpression of MDM2. Leukemia. 2008;22(4):730-739.
24. Bykov VJ, Wiman KG. Mutant p53 reactivation by small molecules makes its way to the clinic. FEBS Lett. 2014;588(16):2622-2627.
25. Martins CP, Brown-Swigart L, Evan GI. Modeling the therapeutic efficacy of p53 restoration in tumors. Cell. 2006;127(7):1323-1334.
26. Xue W, Zender L, Miething C, et al. Senescence and tumour clearance is triggered by p53 restoration in murine liver carcinomas. Nature. 2007;445(7128):656-660.
27. Bykov VJ, Issaeva N, Shilov A, et al. Restoration of the tumor suppressor function to mutant p53 by a low-molecular-weight compound. Nat Med. 2002;8(3):282-288.
28. Lambert JM, Gorzov P, Veprintsev DB, et al. PRIMA-1 reactivates mutant p53 by covalent binding to the core domain. Cancer Cell. 2009;15(5):376-388.
29. Zhang Q, Bykov VJN, Wiman KG, Zawacka-Pankau J. APR-246 reactivates mutant p53 by targeting cysteines 124 and 277. Cell Death Dis. 2018;9(5):439.
30. Tessoulin B, Descamps G, Moreau P, et al. PRIMA-1Met induces myeloma cell death independent of p53 by impairing the GSH/ROS balance. Blood. 2014;124(10):1626-1636.
31. Ali D, Mohammad DK, Mujahed H, et al. Anti-leukaemic effects induced by APR-246 are dependent on induction of oxidative stress and the NFE2L2/HMOX1 axis that can be targeted by PI3K and mTOR inhibitors in acute myeloid leukaemia cells. Br J Haematol. 2016;174(1):117-126.
32. Mohell N, Alfredsson J, Fransson A, et al. APR-246 overcomes resistance to cisplatin and doxorubicin in ovarian cancer cells. Cell Death Dis. 2015;6:e1794.
33. Peng X, Zhang MQ, Conserva F, et al. APR-246/PRIMA-1MET inhibits thioredoxin reductase 1 and converts the enzyme to a dedicated NADPH oxidase. Cell Death Dis. 2013;4:e881.
34. Zandi R, Selivanova G, Christensen CL, Gerds TA, Willumsen BM, Poulsen HS. PRIMA-1Met/APR-246 induces apoptosis and tumor growth delay in small cell lung cancer expressing mutant p53. Clin Cancer Res. 2011;17(9):2830-2841.
35. Nahi H, Merup M, Lehmann S, et al. PRIMA-1 induces apoptosis in acute myeloid leukaemia cells with p53 gene deletion. Br J Haematol. 2006;132(2):230-236.
36. Bykov VJ, Zache N, Stridh H, et al. PRIMA-1(MET) synergizes with cisplatin to induce tumor cell apoptosis. Oncogene. 2005;24(21):3484-3491.
37. Izetti P, Hautefeuille A, Abujamra AL, et al. PRIMA-1, a mutant p53 reactivator, induces apoptosis and enhances chemotherapeutic cytotoxicity in pancreatic cancer cell lines. Invest New Drugs. 2014;32(5):783-794.
38. Liu DS, Read M, Cullinane C, et al. APR-246 potently inhibits tumour growth and overcomes chemoresistance in preclinical models of oesophageal adenocarcinoma. Gut. 2015;64(10):1506-1516.
39. Fransson A, Glaessgen D, Alfredsson J, Wiman KG, Bajalica-Lagercrantz S, Mohell N. Strong synergy with APR-246 and DNA-damaging drugs in primary cancer cells from patients with TP53 mutant high-grade serous ovarian cancer. J Ovarian Res. 2016;9(1):27.
40. Lehmann S, Bykov VJ, Ali D, et al. Targeting p53 in vivo: a first-in-human study with p53-targeting compound APR-246 in refractory hematologic malignancies and prostate cancer. J Clin Oncol. 2012;30(29):3633-3639.
41. Zarin DA, Tse T, Williams RJ, Rajakannan T. Update on trial registration 11 years after the ICMJE policy was established. N Engl J Med. 2017;376(4):383-391.
42. Meyer LH, Eckhoff SM, Queudeville M, et al. Early relapse in ALL is identified by time to leukemia in NOD/SCID mice and is characterized by a gene signature involving survival pathways. Cancer Cell. 2011;19(2):206-217.
43. Bouaoun L, Sonkin D, Ardin M, et al. TP53 variations in human cancers: new lessons from the IARC TP53 database and genomics data. Human Mutat. 2016;37(9):865-876.
44. Bykov VJ, Zhang Q, Zhang M, Ceder S, Abrahmsen L, Wiman KG. Targeting of mutant p53 and the cellular redox balance by APR-246 as a strategy for efficient cancer therapy. Front Oncol. 2016;6:21.
45. Lisek K, Walerych D, Del Sal G. Mutant p53-Nrf2 axis regulates the proteasome machinery in cancer. Mol Cell Oncol. 2017;4(1):e1217967.
46. Liu DS, Duong CP, Haupt S, et al. Inhibiting the system xC(-)/glutathione axis selectively targets cancers with mutant-p53 accumulation. Nat Commun. 2017;8:14844.
47. Haffo L, Lu J, Bykov VJN, et al. Inhibition of the glutaredoxin and thioredoxin systems and ribonucleotide reductase by mutant p53-targeting compound APR-246. Sci Rep. 2018;8(1):12671.
48. Hientz K, Mohr A, Bhakta-Guha D, Efferth T. The role of p53 in cancer drug resistance and targeted chemotherapy. Oncotarget. 2017;8(5):8921-8946.
49. Bykov VJ, Issaeva N, Selivanova G, Wiman KG. Mutant p53-dependent growth suppression distinguishes PRIMA-1 from known anticancer drugs: a statistical analysis of information in the National Cancer Institute database. Carcinogenesis. 2002;23(12):2011-2018.
50. Synnott NC, Murray A, McGowan PM, et al. Mutant p53: a novel target for the treatment of patients with triple-negative breast cancer? Int J Cancer. 2017;140(1):234-246.

Ferrata Storti Foundation

Haematologica 2020
Volume 105(1):182-192

Responsiveness of chronic lymphocytic leukemia cells to B-cell receptor stimulation is associated with low expression of regulatory molecules of the nuclear factor-κB pathway

Ruud W.J. Meijers,[1*] Alice F. Muggen,[1*] Leticia G. Leon, [1]Maaike de Bie,[1] Jacques J.M. van Dongen,[1,2] Rudi W. Hendriks[3#] and Anton W. Langerak[1#]

[1]Laboratory Medical Immunology, Department of Immunology, Erasmus MC, University Medical Center Rotterdam, Rotterdam; [2]Department of Immunohematology and Blood Transfusion, Leiden University Medical Center, Leiden and [3]Department of Pulmonary Medicine, Erasmus MC, Rotterdam, the Netherlands

**RWJM and AFM share equal responsibility and first authorship*

#RWH and AWL share equal responsibility and senior authorship

ABSTRACT

Chronic lymphocytic leukemia (CLL) is a disease with heterogeneous clinical and biological characteristics. Differences in Ca^{2+} levels among cases, both basal and upon B-cell receptor (BCR) stimulation, may reflect heterogeneity in the pathogenesis due to cell-intrinsic factors. Our aim was to elucidate cell-intrinsic differences between BCR-responsive and -unresponsive cases. We therefore determined BCR responsiveness *ex vivo* based on Ca^{2+} influx upon α-IgM stimulation of purified CLL cell fractions from 52 patients. Phosphorylation levels of various BCR signaling molecules, and expression of activation markers were assessed by flow cytometry. Transcription profiling of responsive (n=6) and unresponsive cases (n=6) was performed by RNA sequencing. Real-time quantitative polymerase chain reaction analysis was used to validate transcript level differences in a larger cohort. In 24 cases an α-IgM response was visible by Ca^{2+} influx which was accompanied by higher phosphorylation of PLCγ2 and Akt after α-IgM stimulation in combination with higher surface expression of IgM, IgD, CD19, CD38 and CD43 compared to the unresponsive cases (n=28). Based on RNA sequencing analysis several components of the canonical nuclear factor (NF)-κB pathway, especially those related to NF-κB inhibition, were expressed more highly in unresponsive cases. Moreover, upon α-IgM stimulation, the expression of these NF-κB pathway genes (especially genes coding for NF-κB pathway inhibitors but also NF-κB subunit *REL*) was upregulated in BCR-responsive cases while the level did not change, compared to basal level, in the unresponsive cases. These findings suggest that cells from CLL cases with enhanced NF-κB signaling have a lesser capacity to respond to BCR stimulation.

Correspondence:

ANTON W. LANGERAK
a.langerak@erasmusmc.nl

Received: January 1, 2019.

Accepted: May 15, 2019.

Pre-published: May 16, 2019.

doi:10.3324/haematol.2018.215566

Check the online version for the most updated information on this article, online supplements, and information on authorship & disclosures: www.haematologica.org/content/105/1/182

Introduction

Chronic lymphocytic leukemia (CLL) is a lymphoid malignancy that is characterized by a monoclonal expansion of mature B cells with a homogeneous morphology and a characteristic immunophenotype.[1] CLL is the most common type of leukemia in the Western world and mainly affects the elderly.[1] Based on the somatic hypermutation (SHM) status of the immunoglobulin heavy chain (IGHV) gene, CLL can be divided into unmutated CLL (U-CLL) and mutated CLL (M-CLL), with U-CLL generally being a more aggressive form of the disease and M-CLL a more indolent form.[2,3] Around 30% of all cases can be grouped into subsets based on so-called stereotypic B-cell receptors (BCR), which are identified by their restricted IGHV/IGHD/IGHJ gene usage plus similarities in length and amino acid sequence of their complementarity-determining region 3 (CDR3). [4]

BCR stereotypy would be indicative of the involvement of similar specific antigens and underlines the importance of antigenic stimulation and BCR specificity in the pathogenesis of CLL.[4] In general, most U-CLL express a BCR that is polyreactive and recognizes self- and non-self-antigens with low-affinity binding.[5-8] In addition, for some stereotypic CLL subsets the antigens recognized by their BCR have been identified.[9-13]

However, it was previously shown that the BCR from CLL cells could also be stimulated independently of external antigens, as the CDR3 regions are able to recognize an internal epitope in framework 2 (FR2) of the IGHV domain.[14] This induces a higher level of antigen-independent autonomous BCR signaling, since these cells exhibit a higher Ca^{2+} level in their cytoplasm, as demonstrated *in vitro* using a triple knockout (TKO) cell system.[14]

We previously demonstrated that primary CLL cells generally have higher basal Ca^{2+} levels compared with peripheral B cells from healthy individuals.[15] Basal Ca^{2+} levels correlated with IGHV mutational status, as we found on average higher basal Ca^{2+} levels in M-CLL than in U-CLL.[14,15] However, our data also showed large variation within the subgroups, as cases with high and low basal Ca^{2+} levels could be found in both M-CLL and U-CLL groups.[15] Since there was no correlation with BCR characteristics (e.g., Ig expression level, HCDR3 length, charge and composition) or with cytogenetic aberrations, it is conceivable that high basal Ca^{2+} levels are partly directed by the SHM status and that cell-intrinsic differences caused by cell anergy could explain the variation.[15]

Anergy is an immune state in which the cell is silenced upon low-affinity recognition of self-antigens.[16] Anergic cells remain capable of antigen binding, but have a reduced ability to respond to BCR-dependent antigenic stimulation.[16] Anergy has been linked to CLL based on low surface BCR expression, reduced responsive capability,[17,18] and increased basal Ca^{2+} levels.[15] M-CLL in particular shows these increased basal Ca^{2+} levels in combination with a poorer response to BCR stimulation[15] which is in line with other studies showing that the α-IgM response is associated with IGHV mutational status and with the surface expression of markers of prognosis, such as CD38.[18,19] Moreover, a high level of surface IgM is associated with a clinically aggressive form of the disease, which has potential implications as a diagnostic parameter for disease progression.[20]

However, Ca^{2+} levels, both basal and upon BCR stimulation, vary within the U-CLL and M-CLL groups. We hypothesized that this heterogeneity in BCR responsiveness could reflect a diverse disease pathogenesis involving cell-intrinsic differences. In this study we aimed to elucidate potential cell-intrinsic differences underlying the observed differences in Ca^{2+} levels between CLL cases.

Methods

Study population

Fifty-two patients were included of whom 30 (58%) had U-CLL and 22 (42%) had M-CLL as determined by the IGHV SHM status (*Online Supplementary Methods*). The patients' characteristics are shown in *Online Supplementary Table S1*. The majority of the included patients (n=41, 79%) were treatment-naïve. Purified CLL cells were isolated (*Online Supplementary Methods*) upon informed consent and anonymized for further use, following the guidelines of the institutional review board (METC-2015-741) and in accordance with the Declarations of Helsinki.

Flow cytometry

Flow cytometry was used to assess the responsive capacity upon α-IgM stimulation by measuring Ca^{2+} levels (*Online Supplementary Methods*) and to determine the expression of activation markers by using antibodies listed in *Online Supplementary Table S2*. Phospho-flow analysis was done to study the phosphorylation of Spleen tyrosine kinase (Syk), Phopholipase Cγ2 (PLCγ2) and Protein kinase B (Akt) upon α-IgM stimulation. (*Online Supplementary Methods*).

Cell culture and retroviral transduction of triple knockout cells

TKO cells, derived from a signaling-competent mouse pre-B-cell line lacking the expression of endogenous pre-BCR due to inactivation of *RAG2* and *λ5* genes,[21] and Phoenix cells (ATCC CRL-3214) were both cultured as described by Meixlsperger *et al.*[21] The protocol used for the transduction of TKO cells was also documented before by Meixlsperger *et al.*[21]

RNA sequencing

Twelve cases from our cohort were selected based on their responsiveness to α-IgM stimulation (6 responsive, 6 unresponsive) and their RNA was sequenced. The RNA was extracted using Allprep DNA/RNA/miRNA Universal (Qiagen, Hilden, Germany) according to the manufacturer's instructions. RNA sequencing was performed on a TruSeq platform (Illumina, San Diego, CA, USA) at the Human Genome Facility (Erasmus Medical Center, Rotterdam, the Netherlands). Reads were extracted from the raw sequencing data using CASAVA 1.8.2 (Illumina) and aligned to the human reference genome (UCSC's hg19) using the STAR (2.5.0c) splice aware aligner with gencode v19 transcriptome annotations as an additional template. The BAM files were processed using various tools from the picard software suite (v1.90), as well as tools from the Genome Analysis ToolKit (GATK, v3.5). Quality control metrics were collected at various steps using picard and evaluated, along with coverage metrics using GATK. Read counts per exon/gene were then determined by the featureCounts function of the subread package (v1.4.6-p1) using the gencode v19 annotation as markers. The raw read counts were normalized through the fragments per kilobase of exon model per million reads mapped (FPKM) methodology, normalizing for library yield and gene size.

For classification analysis, the calculated Spearman correlation as a distance (1/similarity) measurement and Ward.D2 for the unsupervised clustering were applied to the samples used. R packages (version 3.4.4) weres used for differential expression analysis and to create plots for visualization. We analyzed the sample fitting with edgeR, the gene-wise negative binomial generalized linear models for contrast.

To validate transcript level differences in a larger cohort, RNA was synthesized to cDNA and real-time quantitative polymerase chain reaction (RQ-PCR) was performed (*Online Supplementary Methods* and *Online Supplementary Table S2*).

Results

Unmutated cases of chronic lymphocytic leukemia are generally more responsive than mutated cases to α-IgM stimulation

To determine whether high basal Ca^{2+} levels are BCR-dependent or caused by cell-intrinsic factors, we selected

a small series of CLL samples with known high (n=3) or low (n=6) basal Ca^{2+} levels from our previous study in 2015,[15] and cloned their BCR into TKO cells as described by Dühren-von Minden *et al.*[14]

Even though we could detect Ca^{2+} signaling by the BCR in TKO cells for all analyzed CLL-derived BCR expressed as IgM, we did not detect any correlation (R^2=0.014, *P*=0.764) between the Ca^{2+} signal in CLL and that in TKO cells (Figure 1B) indicating that the high basal Ca^{2+} levels seen in some CLL samples would result from cell-intrinsic changes rather than from BCR-dependent autonomous signaling.

To determine which cell-intrinsic differences might cause the heterogeneity in Ca^{2+} signaling in basal conditions and upon BCR stimulation, we established a new cohort of patients (n=52, *Online Supplementary Table S1*). CLL cells were isolated from peripheral blood and immediately used for further analysis. First, basal Ca^{2+} levels were assessed (Figure 1B). Similar to the previous study, basal Ca^{2+} levels were heterogeneous in both U-CLL and M-CLL cases.[15]

Next, we examined the responsive capacity of the CLL samples upon BCR stimulation. Figure 1D shows two flow cytometric examples. In line with our previous study,[15] we found that U-CLL cells in general responded significantly (*P*=0.049) better upon α-IgM stimulation compared with M-CLL cells (Figure 1E). Although no differences were found in the response after α-IgD stimulation (Figure 1F), there was a strong correlation between the relative response to α-IgM and α-IgD stimulation (R^2=0.508, *P*<0.0001) (Figure 1G). Based on this, we further defined CLL subgroups based on BCR responsiveness upon α-IgM stimulation. Twenty-four cases were classified as responsive (median fluorescence intensity ratio, response/basal signal: 1.1-6.5; n=17 U-CLL and n=7 M-CLL) and 28 cases were unresponsive (median fluorescence intensity ratio, response/basal signal: <1.1; n=13 U-CLL and n=15 M-CLL).

Higher phosphorylation of PLCγ2 and Akt in chronic lymphocytic leukemia correlated with responsiveness upon B-cell receptor stimulation

In order to gain a better understanding of BCR responsive capacity, as defined by Ca^{2+} influx, we examined phosphorylation of Syk, PLCγ2 and Akt upon α-IgM stimulation. First, we evaluated differences in basal phosphorylation levels of Syk (pSyk), PLCγ2 (pPLCγ2) and Akt (pAkt) (Figure 2A). The responsive cases showed a significantly (*P*=0.0013) higher basal pPLCγ2 level than unresponsive cases but no differences were found in basal pSyk and pAKT levels (Figure 2B). Next we examined the relative response of kinase phosphorylation upon BCR stimulation. Even though no difference in relative response of pSYK after α-IgM stimulation was found, the responsive patients had a higher relative response of pPLCγ2 and pAkt upon α-IgM stimulation (Figure 2C).

Taken together, the α-IgM response as determined by Ca^{2+} influx, is consistent with greater phosphorylation of pPLCy2 and pAkt upon α-IgM stimulation

Chronic lymphocytic leukemia cases showing good B-cell receptor responsiveness have a more activated phenotype

Next we examined whether the expression of activation markers is associated with the response to α-IgM. As expected, CLL cells from responsive cases displayed a significantly (*P*=0.0002) higher expression of surface IgM compared to the unresponsive cases; likewise, IgD (*P*=0.036), CD19 (*P*=0.029), CD38 (*P*=0.035), and CD43 (*P*=0.047) expression levels were also higher in responsive cases than in unresponsive cases (Figure 3A). No differences were found in CD20, CD21, CD27, CD69, CD80, CD86 and CXCR4 expression (*Online Supplementary Figure S1*).

To determine whether the α-IgM responsiveness within the responsive cases correlates with the expression level of these markers, we compared surface expression and relative response. The relative response did correlate with surface IgM (R^2=0.322, *P*=0.0038) and CD21 (R^2=0.469, *P*=0.0002) expression levels (Figure 3B).

IκB-related genes in particular are differentially expressed between B-cell receptor-responsive and -unresponsive cases

Twelve cases from our cohort were selected to evaluate cell-intrinsic differences based on RNA sequencing of total RNA from MACS-purified (>95%) CLL cells. Six patients were classified based on Ca^{2+} levels as responders upon α-IgM stimulation and were compared to another six patients who were unresponsive. (*Online Supplementary Table S3*) First, RNA expression profiles of the 12 cases were compared to each other via Spearman correlation (Figure 4A). Based on these results the patients could be divided into three major clusters, which did not correlate with BCR responsiveness or SHM status. In addition, when comparing the variation in total gene expression levels between the samples, as shown by Z-scores in a heat map (*Online Supplementary Figure S2*), no clear division of responsive and unresponsive cases was found either, probably reflecting the biological heterogeneity of CLL samples, even when classified as BCR-responsive and -unresponsive.

Next, we therefore focused on genes involved in BCR signaling using Qiagen's Ingenuity Pathway Analysis (IPA). As illustrated by the volcano plot, responsive cases demonstrated significantly higher expression of *EBF1*, *FCGR2A*, *SYK* and *FYN* (positive $\log_{FC}$ values), whereas the non-responders showed significantly higher expression of *NFKBID*, *NFKB2*, *CAM2KA*, *NFKBIE*, *RAF1*, *NFKBIB*, *NFKB1*, *RPS6K1*, *PLCG1* and *BCL3* (negative $\log_{FC}$ values) (Figure 4B and *Online Supplementary Figure S2*). Interestingly, the *NFKBIB*, *NFKBID* and *NFKBIE* genes all encode inhibitors of NF-κB (IκB), while *NFKB1*, *NFKB2* and *BCL3* are genes coding for NF-κB components that are associated with inhibition.[22]

B-cell receptor-unresponsive cases have higher expression of genes expressing regulatory molecules of nuclear factor-κB signaling

Additional samples were selected (n=13 unresponsive, n=15 responsive) to validate the differences in transcript levels of NF-κB genes (*NFKB1*, *NFKB2*, *BCL3*, *NFKBIB*, *NFKBID* and *NFKBIE*) using RQ-PCR. RQ-PCR results (displayed as $2^{-deltaCT}$ values) indeed confirmed that responding cases had significantly lower expression of *NFKB1* and *NFKB2* (Figure 5A) *NFKBIB* and *NFKBIE* (Figure 5B). Furthermore, we found a trend towards lower *NFKBID* expression, but no difference in *BCL3* expression between the subgroups (Figure 5B).

In addition, we investigated whether the transcription-

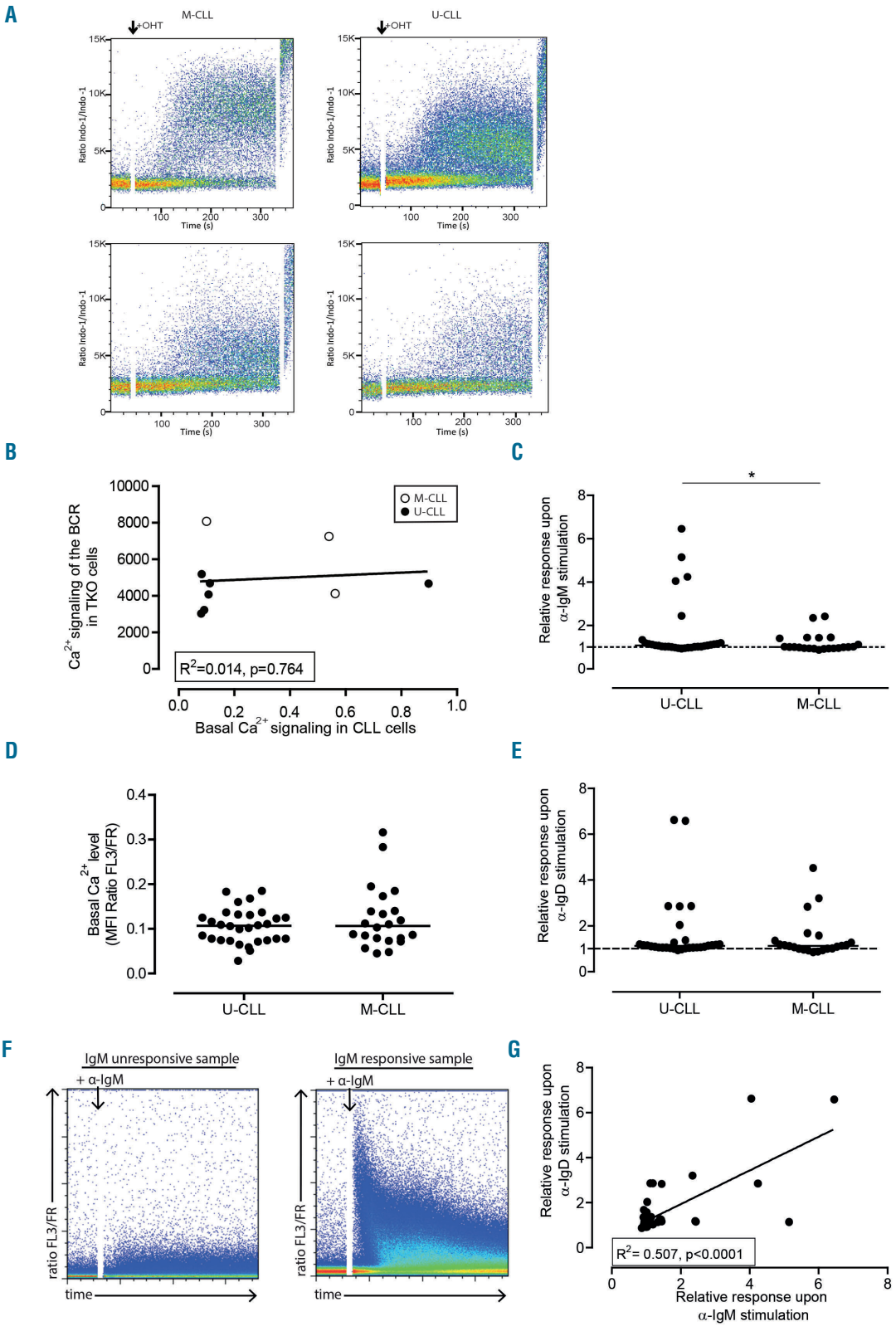

Figure 1. Ca^{2+} signaling in chronic lymphocytic leukemia cells. (A) Flow cytometric analysis of Ca^{2+} flux (ratio Indo-1/Indo-1) after the addition of 4-hydroxytamoxifen (4-OHT) to triple knockout (TKO) cells expressing the B cell receptor (BCR) from two representative samples of mutated chronic lymphocytic leukemia (M-CLL) (left) and two unmutated samples (U-CLL) (right). (B) From nine CLL cases (6 U-CLL, black dots and 3 M-CLL, open dots) in whom the basal Ca^{2+} level (x-axis) had been assessed earlier, the BCR was cloned into TKO cells to determine the autonomous Ca^{2+} signal (y-axis). Linear regression was performed and the R^2 and *P*-value are shown. (C) Basal Ca^{2+} level [median fluorescence intensity (MFI) ratio FI3/FR] was determined in a new cohort of 52 CLL samples (freshly isolated) consisting of 30 U-CLL and 22 M-CLL cases. (D) Responsive capacity upon BCR stimulation. Flow cytometric analysis of a representative CLL sample showing no Ca^{2+} influx (ratio FL3/FR) upon α-IgM stimulation (left) and a representative CLL sample with an increase in Ca^{2+} influx (ratio FL3/FR) upon α-IgM stimulation (right). Based on this analysis the responsive capacity upon α-IgM stimulation (E) and α-IgD stimulation (F) was determined in the 30 U-CLL and 22 M-CLL cases. Individual plots and medians (gray bars) are shown. The Mann-Whitney U-test was performed for statistical analysis between the groups of patients (*P<0.05). (G) Linear regression analysis between the relative response after α-IgM and α-IgD stimulation: R^2 and *P* values are shown.

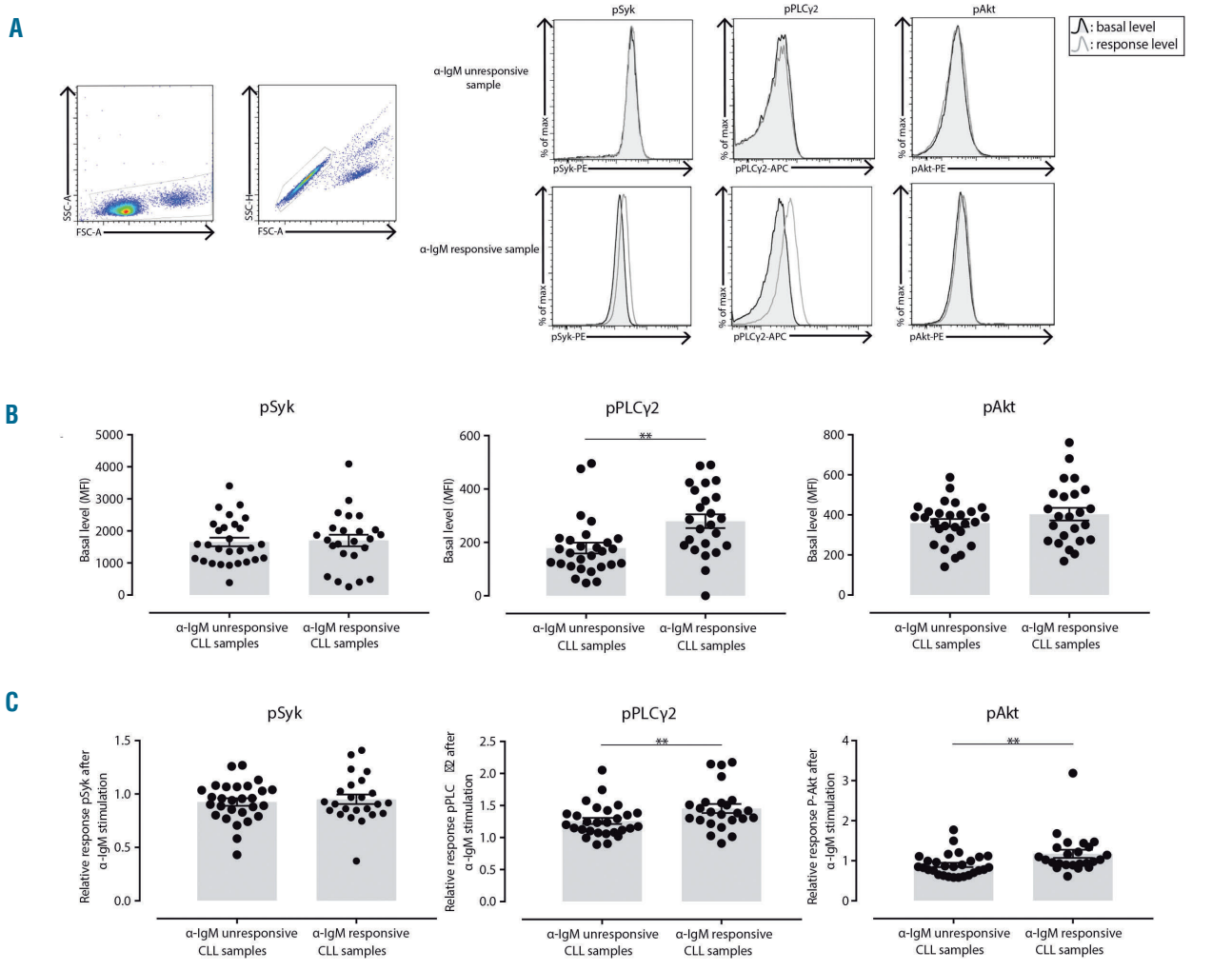

Figure 2. Phosphorylation of Syk, PLCγ2 and Akt. (A) The levels of pSyk, pPLCγ2 and pAkt were determined at baseline and upon stimulation with α-IgM and correlated with the α-IgM response as determined by Ca^{2+} signaling. Representative examples of the analysis in a case of unresponsive chronic lymphocytic leukemia (CLL) (upper histograms) and a responsive CLL case (lower histograms) are shown. After single viable cell selection, the levels of pSyk, pPLCγ2 and pAkt were determined, both at baseline (black line) and upon stimulation with α-IgM (gray line). (B) Differences in basal levels of pSYK, pPLCγ2 and pAKT (x-axis) between α-IgM unresponsive and responsive samples. (C) The relative response after α-IgM stimulation for pSYK, pPLCγ2 and pAKT (x-axis) in the two groups of patients. Individual plots and medians (gray bars) are shown. The Mann-Whitney U-test was performed for statistical analysis between the groups of patients (**P<0.01).

al levels of these NF-κB pathway genes also correlated with basal Ca^{2+} levels (*Online Supplementary Figure S3*). A significant correlation could only be found between basal Ca^{2+} levels and *NFKB1* (R^2=0.163, P=0.033) and *NFKBIE* (R^2=0.234, P=0.0091) transcript levels (*Online Supplementary Figure S3*).

Since loss of IκBε (encoded by *NFKBIE* as caused by an identical 4-bp frameshift deletion in the first exon), has been associated with a progressive form of CLL,[23] we determined whether patients in our cohort with low *NFKBIE* expression carried this identical deletion. Upon sequencing of the first exon of *NFKBIE*, this 4-bp deletion was not observed (*data not shown*).

Expression levels of genes coding for NF-κB regulators (*NFKB1* and *NFKB2*) and coding for IκB that were expressed at lower levels in responsive cases appeared to correlate with each other (*Online Supplementary Figure S4*), implying that unresponsive patients show higher expression of multiple NF-κB inhibitors. Even though we could not detect statistically significant differences in expression levels of genes coding for the NF-κB subunits *RELA*, *RELB* and *REL* between the two subgroups (*data not shown*), we did observe clear correlations between expression levels of genes associated with NF-κB inhibition and expression levels of *RELA* and *REL* (*Online Supplementary Figure S5*), both involved in the canonical NF-κB. No correlations between inhibitor levels and levels of the non-canonical NF-κB subunit *RELB* were found (*data not shown*).

Besides the IκB genes, we also found a difference in expression of tumor necrosis factor-α induced protein 3 (*TNFAIP3*; $\log_{FC}$=-1.70, 10log(Pvalue)=2.24) based on RNA sequencing analysis. *TNFAIP3* encodes for protein A20 that is induced by TNF-α and functions as a negative regulator through inhibition of NF-κB signaling.[24] In addition, RQ-PCR showed significantly (P=0.017) higher expression of *TNFAIP3* in unresponsive cases than in responsive ones (Figure 5C).

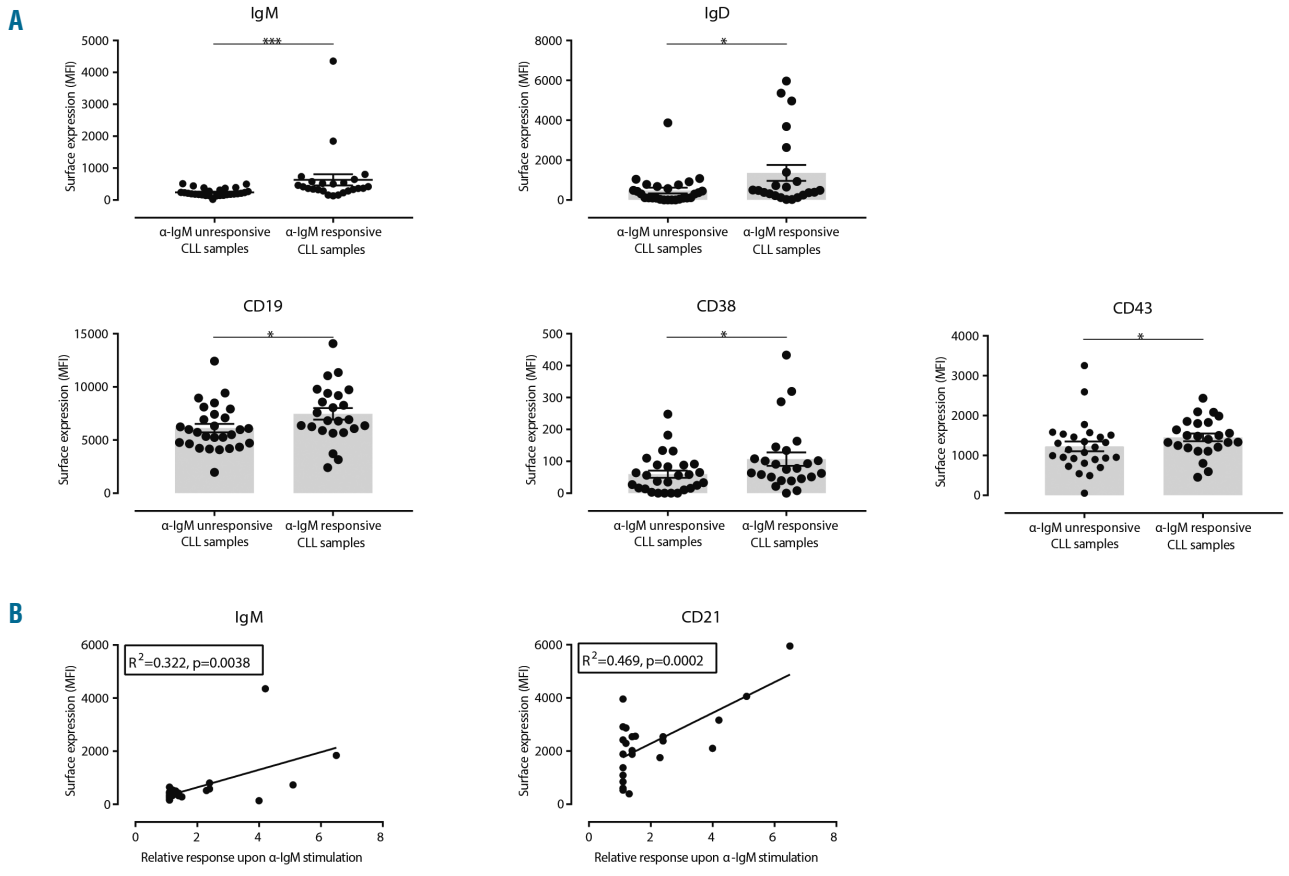

Figure 3. Surface expression of activation-associated markers. The surface expression of several activation-associated markers was measured in 52 patients with chronic lymphocytic leukemia (CLL). (A) Surface expression levels (x-axis) of IgM, IgD, CD19, CD38 and CD43 in α-IgM-unresponsive and α-IgM-responsive cases. Individual plots and medians (gray bars) are shown. The Mann-Whitney U-test was performed for statistical analysis between the groups of patients (*P<0.05). (B) Relative response upon α-IgM stimulation (x-axis) is plotted against the surface expression [median fluorescence intensity (MFI)] expression level of IgM and CD21. Linear regression analysis was performed and R^2 and P values are shown.

Collectively, these results illustrate that unresponsive cases have higher basal gene expression of several regulatory molecules of canonical NF-κB pathway signaling.

Upregulation of nuclear factor-κB pathway genes upon α-IgM stimulation in B-cell receptor-responsive cases

To further study expression of the NF-κB genes upon stimulation, frozen peripheral blood mononuclear cells from 21 cases (unresponsive CLL; n=11 and responsive CLL; n=10) were thawed, after which CLL cells were MACS-isolated and stimulated for 2.5 h with α-IgM (optimal stimulation was defined using normal B cells; *data not shown*). The $2^{-deltaCT}$ values obtained after incubation (α-IgM-stimulated and -unstimulated) were normalized by subtraction of the basal $2^{-deltaCT}$ value to calculate the fold differences in expression between the groups of patients (Figure 6). BCR-responsive cases showed significant upregulation of *NFKB2*, *REL*, *NFKBID*, *NFKBIE* and *TNFAIP3* after stimulation compared with unresponsive cases for which the expression of the NF-κB genes remained roughly equal.

In summary, α-IgM-unresponsive cases had high basal transcription of especially NF-κB inhibitory components, whereas the responsive cases showed clear upregulation of NF-κB inhibitory components, including *TNFAIP3* and NF-κB subunit *REL*, upon stimulation.

Discussion

Here we aimed to study cell-intrinsic differences between unresponsive and responsive CLL, which may underlie differences in Ca^{2+} levels upon α-IgM stimulation. Based on RNA sequencing analysis several components of the canonical NF-κB pathway, especially related to NF-κB inhibition, were expressed more highly in unresponsive cases. Besides these inhibitors, the TNFα-induced NF-κB inhibitor A20 was also significantly more highly expressed in the BCR-unresponsive cases. Lastly we showed that upon α-IgM stimulation, the expression of these NF-κB pathway genes (especially genes coding for NF-κB pathway inhibitors but also NF-κB component *REL*) is upregulated in BCR-responsive cases while for the unresponsive cases the transcriptional level did not change compared to basal levels, indicating that NF-κB signaling is an important pathway for CLL cells in their ability to respond upon BCR stimulation.

Based on the lack of correlation between basal Ca^{2+} lev-

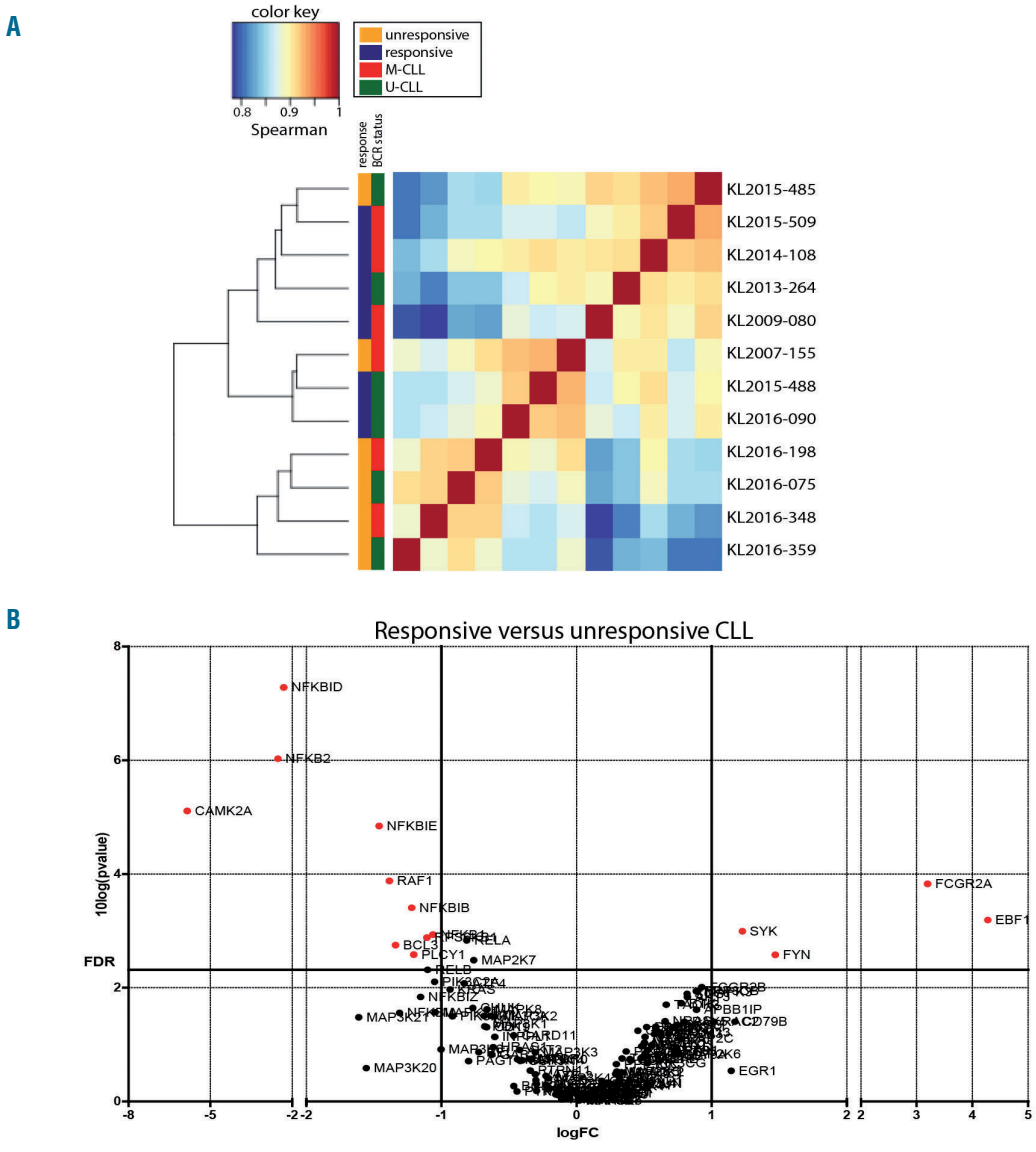

Figure 4. Differential expression analysis based on RNA sequencing data. (A) Results of the Spearman correlation of the RNA expression analysis in different chronic lymphocytic leukemia (CLL) samples (n=6 responsive *vs.* n=6 unresponsive CLL cases). The color scale indicates the degree of correlation varying from blue (low correlation) to red (high correlation). The two panels at the left end indicate the responsiveness (orange = unresponsive, blue = responsive) and the IGHV somatic hypermutation status [red=mutated (M)-CLL, green=unmutated (U)-CLL] of the selected CLL cases. (B) Volcano plot showing differences in transcript levels of genes involved in the B-cell receptor signaling pathway as determined using Qiagen's Ingenuity Pathway Analysis (IPA). A negative $\log_{FC}$ value indicates higher expression of certain genes in unresponsive CLL cases, while a positive $\log_{FC}$ value is indicative of higher expression in responsive CLL cases. The $\log_{FC}$ value was plotted against the 10log(*P*value). False discovery rate (FDR) was calculated and transcriptional differences of genes with a $\log_{FC}$ value of 1 or -1 in combination with a 10log(*P*value) above the FDR are indicated in red.

els and autonomous signaling in TKO cells,[14] we aimed to gain more insight into possible cell-intrinsic differences, although we cannot formally exclude that Ca^{2+} levels could also (partly) have been high due to previous antigenic stimulation in our *ex-vivo* samples. Using a new cohort, Ca^{2+} signaling was determined in freshly isolated cells instead of thawed cells, which on average resulted in lower basal Ca^{2+} levels (*data not shown*). This might be, in combination with the heterogeneity in basal Ca^{2+} levels, an underlying explanation for the fact that in this cohort the basal Ca^{2+} levels were not different between M-CLL and U-CLL cases. Further building on the study of Mockridge *et al.*,[18] who also showed differences in responsiveness to BCR stimulation between CLL cases, we therefore divided our cohort of patients based on their responsive capacity to BCR stimulation. In both the M-CLL and U-CLL groups, there were cases showing a clear α-IgM response based on Ca^{2+} influx, while others did not show such a response, indicating that the level of anergy is independent of the IGHV SHM status of the BCR.

The anergic nature of unresponsive CLL was partly confirmed by the marker profile. IgM responders co-express higher levels of surface IgM and IgD, which explains the response to α-IgM as well as α-IgD stimulation. The higher expression of the prognostic marker CD38 by the responsive cases is also in line with findings of Mockridge *et al.*[18] suggesting that responsive patients in general have a poor prognosis.[2] The strong correlation

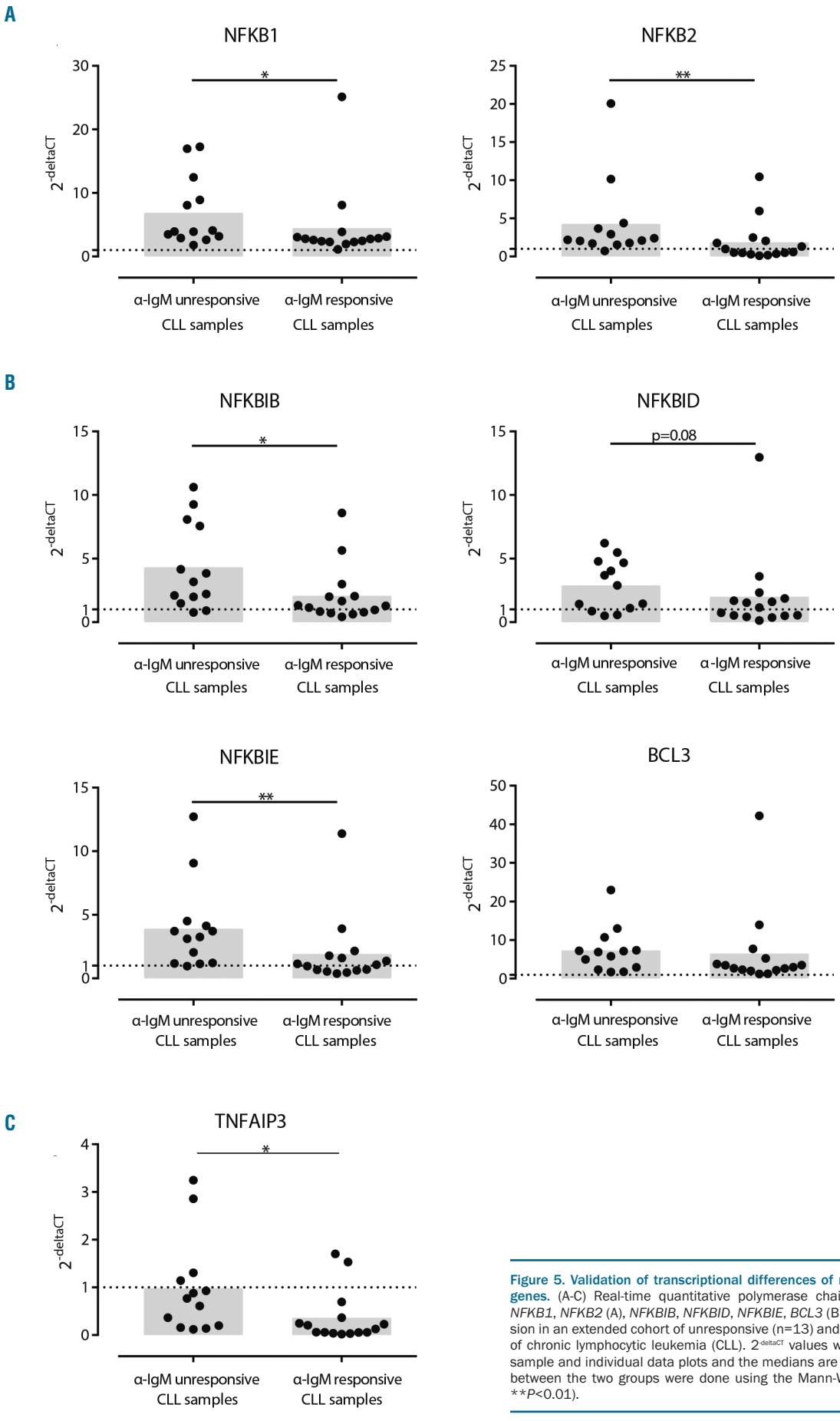

Figure 5. Validation of transcriptional differences of nuclear factor-κB-related genes. (A-C) Real-time quantitative polymerase chain reaction validation of *NFKB1*, *NFKB2* (A), *NFKBIB*, *NFKBID*, *NFKBIE*, *BCL3* (B) and *TNFAIP3* (C) expression in an extended cohort of unresponsive (n=13) and responsive (n=15) cases of chronic lymphocytic leukemia (CLL). $2^{-deltaCT}$ values were determined for each sample and individual data plots and the medians are shown. The comparisons between the two groups were done using the Mann-Whitney U-test (*P<0.05, **P<0.01).

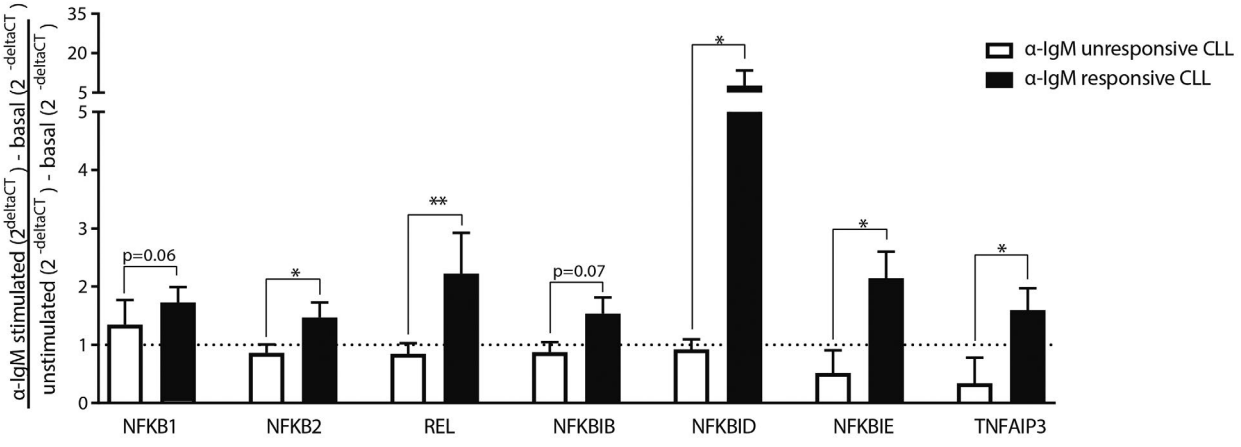

Figure 6. Transcriptional levels of nuclear factor-κB related genes upon α-IgM stimulation. Upon α-IgM stimulation, real-time quantitative polymerase chain reactions were performed to examine the transcriptional levels of multiple nuclear factor (NF)-κB pathway genes (*NFKB1*, *NFKB2*, *REL*, *NFKBIB*, *NFKBID*, *NFKBIE* and *TNFAIP3*) that were differently expressed at baseline between responsive and unresponsive cases of chronic lymphocytic leukemia (CLL). The $2^{-deltaCT}$ value upon α-IgM stimulation was subtracted from the $2^{-deltaCT}$ value at baseline and divided by the $2^{-deltaCT}$ value of the unstimulated condition corrected by the $2^{-deltaCT}$ value at baseline to calculate the net increase or decrease upon α-IgM stimulation. α-IgM unresponsive CLL cases (n=11, white bars) were compared to α-IgM responsive CLL cases (n=10, black bars) and statistical analysis was performed using the Mann-Whitney U-test (*P<0.05, **P<0.01).

between CD21 expression and the responsive capacity upon α-IgM stimulation is striking. In other immune-related diseases, such as rheumatoid arthritis, common variable immunodeficiency[25] and Sjögren syndrome,[26] patients had increased populations of $CD21^{low}$ B cells compared to healthy individuals.[25] These $CD21^{low}$ B cells were found to represent unresponsive cells expressing autoreactive BCR which failed to respond, as determined from Ca^{2+} levels upon BCR stimulation.[25,26] $CD21^{low}$ CLL cells were not found to be autoreactive and are associated with a poor prognosis.[27] Unfortunately we had no access to patients' longitudinal data and we were therefore unable to evaluate progression of the CLL.

RNA sequencing analysis showed that especially genes coding for regulatory molecules involved in NF-κB inhibition are differentially expressed between BCR-responsive and -unresponsive cases. Several studies have shown that CLL cells have higher basal NF-κB levels compared to normal B cells and that they are continuously activated.[28] In addition, it has been shown that NF-κB signaling is important for preventing apoptosis by multiple mechanisms, including CD40L-mediated signaling.[28-30]

We found that the unresponsive cases had higher basal gene expression of several components of the canonical NF-κB pathway, especially those involved in inhibition. Genes coding for the p105/p50 (*NFKB1*) and p100/p52 (*NFKB2*) subunits were expressed more highly in unresponsive CLL. Both are potential inhibitors and allow functional NF-κB activation in which p105/p50 is involved in the canonical NF-κB pathway and p100/p52 in the alternative (non-canonical) NF-κB pathway.[31] In addition, we found that genes coding for IκB were more highly expressed in unresponsive cases. IκBε (coded by *NFKBIE*), which is an important regulator of B-cell proliferation,[32] was found to be mutated in patients with CLL.[23,33] In particular, a recurrent 4-basepair frameshift deletion resulting in functional loss of IκBε and leading to continuous NF-κB activation was detected in progressive forms of CLL [23] as well as in other B-cell malignancies.[34] However, we could not identify this identical deletion as a possible cause for the lower *NFKBIE* gene expression in the responsive cases.

Besides BCR stimulation, the canonical NF-κB pathway can be activated by TNF receptor stimulation.[31] It might thus be that NF-κB signaling in BCR-unresponsive cases is more dependent on TNF-mediated activation. Higher *TNFAIP3* expression, a negative feedback regulator of NF-κB signaling induced by TNFα, as we noted in unresponsive cases, provides a basis for this theory. From B-cell lymphoma patients it is known that increased and sustained NF-κB activation of especially the proto-oncogene c-REL promotes TNFα-induced cell survival.[35] Through this feedback loop mechanism, secretion and uptake of TNFα might result in NF-κB-induced survival of (anergic) CLL cells, independently of BCR signaling. Foa *et al.*[36] reported that CLL cells continuously produce TNFα, especially cells from patients with an indolent form of the disease compared to patients with a progressive form.[36]

Genomic aberrations in the *TNFAIP3* gene resulting in the loss of A20 are linked with autoimmune disease with a humoral component as well as several B-cell lymphomas.[37] In B cells from aged mice it was demonstrated that selective loss of A20 increases the activation threshold and enhances proliferation and survival of B cells causing an inflammatory condition and inducing autoimmunity.[38] Such a loss of A20 caused by genetic aberrations of *TNAIP3* has not been associated with human CLL.[39]

Even though the focus of our study was mostly on those genes that were expressed at higher levels in unresponsive cases, multiple genes, including *SYK*, were found to be expressed more highly in responsive cases. Although *SYK* was differently expressed based on the RNA sequencing analysis between the two groups of patients in the extended cohort of patients with CLL, we did not find a difference in SYK protein level (by phospho-flow analysis; *data not shown*). Another gene of interest that emerged from our analysis is Early B-cell Factor 1 (*EBF1*), a transcription factor important in B-cell differentiation, which was expressed at higher levels by the responsive cases.[40] Seifert *et al.* had earlier shown that

EBF1 was significantly downregulated in patients with CLL compared to conventional B cells.[41] It was suggested that the low expression of *EBF1* might result in reduced levels of B-cell signaling and might contribute to an anergic phenotype of CLL cells.[41] Our results showing a lower level of *EBF1* transcripts in unresponsive cases would support this theory. Future studies are required to elucidate the importance of *EBF1* in CLL pathogenesis.

In summary, our results indicate that responsive CLL cases, irrespective of IGHV SHM status, have a more activated phenotype and reduced basal expression of several regulatory molecules of the canonical NF-κB pathway including those associated with NF-κB inhibition. Upon α-IgM stimulation these responsive cases showed upregulation of NF-κB, including NF-κB inhibitors, whereas transcriptional levels of NF-κB signaling pathway components remained unaltered in unresponsive cases. Our findings suggest that enhanced basal NF-κB inhibition may be strongly associated with a lower capacity of CLL cells to respond to BCR stimulation and the survival of anergic CLL cells.

Acknowledgments

The authors would like to thank: Prof. Andre Uitterlinden, Mila Jahmai, Pascal Arp and Joost Verlouw (HuGeF laboratory, Dept. of Internal Medicine, Erasmus MC) for RNA-sequencing our samples and for the alignment and annotation of the raw data; Prof. Hassan Jumaa and Marcus Dühren-von Minden (Dept. of Molecular Immunology, Biology III, Faculty of Biology, Albert-Ludwigs University, Freiburgny) for helping with the TKO experiments which were performed in their department; Odilia Corneth (Dept. of Pulmonary Diseases, Erasmus MC) for her help in optimizing the Phosphoflow experiments; Larry Mansouri (Dept. of Immunology, Genetics and Pathology, Uppsala University) for sharing information regarding the protocol used for NFKBIE sequencing; and Jorn Assmann (Dept. of Immunology, Erasmus MC) for technical assistance.

AFM was awarded with an EMBO Short Term Fellowship, a Dutch Society for Immunology (NVVI) grant, and an Erasmus Trust Fund grant. This work was financially supported by an unrestricted research grant from F. Hoffmann-La Roche (Basel, Switzerland) to AWL.

References

1. Chiorazzi N, Rai KR, Ferrarini M. Chronic lymphocytic leukemia. N Engl J Med. 2005;352(8):804-815.
2. Damle RN, Wasil T, Fais F, et al. Ig V gene mutation status and CD38 expression as novel prognostic indicators in chronic lymphocytic leukemia. Blood. 1999;94(6):1840-1847.
3. Hamblin TJ, Davis Z, Gardiner A, Oscier DG, Stevenson FK. Unmutated Ig V(H) genes are associated with a more aggressive form of chronic lymphocytic leukemia. Blood. 1999;94(6):1848-1854.
4. Agathangelidis A, Darzentas N, Hadzidimitriou A, et al. Stereotyped B-cell receptors in one-third of chronic lymphocytic leukemia: a molecular classification with implications for targeted therapies. Blood. 2012;119(19):4467-4475.
5. Catera R, Silverman GJ, Hatzi K, et al. Chronic lymphocytic leukemia cells recognize conserved epitopes associated with apoptosis and oxidation. Mol Med. 2008;14(11-12):665-674.
6. Chu CC, Catera R, Zhang L, et al. Many chronic lymphocytic leukemia antibodies recognize apoptotic cells with exposed nonmuscle myosin heavy chain IIA: implications for patient outcome and cell of origin. Blood. 2010;115(19):3907-3915.
7. Herve M, Xu K, Ng YS, et al. Unmutated and mutated chronic lymphocytic leukemias derive from self-reactive B cell precursors despite expressing different antibody reactivity. J Clin Invest. 2005;115(6):1636-1643.
8. Lanemo Myhrinder A, Hellqvist E, Sidorova E, et al. A new perspective: molecular motifs on oxidized LDL, apoptotic cells, and bacteria are targets for chronic lymphocytic leukemia antibodies. Blood. 2008;111(7):3838-3848.
9. Ghia EM, Widhopf GF 2nd, Rassenti LZ, Kipps TJ. Analyses of recombinant stereotypic IGHV3-21-encoded antibodies expressed in chronic lymphocytic leukemia. J Immunol. 2011;186(11):6338-6344.
10. Hoogeboom R, van Kessel KP, Hochstenbach F, et al. A mutated B cell chronic lymphocytic leukemia subset that recognizes and responds to fungi. J Exp Med. 2013;210(1):59-70.
11. Hoogeboom R, Wormhoudt TA, Schipperus MR, et al. A novel chronic lymphocytic leukemia subset expressing mutated IGHV3-7-encoded rheumatoid factor B-cell receptors that are functionally proficient. Leukemia. 2013;27(3):738-740.
12. Kostareli E, Gounari M, Janus A, et al. Antigen receptor stereotypy across B-cell lymphoproliferations: the case of IGHV4-59/IGKV3-20 receptors with rheumatoid factor activity. Leukemia. 2012;26(5):1127-1131.
13. Zwick C, Fadle N, Regitz E, et al. Autoantigenic targets of B-cell receptors derived from chronic lymphocytic leukemias bind to and induce proliferation of leukemic cells. Blood. 2013;121(23):4708-4717.
14. Duhren-von Minden M, Ubelhart R, Schneider D, et al. Chronic lymphocytic leukaemia is driven by antigen-independent cell-autonomous signalling. Nature. 2012;489(7415):309-312.
15. Muggen AF, Pillai SY, Kil LP, et al. Basal Ca(2+) signaling is particularly increased in mutated chronic lymphocytic leukemia. Leukemia. 2015;29(2):321-328.
16. Gauld SB, Benschop RJ, Merrell KT, Cambier JC. Maintenance of B cell anergy requires constant antigen receptor occupancy and signaling. Nat Immunol. 2005;6(11):1160-1167.
17. Apollonio B, Scielzo C, Bertilaccio MT, et al. Targeting B-cell anergy in chronic lymphocytic leukemia. Blood. 2013;121(19):3879-3888, S3871-3878.
18. Mockridge CI, Potter KN, Wheatley I, Neville LA, Packham G, Stevenson FK. Reversible anergy of sIgM-mediated signaling in the two subsets of CLL defined by VH-gene mutational status. Blood. 2007;109(10):4424-4431.
19. Lanham S, Hamblin T, Oscier D, Ibbotson R, Stevenson F, Packham G. Differential signaling via surface IgM is associated with VH gene mutational status and CD38 expression in chronic lymphocytic leukemia. Blood. 2003;101(3):1087-1093.
20. D'Avola A, Drennan S, Tracy I, et al. Surface IgM expression and function are associated with clinical behavior, genetic abnormalities, and DNA methylation in CLL. Blood. 2016;128(6):816-826.
21. Meixlsperger S, Kohler F, Wossning T, Reppel M, Muschen M, Jumaa H. Conventional light chains inhibit the autonomous signaling capacity of the B cell receptor. Immunity. 2007;26(3):323-333.
22. Jost PJ, Ruland J. Aberrant NF-kappaB signaling in lymphoma: mechanisms, consequences, and therapeutic implications. Blood. 2007;109(7):2700-2707.
23. Mansouri L, Sutton LA, Ljungstrom V, et al. Functional loss of IkappaBepsilon leads to NF-kappaB deregulation in aggressive chronic lymphocytic leukemia. J Exp Med. 2015;212(6):833-843.
24. Verstrepen L, Verhelst K, van Loo G, Carpentier I, Ley SC, Beyaert R. Expression, biological activities and mechanisms of action of A20 (TNFAIP3). Biochem Pharmacol. 2010;80(12):2009-2020.
25. Isnardi I, Ng YS, Menard L, et al. Complement receptor 2/CD21- human naive B cells contain mostly autoreactive unresponsive clones. Blood. 2010;115(24):5026-5036.
26. Saadoun D, Terrier B, Bannock J, et al. Expansion of autoreactive unresponsive CD21-/low B cells in Sjogren's syndrome-associated lymphoproliferation. Arthritis Rheum. 2013;65(4):1085-1096.
27. Nichols EM, Jones R, Watson R, Pepper CJ, Fegan C, Marchbank KJ. A CD21 low phenotype, with no evidence of autoantibodies to complement proteins, is consistent with a poor prognosis in CLL. Oncotarget. 2015;6(32):32669-32680.
28. Furman RR, Asgary Z, Mascarenhas JO, Liou HC, Schattner EJ. Modulation of NF-kappa B activity and apoptosis in chronic

lymphocytic leukemia B cells. J Immunol. 2000;164(4):2200-2206.
29. Cuni S, Perez-Aciego P, Perez-Chacon G, et al. A sustained activation of PI3K/NF-kappaB pathway is critical for the survival of chronic lymphocytic leukemia B cells. Leukemia. 2004;18(8):1391-1400.
30. Yu M, Chen Y, He Y, et al. Critical role of B cell lymphoma 10 in BAFF-regulated NF-kappaB activation and survival of anergic B cells. J Immunol. 2012;189(11):5185-5193.
31. Gasparini C, Celeghini C, Monasta L, Zauli G. NF-kappaB pathways in hematological malignancies. Cell Mol Life Sci. 2014;71(11):2083-2102.
32. Alves BN, Tsui R, Almaden J, et al. IkappaBepsilon is a key regulator of B cell expansion by providing negative feedback on cRel and RelA in a stimulus-specific manner. J Immunol. 2014;192(7):3121-3132.
33. Domenech E, Gomez-Lopez G, Gzlez-Pena D, et al. New mutations in chronic lymphocytic leukemia identified by target enrichment and deep sequencing. PLoS One. 2012;7(6):e38158.
34. Mansouri L, Noerenberg D, Young E, et al. Frequent NFKBIE deletions are associated with poor outcome in primary mediastinal B-cell lymphoma. Blood. 2016;128(23):2666-2670.
35. Feuerhake F, Kutok JL, Monti S, et al. NFkappaB activity, function, and target-gene signatures in primary mediastinal large B-cell lymphoma and diffuse large B-cell lymphoma subtypes. Blood. 2005;106(4):1392-1399.
36. Foa R, Massaia M, Cardona S, et al. Production of tumor necrosis factor-alpha by B-cell chronic lymphocytic leukemia cells: a possible regulatory role of TNF in the progression of the disease. Blood. 1990;76(2):393-400.
37. Das T, Chen Z, Hendriks RW, Kool M. A20/tumor necrosis factor alpha-induced protein 3 in immune cells controls development of autoinflammation and autoimmunity: lessons from mouse models. Front Immunol. 2018;9:104.
38. Chu Y, Vahl JC, Kumar D, et al. B cells lacking the tumor suppressor TNFAIP3/A20 display impaired differentiation and hyperactivation and cause inflammation and autoimmunity in aged mice. Blood. 2011;117(7):2227-2236.
39. Frenzel LP, Claus R, Plume N, et al. Sustained NF-kappaB activity in chronic lymphocytic leukemia is independent of genetic and epigenetic alterations in the TNFAIP3 (A20) locus. Int J Cancer. 2011;128(10):2495-2500.
40. Nechanitzky R, Akbas D, Scherer S, et al. Transcription factor EBF1 is essential for the maintenance of B cell identity and prevention of alternative fates in committed cells. Nat Immunol. 2013;14(8):867-875.
41. Seifert M, Sellmann L, Bloehdorn J, et al. Cellular origin and pathophysiology of chronic lymphocytic leukemia. J Exp Med. 2012;209(12):2183-2198.

ARTICLE

Outcome of paraosseous extra-medullary disease in newly diagnosed multiple myeloma patients treated with new drugs

Vittorio Montefusco,[1] Francesca Gay,[2] Stefano Spada,[2] Lorenzo De Paoli,[3] Francesco Di Raimondo,[4] Rossella Ribolla,[5] Caterina Musolino,[6] Francesca Patriarca,[7] Pellegrino Musto,[8] Piero Galieni,[9] Stelvio Ballanti,[10] Chiara Nozzoli,[11] Nicola Cascavilla,[12] Dina Ben-Yehuda,[13] Arnon Nagler,[14] Roman Hajek,[15] Massimo Offidani,[16] Anna Marina Liberati,[17] Pieter Sonneveld,[18] Michele Cavo,[19] Paolo Corradini[20] and Mario Boccadoro[2]

[1]Division of Hematology, Fondazione IRCCS Istituto Nazionale dei Tumori, Milano, Italy; [2]Myeloma Unit, Division of Hematology, University of Torino, Azienda Ospedaliero-Universitaria Città della Salute e della Scienza di Torino, Torino, Italy; [3]Division of Hematology, Department of Translational Medicine, Amedeo Avogadro University of Eastern Piedmont and Maggiore Hospital, Novara, Italy; [4]Division of Hematology, Ospedale Ferrarotto, Azienda Policlinico-Ospedale Vittorio Emanuele, University of Catania, Catania, Italy; [5]Department of Hematology, ASST Spedali Civili di Brescia, Brescia, Italy; [6]Division of Haematology, University of Messina, Messina, Italy; [7]DAME, Udine University, Udine, Italy; [8]Hematology and Stem Cell Transplantation Unit, IRCCS-CROB, Referral Cancer Center of Basilicata, Rionero in Vulture, Italy; [9]U.O.C. Ematologia e Trapianto di Cellule Staminali Emopoietiche, Ospedale Mazzoni, Ascoli Piceno, Italy; [10]Sezione di Ematologia e Immunologia Clinica, Ospedale Santa Maria della Misericordia di Perugia, Perugia, Italy; [11]Cellular therapies and Transfusion Medicine Unit, Careggi University Hospital, Firenze, Italy; [12]Department of Hematology and Stem Cell Transplant Unit, Fondazione IRCCS "Casa Sollievo della Sofferenza", San Giovanni Rotondo, Italy; [13]Division of Hematology, Hadassah Ein-Kerem Medical Center, Jerusalem, Israel; [14]Hematology Division, Chaim Sheba Medical Center, Tel-HaShomer, Israel; [15]Department of Haematooncology, University Hospital Ostrava, Ostrava, Czech Republic and Faculty of Medicine, Ostrava University, Ostrava, Czech Republic; [16]Division of Hematology, Ospedali Riuniti, Ancona, Italy; [17]A O S Maria di Terni, S C Oncoematologia, Terni, Italy; [18]Department of Hematology, Erasmus University Medical Center, Rotterdam, the Netherlands; [19]Institute of Hematology "L. and A. Seràgnoli", Department of Experimental, Diagnostic and Specialty Medicine, University of Bologna, "S. Orsola-Malpighi" Hospital, Bologna, Italy and [20]Hemato-Oncology Department, University of Milan, Division of Hematology, Fondazione IRCCS Istituto Nazionale dei Tumori, Milano, Italy

Ferrata Storti Foundation

Haematologica 2020
Volume 105(1):193-200

ABSTRACT

Extramedullary disease is relatively frequent in multiple myeloma, but our knowledge on the subject is limited and mainly relies on small case series or single center experiences. Little is known regarding the role of new drugs in this setting. We performed a meta-analysis of eight trials focused on the description of extramedullary disease characteristics, clinical outcome, and response to new drugs. A total of 2,332 newly diagnosed myeloma patients have been included; 267 (11.4%) had extramedullary disease, defined as paraosseous in 243 (10.4%), extramedullary plasmocytoma in 12 (0.5%), and not classified in 12 (0.5%) patients. Median progression-free survival was 25.3 months and 25.2 in extramedullary disease and non-extramedullary disease patients, respectively. In multivariate analysis the presence of extramedullary disease did not impact on progression-free survival (hazard ratio 1.15, P=0.06), while other known prognostic factors retained their significance. Patients treated with immunomodulatory drugs, mainly lenalidomide, or proteasome inhibitors had similar progression-free survival and progression-free survival-2 regardless of extramedullary disease presence. Median overall survival was 63.5 months and 79.9 months (P=0.01) in extramedullary and non-extramedullary disease patients, respectively, and in multivariate analysis the presence of extramedullary disease was associated with a reduced overall survival (hazard ratio 1.41, P<0.001), in line with other prognostic factors. With the limits of the use of low sensitivity imaging techniques, that lead to an underestimation of extramedullary disease, we conclude that in patients treated with new drugs the detrimental effect of extramedullary disease at diagnosis is limited, that lenalidomide is effective as are proteasome inhibitors, and that these patients tend to acquire a more aggressive disease in later stages. (EUDRACT2005-004714-32, NCT01063179. NCT00551928, NCT01091831, NCT01093196, NCT01190787, NCT01346787, NCT01857115).

Correspondence:

VITTORIO MONTEFUSCO
vittorio.montefusco@istitutotumori.mi.it

Received: February 13, 2019.

Accepted: June 19, 2019.

Pre-published: June 20, 2019.

doi:10.3324/haematol.2019.219139

Check the online version for the most updated information on this article, online supplements, and information on authorship & disclosures: www.haematologica.org/content/105/1/193

Introduction

Multiple myeloma (MM) is a plasma cell neoplasia characterized by a diffuse tumor infiltration of the bone marrow, resulting, among others, in anemia, bone damage with hypercalcemia, and bone lesions. Occasionally, neoplastic plasma cells acquire a different growth pattern generating tumor masses, that are referred to as extramedullary disease (EMD).[1] EMD can arise from skeletal focal lesions, which disrupt the cortical bone and grow as extra-bone masses, and is referred to as paraosseous plasmocytoma (PO), or derive from hematogenous spread as manifestation in soft tissues, and is called extramedullary plasmocytomas (EMP). Incidence of EMD at diagnosis ranges between 6% and 10%,[2-4] while later in the course of the disease this increases to 13%-26%,[2,4] with a 32-35% peak in case of relapse after allogeneic stem cell transplantation.[5,6] In the final stage of the disease, an extraskeletal involvement is observed in approximately 70% of cases studied with autopsy,[7] with a peculiar involvement of visceral sites.[8] As expected, patients with EMD at diagnosis tend to maintain the same pattern at relapse.[2]

The biological mechanisms behind the acquisition of the EMD-forming phenotype have not yet been fully elucidated. Increased expression of CXCR4 and CXCL12 plays a major role in promoting a bone marrow-independent behavior, favoring dissemination, and homing to distant and unusual sites.[9,10] Other mechanisms are represented by reduced expression of several adhesion molecules, in particular VLA-4, CD44, and CD56, and chemokine receptors, such as CCR1, and CCR2. Diversely, the cyclin D1 pathway seems to favor the bone marrow homing, protecting from extramedullary localizations, as t(11;14) is not observed in MM patients with EMD.[11]

Despite its frequency and clinical relevance, EMD has often been neglected by the medical literature. In fact, almost all the available data derive from retrospective series and single center experiences, mainly reported in the pre-new drug era, with the limitations of this type of studies. In order to fill this gap and clarify the role of new drugs in MM with EMD, we conducted the largest meta-analysis so far reported, based on eight prospective trials by the same sponsors (Fonesa Onlus and Hovon Foundation).

Methods

Study design

Patients with newly diagnosed MM enrolled in eight clinical trials were retrospectively analyzed. Details on trials and treatment regimens are summarized in Table 1. Briefly, three trials enrolled transplant eligible and five trials transplant ineligible patients. Three trials included an immunomodulatory (IMiD) drug in the treatment, lenalidomide in almost all cases, three trials a proteasome inhibitor (PI), and four trials both. Six out of eight trials included maintenance. Trials were approved by the Independent Ethics Committees/Institutional Review Boards at all participating centers. Patients provided written informed consent before entering the study, prepared in accordance with the Declaration of Helsinki. For the purpose of this meta-analysis, we considered the subgroup of patients with EMD, and compared them with patients without EMD.

Extramedullary disease definition and assessment

Extramedullary disease was classified as PO disease, consisting of tumor masses arising directly from bones, or EMP, consisting of masses not contiguous to the bones and derived from hematogenous spread. EMD was identified at study enrollment with the diagnostic procedure required by the patient's study protocol, such as X-ray skeletal survey, magnetic resonance imaging (MRI), computed tomography (CT), and physical examination.

Statistical analysis

Differences in patients' and disease characteristics for EMD patients *versus* non-EMD patients were investigated using Kruskal Wallis test for continuous variables and Fisher's exact test for categorical variables. Data of trials were pooled together and analyzed. Time-to-event data were analyzed using the Kaplan-Meier method; EMD and non-EMD patients were compared with the log-rank test. The Cox proportional hazards models were used to estimate adjusted hazard ratios (HRs) and the 95% confidence intervals (CI) for the main comparisons, EMD patients *versus* non-EMD patients. To account for potential confounders, the Cox models were adjusted for the age, sex, International Staging System (ISS) stage (I *vs.* II; I vs. III), cytogenetic risk defined by fluorescence *in situ* hybridization (FISH) analysis [high, i.e. presence of del(17p), t(4;14), t(14;16), *vs.* standard risk; missing *vs.* standard risk], and autologous stem cell transplantation (ASCT) (ASCT *vs.* non-ASCT; not applicable, i.e. patients not candidate to ASCT, *vs.* non-ASCT). Subgroup analyses were performed to determine the consistency of the overall effect in different subgroups using interaction terms for the comparison between EMD *versus* non-EMD and each of the co-variates included in the Cox model plus Revised ISS stage (RISS) and type of therapies (IMID and PI). All Hazard Ratios (HR) were estimated with their 95%CI and two sided *P*-values. In order to evaluate the impact of different size and types of EMD, further subgroup analyses were performed: EMD size ≤ 3 > 3 cm; EMD size ≤ 5 *vs.* > 5 cm; PO or EMP. Data were analyzed as of December 2018 using and R (Version 3.1.1).

Results

Patients

A total of 2,332 patients were included in this analysis: 267 (11%) had EMD, while 2,065 (89%) had no EMD. Median age of EMD patients was 68 years (IQ range 60-74), and 69 years (IQ range 61-74) in patients without EMD. International Staging System was I in 119 (45%) and 682 (33%), II in 85 (32%) and 782 (38%), and III in 38 (14%) and 509 (25%) patients with or without EMD, respectively. Clinical trials were based on IMiD in 166 (62%) and 1,279 (62%) patients, on a PI in 66 (25%) and 464 (22%) patients, or both in 35 (13%) and 322 (16%) patients with or without EMD, respectively. Patients' characteristics are summarized in Table 2. Patients with EMD had PO in 243 (91%), and an EMP in 12 (4%) cases, while the information was not available for the other 12 (4%) patients. EMD localizations were single in 195 (73%), and multiple in 60 (22%) patients. Median EMD size was 4.2 cm (IQ range 3-7). EMD characteristics are summarized in Table 3. No differences were observed in patients with EMD ≤ or > 3 cm. EMD patients had a lower systemic tumor burden with respect to patients without EMD, as shown by: plasma cell bone marrow infiltration 30% (IQ range 15-50%) *versus* 50% (IQ range

Table 1. Source studies.

Trial	Code	Treatment	Drugs	Maintenance	N. of Patients	Years enrollement	Age population	Outcome PFS	Outcome OS	Pubblication year(s)
GIMEMA-MM-05-05[28]	2005-004714-32	4 PAD induction followed by 2 Mel100 intensification followed by 4 RP consolidation and R maintenance	IMiD-PI	Yes	103	2005-2008	≤75	Median PFS: 48 months	5yrs OS: 63%	2010-2013
GIMEMA-MM-03-05[29]	NCT01063179	9 VMP induction or 9 VMPT induction followed by 2 years VT maintenance	IMiD-PI	Random for FDT or observation	511	2006-2009	≥65	Median PFS: VMPT-VT: 35 months VMP: 25 months	5yrs OS: VMPT-VT: 61% VMP:51%	2010-2014
RV-MM-PI-209[30]	NCT00551928	4 Rd induction, mobilization, 6 MPR or 2 Mel200 intensification followed by R maintenance until PD or observation	PI	Random for maintenance or observation	402	2007-2009	<65	Median PFS: MPR: 22 months ASCT: 43 months	4yrs OS: MPR: 65% ASCT: 81%	2014
RV-MM-EMN-441[31]	NCT01091831	4 Rd induction, mobilization, 6 CPR or 2 Mel200 intensification followed by RP or R maintenance until PD	IMiD	Yes	389	2009-2011	<65	Median PFS: CRD: 29 months ASCT: 43 months	4yrs OS: CRD: 73% ASCT: 86%	2015
EMN01[32]	NCT01093196	9 Rd or MPR or CPR induction followed by RP or R maintenance until PD	IMiD	Yes	654	2009-2012	≥65	Median PFS: MPR: 24 months CPR: 20 months Rd: 21 months	4yrs OS: MPR: 65% CPR: 68% Rd: 58%	2016
MMY2069[33]	NCT01190787	9 VP or CVP or VMP induction followed by V maintenance until PD	PI	Yes	152	2010-2012	≥65	Median PFS: VP: 14 months VCP: 15 months VMP: 17 months	2yrs OS: VP: 60% VCP: 70% VMP: 76%	2016
IST-CAR-506[34]	NCT01346787	9 KCd induction followed by K maintenance until PD	PI	Yes	58	2011-2012	≥65	2yrs PFS: 76%,	2yrs OS: 87%	2014
IST-CAR-561[35]	NCT01857115	9 KCd induction followed by K maintenance until PD	PI	Yes	63	2013-2015	≥65	2yrs PFS: 53%,	2yrs OS: 81%	2018

V: bortezomib; M: melphalan; P: prednisone; T: thalidomide; C: cyclophosphamide; K: carfilzomib; R: lenalidomide; d: dexamethasone; Mel200: high-dose melphalan; PAD: bortezomib-pegylated liposomal doxorubicin -dexamethasone; PD: progression disease; IMiD: immunomodulatory drug; PI: proteasome inhibitor; PFS: progression-free survival; OS: overall survival; FDT: fixed-duration therapy; yrs: years.

30-70%), hemoglobin 12.0 gr/L (IQ range 10.5-13.6) *versus* 10.7 gr/L (IQ range 9.5-12.1), median creatinine clearance 75 mL/min per 1.73 m2 (IQ range 48-98) *versus* 66 (IQ range 41-88), respectively. EMD patients had ISS I stage in 45% of cases, compared to 33% in non-EMD patients (P<0.001).

Efficacy

Progression-free survival. The median follow up was 62 months (IQ range 34-75) in EMD, and 65 months (IQ range 40-77) in non-EMD patients. Median PFS was 25.3 months (95%CI: 21.7-28.7) and 25.2 months (95%CI: 24.2-27.0) in EMD and non-EMD patients, respectively. Five-year PFS was 19% (95%CI: 15-25%) and 22% (95%CI: 20-24%) (P=0.46) in EMD and non-EMD patients, respectively (*Online Supplementary Figure S1*), and there were no differences between EMP, PO, and non-EMD (Figure 1A). In multivariate analysis the presence of EMD did not impact on PFS (HR 1.15, 95%CI: 0.99-1.33; P=0.06), while other known prognostic factors retained their significance: high risk *versus* standard cytogenetic (HR 1.35, 95%CI: 1.20-1.52; P<0.001), and ISS III *versus* I (HR 1.74, 95%CI: 1.53-1.98; P<0.001) (*Online Supplementary Figure S2*). Type of therapy had no impact on PFS: IMiD-based therapy (HR 1.14, 95%CI: 0.96-1.35) and no IMiD (HR 1.18, 95%CI: 0.87-1.59) (interaction P=0.86), PI-based therapy (HR 1.33, 95%CI: 1.04-1.71) and no PI, (HR 1.04, 95%CI: 0.87-1.25) (interaction P=0.12), and ASCT in eligible patients (HR 1.10, 95%CI: 0.81-1.50) and non-ASCT (HR 1.04, 95%CI: 0.73-1.47) (interaction P=0.72). A landmark analysis from maintenance start showed a median PFS of 23.4 months (95%CI: 19.1-30.1) and 23.5 months (95%CI: 21.8-25.7) (P=0.30) in EMD and non-EMD patients, respectively. EMD size was not correlated with median PFS: patients with EMD ≤3 cm 26.0 months (95%CI: 18.5-37.1), patients with EMD >3 cm 23.7 months (95%CI: 18.8-28.2), and patients without EMD 25.2 months (95%CI: 24.2-27.0) (Figure 2). The same results were observed with the EMD size threshold at 5 cm (*Online Supplementary Figure S3*). Median PFS according to EMD number was as follows: single EMD localization 26.1 months (95%CI: 22.5-30.1), multiple EMD localizations 19.4 months (95%CI: 14.9-33.1), and no EMD 25.2 months (95%CI: 24.2-27.0). Median PFS was not correlated with EMD site: PO 24.3 months (95%CI: 21.2-28.2), EMP 26.1 months (95%CI: 8.0-NR), and no EMD 25.2 months (95%CI: 24.2-27.0), PO *versus* no EMD (HR 1.14, 95%CI: 0.98-1.33; P=0.10), and EMP *versus* no EMD (HR

1.23, 95%CI: 0.64-2.37; *P*=0.54) (Figure 1A). Median PFS2 and 5-year PFS2 were 43.2 months (95%CI: 37.0-52.4) and 38% (95%CI: 31-47%) in PO, 27.9 months (95%CI: 4.9-NR) and NR in EMP, and 46.4 months (95%CI: 44.1-48.9) and 40% (95%CI: 37-43%) in non-EMD patients (Figure 3).

Overall survival. Median OS was 63.5 months (95%CI: 48.2-84.7) and 79.9 months (95%CI: 75.8-88.3; *P*=0.01) in EMD and non-EMD patients, respectively. Five-year OS was 51% (95%CI: 45-58%) and 59% (95%CI: 57-61%) (*P*=0.01) in EMD and non-EMD patients, respectively (*Online Supplementary Figure S4*), and there was a significant difference between PO and non-EMD (HR 1.39, 95%CI: 1.13-1.70; *P*=0.001) (Figure 1B). In multivariate analysis the presence of EMD was associated with a reduced OS (HR 1.41, 95%CI: 1.16-1.71; *P*<0.001), in line with other known prognostic factors: high risk *versus* standard cytogenetic (HR 1.68, 95%CI: 1.44-1.96; *P*<0.001), ISS III *versus* I (HR 2.36, 95%CI: 1.98-2.82; *P*<0.001) (*Online Supplementary Figure S5*). Type of therapy did not impact on OS: IMiD-based therapy (HR 1.38, 95%CI: 1.10-1.73) and no IMiD (HR 1.47, 95%CI: 1.01-2.13) (interaction *P*=0.78), PI-based therapy (HR 1.43, 95%CI: 1.04-1.97) and no PI, (HR 1.39, 95%CI: 1.09-1.76) (interaction *P*=0.87), and ASCT in eligible patients (HR 1.45, 95%CI: 0.95-2.20) and non-ASCT (HR 1.40, 95%CI: 0.88-2.25) (interaction *P*=0.99). A landmark analysis by maintenance start showed a median OS of 69.1 months (95%CI: 64.6-NR) and 87.8 months (95%CI: 87.8-NR) (*P*=0.22) in EMD and non-EMD patients, respectively. EMD size was not correlated with median OS: patients with EMD ≤3 cm 58.5 months (95%CI: 38.4-NR), patients with EMD >3 cm 63.7 months (95%CI: 48.2-NR), and patients without EMD 79.9 months (95%CI: 75.8-88.3) (Figure 4). The same analysis was done with the EMD size threshold at 5 cm (*Online Supplementary Figure S6*). Median OS according to EMD number was as follows: single EMD localization 70.1 months (95%CI: 50.4-NR), multiple EMD localizations 45 months (95%CI: 38.2-NR), and no EMD 79.9 months (95%CI: 75.8-88.3), single EMD *versus* no EMD (HR 1.33, 95%CI: 1.07-1.67; *P*=0.01), and multiple EMD localizations *versus* no EMD (HR 1.62, 95%CI: 1.11-2.38; *P*=0.01). Median OS was not correlated with EMD site: PO 67.3 months (95%CI: 50.4-NR), EMP 70.1 months (95%CI: 16.9-NR), and no EMD 79.9 months (95%CI: 75.8-88.3), PO *versus* no EMD (HR 1.39, 95%CI: 1.13-1.70; *P*=0.001), and EMP *versus* no EMD (HR 1.24, 95%CI: 0.55-2.78; *P*=0.60) (Figure 1B).

Discussion

To the best of our knowledge, this is the first meta-analysis of MM clinical trials focusing on patients with EMD so far reported. We included eight Fonesa Onlus and

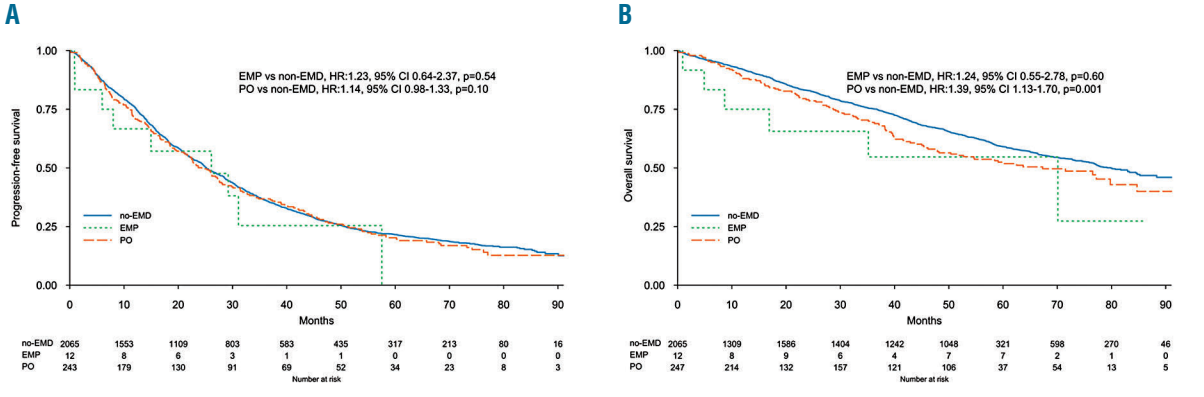

Figure 1. (A) Progression-free survival (PFS) and (B) overall survival (OS) according to extramedullary disease presence and type. EMD: extramedullary disease; EMP: extramedullary plasmocytoma; PO: paraosseous plasmocytoma.

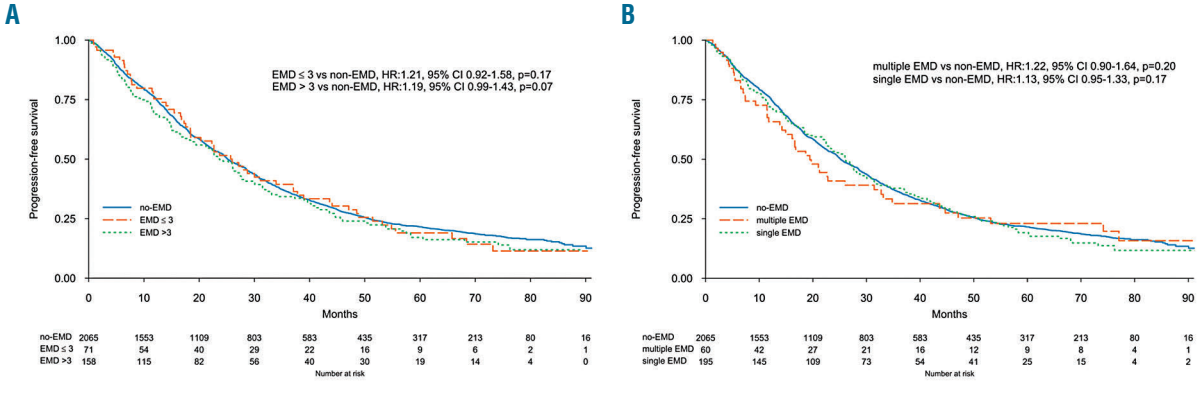

Figure 2. Progression-free survival (PFS) according to extramedullary disease features. (A) PFS according to extramedullary disease (EMD) presence and size. (B) PFS according to single or multiple EMD localizations.

Table 2. Patients' demographics and clinical characteristics.

Characteristic	Patients with extra-medullary disease (N=267)	Control group (N=2065)	*P*
Age			
Median (IQR)-yr	68 (60-74)	69 (61-74)	0.21
Distribution – n. (%)			
<65 yr	108 (40%)	477 (38%)	
65 to 75	105 (39%)	795 (38%)	
≥ 75	54 (21%)	493 (24%)	
ECOG			
0	107 (40%)	847 (41%)	0.35
1	103 (39%)	862 (42%)	
2	39 (15%)	235 (11%)	
3	1 (0%)	7 (0%)	
ISS			
I	119 (45%)	682 (33%)	<0.001
II	85 (32%)	782 (38%)	
III	38 (14%)	509 (25%)	
missing	25 (9%)	92 (4%)	
R-ISS			
I	38 (14%)	294 (14%)	0.62
II	125 (47%)	1132 (55%)	
III	17 (6%)	173 (8%)	
missing	87 (33%)	466 (23%)	
FISH – n. (%)			0.72
Standard risk	115 (43%)	1082 (52%)	
High risk*	51 (19%)	446 (22%)	
del(17p)	32	220	
t(4;14)	22	219	
t(14;16)	6	69	
Missing	101 (38%)	537 (26%)	
LDH – IU/L			0.30
≤450 201	201 (75%)	1567 (76%)	
>450 201	29 (11%)	180 (9%)	
missing	37 (14%)	318 (15%)	
Bone marrow plasma cells, median (IQR)	30% (15% - 50%)	50% (30% - 70%)	<0.001
Hemoglobin, median (IQR) – gr/L	12.0 (10.5 – 13.6)	10.7 (9.5 – 12.1)	<0.001
Creatinine clearance			0.01
Median (IQR) – mL/min per 1.73/m^2	75 (48-98)	66 (41-88)	
< 30 mL/min per 1.73/m^2	45 (17%)	359 (17%)	
30 to 60 mL/min per 1.73/m^2	49 (18%)	544 (26%)	
> 60 mL/min per 1.73/m^2	172 (64%)	1162 (56%)	
Therapy			0.48
IMiD-based	166 (62%)	1279 (62%)	
PI-based	66 (25%)	464 (22%)	
IMiD + PI-based	35 (13%)	322 (16%)	
Autologous stem cell transplantation	155 (58%)	1283 (62%)	0.17
Fixed-duration therapy	31 (12%)	243 (12%)	1.00
Continuous treatment	128 (48%)	1007 (49%)	
No maintenance	108 (40%)	815 (39%)	
Imaging technique			
X-ray skeletal survey	0 (0 %)	989 (42%)	<0.001
CT-scan	0 (0 %)	277 (13 %)	
MRI	115 (43 %)	0 (0 %)	
Physical examination	21 (8 %)	0 (0%)	
Spiral CT	13 (5%)	2 (0%)	
Conventional CT	96 (36%)	675 (33%)	
Unknown	22 (8%)	122 (6 %)	

*More than one fluorescence *in situ* hybridization (FISH) abnormality may occur in the same patient. NS: not significant; NA: not assessable; IQR: interquartile range; IMiD: immunomodulatory drug; PI: proteasome inhibitor; CT: computed tomography; MRI: magnetic resonance imaging. ECOG: Eastern Cooperative Oncology Group.

Hovon Foundation clinical trials that enrolled 2,332 newly diagnosed patients. In this population, we observed 267 (11%) patients with one or more EMD localizations, including 243 PO, 12 EMP, and 12 cases that were not classified. Since none of the clinical trials considered in this study had as primary end point the study of EMD, and a proportion of them were started around ten years ago, the most common imaging procedure performed at enrollment as screening was X-ray skeletal survey, and, only in case of a suspect of EMD, MRI or CT scan. X-ray skeletal survey is clearly suboptimal in detecting extramedullary asymptomatic disease. Nevertheless, the EMD incidence we observed is in line with other case series (in the range of 7-18%),[1] suggesting that our patient population is quite representative of the daily clinical practice. In any case, it is expected that a wider use of more sensitive imaging techniques, such as positron emission tomography (PET), whole-body CT, and MRI will increase EMD detection.[12,13] Interestingly, we observed that EMD patients had less disease burden, as shown by a more favorable ISS, lower bone marrow plasma cell infiltrate, higher hemoglobin levels, and a better renal function. This finding has been observed also by others in the first line setting,[2,14] and may reflect a specific clinical picture, characterized by symptoms attributable to the EMD, rather than to larger disease burden. The presence of EMD at diagnosis did not impair the first line PFS, since EMD patients had a median PFS of 25.3 months, similar to the 25.2 months observed in patients without EMD. This finding is quite remarkable, since presence of EMD has long been recognized as an unfavorable prognostic factor, both in case of PO and EMP.[4] Varettoni *et al*. described 76 EMD patients out of 1,003 MM patients at diagnosis, and with a treatment based on conventional chemotherapy the PFS of EMD was 18 *versus* the 30 months of patients without EMD (P=0.03).[2] Only EMD patients who received an ASCT had a PFS similar to that of patients without EMD. Likewise, Wu *et al*. compared 75 EMD patients at diagnosis with 384 cases without EMD, and observed that EMD patients had an inferior PFS compared to that of patients without EMD, but this difference was overcome when EMD patients received ASCT.[14] Hence, the presence of EMD at diagnosis has been incorporated as an adverse component of the Durie and Salmon PLUS prognostic score.[15] Since we did not observe any significant difference in PFS between EMD and non-EMD patients, it is reasonable to speculate that the incorporation of new drugs in all the regimens tested in the studies included in this meta-analysis was able to overcome the unfavorable prognostic significance of EMD. In this perspective, several case reports, as well as a few trials, have shown that new drugs are effective in MM patients with EMD. In particular, Landau *et al*. have evaluated, in 42 high-risk MM at diagnosis including 14 patients with EMD, an induction with three cycles of bortezomib, liposomal doxorubicin and dexamethasone, followed by ASCT, with an acceptable median time-to-progression of 39 months.[16] In our meta-analysis, 166 EMD patients were treated with IMiD-based therapies (lenalidomide in almost all cases) and have been compared with 1,279 non-EMD patients who received the same treatment. Quite surprisingly, also in this subset there was no difference in PFS between the two groups, suggesting that lenalidomide can be active also in this setting, as suggested by very few case reports.[17] This is in contrast with the observation derived from studies involving thalidomide, the first-in-class IMiD, which resulted in having no effect on EMD,[18] and this may be accounted for by the higher direct cytotoxic effect of lenalidomide respect to thalidomide.[19] Interestingly, in our study EMD patients treated with IMiDs had the same PFS and OS as patients treated with PI (*Online Supplementary Figure S7*).

Previous studies showed that increasing the therapy intensity, i.e. intensifying the treatment with ASCT, overcame the negative prognostic significance of EMD presence.[20] This has been confirmed in a large European Bone Marrow Transplantation registry study that considered 3,744 MM patients, including 353 with EMD, who received ASCT at diagnosis. This study has shown how patients with a single EMD had a similar PFS to patients without EMD.[21] Since intensification seems to be the key to EMD control, it is possible to speculate that new drugs may offer a higher level of treatment intensity than conventional drugs. In the pre-new drug era, this goal was obtained only with ASCT. In order to evaluate whether

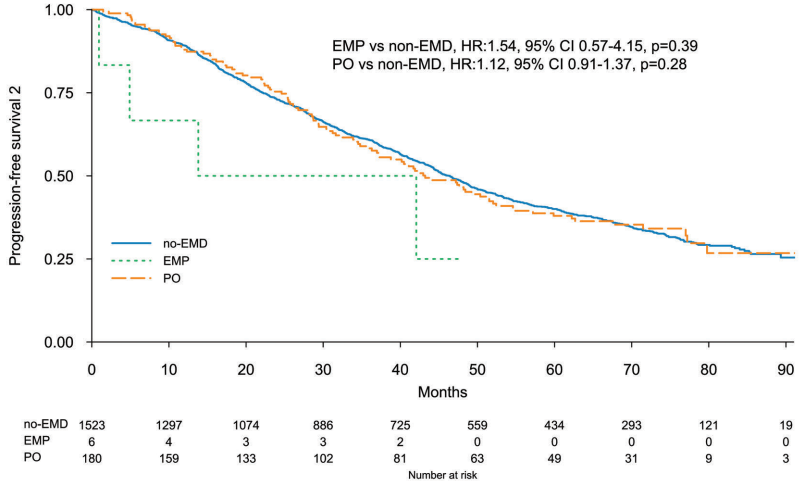

Figure 3. Progression-free survival (PFS2). EMD: extramedullary disease; EMP: extramedullary plasmocytoma; PO: paraosseous plasmocytoma.

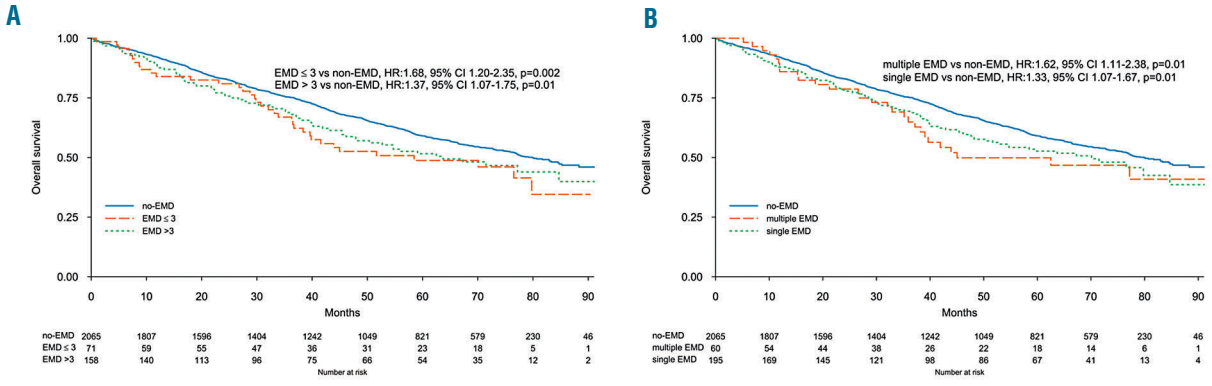

Figure 4. Overall survival (OS) according to extramedullary disease (EMD) features. (A) OS according to EMD presence and size. (B) OS according to single or multiple EMD.

the high efficacy of new drugs results in a more aggressive relapse, we analyzed PFS2, and we observed that EMD patients benefited from a similar disease control when compared to patients without EMD (42.3 *vs.* 46.4 months, respectively). This suggests that patients retain the benefit beyond the first line. Interestingly, also maintenance seems to have a similar efficacy in EMD and non-EMD patients. Median OS of EMD patients was inferior when compared with the control group (63.5 *vs.* 79.9 months, respectively), and this is irrespective of the type of therapy. Since PFS2 is similar between the two groups, it is safe to suggest that MM with EMD may acquire a more aggressive behavior in later stages of the disease.

Doubtless, the most sensitive technique for plasmacytoma identification is PET, which is able to upgrade myeloma-related lesion identification in more than half of patients when compared with X-ray skeletal survey.[22] Unfortunately, in our study, PET was not used, since, at the time the trials were performed, this was not a standard technique. The recent IMAJEM trial, by the Intergroupe Francophone du Myelome (IFM), has shown that spine and pelvis MRI and PET are positive in 95% and 91% of patients at diagnosis, respectively, and that PET has a strong prognostic significance in terms of PFS and OS when evaluated both after the induction phase, represented by three cycles of lenalidomide plus bortezomib plus dexamethasone, and before maintenance start.[23] Moreover, the IFM trial has shown that patients with EMD, evaluated with PET at diagnosis, have an increased risk of EMP relapse, progression or death (HR 3.4, 95%CI: 2.1-5.6; P<0.01). These data reinforce the concept that EMP has a strong detrimental effect on survival, but a specific analysis on the clinical significance of PO disease was not provided.

Surprisingly, we did not find any significant correlation between outcome and EMD size. A similar finding has been reported in the setting of solitary EMD. Eighty-four patients have been evaluated and no differences in terms of outcome have been seen between patients with EMD ≤5 cm, >5 and ≤10 cm, and >10 cm.[24] Probably, the presence of a EMD is detrimental for the relevant biological features that are inherent in this variant of plasma cell neoplasm, rather than EMD size.[25] Also the presence of single or multiple EMD localizations was not prognostically significant. Unfortunately, in our study, EMD was mainly represented by PO disease, since many EMP were probably missed due to the imaging techniques used at the time of trial design. Our observations are in contrast with the study by Rasche *et al.*,[26] who evaluated with diffusion-weighted MRI 404 transplant-eligible patients and showed that the presence of three or more large focal lesions, defined as lesions with a product of the perpendicular diameters >5 cm^2, were strong independent adverse prognostic factors. A possible explanation for this inconsistency can be attributed to the fact that Rasche *et al.* considered all types of focal lesions, including intraosseous focal lesions, while in our study we only analyzed EMD. Finally, we did not observe any significant correlation between EMP and outcome, but this is probably due to the limited number of cases observed in this study.

In conclusion, the main limitation of out study is an underestimation of EMD and, in particular, EMP incidence, caused by the low resolution of the imaging techniques employed at screening. Thus, our findings can be mainly referable to PO localizations, which are known to be less aggressive than EMP;[27] this limits the value of our results. On the other hand, we performed the largest

Table 3. Extramedullary disease characteristics.

Characteristic	N. patients=267
Size, median (IQR)-cm	4.2 (3-7)
Para-skeletal	243 (91%)
Extramedullary plasmocytoma	12 (4.5%)
Not classifiable	12 (4.5%)
Single	195 (73%)
Multiple	60 (22%)
Not classifiable	12 (5%)
Involvement sites*§	
Pelvis	38
Skull	10
Spine	117
Thorax (excluding dorsal spine)	67
Long bones	14
Not classifiable	34

*Sites of extramedullary disease (EMD) localizations were not available. §The sum of the sites is greater than the total number of EMD patients, since one patient could present with more than one localization.

analysis of EMD patients at diagnosis, with the strength of using solid data derived from prospective trials. We confirmed that PI are effective towards EMD, and, for the first time, we provide evidence that also lenalidomide is effective in this difficult setting. We hope that our and other similar studies will draw attention to this unmet clinical need with trials specifically designed for MM patients with EMD.

Acknowledgments

The authors thank Anna De Filippo for assistance in formatting the paper.

References

1. Blade J, Fernandez de Larrea C, Rosinol L, Cibeira MT, Jimenez R, Powles R. Soft-tissue plasmacytomas in multiple myeloma: incidence, mechanisms of extramedullary spread, and treatment approach. J Clin Oncol. 2011;29(28):3805-3812.
2. Varettoni M, Corso A, Pica G, Mangiacavalli S, Pascutto C, Lazzarino M. Incidence, presenting features and outcome of extramedullary disease in multiple myeloma: a longitudinal study on 1003 consecutive patients. Ann Oncol. 2010; 21(2):325-330.
3. Zamagni E, Patriarca F, Nanni C, et al. Prognostic relevance of 18-F FDG PET/CT in newly diagnosed multiple myeloma patients treated with up-front autologous transplantation. Blood. 2011;118(23):5989-5995.
4. Pour L, Sevcikova S, Greslikova H, et al. Soft-tissue extramedullary multiple myeloma prognosis is significantly worse in comparison to bone-related extramedullary relapse. Haematologica. 2014;99(2):360-364.
5. Minnema MC, van de Donk NW, Zweegman S, et al. Extramedullary relapses after allogeneic non-myeloablative stem cell transplantation in multiple myeloma patients do not negatively affect treatment outcome. Bone Marrow Transplant. 2008; 41(9):779-784.
6. Perez-Simon JA, Sureda A, Fernandez-Aviles F, et al. Reduced-intensity conditioning allogeneic transplantation is associated with a high incidence of extramedullary relapses in multiple myeloma patients. Leukemia. 2006;20(3):542-545.
7. Pasmantier MW, Azar HA. Extraskeletal spread in multiple plasma cell myeloma. A review of 57 autopsied cases. Cancer. 1969;23(1):167-174.
8. Thomas FB, Clausen KP, Greenberger NJ. Liver disease in multiple myeloma. Arch Intern Med. 1973;132(2):195-202.
9. Roccaro AM, Mishima Y, Sacco A, et al. CXCR4 Regulates Extra-Medullary Myeloma through Epithelial-Mesenchymal-Transition-like Transcriptional Activation. Cell Rep. 2015; 12(4):622-635.
10. Besse L, Sedlarikova L, Greslikova H, et al. Cytogenetics in multiple myeloma patients progressing into extramedullary disease. Eur J Haematol. 2016;97(1):93-100.
11. Bink K, Haralambieva E, Kremer M, et al. Primary extramedullary plasmacytoma: similarities with and differences from multiple myeloma revealed by interphase cytogenetics. Haematologica. 2008;93(4):623-626.
12. Hillengass J, Moulopoulos LA, Delorme S, et al. Whole-body computed tomography versus conventional skeletal survey in patients with multiple myeloma: a study of the International Myeloma Working Group. Blood Cancer J. 2017;7(8):e599.
13. Cavo M, Terpos E, Nanni C, et al. Role of (18)F-FDG PET/CT in the diagnosis and management of multiple myeloma and other plasma cell disorders: a consensus statement by the International Myeloma Working Group. Lancet Oncol. 2017; 18(4):e206-e217.
14. Wu P, Davies FE, Boyd K, et al. The impact of extramedullary disease at presentation on the outcome of myeloma. Leuk Lymphoma. 2009;50(2):230-235.
15. Durie BG. The role of anatomic and functional staging in myeloma: description of Durie/Salmon plus staging system. Eur J Cancer. 2006;42(11):1539-1543.
16. Landau H, Pandit-Taskar N, Hassoun H, et al. Bortezomib, liposomal doxorubicin and dexamethasone followed by thalidomide and dexamethasone is an effective treatment for patients with newly diagnosed multiple myeloma with Internatinal Staging System stage II or III, or extramedullary disease. Leuk Lymphoma. 2012;53(2):275-281.
17. Masárová K, Stefanikova Z, Mistrik M, Batorova A. Effectiveness of lenalidomide and dexamethasone for the treatment of extramedullary plasmacytoma in patients with multiple myeloma: Report of two cases. Blood. 2014;124(21):5760.
18. Rosinol L, Cibeira MT, Blade J, et al. Extramedullary multiple myeloma escapes the effect of thalidomide. Haematologica. 2004;89(7):832-836.
19. Kotla V, Goel S, Nischal S, et al. Mechanism of action of lenalidomide in hematological malignancies. J Hematol Oncol. 2009;2:36.
20. Touzeau C, Moreau P. How I treat extramedullary myeloma. Blood. 2016; 127(8):971-976.
21. Gagelmann N, Eikema DJ, Iacobelli S, et al. Impact of extramedullary disease in patients with newly diagnosed multiple myeloma undergoing autologous stem cell transplantation: a study from the Chronic Malignancies Working Party of the EBMT. Haematologica. 2018;103(5):890-897.
22. Zamagni E, Nanni C, Patriarca F, et al. A prospective comparison of 18F-fluorodeoxyglucose positron emission tomography-computed tomography, magnetic resonance imaging and whole-body planar radiographs in the assessment of bone disease in newly diagnosed multiple myeloma. Haematologica. 2007;92(1):50-55.
23. Moreau P, Attal M, Caillot D, et al. Prospective evaluation of magnetic resonance imaging and [18F]fluorodeoxyglucose positron emission tomography-computed tomography at diagnosis and before maintenance therapy in symptomatic patients with multiple myeloma included in the IFM/DFCI 2009 Trial: results of the IMAJEM Study. J Clin Oncol. 2017; 35(25):2911-2918.
24. Reed V, Shah J, Medeiros LJ, et al. Solitary plasmacytomas: outcome and prognostic factors after definitive radiation therapy. Cancer. 2011;117(19):4468-4474.
25. Bianchi G, Munshi NC. Pathogenesis beyond the cancer clone(s) in multiple myeloma. Blood. 2015;125(20):3049-3058.
26. Rasche L, Angtuaco EJ, Alpe TL, et al. The presence of large focal lesions is a strong independent prognostic factor in multiple myeloma. Blood. 2018;132(1):59-66
27. Jiménez R, Rosinol L, Cibeira MT, et al. Incidence and outcome of soft-tissue plasmacytomas in patients with multiple myeloma before and after the introduction of novel drugs. Blood. 2017;130(Suppl 1):3140.
28. Gay F, Magarotto V, Crippa C, et al. Bortezomib induction, reduced-intensity transplantation, and lenalidomide consolidation-maintenance for myeloma: updated results. Blood. 2013;122(8):1376-1383.
29. Palumbo A, Bringhen S, Larocca A, et al. Bortezomib-melphalan-prednisone-thalidomide followed by maintenance with bortezomib-thalidomide compared with bortezomib-melphalan-prednisone for initial treatment of multiple myeloma: updated follow-up and improved survival. J Clin Oncol. 2014;32(7):634-640.
30. Palumbo A, Cavallo F, Gay F, et al. Autologous transplantation and maintenance therapy in multiple myeloma. N Engl J Med. 2014;371(10):895-905.
31. Gay F, Oliva S, Petrucci MT, et al. Autologous transplant vs oral chemotherapy and lenalidomide in newly diagnosed young myeloma patients: a pooled analysis. Leukemia. 2017;31(8):1727-1734.
32. Magarotto V, Bringhen S, Offidani M, et al. Triplet vs doublet lenalidomide-containing regimens for the treatment of elderly patients with newly diagnosed multiple myeloma. Blood. 2016;127(9):1102-1108.
33. Larocca A, Bringhen S, Petrucci MT, et al. A phase 2 study of three low-dose intensity subcutaneous bortezomib regimens in elderly frail patients with untreated multiple myeloma. Leukemia. 2016;30(6):1320-1326.
34. Bringhen S, Petrucci MT, Larocca A, et al. Carfilzomib, cyclophosphamide, and dexamethasone in patients with newly diagnosed multiple myeloma: a multicenter, phase 2 study. Blood. 2014;124(1):63-69.
35. Bringhen S, D'Agostino M, De Paoli L, et al. Phase 1/2 study of weekly carfilzomib, cyclophosphamide, dexamethasone in newly diagnosed transplant-ineligible myeloma. Leukemia. 2018;32(4):979-985.

ARTICLE

A real world multicenter retrospective study on extramedullary disease from Balkan Myeloma Study Group and Barcelona University: analysis of parameters that improve outcome

Meral Beksac,[1] Guldane Cengiz Seval,[1] Nicholas Kanellias,[2] Daniel Coriu,[3] Laura Rosiñol,[4] Gulsum Ozet,[5] Vesselina Goranova-Marinova,[6] Ali Unal,[7] Jelena Bila,[8] Hayri Ozsan,[9] Arben Ivanaj,[10] Lejla Ibricevic Balić,[11] Efstathios Kastritis,[2] Joan Bladé,[4] Meletios Athanasios Dimopoulos[2]

[1]Department of Hematology, School of Medicine, Ankara University, Ankara, Turkey; [2]Department of Clinical Therapeutics, National and Kapodistrian University of Athens, School of Medicine, Athens, Greece; [3]University of Medicine and Pharmacy "Carol Davila", Fundeni Clinical Institute, Bucharest, Romania; [4]Hospital Clinic, IDIBAPS, Barcelona, Spain; [5]Clinic of Hematology, Ankara Numune Education and Research Hospital, Ankara, Turkey; [6]University Hospital "Sv. Georgi" and Medical University Plovdiv, Plovdiv, Bulgaria; [7]Department of Hematology, School of Medicine, Erciyes University, Kayseri, Turkey; [8]Faculty of Medicine, University of Belgrade, Belgrade, Serbia; [9]Department of Hematology, School of Medicine, Dokuz Eylül University, Izmir, Turkey; [10]University of Medicine Tirana, Tirana, Albania and [11]Clinical Center of Sarajevo University, Sarajevo, Bosnia and Herzegovina

Ferrata Storti Foundation

Haematologica 2020
Volume 105(1):201-208

ABSTRACT

Here, we report the outcome of 226 myeloma patients presenting with extramedullary plasmacytoma or paraosseous involvement in a retrospective study conducted in 19 centers from 11 countries. Extramedullary disease was detected at diagnosis or relapse between January 2010 and November 2017. Extramedullary plasmacytoma and paraosseous involvement were observed in 130 patients at diagnosis (92 of 38) and in 96 at relapse (84 of 12). The median time from multiple myeloma diagnosis to the development of extramedullary disease was 25.1 months (range 3.1-106.3 months) in the relapse group (median follow up: 15 months). Imaging approach for extramedullary disease was computed tomography (n=133), positron emission tomography combined with computed tomography (n=50), or magnetic resonance imaging (n=35). The entire group received a median two lines of treatment and autologous stem cell transplantation (44%) following the diagnosis of extramedullary disease. Complete response was higher for paraosseous involvement *versus* extramedullary plasmacytoma at diagnosis (34.2% *vs.* 19.3%; *P*=NS.) and relapse (54.5% *vs.* 9%; *P*=0.001). Also paraosseous involvement patients had a better progression-free survival (PFS) when recognized at initial diagnosis of myeloma than at relapse (51.7 *vs.* 38.9 months). In addition, overall survival was better for paraosseous involvement compared to extramedullary plasmacytoma at diagnosis (not reached *vs.* 46.5 months). Extramedullary plasmacytoma at relapse had the worst prognosis with a PFS of 13.6 months and overall survival of 11.4 months. In the multivariate analysis, paraosseous involvement, extramedullary disease at diagnosis, International Staging System (ISS-I), and undergoing autologous stem cell transplantation improved overall survival independently. This cohort demonstrated that extramedullary disease benefits from front-line autologous stem cell transplantation and extramedullary plasmacytoma differs from paraosseous involvement in terms of rate and duration of response, with even worse outcomes when detected at relapse, constituting an unmet clinical need.

Introduction

Multiple myeloma (MM) originates from the proliferation of clonal malignant plasma cells (PC) with a strong interaction with the bone marrow microenvironment. Although the disease is considered generally incurable, overall survival (OS)

Correspondence:

MERAL BEKSAC
meral.beksac@medicine.ankara.edu.tr

Received: February 11, 2019.

Accepted: July 5, 2019.

Pre-published: July 5, 2019.

doi:10.3324/haematol.2019.219295

Check the online version for the most updated information on this article, online supplements, and information on authorship & disclosures: www.haematologica.org/content/105/1/201

has improved substantially in the past 15 years and more than 25% of patients can now expect to live for more than ten years.[1] However, there is still a group of patients presenting with very poor prognostic features whose outcome has not improved; presentation with disease at extramedullary sites is included among these.

Once the plasma cells acquire independence from the cellular microenvironment, plasma cell leukemia or metastasis to soft tissues in the form of plasmacytomas may occur creating an unmet clinical need, even in the era of novel agents.[2,3] Such an escape is driven by pathophysiological alterations including decreased expression of adhesion molecules, low expression of cytokine receptors or increased angiogenesis.[2] Two types of soft tissue involvement in myeloma have been defined: extramedullary plasmacytomas (EMP) resulting from hematogenous spread and involving only soft tissues, and paraskeletal or paraosseous (PO) plasmacytomas, consisting of tumor masses adjacent to bones and arising from focal skeletal lesions.[3,4] The incidence of extra-medullary involvement and paraskeletal plasmacytomas at diagnosis ranges from 1.7% to 3.5% and from 6% to 34.4%, respectively; at relapse, the presence of extramedullary disease (EMD) increases up to 10%.[3-6] There is no clear evidence that the incidence of EMD is higher at relapse after allogeneic transplantation or after exposure to novel anti-myeloma agents.[7,8] At present, there are limited data regarding the basic features of EMD, such as incidence, prevalence, clinical characteristics, laboratory features, and response to novel drugs.[6-11] Two previous publications reported the incidence of EMD at diagnosis and relapse to be 15% and 20%, respectively.[12,13] In the largest study to date, Varettoni *et al*. report the results of 1,003 consecutive MM patients who presented to the University of Pavia in Italy between 1971 and 2007 with an incidence of 13% (7% EMD at diagnosis and 6% at relapse). Of note, cytogenetic data were not available for all patients and were not included in the analysis.[6]

Extramedullary disease both clinically and morphologically resembles lymphoma transformation in terms of laboratory features, such as frequent association with high serum levels of lactate dehydrogenase.[14] In addition, the majority of patients presenting with EMD have highly complex cytogenetic abnormalities and, as found most recently, high-risk features on gene expression profiling.[15] In a classic monoclonal immunoglobulin-secreting tumor, EMD may present as light chain secretory, hypo-secretory, or non-secretory disease as a sign of disease de-differentiation and transformation.[16]

Moreover, an increase in the incidence is probably due to the availability of highly sensitive imaging techniques and the prolongation of survival. Modern imaging techniques, especially 18F-fluorodeoxyglucose (FDG) PET, have become extremely helpful in documenting suspected EMP.[8]

Except for solitary plasmacytoma, there is no standard approach for EMD management.[17] Neither response to EMD within the clinical trials nor case reports have been extensively analyzed and, therefore, no evidence-based consensus has been reached. Therefore, the objectives of this study were to determine the demographic and clinical characteristics of EMD (EMP or PO) among myeloma patients at initial diagnosis or relapse to evaluate its impact on treatment outcomes. The response, progression-free survival (PFS) and overall survival (OS) of this real-world data based on 226 patients will serve as a reference for future studies addressing EMD.

Methods

This is a retrospective, multi-institutional study conducted in 19 centers from 11 countries in Europe. Patients were identified through a database search at each of the participating institutions. Adult (≥18 years) patients with MM who had a pathological and/or radiological diagnosis of extramedullary involvement at any time of follow up between January 2010 and November 2017 were included. Ethical committee approvals and consents were collected from each patient on admission depending on the local regulations of each country. The diagnosis of EMD was made in accordance with the International Myeloma Working Group Guidelines.[18] Eligibility criteria included EMD at any time following the initial diagnosis of MM excluding plasma cell leukemia or solitary plasmacytoma. Those patients with pathological or radiological evidence of neoplastic plasma cells in the soft tissues adjacent to axial skeleton were considered to have PO involvement of locally advanced myeloma, but not EMP. On the basis of type of extramedullary involvement, we defined two groups of myeloma patients: PO group and extramedullary organ/tissue involvement (EMP). Cases with both PO and EMP were included in the EMP group. Disease stage at diagnosis was determined according to the International Staging System (ISS; I-III). Remission, progression, and relapse were defined according to standard International Myeloma Working Group (IMWG) criteria. Progression was calculated from the date of diagnosis of EMD until the date of progression of myeloma or isolated EMD, whichever occurred first.

Clinical data included age at the time of MM diagnosis and at the time of EMD, ISS stage, cytogenetic abnormalities, radiological findings (PET-CT/MRI/CT), number and types of therapies including chemo/radiotherapy, autologous stem cell transplantation (ASCT) for EMD, response, PFS and OS.

Categorical variables were compared with the use of the Fisher's exact test or the χ^2 test. Continuous variables were analyzed using the Kruskal-Wallis test for independent samples. Survival probabilities were estimated by the Kaplan-Meier method,[19] and the Log-Rank test was used for univariate comparison. Outcomes were determined as response to treatment, PFS and OS. We also compared the PFS and OS between the time of EMD diagnosis and PO/EMP cohorts. To assess the multivariate factors for each end point, we used Cox proportional hazard model to estimate hazard ratios (HR) with 95% confidence intervals (CI). All tests were two-sided, with the type 1 error rate fixed at α=0.05. All analyses and graphs were obtained using the statistical software SPSS Statistics 21 (SPSS; IBM Corp., Armonk, NY, USA).

Results

Clinical characteristics

A total of 226 patients met the predetermined criteria for inclusion in this study. Baseline clinical characteristics are summarized in Table 1. Median age at diagnosis of EMD was 62 years (range 34-87 years). EMP/PO were observed in 130 patients at the time of initial diagnose (92 of 38) and in 96 during disease relapse (84 of 12). The median time from MM diagnosis to the development of EMD in the relapsed group was 25.1 months (range 3.1-106.3 months) with relatively faster progression among the EMP patients (PO: median 9.8 months; EMP: median

5.7 months; P=NS). Since Jurczyszyn *et al.*[20] have demonstrated a survival advantage among younger patients, an age cut-off of 45 years was adopted (Table 1) revealing younger age for PO (59 years) *versus* EMP (64 years) (*P*=0.01). Median ages of patients presenting with PO (58.5 years) or EMP (62 years) at diagnosis were not significantly different. The imaging modalities used for the diagnosis were CT (n=133), PET-CT (n=50) and MRI (n=35). The anatomical distribution of EMD is depicted in Table 1. Most patients with EMP (65%) presented with one involved site, 16% had two sites, and 11% had three sites, while involvement in four and five sites was present in 7% of patients, respectively.

Cytogenetic analysis of clonal plasma cells in the bone marrow at the time of MM diagnosis was available for 111 of 226 (49.1%) of the patients with EMD (Table 1).

Table 1. Baseline characteristics of patients.

Characteristics (n=226)		Results
Age, years, Median (range)		62 (34-87)
Age, years, Median (range)		EMP: 64 (34-87) PO: 59 (36-83) *P*=0.01
Age ≤45 *vs.* >45 (at diagnosis)		EMP: 13 *vs.* 79 PO:2 *vs.* 36
Age ≤45 *vs.* >45 (at relapse)		EMP: 3 *vs.* 81 PO:1 *vs.* 11
ISS stage (at myeloma diagnosis)		
Stage I, n (%)		76 (33.6 %)
Stage II, n (%)		68 (30.1 %)
Stage III, n (%)		76 (33.6 %)
Unknown		6 (2.7%)
Number of FISH abnormalities		
No abnormalities, n (%)		57 (51.3 %)
1 abnormality, n (%)		28 (25.2 %)
2 abnormalities, n (%)		12 (10.8 %)
≥3 abnormalities, n (%)		12 (10.8 %)
Del17p, n (%)		10 (9 %)
Del13q, n (%)		20 (18 %)
t (4;14), n (%)		8 (7.2 %)
t (14;16), n (%)		2 (1.8 %)
t (11;14), n (%)		4 (3.6 %)
Anatomical locations of EMP		
Soft tissue (muscle/skin) n (%)		55 (24.3 %)
Lymph nodes, n (%)		23 (10.2 %)
Pleural, n (%)		27 (11.9 %)
Liver, n (%)		21 (9.3 %)
Central nervous system, n (%)		14 (6.2 %)
Abdominal, n (%)		9 (4.0 %)
Oropharynx, n (%)		8 (3.5 %)
Lung, n (%)		7 (3.1 %)
Testis, n (%)		4 (1.8 %)
Others, n (%)		4 (1.8 %)
Initial therapy for EMD (all patients)	At initial diagnosis	At relapse
Only radiotherapy, n (%)	9 (6.9 %)	–
Systemic chemotherapy (without novel agent)		
Thalidomide combinations*, n (%)	34 (26.2%)	23 (24%)
PI combinations*, n (%)	13 (10%)	2 (2.1%)
Len/Pom combinations*, n (%)	63 (48.5%)	40 (41.7%)
PI+IMID combinations:	5 (3.8%)	8 (8.3%)
VDT, n(%)	–	4 (4.2%)
VRD, n(%)	6 (4.6%)	12 (12.5%)
Monoclonal antibodies, n(%)	–	7 (7.3%)
Lines of therapy after EMD diagnosis		
1-2 lines, n (%)	121 (53.8 %)	
>2 lines, n (%)	104 (46.2 %)	
Autologous stem cell transplantation, n (%)	100 (44.2 %)	

*Thalidomide combinations: thalidomide-dexamethasone/TAD/other thalidomide combinations; PI combinations: Vel-Dex/VCD/VMP/other bortezomib combinations or Carfilzomib-Dex; Len/Pom combinations: Len-dex/RCD/Pomalidomide-Dex or other Lenalidomide combinations. TAD: thalidomide-adriamycin-dexamethasone; Vel: bortezomib; dex: dexamethasone; VCD: bortezomib/cyclophosphamide/dexamethasone; VMP: bortezomib/melphalan/prednisolone; Len: lenalidomide; RCD: lenalidomide/cyclophosphamide/dexamethasone; VDT: bortezomib/dexamethasone/thalidomide; VRD: bortezomib/lenalidomide/dexamethasone.

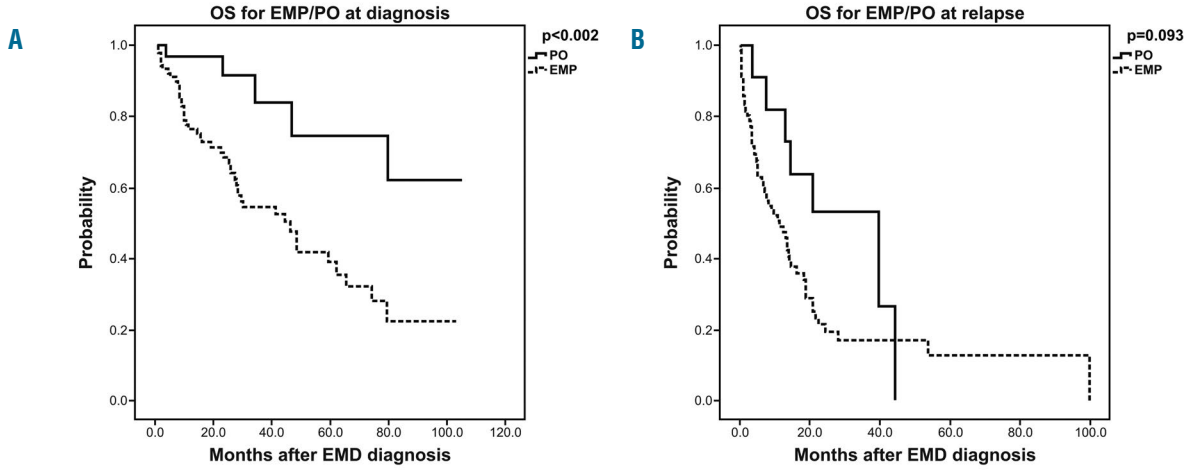

Figure 1. Overall survival (OS) estimates comparing patients with extramedullary plasmacytomas (EMP) to those with paraosseous (PO) lesions (A) at diagnosis and (B) at relapse. EMD: extramedullary disease.

Table 2. Comparison of response, survival outcomes of extramedullary plasmacytomas (EMP) or paraosseous (PO) patients either at diagnosis or at relapse.

	CR (%)		PFS (mos)		OS (mos)	
EMP						
diagnosis (n=92)	19.3		38.9 (95% CI: 23.6-54.2)	*P*<0.001	46.5 (95% CI: 25.5-67.5)	*P*<0.001
relapse (n=84)	9	*P*=0.034	13.6 (95% CI: 11.6-15.6)		11.4 (95% CI:*.6-16.2)	
PO						
diagnosis (n=38)	34.2	*P*=0.001	51.7 95% CI: 13.5-89.9)	*P*=0.005	NR	*P*<0.001
relapse (n=12)	54.5		20.9 (95% CI: 10.3-31.5)		39.8 (95% CI: 12.7-66.9)	

CR: complete remission; PFS: progression-free survival; OS: overall survival; n: number.

Therapeutic interventions and response

Treatments of patients are summarized in Table 1. The most commonly used treatment was combination chemotherapy with or without radiotherapy followed by cyclophosphamide/bortezomib/dexamethasone (45.6%). A total of 100 patients received ASCT, of which 67 (51.5%) with EMD at diagnosis. Median interval from EMD diagnosis to ASCT was 11.3 months (2-91 months). Transplant was a more frequent treatment approach among patients presenting with PO (31 of 38) compared to those with EMP (36 of 92) In addition, 29 patients (12.8%) had already been transplanted prior to the diagnosis of EMD, which developed after a median of 30.8 months post ASCT. Only four EMD patients diagnosed at relapse underwent ASCT. The entire group received a median of two lines of treatment following the diagnosis of EMD. Seventy-five (57.7%) myeloma patients with EMD at diagnosis went on to receive second line of therapy and 48 (37.2%) received more than two lines of therapy. Among 96 patients with EMD at relapse, 56 (58.3%) of them received more than two lines therapy.

As can be seen in Table 2 there were significant differences in outcomes when EMP was compared with PO. A statistically significant difference in complete response rate (CR) (PO: 38.8% *vs.* EMP: 14.8%; *P*=0.001) was observed following first line of treatment (not shown in Table 2). Of the 88 newly diagnosed EMP patients, with response to induction available, 35 had received radiotherapy without (n=6) or with (n=29) systemic treatment. These patients achieved a CR rate (11.4 %) that was considerably less than the CR (24.5%) achieved with chemotherapy alone. Among those who received ASCT, there was an improved CR rate of 29% *versus* 19% (at diagnosis) 41.7% *versus* 9.5% (at relapse). However, regardless of treatment, 51.4% of even those who achieved CR progressed within median 18.1 months *versus* 12.1 months in PO and EMP groups, respectively (*P*=NS). Among the newly diagnosed patients who underwent ASCT (n=67), the median PFS from diagnosis was 49 months (95%CI: 22.7-75.3) (PO: 51.7 months (95%CI: 18.3-85.1) and EMP: 46.5 months (95%CI: 32.8-60.2); *P*=NS). Among those who did not receive ASCT the median PFS was 28.1 months (95%CI: 20.3-35.9) (*P*<0.001). Post-ASCT depth of response (>VGPR *vs.* <VGPR) did not

Table 3. Univariate and multivariate analysis for overall survival in myeloma patients with extramedullary disease (EMD).

Factors	Median OS (months)	Univariate HR (95 % CI)	P	Multivariate HR (95 % CI)	P
Age in years, >45					
<45	68.3 months	0.77 (0.36-1.6)	NS		
>45	28.4 months	1.00			
Extramedullary involvement type					
PO	Not reached	0.44 (0.21-0.93)	0.032	0.44 (0.21-0.92)	0.029
EMP	19.2 months	1.00		1.00	
Timing of EMD					
At initial diagnosis	59.2 months	0.33 (0.21-0.50)	<0.001	0.34 (0.23-0.51)	<0.001
At relapse	8.4 months	1.00		1.00	
ISS					
ISS stage I	Not reached	0.45 (0.28-0.72)	0.001	0.45 (0.28-0.73)	0.001
ISS stage II-III	16.1 months	1.00		1.00	
Previous lines of therapy					
1-2 previous line	33.4 months	1.00	NS		
2+ previous lines	28.6 months	1.26 (0.84-1.89)			
ASCT (all patients)					
Yes	79.5 months	0.61 (0.39-0.94)	0.026	0.58 (0.38-0.89)	0.013
No	34.7 months	1.00		1.00	

PO: paraosseous; OS: overall survival; ISS: International Staging System; ASCT: autologous stem cell transplantation.

affect PFS. Type of therapy did not significantly impact PFS: immunomodulatory drug (IMID)-based (median 18.4 months, 95%CI: 6-32) or proteasome inhibitors (PI)-based (median 24.3 months, 95%CI: 20-29).

Survival analyses and prognostic factors

We did not find any association between EMP, ISS or age (Table 3). At the time of this report, 118 patients (52.2%) have died and the median follow up after EMD diagnosis is 15 months (range: 2-105 months). The estimated median PFS and OS from initial diagnosis of myeloma for the EMP and PO groups with a median follow up of 24.4 months are summarized (Table 2 and Figure 1). At initial MM diagnosis, PFS and OS were 38.9 months and 46.5 months for EMP, whereas 51.7 months (P=0.034) and not reached (P=0.002) for PO, respectively. However, if diagnosed at relapse, PFS and OS were 13.6 months and 11.4 months for EMP compared to 20.9 months (P=0.249) and 39.8 months (P=0.093) for PO, respectively (Table 2 and Figure 1).

In the group of patients with EMD at initial diagnosis, the OS was 46.5 months (95%CI: 10.3-31.5) with 2- and 5-year OS rates of 74.1±0.4 % and 47.1±0.6 %, respectively (P<0.001). For the PO group, median OS after ASCT was not reached *versus* 43.5 months in the EMP group (P=0.018).

In the univariate analysis, ISS staging (II/III *vs.* I) at the time of initial MM diagnosis (Figure 2A), time of EMD diagnosis (relapse *vs.* initial diagnosis) (Figure 2B), type of extra-medullary involvement (EMP *vs.* PO) (Figure 2C), and not undergoing ASCT (all patients) (Figure 2D) were associated with a worse OS. In the multivariate analysis, ISS stage I *versus* II-III, EMD at diagnosis *versus* relapse, PO *versus* EMP and yes *versus* no for ASCT were independently associated with better OS. The univariate and multivariate models are shown in Table 3.

Discussion

Extramedullary disease (EMD) is generally considered to be a poor prognostic factor. This multi-institutional real-world retrospective analysis on 226 patients has shown PFS/OS similar to the general myeloma population for those presenting with PO but not EMP.[9] However, EMD at diagnosis when treated with ASCT was able to reach a median PFS of 79.5 months (95%CI: 42.4-116.6) *versus* 30.1 months (95%CI: 11.2-48.9) depending on the depth of response (≥VGPR). Thus, although deep responses are reachable they are not sustainable for EMP even with ASCT.

In a report from the Spanish PETHEMA group, an upfront comparison was made of patients treated with three induction regimens: (i) thalidomide/dexamethasone; (ii) bortezomib/ thalidomide/dexamethasone; and (iii) vincristine/carmustine/melphalan/cyclophosphamide plus prednisone/vincristine/carmustine/adriamycin/bortezomib with the lowest rate of progressive disease being observed in the bortezomib/ thalidomide/ dexamethasone arm. EMD was reported in 18% of patients across this study and the response among EMD patients were not specified.[9] There are limited data concerning the efficacy of novel agents in myeloma patients with EMD. Different groups reported successful use of bortezomib.[21,22,23] The efficacy of other proteasome inhibitor (PI) (carfilzomib and ixazomib) is still unknown. The efficacy of IMID is also limited. Rosinòl *et al.* reported the data on the lack of efficacy of thalidomide in myeloma patients with EMD in different series.[24,25] In addition, Anagnostopoulos *et al.* recently demonstrated that relapses may occur under thalidomide maintenance with an increase in bone marrow plasma cells and no increase in the M-protein size.[26] The efficacy of lenalidomide on plasmacytomas has not yet been reported. Concerning pomalidomide and dexam-

ethasone, different groups have reported conflicting results.[27]

In a retrospective study, a subset of 101 EMD patients (66 at diagnosis and 35 at relapse), were compared to patients without any EMD but enrolled in Total Therapy (TT) or non-TT protocols.[28] Regardless of therapy, EMD was associated with shorter PFS and OS: EMP at diagnosis was associated with poor PFS (TT: 27%, non-TT: 12% after 5 years) and OS (TT: 35%, non-TT: 34% after 5 years) regardless of whether or not the patients were treated on TT protocols.[14] The PFS and OS in our study is comparable to the survival durations reported by the Arkansas group. Usmani *et al.*, but not Pour *et al.*, found fluorescence *in situ* hybridization (FISH) detectable abnormalities to be associated with EMD and poor outcome.[21,24] In our study, FISH analysis was available in half of the patients and was similar to the experience of the Czech group revealing results comparable to the general myeloma population. In our experience, only 13q del (18%), was observed less frequently than expected.

In a recent paper, Kumar *et al.* have analyzed data of 44 (16.2%) EMD out of 271 consecutive ASCT recipients. Although they did not discriminate EMP from PO, both OS and PFS was shorter for patients with EMD; median OS was 19.2 months (95%CI: 10.6-27.8) with a median PFS of 19 months (95%CI: 12.6-25.4). Achievement of CR post transplant was found to be the most important predictor for OS and PFS in this study.[29] In our cohort, 67 myeloma patients with EMD at diagnosis underwent ASCT within a median of 10.7 months and 39 patients (66.1%) achieved ≥very good partial response (VGPR) following ASCT. We were also able to demonstrate the impact of transplant on OS in our newly diagnosed EMD ASCT cohort in univariate and multivariate analysis. Although PFS was comparable to the standard myeloma population, we were not able to see the impact of response ≥VGPR, which may be attributable to the differences among the imaging tools used.

The European Group of Blood and Marrow Transplantation (EBMT) recently reported on 682 EMD subjects (EMP/PO: 139/543) who have received ASCT. In this report, PO (14.5%) involvement was found to be more frequent compared to EMP (3.7%). They noted a gradual increase in frequency of EMD from 2005 to 2014.[30] Similar to our results, they also report ISS to have a poor

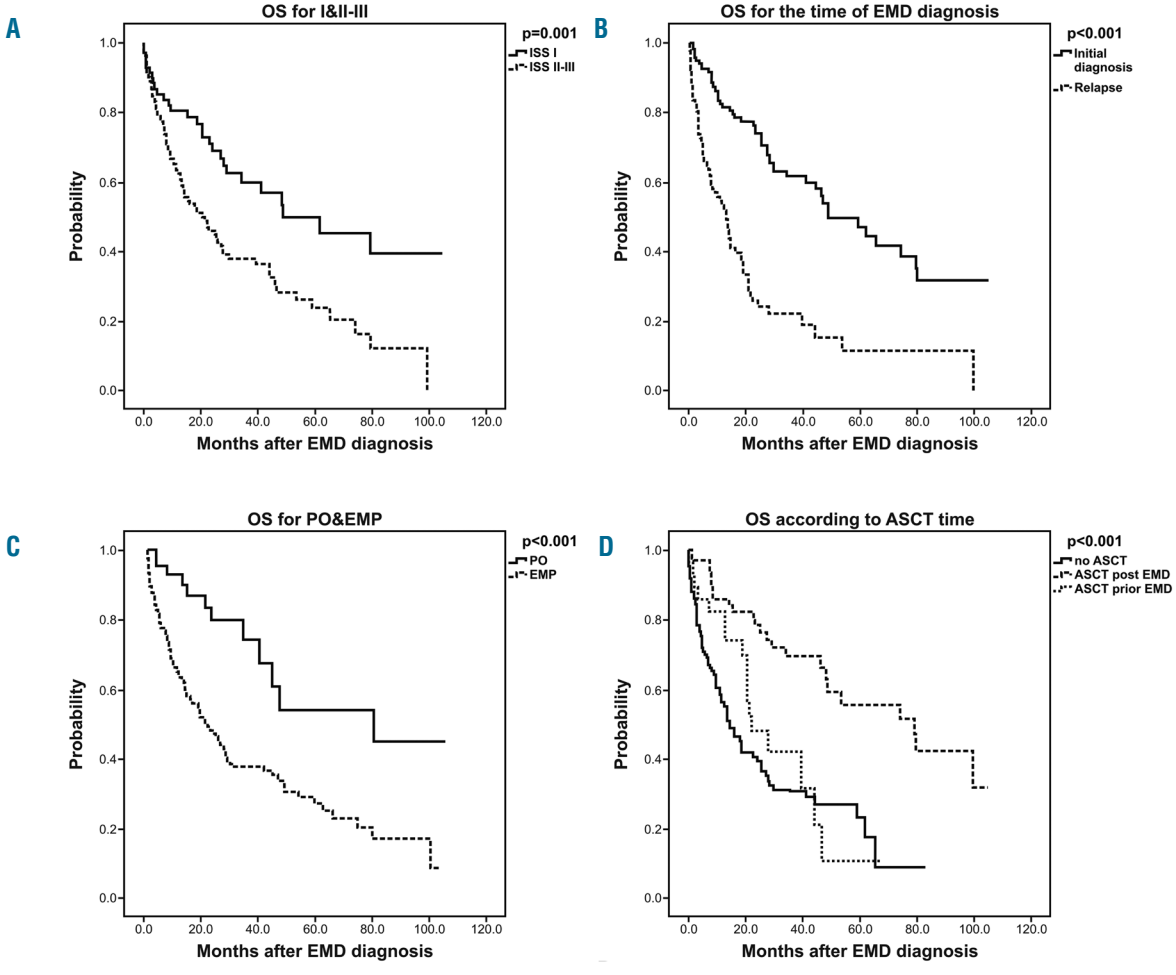

Figure 2. Overall survival (OS) estimates comparing the risk factors in (A) extramedullary disease (EMD) patients at diagnosis according to International Staging System (ISS) stage, (B) EMD patients according to disease stage, (C) all patients according to paraosseous (PO) *versus* extramedullary plasmacytomas (EMP) and (D) all patients according to autologous stem cell transplantation (ASCT) treatment at diagnosis *versus* at relapse *versus* no ASCT.

prognostic effect on PFS and OS. Organ distributions are similar between the EBMT report and ours. We have to consider selection bias in their report, as elderly patients not transplanted are not included. Our study did not aim to analyze the frequency of EMD, but rather the response and survival outcomes. Our results for patients detected at diagnosis differ from the EBMT report as their median PFS (PO *vs.* EMP) values were 36 *versus* 24 months, compared to our results, which were 51.7 *versus* 38.9 months, respectively. In our study, ASCT was performed among 44% of our patients. Among the EMD following ASCT cases, a shorter 3-year PFS: 28.4±1.6% was observed compared to the PFS of those who were transplanted with EMD at diagnosis (55.8±6.7%; P<0.001). Usmani *et al*. have also concluded that even with the Total Therapy approach EMD is not controllable. In their study, non-EMD patients were able to improve their PFS from four to six years, but PFS of patients with EMD were approximately one year regardless of being included in the TT programs with a 5-year PFS of 50% *versus* 21% in no EMD *versus* EMD prior to ASCT groups, respectively (P=0.08).[28] Pour *et al*. reported on 55 cases in an extramedullary relapse setting and the most important finding in their study was the significant difference in prognosis for PO and EMP. If the extramedullary myeloma infiltration was not bone-related, the OS was extremely short and not longer than four months. They were not able to observe any association between EMD relapse and novel agents (thalidomide or bortezomib).[31] This multi-national study includes widely heterogeneous drug approvals and access to novel agents. In our relapsed EMD cohort, 24% (23 of 96) of patients received initial therapy without any novel agents. Although there was a trend in favor of PI, we were not able to observe an effect of novel agents on PFS. In addition, our cohort of relapsed EMP also had the worst prognosis with an OS of 11.4 months.

Our study results highlight a lack of an association between EMD and younger age at diagnosis. In our study, the age cut-off of 45 years was selected arbitrarily to distinguish younger patients from the general myeloma population (65+/- 20 years). In general, the outcome of younger patients is better than that of elderly myeloma patients because of their better performance status and treatment tolerability. Median ages of EMP and PO of our patients were similar to the median value of 59 years reported in the EBMT study (EMP/PO: 64/59 years).[30]

A standard approach for EMD has still not been established. Neither response to EMD within the clinical trials nor case reports have been extensively analyzed in order to arrive at an evidence-based consensus. The most standardized modality is to give radiotherapy and treat patients with multiple agents as if treating lymphoma. Given the dismal outcome of EMD reported by others and us, there is an unmet need to improve PFS and OS. Prospective clinical trials focusing on EMD are needed. Despite the limitations of a retrospective approach, the response kinetics reported in our real-world study may provide guidance in designing future EMD clinical trials. Since PO *versus* EMP, EMP at initial diagnosis *versus* relapse, ISS I *versus* II and III, ASCT yes/no are found to improve OS, these parameters need to be balanced in future studies comparing novel treatment approaches.

Acknowledgments

Authors are grateful to additional members of Balkan Myeloma Study Group who also participated but could not qualify for authorship: Guenova M, Markovic O, Djurdjevic P, Kinda SB, Karanfilsky O, Dapcevic M, Zver S.

References

1. Kumar SK, Rajkumar SV, Dispenzieri A, et al. Improved survival in multiple myeloma and the impact of novel therapies. Blood. 2008;111(5):2516-2520.
2. Palumbo A, Anderson K. Multiple myeloma. N Eng J Med. 2011;364(11):1046-1060.
3. Blade J, Larrea CF, Rosinol L, et al. Soft-tissue plasmacytomas in multiple myeloma: incidence, mechanisms of extramedullary spread, ad treatment approach. J Clin Oncol. 2011;29(28):3805-3812.
4. Touzeau C, Moreau P. How I treat extramedullary myeloma. Blood. 2016; 127(8):971-976.
5. Oriol A. Multiple myeloma with extramedullary disease. Adv Ther. 2011; 28(Suppl 7):1-6.
6. Varettoni M1, Corso A, Pica G, Mangiacavalli S, Pascutto C, Lazzarino M. Incidence, presenting features and outcome of extramedullary disease in multiple myeloma: a longitudinal study on 1003 consecutive patients. Ann Oncol. 2010; 21(2):325-330.
7. Varga C, XieW, Laubach J, et al. Development of extramedullary myeloma in the era of novel agents: no evidence of increased risk with lenalidomide-bortezomib combinations. Br J Haematol. 2015;169(6):843-850.
8. Weinstock M, Aljwai Y, Morgan EA, et al. Incidence and clinical features of extramedullarty multiple myeloma in patents who underwent stem cell transplantation. Br Hematol. 2015;169(6):851-858.
9. Rosiñol L, Oriol A, Teruel AI, et al. Superiority of bortezomib, thalidomide, and dexamethasone (VTD) as induction pre- transplantation therapy in multiple myeloma: a randomized phase 3 PETHEMA/GEM study. Blood. 2012; 12:120(8):1589-1596.
10. Usmani SZ, Rodriguez-Otero P, Bhutani M, Mateos MV, Miguel JS. Defining and treating high-risk myeloma. Leukemia. 2015; 29(11):2119-2125.
11. Sonneveld P, Avet-Loiseau H, Lonial S, et al. Treatment of multiple myeloma with high risk cytogenetics: a consensus of the International Myeloma Working Group. Blood. 2016;127(24):2955-2962.
12. Bladé J, Lust J, Kyle RA. Immunoglobulin D multiple myeloma: presenting features response to therapy, and survival in a series of 53 cases. J Clin Oncol. 1994;12(11):2398-2404.
13. Bladé J, Kyle RA, Greipp PR. Presenting features and prognosis in 72 patients with multiple myeloma who were younger than 40 years. Br J Haematol. 1996;93:345-351.
14. Barlogie B, Smallwood L, Smith T, et al. High serum levels of lactic dehydrogenase identify a high-grade lymphoma-like myeloma. Ann Intern Med. 1989; 110(7):521-525.
15. Rasche L, Bernard C, Topp M, et al. Features of extramedullary myeloma relapse: high proliferation, minimal marrow nvolvement, adverse cytogenetics: a retrospective single centre study of 24 cases. Ann Hematol. 2012;91(7):1031-1037.
16. Weinstock M, Ghobrial IM. Extramedullary multiple myeloma. Leuk Lymphoma. 2013; 54(6):1135-1141.
17. Caers J, Paiva B, Zamagni E, et al. Diagnosis, treatment, and response assessment in solitary plasmacytoma: updated recommendations from a European Expert Panel. J Hematol Oncol. 2018;11(1):10.
18. Rajkumar SV, Dimopoulos MA, Palumbo A, et al. International Myeloma Working Group updated criteria fort he diagnosis of multiple myeloma. Lancet Oncol. 2014; 15(12):PE538-E5448.
19. Kaplan E, Meier P. Nonparametric estimation from incomplete observations. J Am Stat Assoc. 1958;53(282):457-481.
20. Jurczyszyn A, Nahi H, Avivi I, et al. Characteristics and outcomes of patients with multiple myeloma aged 21-40 years versus 41-60 years: a multi-institutional case-control study. Br J Haematol. 2016;175(5):884-891.
21. Patriarca F, Prosdocimo S, Tomadini V, et al. Efficacy of bortezomib therapy for extramedullary relapse of myeloma after autologous and non-myeloablative allogeneic transplantation. Haematologica. 2005;90(2):278-279.

22. Paubelle E, Coppo P, Garderet L, et al. Complete remission with bortezomib on plasmacytomas in an end-stage patient with refractory multiple myeloma who failed all other therapies including haematopoietic stem cell transplantation: possible enhancement of graft-vs-tumor effect. Leukemia. 2005;19(9):1702-1704.
23. Rosiñol L, Cibeira MT, Uriburu C, et al. Bortezomib: an effective agent in extramedullary disease in multiple myeloma. Eur J Haematol. 2006;76(5):405-408.
24. Rosiñol L, Cibeira MT, Bladé J, et al. Extramedullary multiple myeloma escapes the effect of thalidomide. Haematologica. 2004;89(7):832-836.
25. Bladé J, Perales M, Rosiñol L, et al. Thalidomide in multiple myeloma: lack of response of soft-tissue plasmacytomas. Br J Haematol. 2001;113(2):422-425.
26. Anagnostopoulos A, Gika D, Hamilos G, et al. Treatment of relapsed refractory multiple myeloma with thalidomide-based regimens: identification of prognostic factors. Leuk Lymphoma. 2004;45(11):2275-2279.
27. Jiménez-Segura R, Granell M, Gironella M, et al. Pomalidomida/dexametasona en el tratamiento de la enfermedad extramedular en pacientes con myeloma multiple en recaída/refractario: análisis de 16 casos. Haematologica. 2016;101(s4):103.
28. Usmani SZ, Heuck C, Mitchell A, et al. Extramedullary disease portends poor prognosis in multiple myeloma and is over-represented in high-risk disease even in the era of novel agents. Haematologica. 2012;97(11):1761-1767.
29. Kumar L, Gogi R, Patel AK, et al. Multiple myeloma with extramedullary disease: impact of autologous stem cell transplantation on outcome. Bone Marrow Transplant. 2017;52(10):1473-1475.
30. Gagelmann N, Eikerna DJ, Iacobelli S, et al. Impact of extramedullary disease in patients with newly diagnosed multiple myeloma undergoing autologous stem cell transplantation: a study from the Chronic Malignancies Working Party of the EBMT. Haematologica. 2018;103(5):890-897.
31. Pour L, Sevcikova S, Greslikova H, et al. Soft-tissue extramedullary multiple myeloma prognosis is significantly worse in comparison to bone-related extramedullary relapse. Hematologica. 2014;99(2):360-364.

ARTICLE

Extracellular mitochondria released from traumatized brains induced platelet procoagulant activity

Zilong Zhao,[1,2] Yuan Zhou,[1,2] Tristan Hilton,[1] Fanjian Li,[2] Cha Han,[1] Li Liu,[2] Hengjie Yuan,[2] Ying Li,[2] Xin Xu,[1] Xiaoping Wu,[1] Fangyi Zhang,[3] Perumal Thiagarajan,[4] Andrew Cap,[5] Fu-Dong Shi,[2,6] Jianning Zhang[2] and Jing-fei Dong[1,7]

[1]BloodWorks Research Institute, Seattle, WA, USA; [2]Tianjin Institute of Neurology, Departments of Neurosurgery and Neurology, Tianjin Medical University General Hospital, Tianjin, China; [3]Department of Neurosurgery, University of Washington School of Medicine, Seattle, WA, USA; [4]Departments of Medicine and Pathology, Michael E. DeBakey VA Medical Center and Baylor College of Medicine, Houston, TX, USA; [5]US Army Institute of Surgical Research, San Antonio, TX, USA; [6]Department of Neurology, Barrow Neurological Institute, St. Joseph's Hospital and Medical Center, Phoenix, AZ, USA and [7]Division of Hematology, Department of Medicine, University of Washington, School of Medicine, Seattle, WA, USA

Ferrata Storti Foundation

Haematologica 2020
Volume 105(1):209-217

ABSTRACT

Coagulopathy often develops soon after acute traumatic brain injury and its cause remains poorly understood. We have shown that injured brains release cellular microvesicles that disrupt the endothelial barrier and induce consumptive coagulopathy. Morphologically intact extracellular mitochondria accounted for 55.2% of these microvesicles, leading to the hypothesis that these extracellular mitochondria are metabolically active and serve as a source of oxidative stress that activates platelets and renders them procoagulant. In testing this hypothesis experimentally, we found that the extracellular mitochondria purified from brain trauma mice and those released from brains subjected to freeze-thaw injury remained metabolically active and produced reactive oxygen species. These extracellular mitochondria bound platelets through the phospholipid-CD36 interaction and induced α-granule secretion, microvesiculation, and procoagulant activity in an oxidant-dependent manner, but failed to induce aggregation. These results define an extracellular mitochondria-induced and redox-dependent intermediate phenotype of platelets that contribute to the pathogenesis of traumatic brain injury-induced coagulopathy and inflammation.

Introduction

Traumatic brain injury (TBI) induces coagulopathy that promotes secondary bleeding and propagates cerebral injury,[1] resulting in poor clinical outcomes of the patients.[2-6] Laboratory findings suggest that coagulopathy results from a hypercoagulable state that rapidly develops into consumptive coagulopathy.[1,7] This consumptive coagulopathy has been recapitulated in animal models of TBI with thrombotic and hemorrhagic manifestations in the pulmonary and cerebral microvasculature.[8,9] Despite strong clinical and laboratory evidence of its presence and association with poor clinical outcomes, the pathogenesis of TBI-associated coagulopathy remains poorly understood.

We have recently shown in mouse models that cellular microvesicles released from traumatically injured brains disrupt endothelial cell junctions through a synergistic action with platelets.[8] These brain-derived microvesicles are highly procoagulant due to the abundant expression of surface-exposed anionic phospholipids and tissue factor. The sudden and substantial release of brain-derived microvesicles into the circulation results in a consumptive coagulopathy that is characterized by progressive fibrinogen depletion from plasma and fibrin deposition in the vasculature.[8]

Correspondence:

JING-FEI DONG
jfdong@bloodworksnw.org

JIANNING ZHANG
jianningzhang@hotmail.com

Received: December 18, 2018.

Accepted: April 9, 2019.

Pre-published: April 11, 2019.

doi:10.3324/haematol.2018.214932

Check the online version for the most updated information on this article, online supplements, and information on authorship & disclosures: www.haematologica.org/content/105/1/207

We also found that 55.2±12.6% of annexin-V-binding microvesicles in peripheral blood of TBI mice were morphologically intact extracellular mitochondria (exMT).[9] These exMT promoted coagulation through the surface-exposed anionic phospholipid cardiolipin. The findings raise an important question: are these exMT metabolically active and, if so, do they affect platelet function through redox-dependent mechanisms? The question is raised because exMT can be viable, transferred between cells, and influence the function of target cells.[10-13] The influence of mitochondria on target cells has mostly been reported as protective,[10,12,13] likely due to increased energy supply. However, reactive oxygen species (ROS) are generated during ATP production in mitochondria[14] and are known to activate platelets.[15-17] Several studies have shown that platelets in patients with TBI are activated but aggregate poorly.[18] This platelet phenotype has also been reproduced in rat and swine models of TBI, in which platelets are activated,[19,20] accumulate on the pia mater,[21] and contribute to thrombosis in the lesion boundary zone.[22] The underlying mechanism for this unique TBI-associated platelet phenotype remains poorly understood. Here we discuss results from a study that was designed to investigate the effect of exMT on platelet activation and procoagulant activity through *in vitro* experiments and in mouse models.

Methods

Mouse models

C57BL/6J male mice (12-20 weeks and 22-25 g), obtained from the Jackson Laboratory (Bar Harbor, ME, USA) were subjected to fluid percussion injury[8] and blood samples were collected to quantify plasma exMT (*Online Supplementary Methods*).[9] This mouse protocol was approved by the Institutional Animal Care and Use Committee of the BloodWorks Research Institute.

Flow cytometry

Platelet activation

We used an LSR II flow cytometer (Beckon Dickinson, San Jose, CA, USA) to detect platelet activation through several measurements: CD62p expression, the binding of PAC-1 antibody (BD Biosciences), which recognizes the active conformation of the fibrinogen receptor αIIbβ3, annexin V binding,[9] platelet-bound fibrinogen and coagulation factor V,[25,26] and the formation of platelet-leukocyte complexes (*Online Supplementary Methods*).

Calcium influx

We used flow cytometry to measure the exMT-induced calcium influx in platelets labeled with 5 μM eFluor 514 Calcium Sensor Dye (Bioscience, San Diego, CA, USA) for 10 min at 37°C.[8]

Reactive oxygen species production

ExMT were suspended in Ca^{2+}-free HEPES buffered Tyrode solution (138 mM NaCl, 5.5 mM glucose, 10 mM HEPES, 12 mM $NaHCO_3$, 2.9 mM KCl, 0.4 mM NaH_2PO_4, 0.4 mM $MgCl_2$, and 0.1% BSA; pH 7.2) and incubated for 30 min at 37°C with 10 μM of DCFH-DA dye (ThermoFisher).[24] As controls, labeled exMT were treated with either 50 μM N-acetylcysteine (NAC, Life Technologies, Grand Island, NY, USA), which is a precursor of the antioxidant glutathione, or 200 μM tert-butyl hydroperoxide (TBHP, Life Technologies), which increases intracellular ROS production.[27] ExMT fixed with 5% paraformaldehyde were also examined as a control.

Image flow cytometry for the extracellular mitochondria-platelet interaction

As we previously described,[28] platelet-rich plasma was incubated for 30 min at 37°C with exMT labeled with MitoTracker Green and an APC-conjugated CD41a antibody (BD Bioscience). The platelets were washed in phosphate-buffered saline and fixed in 1% paraformaldehyde. Images were acquired at 60 x magnification to collect ≥20,000 cells from each sample using the Amnis ImageStream® X Mk II system (Amnis, Seattle, WA, USA). To distinguish exMT bound to the platelet surface from those internalized, platelets were digested with 1% trypsin for 10 min at 37°C after incubation with exMT. Mouse mitochondrial-specific DNA was then amplified from these exMT-treated and trypsinized platelets using a protocol modified from our previous study.[9]

CD36-extracellular mitochondria interaction

For *in vitro* experiments, platelet-rich plasma was incubated for 30 min at 37°C with a monoclonal CD36 antibody (Abcam, ab17044, Cambridge, MA, USA) or isotype IgG, followed by incubation with MitoTracker Green-labeled exMT and a PE-CD41a antibody for 30 min. For *in vivo* experiments, blood samples from non-injured mice infused with MitoTracker Green-labeled exMT were analyzed for exMT-bound platelets (MitoTracker Green$^+$/CD41a$^+$), platelet counts (CD41a$^+$ platelet counts in 60 s), platelet CD62p expression, and platelet-leukocyte complexes (CD41a$^+$/ CD45$^+$). The CD36 antibody used in this study recognizes both mouse and human CD36.[29,30]

Statistical analysis

Categorical (frequency) variables were expressed as percentages and continuous variables were expressed as the mean ± standard error of mean. The quantitative data were analyzed using SigmaPlot V. 11.2 (SYSTAT Software Inc., San Jose, CA, USA) for paired *t* tests, one way or repeated measures analysis of variance (ANOVA) as specified in each analysis. A *P* value of ≤0.05 was considered statistically significant.

Results

Extracellular mitochondria bound platelets *in vivo* and *in vitro*

Structurally intact (MitoTracker Green$^+$) (Figure 1A) and cardiolipin-exposed (Figure 1B) exMT were detected in the peripheral blood of mice with acute TBI. The exMT formed complexes with approximately 12.3 ± 5.8% of circulating platelets that remained detectable for 6 h after TBI (Figure 1C). Low levels of exMT-platelet complexes were also detected in sham-treated mice and likely resuited from surgery-induced injuries. When co-incubated for 30 min at 37°C *in vitro*, purified exMT from brains subjected to freeze-thaw injury also formed complexes with platelets (Figure 1D) in a dose-dependent manner (Figure 1E). Transmission electron microscopy showed that exMT interacted with the body (Figure 1F) and filopodia (Figure 1G) of platelets.

The Amnis® imaging flow cytometer detected exMT on the surface of platelets (Figure 2A, top panel), being endocytosed by platelets (Figure 2A, middle panel) and fused with platelet membranes (Figure 2A, bottom panel). The internalization of exMT by platelets was further validated by co-incubation of human platelets with mouse exMT for 30 min at 37°C followed by the amplification of mouse mitochondria-derived DNA from exMT-treated platelets that were trypsinized to remove surface-bound exMT

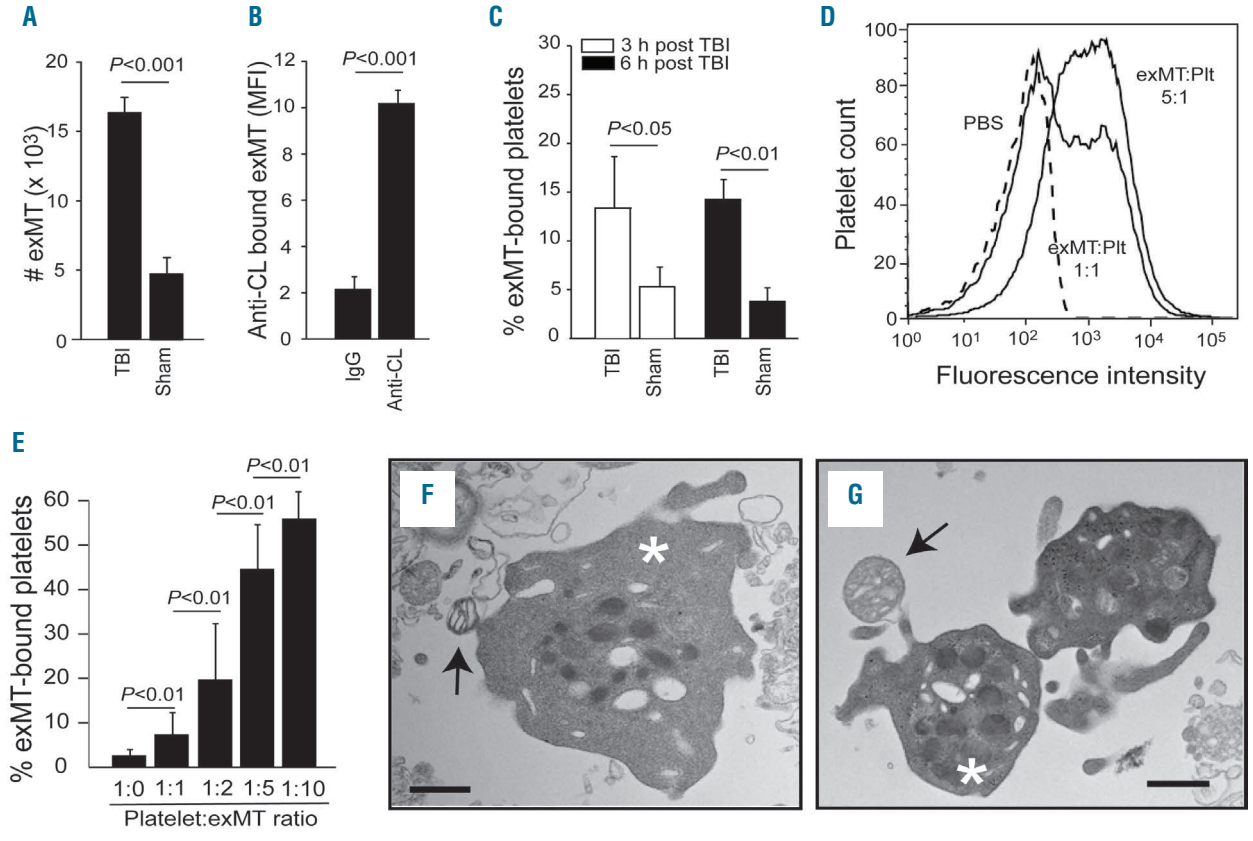

Figure 1. Extracellular mitochondria were released from injured cells and bound platelets. (A, B) Extracellular mitochondria (exMT) from mice with traumatic brain injury (TBI) were detected by MitoTracker Green (# exMT/100 μL plasma) (A) and anti-cardiolipin antibody (n=12, paired *t* test) (B). (C) Platelet-exMT complexes were detected in the blood of TBI mice using CD41a and TOM22 antibodies (n=8, paired *t* test). (D, E) After co-incubation for 30 min at 37 °C, exMT also bound platelets *in vitro,* as shown by a representative histogram (D) in a dose-dependent manner (n=30, one-way analysis of variance) (E). (F, G) Transmission electron microscopy (see *Online Supplementary Methods*) showed exMT binding to the body (F) and filopodia (G) of platelets (bar = 500 nm; arrow: mitochondria; *: platelet; representatives of 98 images reviewed).

(Figure 2B). Quantitatively, 13.7 ± 9.1% of platelets were exMT-bound after 30 min co-incubation (Figure 2C), which was consistent with the level of exMT-bound platelets found in TBI mice (Figure 1C). This exMT-platelet interaction was blocked by the phosphatidylserine-binding proteins annexin V and lactadherin (Figure 2C)[28,31] and partially by a CD36 antibody (Figure 2D), which blocks the CD36-mediated binding of endothelial microvesicles to platelets,[29] suggesting that exMT bind platelets through cardiolipin exposed on the mitochondria and CD36 expressed on platelets. Furthermore, ATP production was dose-dependently increased in the exMT-treated platelets at levels that were significantly higher than in platelets activated with ADP (Figure 2E). We were unable to determine whether the ATP increase was caused by platelet-bound exMT or by exMT-induced ATP production of platelets. Finally, when added to platelets that had been treated with exMT, FITC-conjugated annexin V bound 16.2 ± 6.3% of platelets (Figure 2F).

Extracellular mitochondria were metabolically viable and activated platelets

We found that exMT from TBI mice stimulated platelets to express CD62p and this activity was partially blocked by the antioxidant glutathione (GSH) (Figure 3A). One pitfall of this experiment was that exMT purified from plasma of TBI mice were derived from multiple cells. It was technically challenging to separate brain-derived exMT from those of other cells, without damaging the viability of exMT. To address this concern, we tested exMT from brains subjected to freeze-thaw injury *in vitro*.[9] These exMT produced ATP (Figure 3B) and ROS (Figure 3C). The ROS production was blocked by 50 μM of the anti-oxidant NAC and enhanced by 200 μM of the oxidant TBHP. The two agents have previously been shown to block and enhance ROS production of mammalian cells, respectively.[32,27] This metabolic viability was further validated by the lack of ROS production from paraformaldehyde-fixed exMT (Figure 3C). After 30 min of incubation with exMT, both mouse (*Online Supplementary Figure S2*) and human platelets (Figure 3D) expressed CD62p on their surfaces. The exMT-induced CD62p expression was reduced by the antioxidants GSH (20 μM), L-cysteine (0.5 mM), and NEM (2 mM) (Figure 3E). Testing the three thiol-modifying agents was necessary because GSH and L-cysteine reversibly interact with extracellular and intracellular oxidants, respectively, whereas NEM forms irreversible sulfur bonds with thiols. The exMT-treated platelets also increased calcium influx (*Online Supplementary Figure S3*), formed complexes with leukocytes (Figure 3F), and

released von Willebrand factor (Figure 3G). The exMT-induced CD62 expression and platelet-leukocyte aggregation were detected in 10-23% of platelets, which was consistent with the percentages of exMT-bound platelets found in TBI mice (Figure 1). We used platelets stimulated with collagen and thrombin as the control because this exMT-induced platelet phenotype resembled that of "coated platelets".[33,34] Together, these data suggested that exMT from TBI mice and those released from brains subjected to freeze-thaw injury *in vitro* were metabolically viable and activated platelets in an oxidant-dependent manner.

Using hopping probe ion conductance microscopy, we continuously monitored morphological changes of platelets adherent to fibrinogen in real-time (Figure 4A, top panel). After stimulation with exMT, adherent platelets underwent drastic membrane disintegration as exemplified in the middle panel of Figure 4A. This exMT-induced membrane disintegration was prevented by 20 μM GSH (Figure 4A, bottom row). Consistent with the exMT-induced platelet disruption, $CD41a^+$ platelet-derived membrane microvesicles were detected in the supernatant of exMT-treated platelets (Figure 4B) and platelet counts were reduced after treatment with exMT (Figure 4C). The production of platelet microvesicles and the reduction of platelet counts were partially blocked by the anti-oxidant GSH.

In contrast to their induction of α-granule secretion, exMT at comparable doses failed to induce platelet aggregation (Figure 4D) and did not enhance the formation of platelet thrombosis on the collagen matrix under arterial shear stress (*Online Supplementary Figure S4A-C*). Furthermore, the exMT-treated platelets aggregated normally in response to collagen (Figure 4E) and ADP (Figure 4F), and were moderately primed for activation by sub-threshold concentrations of ADP and collagen (*Online Supplementary Figure S4D*). Neither the binding of PAC-1 antibody (*Online Supplementary Figure S5*), which recognizes the active conformation of integrin αIIbβ3, nor the surface density of the integrin αIIbβ3 (Figure 4G) was changed after exMT treatment, as compared to platelets stimulated with collagen.

Extracellular mitochondria-treated platelets were procoagulant

ExMT-treated platelets also expressed anionic phos-

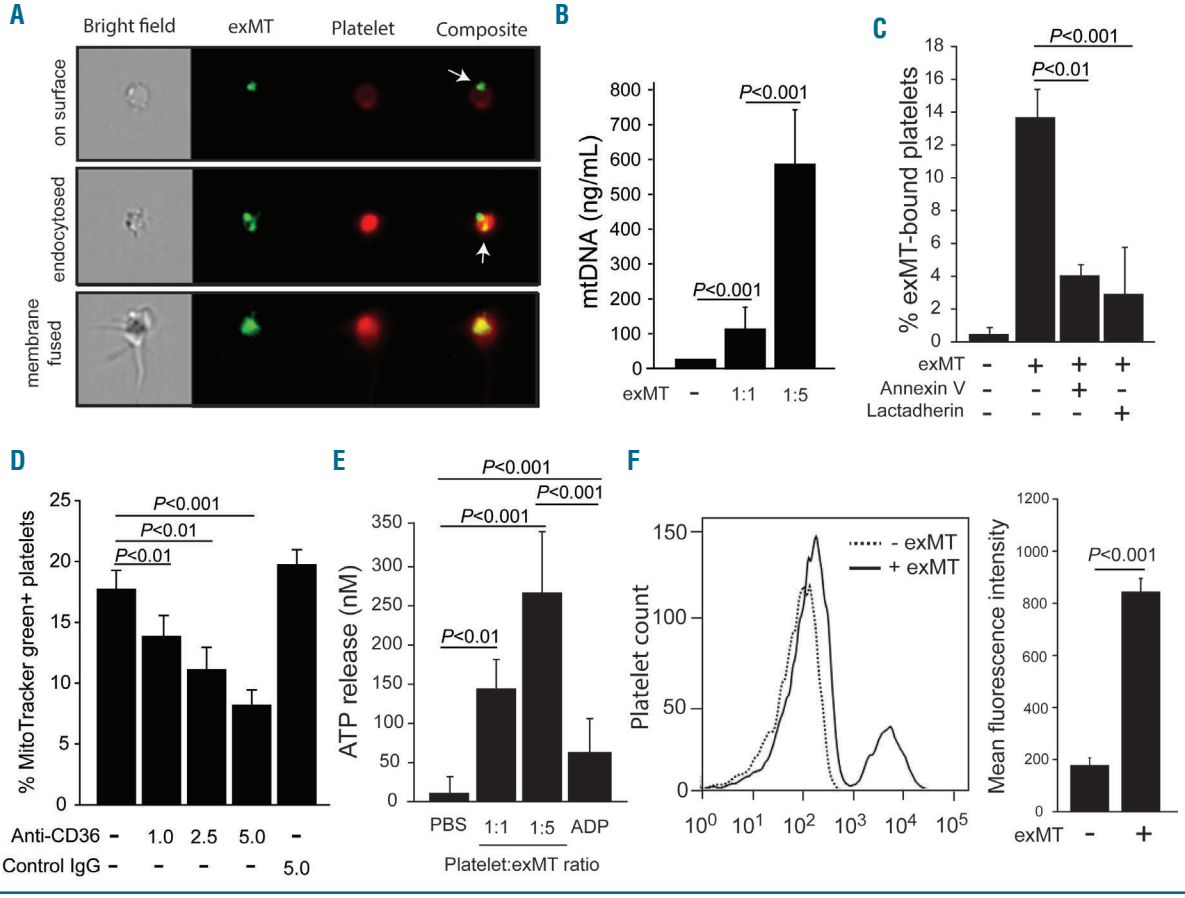

Figure 2. Anionic phospholipid and CD36 mediated the extracellular mitochondria-platelet interaction. (A) Amnis® flow cytometric images show extracellular mitochondria (exMT) binding a platelet (top panel), endocytosed by a platelet (middle panel), and fused with platelet membrane (bottom panel) after 30 min co-incubation at 37°C (representative images from 20,000 images randomly selected). (B) Platelets internalized exMT in a dose dependent manner, as determined by the presence of mouse mitochondrial DNA in mouse exMT-treated human platelets that were trypsinized to remove surface-bound exMT (n=20, one-way analysis of variance, ANOVA). (C, D) The formation of complexes between platelets and MitoTracker-Green$^+$ exMT (1:1 ratio) was blocked by 20 μg/mL of annexin V or 200 μg/mL of lactadherin (n=56, one-way ANOVA) (C) and by an anti-CD36 antibody (n=20, one-way ANOVA) (D). (E) ATP production was increased in exMT-treated platelets (n=24, one-way ANOVA). (F) FITC-conjugated annexin V bound platelets that were pretreated with exMT (left: a representative flow cytometric histogram; right: a summary from 12 experiments; paired Student *t* test).

pholipids as indicated by annexin V binding (Figure 2F) and had elevated levels of fibrinogen (Figure 5A) and coagulation factor Va on their surfaces (Figure 5B), suggesting that exMT-treated platelets could promote coagulation.[33,34] Consistent with this notion, exMT-treated platelets accelerated clot formation at a level comparable to that of collagen-activated platelets but lower than that of purified phosphatidylserine micelles (Figure 5C). When added to platelet-rich plasma, exMT-treated platelets significantly accelerated and enhanced thrombin-induced clot retraction (Figure 5D), which measures the integrin αIIbβ3-dependent retraction of platelet-bound fibrin fibers.[35,36] The effect of exMT was comparable to that of collagen-stimulated platelets. This procoagulant activity was independent of tissue factor, which was not detected on the surface of exMT-treated platelets (*Online Supplementary Figure S6*).

Anti-CD36 antibody blocked extracellular mitochondria-induced platelet activation

To measure exMT-induced platelet activation *in vivo*, non-injured mice were infused with purified exMT. Thirty minutes after infusion, platelets became exMT-bound (Figure 6A), expressed CD62p (Figure 6B), and formed complexes with leukocytes (Figure 6C). Mice infused with exMT also developed thrombocytopenia (Figure 6D). MitoTracker-Green-labeled exMT were detected in approximately 50% of platelet-leukocyte aggregates (Figure 6E). These phenotypic changes of platelets were prevented by infusing mice with exMT, together with a CD36 antibody but not isotype IgG.

Discussion

We investigated whether morphologically intact but cardiolipin-exposed exMT are metabolically active and, if so, whether they activate platelets through ROS. We have made several novel observations that define an exMT-induced and redox-dependent intermediate phenotype of platelets.

First, despite the cardiolipin translocation,[9] exMT found in TBI mice or released from brains subjected to freeze-thaw injury produced ATP and ROS (Figure 3B, C). Because metabolic activity of mitochondria requires a functional membrane, exMT that interact with platelets

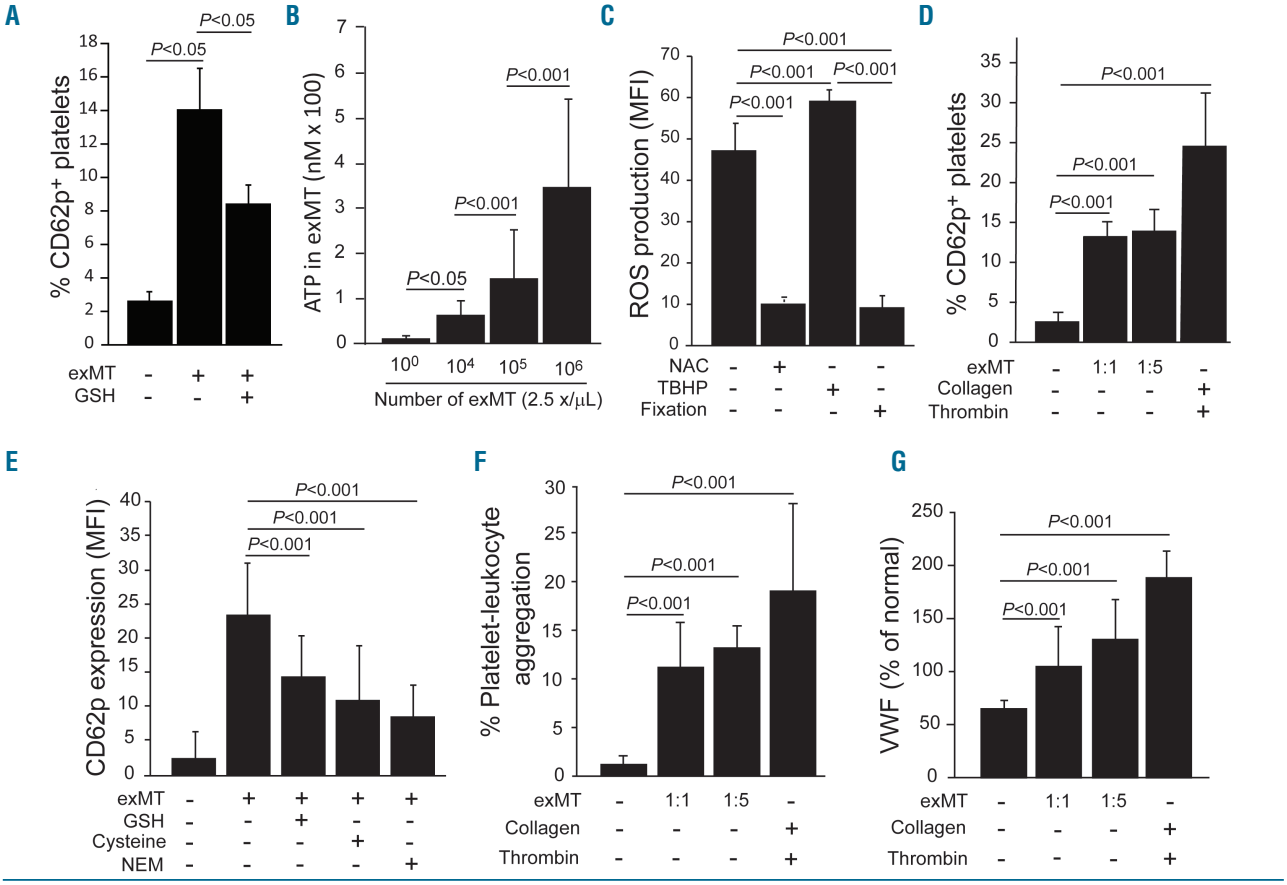

Figure 3. Extracellular mitochondria induced α-granule secretion of platelets through reactive oxygen species. (A) Extracellular mitochondria (exMT) purified from mice with traumatic brain injury stimulated platelets to express CD62 and this effect was blocked by 20 μM of glutathione (GSH) (n=45, one-way analysis of variance, ANOVA). (B, C) ExMT released from brains subjected to freeze-thaw injury produced ATP (n=4, one-way ANOVA) (B) and reactive oxygen species (ROS) ($2.5x10^8$/mouse of exMT; mean fluorescence intensity) at 37°C *in vitro*. The ROS production was blocked by the antioxidant N-acetylcysteine, enhanced by the oxidant tert-butyl hydroperoxide, and not detected in paraformaldehyde-fixed exMT (n=18, one-way ANOVA) (C). (D) Platelets incubated with exMT at a ratio of 1:1 or 1:5 for 30 min at 37°C expressed CD62p (n=24, one-way ANOVA). (E) The CD62p expression was reduced by 20 μM of GSH, 200 μM of L-cysteine, or 2 mM of NEM (n=30, one-way ANOVA). (F, G) ExMT-treated platelets formed complexes with leukocytes (n=24, one-way ANOVA) (F) and released von Willebrand factor (n=24, one-way ANOVA, *Online Supplementary Methods)* (G). For platelet activation, platelets stimulated with 5 μg/mL of collagen or 50 nM of thrombin were used as controls to mimic "coated platelets".[33] NAC: N-acetylcysteine; TBHP: tert-butyl hydroperoxide; MFI: mean fluorescence intensity; NEM: N-ethylmaleimide; vWF: von Willebrand factor.

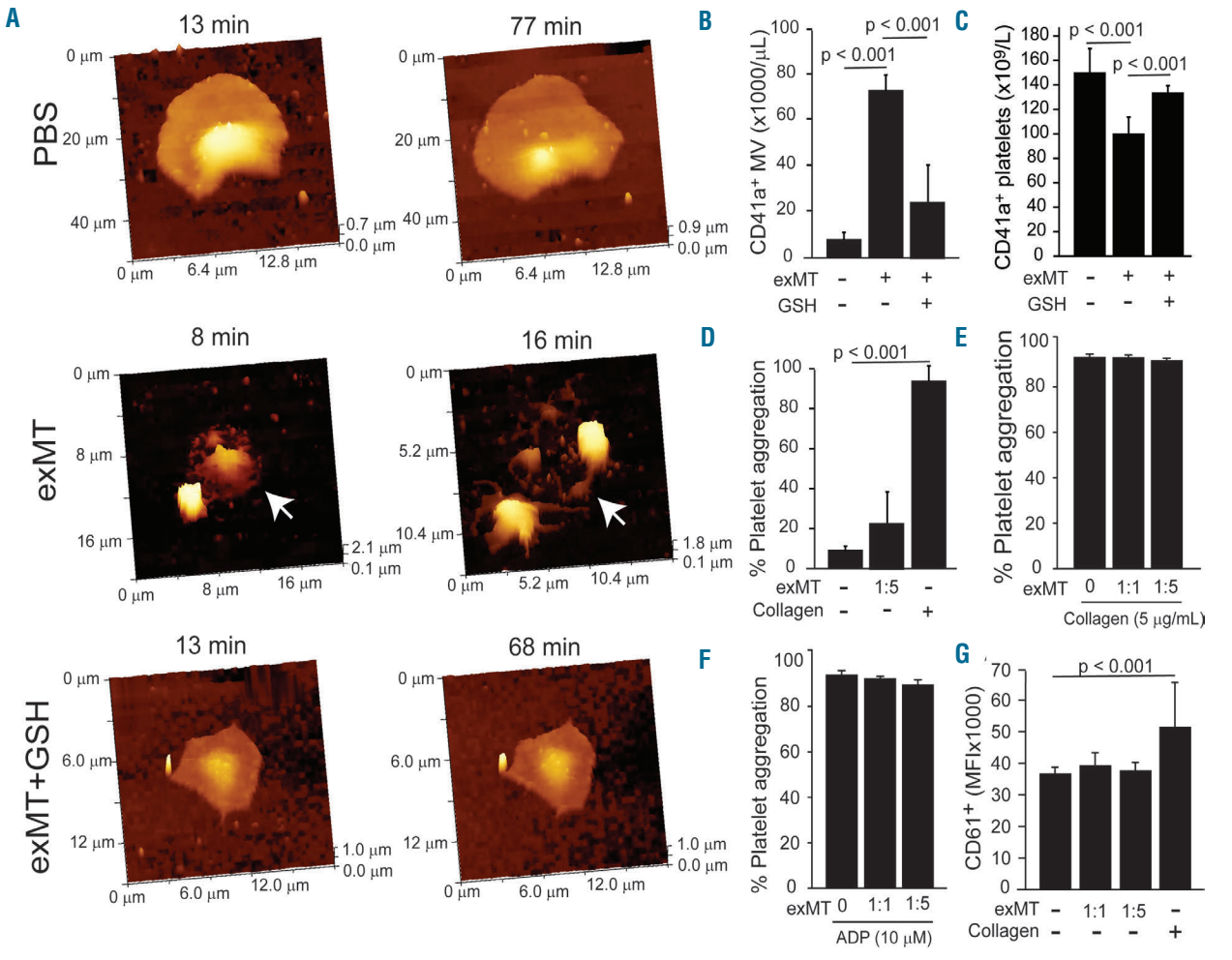

Figure 4. Extracellular mitochondria induced platelet disintegration, not aggregation. Platelets adherent to immobilized fibrinogen were treated with phosphate-buffered saline (PBS), extracellular mitochondria (exMT), or exMT + 20 µM of glutathione (GSH) for 30 min at 37 °C and repeatedly scanned for up to 80 min by hopping probe ion conductance microscopy. (A) The images show adherent platelets treated with PBS (top panel), exMT at a 1:1 ratio with platelets (middle panel; arrow: membrane disintegration of an adherent platelet), and GSH-treated exMT (bottom panel). The images are representative of three to six independent experiments. (B) The supernatants were collected and stained for CD41a+ microvesicles by flow cytometry (n=18, one-way analysis of variance, ANOVA). (C) Platelet counts before and after exMT treatment either alone or with GSH (n=15, one-way ANOVA). (D-F) ExMT induced minimal platelet aggregation (D) (n=24, one-way ANOVA), but exMT-treated platelets aggregated normally when stimulated with collagen (E) or ADP (F) (n=54, repeated measures ANOVA). (G) CD61 expression on exMT-treated platelets was comparable to that on untreated platelets but increased upon stimulation with 5 µg/mL of collagen (n=24, one-way ANOVA). MV: microvesicles; MFI: mean fluorescence intensity.

are likely those with an intact membrane. The metabolically active exMT formed complexes with platelets (Figures 1 and 2) which remained detectable in the circulation for at least 6 h after TBI (Figure 1C).[9] Cardiolipin on exMT and CD36 on platelets mediated the exMT-platelet interaction because: (i) cardiolipin is the dominant anionic phospholipid expressed on exMT[9] and (ii) the exMT-platelet interaction was blocked by the phospholipid binding proteins annexin V and lactadherin (Figure 2C) and by an antibody against CD36 (Figure 2D), which is a phospholipid receptor[37] that is expressed on platelets[38,39] and promotes phospholipid-mediated endocytosis.[40]

Second, exMT induced platelets to secrete their α-granule proteins (Figures 3 and 5) but failed to induce them to aggregate (Figure 4D) or promote platelet thrombus formation on the collagen matrix under arterial shear stress (*Online Supplementary Figure S4A-C*). There are several possible explanations for this apparent discrepancy. (i) Platelet-bound exMT may have interfered with the fibrinogen coupling of platelets through steric hindrance. This is unlikely because exMT-bound platelets aggregated after stimulation with collagen or ADP at levels comparable to those of platelets that had not been treated with exMT (Figure 4E, F). (ii) ExMT only activated 10-25% of platelets, insufficient to induce platelet aggregation. A similar effect was observed with platelets simultaneously treated with two antibodies against the integrins αIIb and β3,[41] suggesting that α-granule secretion alone is insufficient to induce platelet aggregation, but may prime platelets for activation by other agonists. (iii) Some or all exMT-stimulated platelets underwent drastic membrane disintegration to produce microvesicles (Figure 4A, B), thereby becoming unavailable for aggregation. The third possibility is supported by the reduction of platelet counts after exMT treatment (Figure 4C). This exMT-induced intermediate platelet phenotype resembles "coat-

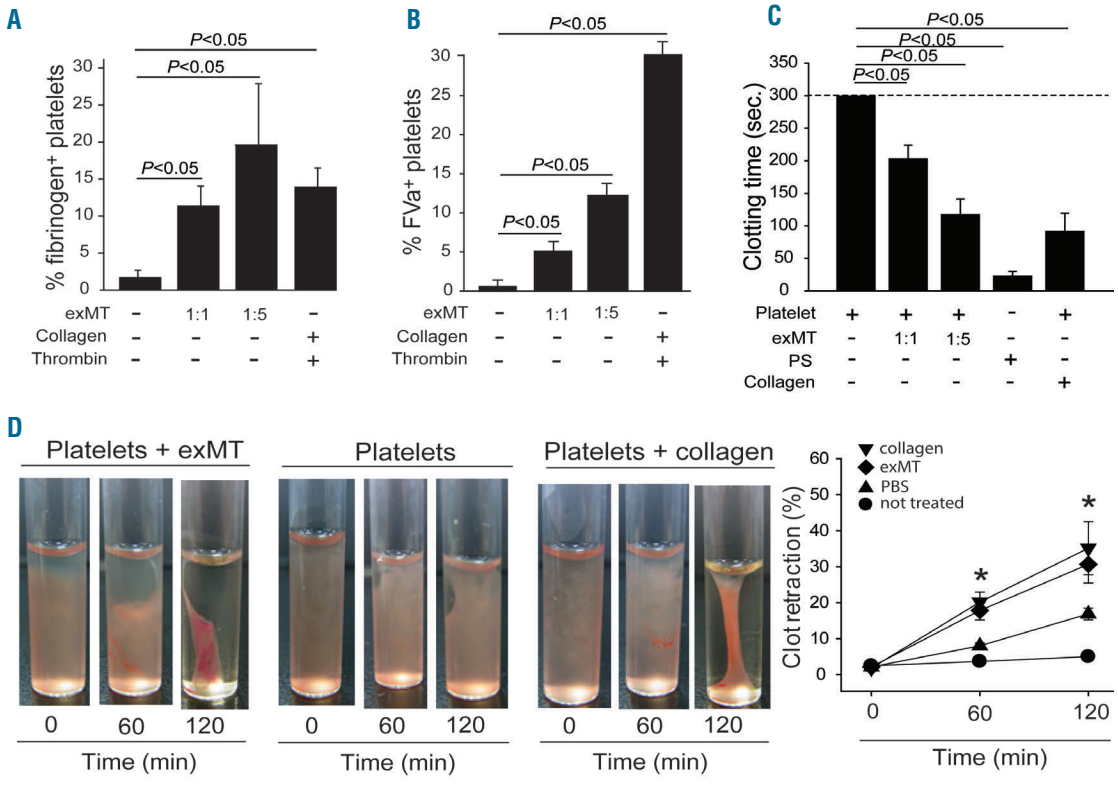

Figure 5. Extracellular mitochondria induced procoagulant activity of platelets and enhanced clot retraction. (A-C) Platelets incubated with extracellular mitochondria (exMT) at a ratio of 1:1 or 1:5 for 30 min at 37°C expressed increased amounts of fibrinogen (A) (n=24, one-way analysis of variance, ANOVA) and coagulation factor Va (B) (n=24, one-way ANOVA), and had shortened clotting time (C) (n=24, one-way ANOVA). Platelets stimulated with 5 μg/mL of collagen or 50 nM of thrombin were again used as controls to mimic "coated platelets." (D) Clot retraction in platelet-rich plasma was induced by 1 U/mL of thrombin in the presence of phosphate-buffered saline (PBS, left panel), exMT (1:1 ratio to platelets, middle panel), or 5 μg/mL of collagen (right panel). The graph in the right panel summarizes the results from multiple experiments (n=27, one-way ANOVA, *P<0.05 *vs.* PBS-treated). FVa: activated factor V; PS: phosphatidylserine.

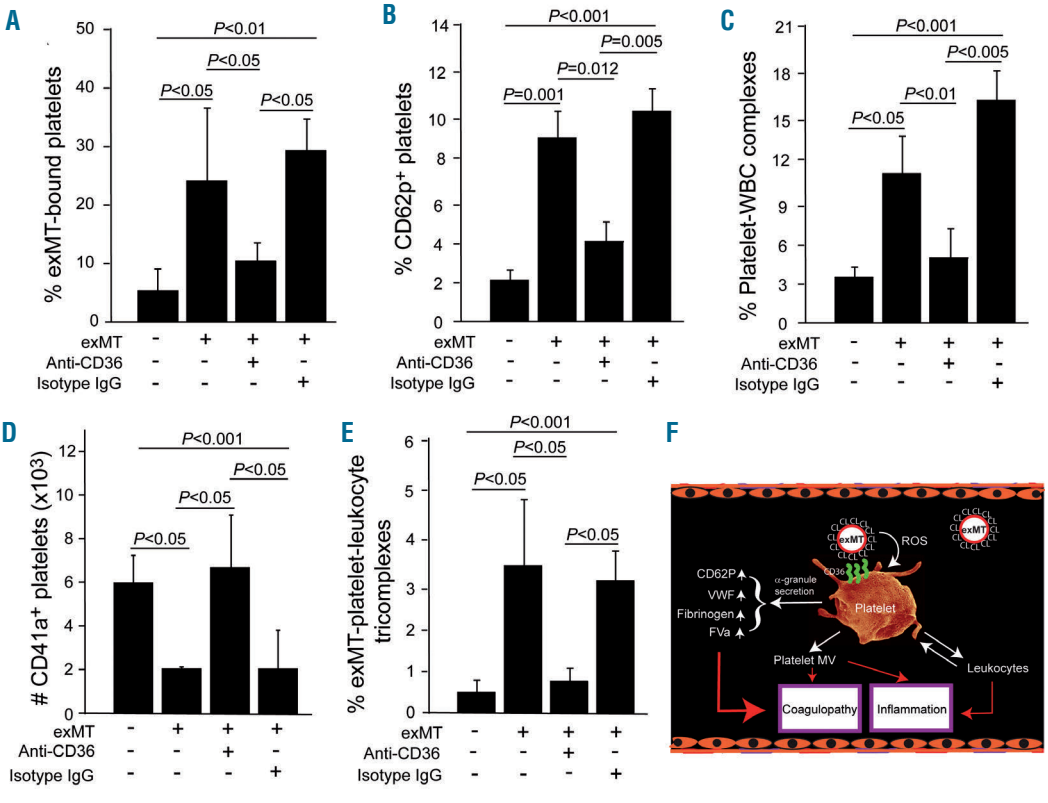

Figure 6. CD36 antibody reduced extracellular mitochondria-induced platelet activation. Non-injured mice were infused with 2 x 10^8/mouse of MitoTracker-Green-labeled extracellular mitochondria (exMT), together with CD36 antibody or isotype IgG. (A-F) Blood samples were collected 30 min after infusion to measure levels of exMT-bound platelets (A), CD62p+ platelets (B), platelet-leukocyte complexes (C), platelet counts (D), and platelet-leukocyte-exMT tri-complexes (E) by flow cytometry (n=16, one-way analysis of variance). (F) Schematic summary of the study. An injured brain releases metabolically active exMT that interact with platelets. These exMT induce α-granule secretion by platelets, but do not induce platelet aggregation. As a result, the exMT-bound platelets and platelet-derived microvesicles promote the systemic consumptive coagulopathy and inflammation that are consistently found during the acute phase of traumatic brain injury. WBC: white blood cell; ROS: reactive oxygen species; VWF: von Willebrand factor; FVa: activated factor V; MV: microvesicles.

ed platelets", which are defined as a subpopulation (12-30%) of platelets that express procoagulant activity upon stimulation by collagen and thrombin.[25,42] This procoagulant activity was also detected in exMT-treated platelets (Figure 5).

Third, the metabolic viability of exMT also suggests a potential role of ROS in the development of this intermediate platelet phenotype because ROS are known to activate platelets.[15-17] We have shown that ROS from exMT activated platelets (Figure 3) and induced platelet microvesiculation (Figure 4) in an oxidant-dependent manner. A physical contact between exMT and platelets appears to be required for the ROS-induced platelet secretion because ROS primarily affect exMT-bound platelets. This direct exMT-platelet interaction may concentrate ROS activity on exMT-bound cells or protect the oxidants from plasma antioxidants.

In summary, we have shown that exMT-bound platelets develop an intermediate phenotype using ROS as mediators. This intermediate phenotype is characterized by α-granule secretion, procoagulant activity and poor aggregation (Figure 6F). As a result, these procoagulant platelets remain in the circulation to promote non-focal coagulation, similar to the consumptive coagulopathy found in TBI patients[43,44] and mouse models.[9] While previous studies have found protective effects of exMT on target cells,[10,12,13] our study demonstrates that these exMT could also have detrimental effects by making platelets procoagulant and prothrombotic. The findings from this study could have much broader implications regarding exMT in other pathologies in which hypercoagulable and inflammatory states develop, such as severe infections, autoimmune diseases, and cancer.

Funding

This study was supported by NIH grants NS087296 and HL71895 (JFD), National Natural Science Foundation of China State Key Program grant 81330029 (JNZ), National Natural Science Foundation of China Major International Joint Research Project 81720108015 (JNZ), National Natural Science Foundation of China Research grants 81271361, 81271359 (JNZ) and 81601068 (ZLZ), Natural Science Foundation of Tianjin 17JCQNJC12100 (ZLZ) and a regional scientific grant 16PTSTJC00180 (JNZ).

References

1. Cap AP, Spinella PC. Severity of head injury is associated with increased risk of coagulopathy in combat casualties. J Trauma. 2011;71(1 Suppl):S78-81.
2. Sun Y, Wang J, Wu X, et al. Validating the incidence of coagulopathy and disseminated intravascular coagulation in patients with traumatic brain injury--analysis of 242 cases. Br J Neurosurg. 2011;25(3):363-368.
3. Talving P, Benfield R, Hadjizacharia P, Inaba K, Chan LS, Demetriades D. Coagulopathy in severe traumatic brain injury: a prospective study. J Trauma. 2009;66(1):55-63.
4. Stein SC, Young GS, Talucci RC, Greenbaum BH, Ross SE. Delayed brain injury after head trauma: significance of coagulopathy. Neurosurgery. 1992;30(2):160-165.
5. Kaufman HH, Moake JL, Olson JD, et al. Delayed and recurrent intracranial hematomas related to disseminated intravascular clotting and fibrinolysis in head injury. Neurosurgery. 1980;7(5):445-449.
6. Wafaisade A, Lefering R, Tjardes T, et al. Acute coagulopathy in isolated blunt traumatic brain injury. Neurocrit Care. 2010;12(2):211-219.
7. Stein SC, Chen XH, Sinson GP, Smith DH. Intravascular coagulation: a major secondary insult in nonfatal traumatic brain injury. J Neurosurg. 2002;97(6):1373-1377.
8. Tian Y, Salsbery B, Wang M, et al. Brain-derived microparticles induce systemic coagulation in a murine model of traumatic brain injury. Blood. 2015;125(13):2151-2159.
9. Zhao Z, Wang M, Tian Y, et al. Cardiolipin-mediated procoagulant activity of mitochondria contributes to traumatic brain injury-associated coagulopathy in mice. Blood. 2016;127(22):2763-2772.
10. Hayakawa K, Esposito E, Wang X, et al. Transfer of mitochondria from astrocytes to neurons after stroke. Nature. 2016;535(7613):551-555.
11. Davis CH, Kim KY, Bushong EA, et al. Transcellular degradation of axonal mitochondria. Proc Natl Acad Sci U S A. 2014;111(26):9633-9638.
12. Islam MN, Das SR, Emin MT, et al. Mitochondrial transfer from bone-marrow-derived stromal cells to pulmonary alveoli protects against acute lung injury. Nat Med. 2012;18(5):759-765.
13. Moschoi R, Imbert V, Nebout M, et al. Protective mitochondrial transfer from bone marrow stromal cells to acute myeloid leukemic cells during chemotherapy. Blood. 2016;128(2):253-264.
14. Schon EA, DiMauro S, Hirano M. Human mitochondrial DNA: roles of inherited and somatic mutations. Nat Rev Genet. 2012;13(12):878-890.
15. Begonja AJ, Gambaryan S, Geiger J, et al. Platelet NAD(P)H-oxidase-generated ROS production regulates alphaIIbbeta3-integrin activation independent of the NO/cGMP pathway. Blood. 2005;106(8):2757-2760.
16. Arthur JF, Qiao J, Shen Y, et al. ITAM receptor-mediated generation of reactive oxygen species in human platelets occurs via Syk-dependent and Syk-independent pathways. J Thromb Haemost. 2012;10(6):1133-1141.
17. Bosin TR, Schaltenbrand SL. Stimulation of platelet serotonin transport by substituted 1,4-naphthoquinone-induced oxidant stress. Biochem Pharmacol. 1991;41(6-7):967-974.
18. Lorente L, Martin MM, Gonzalez-Rivero AF, et al. Serum soluble CD40 ligand levels are associated with severity and mortality of brain trauma injury patients. Thromb Res. 2014;134(4):832-836.
19. Castellino FJ, Chapman MP, Donahue DL, et al. Traumatic brain injury causes platelet adenosine diphosphate and arachidonic acid receptor inhibition independent of hemorrhagic shock in humans and rats. J Trauma Acute Care Surg. 2014;76(5):1169-1176.
20. Sillesen M, Johansson PI, Rasmussen LS, et al. Platelet activation and dysfunction in a large-animal model of traumatic brain injury and hemorrhage. J Trauma Acute Care Surg. 2013;74(5):1252-1259.
21. Dietrich WD, Alonso O, Busto R, et al. Posttraumatic cerebral ischemia after fluid percussion brain injury: an autoradiographic and histopathological study in rats. Neurosurgery. 1998;43(3):585-593.
22. Lu D, Mahmood A, Goussev A, Qu C, Zhang ZG, Chopp M. Delayed thrombosis after traumatic brain injury in rats. J Neurotrauma. 2004;21(12):1756-1766.
23. Zhang JN, Bergeron AL, Yu Q, et al. Duration of exposure to high fluid shear stress is critical in shear-induced platelet activation-aggregation. Thromb Haemost. 2003;90(4):672-678.
24. Yuan H, Houck KL, Tian Y, et al. Piperlongumine blocks JAK2-STAT3 to inhibit collagen-induced platelet reactivity independent of reactive oxygen species. PLoS One. 2015;10(12):e0143964.
25. Alberio L, Safa O, Clemetson KJ, Esmon CT, Dale GL. Surface expression and functional characterization of alpha-granule factor V in human platelets: effects of ionophore A23187, thrombin, collagen, and convulxin. Blood. 2000;95(5):1694-1702.
26. Tracy PB, Mann KG. Prothrombinase complex assembly on the platelet surface is mediated through the 74,000-dalton component of factor Va. Proc Natl Acad Sci U S A. 1983;80(8):2380-2384.
27. Hierso R, Waltz X, Mora P, et al. Effects of oxidative stress on red blood cell rheology in sickle cell patients. Br J Haematol. 2014;166(4):601-606.
28. Zhou Y, Cai W, Zhao Z, et al. Lactadherin promotes microvesicle clearance to prevent coagulopathy and improves survival of severe TBI mice. Blood. 2018;131(5):563-572.
29. Ghosh A, Li W, Febbraio M, et al. Platelet CD36 mediates interactions with endothelial cell-derived microparticles and contributes to thrombosis in mice. J Clin Invest. 2008;118(5):1934-1943.

30. Pascual G, Avgustinova A, Mejetta S, et al. Targeting metastasis-initiating cells through the fatty acid receptor CD36. Nature. 2017;541(7635):41-45.
31. Saliba AE, Vonkova I, Gavin AC. The systematic analysis of protein-lipid interactions comes of age. Nat Rev Mol Cell Biol. 2015;16(12):753-761.
32. Samuni Y, Goldstein S, Dean OM, Berk M. The chemistry and biological activities of N-acetylcysteine. Biochim Biophys Acta. 2013;1830(8):4117-4129.
33. Dale GL, Friese P, Batar P, et al. Stimulated platelets use serotonin to enhance their retention of procoagulant proteins on the cell surface. Nature. 2002;415(6868):175-179.
34. Prodan CI, Vincent AS, Dale GL. Coated-platelet levels increase with number of injuries in patients with mild traumatic brain injury. J Neurotrauma. 2016;33(9):818-824.
35. Carr ME, Jr., Carr SL. Fibrin structure and concentration alter clot elastic modulus but do not alter platelet mediated force development. Blood Coagul Fibrinolysis. 1995;6(1):79-86.
36. Carr ME, Jr., Carr SL, Hantgan RR, Braaten J. Glycoprotein IIb/IIIa blockade inhibits platelet-mediated force development and reduces gel elastic modulus. Thromb Haemost. 1995;73(3):499-505.
37. Fadok VA, Bratton DL, Frasch SC, Warner ML, Henson PM. The role of phosphatidylserine in recognition of apoptotic cells by phagocytes. Cell Death Differ. 1998;5(7):551-562.
38. Rigotti A, Acton SL, Krieger M. The class B scavenger receptors SR-BI and CD36 are receptors for anionic phospholipids. J Biol Chem. 1995;270(27):16221-16224.
39. Podrez EA, Byzova TV, Febbraio M, et al. Platelet CD36 links hyperlipidemia, oxidant stress and a prothrombotic phenotype. Nat Med. 2007;13(9):1086-1095.
40. Tait JF, Smith C. Phosphatidylserine receptors: role of CD36 in binding of anionic phospholipid vesicles to monocytic cells. J Biol Chem. 1999;274(5):3048-3054.
41. Newman PJ, McEver RP, Doers MP, Kunicki TJ. Synergistic action of two murine monoclonal antibodies that inhibit ADP-induced platelet aggregation without blocking fibrinogen binding. Blood. 1987;69(2):668-676.
42. Hamilton SF, Miller MW, Thompson CA, Dale GL. Glycoprotein IIb/IIIa inhibitors increase COAT-platelet production in vitro. J Lab Clin Med. 2004;143(5):320-326.
43. Bulstrode H, Nicoll JA, Hudson G, Chinnery PF, Di Pietro V, Belli A. Mitochondrial DNA and traumatic brain injury. Ann Neurol. 2014;75(2):186-195.
44. Walko TD 3rd, Bola RA, Hong JD, et al. Cerebrospinal fluid mitochondrial DNA: a novel DAMP in pediatric traumatic brain injury. Shock. 2014;41(6):499-503.

Ferrata Storti Foundation

Haematologica 2019
Volume 105(1):218-225

Neutrophils and neutrophil extracellular traps enhance venous thrombosis in mice bearing human pancreatic tumors

Yohei Hisada,[1] Steven P. Grover,[1] Anaum Maqsood,[1] Reaves Houston,[1] Cihan Ay,[2] Denis F. Noubouossie,[1] Brian C. Cooley,[3] Håkan Wallén,[4] Nigel S. Key,[1] Charlotte Thålin,[5] Ádám Z. Farkas,[6] Veronika J. Farkas,[6] Kiril Tenekedjiev,[7,8] Krasimir Kolev[6] and Nigel Mackman[1]

[1]Department of Medicine, Division of Hematology and Oncology, University of North Carolina at Chapel Hill, Chapel Hill, NC, USA; [2]Department of Medicine I, Clinical Division of Hematology and Hemostaseology, Medical University of Vienna, Vienna, Austria; [3]Department of Pathology and Laboratory Medicine, University of North Carolina at Chapel Hill, Chapel Hill, NC, USA; [4]Department of Clinical Sciences, Danderyd Hospital, Division of Cardiovascular Medicine, Karolinska Institutet, Stockholm, Sweden; [5]Department of Clinical Sciences, Danderyd Hospital, Division of Internal Medicine, Karolinska Institutet, Stockholm, Sweden; [6]Department of Medical Biochemistry, Semmelweis University, Budapest, Hungary; [7]Australian Maritime College, University of Tasmania, Launceston, Australia and [8]Department of Information Technology, Nikola Vaptsarov Naval Academy, Varna, Bulgaria

ABSTRACT

Pancreatic cancer is associated with a high incidence of venous thromboembolism. Neutrophils have been shown to contribute to thrombosis in part by releasing neutrophil extracellular traps (NET). A recent study showed that increased plasma levels of the NET biomarker, citrullinated histone H3 (H3Cit), are associated with venous thromboembolism in patients with pancreatic and lung cancer but not in those with other types of cancer, including breast cancer. In this study, we examined the contribution of neutrophils and NET to venous thrombosis in nude mice bearing human pancreatic tumors. We found that tumor-bearing mice had increased circulating neutrophil counts and levels of granulocyte-colony stimulating factor, neutrophil elastase, H3Cit and cell-free DNA compared with controls. In addition, thrombi from tumor-bearing mice contained increased levels of the neutrophil marker Ly6G, as well as higher levels of H3Cit and cell-free DNA. Thrombi from tumor-bearing mice also had denser fibrin with thinner fibers consistent with increased thrombin generation. Importantly, either neutrophil depletion or administration of DNase I reduced the thrombus size in tumor-bearing but not in control mice. Our results, together with clinical data, suggest that neutrophils and NET contribute to venous thrombosis in patients with pancreatic cancer.

Correspondence:

NIGEL MACKMAN
nmackman@med.unc.edu

Received: January 18, 2019.

Accepted: April 24, 2019.

Pre-published: May 2, 2019.

doi:10.3324/haematol.2019.217083

Check the online version for the most updated information on this article, online supplements, and information on authorship & disclosures: www.haematologica.org/content/105/1/218

Introduction

Cancer patients have a 4- to 7-fold increased risk of venous thromboembolism (VTE) compared with the general population.[1] However, the rates of VTE vary in different cancer types. For instance, breast cancer has a low rate whereas pancreatic cancer has a high rate of VTE.[2] This variability suggests that there may be cancer type-specific mechanisms of VTE.[3] For instance, we found an association between levels of circulating extracellular vesicle tissue factor activity and VTE in pancreatic cancer in two studies and a borderline significance in a third study.[4-6] Circulating tumor-derived, tissue factor-positive extracellular vesicles are also observed in mice bearing human pancreatic tumors[7-10] Importantly, we have shown that these tumor-derived, human tissue factor-positive extracellular vesicles enhance venous thrombosis in mice.[10]

Leukocytosis is often observed in cancer patients, particularly patients with lung and colorectal cancer.[3] Leukocytosis is also associated with VTE in cancer patients, and is a component of the Khorana Risk Score for predicting chemotherapy-asso-

ciated thrombosis in ambulatory cancer patients.[11-13] In addition, some patients have increased circulating levels of hematopoietic cytokines, such as granulocyte-colony stimulating factor (G-CSF).[14] The coagulation cascade is activated by pathogens as part of the innate immune system to limit dissemination of infection.[15] Recently, the term "immunothrombosis" was introduced to describe the contribution of immune cells to thrombus.[16] Activated monocytes can trigger thrombosis by expressing tissue factor.[17] Activated neutrophils release proteases, such as neutrophil elastase (NE), which enhance thrombosis by degrading the anticoagulant protein tissue factor pathway inhibitor.[18] In addition, neutrophils release neutrophil extracellular traps (NET). NET are composed of extracellular chromatin components and neutrophil granule proteins that enhance thrombosis by capturing platelets and procoagulant extracellular vesicles.[19-22] NET are present in both arterial and venous thrombi.[19,23,24] NET can also obstruct smaller blood vessels in a coagulation-independent manner.[25] Interestingly, two studies showed that neutrophils contribute to thrombosis in the mouse inferior vena cava (IVC) stenosis model, although this was not observed in a third study.[20,26,27] In contrast, neutrophil depletion did not affect thrombosis in the IVC stasis model.[28]

There is a wide range of agonists that can induce NET formation.[29] In neutrophils histone citrullination by peptidylarginine deiminases (PAD), including PAD4, is considered a driver of chromatin decondensation and subsequent NET formation.[30] PAD4 is also expressed by the human breast cancer cell line MCF7.[31] Citrullinated histones, such as citrullinated histone H3 (H3Cit), are therefore widely used as a biomarker of NET formation. In mice, it has been proposed that PAD4 is required for NET formation.[32] Indeed, PAD4$^{-/-}$ mice have smaller thrombi in the IVC stenosis model.[33] However, a recent study found that inhibition of PAD did not affect human neutrophil NET formation induced by a variety of pathogens,[29] suggesting that certain forms of NET formation can occur without PAD. Interestingly, a recent study found an association between plasma levels of H3Cit and VTE in patients with pancreatic and lung cancer but not in those with other types of cancer, such as breast cancer.[34] In another study plasma levels of nucleosomes and cell-free DNA (cfDNA) were higher in cancer patients than in healthy controls, but these are not NET-specific biomarkers.[35]

Neutrophilia was observed in mice bearing murine breast 4T1 tumors and human pancreatic BxPc-3 tumors.[10,36-38] In addition, mice bearing 4T1 breast tumors had increased levels of circulating markers of neutrophil activation and NET, such as H3Cit and myeloperoxidase.[37,38] Furthermore, tumor-bearing mice had more rapid thrombotic occlusion in a jugular vein Rose Bengal/laser-induced injury model.[38] Interestingly, administration of DNase I to degrade cfDNA and NET did not affect thrombotic occlusion in control mice but provided protection from the enhanced venous thrombosis observed in tumor-bearing mice.[38] These studies suggest that neutrophils and NET contribute to venous thrombosis in a murine breast cancer model.

In the light of recent clinical data suggesting a role of NET in VTE in patients with pancreatic cancer,[34] we investigated the contribution of neutrophils and NET to venous thrombosis in mice bearing human pancreatic BxPc-3 tumors.

Methods

Cells and the mouse tumor model

We used a human pancreatic cancer cell line BxPc-3 expressing the firefly luciferase reporter.[10] BxPc-3 tumors were grown in the pancreas of Crl:NU-*Foxn1*^{nu} male mice (nude mice) and monitored by measuring luciferase expression.[10] We used mice with tumors weighing from 1.5 to 3.9 grams. All animal studies were approved by the University of North Carolina at Chapel Hill Animal Care and Use Committee, and complied with National Institutes of Health guidelines.

Measurement of blood cells

A Hemavet HV950FS (Drew Scientific, Miami Lakes, FL, USA) was used to count neutrophils.

Preparation of plasma and measurement of plasma biomarkers

Blood was collected[39] and plasma was prepared by centrifuging the blood at 4500 x *g* for 15 min. CfDNA was quantified as described elsewhere.[40] Mouse G-CSF and NE were measured using commercially available enzyme-linked immunosorbent assays (R&D systems, Minneapolis, MN, USA). H3Cit was measured using an in-house enzyme-linked immunosorbent assay.[41]

Thrombosis model

We used the IVC stasis model of thrombosis.[10]

Western blot analysis of thrombus samples

Processing of thrombi and detection of primary antibodies is described in the *Online Supplementary Methods*. Membranes were probed with 2 μg/mL anti-Ly6G (BioXCell, West Lebanon, NH, USA), a 1,000-fold dilution of anti-β-actin (Abgent, San Diego, CA, USA), a 2,000-fold dilution of anti-PAD4 (Abcam), 1 μg/mL anti-H3Cit (Abcam) or 0.5 μg/mL anti-histone H3 (Abcam) primary antibody.

Immunofluorescence

Analysis of thrombi by immunofluorescence is described in the *Online Supplementary Methods*. Areas of different fluorescent signals were quantified using Image J software.

Scanning electron microscopy

Analysis of thrombi by scanning electron microscopy is described in the *Online Supplementary Methods*.

Neutrophil depletion

Neutrophils were depleted by intravenous administration of 5 mg/kg anti-Ly6G antibody (BioXCell) 24 h and 1 h before IVC stasis. A rat IgG (Sigma-Aldrich) was used as a control.

DNase I treatment

DNase I (50 U/mouse (Genentech, South San Francisco, CA, USA) or phosphate-buffered saline was intravenously administered to mice 1 h before and 24 h after IVC stasis.

Statistical analysis

Data are shown as mean ± standard error of the means for normally distributed data or median ± interquartile range for non-normally distributed data. The Shapiro-Wilk test was used to determine normality. For the majority of the studies two-group comparisons, the unpaired two-tailed Student t-test or the Mann-Whitney U-test was used depending on the data distribution. For the ultrasound data, two-way analysis of variance with the Sidak multiple comparison test was used. These statistical analyses were

performed with GraphPad PRISM version 7.03 (GraphPad Software, La Jolla, CA, USA). For immunofluorescence data and scanning electron microscopy data, bootstrap simulations of the chosen quantiles of the distribution of the measured values were performed[42] followed by a Bootstrap Kuiper test for identity of the quantile distributions.[43] These statistical analyses are described in detail in the *Online Supplementary Material*. *P* values <0.05 were considered statistically significant for all experiments.

Results

Measurement of circulating neutrophil counts and different biomarkers in mice bearing human pancreatic tumors

We measured the numbers of neutrophils in whole blood and various circulating biomarkers in the plasma of mice bearing human BxPc-3 pancreatic tumors (1.5-3.9 grams) and in control mice. We observed significant increases in neutrophil numbers and mouse G-CSF levels in tumor-bearing mice compared with those in controls (Figure 1A, B). We did not observe an increase in human G-CSF (*data not shown*). We found a significant correlation between circulating neutrophil count and mouse G-CSF level (r = 0.83, *P*=0.02, Spearman test). In addition, we found significant increases in the neutrophil biomarker NE and the NET biomarker H3Cit in tumor-bearing mice compared with controls (Figure 1C, D). Finally, the amount of cfDNA was significantly greater in tumor-bearing mice than in controls (Figure 1E).

The human breast cancer cell line MCF7 expresses PAD4.[31] We therefore determined whether BxPc-3 cells also express PAD4. Western blotting showed that the BxPc-3 cells did express PAD4 protein (*data not shown*). Tumor cells may, therefore, also contribute to plasma H3Cit.

Measurement of neutrophils, histone H3 and citrullinated histone H3 in thrombi from mice bearing human pancreatic tumors

We generated thrombi in control and tumor-bearing mice using the IVC stasis model. Using western blotting, we measured levels of Ly6G (a neutrophil marker), β-actin (a housekeeping gene), histone H3 (a marker of cellular content), and H3Cit (a NET biomarker) in thrombi from mice bearing human pancreatic tumors and control mice (Figure 2A). Thrombi from tumor-bearing mice had higher levels of Ly6G, β-actin, histone H3, and H3Cit compared with the levels in thrombi from control mice (Figure 2 B-E). The H3Cit/H3 ratio for thrombi from control mice was ~1 (Figure 2F). Interestingly, there was significant variation in the H3Cit/H3 ratio in thrombi from tumor-bearing mice (Figure 2F).

Next, we measured the cfDNA and H3Cit content in thrombi from mice bearing human pancreatic tumors and in thrombi from controls using immunofluorescence. Consistent with the data from the western blot analysis, thrombi from tumor-bearing mice had increased levels of cfDNA and H3Cit compared with levels of these biomarkers in thrombi from control mice (Figure 3).

Finally, we analyzed the composition of thrombi from control and tumor-bearing mice by scanning electron microscopy. Red blood cells were decreased in thrombi from tumor-bearing mice compared with thrombi from control mice (Figure 4A). In addition, we observed an increase in fibrin density and a decrease in fibrin fiber thickness in thrombi from tumor-bearing mice compared with thrombi from controls (Figure 4B). Previous studies

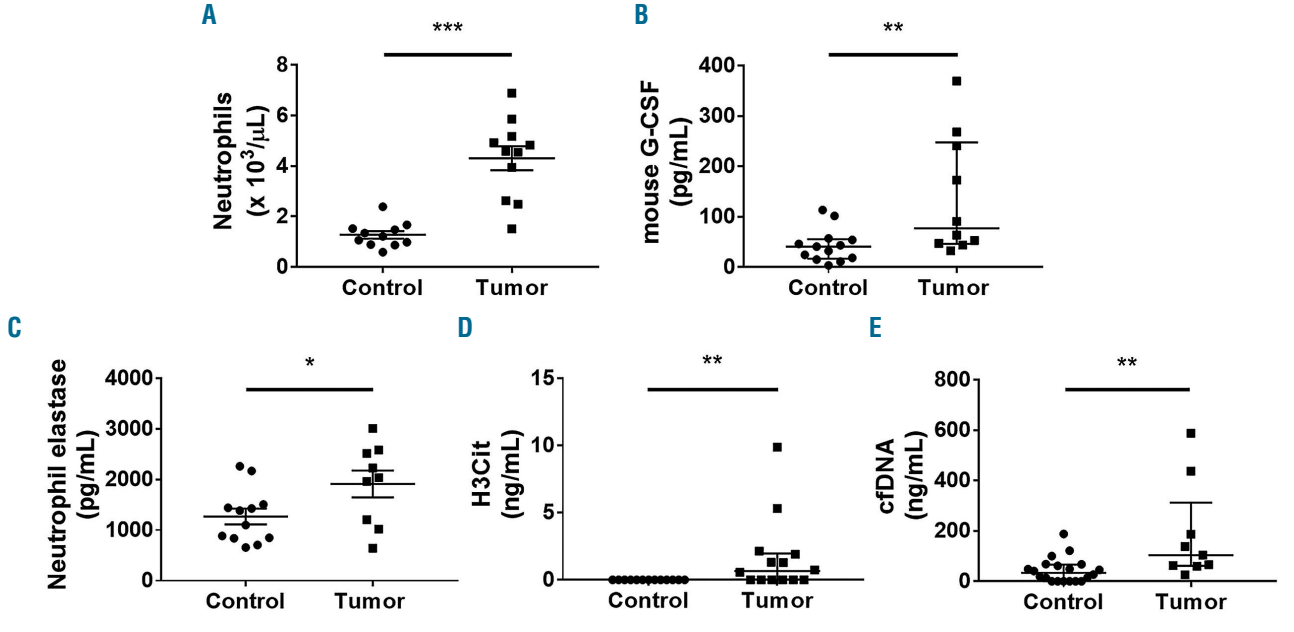

Figure 1. Levels of neutrophils and circulating biomarkers in blood samples. (A-E) Neutrophil counts in whole blood (A) and circulating mouse granulocyte-colony stimulating factor (G-CSF) (B), neutrophil elastase (C), citrullinated histone H3 (H3Cit) (D), and cell-free (cf) DNA (E) in plasma of control and tumor-bearing mice. Nine to 20 mice were used for each group. Data were analyzed with either the unpaired *t*-test or the Mann-Whitney U-test, depending on the type of data distribution. **P*<0.05, ***P*<0.01, ****P*<0.001.

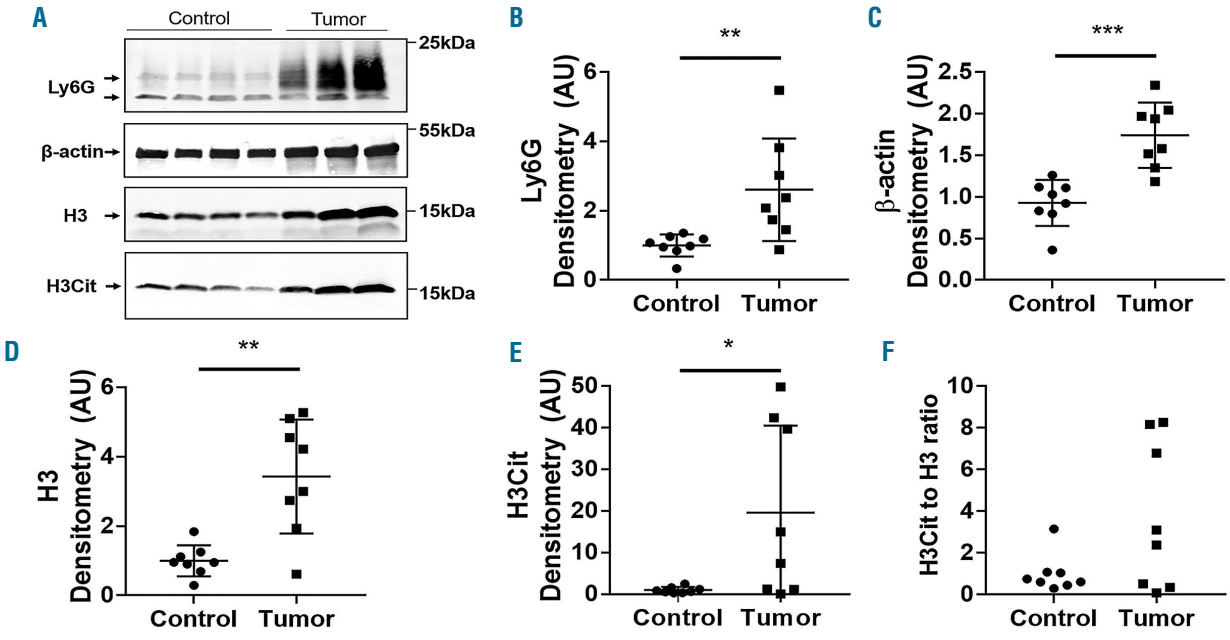

Figure 2. Analysis of thrombus constituents. (A) Representative western blot of Ly6G, β-actin, histone H3, and citrullinated histone H3 (H3Cit) in thrombi from control and tumor-bearing mice. Arrows on the left of the panel indicate the target proteins and the size of the molecular weight markers are shown on the right. (B-E) Levels of the different markers were quantified by densitometric analysis. (F) The H3Cit/H3 ratio for thrombi from control and tumor-bearing mice are shown. AU: arbitrary unit. Eight mice were used for each group. Data were analyzed with the unpaired *t*-test or the Mann-Whitney U-test depending on the type of data distribution. **P*<0.05, ***P*<0.01, ****P*<0.001.

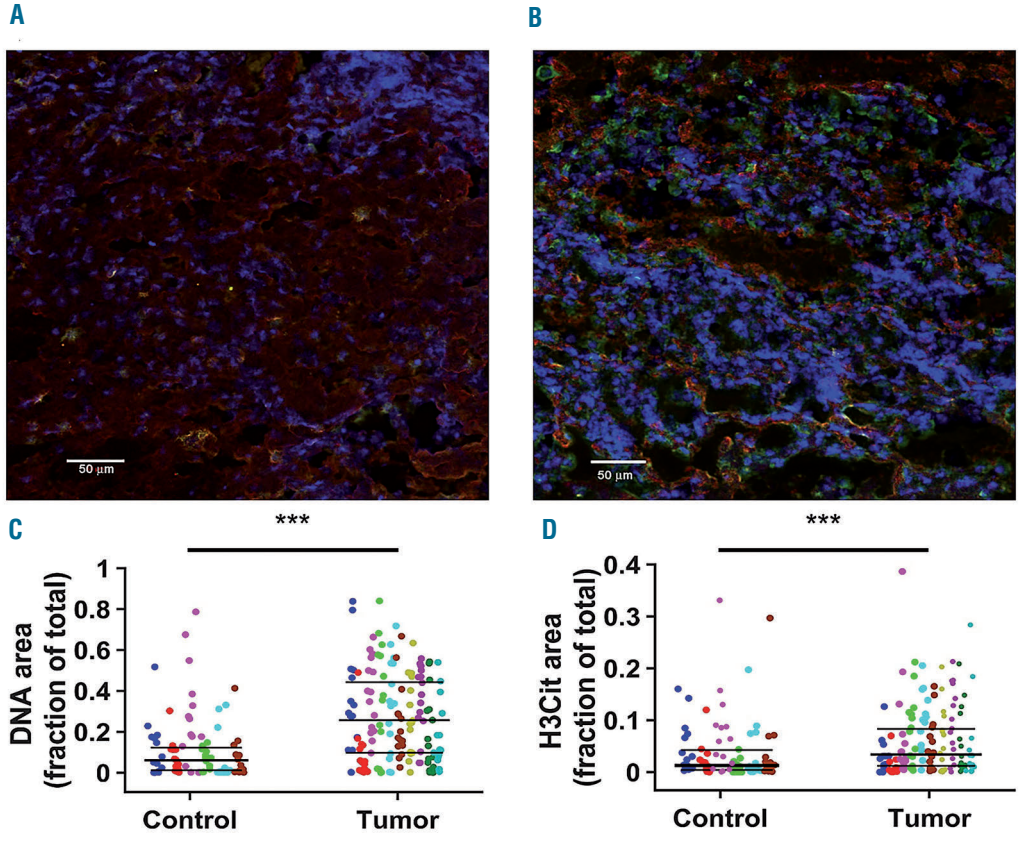

Figure 3. Analysis of thrombi by immunofluorescence. (A, B) Thrombus sections from control (A) and tumor-bearing (B) mice were stained for cell-free DNA (TOTO-3, blue), citrullinated histone H3 (H3Cit; immunostained, green) and fibrin (immunostained, red) and examined with confocal laser scanning microscopy (Zeiss LSM 710, Carl Zeiss, Jena, Germany). (C, D) The area occupied by the DNA (C) and H3Cit (D) signal was quantified in 15 randomly selected images from each thrombus shown with the same color. Lines indicate the median values of the bottom, median and top quartiles calculated from the data of 90 images from six animals of the control group (shown in different colors) and 150 images from ten animals of the tumor group (shown in different colors). The statistical analysis was performed using 90 or 150 input data according to the two-step procedure described in the *Online Supplement* (Bootstrap Kuiper test *P*<0.001 for all three quartiles of the datasets in panels C and D).

have shown that increased levels of thrombin lead to the generation of denser fibrin with thinner fibers.[44]

Effect of neutrophil depletion on thrombus size in mice bearing human pancreatic tumors

Thrombi in the group of tumor-bearing mice treated with IgG weighed significantly more than those in controls [controls *vs.* tumor-bearing mice (median [range]): 16.4 [13.8-22.4] g *vs.* 31.9 [29.1-36.5] g; $P<0.001$, n=4-5]. Next, we investigated the role of neutrophils in thrombus formation in tumor-bearing mice and control mice by depleting neutrophils using the anti-Ly6G antibody 1A8. Administration of 1A8 significantly decreased levels of circulating neutrophils in both control mice [IgG *vs.* 1A8 (median [range]): 2.9 [1.9-4.4] x 10^3/μL *vs.* 0.3 [0.2-1.3] x 10^3/μL; $P<0.05$, n=4-5] and mice bearing human pancreatic tumors [IgG *vs.* 1A8 (median [range]): 6.7 [3.8-8.5] x 10^3/μL *vs.* 1.1 [1.0-3.7] x 10^3/μL; $P<0.05$, n=4-5]. Depletion of neutrophils decreased thrombus weight in tumor-bearing mice but not in control mice (Figure 5).

Effect of DNase I administration on thrombus size in mice bearing human pancreatic tumors

Thrombus weight was significantly increased in the vehicle treatment group of tumor-bearing mice compared with that of control mice [controls *vs.* tumor-bearing mice (median [range]): 15.7 [12.1-25.2] g *vs.* 27.25 [22.8-47.8] g; $P<0.05$, n=5-6]. We determined the effect of DNase I administration on the size of thrombi in mice bearing human pancreatic tumors. DNase I degrades both cfDNA and NET. We found that administration of DNase I significantly reduced thrombus weight in tumor-bearing mice but did not affect thrombus weight in control mice (Figure 6).

Discussion

We observed a striking increase in neutrophils in the circulation of nude mice bearing human pancreatic tumors compared with controls. In addition, we found increased levels of plasma biomarkers that either increase neutrophil

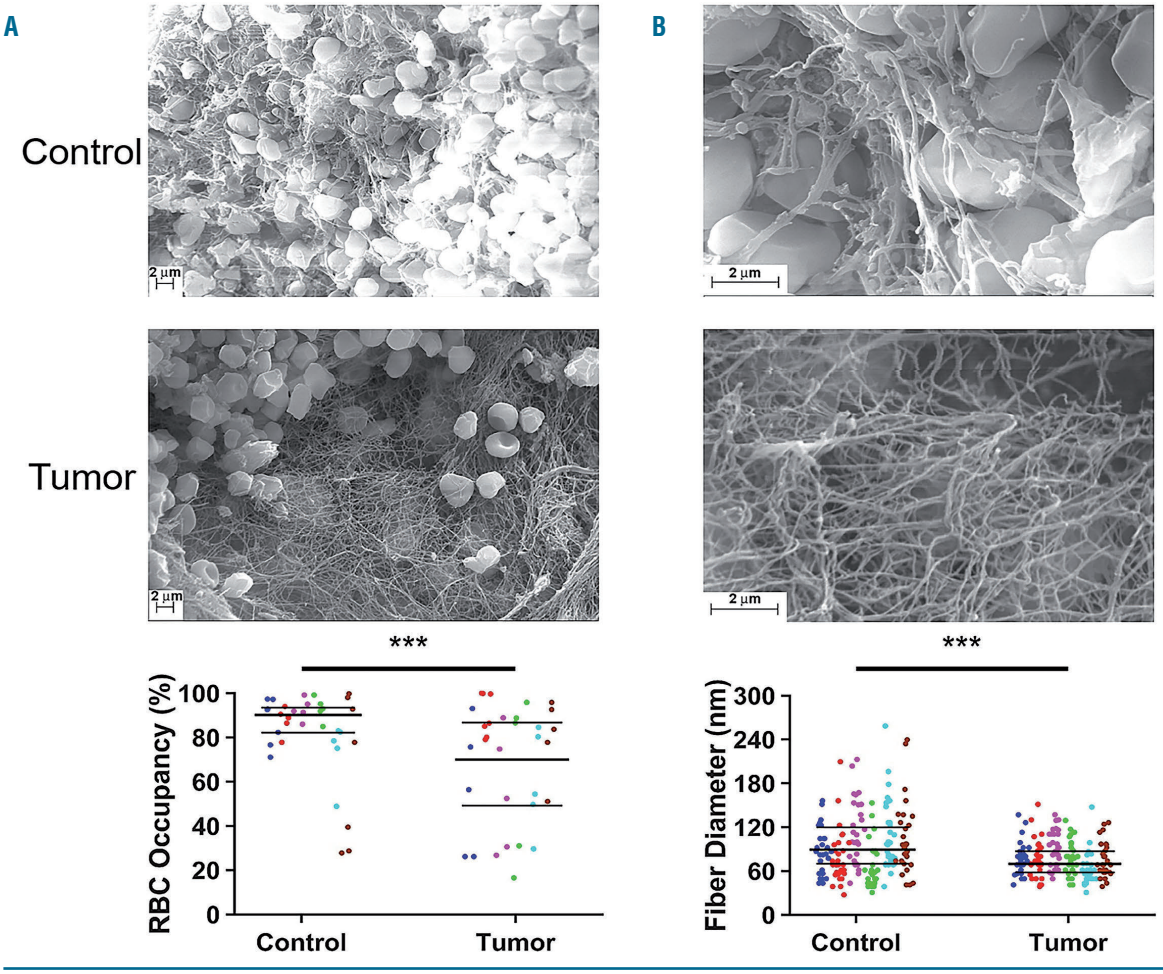

Figure 4. Analysis of thrombi by scanning electron microscopy. (A, B) The red blood cell (RBC) and fibrin content in thrombi from control and tumor-bearing mice were assessed by scanning electron microscopy using a SEM EVO40 (Carl Zeiss GmbH, Oberkochen, Germany). Upper panels are representative images of thrombi from control and tumor-bearing mice. RBC occupancy was quantified in five to seven randomly selected images from each animal (A, data from each thrombus are shown with the same color in the lower panel). The diameter of 300 fibrin fibers from separate parts of each thrombus was measured (B, every 10th measured value is plotted in the same color for each thrombus in the lower panel). Lines indicate the median values of the bottom, median and top quartiles calculated from the data of six animals from each group (shown in different colors) based on 35 images in the control group and 32 images in the tumor group. The statistical analysis was performed using 35 or 32 input data for RBC occupancy and 1,800 data for fiber diameter according to the two-step procedure described in the *Online Supplement* (Bootstrap Kuiper test $P<0.001$ for all three quartiles of the datasets in the lower panels).

counts, such as G-CSF, or are biomarkers of activated neutrophils and NET, such as NE and H3Cit, in tumor-bearing mice compared with controls. We also observed increased levels of the neutrophil biomarker Ly6G and the NET biomarker H3Cit in thrombi from tumor-bearing mice. Finally, depletion of neutrophils reduced thrombus size in tumor-bearing mice but not in control mice. The lack of effect on thrombus size in neutrophil-depleted control mice is consistent with a previous study showing that neutrophil depletion did not reduce thrombus size in mice in an IVC stasis model.[28] Taken together, these data suggest that neutrophils contribute to increased venous thrombosis observed in tumor-bearing mice.

We found that tumor-bearing mice have increased levels of mouse G-CSF and there was a significant positive correlation between levels of mouse G-CSF and neutrophil numbers. This suggests that increased levels of G-CSF drive the increase in neutrophil numbers. At present, we do not know the cellular source of G-CSF in tumor-bearing mice but this cytokine is normally expressed by endothelial cells, macrophages and immune cells.[45] In support of this, mice with murine breast 4T1 tumors exhibit increased plasma levels of G-CSF and administration of an anti-G-CSF antibody reduces neutrophil counts.[37] G-CSF level and neutrophil count may, therefore, represent novel biomarkers of VTE risk in cancer patients.

It has been hypothesized that G-CSF primes neutrophils to undergo NET formation in tumor-bearing mice.[37,46] In one study it was found that the percentage of H3Cit-positive neutrophils was increased in tumor-bearing mice compared with controls.[37] Furthermore, neutrophils isolated from mice bearing murine 4T1 tumors treated with an anti-G-CSF antibody had significantly less NET formation compared with those from tumor-bearing mice treated with an isotype control.[37] In addition, administration of recombinant G-CSF to mice bearing murine melanoma

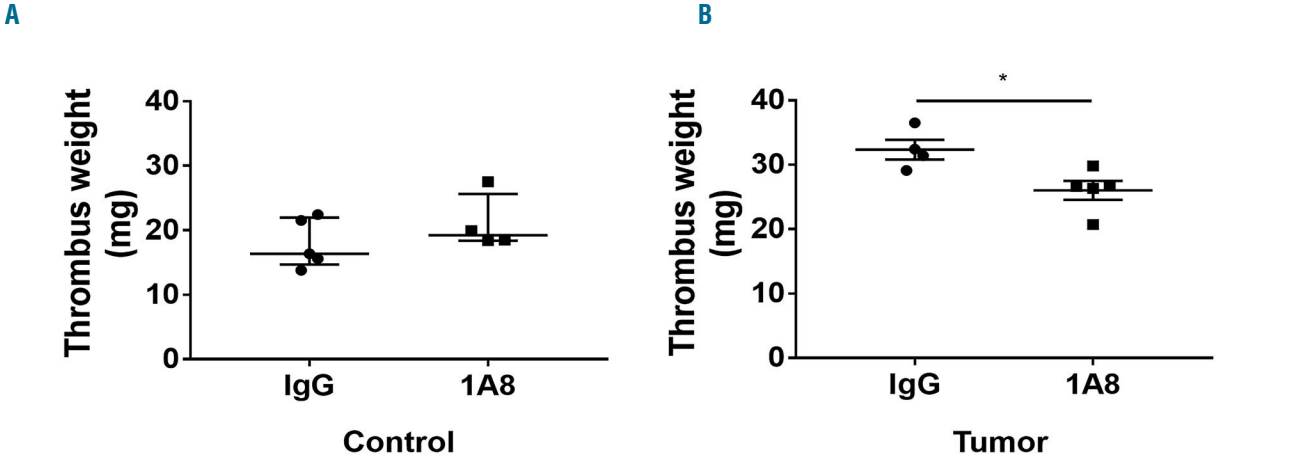

Figure 5. Effect of neutrophil depletion on venous thrombosis in control and tumor-bearing mice. (A, B) Control and tumor-bearing mice received an anti-mouse Ly6G antibody (clone: 1A8) or a control IgG (5 mg/kg) 24 h and 1 h before inferior vena cava stasis. Thrombi from control (A) and tumor-bearing mice (B) were collected at 48 h and weighed. Four to five mice were used for each group. Data were analyzed with either the unpaired *t*-test or the Mann-Whitney U-test depending on the type of data distribution. *P<0.05.

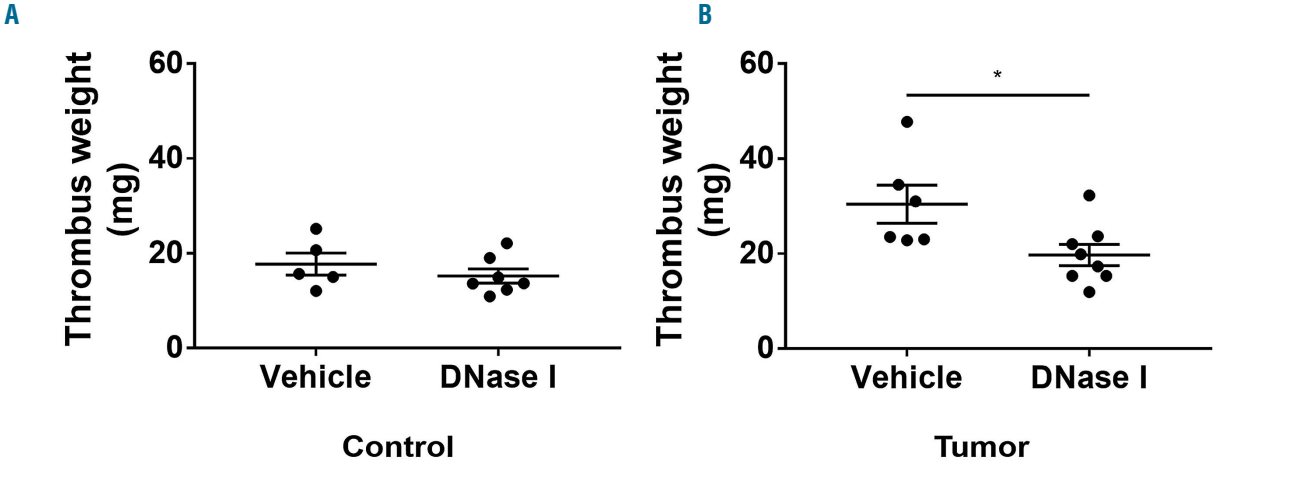

Figure 6. Effect of DNase I treatment on venous thrombosis in control and tumor-bearing mice. Mice received vehicle or DNase I (50 U/mouse) 1 h before and 24 h after inferior vena cava stasis. Thrombi from control (A) and tumor-bearing mice (B) were collected at 48 h and weighed. Five to seven mice were used for each group. Data were analyzed with the unpaired *t*-test. *P<0.05.

B16 tumors, which do not produce G-CSF, increased H3Cit in tumors in a PAD4-dependent manner.[46,47] We observed a large variation in the H3Cit/H3 ratio in thrombi from tumor-bearing mice which appears to be due to different levels of H3Cit in the thrombi. At present, we do not know the reason for this range of H3Cit in thrombi from tumor-bearing mice but it may reflect differences in G-CSF levels and the degree of neutrophil priming in the different tumor-bearing mice.

Plasma cfDNA and the NET biomarker, H3Cit, were increased in tumor-bearing mice compared with controls. Tumors are known to release cfDNA into the blood.[48] In addition, we observed that BxPc-3 cells express PAD4 and therefore tumors may also contribute to the plasma levels of H3Cit. Thrombi from tumor-bearing mice also had increased levels cfDNA and H3Cit compared with thrombi from controls. Importantly, administration of DNase I reduced thrombus size in tumor-bearing mice but not in control mice. Similarly, a previous study showed that DNase I did not affect jugular vein occlusion times in control mice but prolonged the time to occlusion in 4T1 tumor-bearing mice.[38] We observed that DNase I reduced thrombus size more effectively than depletion of neutrophils. It is possible that DNase I is more effective than neutrophil depletion because it digests not only NET but also cfDNA which may also be released by cancer cells and may enhance thrombosis by activating factor XII.[40,49]

In the present study, we observed decreased numbers of red blood cells in thrombi from tumor-bearing mice compared with controls. This is consistent with our recent study that showed a decrease in red blood cell-rich areas and an increase in inflammatory cell-rich areas in thrombi from tumor-bearing mice compared with controls.[10] In the current study, we did not observe an increase in neutrophils in thrombi of tumor-bearing mice because these cells were not preserved during the preparation of the samples for scanning electron microscopy. In addition, thrombi from tumor-bearing mice had a denser fibrin network with thinner fibrin fibers compared with thrombi from control mice. *In vitro* experiments showed that higher thrombin produces thrombi with a denser fibrin network with thinner fibrin fibers.[44] In our model of cancer-associated thrombosis, it is likely that tumor-derived, tissue factor-positive extracellular vesicles increase the thrombin concentration in thrombi and this results in the formation of a denser fibrin network with thinner fibers. Indeed, in our previous study,[10] we observed that thrombi from BxPc-3 tumor-bearing mice had increased levels of human tissue factor activity derived from extracellular vesicles released from BxPc-3 tumors. In addition, a previous study showed that extracellular vesicles bind to NET via a phosphatidylserine-histone interaction.[50]

In summary, we have demonstrated a contribution of neutrophils to venous thrombosis in a mouse model of pancreatic cancer-associated venous thrombosis. Our data, taken together with a clinical study showing an association between circulating H3Cit and VTE in pancreatic cancer, support the notion that neutrophils and NET formation enhance venous thrombosis in pancreatic cancer.

Acknowledgments

The Animal Surgery Core Laboratory of the McAllister Heart Institute at UNC performed the thrombosis experiments. This work was supported by grants from the National Institutes of Health (to YH T32 HL007149), the John C. Parker Professorship (to NM), the Jochnick Foundation (to CT and HW), the Hungarian National Research, Development and Innovation Office (NKFIH) (129528, to KK) and the Higher Education Institutional Excellence Programme of the Ministry of Human Capacities in Hungary for the Molecular Biology thematic programme of Semmelweis University (to KK).

References

1. Timp JF, Braekkan SK, Versteeg HH, Cannegieter SC. Epidemiology of cancer-associated venous thrombosis. Blood. 2013;122(10):1712-1723.
2. Horsted F, West J, Grainge MJ. Risk of venous thromboembolism in patients with cancer: a systematic review and meta-analysis. PLoS Med. 2012;9(7):e1001275.
3. Hisada Y, Mackman N. Cancer-associated pathways and biomarkers of venous thrombosis. Blood. 2017;130(13):1499-1506.
4. Khorana AA, Francis CW, Menzies KE, et al. Plasma tissue factor may be predictive of venous thromboembolism in pancreatic cancer. J Thromb Haemost. 2008;6(11):1983-1985.
5. Thaler J, Ay C, Mackman N, et al. Microparticle-associated tissue factor activity, venous thromboembolism and mortality in pancreatic, gastric, colorectal and brain cancer patients. J Thromb Haemost. 2012;10(7):1363-1370.
6. Bharthuar A, Khorana AA, Hutson A, et al. Circulating microparticle tissue factor, thromboembolism and survival in pancreaticobiliary cancers. Thromb Res. 2013;132(2):180-184.
7. Davila M, Amirkhosravi A, Coll E, et al. Tissue factor-bearing microparticles derived from tumor cells: impact on coagulation activation. J Thromb Haemost. 2008;6(9):1517-1524.
8. Wang JG, Geddings JE, Aleman MM, et al. Tumor-derived tissue factor activates coagulation and enhances thrombosis in a mouse xenograft model of human pancreatic cancer. Blood. 2012;119(23):5543-5552.
9. Geddings JE, Hisada Y, Boulaftali Y, et al. Tissue factor-positive tumor microvesicles activate platelets and enhance thrombosis in mice. J Thromb Haemost. 2016;14(1):153-166.
10. Hisada Y, Ay C, Auriemma AC, Cooley BC, Mackman N. Human pancreatic tumors grown in mice release tissue factor-positive microvesicles that increase venous clot size. J Thromb Haemost. 2017;15(11):2208-2217.
11. Khorana AA, Kuderer NM, Culakova E, Lyman GH, Francis CW. Development and validation of a predictive model for chemotherapy-associated thrombosis. Blood. 2008;111(10):4902-4907.
12. Pabinger I, Posch F. Flamethrowers: blood cells and cancer thrombosis risk Hematology. 2014. 2014;1):410-417.
13. Blix K, Jensvoll H, Braekkan SK, Hansen JB. White blood cell count measured prior to cancer development is associated with future risk of venous thromboembolism--the Tromso study. PLoS One. 2013;8(9):e73447.
14. Kasuga I, Makino S, Kiyokawa H, Katoh H, Ebihara Y, Ohyashiki K. Tumor-related leukocytosis is linked with poor prognosis in patients with lung carcinoma. Cancer. 2001;92(9):2399-2405.
15. Esmon CT. Interactions between the innate immune and blood coagulation systems. Trends Immunol. 2004;25(10):536-542.
16. Engelmann B, Massberg S. Thrombosis as an intravascular effector of innate immunity. Nat Rev Immunol. 2013;13(1):34-45.
17. Osterud B. Tissue factor expression by monocytes: regulation and pathophysiological roles. Blood Coagul Fibrinolysis. 1998;9(Suppl 1):S9-14.
18. Massberg S, Grahl L, von Bruehl ML, et al. Reciprocal coupling of coagulation and innate immunity via neutrophil serine proteases. Nat Med. 2010;16(8):887-896.
19. Fuchs TA, Brill A, Duerschmied D, et al. Extracellular DNA traps promote thrombosis. Proc Natl Acad Sci U S A. 2010;107(36):15880-15885.
20. Brill A, Fuchs TA, Savchenko AS, et al. Neutrophil extracellular traps promote deep vein thrombosis in mice. J Thromb

Haemost. 2012;10(1):136-144.
21. Fuchs TA, Brill A, Wagner DD. Neutrophil extracellular trap (NET) impact on deep vein thrombosis. Arterioscler Thromb Vasc Biol. 2012;32(8):1777-1783.
22. Noubouossie DF, Reeves BN, Strahl BD, Key NS. Neutrophils: back in the thrombosis spotlight. Blood. 2019;133(23):2529-2541.
23. Longstaff C, Varju I, Sotonyi P, et al. Mechanical stability and fibrinolytic resistance of clots containing fibrin, DNA, and histones. J Biol Chem. 2013;288(10):6946-6956.
24. Mangold A, Alias S, Scherz T, et al. Coronary neutrophil extracellular trap burden and deoxyribonuclease activity in ST-elevation acute coronary syndrome are predictors of ST-segment resolution and infarct size. Circ Res. 2015;116(7):1182-1192.
25. Jimenez-Alcazar M, Rangaswamy C, Panda R, et al. Host DNases prevent vascular occlusion by neutrophil extracellular traps. Science. 2017;358(6367):1202-1206.
26. von Bruhl ML, Stark K, Steinhart A, et al. Monocytes, neutrophils, and platelets cooperate to initiate and propagate venous thrombosis in mice in vivo. J Exp Med. 2012;209(4):819-835.
27. Meng H, Yalavarthi S, Kanthi Y, et al. In vivo tole of neutrophil extracellular traps in antiphospholipid antibody-mediated venous thrombosis. Arthritis Rheumatol. 2017;69(3):655-667.
28. El-Sayed OM, Dewyer NA, Luke CE, et al. Intact Toll-like receptor 9 signaling in neutrophils modulates normal thrombogenesis in mice. J Vasc Surg. 2016;64(5):1450-1458.e1.
29. Kenny EF, Herzig A, Kruger R, et al. Diverse stimuli engage different neutrophil extracellular trap pathways. Elife. 2017;6.
30. Li P, Li M, Lindberg MR, Kennett MJ, Xiong N, Wang Y. PAD4 is essential for antibacterial innate immunity mediated by neutrophil extracellular traps. J Exp Med. 2010;207(9):1853-1862.
31. Stadler SC, Vincent CT, Fedorov VD, et al. Dysregulation of PAD4-mediated citrullination of nuclear GSK3beta activates TGF-beta signaling and induces epithelial-to-mesenchymal transition in breast cancer cells. Proc Natl Acad Sci U S A. 2013;110(29):11851-11856.
32. Wang Y, Li M, Stadler S, et al. Histone hypercitrullination mediates chromatin decondensation and neutrophil extracellular trap formation. J Cell Biol. 2009;184(2):205-213.
33. Martinod K, Demers M, Fuchs TA, et al. Neutrophil histone modification by peptidylarginine deiminase 4 is critical for deep vein thrombosis in mice. Proc Natl Acad Sci U S A. 2013;110(21):8674-8679.
34. Mauracher LM, Posch F, Martinod K, et al. Citrullinated histone H3, a biomarker of neutrophil extracellular trap formation, predicts the risk of venous thromboembolism in cancer patients. J Thromb Haemost. 2018;16(3):508-518.
35. Oklu R, Sheth RA, Wong KHK, Jahromi AH, Albadawi H. Neutrophil extracellular traps are increased in cancer patients but does not associate with venous thrombosis. Cardiovasc Diagn Ther. 2017;7(Suppl 3):S140-S149.
36. DuPre SA, Redelman D, Hunter KW Jr. The mouse mammary carcinoma 4T1: characterization of the cellular landscape of primary tumours and metastatic tumour foci. Int J Exp Pathol. 2007;88(5):351-360.
37. Demers M, Krause DS, Schatzberg D, et al. Cancers predispose neutrophils to release extracellular DNA traps that contribute to cancer-associated thrombosis. Proc Natl Acad Sci U S A. 2012;109(32):13076-13081.
38. Leal AC, Mizurini DM, Gomes T, et al. Tumor-derived exosomes induce the formation of neutrophil extracellular traps: implications for the establishment of cancer-associated thrombosis. Sci Rep. 2017;7(1):6438.
39. Sommeijer DW, van Oerle R, Reitsma PH, et al. Analysis of blood coagulation in mice: pre-analytical conditions and evaluation of a home-made assay for thrombin-antithrombin complexes. Thromb J. 2005;3:12.
40. Noubouossie DF, Whelihan MF, Yu YB, et al. In vitro activation of coagulation by human neutrophil DNA and histone proteins but not neutrophil extracellular traps. Blood. 2017;129(8):1021-1029.
41. Thalin C, Daleskog M, Goransson SP, et al. Validation of an enzyme-linked immunosorbent assay for the quantification of citrullinated histone H3 as a marker for neutrophil extracellular traps in human plasma. Immunol Res. 2017;65(3):706-712.
42. Efron B, Tibshirani RJ. An Introduction to the Bootstrap. New York, NY, USA: Taylor & Francis, 1993.
43. Nikolova N, Chai SH, Ivanova SD, Kolev K, Tenekedjiev K. Bootstrap Kuiper testing of the identity of 1D continuous distributions using fuzzy samples. International Journal of Computational Intelligence Systems. 2015;8:63-75.
44. Wolberg AS. Thrombin generation and fibrin clot structure. Blood Rev. 2007;21(3):131-142.
45. von Vietinghoff S, Ley K. Homeostatic regulation of blood neutrophil counts. J Immunol. 2008;181(8):5183-5188.
46. Demers M, Wong SL, Martinod K, et al. Priming of neutrophils toward NETosis promotes tumor growth. Oncoimmunology. 2016;5(5):e1134073.
47. Cedervall J, Zhang Y, Huang H, et al. Neutrophil extracellular traps accumulate in peripheral blood vessels and compromise organ function in tumor-bearing animals. Cancer Res. 2015;75(13): 2653-2662.
48. Schwarzenbach H, Hoon DS, Pantel K. Cell-free nucleic acids as biomarkers in cancer patients. Nat Rev Cancer. 2011;11(6):426-437.
49. Swystun LL, Mukherjee S, Liaw PC. Breast cancer chemotherapy induces the release of cell-free DNA, a novel procoagulant stimulus. J Thromb Haemost. 2011;9(11):2313-2321.
50. Wang Y, Luo L, Braun OO, et al. Neutrophil extracellular trap-microparticle complexes enhance thrombin generation via the intrinsic pathway of coagulation in mice. Sci Rep. 2018;8(1):4020.

Ferrata Storti Foundation

Haematologica 2020
Volume 105(1):226-234

Myeloid differentiation factor 88 signaling in donor T cells accelerates graft-*versus*-host disease

Satomi Matsuoka,[1] Daigo Hashimoto,[1] Masanori Kadowaki,[2] Hiroyuki Ohigashi,[1] Eiko Hayase,[1] Emi Yokoyama,[1] Yuta Hasegawa,[1] Takahiro Tateno,[1] Xuanzhong Chen,[1] Kazutoshi Aoyama,[2] Hideyo Oka,[2] Masahiro Onozawa,[1] Kiyoshi Takeda,[3] Koichi Akashi[2] and Takanori Teshima[1]

[1]Department of Hematology, Faculty of Medicine, Hokkaido University, Sapporo; [2]Department of Medicine and Biosystemic Science, Kyushu University Graduate School of Medical Sciences, Fukuoka and [3]Department of Microbiology and Immunology, Graduate School of Medicine, WPI Immunology Frontier Research Center, Osaka University, Suita, Japan

ABSTRACT

Myeloid differentiation factor 88 (MyD88) signaling has a crucial role in activation of both innate and adoptive immunity. MyD88 transduces signals *via* Toll-like receptor and interleukin-1 receptor superfamily to the NFκB pathway and inflammasome by forming a molecular complex with interleukin-1 receptor-associated kinase 4. The MyD88/interleukin-1 receptor-associated kinase 4 pathway plays an important role, not only in innate immunity, but also T-cell immunity; however, its role in donor T cells on the pathophysiology of graft-*versus*-host disease (GvHD) remains to be elucidated. We addressed this issue by using MyD88-deficient T cells in a mouse model of allogeneic hematopoietic stem cell transplantation (allo-SCT). While MyD88-deficient and wild-type T cells proliferated equivalently after transplantation, MyD88-deficient T cells demonstrated impaired survival and differentiation toward Th1, Tc1, and Th17, and induced less severe GvHD compared to wild-type T cells. Administration of interleukin-1 receptor-associated kinase 4 inhibitor PF-06650833 significantly ameliorated GvHD after allo-SCT. These results thus demonstrate that donor T-cell MyD88/ interleukin-1 receptor-associated kinase 4 pathway is a novel therapeutic target against GvHD after allo-SCT.

Correspondence:

TAKANORI TESHIMA
teshima@med.hokudai.ac.jp

Received: August 2, 2018.

Accepted: April 30, 2019.

Pre-published: May 2, 2019.

doi:10.3324/haematol.2018.203380

Check the online version for the most updated information on this article, online supplements, and information on authorship & disclosures: www.haematologica.org/content/105/1/226

Introduction

Myeloid differentiation factor 88 (MyD88) is a critical adaptor molecule to transduce the signals through receptors belonging to most of the TLR and IL-1R family (TLR/IL-1R superfamily) to NFκB pathway and inflammasome by recruiting IL-1R-associated kinase 4 (IRAK4).[1] The TLR/MyD88 pathway in myeloid cells plays an essential role in innate immunity by recognizing pathogen-associated molecular patterns (PAMP) released by microbes and damage-associated molecular patterns (DAMP) produced by stressed or dying cells.[2] MyD88 dependent signaling in myeloid cells plays proinflammatory roles by secreting proinflammatory cytokines and enhancing antigen presentation, and also homeostatic roles by maintaining regulatory T cells (Tregs) and myeloid-derived suppressor cells (MDSC).[3,4] In addition, there is growing evidence to indicate that MyD88 signaling in T cells also plays a critical role in T-cell proliferation, survival, and differentiation upon TCR-stimulation.[5-13]

Graft-*versus*-host disease (GvHD), the major complication of allogeneic hematopoietic stem cell transplantation (allo-SCT), is mediated by donor T cells recognizing host-derived alloantigens expressed on professional or non-professional APC and further accelerated by pre-transplant conditioning-mediated inflammatory milieu and tissue injury.[14,15] In particular, damage of the epithelial and mucous barrier allows translocation of bacteria and its immunostimulatory molecules into systemic circulation, leading to subsequent activation of innate immune responses

through TLR stimulation towards production of inflammatory cytokines such as tumor necrosis factor (TNF)-α and IL-1 family cytokines.[16-19]

In this study, we evaluated the role of MyD88 signaling in donor T cells by using a well-established mouse model of allogeneic bone marrow transplantation (allo-BMT), in which lethally irradiated recipient mice were transplanted with *MyD88*$^{-/-}$ T cells and T cell-depleted bone marrow cells (TCD-BM) from *WT* mice. We found that lack of MyD88 signaling in donor T cells directly modulated adaptive T-cell responses and reduced severity of GvHD in association with profoundly impaired donor Th1, Tc1, and Th17 responses. Administration of a pharmacological IRAK4 inhibitor, PF-06650833, significantly ameliorated GvHD. MyD88 in donor T cells was not essential for graft-*versus*-leukemia (GvL) effects, suggesting that MyD88 in T cells is a potential therapeutic target of GvHD, while sparing GvL effects.

Methods

Mice

Female C57BL/6 (B6, H-2^{b}) and B6D2F1 (H-2$^{b/d}$) mice were purchased from Charles River Japan (Yokohama, Japan). *TLR2*$^{-/-}$ and *TLR7*$^{-/-}$ mice with a B6 genetic background were purchased from Oriental Bioservice (Chiba, Japan). B6-*MyD88*$^{-/-}$ mice were produced and maintained as previously described.[20] Age of the mice was 8-10 weeks. All animal experiments were performed under the auspices of the Institutional Animal Care and Research Advisory Committee (approval n: 12-0106).

Bone marrow transplantation

Mice were transplanted as previously described.[21] In brief, recipient B6D2F1 mice were intravenously (i.v.) injected with 5x10^{6} TCD-BM cells form WT B6 donors plus 1x10^{6} T cells purified from either wild-type (WT) or *MyD88*$^{-/-}$ B6 donors on day 0 following lethal total body irradiation (TBI, 12Gy) delivered in two doses at 3-hour intervals. BALB/c recipients were transplanted with 5x10^{6} TCD-BM cells from WT B6 donors plus 1x10^{6} T cells purified from either WT or *MyD88*$^{-/-}$ B6 donors on day 0 following 6 Gy TBI. Isolation of T cells and TCD were performed using a Pan T cell Isolation kit II and anti-CD90-MicroBeads, respectively, and the autoMACS Pro system (Miltenyi Biotec, Bergisch Gladbach, Germany) according to the manufacturer's instructions. Mice were housed in sterilized microisolator cages and received autoclaved hyperchlorinated drinking water for the first three weeks after BMT, and filtered water thereafter.

Assessment of graft-*versus*-host disease and graft-*versus*-leukemia effect

Clinical GvHD scores were assessed as previously described.[22] GvL was assessed by postmortem examination or on *in vivo* bioluminescent imaging.[23,24] Detailed protocols are described in the *Online Supplementary Methods*.

Quantitative-polymerase chain reaction

RNA extraction and quantitative-polymerase chain reaction (Q-PCR) were performed as described in the *Online Supplementary Methods*. Specific primers and probes used for Q-PCR are listed in *Online Supplementary Table S1*.

Flow cytometric analysis

Flow cytometric analysis was performed as previously described.[21] The cells isolated from the thymus or spleen were incubated with antibodies (Abs) (listed in *Online Supplementary Table S2*) at 4°C for 30 minutes (min). Detailed protocols are described in the *Online Supplementary Methods*.

Cell cultures

All culture media and incubation conditions have been previously described.[21] TCR on purified T cells (5x10^{4} T cells/well) were stimulated with 5x10^{4} /well of Dynabeads Mouse T-Activator CD3/CD28 for T-cell expansion and activation (ThermoFisher Scientific, Waltham, MA, USA) in the presence or absence of TLR ligands at concentrations listed in *Online Supplementary Table S3* or PF-06650833 (20 μM) for up to 96 hours.

T-cell proliferation

To assess T-cell proliferation, purified T cells were labeled using a CellTrace Violet Cell Proliferation Kit (ThermoFisher Scientific) according to the manufacturer's instructions. To measure cellular uptake of BrdU, recipients were intraperitoneally (i.p.) injected with 1 mg of BrdU 2 hours before analyses.

Statistical analysis

Mann-Whitney U tests were used to analyze cell counts, the cytokine data, and the clinical scores. We used the Kaplan-Meier product limit method to obtain the survival probability. and the log-rank test was applied to compare the survival curves. $P<0.05$ was considered statistically significant.

Results

Donor T cells lacking MyD88 pathway induce attenuated graft-*versus*-host disease

We investigated whether ablation of MyD88 signaling in donor cells influenced GvHD in a well-established mouse model of haploidentical BMT. Lethally irradiated B6D2F1 mice were i.v. injected with 5x10^{6} BM plus 5x10^{6} splenocytes from either WT or *MyD88*$^{-/-}$ B6 donors. Frequencies and absolute numbers of CD4^{+} T cells, CD8^{+} T cells, memory T cells, and Foxp3^{+} Tregs in the spleen were equivalent in donor WT and *MyD88*$^{-/-}$ B6 mice (*Online Supplementary Figure S1*). While GvHD was severe in allogeneic controls with 80% mortality by day 50, 67% of recipients of *MyD88*$^{-/-}$ donors survived this period (Figure 1A). Clinical GvHD scores were also significantly lower in recipients of *MyD88*$^{-/-}$ graft compared to those of WT graft (Figure 1B).

Next, we evaluated if effects of MyD88 signaling in donor cells on GvHD could reside in the T-cell compartment of the donor graft. Lethally irradiated B6D2F1 mice were injected with 5x10^{6} TCD-BM from WT B6 mice plus 1x10^{6} T cells from either WT or *MyD88*$^{-/-}$ B6 mice. MyD88 deficiency in donor T cell alone significantly ameliorated mortality and morbidity of GvHD (Figure 1C and D). Histopathological examination of the small intestine and colon performed 6-8 weeks after BMT confirmed attenuated GvHD pathology in recipients of *MyD88*$^{-/-}$ T cells. GvHD pathology in the small intestine, including villous blunting, epithelial apoptosis, and Paneth-cell loss accom-

panied by inflammatory-cell infiltration, was significantly less severe in recipients of *MyD88*$^{-/-}$ T cells (Figure 1E-G), although liver GvHD was the same as in controls. The thymic GvHD characterized by the loss of CD4^{+}CD8^{+} double positive (DP) thymocytes was also less severe in *MyD88*$^{-/-}$ T-cell recipients than in controls (Figure 1H-J). The role of donor T-cell MyD88 signaling in GvHD was not strain dependent, as MyD88 deficiency in donor T cells ameliorates GvHD in the B6 into BALB/c model (Figure 1K).

Absence of MyD88 signaling impairs donor Th1/Tc1/Th17 differentiation

Induction of GvHD is primarily dependent on donor T-cell reactivity to host alloantigens.[14] To evaluate the effects of MyD88 signaling in donor T-cell activation *in vivo*, donor T-cell expansion was evaluated in the spleen early after BMT. Numbers of CD8^{+} T cells were significantly less in *MyD88*$^{-/-}$ T-cell recipients than those in controls seven days after BMT (Figure 2A). Both groups showed complete donor T-cell chimerism, ruling out mixed chimerism as a cause of reduced numbers of donor T cells (Figure 2B). Analysis of cell division using CellTrace Violet-labeled T cells showed equivalent cell division between WT and *MyD88*$^{-/-}$ T cells at both 72 and 96 hours after BMT (Figure 2C and D). Donor T-cell proliferation determined by BrdU uptake on day 6 also showed equivalent T-cell uptake of BrdU in both groups (Figure 2E and F). Proliferative response of WT and *MyD88*$^{-/-}$ T cells to CD3/CD28 stimulation *in vitro* and after allogeneic SCT *in*

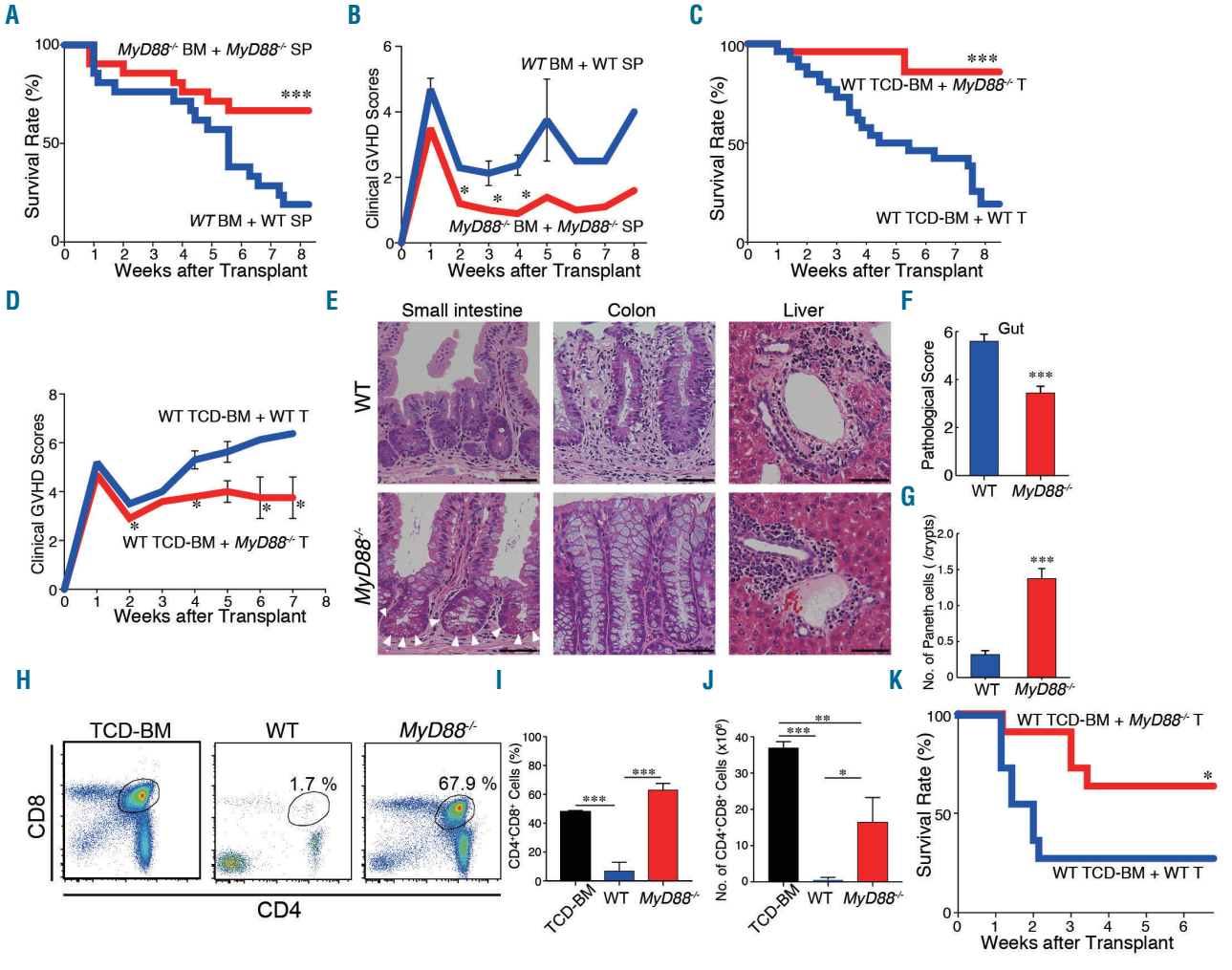

Figure 1. MyD88 signaling in donor T cells exaggerates graft-versus-host disease (GvHD). (A and B) Lethally irradiated B6D2F1 mice were transplanted with 5x10^{6} bone marrow (BM) cells plus 5x10^{6} splenocytes from wild-type (WT) (n=21) or *MyD88*$^{-/-}$ (n=21) B6 donors on day 0. Survival (A) and clinical GvHD scores (B) from four independent experiments are combined. (C-H) Lethally irradiated B6D2F1 mice were transplanted with 5x10^{6} T-cell-depleted bone marrow cells (TCD-BM) cells from WT B6 mice plus 1x10^{6} purified T cells from WT or *MyD88*$^{-/-}$ B6 donors. Survival (C) and clinical GvHD scores (D) from five independent experiments are combined (n=25-26 / group). (E) Representative Hematoxylin & Eosin (H&E) images of the small intestine, colon, and liver harvested 6-8 weeks after BM transplantation (BMT). (F) Pathological GvHD scores of the liver and total pathological scores in the gut which is the sum of the scores of the small intestine and colon. Data from three independent experiments are combined and shown as means ± Standard Error (SE) (n=8-14/group). (G) Numbers of Paneth cells morphologically identified as cells containing eosinophilic granules at crypt base of the small intestines (white arrow heads in Figure 1E) on day +7 after BMT. Data from two similar experiments were combined and shown as means ± SE (n=12 / group). (H-J) CD4^{+}CD8^{+} double positive thymocytes were assessed 6-8 weeks after BMT. Representative dot plots (H), frequencies (I) (means±SE), and absolute numbers (J) (means±SE) of CD4^{+}CD8^{+} thymocytes from one of two similar experiments were shown (n=5/group). (K) BALB/c mice recipients were transplanted with 5x10^{6} TCD-BM cells from WT B6 mice plus 1x10^{6} purified T cells from WT or *MyD88*$^{-/-}$ B6 donors following total body irradiation on day 0 (n=11/group). Data from two similar experiments were combined. Bar, 50 μm. ***P*<0.01; ****P*<0.005.

vivo was also equivalent (Figure S2A and B). T-cell proliferation was much more robust *in vivo* compared to *in vitro*, probably due to the presence of potent inflammatory milieu induced by TBI. On the other hand, annexin V+ apoptotic donor CD8$^+$ T cells were significantly increased in the recipients of *MyD88*$^{-/-}$ T cells on day +7, suggesting that MyD88 is an intrinsic survival factor of donor T cells after allo-BMT (Figure 2G).

To assess the role of MyD88 in donor T-cell differentiation after allo-BMT, cytokine production was evaluated in donor T cells isolated on day +7 after BMT. *MyD88*$^{-/-}$ CD4$^+$ T cells produced significantly less IFN-γ and IL-17, and *MyD88*$^{-/-}$ donor CD8$^+$ T cells produced less INF-γ than their WT counterpart, indicating that MyD88 signaling is critical for Th1, Th17, and Tc1 differentiation (Figure 3A-D). In contrast, IL-4 production from *MyD88*$^{-/-}$ donor CD4$^+$ T cells tend to be greater than that from WT CD4$^+$ T cells (Figure 3E and F). Impaired Th1/Tc1, not Th2, differentiation in *MyD88*$^{-/-}$ T cells was also confirmed *in vitro* after CD3/CD28 stimulation (Figure S2C-F). Furthermore, flow cytometric analysis on day +7 demonstrated that absolute numbers of donor CD4$^+$ Foxp3$^+$ Tregs and pro-

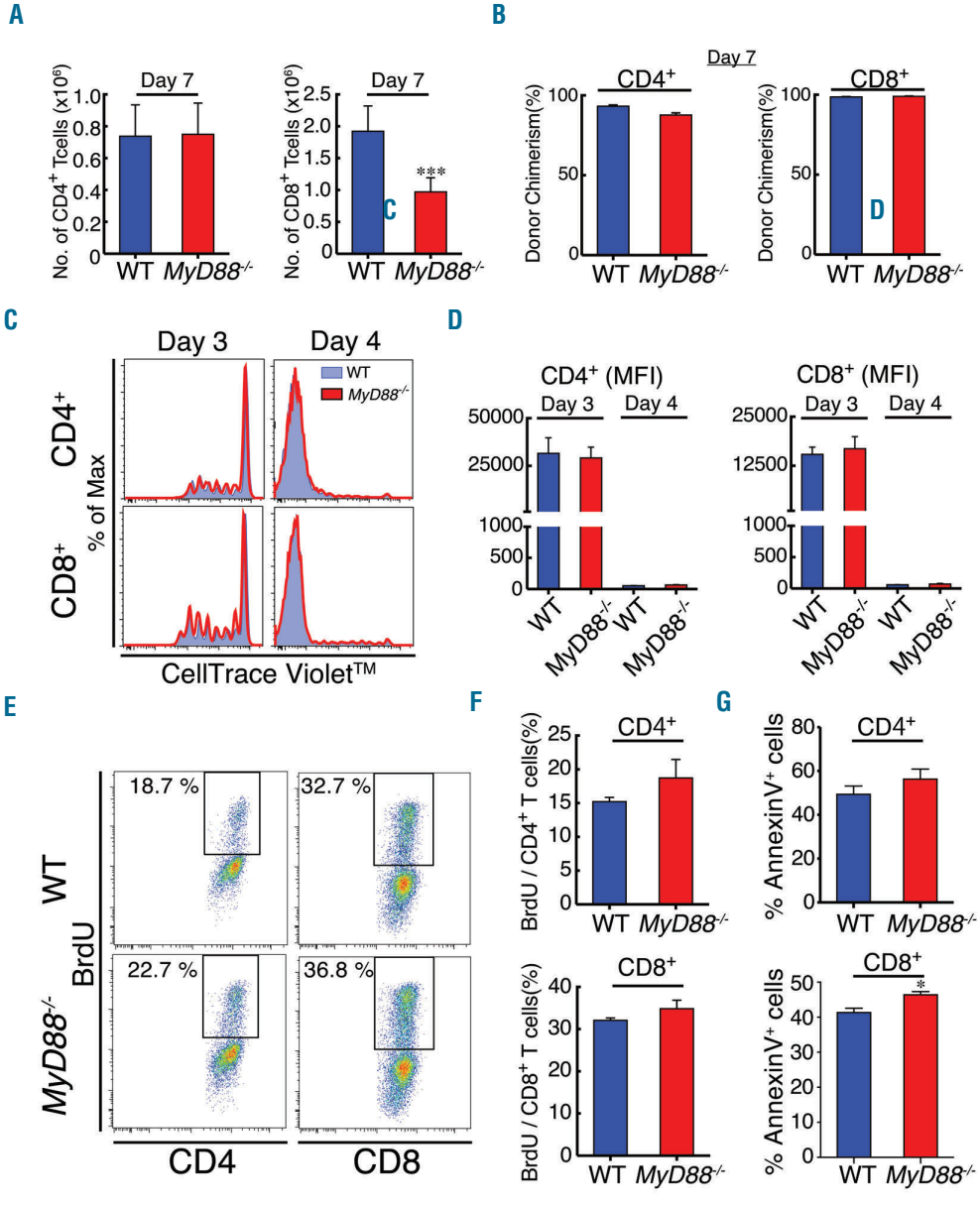

Figure 2. MyD88 is not essential for T-cell proliferation and survival after allogeneic bone marrow transplantation (alloBMT). (A,B,E-H) Mice were transplanted as in Figure 1C. Absolute numbers of donor CD4$^+$ and CD8$^+$T cells (A) and donor chimerism (B) in the spleen on day +7. Data from four independent experiments were combined and shown as means±Standard Error (SE) (n=17-18/group). (C and D) CellTrace Violet-labeled T cells from *WT* or *MyD88*$^{-/-}$ B6 mice were injected and dilution of CellTrace Violet in donor CD4$^+$ and CD8$^+$ T cells in the spleen were assessed on days 3 and 4. Representative histograms (C) and MFI of Cell Trace Violet (D) (means±SE) from two experiments were combined (n=4-6 group). (E and F) Recipients were intraperitoneally injected with 1 mg BrdU on day +6 and BrdU taken up by donor T cells was evaluated two hours later. Representative dot plots (E) and proportions of BrdU positive cells among donor T cells (F) (means±SE). Data from two experiments were combined (n=10/group). (G) Proportion of Annexin V$^+$ cells among donor T cells in the spleen on day +7. Data from a representative experiment of two similar experiments were combined and shown as means±SE (n=9-11 / group). *P<0.05; ***P<0.005.

portions of Foxp3$^+$ cells among donor CD4$^+$ T cells were significantly greater in the spleen of recipients of *MyD88*$^{-/-}$ T cells than those in controls (Figure 3G and H). Taken together, donor T cells require MyD88 signaling to differentiate into Th1, Th17, and Tc1, while it is dispensable for Th2 and Treg differentiation after allo-SCT.

IRAK4 inhibition, but not single TLR deficiency, mitigates lethal graft-*versus*-host disease

MyD88 transduces signals from both TLR and IL-1 family cytokines, such as IL-1, IL-18 and IL-33. Although roles of IL-1, IL-18, and IL-33 in GvHD have been well studied, role of T-cell TLR remained to be clarified. First, we examined expression of MyD88-related TLR and IL-1 family cytokine receptors on CD4$^+$ and CD8$^+$ T cells. Q-PCR demonstrated that resting CD4$^+$ and CD8$^+$ T cells expressed TLR2 and TLR7, but to a lesser extent to the levels in macrophages (Figure 4A). In addition, CD4$^+$ T cells also expressed IL-1R, IL-18R and IL-33R, and CD8$^+$ T cells did IL-18R. Flow cytometric analysis confirmed expression of TLR2 and TLR7 both on CD4$^+$ and CD8$^+$ T cells (Figure 4B). Expression of TLR2 and TLR7 on T cells were functional, such as TLR2 ligand, Pam3CSK4, and TLR7 ligands, ssRNA40 and R848 enhanced T-cell proliferative response to CD3/CD28 stimulation *in vitro*, indicating that TLR2 and TLR7 on T cells have co-stimulatory function in T-cell responses (Figure 4C). In contrast, LPS, flagellin, or CpG-ODN did not enhance T-cell expansion. Next, we evaluated the role of TLR2 and TLR7 in GvHD by transplanting *TLR2*$^{-/-}$ or TLR7$^{-/-}$ T cells plus WT TCD-BM. Mortality and morbidity of GvHD in recipients of *TLR2*$^{-/-}$ or TLR7$^{-/-}$ T cells were identical to those of WT T cells, suggesting that inhibition of single TLR signaling was insufficient to ameliorate GvHD (Figure 4D and E).

Next, we tested if pharmacological inhibition of MyD88 signaling could ameliorate GvHD, using IRAK4 inhibitor PF-06650833 that inhibits signal transduction through MyD88. First, we found that addition of PF-06650833 to culture significantly suppressed T-cell production of IFN-γ after CD3/CD28 stimulation without affecting T-cell proliferative response *in vitro* (Figure 5A-D). PF-06650833 administered daily for three weeks after allogeneic BMT significantly ameliorated morbidity and mortality of GvHD, indicating that MyD88/IRAK4 is a potential pharmacological therapeutic target of GvHD (Figure 5E and F).

MyD88 signaling is dispensable for graft-*versus*-leukemia activity of donor T cells

Considering the significant reduction of GvHD in the absence of MyD88 signaling in donor T cells, it is of interest to evaluate the impact of MyD88 signaling in donor T cells on GvL effect after allogeneic BMT. Lethally irradiat-

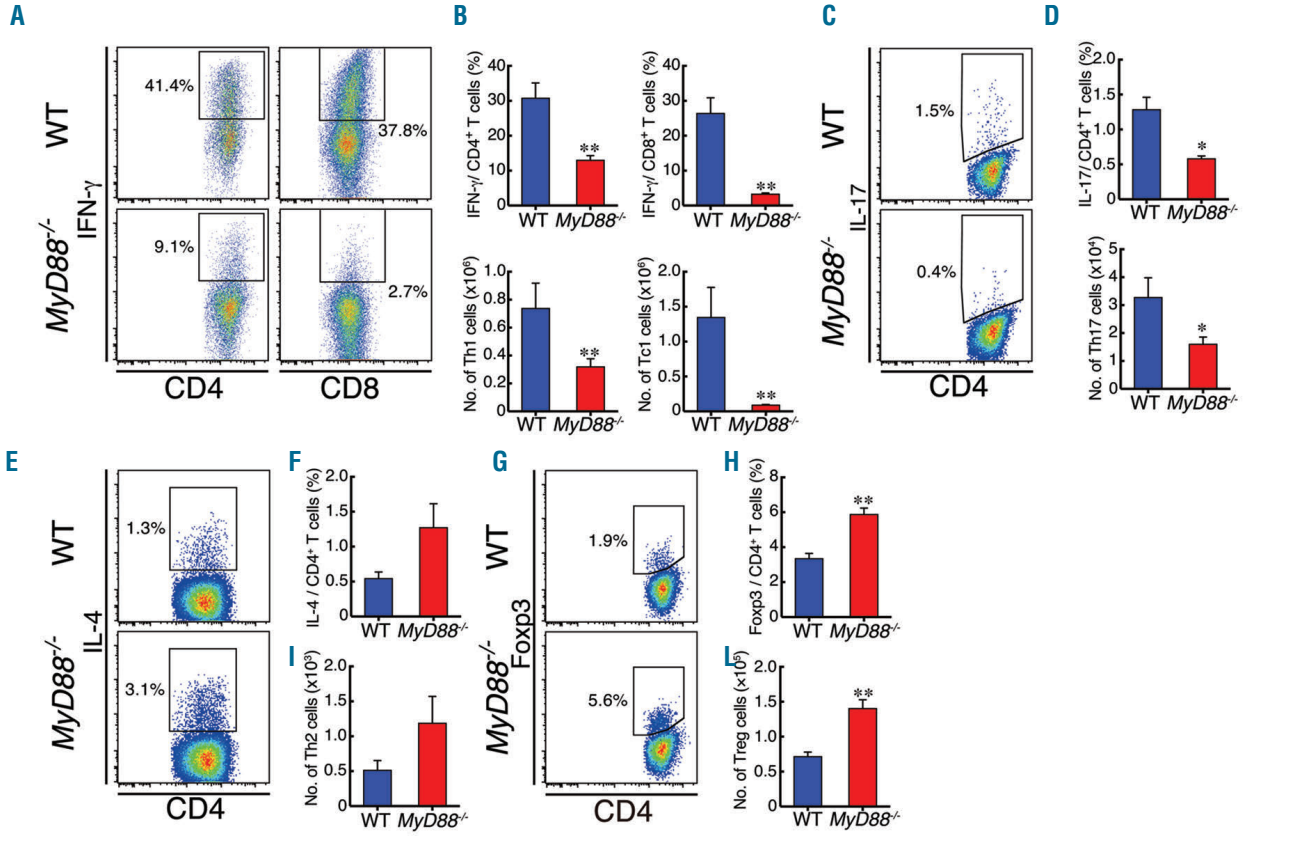

Figure 3. MyD88 deficient donor T cells skew from Th1, Tc1 and Th17 toward T regulatory cell (Treg) differentiation after allogeneic bone marrow transplantation (alloBMT). Mice were transplanted as in Figure 1C. (A-H) Donor T cells harvested from spleens on day +7 were stimulated with PMA/ionomycin and intracellular IFN-γ (A-B), IL-17 (C-D), and IL-4 (E-F) were stained. Representative dot plots (A, C, E), frequencies (B, D, F; top panels) means±Standard Error (SE) and absolute numbers (B, H, E; bottom panels) (means±SE) of cytokine producing donor T cells are shown. Data from two similar experiments were combined (n=10/group). Representative dot plots (G), frequencies (H; top panels) (means±SE), and absolute numbers (H; bottom panels) (means±SE) of donor CD4$^+$Foxp3$^+$ Tregs from a representative experiment of three similar experiments are shown (n=5/group). *P<0.05; **P<0.01.

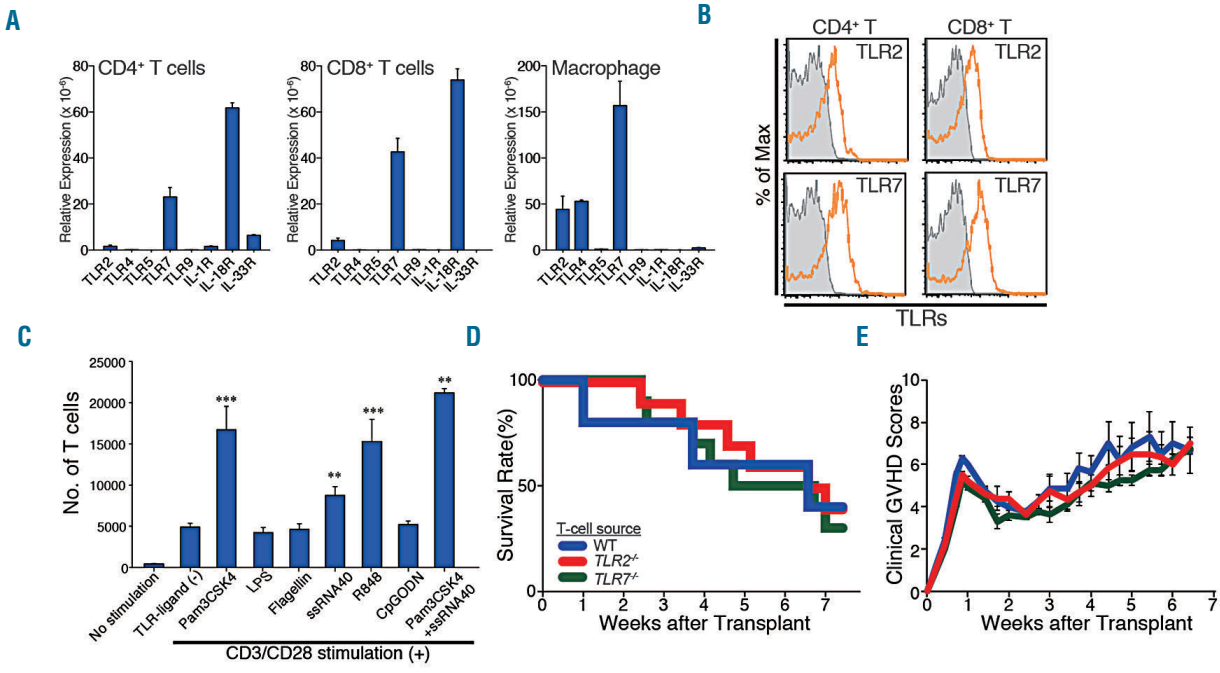

Figure 4. Single TLR blockade is not sufficient to mitigate lethal graft-*versus*-host disease (GvHD). (A) mRNA from CD4+ T cells, CD8+ T cells, and macrophages of naïve *WT* B6 mice was subjected to quantitative polymerase chain reaction of MyD88-related TLRs and cytokine receptors. Data from three similar experiments were combined and shown as means±Standard Error (SE). (B) Flow cytometric analysis of TLR2 (top panels) and TLR7 on T cells (bottom panels) were performed. Representative histograms from one of three similar experiments were shown. (C) 5x10^4 T cells were stimulated with CD3/28 mAb-coated beads in the presence or absence of TLR-ligands for three days (n=12/group). Absolute numbers of T cells after stimulation from four similar experiments were combined and shown as means±SE. (D and E) Lethally irradiated B6D2F1 mice were transplanted with 5x10^6 T cell-depleted bone marrow cells (TCD-BM) cells from *WT* B6 mice plus 1x10^6 purified T cells from *WT*, TLR2$^{-/-}$, or TLR7$^{-/-}$ B6 donors. Survivals (D) and clinical GvHD scores (E) from two independent experiments are combined and shown (n=10/group).

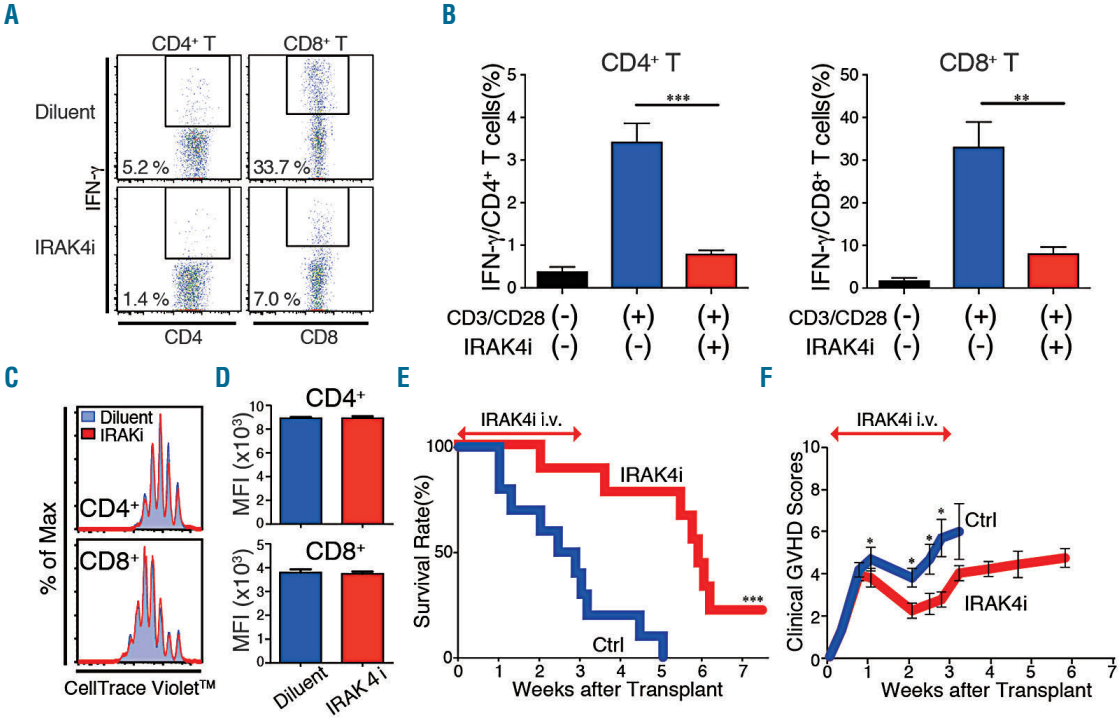

Figure 5. IRAK4 inhibitor PF-06650833 ameliorates graft-*versus*-host disease (GvHD). (A and B) Sorted 5x10^4 T cells from B6 mice were incubated with Dynabeads coated with anti-CD3/CD28 mAbs in the presence or absence of PF-06650833 at a concentration of 20 μM for 96 hours. Representative dot plots (A) and frequency (B), means±Standard Error (SE), of IFN-γ producing T cells from two similar experiments are combined (n=8/group). (C and D) T cells were labeled with CellTrace Violet and stimulated with Dynabeads coated with anti-CD3/CD28 mAbs for 72 hours. Representative histograms (C) and MFI of CellTrace Violet (D) (means±SE) from one of two similar experiments were shown (n=4/group). (E and F) Mice were transplanted as in Figure 1C. A group of mice were intravenously injected with 12.0 mg/kg PF-06650833 daily from day 0 to day 20 after BMT. Survival curves (E) and clinical GvHD scores (F) from two independent experiments are combined (n=10/group). Ctrl: control.

ed B6D2F1 mice were injected with $5x10^6$ TCD-BM from WT B6 plus $1x10^6$ T cells from either WT or *MyD88*$^{-/-}$ B6 mice, with the addition of $1x10^3$ host-type P815 leukemia cells to the donor inoculum. All allogeneic TCD-BM recipients died from leukemia within two weeks after BMT, whereas leukemia mortality was significantly suppressed in the recipients of both WT and *MyD88*$^{-/-}$ T cells. While leukemia mortality was not significantly different between the allogeneic recipients of WT and *MyD88*$^{-/-}$ T cells, overall survival time was significantly prolonged in recipients of *MyD88*$^{-/-}$ T cells compared to controls, suggesting that MyD88 signaling in donor T cells is dispensable for GvL effect and T-cell MyD88 is a therapeutic target of GvHD without GvL reduction (Figure 6A and B). To further assess GvL effects, we have performed *in vivo* bioluminescent imaging (BLI) to track luciferase-transfected P815 (P815-luc) cells after BMT. Survivals were again significantly prolonged in recipients of *MyD88*$^{-/-}$ T cells compared to those of WT T cells (Figure 6C). Whole body BLI clearly demonstrated that growth of P815-luc cells were suppressed both in the recipients of *MyD88*$^{-/-}$ T cells and WT T cells, while P815-luc expanded vigorously in the recipients of TCD-BM alone (Figure 6D). Taken together, we concluded that GvL effects were preserved without donor T-cell MyD88 signaling.

Discussion

The expanding IL-1R/TLR superfamily now consists of more than ten TLR and IL-1R, IL-18R, and IL-33R. TLR are expressed on a wide range of myeloid cells such as macrophages and dendritic cells. However, emerging evidence demonstrates that TLR are also expressed on T cells.[25] Signaling from TLR2, TLR3, TLR5, TLR7/8, and TLR9 has co-stimulatory role in T-cell activation, leading to enhancement of proliferation, survival, and differentiation towards Th1, Th17 and memory CD4$^+$ T cells.[8,25-28] TLR2 is required for expansion and differentiation of virus-specific CD8$^+$ memory T cells.[29,30] TLR4 engagement on CD4$^+$ T cells is required for their effector functions in experimental autoimmune encephalomyelitis.[9] Members of the IL-1R family including IL-1R, IL-18R, and IL-33R are also expressed in T cells and regulate various T-cell functions.[7] IL-1R or IL-18R signaling in T cells is critical for Th1, Th17 and antigen-specific CD8$^+$ T-cell responses.[12,13,31] A previous study demonstrated an impaired proliferation of MyD88-deficient T cells upon antigen stimulation.[12] However, in our study, proliferation of WT T cells and MyD88-deficient T cells were comparable early after allogeneic transplantation or *in vitro* upon CD3/CD28 stimulation, suggesting that the pres-

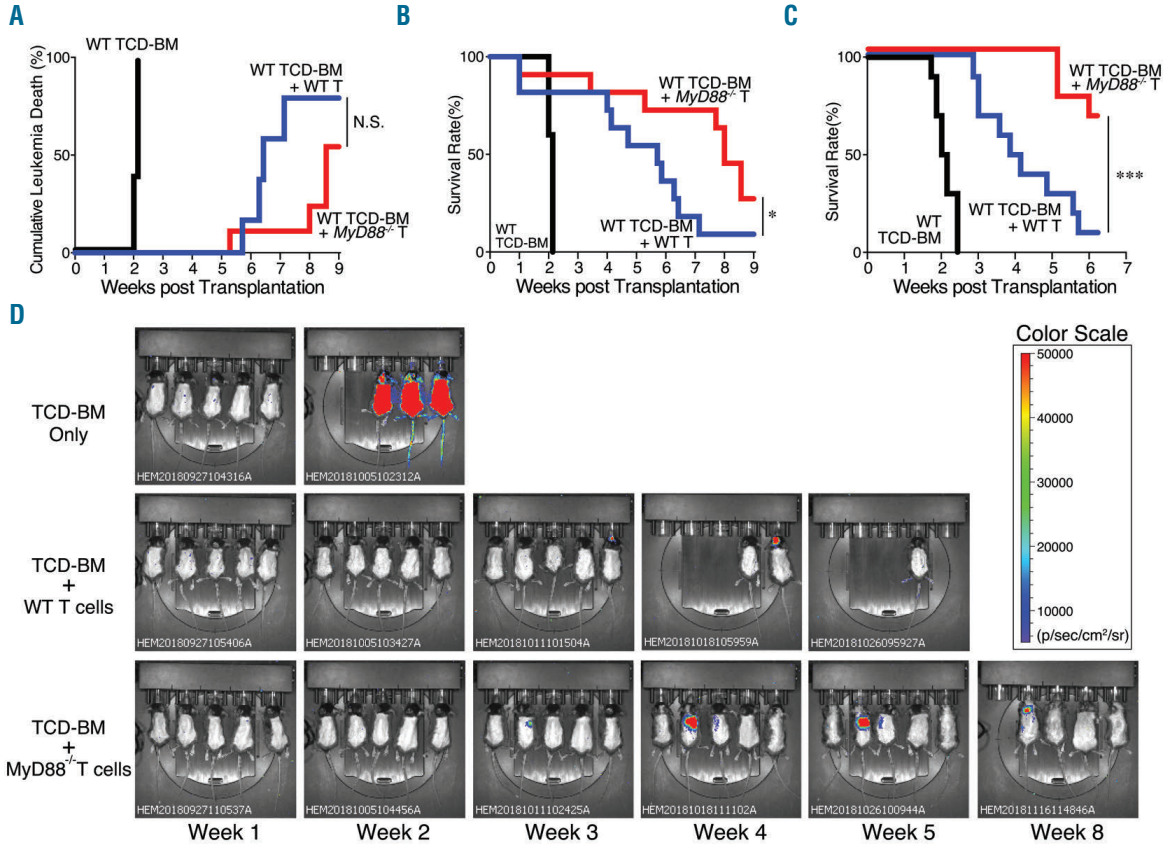

Figure 6. MyD88 signaling in donor T cells is not essential for significant graft-*versus*-leukemia (GvL) effects. (A and B) Lethally irradiated B6D2F1 mice were transplanted with wild-type (WT) T-cell-depleted bone marrow cells (TCD-BM) alone (n=5) or in combination with either WT (n=11) or *MyD88*$^{-/-}$ (n=11) T cells from B6 together with $1x10^3$ P815 leukemia cells (H-2Kd+) on day 0. Cumulative leukemia mortality (A) and overall survival (B) after bone marrow transplantation (BMT) from two experiments are combined. (C and D) Lethally irradiated B6D2F1 mice were transplanted with WT TCD-BM alone (n=10) or in combination with either WT (n=10) or *MyD88*$^{-/-}$ (n=10) T cells from B6 donors together with $5x10^3$ P815-luc cells on day 0. Bioluminescent imaging (BLI) was performed weekly after allogeneic BMT. (C) Overall survival from two independent experiments were combined. (D) The whole body bioluminescent images from 1 of 2 similar experiments are shown.

ence of inflammatory milieu or potent co-stimulation induced robust T-cell proliferation even without T-cell MyD88 signaling. Although we detected only TLR2, TLR7, IL-1R, IL-18R, IL-33R but not TLR4, TLR5, or TLR9 in resting T cells, a diverse combination of expression of the TLR/IL-1R superfamily in T cells including TLR4 and TLR5 has been demonstrated, indicating that the range of TLR/IL-1R expression could be context dependent, such as differentiation and activation status and subtype of T cells, as well as environmental milieu, such as type of inflammation and microbiota.

Although we demonstrated the T-cell co-stimulatory functions of both TLR2 and TLR7 signaling *in vitro*, absence of TLR2 or TLR7 in donor T cells did not change the severity of GvHD. Our results are consistent with previous studies showing that neither TLR2 or TLR7 deficiency in donor cells nor pharmacological inhibition of TLR2 altered morbidity and mortality of GvHD.[32,33] These results suggest that TLR have no role in GvHD. IL-18R and IL-33R signaling in donor T cells has also conflicting roles in GvHD, depending on the experimental models used and the timing of administration of their ligands.[34-37] Given this redundancy and conflicting role of each of IL-1R/TLR superfamily in T cells, we took advantage of *MyD88*$^{-/-}$ T cells that enabled us to block most of the signals from receptors belonging to the TLR/IL-1R superfamily. We found that *MyD88*$^{-/-}$donor T cells showed significantly impaired survival and differentiation toward Th1, Tc1, and Th17 cells, while preserving Foxp3^{+} Treg expansion after allo-SCT, resulting in significant improvement of GvHD. This impairment of *MyD88*$^{-/-}$ T-cell functions after allo-SCT was confirmed in *in vitro* culture. It has been shown that impairment of Th1, Tc1, and Th17 results in mitigated GvHD.[38] A recent study by Lim *et al*. showed that MyD88 deficiency in donor T cells did not ameliorate GvHD, but decreased GvL using a similar model of BMT, even though they also showed impaired Th1 differentiation of *MyD88*$^{-/-}$ T cells after BMT.[39] It should be noted that GvHD of allogeneic controls was less severe with 30% mortality in that study compared to severe GvHD with 80% mortality in our study. Thus, the mild experimental condition in that study may compromise our seeing a reduction in GvHD. GvL activity determined by leukemia mortality and *in vivo* BLI was preserved in the absence of T-cell MyD88, suggesting that T-cell MyD88 signaling plays a more important role on GvHD than on GvL effects in our model. However, its contribution to GvHD and GvL may change in allo-SCT following reduced intensity conditioning, as shown in the Lim *et al*. study.[39]

Pharmacological inhibition of TLR/IL-1R has been studied in murine models and clinical studies. Pharmacological blockade of IL-1/IL-1R or IL-33/IL-33R interaction ameliorates experimental GvHD;[40] however, a randomized trial failed to show any protective effect of the IL-1R antagonist Anakinra against clinical GvHD.[41-43] MyD88 is an adopter molecule to recruit IRAK to most of the receptors belonging to the IL-1R/TLR superfamily to relay signals to downstream proinflammatory pathways.[44,45] Given the redundant roles of a wide range of TLR/IL-1R, inhibition of multiple TLR/IL-1R signals by MyD88 or IRAK4 inhibitors would be more effective than a single pathway blockade. We showed that pharmacological inhibition of MyD88/IRAK4 pathway using IRAK4 inhibitor ameliorated experimental GvHD. IRAK4 also plays a critical role in T-cell activation[46] and IRAK4-deficient T cells showed significantly delayed allogeneic skin graft rejection.[46] The IRAK4 inhibitor could not only affect donor T cells, but also donor accessory cells and recipient cells; however, it has been reported that MyD88 signaling in the donor BM cells or recipient cells did not enhance GvHD, thus it is likely that IRAK4 inhibitor ameliorated GvHD by acting on donor T cells.[4,47] There are several MyD88 or IRAK4 inhibitors that demonstrated anti-inflammatory effects in pre-clinical models. PF-06650833 is one of IRAK4 inhibitors in clinical development, that was previously tested in a phase I trial for patients with systemic lupus erythematosus and phase II clinical study for patients with rheumatoid arthritis is ongoing (*https://clinicaltrials.gov/ct2/show/NCT02996500?term=06650833&rank=3*).[48,49]

In conclusion, our results demonstrate a previously unrevealed role of T-cell MyD88 signaling in the development of GvHD. Because GvL effects were at least preserved in the absence of donor MyD88 signaling, the IRAK-4 inhibitor PF-06650833 is an ideal agent to ameliorate GvHD, likely by inhibiting MyD88/IRAK4 signaling in donor T cells with sparing. Furthermore, the IRAK4 inhibitor is also under development as a therapeutic reagent against B-cell neoplasms with MyD88 mutation, indicating that therapeutic or prophylactic administration of IRAK4 inhibitor after allo-SCT could ameliorate GvHD with enhancing tumor control of B-cell neoplasms.[50] Signaling molecules such as JAK, MEK, AURKA, and many other molecules that integrate the signals from multiple receptors of cytokines or growth factors, are promising therapeutic targets of GvHD.[51,52] Given the critical role of IRAK4 in activation of human T cells, MyD88 and IRAK4 inhibitors that could inhibit signaling from more than ten receptors belonging to the TLR/IL-1R superfamily should be tested in clinical studies to explore their prophylactic and therapeutic potentials against GvHD.[53]

Funding

This study was supported by JSPS KAKENHI (21390295 and 17H04206 to TT, 17K09945 to DH), Japan Society of Hematology Research Fund (TT), the Center of Innovation Program from JST (TT), and research grants from the Mochida Memorial Foundation for Medical and Pharmaceutical Research (DH).

References

1. Garlanda C, Dinarello CA, Mantovani A. The interleukin-1 family: back to the future. Immunity. 2013;39(6):1003-1018.
2. Kono H, Rock KL. How dying cells alert the immune system to danger. Nat Rev Immunol. 2008;8(4):279-289.
3. Mortha A, Chudnovskiy A, Hashimoto D, et al. Microbiota-dependent crosstalk between macrophages and ILC3 promotes intestinal homeostasis. Science. 2014; 343(6178):1249288.
4. Lim JY, Lee YK, Lee SE, et al. MyD88 in donor bone marrow cells is critical for protection from acute intestinal graft-vs.-host disease. Mucosal Immunol. 2016;9(3):730-743.
5. Jin B, Sun T, Yu XH, Yang YX, Yeo AE. The effects of TLR activation on T-cell development and differentiation. Clin Dev Immunol. 2012;2012:836485.
6. Rahman AH, Taylor DK, Turka LA. The contribution of direct TLR signaling to T cell responses. Immunol Res. 2009; 45(1):25-36.
7. Li W, Kashiwamura S, Ueda H, Sekiyama A, Okamura H. Protection of CD8+ T cells from activation-induced cell death by IL-

18. J Leukoc Biol. 2007;82(1):142-151.
8. Imanishi T, Hara H, Suzuki S, Suzuki N, Akira S, Saito T. Cutting edge: TLR2 directly triggers Th1 effector functions. J Immunol. 2007;178(11):6715-6719.
9. Reynolds JM, Martinez GJ, Chung Y, Dong C. Toll-like receptor 4 signaling in T cells promotes autoimmune inflammation. Proc Natl Acad Sci U S A. 2012;109(32):13064-13069.
10. Chang J, Burkett PR, Borges CM, Kuchroo VK, Turka LA, Chang CH. MyD88 is essential to sustain mTOR activation necessary to promote T helper 17 cell proliferation by linking IL-1 and IL-23 signaling. Proc Natl Acad Sci U S A. 2013;110(6):2270-2275.
11. Zhang Y, Jones M, McCabe A, Winslow GM, Avram D, MacNamara KC. MyD88 signaling in CD4 T cells promotes IFN-gamma production and hematopoietic progenitor cell expansion in response to intracellular bacterial infection. J Immunol. 2013;190(9):4725-4735.
12. Schenten D, Nish SA, Yu S, et al. Signaling through the adaptor molecule MyD88 in CD4+ T cells is required to overcome suppression by regulatory T cells. Immunity. 2014;40(1):78-90.
13. O'Donnell H, Pham OH, Li LX, et al. Toll-like receptor and inflammasome signals converge to amplify the innate bactericidal capacity of T helper 1 cells. Immunity. 2014;40(2):213-224.
14. Shlomchik WD, Couzens MS, Tang CB, et al. Prevention of graft versus host disease by inactivation of host antigen-presenting cells. Science. 1999;285(5426):412-415.
15. Koyama M, Kuns RD, Olver SD, et al. Recipient nonhematopoietic antigen-presenting cells are sufficient to induce lethal acute graft-versus-host disease. Nat Med. 2011;18(1):135-142.
16. Hill GR, Crawford JM, Cooke KR, Brinson YS, Pan L, Ferrara JL. Total body irradiation and acute graft-versus-host disease: the role of gastrointestinal damage and inflammatory cytokines. Blood. 1997;90(8):3204-3213.
17. Ferrara JL, Cooke KR, Teshima T. The pathophysiology of acute graft-versus-host disease. Int J Hematol. 2003;78(3):181-187.
18. Cooke KR, Hill GR, Crawford JM, et al. Tumor necrosis factor- alpha production to lipopolysaccharide stimulation by donor cells predicts the severity of experimental acute graft-versus-host disease. J Clin Invest. 1998;102(10):1882-1891.
19. Cooke KR, Gerbitz A, Crawford JM, et al. LPS antagonism reduces graft-versus-host disease and preserves graft-versus-leukemia activity after experimental bone marrow transplantation. J Clin Invest. 2001;107(12):1581-1589.
20. Yamamoto M, Sato S, Hemmi H, et al. Role of adaptor TRIF in the MyD88-independent toll-like receptor signaling pathway. Science. 2003;301(5633):640-643.
21. Uryu H, Hashimoto D, Kato K, et al. alpha-Mannan induces Th17-mediated pulmonary graft-versus-host disease in mice. Blood. 2015;125(19):3014-3023.
22. Cooke KR, Kobzik L, Martin TR, et al. An experimental model of idiopathic pneumonia syndrome after bone marrow transplantation: I. The roles of minor H antigens and endotoxin. Blood. 1996;88(8):3230-3239.
23. Teshima T, Hill GR, Pan L, et al. IL-11 separates graft-versus-leukemia effects from graft-versus-host disease after bone marrow transplantation. J Clin Invest. 1999;104(3):317-325.
24. Edinger M, Hoffmann P, Ermann J, et al. CD4(+)CD25(+) regulatory T cells preserve graft-versus-tumor activity while inhibiting graft-versus-host disease after bone marrow transplantation. Nat Med. 2003;9(9):1144-1150.
25. Gelman AE, Zhang J, Choi Y, Turka LA. Toll-like receptor ligands directly promote activated CD4+ T cell survival. J Immunol. 2004;172(10):6065-6073.
26. Komai-Koma M, Jones L, Ogg GS, Xu D, Liew FY. TLR2 is expressed on activated T cells as a costimulatory receptor. Proc Natl Acad Sci U S A. 2004;101(9):3029-3034.
27. Caron G, Duluc D, Fremaux I, et al. Direct stimulation of human T cells via TLR5 and TLR7/8: flagellin and R-848 up-regulate proliferation and IFN-gamma production by memory CD4+ T cells. J Immunol. 2005;175(3):1551-1557.
28. Reynolds JM, Pappu BP, Peng J, et al. Toll-like receptor 2 signaling in CD4(+) T lymphocytes promotes T helper 17 responses and regulates the pathogenesis of autoimmune disease. Immunity. 2010;32(5):692-702.
29. Quigley M, Martinez J, Huang X, Yang Y. A critical role for direct TLR2-MyD88 signaling in CD8 T-cell clonal expansion and memory formation following vaccinia viral infection. Blood. 2009;113(10):2256-2264.
30. Mercier BC, Cottalorda A, Coupet CA, Marvel J, Bonnefoy-Berard N. TLR2 engagement on CD8 T cells enables generation of functional memory cells in response to a suboptimal TCR signal. J Immunol. 2009;182(4):1860-1867.
31. Ben-Sasson SZ, Hogg A, Hu-Li J, et al. IL-1 enhances expansion, effector function, tissue localization, and memory response of antigen-specific CD8 T cells. J Exp Med. 2013;210(3):491-502.
32. Heimesaat MM, Nogai A, Bereswill S, et al. MyD88/TLR9 mediated immunopathology and gut microbiota dynamics in a novel murine model of intestinal graft-versus-host disease. Gut. 2010;59(8):1079-1087.
33. Lee WS, Kim JY, Won HJ, et al. Effect of upregulated TLR2 expression from G-CSF-mobilized donor grafts on acute graft-versus-host disease. Int Immunopharmacol. 2015;29(2):488-493.
34. Reddy P, Teshima T, Kukuruga M, et al. Interleukin-18 regulates acute graft-versus-host disease by enhancing Fas-mediated donor T cell apoptosis. J Exp Med. 2001;194(10):1433-1440.
35. Okamoto I, Kohno K, Tanimoto T, et al. IL-18 prevents the development of chronic graft-versus-host disease in mice. J Immunol. 2000;164(11):6067-6074.
36. Min CK, Maeda Y, Lowler K, et al. Paradoxical effects of interleukin-18 on the severity of acute graft-versus-host disease mediated by CD4+ and CD8+ T-cell subsets after experimental allogeneic bone marrow transplantation. Blood. 2004;104(10):3393-3399.
37. Matta BM, Reichenbach DK, Zhang X, et al. Peri-alloHCT IL-33 administration expands recipient T-regulatory cells that protect mice against acute GVHD. Blood. 2016;128(3):427-439.
38. Yu Y, Wang D, Liu C, et al. Prevention of GVHD while sparing GVL by targeting Th1 and Th17 transcription factor T-bet and ROR{gamma}t in mice. Blood. 2011;118(18):5011-5020.
39. Lim JY, Ryu DB, Lee SE, Park G, Choi EY, Min CK. Differential Effect of MyD88 Signal in Donor T Cells on Graft-versus-Leukemia Effect and Graft-versus-Host Disease after Experimental Allogeneic Stem Cell Transplantation. Mol Cells. 2015;38(11):966-974.
40. Zhang J, Ramadan AM, Griesenauer B, et al. ST2 blockade reduces sST2-producing T cells while maintaining protective mST2-expressing T cells during graft-versus-host disease. Sci Transl Med. 2015;7(308):308ra160.
41. Jankovic D, Ganesan J, Bscheider M, et al. The Nlrp3 inflammasome regulates acute graft-versus-host disease. J Exp Med. 2013;210(10):1899-1910.
42. Park MJ, Lee SH, Lee SH, et al. IL-1 Receptor Blockade Alleviates Graft-versus-Host Disease through Downregulation of an Interleukin-1beta-Dependent Glycolytic Pathway in Th17 Cells. Mediators Inflamm. 2015;2015:631384.
43. Antin JH, Weisdorf D, Neuberg D, et al. Interleukin-1 blockade does not prevent acute graft-versus-host disease: results of a randomized, double-blind, placebo-controlled trial of interleukin-1 receptor antagonist in allogeneic bone marrow transplantation. Blood. 2002;100(10):3479-3482.
44. Hultmark D. Macrophage differentiation marker MyD88 is a member of the Toll/IL-1 receptor family. Biochem Biophys Res Commun. 1994;199(1):144-146.
45. Muzio M, Ni J, Feng P, Dixit VM. IRAK (Pelle) family member IRAK-2 and MyD88 as proximal mediators of IL-1 signaling. Science. 1997;278(5343):1612-1615.
46. Suzuki N, Suzuki S, Millar DG, et al. A critical role for the innate immune signaling molecule IRAK-4 in T cell activation. Science. 2006;311(5769):1927-1932.
47. Li H, Matte-Martone C, Tan HS, et al. Graft-versus-host disease is independent of innate signaling pathways triggered by pathogens in host hematopoietic cells. J Immunol. 2011;186(1):230-241.
48. Wu YW, Tang W, Zuo JP. Toll-like receptors: potential targets for lupus treatment. Acta Pharmacol Sin. 2015;36(12):1395-1407.
49. Lee KL, Ambler CM, Anderson DR, et al. Discovery of Clinical Candidate 1-{[(2S,3S,4S)-3-Ethyl-4-fluoro-5-oxopyrrolidin-2-yl]methoxy}-7-methoxyisoquinoline-6-carboxamide (PF-06650833), a Potent, Selective Inhibitor of Interleukin-1 Receptor Associated Kinase 4 (IRAK4), by Fragment-Based Drug Design. J Med Chem. 2017;60(13):5521-5542.
50. Kelly PN, Romero DL, Yang Y, et al. Selective interleukin-1 receptor-associated kinase 4 inhibitors for the treatment of autoimmune disorders and lymphoid malignancy. J Exp Med. 2015;212(13):2189-2201.
51. Teshima T, Reddy P, Zeiser R. Acute Graft-versus-Host Disease: Novel Biological Insights. Biol Blood Marrow Transplant. 2016;22(1):11-16.
52. Zeiser R, Blazar BR. Acute Graft-versus-Host Disease - Biologic Process, Prevention, and Therapy. N Engl J Med. 2017;377(22):2167-2179.
53. McDonald DR, Goldman F, Gomez-Duarte OD, et al. Impaired T-cell receptor activation in IL-1 receptor-associated kinase-4-deficient patients. J Allergy Clin Immunol. 2010;126(2):332-337.

ARTICLE

Rapid generation of multivirus-specific T lymphocytes for the prevention and treatment of respiratory viral infections

Spyridoula Vasileiou, Anne M. Turney, Manik Kuvalekar, Shivani S. Mukhi, Ayumi Watanabe, Premal Lulla, Carlos A. Ramos, Swati Naik, Juan F. Vera, Ifigeneia Tzannou and Ann M. Leen

Center for Cell and Gene Therapy, Baylor College of Medicine, Texas Children's Hospital and Houston Methodist Hospital, Houston, TX, USA

Ferrata Storti Foundation

Haematologica 2020
Volume 105(1):235-243

ABSTRACT

Respiratory tract infections due to community-acquired respiratory viruses including respiratory syncytial virus, Influenza, parainfluenza virus 3 and human metapneumovirus are detected in up to 40% of allogeneic hematopoietic stem cell transplant recipients in whom they cause severe symptoms including pneumonia and bronchiolitis and can be fatal. Given the lack of effective antivirals and the data from our group demonstrating that adoptively transferred *ex vivo*-expanded virus-specific T cells can be clinically beneficial for the treatment of both latent (Epstein-Barr virus, cytomegalovirus, BK virus, human herpesvirus 6) and lytic (adenovirus) viruses, we investigated the potential for extending this immunotherapeutic approach to respiratory viruses. We now describe a system that rapidly generates a single preparation of polyclonal ($CD4^+$ and $CD8^+$) virus-specific T cells reactive against 12 antigens derived from four viruses (respiratory syncytial virus, Influenza, parainfluenza virus 3 and human metapneumovirus) that commonly cause post-transplant morbidity and mortality. With a single *in vitro* stimulation we consistently generated Th1-polarized T-cell lines that produced multiple effector cytokines and were selectively reactive against viral-expressing targets, with no evidence of "off target" auto- or allo-reactivity. Finally, we demonstrated the clinical relevance of these virus-specific T cells by measuring responses in transplant recipients who successfully controlled active infections. These results support the clinical importance of T-cell immunity in mediating protective antiviral effects against community-acquired respiratory viruses and demonstrate the feasibility of utilizing a broad-spectrum immunotherapeutic in immunocompromised patients with uncontrolled infections.

Introduction

Acute upper and lower respiratory tract infections (RTI) due to community-acquired respiratory viruses (CARV) including respiratory syncytial virus (RSV), influenza, parainfluenza virus (PIV) and human metapneumovirus (hMPV) are a major public health problem.[1] For example, RSV-induced bronchiolitis is the most common reason for hospital admission in children under one year of age,[2-4] while the Center for Disease Control (CDC) estimates that, annually, Influenza accounts for up to 35.6 million illnesses worldwide, between 140,000 and 710,000 hospitalizations, annual costs of approximately $87.1 billion in disease management in the US alone, and between 12,000 and 56,000 deaths.

Thus, CARV are a leading cause of morbidity and mortality worldwide, with individuals whose immune systems are naïve (e.g. young children) or compromised being the most vulnerable. For example, in allogeneic hematopoietic stem cell transplant (HSCT) recipients, the incidence of CARV-related respiratory viral diseases is as high as 40%.[5] While most patients initially present with rhinorrhea, cough and fever, in approximately 50% of cases, infections progress to the lower respiratory tract and are characterized by severe symptoms including pneumonia and bronchiolitis and mortality rates of 23-50%.[6-9] There are neither approved preventative vaccines nor antiviral drugs for hMPV[10] and PIV[11] and for Influenza the preventative vaccine is not indi-

Correspondence:

ANN M. LEEN
amleen@txch.org

Received: September 14, 2018.

Accepted: April 16, 2019.

Pre-published: April 19, 2019.

doi:10.3324/haematol.2018.206896

Check the online version for the most updated information on this article, online supplements, and information on authorship & disclosures: www.haematologica.org/content/105/1/235

cated unless patients are at least six months post-HSCT.[12] Aerosolized ribavirin (RBV) has been approved by the US Food and Drug Administration (FDA) for the treatment of RSV, but it is extremely costly (5-day course = $149,756) and logistically difficult to administer, requiring a specialized nebulization device that connects to an aerosol tent surrounding the patient.[13-16] Thus, the lack of approved antiviral agents for many clinically problematic CARV, and the high cost and complexity of administering aerosolized RBV, underscores the need for alternative treatment strategies.

Our group has previously demonstrated that the adoptive transfer of *in vitro*-expanded virus-specific T cells (VST) can safely and effectively prevent and treat infections associated with both latent [Epstein-Barr virus (EBV), cytomegalovirus (CMV), BK virus (BKV), human herpesvirus 6 (HHV6)] and lytic [adenovirus (AdV)] viruses in allogeneic HSCT recipients.[17,18] Given that susceptibility to CARV is associated with underlying cellular immune deficiency,[1,5,6] in the current study, we explored the feasibility of extending the therapeutic range of VST therapy to include Influenza, RSV, hMPV and PIV-3.

We here describe a mechanism by which we can rapidly generate a single preparation of polyclonal ($CD4^+$ and $CD8^+$) VST with specificity for 12 immunodominant antigens derived from our four target viruses using Good Manufacturing Practices (GMP)-compliant manufacturing methodologies. The viral proteins used for stimulation were chosen on the basis of both their immunogenicity to T cells and their sequence conservation.[19-21] The expanded cells are Th1-polarized, polyfunctional and selectively able to react to and kill, viral antigen-expressing target cells with no activity against non-infected autologous or allogeneic targets, attesting to both their selectivity for viral targets and their safety for clinical use. We anticipate such multi-respiratory virus-targeted cells (multi-R-VST) will provide broad spectrum benefit to immunocompromised individuals with uncontrolled CARV infections.

Methods

Donors and cell lines

Peripheral blood mononuclear cells (PBMC) were obtained from healthy volunteers and HSCT recipients with informed consent using Baylor College of Medicine institutional review board-approved protocols (H-7634, H-7666) and were used to generate phytohemagglutinin (PHA) blasts and multi-R-VST. PHA blasts were generated as previously reported[20] and cultured in VST medium [45% RPMI 1640 (HyClone Laboratories, Logan, UT, USA), 45% Click's medium (Irvine Scientific, Santa Ana, CA, USA), 2 mM GlutaMAX TM-I (Life Technologies, Grand Island, New York, NY, USA), and 10% human AB serum (Valley Biomedical, Winchester, VA, USA)] supplemented with interleukin 2 (IL2) (100 U/mL; NIH, Bethesda, MD, USA), which was replenished every two days.

Multi-respiratory virus-targeted cell generation

Pepmixes

Peripheral blood mononuclear cells were stimulated with peptide libraries (15mers overlapping by 11aa) spanning Influenza A (NP1, MP1), RSV (N, F), hMPV (F, N, M2-1, M) (JPT Peptide Technologies, Berlin, Germany) and PIV-3 antigens (M, HN, N, F) (Genemed Synthesis, San Antonio, TX, USA). Lyophilized pepmixes were reconstituted in dimethyl sulfoxide (DMSO) (Sigma-Aldrich) and stored at -80°C.

Generation of virus-specific T cells

To generate multi-R-VST, PBMC ($2.5x10^7$) were transferred to a G-Rex10 (Wilson Wolf Manufacturing Corporation, St. Paul, MN, USA) with 100 mL of VST medium supplemented with IL7 (20 ng/mL), IL4 (800 U/mL) (R&D Systems, Minneapolis, MN, USA) and pepmixes (2 ng/peptide/mL) and cultured for 10-13 days at 37°C, 5% CO_2.

Flow cytometry

Immunophenotyping

Multi-R-VST were surface-stained with monoclonal antibodies to: CD3, CD25, CD28, CD45RO, CD279 (PD-1) [Becton Dickinson (BD), Franklin Lakes, NJ, USA], CD4, CD8, CD16, CD62L, CD69 (Beckman Coulter, Brea, CA, USA) and CD366 (TIM-3) (BioLegend, San Diego, CA, USA). Cells were acquired on a Gallios™ Flow Cytometer and analyzed with Kaluza® Flow Analysis Software (Beckman Coulter). See *Online Supplementary Appendix* for details.

Intracellular cytokine staining

Multi-R-VST were harvested, resuspended in VST medium ($2x10^6$/mL) and 200 μL added per well of a 96-well plate. Cells were incubated overnight with 200 ng of individual test or control (irrelevant non-viral, e.g. SURVIVIN, WT1) pepmixes, along with Brefeldin A (1 μg/mL), monensin (1 μg/mL), CD28 and CD49d (1 μg/mL) (BD). Intracellular cytokine staining (ICS) for IFNγ and TNFα was performed as described in the *Online Supplementary Appendix*.

FoxP3 staining

FoxP3 staining was performed using the eBioscience FoxP3 kit (Thermo Fisher Scientific, Waltham, MA, USA), per manufacturers' instructions and as detailed in the *Online Supplementary Appendix*.

Functional studies

Enzyme-linked immunospot

Enzyme-linked immunospot (ELIspot) analysis was used to quantitate the frequency of IFNγ and Granzyme B-secreting cells. PBMC and multi-R-VST were resuspended at $5x10^6$ and $2x10^6$ cells/mL, respectively, in VST medium and 100 μL of cells added to each ELIspot well. Antigen-specific activity was measured as previously described after direct stimulation (500 ng/peptide/mL) with the individual test or control pepmixes. See the *Online Supplementary Appendix* for more details.

Multiplex

The multi-R-VST cytokine profile was evaluated using the MILLIPLEX High Sensitivity Human Cytokine Panel (Millipore, Billerica, MA, USA), per manufacturer's instructions (see the *Online Supplementary Appendix*).

Chromium release assay

A standard 4-hour chromium (Cr^{51}) release assay was used to measure the specific cytolytic activity of multi-R-VST with autologous antigen-loaded PHA blasts as targets (20 ng/pepmix/$1x10^6$ target cells). Effector:Target (E:T) ratios of 40:1, 20:1, 10:1, and 5:1 were used to analyze specific lysis. The percentage of specific lysis was calculated [(experimental release - spontaneous release)/(maximum release - spontaneous release)] x 100. In order to measure the autoreactive and alloreactive potential of multi-R-VST lines, autologous and allogeneic PHA blasts alone were used as targets.

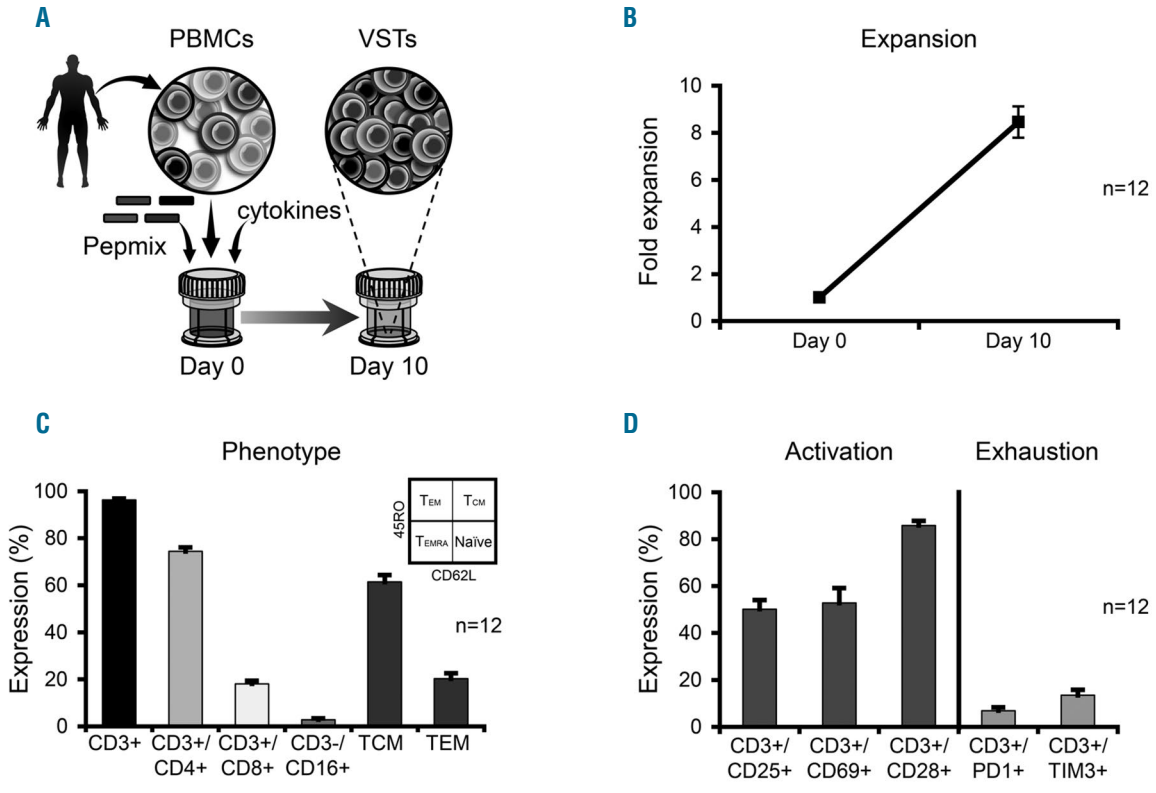

Figure 1. Generation of polyclonal multi-respiratory virus-targeted cells (multi-R-VST) from healthy donors. (A) A schematic representation of the multi-R-VST generation protocol. (B) Fold expansion achieved over a 10-13 day period based on cell counting using trypan blue exclusion (n=12). (C and D) Phenotype of the expanded cells (mean±Standard Error of Mean, n=12) (SEM).

Results

Generation of polyclonal multi-respiratory virus-targeted cells from healthy donors

To investigate the feasibility of generating VST-specific T-cell lines containing sub-populations of cells reactive against Influenza, RSV, hMPV, and PIV-3 we utilized a pool of overlapping peptide libraries spanning immunogenic antigens from each of the target viruses (Influenza – NP1 and MP1; RSV – N and F; hMPV – F, N, M2-1 and M; PIV-3 – M, HN, N and F) to stimulate PBMC before culture in a G-Rex10 in cytokine-supplemented VST medium (Figure 1A). Over 10-13 days we achieved an average 8.5-fold increase in cells (Figure 1B) [increase from $0.25x10^7$ PBMC/cm^2 to mean $1.9±0.2x10^7$ cells/cm^2 (median: $2.05x10^7$, range: $0.6\text{-}2.82x10^7$ cells/cm^2; n=12)], which were comprised almost exclusively of $CD3^+$ T cells (96.2±0.6%; mean±SEM), with a mixture of cytotoxic ($CD8^+$; 18.1±1.3%) and helper ($CD4^+$; 74.4±1.7%) T cells (Figure 1C), with no evidence of regulatory T-cell outgrowth, as assessed by CD4/CD25/$FoxP3^+$ staining (*Online Supplementary Figure S1*). Furthermore, the expanded cells displayed a phenotype consistent with effector function and long-term memory as evidenced by upregulation of the activation markers CD25 (50.2±3.8%), CD69 (52.8±6.3%), CD28 (85.8±2%) as well as expression of central ($CD45RO^+$/$CD62L^+$: 61.4±3%) and effector memory markers ($CD45RO^+$/$CD62L^-$: 20.3±2.3%), with minimal PD1 (6.9±1.4%) or Tim3 (13.5±2.3%) surface expression (Figure 1C and D).

Anti-viral specificity of multi-respiratory virus-targeted cells

To next determine whether the expanded populations were antigen-specific, we performed an IFNγ ELIspot assay using each of the individual stimulating antigens as an immunogen. All 12 lines generated proved to be reactive against all of the target viruses (Table 1 and *Online Supplementary Figure S2*). Figure 2A summarizes the magnitude of activity against each of the stimulating antigens, while *Online Supplementary Figure S3* shows the response of our expanded VST to titrated concentrations of viral antigen. Of note, over the 10-13 days in culture we achieved an enrichment in VST of between 14.6±4.3-fold (PIV-3-HN) and 50.4±9.9-fold (RSV-N) (Figure 2B). The precursor frequencies of CARV-reactive T cells within donor PBMC are summarized in *Online Supplementary Figures S4* and *S5*. Taken together these data suggest that respiratory VST reside in the memory pool and can be readily amplified *ex vivo* using GMP-compliant manufacturing methodologies.

To next evaluate whether viral specificity was contained within the $CD4^+$ or $CD8^+$ or both T-cell subsets we performed ICS, gating on $CD4^+$ and $CD8^+$ IFNγ-producing cells. Figure 2C shows representative results from one donor with activity against all four viruses detected in both T-cell compartments [($CD4^+$: Influenza – 5.28%; RSV – 11%; hMPV – 6.57%; PIV-3 – 3.37%), ($CD8^+$: Influenza – 2.26%; RSV – 4.36%; hMPV – 2.69%; PIV-3 – 2.16%)] while Figure 2D shows a summary of results for nine donors screened, confirming that our multi-R-VST are polyclonal and poly-specific.

Table 1. Reactivity of expanded virus-specific T cells lines against individual stimulating antigens.

	Influenza		RSV		hMPV				PIV-3			
Donor	NP1	MP1	N	F	M	M2-1	F	N	M	F	N	HN
1	✓	✓	✓	✓	✓	✓	✓	x	✓	x	✓	✓
2	✓	✓	✓	✓	✓	✓	✓	✓	✓	✓	✓	✓
3	✓	✓	✓	✓	✓	✓	✓	✓	✓	✓	✓	✓
4	✓	✓	✓	✓	✓	x	✓	✓	✓	✓	x	x
5	✓	✓	✓	✓	✓	✓	✓	✓	✓	✓	✓	✓
6	✓	✓	✓	✓	✓	✓	✓	x	✓	x	x	✓
7	✓	✓	✓	✓	✓	x	✓	x	✓	✓	x	x
8	✓	✓	✓	✓	✓	✓	✓	x	✓	✓	✓	x
9	✓	✓	✓	✓	✓	✓	✓	✓	✓	x	x	x
10	✓	✓	✓	✓	x	✓	x	x	✓	x	x	x
11	✓	✓	✓	✓	✓	✓	✓	✓	✓	✓	x	✓
12	✓	✓	✓	✓	✓	✓	x	✓	✓	✓	✓	x

Functional characterization of multi-respiratory virus-targeted cells

The production of multiple proinflammatory cytokines and expression of effector molecules has been shown to correlate with enhanced cytolytic function and improved *in vivo* T-cell activity. Hence, we next examined the cytokine profile of our multi-R-VST following antigen exposure. The majority of IFNγ-producing cells also produced TNFα (see Figure 3A for detailed ICS results from 1 donor, and Figure 3B, for summary results for 9 donors), in addition to GM-CSF, as measured by Luminex array (Figure 3C, left panel) with baseline levels of prototypic Th2/suppressive cytokines (Figure 3C, right panel). Furthermore, upon antigenic stimulation our cells produced the effector molecule Granzyme B, suggesting the cytolytic potential of these expanded cells (Figure 3D, n=9). Taken together, these data demonstrate the Th1-polarized and polyfunctional characteristics of our multi-R-VST.

Multi-respiratory virus-targeted cells are cytolytic and kill virus-loaded targets

To investigate the cytolytic potential of these expanded cells *in vitro*, we co-cultured multi-R-VST with autologous Cr^{51}-labeled PHA blasts, which were loaded with viral pepmixes with unloaded PHA blasts serving as a control. Viral antigen-loaded targets were specifically recognized and lysed by our expanded multi-R-VST (40:1 E:T - Influenza: 13±5%, RSV: 36±8%, hMPV: 26±7%, PIV-3: 22±5%, n=8) (Figure 4A and *Online Supplementary Figure S6*). Finally, even though these VST had received only a single stimulation, there was no evidence of activity against non-infected autologous targets nor of alloreactivity (graft-*versus*-host potential) using HLA-mismatched PHA blasts as targets (Figure 4B), an important consideration if these cells are to be administered to allogeneic HSCT recipients.

Detection of CARV-specific T cells in hematopoietic stem cell transplant recipients

Finally, to assess the potential clinical relevance of multi-R-VST we investigated whether allogeneic HSCT recipients with active/recent CARV infections exhibited elevated levels of reactive T cells during/following an active viral episode. Figure 5A shows the results of Patient #1, a 64-year old male with acute myeloid leukemia (AML) who received a matched related donor (MRD) transplant with reduced intensity conditioning. The patient developed a severe upper respiratory tract infection (URTI) nine months post-HSCT that was confirmed to be RSV-related by polymerase chain reaction (PCR) analysis. He was not on any immunosuppression at the time of infection but was placed on prednisone the day of infection diagnosis to control pulmonary inflammation. Within four weeks his symptoms resolved without specific antiviral treatment. To assess whether T-cell immunity contributed to viral clearance, we analyzed the circulating frequency of RSV-specific T cells over the course of his infection. Immediately prior to infection this patient exhibited a very weak response to the RSV antigens N and F (6.5 SFC/5x10^5 PBMC). However, within a month of viral exposure, RSV-specific T cells had expanded *in vivo* (527 SFC/5x10^5 PBMC), representing an 81-fold increase in reactive cells (Figure 5A) which declined thereafter, coincident with viral clearance. Of note, the observed RSV-specific responses did not follow the overall increase in lymphocyte/$CD4^+$ counts, thus indicating that T-cell expansion was virus-driven and not due to general immune reconstitution. Similarly, Patient #2, a 23-year old male with acute lymphoblastic leukemia (ALL) who received a matched unrelated donor (MUD) transplant with myeloablative conditioning, and developed a severe RSV-related URTI five months post HSCT while on tapering doses of tacrolimus. His infection symptomatically resolved within one week, coincident with the administration of ribavirin. To investigate whether endogenous immunity also played a role in viral clearance we monitored reactive T-cell numbers over time. Viral clearance was accompanied by an increase in the circulating frequency of RSV-specific T cells (peak 93 SFC/5x10^5 PBMC) with subsequent return to baseline levels (Figure 5B). The same patient was hospitalized seven months

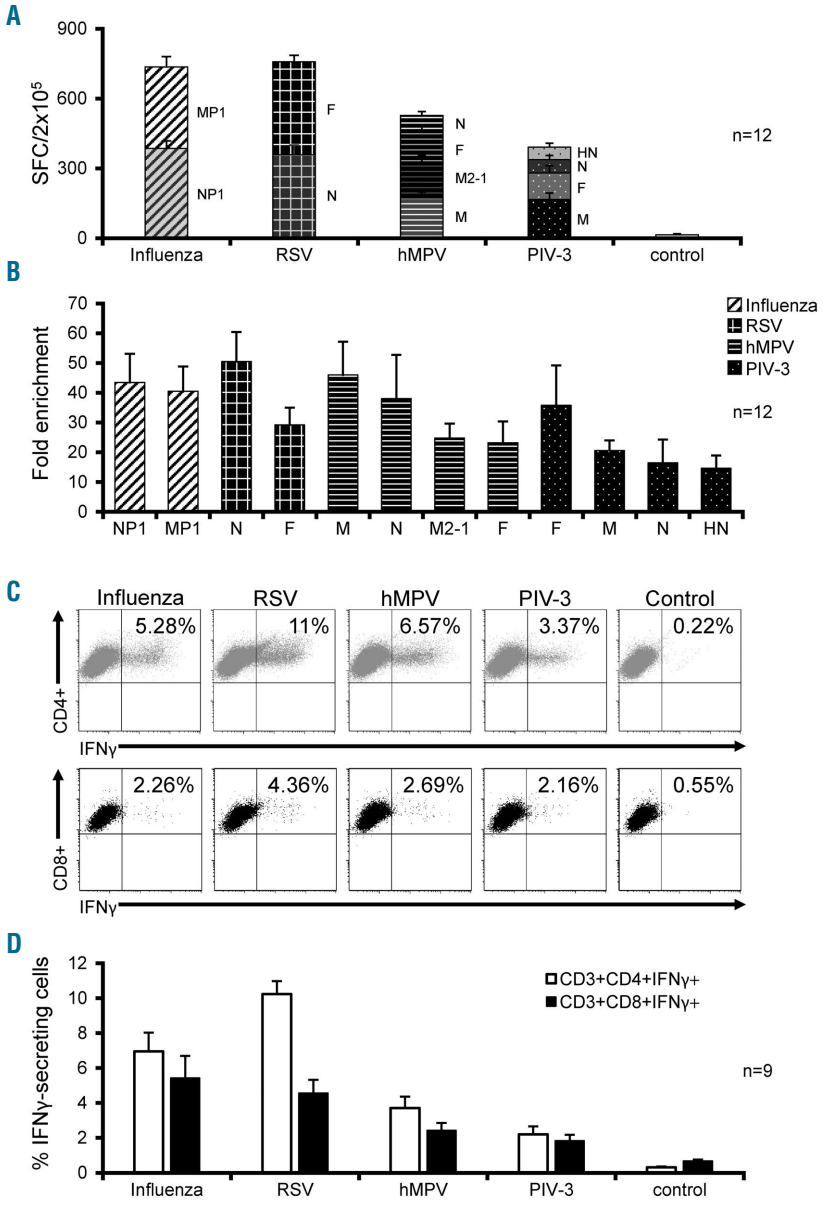

Figure 2. Specificity and enrichment of multi-respiratory virus-targeted cells (multi-R-VST). (A) The specificity of virus-reactive T cells within the expanded T-cell lines following exposure to individual stimulating antigens from each of the target viruses. Data are presented as mean± Standard Error of Mean (SEM) SFC/2x10^5 (n=12). (B) Fold enrichment of specificity [peripheral blood mononuclear cels (PBMC) *vs.* multi-R-VST; n=12]. (C) IFNγ production, as assessed by ICS from CD4 helper (top) and CD8 cytotoxic T cells (bottom) after viral stimulation in one representative donor (dot plots were gated on CD3$^+$ cells). (D) Summary results for nine donors screened (mean±SEM).

post transplant for a subsequent pneumococcal pneumonia with concurrent detection (by PCR) of hMPV in sputum. His pneumonia was treated with antibiotics with subsequent resolution of disease and viral clearance, coincident with a marked expansion of hMPV-specific T cells (reactive against F, N, M2-1 and M), which increased from 4 SFC to a peak of 70 SFC and subsequent decline to baseline levels (Figure 5C). Again, the observed RSV-and hMPV-specific responses were independent of the overall increase in lymphocyte/CD4$^+$ counts.

Online Supplementary Figure S7 shows the results of three additional HSCT recipients who developed CARV infections. Patient #3 is a 15-year old female with AML who received a haplo-identical transplant with reduced intensity conditioning, and developed an RSV-induced URTI and LRTI while on tacrolimus five weeks post transplant. The patient was administered ribavirin and the infection resolved within four weeks. We monitored RSV-reactive T cells over time and viral clearance coincided with a striking increase in the frequency of RSV-specific T cells (from 0 to 506 SFC/5x10^5 PBMC) (*Online Supplementary Figure S7A*). Similarly, Patient #4, a 10-year old male patient with ALL who received a MUD transplant with myeloablative conditioning, developed a PIV3-related URTI and LRTI one month after HSCT while on tacrolimus. His infection symptomatically resolved within five weeks, coincident with the administration of ribavirin. To investigate whether endogenous immunity also played a role in viral clearance, we monitored PIV3-reactive T-cell numbers over time. Viral clearance was accompanied by an increase in the circulating frequency of T cells specific for the PIV-3 antigens M, HN, N and F (peak 38 SFC/5x10^5 PBMC) with subsequent decline (*Online Supplementary Figure S7B*). Finally, we show Patient #5, a 3-year old male with chronic granulomatous disease who received a MRD transplant with myeloablative conditioning and developed a severe PIV-3-related URTI four months post HSCT while on cyclosporine. The patient received ribavirin but (at last timepoint assessed) continued to exhibit disease symptoms and failed to demonstrate PIV-3-specific T cells (*Online Supplementary Figure S7C*). Taken together, these data suggest the *in vivo* rele-

vance of CARV-specific T cells in the control of viral infections in immunocompromised patients.

Discussion

In the present study, we explored the feasibility of targeting multiple clinically problematic respiratory viruses using *ex vivo* expanded T cells. We have now shown that we can rapidly generate polyclonal, $CD4^+$ and $CD8^+$ T cells with specificities directed to a total of 12 antigens derived from four seasonal CARV [Influenza, RSV, hMPV and PIV-3] that are responsible for upper and lower respiratory tract infections in the immunocompromised host. These broad spectrum VST, generated using GMP-compliant methodologies, were Th1-polarized, produced multiple effector cytokines upon stimulation, and killed virus-infected targets without auto- or allo-reactivity. Finally, the detection of reactive T-cell populations in the peripheral blood of allogeneic HSCT recipients who successfully cleared active CARV infections suggests the potential for clinical benefit following the adoptive transfer of such multi-R-VST.

Community-acquired respiratory virus-associated acute upper and lower RTI are a major public health problem with young children, the elderly and those with suppressed or compromised immune systems being the most vulnerable.[1-3] These infections are associated with symptoms including cough, dyspnea, and wheezing, and

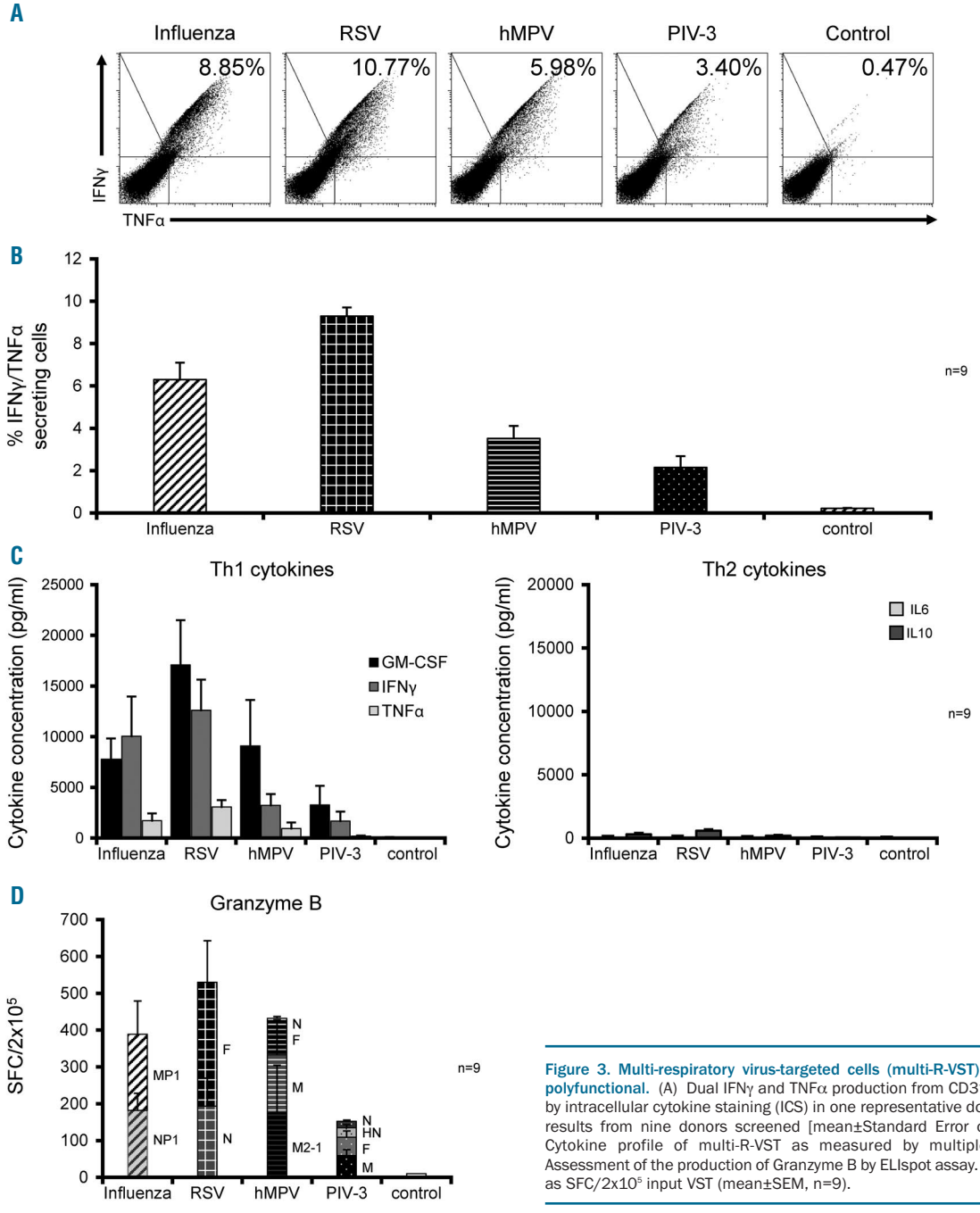

Figure 3. Multi-respiratory virus-targeted cells (multi-R-VST) are polyclonal and polyfunctional. (A) Dual IFNγ and TNFα production from $CD3^+$ T cells as assessed by intracellular cytokine staining (ICS) in one representative donor. (B) Summary of results from nine donors screened [mean±Standard Error of Mean (SEM)]. (C) Cytokine profile of multi-R-VST as measured by multiplex bead array. (D) Assessment of the production of Granzyme B by ELIspot assay. Results are reported as SFC/2x10^5 input VST (mean±SEM, n=9).

dual/multiple co-existing infections are common, with frequencies that may exceed 40% among children under 5-years of age and are associated with increased risk of morbidity and hospitalization.[22-26] Among immunocompromised allogeneic HSCT recipients up to 40% experience CARV infections that can range from mild (associated symptoms including rhinorrhea, cough and fever) to severe (bronchiolitis and pneumonia) with associated mortality rates as high as 50% in those with LRTI.[5-9] The therapeutic options are limited. For hMPV and PIV-3, there are currently no approved preventative vaccines nor therapeutic antiviral drugs, while the off-label use of the nucleoside analog RBV and the investigational use of DAS-181 (a recombinant sialidase fusion protein) have had limited clinical impact.[10,11,27,28] The preventative annual Influenza vaccine is not recommended for allogeneic HSCT recipients until at least six months post transplant (and excluded in recipients of intensive chemotherapy or anti-B-cell antibodies), while neuraminidase inhibitors are not always effective for the treatment of active infections.[12] For RSV, aerosolized RBV is FDA-approved for the treatment of severe bronchiolitis in infants and children, and it is also used off-label for the prevention of upper or lower RTI and treatment of RSV pneumonia in HSCT recipients.[13,15,16] However, its widespread use is limited by the cumbersome nebulization device and ventilation system required for drug delivery, as well as the considerable associated cost. For example, in 2015, aerosolized RBV cost $29,953 per day, with five days representing a typical treatment course.[14] Thus, the lack of approved treatments combined with the high cost of antiviral agents led us to explore the potential for using adoptively-transferred T cells to prevent and/or treat CARV infections in this patient population.

The pivotal role of functional T-cell immunity in mediating viral control of CARV has only recently attracted attention. For example, a retrospective study of 181 HSCT patients with RSV URTI, reported lymphopenia (defined as ALC ≤100/mm^3) as a key determinant in identifying patients whose infections would progress to LRTI, while RSV neutralizing antibody levels were not significantly associated with disease progression.[29] Furthermore, in a recent retrospective analysis of 154 adult patients with hematologic malignancies with or without HSCT treated for RSV LRTI, lymphopenia was significantly associated with higher mortality rates.[30] Both of these studies are suggestive of the importance of cellular immunity in mediating protective immunity *in vivo*.

Our group has previously demonstrated the feasibility and clinical utility of *ex vivo*-expanded VST to treat a range of clinically problematic viruses including the latent viruses CMV, EBV, BKV, HHV-6 and AdV.[17,31-33] Our initial studies (and those of others)[34-37] explored the safety and activity of donor-derived T-cell lines, but more recently we have developed an "off the shelf" universal T-cell platform whereby VST specific for all five viruses (CMV, EBV, BKV, HHV-6, AdV) were prospectively generated and banked, thus ensuring their immediate availability for administration to immunocompromised patients with uncontrolled infections. Indeed, in our recent phase II clinical trial, we administered these partially HLA-matched VST to 38 patients with a total of 45 infections that had proven refractory to conventional antiviral agents and achieved an overall response rate of 92%, with no significant toxicity.[18] This precedent of clinical success using adoptively transferred T cells, as well as the absence of effective therapies for a range of CARV, prompted us to explore the potential for extending the therapeutic scope of VST therapy to Influenza, RSV, hMPV and PIV-3 infections post HSCT. In this context, one could consider the option of prophylactic VST administration seasonally to high-risk patients [e.g. young (<5 years) and elderly adults, patients with impaired immune systems]. Alternatively, these cells could be used therapeutically in patients with URTI who have failed conventional antiviral medications in order to prevent LRT progression.

Thus, using our established, GMP-compliant VST manufacturing methodology, we demonstrated the feasibility of generating VST reactive against a spectrum of CARV-derived antigens chosen on the basis of both their immunogenicity to T cells and their sequence conservation [Influenza – NP1 and MP1;[20,38,39] RSV – N and F;[15,16,20] hMPV – F, N, M2-1 and M;[21] PIV3 – M, HN, N and F[19]] from 12 donors with diverse haplotypes. The expanded cells were polyclonal (CD4$^+$ and CD8$^+$), Th1-polarized and polyfunctional, and were able to lyse viral antigen-expressing targets while sparing non-infected autologous or allogeneic targets, attesting to both their virus specificity and their safety for clinical use. Finally, to assess the clinical significance of these findings we examined the

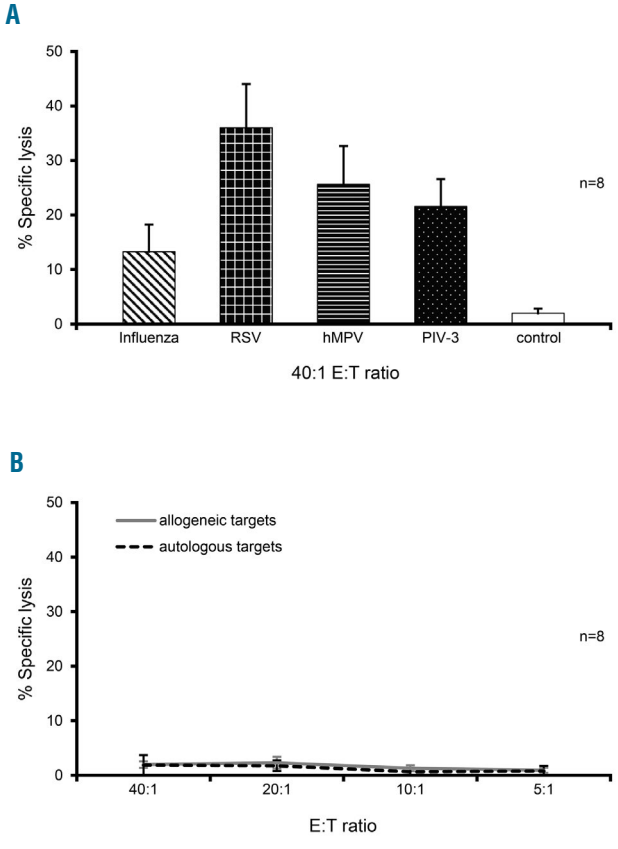

Figure 4. Multi-respiratory virus-targeted cells (multi-R-VST) are exclusively reactive against virus-infected targets. (A) Cytolytic potential of multi-R-VST evaluated by standard 4-hour Cr^{51} release assay using autologous pepmix-pulsed PHA blasts as targets (E:T 40:1; n=8) with unloaded phytohemagglutinin (PHA) blasts as a control. Results are presented as percentage of specific lysis (mean±SEM). (B) Demonstration that multi-R-VST show no activity against either non-infected autologous or allogeneic PHA blasts, as assessed by Cr^{51} release assay.

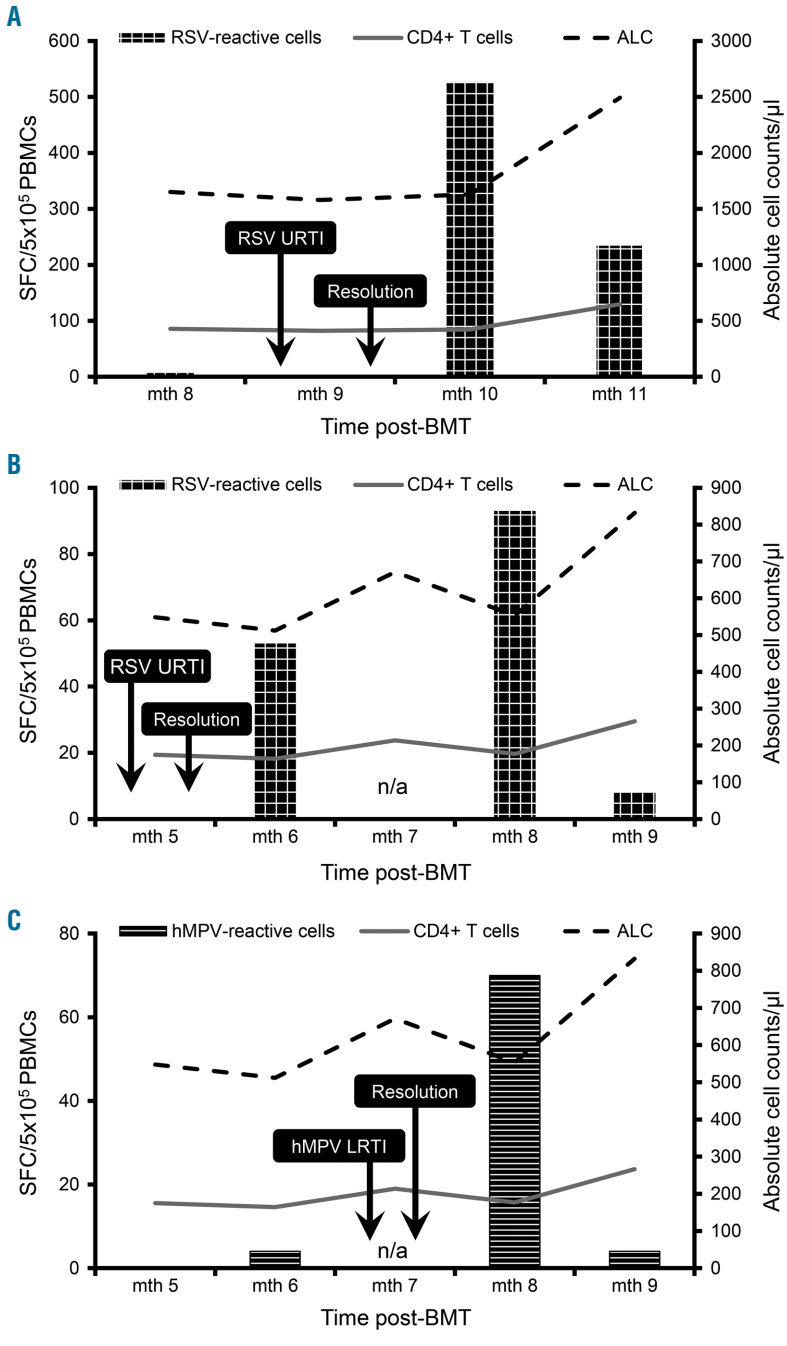

Figure 5. Detection of respiratory virus-targeted (RSV)- and human metapneumovirus (hMPV)-specific T cells in the peripheral blood of hematopoietic stem cell transplant (HSCT) recipients. Peripheral blood mononuclear cells (PBMC) isolated from two HSCT recipients with three infections were tested for specificity against the infecting viruses, using IFNγ ELIspot as a readout. (A and B) Results from two patients with RSV-associated upper respiratory tract infection (URTI) which was controlled, coincident with a detectable rise in endogenous RSV-specific T cells. (C) Clearance of an hMPV-lower respiratory tract infection (LRTI) with expansion of endogenous hMPV-specific T cells. ALC: absolute lymphocyte count.

peripheral blood of five allogeneic HSCT recipients with active RSV, hMPV and PIV-3 infections. Four of these patients successfully controlled the viruses within 1-5 weeks, coincident with an amplification of endogenous reactive T cells and subsequent return to baseline levels upon viral clearance, while one patient failed to mount an immune response against the infecting virus and has equally failed to clear the infection to date. These data suggests that the adoptive transfer of *ex vivo*-expanded cells should be clinically beneficial in patients whose own cellular immunity is lacking.

In conclusion, we have shown that it is feasible to rapidly generate a single preparation of polyclonal multi-respiratory (multi-R)-VST with specificities directed to Influenza, RSV, hMPV and PIV-3 in clinically relevant numbers using GMP-compliant manufacturing methodologies. These data provide the rationale for a future clinical trial of adoptively transferred multi-R-VST for the prevention or treatment of CARV infections in immunocompromised patients.

Funding

This work was supported by the Flow Cytometry and Cell and Vector Production shared resources in the Dan L. Duncan Comprehensive Cancer Center (support grant P30 CA125123).

SV was funded in part by an educational grant from the Hellenic Foundation of Hematology. PL is supported by the American Society of Hematology Junior Faculty Scholar grant and the Leukemia Texas Research grant. J. F. V. is supported by a Mentored Research Scholars Grant in Applied and Clinical Research (grant number MRSG-14-197-01-LIB) from the American Cancer Society.

References

1. Hodinka RL. Respiratory RNA Viruses. Microbiol Spectr. 2016;4(4).
2. Gill PJ, Richardson SE, Ostrow O, et al. Testing for Respiratory Viruses in Children: To Swab or Not to Swab. JAMA Pediatr. 2017;171(8):798-804.
3. Nair H, Simoes EA, Rudan I, et al. Global and regional burden of hospital admissions for severe acute lower respiratory infections in young children in 2010: a systematic analysis. Lancet. 2013;381(9875):1380-1390.
4. Shi T, McAllister DA, O'Brien KL, et al. Global, regional, and national disease burden estimates of acute lower respiratory infections due to respiratory syncytial virus in young children in 2015: a systematic review and modelling study. Lancet. 2017; 390(10098):946-958.
5. Paulsen GC, Danziger-Isakov L. Respiratory Viral Infections in Solid Organ and Hematopoietic Stem Cell Transplantation. Clin Chest Med. 2017; 38(4):707-726.
6. Abbas S, Raybould JE, Sastry S, et al. Respiratory viruses in transplant recipients: more than just a cold. Clinical syndromes and infection prevention principles. Int J Infect Dis. 2017;62:86-93.
7. Hutspardol S, Essa M, Richardson S, et al. Significant Transplantation-Related Mortality from Respiratory Virus Infections within the First One Hundred Days in Children after Hematopoietic Stem Cell Transplantation. Biol Blood Marrow Transplant. 2015;21(10):1802-1807.
8. Lin R, Liu Q. Diagnosis and treatment of viral diseases in recipients of allogeneic hematopoietic stem cell transplantation. J Hematol Oncol. 2013;6:94.
9. Renaud C, Xie H, Seo S, et al. Mortality rates of human metapneumovirus and respiratory syncytial virus lower respiratory tract infections in hematopoietic cell transplantation recipients. Biol Blood Marrow Transplant. 2013;19(8):1220-1226.
10. Shah DP, Shah PK, Azzi JM, et al. Human metapneumovirus infections in hematopoietic cell transplant recipients and hematologic malignancy patients: A systematic review. Cancer Lett. 2016;379(1):100-106.
11. Shah DP, Shah PK, Azzi JM, et al. Parainfluenza virus infections in hematopoietic cell transplant recipients and hematologic malignancy patients: A systematic review. Cancer Lett. 2016; 370(2):358-364.
12. Chemaly RF, Shah DP, Boeckh MJ. Management of respiratory viral infections in hematopoietic cell transplant recipients and patients with hematologic malignancies. Clin Infect Dis. 2014;59 Suppl 5:S344-351.
13. Beaird OE, Freifeld A, Ison MG, et al. Current practices for treatment of respiratory syncytial virus and other non-influenza respiratory viruses in high-risk patient populations: a survey of institutions in the Midwestern Respiratory Virus Collaborative. Transpl Infect Dis. 2016; 18(2):210-215.
14. Chemaly RF, Aitken SL, Wolfe CR, et al. Aerosolized ribavirin: the most expensive drug for pneumonia. Transpl Infect Dis. 2016;18(4):634-636.
15. Griffiths C, Drews SJ, Marchant DJ. Respiratory Syncytial Virus: Infection, Detection, and New Options for Prevention and Treatment. Clin Microbiol Rev. 2017;30(1):277-319.
16. Walsh EE. Respiratory Syncytial Virus Infection: An Illness for All Ages. Clin Chest Med. 2017;38(1):29-36.
17. Papadopoulou A, Gerdemann U, Katari UL, et al. Activity of broad-spectrum T cells as treatment for AdV, EBV, CMV, BKV, and HHV6 infections after HSCT. Sci Transl Med. 2014;6(242):242ra83.
18. Tzannou I, Papadopoulou A, Naik S, et al. Off-the-Shelf Virus-Specific T Cells to Treat BK Virus, Human Herpesvirus 6, Cytomegalovirus, Epstein-Barr Virus, and Adenovirus Infections After Allogeneic Hematopoietic Stem-Cell Transplantation. J Clin Oncol. 2017;35(31):3547-3557.
19. Aguayo-Hiraldo PI, Arasaratnam RJ, Tzannou I, et al. Characterizing the cellular immune response to parainfluenza virus 3. J Infect Dis. 2017; 216(2):153-161.
20. Gerdemann U, Keirnan JM, Katari UL, et al. Rapidly generated multivirus-specific cytotoxic T lymphocytes for the prophylaxis and treatment of viral infections. Mol Ther. 2012;20(8):1622-1632.
21. Tzannou I, Nicholas SK, Lulla P, et al. Immunologic Profiling of Human Metapneumovirus for the Development of Targeted Immunotherapy. J Infect Dis. 2017;216(6):678-687.
22. Goka E, Vallely P, Mutton K, et al. Influenza A viruses dual and multiple infections with other respiratory viruses and risk of hospitalisation and mortality. Influenza Other Respir Viruses. 2013;7(6):1079-1087.
23. Goka EA, Vallely PJ, Mutton KJ, et al. Single, dual and multiple respiratory virus infections and risk of hospitalization and mortality. Epidemiol Infect. 2015;143(1):37-47.
24. Kouni S, Karakitsos P, Chranioti A, et al. Evaluation of viral co-infections in hospitalized and non-hospitalized children with respiratory infections using microarrays. Clin Microbiol Infect. 2013;19(8):772-777.
25. Lim FJ, de Klerk N, Blyth CC, et al. Systematic review and meta-analysis of respiratory viral coinfections in children. Respirology. 2016;21(4):648-655.
26. Stefanska I, Romanowska M, Donevski S, et al. Co-infections with influenza and other respiratory viruses. Adv Exp Med Biol. 2013;756:291-301.
27. Salvatore M, Satlin MJ, Jacobs SE, et al. DAS181 for treatment of parainfluenza Virus infections in hematopoietic stem cell Transplant recipients at a single center. Biol Blood Marrow Transplant. 2016;22(5):965-970.
28. Zenilman JM, Fuchs EJ, Hendrix CW, et al. Phase 1 clinical trials of DAS181, an inhaled sialidase, in healthy adults. Antiviral Res. 2015;123:114-119.
29. Kim YJ, Guthrie KA, Waghmare A, et al. Respiratory syncytial virus in hematopoietic cell transplant recipients: factors determining progression to lower respiratory tract disease. J Infect Dis. 2014;209(8):1195-1204.
30. Vakil E, Sheshadri A, Faiz SA, et al. Risk factors for mortality after respiratory syncytial virus lower respiratory tract infection in adults with hematologic malignancies. Transpl Infect Dis. 2018;20(6):e12994.
31. Gerdemann U, Katari UL, Papadopoulou A, et al. Safety and clinical efficacy of rapidly-generated trivirus-directed T cells as treatment for adenovirus, EBV, and CMV infections after allogeneic hematopoietic stem cell transplant. Mol Ther. 2013;21(11):2113-2121.
32. Heslop HE, Slobod KS, Pule MA, et al. Long-term outcome of EBV-specific T-cell infusions to prevent or treat EBV-related lymphoproliferative disease in transplant recipients. Blood. 2010;115(5):925-935.
33. Leen AM, Christin A, Myers GD, et al. Cytotoxic T lymphocyte therapy with donor T cells prevents and treats adenovirus and Epstein-Barr virus infections after haploidentical and matched unrelated stem cell transplantation. Blood. 2009; 114(19):4283-4292.
34. Doubrovina E, Oflaz-Sozmen B, Prockop SE, et al. Adoptive immunotherapy with unselected or EBV-specific T cells for biopsy-proven EBV+ lymphomas after allogeneic hematopoietic cell transplantation. Blood. 2012;119(11):2644-2656.
35. Feucht J, Opherk K, Lang P, et al. Adoptive T-cell therapy with hexon-specific Th1 cells as a treatment of refractory adenovirus infection after HSCT. Blood. 2015; 125(12):1986-1994.
36. Feuchtinger T, Opherk K, Bethge WA, et al. Adoptive transfer of pp65-specific T cells for the treatment of chemorefractory cytomegalovirus disease or reactivation after haploidentical and matched unrelated stem cell transplantation. Blood. 2010; 116(20):4360-4367.
37. Peggs KS, Verfuerth S, Pizzey A, et al. Cytomegalovirus-specific T cell immunotherapy promotes restoration of durable functional antiviral immunity following allogeneic stem cell transplantation. Clin Infect Dis. 2009;49(12):1851-1860.
38. Chen L, Zanker D, Xiao K, et al. Immunodominant CD4+ T-cell responses to influenza A virus in healthy individuals focus on matrix 1 and nucleoprotein. J Virol. 2014;88(20):11760-11773.
39. Grant EJ, Quinones-Parra SM, Clemens EB, et al. Human influenza viruses and CD8(+) T cell responses. Curr Opin Virol. 2016; 16:132-142.

haematologica
Journal of the Ferrata Storti Foundation

The origin of a name that reflects Europe's cultural roots.

Ancient Greek

αἷμα [haima] = blood
αἵματος [haimatos] = of blood
λόγος [logos]= reasoning

Scientific Latin

haematologicus (adjective) = related to blood

Scientific Latin

haematologica (adjective, plural and neuter, used as a noun) = hematological subjects

Modern English

The oldest hematology journal, publishing the newest research results.
2018 JCR impact factor = 7.570

RESEARCH, READ & CONNECT

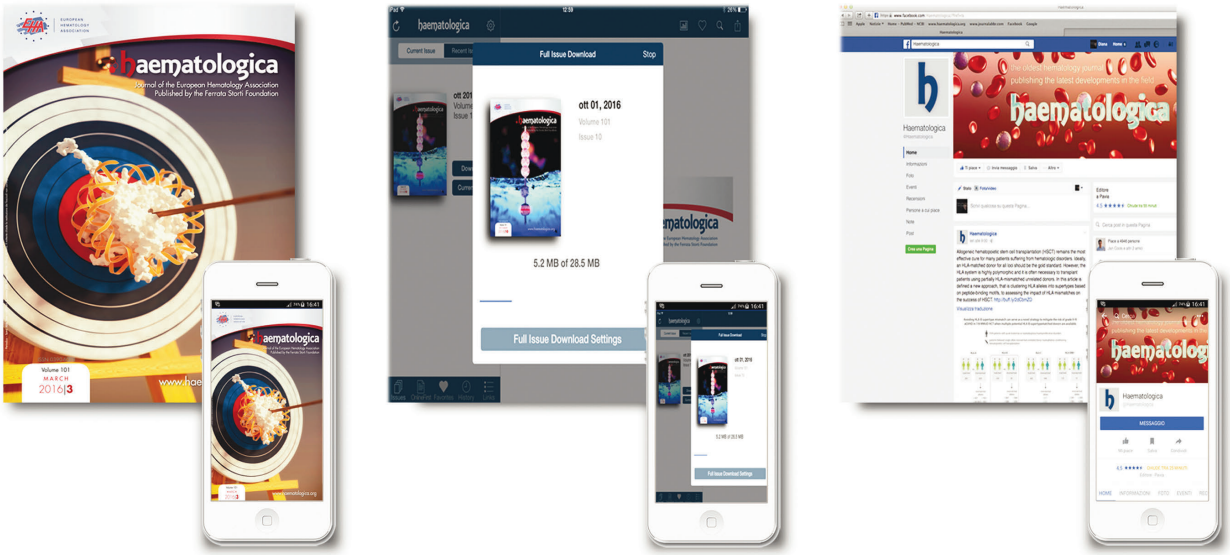

We reach more than
6 hundred thousand readers each year

The first Hematology Journal in Europe

Impressions YTD

9,621,645

Digital Readers

4,431

Total Audience

554,484

Worldwide rank	Impact factor	Total citations
7 th	7.570	16,255

haematologica

Journal of the Ferrata Storti Foundation

haematologica — Vol. 105 n. 1 — January 2020 — 1-244